Advances in Visual Science and Eye Diseases 1
Series Editor: Ningli Wang

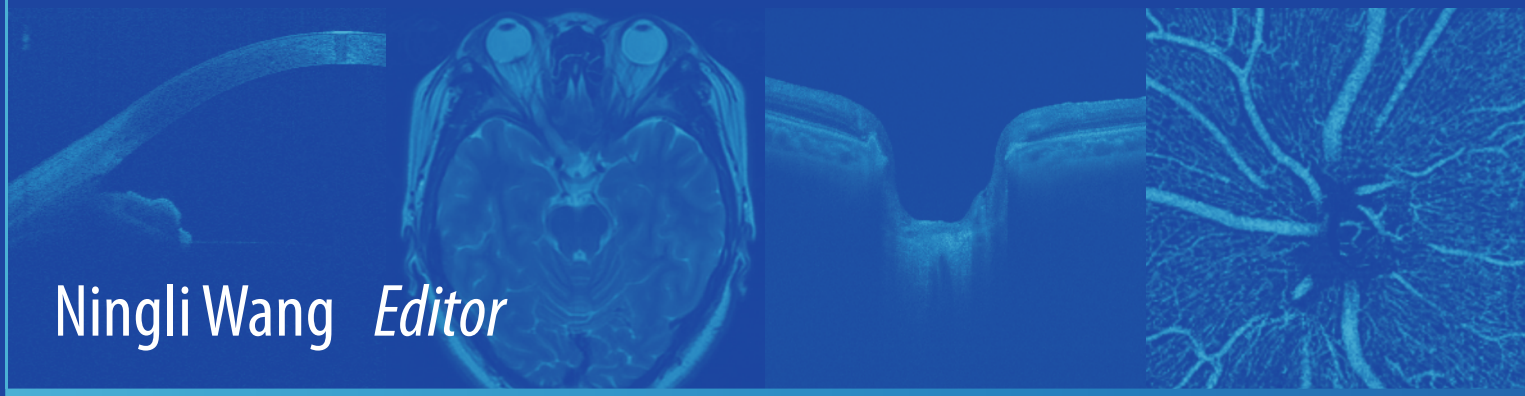

Ningli Wang *Editor*

Intraocular and Intracranial Pressure Gradient in Glaucoma

Springer

Advances in Visual Science and Eye Diseases

Series Editor

Ningli Wang
Beijing Tongren Hospital
Capital Medical University
Beijing, China

Advances in Visual Science and Eye Diseases presents the latest progress and achievement made in visual science and eye diseases for eye care health professionals at different links in the chain of eye care delivery including ophthalmologists, researchers, eye care service providers, health policy makers, and medical students.

The series firstly covers major blinding eye diseases, expounding on their characteristics and the latest development in pathogenesis, up-to-date researches and treatment options of the diseases in detail. Then, the series unfolds the pathogenesis, new diagnosis methods, latest surgery techniques, genetic research, animal modelling studies and translational medicine in glaucoma. Next, the series provides an overall picture on 000. the development of ophthalmology in China along with the contribution of Chinese ophthalmologists to the international community from historical perspective and sheds light on its future development directions; 2. eye epidemiological studies and achievements in blindness prevention in China; 4. holistic view on the systematic relationship between the eye and other organs as well as the relationship between eye diseases and systematic diseases. We hope readers can benefit from this series by enriching their latest knowledge in no matter visual science or clinical management of eye diseases.

Ningli Wang is a professor at Beijing Tongren Hospital affiliated to Capital Medical University, Beijing, China. He is also the director of Tongren Eye Center, Beijing, China.

More information about this series at http://www.springer.com/series/16143

Ningli Wang
Editor

Intraocular and Intracranial Pressure Gradient in Glaucoma

Springer

Editor
Ningli Wang
Beijing Tongren Hospital
Capital Medical University
Beijing
China

ISSN 2524-566X ISSN 2524-5678 (electronic)
Advances in Visual Science and Eye Diseases
ISBN 978-981-13-2136-8 ISBN 978-981-13-2137-5 (eBook)
https://doi.org/10.1007/978-981-13-2137-5

This Springer imprint is published by the registered company Springer Nature Singapore Pte Ltd.
The registered company address is: 152 Beach Road, #21-01/04 Gateway East, Singapore 189721, Singapore

Preface

Glaucoma is well recognized as a pressure-related disease. Although many traditional theories have been brought up to explain the mechanism of glaucomatous optic nerve damage, such as mechanical theory and vascular theory, none of them succeeded in revealing the whole truth about the pathogenesis of glaucoma. More importantly, it was noticed in recent years that, in Asia, especially in East Asia, the intraocular pressure (IOP) of 60–80% patients with open angle glaucoma (OAG) was within the normal range. Why would the optic nerve damage still occur even when the IOP is within the normal range? This challenging yet significant question has remained unanswered.

In 1976, the effect of low cerebrospinal fluid pressure (CSFP) on glaucoma was, for the first time, discussed by Volkov V.V. In 1979, Yablonski M.E., Ritch R. and Pokorny K.S. found that chronic lowering of intracranial pressure (ICP) led to glaucomatous damage in the optic nerve and put forward the hypothesis that low CSFP might be involved in glaucoma. Yablonski and colleagues lowered the CSFP to 4 mmHg in the cat model. One eye of the cat was cannulated to achieve 0 mmHg of pressure, while the other eye was the control. Three weeks later, the non-cannulated eye developed glaucomatous neuropathy, while the fundus of the eye that was maintained a lower pressure as similar to the CSFP remained normal. This is the first animal model that suggested the role of the intraocular and intracranial pressure gradient in glaucoma. About three decades later, a retrospective study by John Berdahl et al. in 2008 and a prospective study by Beijing iCOP Study Group in 2010 found that 70–80% patients with normal tension glaucoma (NTG) had a relatively low ICP, which was the first time that the elevated trans-lamina cribrosa pressure difference (TLPD) caused by low ICP in NTG was identified through a clinical observational study. After this breakthrough, a series of studies based on primate and rat models were carried out worldwide, providing growing evidence that the intraocular and intracranial pressure gradient or TLPD plays an essential role in the mechanism of optic nerve damage in OAG. However, at the same time, a number of studies have also proved that the pressure gradient theory or TLPD theory alone cannot explain the development of all types of glaucoma, and it only serves as a potential pathogenesis for a certain proportion of NTG patients.

In 2016, the Beijing iCOP Study Group organized the first "Intraocular and Intracranial Pressure Gradient Related Diseases International Summit" (IIPGD Summit) and invited top experts in this field from all over the world to introduce and share their research results. After candid and spirited discussion, all the speakers reached an agreement on publishing a book that covers all the presented research results. The book reviews all the research results in this field from the beginning to the present, summarizes the consensus built, presents different viewpoints and proposes future research directions in the field.

Recently, there were several important articles on this theme published. Linda et al. used a more accurate method to calculate the TLPD and reported that NTG patients have normal ICP. This inconsistency between our research results was caused by difference in small sample sizes in all studies, and racial difference should also be considered, which has inspired us that an international cooperative study covering different ethnic groups based on a standard protocol would be of great interest. In addition, Gallina et al. reported that 9 out of 22 patients with normal pressure hydrocephalus who were treated with ventriculoperitoneal shunt placement to

lower the cerebrospinal fluid pressure developed NTG, which provides stronger evidence on the role of CSFP in glaucomatous optic neuropathy. More recently, Sawada et al. observed focal lamina cribrosa (LC) defect in patients with myopia. The results showed that compared with progressive visual field defect group, non-progressive visual field defect group had more eyes with LC defect. Meanwhile, the baseline IOP was lower in eyes with LC defect. These findings suggested that LC defect may have contributed to the pressure balance between IOP and CSFP, resulting in a lower TLPD and thereby protecting LC from mechanical force. Unfortunately, all the manuscripts have already been submitted to the publisher when these articles were published. Therefore, the results of these remarkable researches were not included in this book.

This is a fascinating field with many possibilities to explore: Is there a non-invasive method for TLPD measurement? Is it possible to achieve simultaneous measurement of IOP and ICP fluctuations? Is a treatment that reduces the TLPD by appropriately increasing ICP feasible? Can we develop a surgery that can resume the pressure balance between IOP and ICP?

The successful publication of this book would not have been possible without the input, help and support from many. To start with, I would like to convey my sincere gratitude to all the authors for their hard work and their incredible support. In addition, my heartfelt appreciation goes to all the members of the preparation working group (Dr. Liu Xiangxiang, Ms. Mayinuer Yusufu, Dr. Zhang Ye) who have put a great amount of effort and time in the preparation of this book. I also thank all my family members and friends, especially my loving wife and lovely daughter, whose moral support has been a great motivation. At the time that this book is officially published, it will have been 3 years since the first “IIPGD Summit” was held. According to the agreement reached at the meeting, we are about to host the second “IIPGD Summit”. I would like to take this opportunity to invite all the readers who are interested in this theme to attend the meeting.

Last but not least, with this book, I would like to pay the highest respect to all the researchers who have made their unique contribution to the advancement of this field by proposing hypotheses and carrying out a great amount of research work!

Beijing, China Ningli Wang

Contents

Part VIII System Disease and POAG

Contributors

R. Rand Allingham Duke University Eye Center, Durham, NC, USA

Bang V. Bui Department of Optometry and Vision Sciences, University of Melbourne, Parkville, VIC, Australia

Claude F. Burgoyne Devers Eye Institute, Optic Nerve Head Research Laboratory, Legacy Research Institute, Portland, OR, USA

Weiwei Chen Beijing Institute of Ophthalmology, Beijing Tongren Eye Center, Beijing Tongren Hospital, Capital Medical University, Beijing, China

Beijing Ophthalmology & Visual Sciences Key Laboratory, Beijing, China

Chao Dai Southwest Eye Hospital, Southwest Hospital, Third Military Medical University, Chongqing, China

Shaban Demirel Devers Eye Institute, Optic Nerve Head Research Laboratory, Legacy Research Institute, Portland, OR, USA

Jialing Du Beijing Institute of Ophthalmology, Beijing Tongren Eye Center, Beijing Tongren Hospital, Capital Medical University, Beijing, China

Beijing Ophthalmology & Visual Sciences Key Laboratory, Beijing, China

Ning Fan Shenzhen Eye Hospital, Jinan University, Guangdong, China

Yubo Fan Key Laboratory for Biomechanics and Mechanobiology of Ministry of Education, School of Biological Science, and Medical Engineering, Beijing Advanced Innovation Centre for Biomedical Engineering, Beihang University, BeijingChina

Zhigang Fan Zhongshan Ophthalmic Center, Sun Yet-sen University, Guangdong, China

David Fleischman Department of Ophthalmology, University of North Carolina at Chapel Hill, Chapel Hill, NC, USA

Stuart Gardiner Devers Eye Institute, Optic Nerve Head Research Laboratory, Legacy Research Institute, Portland, OR, USA

Josh Gross Department of Ophthalmology, Glaucoma Research and Diagnostic Center, Eugene and Marilyn Glick Eye Institute, Indiana University School of Medicine, Indianapolis, IN, USA

Giovanna Guidoboni Department of Electrical Engineering and Computer Science, University of Missouri, Columbia, MO, USA

Department of Mathematics, University of Missouri, Columbia, MO, USA

Chunyu Guo Department of Epidemiology, School of Public Health, University of Michigan, Ann Arbor, MI, USA

Neeru Gupta Department of Ophthalmology and Vision Sciences, University of Toronto, TorontoONCanada

Jie Hao Beijing Institute of Ophthalmology, Beijing Tongren Eye Center, Beijing Tongren Hospital, Capital Medical University, Beijing, China

Beijing Ophthalmology & Visual Sciences Key Laboratory, Beijing, China

Christy Hardin Devers Eye Institute, Optic Nerve Head Research Laboratory, Legacy Research Institute, Portland, OR, USA

Alon Harris Department of Ophthalmology, Glaucoma Research and Diagnostic Center, Eugene and Marilyn Glick Eye Institute, Indiana University School of Medicine, IndianapolisINUSA

Zheng He Department of Optometry and Vision Sciences, University of Melbourne, ParkvilleVICAustralia

Ruowu Hou Department of Neurosurgery, Beijing Tongren Hospital, Capital Medical University, Beijing, China

Jost B. Jonas Department of Ophthalmology, Medical Faculty Mannheim of the Ruprecht-Karls-University, Seegartenklinik Heidelberg, HeidelbergGermany

Jae Hee Kang Brigham and Women's Hospital/Harvard Medical School, Boston, MA, USA

Hanspeter E. Killer Department of Ophthalmology Kantonsspital Aarau, University of Basel, Basel, Switzerland

Christopher Leung Department of Ophthalmology and Visual Sciences, The Chinese University of Hong Kong, Hong Kong, China

Jing Li Beijing Institute of Ophthalmology, Beijing Tongren Eye Center, Beijing Tongren Hospital, Capital Medical University, Beijing, China

Beijing Ophthalmology & Visual Sciences Key Laboratory, Beijing, China

Xiaoxia Li Beijing Institute of Ophthalmology, Beijing Tongren Eye Center, Beijing Tongren Hospital, Capital Medical University, Beijing, China

Beijing Ophthalmology & Visual Sciences Key Laboratory, Beijing, China

Ying Li UCL Department of Cell and Developmental Biology and Spinal Repair Unit, Department of Brain Repair and Rehabilitation, UCL Institute of Neurology, LondonUK

Zhen Li Department of Ophthalmology, Xuanwu Hospital, Capital Medical University, Beijing, China

Jeremiah K.H. Lim Department of Optometry and Vision Sciences, University of Melbourne, Parkville, VIC, Australia

Caixia Lin Beijing Institute of Ophthalmology, Beijing Tongren Eye Center, Beijing Tongren Hospital, Capital Medical University, Beijing, China

Beijing Ophthalmology & Visual Sciences Key Laboratory, Beijing, China

Dachuan Liu Department of ophthalmology, Xuanwu Hospital, Capital medical University, BeijingChina

Guo Liu Shenzhen Eye Hospital, Jinan University, GuangdongChina

Hanruo Liu Beijing Institute of Ophthalmology, Beijing Tongren Eye Center, Beijing Tongren Hospital, Capital Medical University, Beijing, China

Beijing Ophthalmology & Visual Sciences Key Laboratory, Beijing, China

John H.K. Liu Department of Ophthalmology, Shiley Eye Institute, University of California, San Diego, CA, USA

Lu Liu Beijing Institute of Ophthalmology, Beijing Tongren Eye Center, Beijing Tongren Hospital, Capital Medical University, Beijing, China

Beijing Ophthalmology & Visual Sciences Key Laboratory, Beijing, China

Si'an Liu Zhongshan Ophthalmic Center, Sun Yet-sen University, Guangdong, China

Xiangxiang Liu Beijing Institute of Ophthalmology, Beijing Tongren Eye Center, Beijing Tongren Hospital, Capital Medical University, Beijing, China

Beijing Ophthalmology & Visual Sciences Key Laboratory, Beijing, China

Xiaoyu Liu Key Laboratory for Biomechanics and Mechanobiology of Ministry of Education, School of Biological Science, and Medical Engineering, Beijing Advanced Innovation Centre for Biomedical Engineering, Beihang University, Beijing, China

Xuyang Liu Shenzhen Eye Hospital, Jinan University, Guangdong, China

Yan Lu Department of Ophthalmology, Beijing Shijitan Hospital, Capital Medical University, BeijingChina

Yingyan Mao Beijing Institute of Ophthalmology, Beijing Tongren Eye Center, Beijing Tongren Hospital, Capital Medical University, Beijing, China

Beijing Ophthalmology & Visual Sciences Key Laboratory, Beijing, China

Teng Ma Beijing Institute of Ophthalmology, Beijing Tongren Eye Center, Beijing Tongren Hospital, Capital Medical University, Beijing, China

John M. McGregor Department of Neurological Surgery, The Ohio State University, Columbus, OH, USA

Nancy J. Newman Department of Ophthalmology, Neurology and Neurological Surgery, Emory University School of Medicine, Atlanta, GA, USA

Christine T.O. Nguyen Department of Optometry and Vision Sciences, University of Melbourne, Parkville, VIC, Australia

Louis R. Pasquale Department of Ophthalmology, Icahn School of Medicine at Mount Sinai, New York, NY, USA

April Peszel The First Affiliated Hospital of Anhui Medical University, Hefei, China

Daniele Prada Istituto di Matematica Applicata e Tecnologie Informatiche "Enrico Magenes", Centro Nazionale delle Ricerche, Pavia, Italy

Zhu Qiang Beijing Institute of Ophthalmology, Beijing Tongren Eye Center, Beijing Tongren Hospital, Capital Medical University, Beijing, China

Geoffrey Raisman UCL Department of Cell and Developmental Biology and Spinal Repair Unit, Department of Brain Repair and Rehabilitation, UCL Institute of Neurology, London, UK

Ruojin Ren Devers Eye Institute, Optic Nerve Head Research Laboratory, Legacy Research Institute, Portland, OR, USA

Feras Kamel Rizeq Avalon University School of Medicine, Willemstad, Curacao

Cynthia J. Roberts Ophthalmology & Visual Science and Biomedical Engineering, The Ohio State University, Columbus, OH, USA

Lauren Saint Department of Ophthalmology, Glaucoma Research and Diagnostic Center, Eugene and Marilyn Glick Eye Institute, Indiana University School of Medicine, Indianapolis, IN, USA

Jinghong Sang Beijing Institute of Ophthalmology, Beijing Tongren Eye Center, Beijing Tongren Hospital, Capital Medical University, Beijing, China

Beijing Ophthalmology & Visual Sciences Key Laboratory, Beijing, China

Wenyuan Shi Beijing Institute of Ophthalmology, Beijing Tongren Eye Center, Beijing Tongren Hospital, Capital Medical University, Beijing, China

Brent Siesy Department of Ophthalmology, Glaucoma Research and Diagnostic Center, Eugene and Marilyn Glick Eye Institute, Indiana University School of Medicine, Indianapolis, IN, USA

Chenyu Sun The First Affiliated Hospital of Anhui Medical University, Hefei, China

Yunxiao Sun Beijing Institute of Ophthalmology, Beijing Tongren Eye Center, Beijing Tongren Hospital, Capital Medical University, BeijingChina

Beijing Ophthalmology & Visual Sciences Key Laboratory, BeijingChina

Ning Tian Beijing Institute of Ophthalmology, Beijing Tongren Eye Center, Beijing Tongren Hospital, Capital Medical University, Beijing, China

Beijing Ophthalmology & Visual Sciences Key Laboratory, Beijing, China

Anna Van Koeverden Department of Optometry and Vision Sciences, University of Melbourne, ParkvilleVICAustralia

Alice C. Verticchio Vercellin Department of Ophthalmology, Glaucoma Research and Diagnostic Center, Eugene and Marilyn Glick Eye Institute, Indiana University School of Medicine, Indianapolis, IN, USA

Algis J. Vingrys Department of Optometry and Vision Sciences, University of Melbourne, Parkville, VIC, Australia

Huaizhou Wang Beijing Institute of Ophthalmology, Beijing Tongren Eye Center, Beijing Tongren Hospital, Capital Medical University, BeijingChina

Beijing Ophthalmology & Visual Sciences Key Laboratory, Beijing, China

Jiawei Wang Department of Neurology and Medical Research Center, Beijing Tongren Hospital, Capital Medical University, Beijing, China

Ningli Wang Beijing Institute of Ophthalmology, Beijing Tongren Eye Center, Beijing Tongren Hospital, Capital Medical University, Beijing, China

Beijing Ophthalmology & Visual Sciences Key Laboratory, Beijing, China

Yaxing Wang Beijing Institute of Ophthalmology, Beijing Tongren Eye Center, Beijing Tongren Hospital, Capital Medical University, Beijing, China

Beijing Ophthalmology & Visual Sciences Key Laboratory, Beijing, China

Yue Wan Beijing Institute of Ophthalmology, Beijing Tongren Eye Center, Beijing Tongren Hospital, Capital Medical University, Beijing, China

Beijing Ophthalmology & Visual Sciences Key Laboratory, BeijingChina

Robert N. Weinreb Hamilton Glaucoma Center and the Department of Ophthalmology, University of California, San Diego, La Jolla, CA, USA

Vickie H.Y. Wong Department of Optometry and Vision Sciences, University of Melbourne, Parkville, VIC, Australia

Shen Wu Beijing Institute of Ophthalmology, Beijing Tongren Eye Center, Beijing Tongren Hospital, Capital Medical University, Beijing, China

Beijing Ophthalmology & Visual Sciences Key Laboratory, BeijingChina

Junfang Xian Department of Radiology, Beijing Tongren Hospital, Capital Medical University, Beijing, China

Xiaobin Xie Eye Hospital, China Academy of Chinese Medical Sciences, Beijing, China

Chen Xin Beijing Institute of Ophthalmology, Beijing Tongren Eye Center, Beijing Tongren Hospital, Capital Medical University, Beijing, China

Beijing Ophthalmology & Visual Sciences Key Laboratory, BeijingChina

Diya Yang Beijing Institute of Ophthalmology, Beijing Tongren Eye Center, Beijing Tongren Hospital, Capital Medical University, Beijing, China

Beijing Ophthalmology & Visual Sciences Key Laboratory, Beijing, China

Hongli Yang Devers Eye Institute, Optic Nerve Head Research Laboratory, Legacy Research Institute, Portland, OR, USA

Yiquan Yang Beijing Institute of Ophthalmology, Beijing Tongren Eye Center, Beijing Tongren Hospital, Capital Medical University, Beijing, China

Beijing Ophthalmology & Visual Sciences Key Laboratory, Beijing, China

Yeni Yucel Department of Ophthalmology and Vision Sciences, Laboratory Medicine and Pathobiology, Keenan Research Centre for Biomedical Science, Li Ka Shing Knowledge Institute of St. Michael's Hospital, University of Toronto, Toronto, ON, Canada

Jing Yu Beijing Institute of Ophthalmology, Beijing Tongren Eye Center, Beijing Tongren Hospital, Capital Medical University, Beijing, China

Beijing Ophthalmology & Visual Sciences Key Laboratory, Beijing, China

Mayinuer Yusufu Beijing Institute of Ophthalmology, Beijing Tongren Eye Center, Beijing Tongren Hospital, Capital Medical University, Beijing, China

Jingxue Zhang Beijing Institute of Ophthalmology, Beijing Tongren Eye Center, Beijing Tongren Hospital, Capital Medical University, Beijing, China

Beijing Ophthalmology & Visual Sciences Key Laboratory, Beijing, China

Qian Zhang Department of Nutrition, Beijing Tongren Hospital, Capital Medical University, Beijing, China

Qing Zhang Beijing Institute of Ophthalmology, Beijing Tongren Eye Center, Beijing Tongren Hospital, Capital Medical University, Beijing, China

Beijing Ophthalmology & Visual Sciences Key Laboratory, Beijing, China

Xiaoguang Zhang Shenzhen Eye Hospital, Jinan University, Guangdong, China

Xuxiang Zhang Department of Ophthalmology, Xuanwu Hospital, Capital Medical University, Beijing, China

Ye Zhang Beijing Institute of Ophthalmology, Beijing Tongren Eye Center, Beijing Tongren Hospital, Capital Medical University, Beijing, China

Beijing Ophthalmology & Visual Sciences Key Laboratory, Beijing, China

Zheng Zhang Beijing Institute of Ophthalmology, Beijing Tongren Eye Center, Beijing Tongren Hospital, Capital Medical University, Beijing, China

Beijing Ophthalmology & Visual Sciences Key Laboratory, Beijing, China

Da Zhao Department of Optometry and Vision Sciences, University of Melbourne, Parkville, VIC, Australia

Zhenni Zhao Zhongshan Ophthalmic center, Sun Yet-sen University, Guangdong, China

Part I

Review of the Study of Trans-laminar Cribrosa Pressure Difference

Road Map for the Pathogenesis of Glaucomatous Optic Neuropathy

1

Ningli Wang

Glaucoma has been recognized for several hundred years. Initially, it was defined as an eye disease of characteristic structural change of optic nerves and specific visual field change caused by increased intraocular pressure (IOP). However, when we comprehended the development and progress of glaucoma only limiting to the perspective of the eye itself, we could hardly interpret some problems we encountered clinically. For example, some glaucoma patients' IOP is in the normal range (normal-tension glaucoma); some people have long-term IOP higher than the normal range, and there is no pathological change of their optic nerves though; some glaucoma patients have IOP controlled in normal range by drugs or surgeries, while impairment of their optic nerves and vision is still gradually worsening; and some patients with disease of the nervous system have glaucoma at the same time. Are those phenomena occasional, or are there some correlations not yet discovered? In order to answer above questions, the ophthalmologist have started to explore the structures beyond the eyeball per se, and proposed an innovative theory of "trans-lamina cribrosa pressure gradient", a concept that defines glaucoma as "a disease of central visual pathway" by considering both ocular pathological changes and body fluid circulation, which shall open a new chapter in glaucoma study.

In this article, we reviewed some milestone studies of "trans-lamina cribrosa pressure gradient in glaucoma" to retrospect the road map for the pathogenesis of glaucomatous optic neuropathy (Fig. 1.1).

In 1976, Volkov VV first discussed about the effect of low CSF pressure on glaucoma [1]. In 1979, Yablonski ME, Ritch R, and Pokorny KS found chronic lowering of intracranial pressure led to glaucoma damage of the optic nerve and that simultaneous lowering of IOP prevented damage [2]. At this time, the hypothesis that low cerebrospinal fluid pressure (CSFp) might be involved in glaucoma was proposed.

Thirty years later, two clinical studies, a prospective study from Tongren Hospital [3] and a retrospective study from Duke [4], both found that cerebrospinal fluid pressure was low in NTG patients. These are pioneer clinical studies focusing on the role of CSFp in the pathogenesis of glaucoma. The same study groups did some further studies based on the concept of trans-lamina cribrosa pressure difference (TLPD). The results suggested that the TLPD as compared to the IOP was significantly better correlated with cup to disc ratio, rim width, and visual field loss [5]. This may provide some indirect evidence that the CSFp might play some role in the pathogenesis of glaucomatous optic neuropathy.

Followed by this lead, the same study groups found that body mass index (BMI) had a positive linear relationship with CSFp, whereas IOP was unaffected by BMI and CSFp [6, 7]. This finding indicated that the higher BMI may be a protective factor for glaucoma.

In 2011, Mader et al. [8] first reported that after long-duration space flight, optic disc edema, globe flattening, choroidal folds, and hyperopic shifts were observed in astronauts. This finding proved that zero-gravity environment may cause CSFp elevation and a reversal TLPD. As the optic change of the astronauts was opposite of the glaucomatous neuropathy, we may speculate that the TLPD-related conditions existed and breaking the balance of difference between IOP and CSFp may cause either side of the optic neuropathy.

In practice, lumbar puncture is often used to measure the CSFp. However, the CSFp at the lumbar area cannot represent the CSFp around the optic nerve. In addition, there's no indication for POAG patients to perform the lumber puncture. Therefore, our team proposed a noninvasive method to measure the orbital CSFp with MRI [9]. According to the image, we found that CSFp around the optic nerve was decreased in NTG patients, which further approved our former findings (Fig. 1.2).

N. Wang
Beijing Institute of Ophthalmology, Beijing Tongren Eye Center, Beijing Tongren Hospital, Capital Medical University, Beijing, China

Beijing Ophthalmology & Visual Sciences Key Laboratory, Beijing, China
e-mail: wningli@vip.163.com

N. Wang (ed.), *Intraocular and Intracranial Pressure Gradient in Glaucoma*,
Advances in Visual Science and Eye Diseases 1, https://doi.org/10.1007/978-981-13-2137-5_1

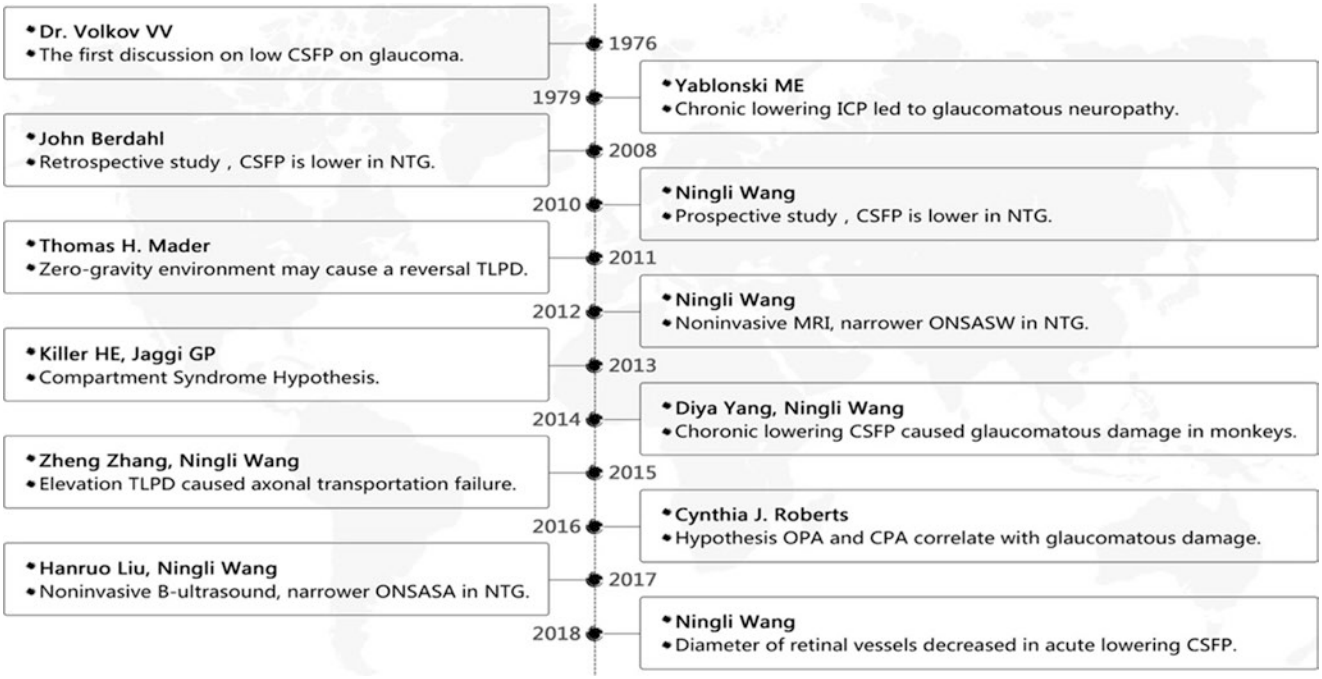

Fig. 1.1 Milestone studies of trans-lamina cribrosa pressure difference

At the same time, Dr. Killer et al. [10] described a compartment syndrome of subarachnoid space of the nerve in glaucoma first. In the study, they found that the circulation of CSF in the subarachnoid space of the nerve and the brain cannot communicate with the CSF around the ventricle, so the CSF there just keep static around the optic nerve. This is the new hypothesis that CSF circulation may be disrupted and a chemical toxic effect may damage the optic nerve.

Recently, our team analyzed the correlation between ICP and IOP in normal dog models and found three different stages of the ICP-IOP relationship [11]. There is an ICP-IOP dependent zone where ICP and IOP change in parallel, so the TLPD is unchanged. Right below the breakpoint, which is the second stage, there is also an ICP-IOP independent zone, where IOP changes no longer parallel ICP changes and lead to an increasing TLPD. We proposed that the imbalanced relationship between ICP and IOP may play a role in the glaucomatous optic neuropathy in patients with lower ICP.

Beijing iCOP study group made the monkey model by lowering of CSFp by placing the lumbar peritoneal shunt [12]. After 1 year, we found five out of eight eyes show optic neuropathy changes similar to glaucoma (Fig. 1.3). Then, we did the comparative study between high IOP and low ICP monkey model and found that nearly all the glaucomatous optic neuropathy-related parameters showed similar changes; however, the deformation and thinning of lamina cribrosa only existed in the high IOP model. Moreover, after another year of observation, there were no any further changes or damages in the optic nerve and nerve fiber layers in monkeys. Why does optic damage ceased?

The same study group used the infinite analysis method to answer the question. In the infinite model, at the same level of TLPD, elevated IOP caused more severe deformation than that in reduced CSFp condition. Moreover, lower CSFp group exhibited less cup to disc ratio change than that in the higher IOP group.

Zhang et al. [13] used the lower CSFp rats to observe the optic changes without the deformation of lamina cribrosa. They found that both short-term lowering CSFp and acute rising in IOP were all associated with a disturbance of both the orthograde and retrograde axonal transport (Fig. 1.4). Furthermore, the results showed an accumulation of dynein IC (intermediate chain) at the optic nerve head and retina when the TLPD dramatically increased. Meanwhile, the kinesin HC (heavy chain) immunoreactivity in the optic nerve fiber axons reduced. From this study, we note that the low CSFp or mild IOP elevation can cause the failure of axonal transport, while high IOP cannot just cause the failure of axonal transport but also the direct stress on laminar RGC loss. Therefore, a new hypothesis was proposed that lower CSFp may only affect axonal transport but have no effect on lamina cribrosa structure, although TLPD increased with higher IOP or lower CSFp.

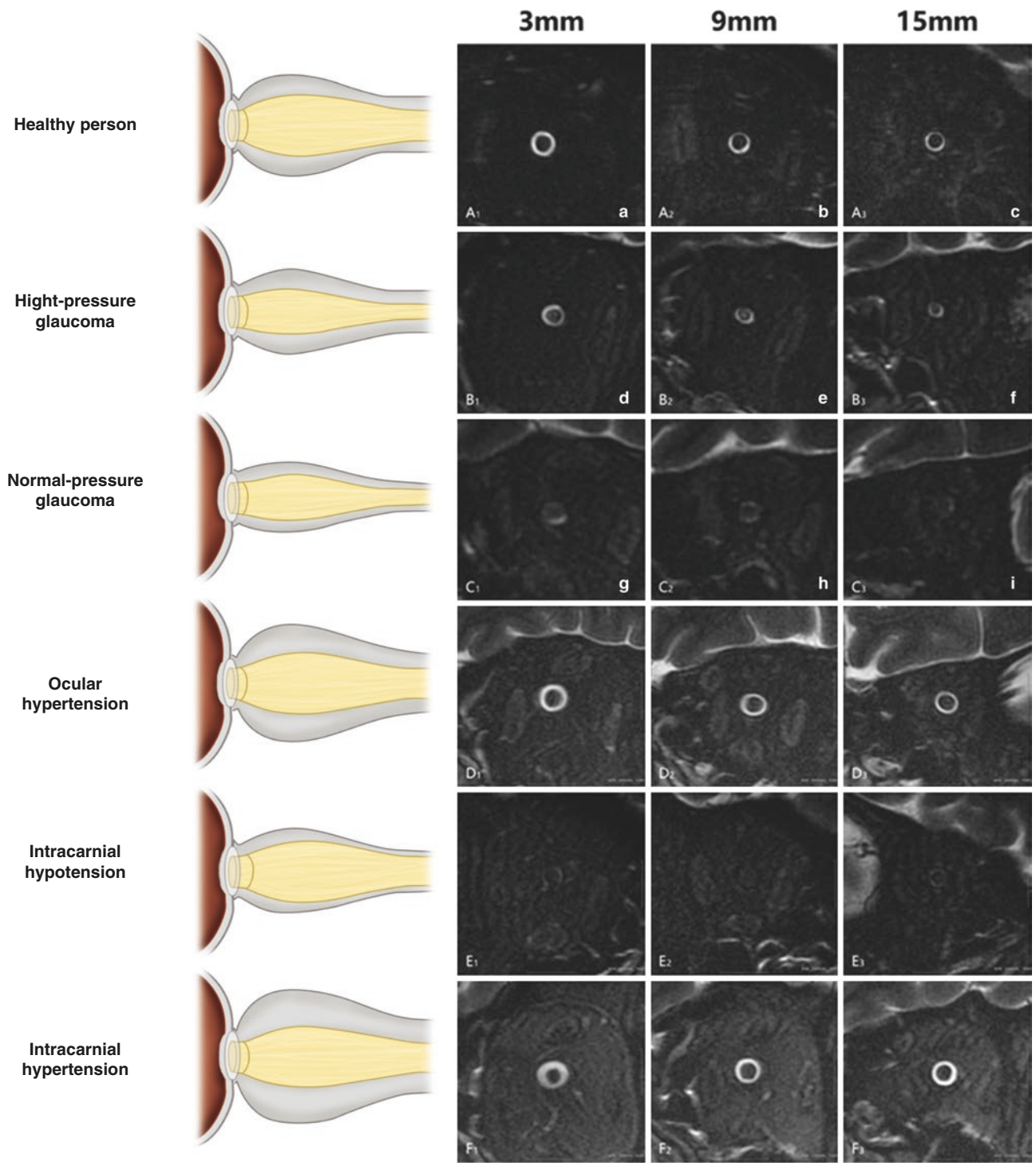

Fig. 1.2 Oblique magnetic resonance coronal T2WI-FRFSE image with fat suppression for demonstrating the optic nerve sheath complex (digital field of view 4, window width 2000, window level 1000), taken at 3 mm (**a**, **d**, **g**), 9 mm (**b**, **e**, **h**), and 15 mm (**c**, **f**, **i**) behind the globe. (**a**–**c**) A 57-year-old healthy man. Note the decreasing optic nerve diameter and ONSASW with increasing distance to the globe. (**d**–**f**) A 45-year-old man with high-pressure glaucoma. Note the optic nerve diameter is smaller than in (**a**–**c**). The ONSASW relatively wide and bright. (**g**–**i**) A 40-year-old man with normal-pressure glaucoma. Note the faint optic nerve subarachnoid space (Reprinted with permission from Wang N, Xie X, Yang D, Xian J, Li Y, Ren R, Peng X, Jonas JB, Weinreb RN. Orbital cerebrospinal fluid space in glaucoma: the Beijing intracranial and intraocular pressure (iCOP) study. Ophthalmology, 2012, 119: 2065-2073 e2061)

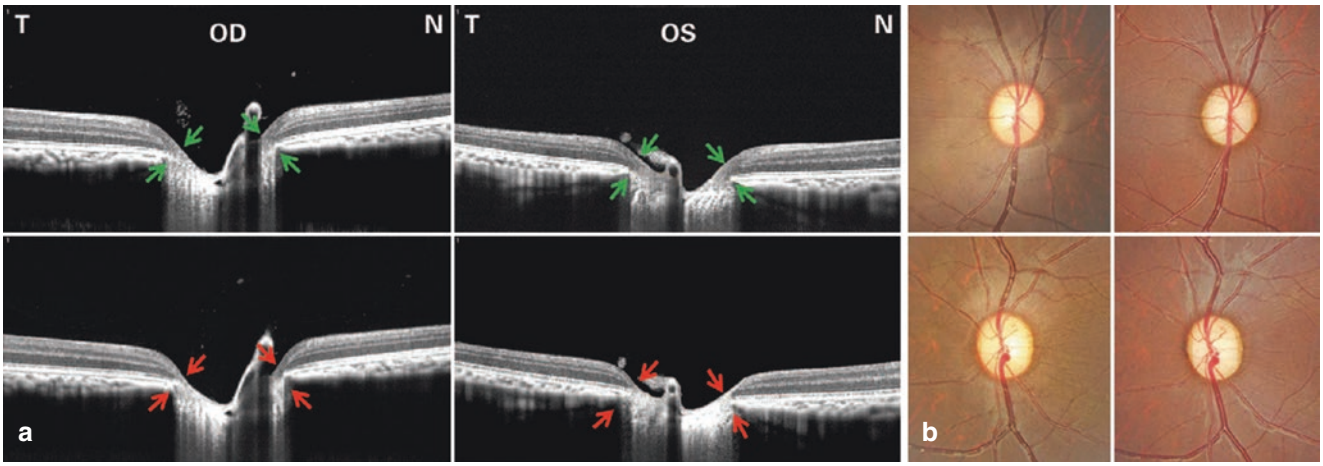

Fig. 1.3 (**a**) Optical coherence tomograms of the optic nerve head in monkey 1 (OD) and monkey 3 (OS) after lumbar-peritoneal shunting and reduction of cerebrospinal fluid pressure, taken at baseline (upper row) and at 12 months of follow-up (lower row). Note reduction in neuroretinal rim tissue. (**b**) Fundus photograph at baseline (left column) and at 12 months after lowering of cerebrospinal fluid pressure (right column) of monkey 1. Note decreased visibility of the retinal nerve fiber layer (Reprinted with permission from Yang D, Fu J, Hou R, et al. Optic neuropathy induced by experimentally reduced cerebrospinal fluid pressure in monkeys.[J]. Invest Ophthalmol Vis Sci, 2014, 55(5):3067–3073)

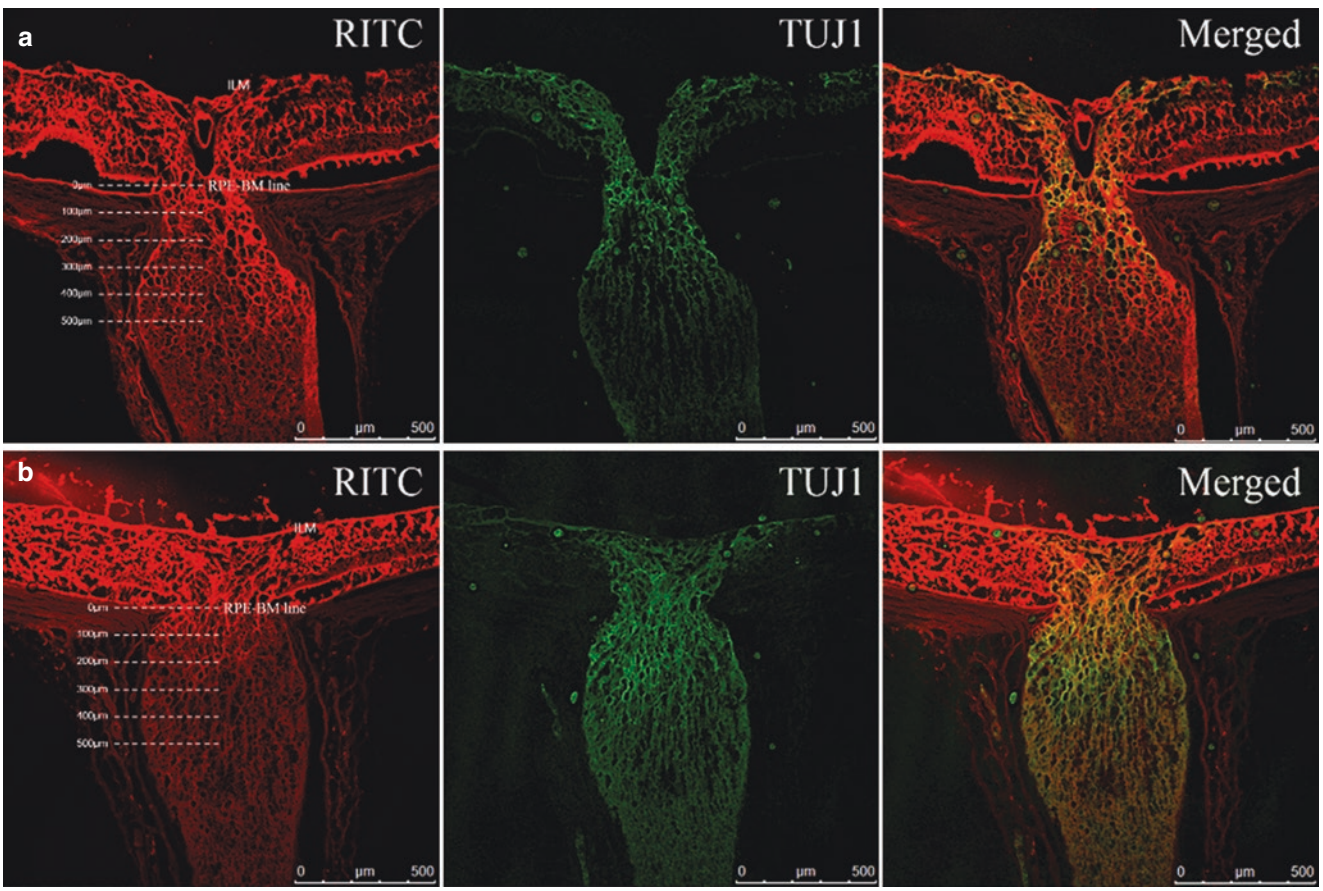

Fig. 1.4 Orthograde axonal transport of rhodamine isothiocyanate (RITC) in the optic nerve of rats of the control group (**a**) and in the optic nerve of rats with an experimental short-term (6 h) reduction in cerebrospinal fluid pressure (**b**), imaged at 1 day after baseline (Reprinted with permission from Zhang Z, Liu D, Jonas J B, et al. Axonal Transport in the Rat Optic Nerve Following Short-Term Reduction in Cerebrospinal Fluid Pressure or Elevation in Intraocular Pressure.[J]. Investigative Ophthalmology & Visual Science, 2015, 56(8):4257–66)

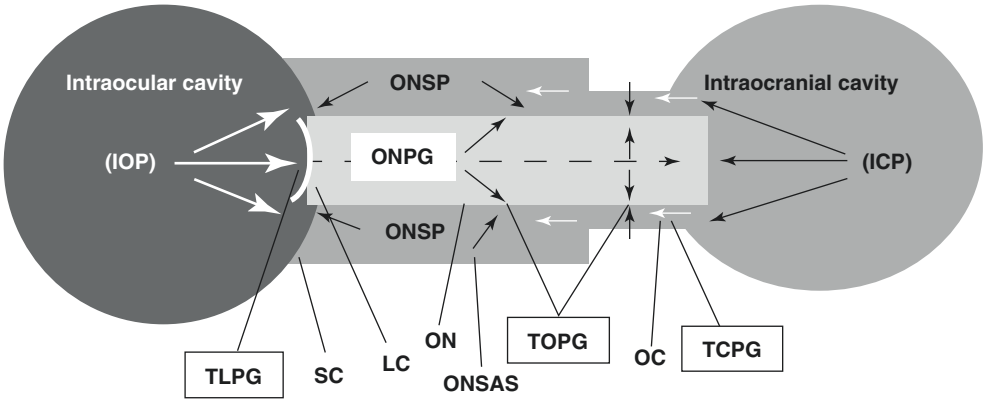

Fig. 1.5 The scheme of the pressures around the optic nerve (Reprinted with permission from Hou R, Zheng Z, Yang D, et al. Pressure balance and imbalance in the optic nerve chamber: The Beijing Intracranial and Intraocular Pressure (iCOP) Study[J]. Science China, 2016, 59(5):495–503)

So far, the pressure difference we study now is static. As we know, IOP and ICP change with the heartbeats and respiratory rhythm. Professor Cynthia Roberts et al. (unpublished) proposed another hypothesis that ocular pulse amplitude (OPA) that interacts with cerebral pulse amplitude (CPA) would cause nerve damage. Of these, the sclera stiffness plays an important risk factor. So we get the new ideas about the TLPD; we should not only think it in static but also in dynamics. What's more, the optic nerve damage has not only happened in the site of the laminar cribrosa but all along the optic nerve, where pressure gradients exist. So the concept of "trans-lamina cribrosa pressure difference" may be changed into "optic nerve pressure gradient (ONPG)" to be more precise (Fig. 1.5).

In review of the literatures, either in the prospective study or retrospective study, we found that not every normal-tension glaucoma patient had lower CSFp [3, 14–17]. Besides the different ICP measurements, some other possible factors should be considered, such as the different definitions of NTG and racial differences as BMI is related to the CSFp which was mentioned before. Since all the related studies have small sample sizes, we suggested that a further international cooperative study among different ethnic groups based on standard protocol is in need.

In conclusion, POAG is an entity of diseases that is caused by various reasons but with characterized optic neuropathy. The future directions include noninvasive measurement of CSFp and IOP dynamics and the change of optic blood flow; therefore, we may have the new classification or the formula to calculate the risk factors and the technique to rebalance the IOP and ICP.

References

1. Volkov VV. Essential element of the glaucomatous process neglected in clinical practice. Oftalmol Zh. 1976;31:500–4.
2. Yablonski MRR, Pokorny KS. Effect of decreased intracranial pressure on optic disc. Invest Ophthalmol Vis Sci. 1979;18(Suppl):165.
3. Ren R, Jonas JB, Tian G, Zhen Y, Ma K, Li S, et al. Cerebrospinal fluid pressure in glaucoma: a prospective study. Ophthalmology. 2010;117(2):259–66.
4. Berdahl JP, Fautsch MP, Stinnett SS, Allingham RR. Intracranial pressure in primary open angle glaucoma, normal tension glaucoma, and ocular hypertension: a case-control study. Invest Ophthalmol Vis Sci. 2008;49(12):5412–8.
5. Ren R, Wang N, Zhang X, Cui T, Jonas JB. Trans-lamina cribrosa pressure difference correlated with neuroretinal rim area in glaucoma. Graefes Arch Clin Exp Ophthalmol. 2011;249(7):1057–63.
6. Ren R, Wang N, Zhang X, Tian G, Jonas JB. Cerebrospinal fluid pressure correlated with body mass index. Graefes Arch Clin Exp Ophthalmol. 2012;250(3):445–6.
7. Berdahl JP, Fleischman D, Zaydlarova J, Stinnett S, Allingham RR, Fautsch MP. Body mass index has a linear relationship with cerebrospinal fluid pressure. Investig Ophthalmol Vis Sci. 2012;53:1422e7.
8. Mader TH, Gibson CR, Pass AF, Kramer LA, Lee AG, Fogarty J, et al. Optic disc edema, globe flattening, choroidal folds, and hyperopic shifts observed in astronauts after long-duration space flight. Ophthalmology. 2011;118(10):2058–69.
9. Wang N, Xie X, Yang D, Xian J, Li Y, Ren R, et al. Orbital cerebrospinal fluid space in glaucoma: the Beijing intracranial and intraocular pressure (iCOP) study. Ophthalmology. 2012;119(10):2065–73. e1
10. Killer HE. Compartment syndromes of the optic nerve and open-angle glaucoma. J Glaucoma. 2013;22(Suppl 5):S19–20.
11. Hou R, Zhang Z, Yang D, Wang H, Chen W, Li Z, et al. Pressure balance and imbalance in the optic nerve chamber: The Beijing Intracranial and Intraocular Pressure (iCOP) Study. Sci China Life Sci. 2016;59(5):495–503.
12. Yang D, Fu J, Hou R, Liu K, Jonas JB, Wang H, et al. Optic neuropathy induced by experimentally reduced cerebrospinal fluid pressure in monkeys. Invest Ophthalmol Vis Sci. 2014;55(5):3067–73.
13. Zhang Z, Wu S, Jonas JB, Zhang J, Liu K, Lu Q, et al. Dynein, kinesin and morphological changes in optic nerve axons in a rat model with cerebrospinal fluid pressure reduction: the Beijing Intracranial and Intraocular Pressure (iCOP) study. Acta Ophthalmol. 2016;94(3):266–75.
14. Berdahl JPAR, Johnson DH. Cerebrospinal fluid pressure is decreased in primary open-angle glaucoma. Ophthalmology. 2008;115(5):763–8.
15. Linden C, Qvarlander S, Johannesson G, Johansson E, Ostlund F, Malm J, et al. Normal-Tension Glaucoma Has Normal Intracranial Pressure: A Prospective Study of Intracranial Pressure and Intraocular Pressure in Different Body Positions. Ophthalmology. 2018;125(3):361–8.
16. Pircher A, Remonda L, Weinreb RN, Killer HE. Translaminar pressure in Caucasian normal tension glaucoma patients. Acta Ophthalmol. 2017;95(7):e524–e31.
17. Siaudvytyte L, Januleviciene I, Ragauskas A, Bartusis L, Meiliuniene I, Siesky B, et al. The difference in translaminar pressure gradient and neuroretinal rim area in glaucoma and healthy subjects. J Ophthalmol. 2014;2014:937360.

Time to Eliminate "Normal Tension" in Primary Open-Angle Glaucoma

2

Diya Yang and Robert N. Weinreb

2.1 Introduction

Glaucoma affects more than 70 million people worldwide with approximately 10% being bilaterally blind. It is the leading cause of irreversible blindness in the world [1]. Primary open-angle glaucoma (POAG), perhaps the most common type of glaucoma, is an optic neuropathy characterized by an accelerated loss of retinal ganglion cells [2]. There is a characteristic excavated appearance of the optic disc associated with visual field loss.

The biological basis of glaucoma is poorly understood, and the factors contributing to its progression have not been fully characterized. A recent JAMA Rational Clinical Examination systematic review found that the risk of glaucoma was highest when there is increased cup-disc ratio (CDR), CDR asymmetry, disc hemorrhage, or high intraocular pressure [3].

Although intraocular pressure (IOP) is the most important risk factor for POAG, glaucomatous optic neuropathy can occur in individuals with IOP within "the normal" range. Normal-tension glaucoma (NTG) is a term that has arisen to distinguish such individuals from individuals with high intraocular pressure [4]. However, considerable evidence has accumulated suggesting that the term "normal-tension glaucoma" may not be a separate clinical entity. Rather, it has been suggested that it is a statistical construct. It is possible that this term has done more to confuse the diagnosis and management of POAG than it has done to enhance it. The criteria that have been used to define NTG during the past have been highly variable [4]. Perhaps, this term should be abandoned [5].

2.2 Origin of Normal-Tension Glaucoma

Von Graefe in 1857 first recognized the features of excavation of optic disc without high IOP and described it as "amaurosis with excavation" [6]. However, he retracted it as an entity, as he later acknowledged that optic nerves may vary in their resistance to high IOP and believed that all excavation of optic disc was due to high IOP [7]. However, it was not until the advent of the indentation tonometer, several decades later in 1905, that there was a reliable instrument to measure IOP [8]. And it only was subsequently that the term "low-tension glaucoma" [9–11] appeared. A few decades later, a similar term "normal-tension glaucoma" [12–14] appeared as well.

Since the IOP among subjects without glaucoma had a mean of ~16 mmHg and a SD of 2.5 mm Hg, less than 2% of the general population was expected to have an IOP greater than ~21 mmHg (mean ± 2 SD). It was assumed that those whose IOP was higher than 21 mmHg either had POAG or were likely to develop it. As those with high IOP were "uncommon" in the general population, they were unlikely to be "normal." And, "uncommon" became "abnormal" [5].

However, this approach is flawed because IOP distribution in the population is non-Gaussian and skewed toward higher pressures. Moreover, population surveys found that a substantial number of individuals with otherwise typical POAG had pressure that did not exceed 21 mmHg. Normal-tension glaucoma then entered our lexicon as a new distinct clinical entity [15].

D. Yang
Beijing Institute of Ophthalmology, Beijing Tongren Eye Center, Beijing Tongren Hospital, Capital Medical University, Beijing, China

Beijing Ophthalmology & Visual Sciences Key Laboratory, Beijing, China

R. N. Weinreb (✉)
Hamilton Glaucoma Center and the Department of Ophthalmology, University of California, San Diego, La Jolla, CA, USA
e-mail: rweinreb@ucsd.edu

N. Wang (ed.), *Intraocular and Intracranial Pressure Gradient in Glaucoma*,
Advances in Visual Science and Eye Diseases 1, https://doi.org/10.1007/978-981-13-2137-5_2

2.3 Pathogenesis of Primary Open-Angle Glaucoma

Although the pathogenesis of POAG is not fully understood, the elevation of IOP is clearly an important and modifiable risk factor for POAG that is related to retinal ganglion cell death. Higher IOP can cause mechanical stress and strain on the sclera and the lamina cribrosa where the optic nerve fibers (retinal ganglion cell axons) exit the eye. Thus, retinal ganglion cell death is associated with high IOP [2].

However, there are several multifactorial disease processes in which IOP-independent processes have a role. For example, local ischemia-hypoxia, excessive glutamate stimulation, oxidative stress and formation of free radicals, inflammatory cytokines, and aberrant immunity might increase the vulnerability of the retinal ganglion cells [1]. However, there is still debate on whether these processes are primary insults along with elevated IOP or they are the result of an initial optic nerve injury. Such factors are likely to be different among individuals with respect to the underlying pathophysiology.

It should be noted that the IOP is not the only pressure at the lamina cribrosa. Posterior to the lamina, there is another relevant pressure, the intracranial pressure (ICP). It may act to counteract IOP. And the pressure difference between IOP and ICP, the so-called trans-laminar pressure difference [16], perhaps causes compression, deformation, and remodeling of the lamina cribrosa with consequent mechanical axonal damage and disruption of axonal transport. This would cause a blockade of retrograde delivery of essential trophic factors to retinal ganglion cells from their brainstem target [17].

Numerous studies have demonstrated the relationship between ICP and POAG. Wang et al. from the Beijing iCOP (intracranial and intraocular pressure) study group first demonstrated a low ICP in glaucoma patients with IOP in the normal range [18]. They also demonstrated by means of both MRI and ultrasound scan that in those patients the subarachnoid space of the optic nerve is significantly narrow or collapsed in comparison with normal subjects and glaucoma patients with high IOP [19, 20].

More importantly, Yang et al. from the iCOP group lowered the ICP in nonhuman primates by continuous shunting of cerebrospinal fluid (lowering ICP) for 1 year, and observed an appearance that mimics that of glaucomatous optic neuropathy with retinal nerve fiber layer loss and neuroretinal rim defects on the monkeys [21]. Beyond the association between low ICP and glaucoma, this study showed a causal relationship between them.

Most recently, studies with experimentally induced low ICP have demonstrated blockade of both orthograde and retrograde axonal transport at the level of the lamina cribrosa, similar to what has been found in experimental ocular hypertension studies [17]. Disrupted axonal transport occurs early in the pathogenesis of experimental glaucoma with resulting disorganization of microtubules in the prelaminar and postlaminar regions. Because there also might be mitochondrial dysfunction, high levels of energy demand may not be satisfied during periods of stress caused by either high IOP or low ICP.

Although the trans-laminar cribrosa pressure difference has been suggested as a risk factor for glaucoma, factors like impaired microcirculation, altered immunity, excitotoxicity, and oxidative stress also may be related.

2.4 Genetics of POAG

The discovery of the genes that cause glaucoma may help assess the risk for disease and develop new treatment strategies. Several genes, including myocilin (MYOC, GLC1A), optineurin (OPTN, GLC1E), and WD repeat domain 36 (GLC1G), are identified as a monogenic, autosomal dominant inheritance (Mendelian) trait for POAG. However, there are only less than 10% cases of POAG that can be attributed to the action of monogenic causing gene [2].

Myocilin was the first reported gene that "causes" POAG in many juvenile pedigrees, which is usually characterized by early onset, very high level IOP and greater resistance to medical therapies [22]. The prevalence of myocilin mutations varies from 3 to 5% in adults with POAG [22–24]. And, it was estimated that 90% of carriers of myocilin mutations develop glaucoma phenotype. However, little is known about the mechanism of myocilin-related glaucoma. It appears that mutations-altered myocilin protein may be toxic to trabecular meshwork cells and may lead to dysfunction or death of the cells, which ultimately disrupted aqueous outflow, elevated IOP [2].

In contrast to myocilin, optineurin was identified as a glaucoma-causing gene with a pedigree of POAG with normal level of IOP [25]. Mutations in optineurin lead to malfunction of neuroprotective role of wild-type optineurin. It has yet to be identified if optineurin is related to the above-mentioned trans-laminar cribrosa pressure difference in POAG [2].

The known glaucoma-causing gene only accounts for <10% POAG cases. The remaining are likely due to combined actions of several genes and environmental factors. A growing number of genome-wide association studies (GWAS) find gene sequences that are statistically more common in POAG patients than in normal subjects [2]. As the magnitudes of most quantitative traits are generally

controlled by a number of genes, it is expected that phenotypes like POAG with normal level of IOP or low ICP traits can be identified by large-scale GWAS of POAG to provide more insights into the pathophysiology of glaucoma.

2.5 Is NTG Clinically Distinguishable from POAG?

POAG patients with "normal" pressure share the same characteristics of glaucomatous optic neuropathy as those with "high" pressure. Those patients with "normal" pressure has been reported in some studies to present with more prevalent disc hemorrhages and visual field defects in the central region [10, 26, 27]. However, it is possible that these observations may be the result of biased ascertainment, as such patients may be more likely to seek examination.

Moreover, IOP is not a static measure and may well rise or fall on subsequent examinations. It is reported that subjects in the Baltimore Eye Survey with an IOP lower than 21 mmHg on their initial examination had a 40% chance of it being greater on their follow-up examination [28]. For those in whom it had been higher than 21 mmHg on initial examination, there was a 20% chance of it being lower. And, IOP fluctuates throughout day and night [29]. IOP behavior at specific times on a given day does not provide meaningful information regarding IOP at the same times on other days. For any given patient, the clinical findings and differential diagnosis of glaucoma with low and high IOP are indistinguishable.

In 63 articles that defined the disease entity NTG [4], the maximum IOP values acceptable for NTG ranged from 17 to 26 mmHg. A significantly greater proportion of recent studies required maximum IOP values ≤21 mmHg. Inclusion criteria based on structural characteristics of the glaucomatous optic disc or on the glaucomatous visual field were present in 55 (87%) and 56 (89%) articles, respectively. So, many of the criteria used previously to define NTG have been highly variable.

And for the management of glaucoma, the treatment strategies for glaucoma with low and high IOP are also similar. Lowering of IOP is the only proven effective way for managing of glaucoma.

2.6 Conclusion

The so-called normal-tension glaucoma is a statistical construct that obfuscates the diagnosis and management of POAG. Measurement of the trans-laminar cribrosa pressure difference may provide a better understanding of the physiologic basis of glaucoma. More evidence, particularly the elucidation of underlying genetics, may enhance our understanding of glaucoma. At present, the evidence for a distinct entity of "normal-tension" glaucoma is limited.

References

1. Weinreb RN, Aung T, Medeiros FA. The pathophysiology and treatment of glaucoma: a review. JAMA. 2014;311(18):1901–11.
2. Weinreb RN, Khaw PT. Primary open-angle glaucoma. Lancet. 2004;363(9422):1711–20.
3. Hollands H, Johnson D, Hollands S, Simel DL, Jinapriya D, Sharma S. Do findings on routine examination identify patients at risk for primary open-angle glaucoma? JAMA. 2013;309(19):2035–42.
4. Lee BL, Bathija R, Weinreb RN. The definition of normal-tension glaucoma. J Glaucoma. 1998;7(6):366–71.
5. Sommer A. Ocular hypertension and normal-tension glaucoma: time for banishment and burial. Arch Ophthalmol. 2011;129(6):785–7.
6. Von Graefe A. Uber die iridectomie bei glaucoma und uber den glaucomatosen prozess. Graefes Arch Clin Exp Ophthalmol. 1857;3:456–65.
7. Von Graefe A. Uber die glaucomatose Natur der "Amaurosen mit Sehnervenexkavation" und uber das Wesen und die Classification des Glaucoms. Graefe. Arch Ophthalmol. 1862;8:271.
8. Schiotz H. Ein neuer Tonometer: Tonometrie. Arch Augenheilkd. 1905;52:401.
9. Pickard R. Glaucoma and low tension disc cup enlargements. Br J Ophthalmol. 1931;15(6):323–33.
10. Drance SM, Sweeney VP, Morgan RW, Feldman F. Studies of factors involved in the production of low tension glaucoma. Arch Ophthalmol. 1973;89(6):457–65.
11. Drance SM, Morgan RW, Sweeney VP. Shock-induced optic neuropathy: a cause of nonprogressive glaucoma. N Engl J Med. 1973;288(8):392–5.
12. King D, Drance SM, Douglas G, Schulzer M, Wijsman K. Comparison of visual field defects in normal-tension glaucoma and high-tension glaucoma. Am J Ophthalmol. 1986;101(2):204–7.
13. Cartwright MJ, Anderson DR. Correlation of asymmetric damage with asymmetric intraocular pressure in normal-tension glaucoma (low-tension glaucoma). Arch Ophthalmol. 1988;106(7):898–900.
14. Shields MB. Textbook of glaucoma. Lippincott, Williams & Wilkins, 1992.
15. Hollows FC, Graham PA. Intra-ocular pressure, glaucoma, and glaucoma suspects in a defined population. Br J Ophthalmol. 1966;50(10):570–86.
16. Jonas JB, Wang N, Yang D, Ritch R, Panda-Jonas S. Facts and myths of cerebrospinal fluid pressure for the physiology of the eye. Prog Retin Eye Res. 2015;46:67–83.
17. Zhang Z, Liu D, Jonas JB, Wu S, Kwong JM, Zhang J, Liu Q, Li L, Lu Q, Yang D, Wang J, Wang N. Axonal transport in the rat optic nerve following short-term reduction in cerebrospinal fluid pressure or elevation in intraocular pressure. Invest Ophthalmol Vis Sci. 2015;56(8):4257–66.
18. Ren R, Jonas JB, Tian G, Zhen Y, Ma K, Li S, Wang H, Li B, Zhang X, Wang N. Cerebrospinal fluid pressure in glaucoma: a prospective study. Ophthalmology. 2010;117(2):259–66.
19. Wang N, Xie X, Yang D, Xian J, Li Y, Ren R, Peng X, Jonas JB, Weinreb RN. Orbital cerebrospinal fluid space in glaucoma:

the Beijing intracranial and intraocular pressure (iCOP) study. Ophthalmology. 2012;119(10):2065–73.
20. Liu H, Yang D, Ma T, Shi W, Zhu Q, Kang J, Wang N. Measurement and associations of the optic nerve subarachnoid space in Normal tension and primary open-angle Glaucoma. Am J Ophthalmol. 2018;186:128–37.
21. Yang D, Fu J, Hou R, Liu K, Jonas JB, Wang H, Chen W, Li Z, Sang J, Zhang Z, Liu S, Cao Y, Xie X, Ren R, Lu Q, Weinreb RN, Wang N. Optic neuropathy induced by experimentally reduced cerebrospinal fluid pressure in monkeys. Invest Ophthalmol Vis Sci. 2014;55(5):3067–73.
22. Stone EM, Fingert JH, Alward WL, Nguyen TD, Polansky JR, Sunden SL, Nishimura D, Clark AF, Nystuen A, Nichols BE, Mackey DA, Ritch R, Kalenak JW, Craven ER, Sheffield VC. Identification of a gene that causes primary open angle glaucoma. Science. 1997;275(5300):668–70.
23. Wiggs JL, Allingham RR, Vollrath D, Jones KH, De La Paz M, Kern J, Patterson K, Babb VL, Del Bono EA, Broomer BW, Pericak-Vance MA, Haines JL. Prevalence of mutations in TIGR/Myocilin in patients with adult and juvenile primary open-angle glaucoma. Am J Hum Genet. 1998;63(5):1549–52.
24. Fingert JH, Héon E, Liebmann JM, Yamamoto T, Craig JE, Rait J, Kawase K, Hoh ST, Buys YM, Dickinson J, Hockey RR, Williams-Lyn D, Trope G, Kitazawa Y, Ritch R, Mackey DA, Alward WL, Sheffield VC, Stone EM. Analysis of myocilin mutations in 1703 glaucoma patients from five different populations. Hum Mol Genet. 1999;8(5):899–905.
25. Rezaie T, Child A, Hitchings R, Brice G, Miller L, Coca-Prados M, Héon E, Krupin T, Ritch R, Kreutzer D, Crick RP, Sarfarazi M. Adult-onset primary open-angle glaucoma caused by mutations in optineurin. Science. 2002;295(5557):1077–9.
26. Thonginnetra O, Greenstein VC, Chu D, Liebmann JM, Ritch R, Hood DC. Normal versus high tension glaucoma: a comparison of functional and structural defects. J Glaucoma. 2010;19(3):151–7.
27. Shields MB. Normal-tension glaucoma: is it different from primary open-angle glaucoma? Curr Opin Ophthalmol. 2008;19(2):85–8.
28. Sommer A, Tielsch JM, Katz J, Quigley HA, Gottsch JD, Javitt J, Singh K. Relationship between intraocular pressure and primary open angle glaucoma among white and black Americans. The Baltimore Eye Survey. Arch Ophthalmol. 1991;109(8):1090–5.
29. Liu JH, Zhang X, Kripke DF, Weinreb RN. Twenty-four-hour intraocular pressure pattern associated with early glaucomatous changes. Invest Ophthalmol Vis Sci. 2003;44(4):1586–90.

Intracranial and Intraocular Pressure-Related Diseases

3

Diya Yang and Ningli Wang

3.1 Anatomy

The optic nerve is the only pair of cranial nerves that pass through three sealing containers with pressure. First, the retinal ganglion cell bodies and its gathering of the axons belong to the ocular container. Then, the rest part of the axons is surrounded by cerebrospinal fluid along its pathway, until into the third container, the intracranial container. The connection between the first two containers is called the laminar cribrosa, which is the part of the sclera that is pierced by the axons. The intracranial container is a bone structure without space to expand. So, the intracranial pressure change can severely impair the neuro structures. At the same time, the ocular container is constructed with compact fiber tissues, also with no space to expand.

Normally, the intraocular pressure is higher than the intracranial pressure (5–11 mmHg). When the pressure changes in the intracranial or intraocular container, the pressure difference or the pressure gradient can impose a sheared force on the site that the two pressures meet. Thus, the laminar cribrosa plays an important role in the pressure-related disease either from intraocular or from intracranial, as it is the weakest point of the conjunction.

3.2 Epidemiology

Most of the neurology diseases can affect the intracranial pressure, such as the tumor, intracranial infectious disease, trauma, cerebral hemorrhage, etc. Brain tumor is ranked among the top ten tumors that cause death. The prevalence rate of the brain tumor is 130.8 every 100,000 people. It was estimated that there are two million brain tumor patients in China. Besides the tumor, with the rapid development of architectural industry and high-speed vehicles, traumatic brain injury has become one of the most important causes of death among young people (250 every 100,000 people per year). It was estimated that among the patients with traumatic brain injury, 40% of them are dead or disabled due to uncontrollable high intracranial pressure. Besides the secondary intracranial pressure change, the idiopathic intracranial hypertension (IIH) affects more and more people with the rate of obesity rising in China.

On the other hand, many diseases can lead to low intracranial pressure, such as Alzheimer's disease, idiopathic intracranial hypotension, etc. For example, there are currently six million patients suffering from Alzheimer's disease in China, and the number would grow up to 20 million by 2050. The change of the intracranial pressure impairs the optic nerve and causes irreversible vision loss.

Obviously, intraocular pressure causes optic nerve damages, like glaucoma. And with the development of ocular surgery, more cases of ocular hypotension also have been seen. It can be estimated that for diseases that were caused by intracranial and intraocular pressure change, the blindness rate is 10%. Therefore, in our country, nearly 30 million people's visions are threatened by intracranial and intraocular pressure-related diseases. And among them, 300 are blind, which account for half of the blind population in China.

What's even worse is that the pressure-related optic nerve impairment is irreversible. Hence, more actions should be taken to study this kind of disease. It means a brighter and better life quality for all the patients.

D. Yang · N. Wang (✉)
Beijing Institute of Ophthalmology, Beijing Tongren Eye Center, Beijing Tongren Hospital, Capital Medical University, Beijing, China

Beijing Ophthalmology & Visual Sciences Key Laboratory, Beijing, China
e-mail: wningli@vip.163.com

N. Wang (ed.), *Intraocular and Intracranial Pressure Gradient in Glaucoma*,
Advances in Visual Science and Eye Diseases 1, https://doi.org/10.1007/978-981-13-2137-5_3

3.3 IOP: A Dilemma in Glaucoma Diagnosis and Treatment

Glaucomatous optic neuropathy is the primary cause of irreversible blindness worldwide. The main features of primary open-angle glaucoma (POAG) are the excavation of optic disk and the thinning of the rim [1]. Elevated intraocular pressure (IOP) has long been considered responsible for the development and progression of glaucomatous optic nerve damage [2]. However, a relatively large number of glaucomatous optic neuropathy have an IOP in the normal range (<21 mmHg) [3]. In population-based Handan Eye Study, it was found that about 80% of Chinese POAG patients had maximum IOPs less than 21 mmHg over a 24-h period [4]. More interestingly, it was found by the Ocular Hypertension Treatment Study Group (OHTS) that only 9.5% of ocular hypertension patients would develop into glaucomatous optic neuropathy during 5-year follow-up [5].

Why would NTG patients still develop into glaucoma without high IOP? Are there factors other than IOP contributing to the pathogenesis of NTG, as the role of IOP in the pathogenesis of POAG becomes vague and controversial?

3.4 Cerebrospinal Fluid Pressure: The New Dangerous Factor

Other factors, like vascular dysregulation or impaired blood flow to the optic nerve, were also hypothesized as the risk factor for NTG [3, 6], but a purely vasogenic pathogenesis of optic nerve damage contradicted with the optic disk appearance in NTG [7].

Volkov in the 1970s [8] hypothesized that CSF-P could be a counterpressure of IOP and may be associated with glaucoma. Yablonsky et al. [9] also postulated that an abnormally low CSF-P may be the reason for barotraumatically induced glaucomatous nerve damage in NTG.

Until recently, both retrospective studies by Berdahl et al. [10, 11] and prospective studies by iCOP study group [12, 13] found that the CSF-P is lower in NTG. Moreover, the CSF-P data in POAG with normal IOP from another study by Jaggi et al. [14] also revealed a lower CSF-P. Therefore, seemingly the lower CSF-P better resolves the dilemma of IOP, and a classification of POAG with high IOP and POAG with low CSF-P can be adopted.

3.5 Trans-laminar Cribrosa Pressure Difference (TLPD): The Pathogenesis for Glaucoma?

Mechanically, CSF-P can act as a counterpressure of IOP, so the pressure difference between IOP and CSF-P (translamina cribrosa pressure difference, TLPD) may play an important role in glaucoma. It is found that the TLPD is correlated with neuroretinal rim area (P = 0.006; correlation coefficient $r = -0.38$) and mean visual field defect ($P = 0.008$; $r = 0.38$). Moreover, the correlation coefficients of rim area/visual field defect and TLPD were higher than for the associations between rim area/visual field defect and IOP or lumbar CSF-P alone. Berdahl et al. also described that TLPD was significantly correlated with cup-to-disk (C/D) ratio ($P < 0.0001$; $r = 0.34$) [15]. These evidence may suggest that TLPD may play a stronger role than IOP or CSF-P alone in glaucoma.

However, there is no method for assessment of the translaminar cribrosa pressure difference in the clinic. A single lumbar CSF-P measurement can be used for calculating of TLPD, but it is not a real measurement of the CSF-P in the retrobulbar space of the orbit. It is urgent to develop a noninvasive way to get an estimate of the orbital CSF-P, since the direct measurement of the orbital CSF-P is not applicable in clinic. Due to the principles of elasticity according to Poisson's effect, the shape of optic nerve sheaths can be changed with the change of orbital CSF-P. So, patients with brain tumors or other diseases that elevate CSF-P can have a widened orbital CSF space, and patients with intracranial hypotension have a smaller orbital CSF space. Thus, measuring of the optic nerve subarachnoid space width through noninvasive imaging technologies can be a surrogate for the orbital CSF-P. And we found a narrower orbital optic nerve subarachnoid space in NTG patients as compared with high-pressure glaucoma [16]. The results suggest a lower orbital CSF-P in NTG.

3.6 Mechanisms and Clinical Implications

However, it is still hard to say whether the increase of TLPD is the hypostasis for POAG or just a manifestation. Many results can be provoked beyond the mechanical environment change by an increased trans-laminar cribrosa pressure difference. For example, the increased TLPD may also increase the strain power of the laminar pore and change the ocular perfusion status; in addition, reduced CSF flow in the optic nerve subarachnoid space may cause accumulation of metabolites and conglutination between optic nerve and its sheath. Although Killer et al. [17] suggested compartment of subarachnoid space and showed CSF composition difference in POAG patients with normal IOP, it is still hard to say whether the lowering of CSF-P or CSF flow in the optic nerve subarachnoid space happens first or the optic nerve sheath compartment happens first. It is rather important in the future to explore the downstream pathophysiology of the increased TLPD in POAG to find the true hypostasis.

Moreover, in the context of an increased TLPD in the pathogenesis of POAG, one may infer that the diagnostic and therapy patterns for POAG patients may be changed. Thus, it

seems essential to examine the TLPD in POAG patients. However, currently, lumbar puncture for POAG patients is controversial and not applicable in the clinic. Although some noninvasive ways of measuring intracranial pressure have been developed, the accuracy and efficacy of these methods remain dim. More importantly, for TLPD, orbital CSF-P is the key, but the invasiveness ethically restrains us from directly measuring it. Finding a noninvasive way to measure the orbital CSF-P seems essential and applicable. We used the 3.0 T MRI to measure the optic nerve subarachnoid space width (ONSASW) as a surrogate for orbital CSF-P in 72 neurological patients with lumbar CSF-P measurement results and found the algorithms for the associations between CSF-P and OSASW. Applying these algorithms in the independent test group, the measured lumbar CSF-P significantly matched with the calculated MRI-derived CSF-P. The intraclass correlation coefficients (ICCs) for the CSF-P assessment based on OSASW were 0.87 [18]. However, the resolution of MRI and the accuracy and efficacy of this method should be further examined. Large-scale multicenter verification of this method should also be explored.

Meanwhile, lowering of IOP still seems the most applicable way of decreasing trans-laminar cribrosa pressure difference for POAG patients. It may be of interest to see if there is a way to increase CSF-P noninvasively. However, surgical procedure which shunts the aqueous humor from the eye to the optic nerve subarachnoid space can be imagined, and actually there already have been some similar surgery cases [19, 20].

3.7 Conclusion

Imbalance of the trans-laminar cribrosa pressure difference may play an important role in the pathogenesis of glaucomatous optic nerve damage and other intracranial and intraocular pressure-related diseases. Animal model researches are of importance and yet to be continued to elucidate the downstream mechanisms of increased trans-laminar cribrosa pressure difference in glaucoma optic neuropathy. Rational and precise procedure of diagnosis and management of POAG based on trans-laminar cribrosa pressure difference is not applicable currently, obstacles and problems should be conquered, and intensive investigations should be conducted.

References

1. Hitchings RA, Spaeth GL. The optic disc in glaucoma. I: classification. Br J Ophthalmol. 1976;60:778–85.
2. Leske MC, Heijl A, Hussein M, et al. Factors for glaucoma progression and the effect of treatment: the Early Manifest Glaucoma Trial. Arch Ophthalmol. 2003;121:48–56.
3. Drance SM. Some factors in the production of low tension glaucoma. Br J Ophthalmol. 1972;56:229–42.
4. Wang NL, Friedman DS, et al. A population-based assessment of 24-hour intraocular pressure among subjects with primary open-angle glaucoma: the handan eye study. Invest Ophthalmol Vis Sci. 2011;52(11):7817–21.
5. Kass MA, Heuer DK, Higginbotham EJ, Johnson CA, Keltner JL, Miller JP, Parrish RK 2nd, Wilson MR, Gordon MO. The Ocular Hypertension Treatment Study: a randomized trial determines that topical ocular hypotensive medication delays or prevents the onset of primary open-angle glaucoma. Arch Ophthalmol. 2002;120(6):701–13. discussion 829-730
6. Flammer J, Orgül S, Costa VP, Orzalesi N, Krieglstein GK, Serra LM, Renard JP, Stefánsson E. The impact of ocular blood flow in glaucoma. Prog Retin Eye Res. 2002;21:359e93.
7. Jonas JB, Hayreh SS. Optic disk morphology in experimental central retinal artery occlusion in rhesus monkeys. Am J Ophthalmol. 1999;127:523–30.
8. Volkov VV. Essential element of the glaucomatous process neglected in clinical practice [in Russian]. Oftalmol Zh. 1976;31:500–4.
9. Yablonski M, Ritch R, Pokorny KS. Effect of decreased intracranial pressure on optic disc. Invest Ophthalmol Vis Sci. 1979;18(Suppl):165.
10. Berdahl JP, Allingham RR, Johnson DH. Cerebrospinal fluid pressure is decreased in primary open-angle glaucoma. Ophthalmology. 2008;115:763–8.
11. Berdahl JP, Fautsch MP, Stinnett SS, Allingham RR. Intracranial pressure in primary open angle glaucoma, normal tension glaucoma, and ocular hypertension: a case-control study. Invest Ophthalmol Vis Sci. 2008;49:5412–8.
12. Ren R, Jonas JB, Tian G, et al. Cerebrospinal fluid pressure in glaucoma. A prospective study. Ophthalmology. 2010;117:259–66.
13. Ren R, Zhang X, Wang N, Li B, Tian G, Jonas JB. Cerebrospinal fluid pressure in ocular hypertension. Acta Ophthalmol. 2011;89:E142–8.
14. Jaggi GP, Miller NR, Flammer J, Weinreb RN, Remonda L, Killer HE. Optic nerve sheath diameter in normal-tension glaucoma patients. Br J Ophthalmol. 2012;96(1):53–6.
15. Ren R, Wang NL, Zhang X, Cui T, Jonas JB. Trans-lamina cribrosa pressure difference correlated with neuroretinal rim area in glaucoma. Graefes Arch Clin Exp Ophthalmol. 2011;249(7):1057–63.
16. Wang NL, Xie XB, Yang DY, et al. Orbital Cerebrospinal Fluid Space in Glaucoma: The Beijing iCOP Study. Ophthalmology. 2012;119(10):2065–73.
17. Killer HE, Jaggi GP, et al. Cerebrospinal fluid dynamics between the intracranial and the subarachnoid space of the optic nerve. Is it always bidirectional? Brain. 2007;130(Pt 2):514–20.
18. Xie XB, Zhang XJ, Fu J, et al. Intracranial pressure estimation by orbital subarachnoid space measurement. Crit Care. 2013;17:R162.
19. Berdahl JP, Allingham RR. Intracranial pressure and glaucoma. Curr Opin Ophthalmol. 2010;21(2):106–11.
20. Quiroz-Mercado H, Alvarez-Celorio D, Martinez-Jardon S, et al. Pars plana vitrectomy and lamina cribrosa puncture in absolute glaucoma. Ophthalmic Surg Lasers Imaging. 2004;35:244–6.

4 Conciliation of Discrepancy of Hypertensive Glaucoma and Normal-Tension Glaucoma Through Intraocular-Intracranial Pressure Gradient

Zhigang Fan, Si'an Liu, and Zhenni Zhao

Glaucoma is the first leading cause of irreversible blindness worldwide. It is estimated that by the year 2020, 79.6 million people will suffer from primary glaucoma with 11.2 million sufferers of bilateral blindness throughout the world [1]. The key to preventing blindness caused by glaucoma is early diagnosis and treatment. Clarification of the definition of glaucoma is important for guiding researches in this field.

Intraocular pressure (IOP) and optic neuropathy have always been two of the essential core concepts about glaucoma. As the ophthalmology community is gaining a deeper and profounder understanding of the relationship between IOP and glaucoma, the definition of primary glaucoma has undergone a series of transitions.

4.1 The Historical Evolution of the Definition of Glaucoma

The evolution of the definition of glaucoma can be classified into three historical periods:

1. In 1745 *Johann Zacharias Platner* found the eyeballs of glaucoma patients were harder than normal; in 1830 *William Mackenzie* highlighted the importance of elevated IOP in the identification of glaucoma. In this period, glaucoma was defined as "a disease in which IOP is elevated."
2. In 1857 *Von Graefe* discovered the pitting atrophy of optic nerve head (ONH) in glaucoma patients by ophthalmoscopy and named it "glaucomatous optic neuropathy (GON)." Then glaucoma was defined as "optic neuropathy caused by elevated IOP."
3. In the late twentieth century, the recognition of normal tension glaucoma (NTG) and ocular hypertension (OHT) suggested that elevation of IOP is not equal to glaucoma, and researchers pointed out that the essence of glaucoma is GON.

4.2 The Transitions of the Definition of Primary Glaucoma in Recent Guidelines and Expert Consensuses

4.2.1 Transitions of the Definition of Primary Open–Angle Glaucoma (POAG)

The recognition of NTG and OHT made researchers come to realize the complexity of the relationship between IOP and glaucoma; thus the definition of POAG has been changed.

4.2.1.1 POAG Definition in the Expert Consensuses in China

In 1987, the diagnostic criteria of POAG were put forward in a Chinese expert consensus *The Preliminary Proposals for Early Diagnosis of Primary Glaucoma* as follows: "Only in the condition when the anterior chamber angle is open and IOP >21 mmHg (measured with Goldmann applanation tonometer) together with GON and/or glaucomatous visual field defects can POAG be diagnosed." Also *The Preliminary Proposals* mentioned: "In the condition when GON and visual field defects occur without known reasons, and IOP keeps in normal range, a diagnosis of NTG can be committed. In the condition when IOP is greater than the upper limit of normal range through multiple measurements, yet GON and visual field defects are not detectable, a diagnosis of OHT can be committed" [2].

The Preliminary Proposals emphasized that elevated IOP was necessary for the diagnosis of POAG. On the one hand, diagnostic criteria of NTG and OHT were described in the

Z. Fan (✉) · S. Liu · Z. Zhao
Zhongshan Ophthalmic center, Sun Yet-sen University, Guangdong, China
e-mail: fanzhg3@mail.sysu.edu.cn

N. Wang (ed.), *Intraocular and Intracranial Pressure Gradient in Glaucoma*,
Advances in Visual Science and Eye Diseases 1, https://doi.org/10.1007/978-981-13-2137-5_4

section titled with "POAG" in the article; on the other hand, NTG and OHT could not meet the criteria of POAG described in this article. Therefore, *The Preliminary Proposals* did not make the relationship among NTG, OHT, and POAG clear, which reflected the confusion of the whole glaucoma community at that time.

In 2008, *The Expert Consensuses on Diagnosis and Treatments of Primary Glaucoma in China (2008)* was published. In this article, POAG was classified into three subtypes: (1) high-tension POAG (anterior chamber angle stays open, IOP >21 mmHg together with GON, and/or glaucomatous visual field defects without other known reasons which can cause IOP elevation), (2) NTG, and (3) OHT. The diagnostic criteria of NTG and OHT are almost identical to those in *The Preliminary Proposals* [3].

The latest version of *The Expert Consensuses on Diagnosis and Treatments of Primary Glaucoma in China* was published in 2014. It gave a definition of POAG as follow: "POAG is a chronic and progressive optic neuropathy, for which pathologically elevated IOP is an important risk factor. The defining characteristics of POAG include the acquired atrophy of optic nerve and the loss of retinal ganglion cells and their axons." However, *The Expert Consensuses 2014* kept the same as *The Expert Consensuses 2008* in regard to the classification of POAG [4].

The Expert Consensuses 2008 did not provide a definition of POAG; it implicated that both elevated IOP and GON could be the defining feature of POAG since OHT and NTG were both regarded as subtypes of POAG. *The Expert Consensuses 2014* defined POAG as "optic neuropathy" and took elevated IOP as a "risk factor," but what seems paradoxical is that it still regarded OHT as a subtype of POAG.

4.2.1.2 POAG Definition by the American Academy of Ophthalmology (AAO)

In 1996, AAO published their second version of *POAG Preferred Practice Pattern (PPP)*. For the first time, neither a visual field defect nor a level of IOP was part of the definition of POAG. Instead, optic nerve or nerve fiber defects characteristic of glaucoma were regarded sufficient for defining glaucoma. *PPP 1996* went on to provide a list of presumed characteristic defects of the optic nerve or nerve fiber layer: asymmetry, notching, thinning, progressive change, and nerve fiber layer defects [5]. Later versions of *PPP* always keep to the rule that "GON is the only defining feature of glaucoma."

In *PPP 2016*, the definition of POAG is POAG is a chronic, progressive optic neuropathy suffered by adults, in which there are a characteristic acquired atrophy of the optic nerve and loss of retinal ganglion cells and their axons, and this condition is associated with an open anterior chamber angle by gonioscopy [6]. The definition of POAG suspect is: a POAG suspect is an individual with clinical findings and/or a constellation of risk factors that indicate an increased likelihood of developing POAG. Any of the following clinical findings in one or both eyes of an individual with an open anterior chamber angle can define a POAG suspect patient: (1) an appearance of the optic disc or retinal nerve fiber layer (RNFL) that is suspicious for glaucomatous damage; (2) a visual field suspicious for glaucomatous damage in the absence of clinical signs of other optic neuropathies; or (3) consistently elevated IOP associated with normal appearance of the optic disc, RNFL, and visual field. This definition excludes the angle-closure glaucoma and known secondary causes for open-angle glaucoma, such as pseudoexfoliation, pigment dispersion, and traumatic angle recession [7] (Fig. 4.1).

4.2.1.3 Contrast of POAG Definitions Between China and America

According to the classification methods proposed by AAO, the "high-tension POAG" and "NTG" should be collectively named "POAG," and "OHT" should be classified as "POAG suspect."

The definition and classification of POAG in China put more emphasis on the important role of IOP. Not only do they highlight that "pathologically elevated IOP is an important risk factor" but also they regard OHT as a subtype of POAG.

The worry that OHT patients may develop GON and visual field defects in a period of time is another reason why OHT is regarded as a subtype of POAG in China. But according to "the Ocular Hypertension Treatment Study (OHTS)," 90–95% of patients with OHT will not go on to develop glaucoma over 5 years [8], and this suggests OHT should be regarded as a separate diagnosis.

Although a consensus about the definition and classification of POAG has not been reached, there is no controversy about the treatments of the disease. It is universally accepted that IOP reduction is the only evidence-based treatment strategy for both POAG and POAG suspect [7, 9]. OHT patients who are not supposed to suffer from optic injury in a long time should also reduce their IOP, because this treatment can reduce their risk of developing POAG by 9.5% to 4.5% [8].

4.2.2 Transitions of the Definition of Primary Angle–Closure Glaucoma (PACG)

The traditional definition of PACG is "the elevation of IOP caused by the primary closure of anterior chamber angle" [2]. Inspired by the transitions of POAG definition,

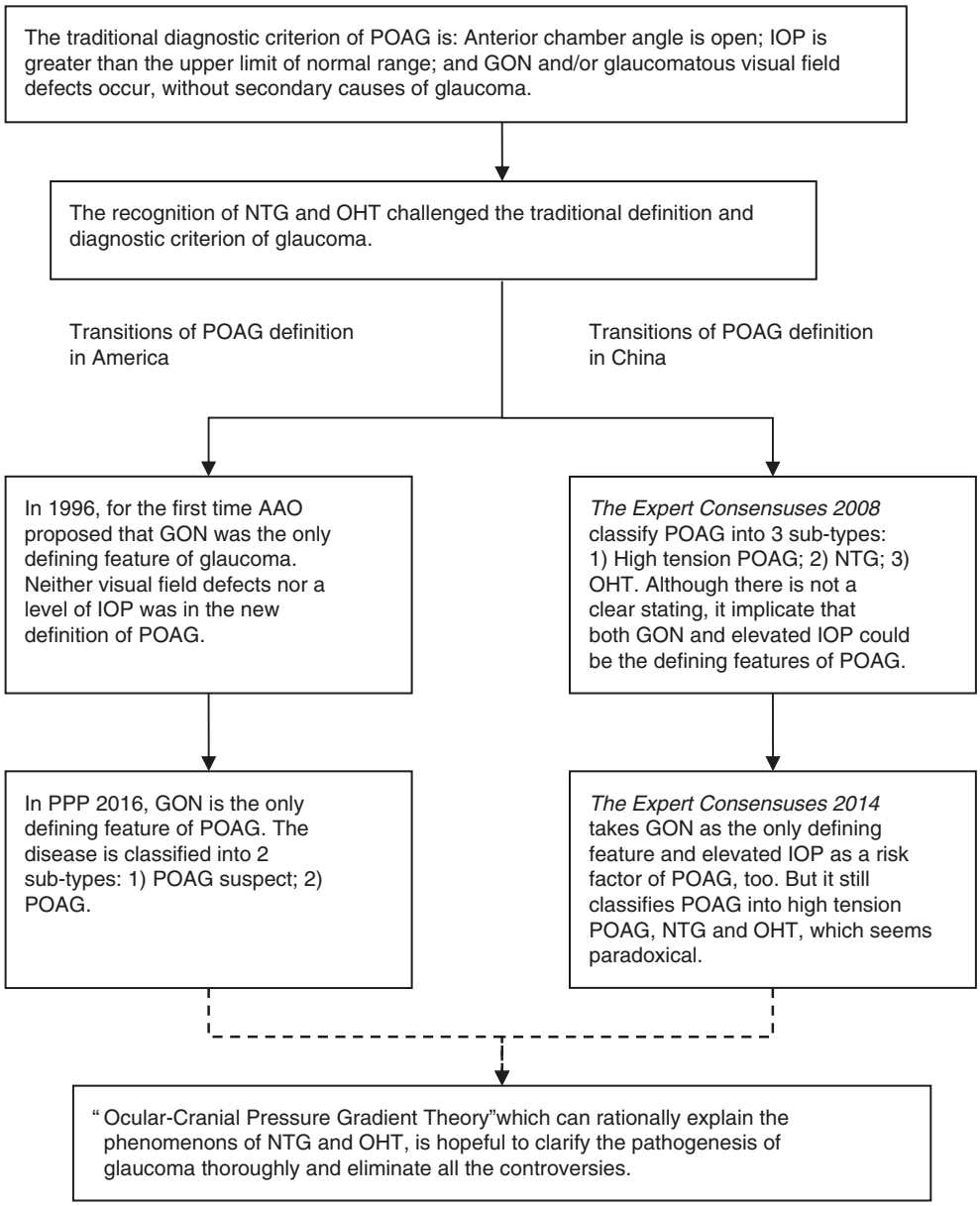

Fig. 4.1 Transitions of the definition and classification of POAG in America and China

researchers proposed to replace elevated IOP with GON as the defining feature of PACG.

4.2.2.1 The Classification System by the International Society of Geographical and Epidemiological Ophthalmology (ISGEO)

In 2002, ISGEO proposed a new definition and classification system of PACG, in which the traditional PACG was classified into three subtypes: (1) primary angle-closure suspect (PACS), (2) primary angle closure (PAC), and (3) primary angle-closure glaucoma (PACG). The new definition and classification highlighted "only when GON occurs can glaucoma be diagnosed" [10].

ISGEO defined PACS, PAC, and PACG as follows:

1. PACS: Appositional contact between the peripheral iris and posterior trabecular meshwork in the eye is considered possible;
2. PAC: An occludable drainage angle and features indicating that trabecular obstruction by the peripheral iris has occurred in the eye, such as peripheral anterior synechiae, elevated IOP, iris whorling (distortion of the radially orientated iris fibers), glaukomflecken lens opacities, or excessive pigment deposition on the trabecular surface. The optic disc does not have glaucomatous damage.
3. PACG: PAC occurs together with evidence of GON [10].

AAO accepted the ISGEO classification, and in *PPP 2016*, the diagnostic criteria of PACS, PAC, and PACG were listed [11] in the following chart:

Table 1 Clinical findings that define patients seen with angle-closure disease

	PACS	PAC	PACG
≥180°ITC	Present	Present	Present
Elevated IOP or PAS	Absent	Present	Present
Optic nerve damage	Absent	Absent	Present

ITC iridotrabecular contact, *PAS* peripheral anterior synechiae

4.2.2.2 PACG Definition in China

The traditional definition and classification of PACG are still adopted in China, while ISGEO definition has been proposed for more than a decade.

The Expert Consensuses 2008 defined PACG as acute or chronic elevation of IOP caused by primary closure of anterior chamber angle with or without GON and visual field defects. Based on clinical manifestations, it classified PACG into acute PACG and chronic PACG. Acute PACG was divided by the traditional approach into preclinical stage, portent stage, acute episode stage, symptomatic relief stage, and chronic stage. Chronic PACG was divided into early stage, progressing stage, and late stage. Complete blindness was the absolute stage [3]. Meanwhile, Chinese researchers proposed to classify PACG into pupillary blocking type, non-pupillary blocking type, and multi-mechanism type based on the mechanisms in which angle closure happens [12].

The Expert Consensuses 2014 kept the same as *The Expert Consensuses 2008* in regard to the definition and classification of PACG. But it suggested Chinese ophthalmologists to adopt ISGEO classification and advocated the combination of ISGEO classification, classification based on clinical manifestations, and classification based on angle-closure mechanisms [4] (Fig. 4.2).

4.2.2.3 Contrast of PACG Definitions and Classifications Between China and America

The basic logic of ISGEO definition of PACG is PAC is a special disease of anterior ocular chamber, which can increase the risk of developing PACG but itself is not equal to PACG; only when GON occurs can glaucoma be diagnosed [13]. This has been supported by several researches. Surveys found that acute, symptomatic phase occurs in only a minority of those with PACG, while a chronic, asymptomatic form of PACG predominates [14–17]; thus ISGEO proposed that emphasis should be placed on optic nerve injury and visual loss rather than symptomatic disease [10]. Other researches indicated that as many as 60–75% of people suffering from an acute, symptomatic episode of angle closure recovered without optic disc or visual field damage at least in the short term [18, 19], which suggests that PAC should be a separate diagnosis.

Some Chinese researchers found the ISGEO definition disputable and pointed out that: "There is a causal relationship among PAC, elevation of IOP and occurrence of GON, although PAC cannot cause GON immediately, but the occurrence of GON is almost inevitable. So it's not suitable to regard PAC as a separate diagnosis" [20]. In a cohort study, 28.5% of PAC patients developed GON in a 5-year time [21]. In another study, several years after suffering from acute primary angle closure, 17.8% of subjects examined were blind in the attack eye, and almost half had glaucomatous optic nerve damage [22].

Jian Ge [23] commented: "The radical divergence between these two definitions is whether PACS and PAC are separate diagnoses or just the early stages in the course of PACG. But it's hard to get a conclusion because the studies about the natural history of PACG are still scarce. Besides, ISGEO definition does not reduce clinical interventions since both PACS and PAC need to be treated too."

ISGEO classification has its advantages because it highlights the dynamic development in the genesis and progression of the disease and reflects the important significance of early screening [23]. The fundamental of ISGEO classification is adequate early screening for glaucoma which has been achieved in developed countries. In China, since the early screening of glaucoma has not been achieved adequately, researchers prefer the traditional classification of PACG which pays more consideration to the clinical manifestations after diagnosis of the disease. Besides, the classification based on angle-closure mechanisms is an important complement to the current classification of PACG because different treatments should be employed in PACG with different angle-closure mechanisms [12].

4.3 New Hypotheses and Theories About the Relationship Between Pressure and Glaucoma

In recent years, researchers have put forward some new hypotheses and theories trying to explain the pathogenesis of glaucoma, such as "safe IOP hypothesis" and "ocular-cranial pressure gradient theory" which have provided a deeper understanding of the relationship between pressure and glaucoma.

4.3.1 "Safe IOP Hypothesis"

The existence of NTG and OHT has demonstrated the falseness of defining glaucoma with a specific range of IOP value, but some researchers came up with the "safe IOP hypothesis" trying to keep "pathologically elevated IOP" as the pathogenesis and defining feature of glaucoma. "Safe

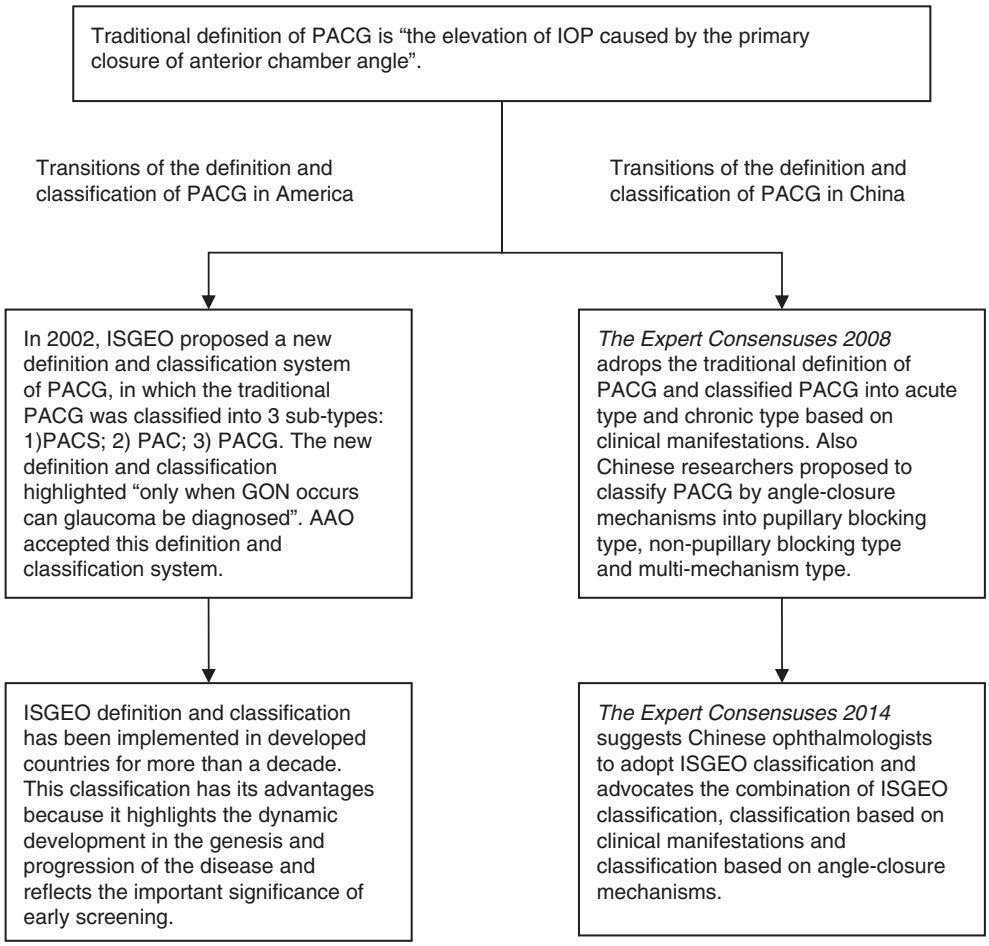

Fig. 4.2 Transitions of the definition and classification of POAG in America and China

IOP hypothesis" says "safe IOP" is a range of IOP that will not cause optic neuropathy in individuals, and "safe IOP" is individualized and different from the statistically normal IOP. The occurrence of NTG and OHT can be explained with this hypothesis: the "safe IOP" is lower for NTG patients than the normal population; thus statistically normal IOP can cause GON; while the "safe IOP" is higher for OHT patients, thus GON does not occur under the high IOP. However, relevant studies of this hypothesis are still scarce [24].

4.3.2 "Ocular-Cranial Pressure Gradient Theory"

The Consensuses and Suggestions on POAG Ocular-Cranial Pressure Gradient in China (2017) says: "The optic nerve is located in both intraocular cavity and intracranial cavity, and the difference between IOP and intracranial pressure (ICP) exists at the lamina cribrosa and forms a pressure gradient along the optic nerve, which is called ocular-cranial pressure gradient, also named 'trans-lamina cribrosa pressure difference (TLPD)'" [25].

In conventional opinions, squeezing of ONH and degeneration of lamina cribrosa caused by elevated IOP are the causes of GON. But in the opinions of TLPD theory, it is the elevated TLPD that causes the squeezing of ONH and the degeneration of lamina cribrosa rather than elevated IOP; not only elevated IOP but also decreased ICP can result in an elevated TLPD and induce GON [26]. The occurrence of NTG and OHT can be explained rationally in this new theory: when ICP is lower than normal, TLPD gets higher under the normal IOP and causes NTG; when ICP is higher than normal, TLPD can stay normal even if IOP is elevated; thus OHT is caused rather than GON.

A series of researches have collected supportive evidences for this theory. In case-control studies, ICP was lower in POAG and NTG and elevated in OHT [27, 28]. A prospective study found that lumbar cerebrospinal fluid pressure (CSFP) was significantly lower in the NTG group than in the high-tension POAG group or the control group and that the TLPD (IOP minus CSFP) was significantly higher in the NTG group and the high-tension POAG group than in the control group [29]. Multiple researches indicated that TLPD was more significantly correlated with the amount of glaucomatous optic nerve damage other than IOP and ICP alone

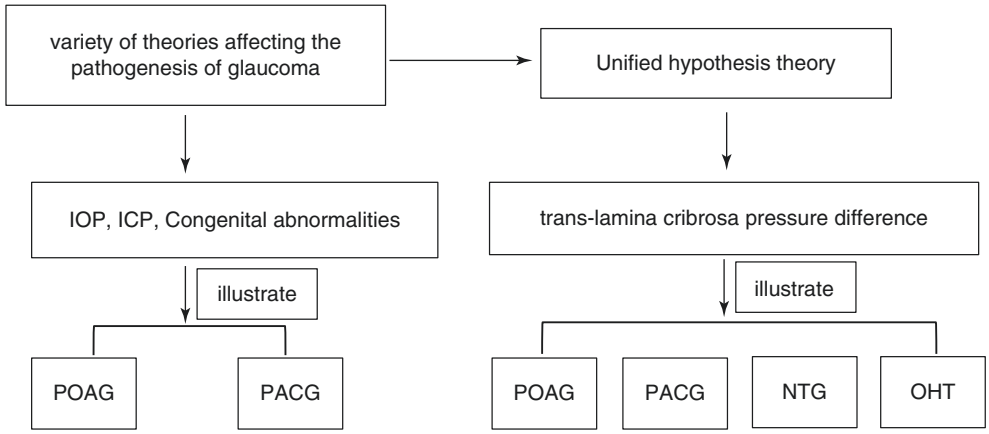

Fig. 4.3 We integrate varieties of theories that affect the pathogenesis and development of glaucoma into a unified hypothesis of ocular-cranial pressure gradient

[30, 31]. Another study proved that lowering CSFP could induce glaucoma-like optic neuropathy in monkeys [32]. *Ning-Li Wang* et al. found that increasing TLPD by lowering CSFP could cause axonal transport failure of optic nerve and affect optic blood supply, which led to optic neuropathy [33].

Ning-Li Wang et al. further proposed the optic nerve is under different pressures imposed by the surrounding tissues and fluid along its whole length, so the optic nerve damage not only happened in the site of lamina cribrosa but all along the optic nerve, where pressure gradients exist. Thus they suggested that the concept of TLPD should be expanded to a new concept "optic nerve pressure gradient (ONPG)" [26]. Several researches on this topic have obtained inspiring achievements [26, 34].

The blood of the retina is mainly supplied by the central retinal artery and the posterior ciliary artery. The fluctuations in TLPD not only cause the changes in retinal microvascular flow and the local elastic organization beyond their limits but also can lead to the changes in the microenvironment of the retina. Resulting from these facts, the axoplasm transport of the optic nerve will be affected, which eventually bring about the occurrence and development of glaucoma.

On the whole, "ocular-cranial pressure gradient theory" not only can explain the occurrence of NTG and OHT perfectly but also has got many supportive evidences; thus this new theory becomes one of the most convincing theories on the pathogenesis of glaucoma. The former chairman of the World Glaucoma Association, Professor Weinreb, commended this theory as a "landmark" in the research field of glaucoma [35]. Conclusively, we integrate varieties of theories that affect the pathogenesis and development of glaucoma into a unified hypothesis of ocular-cranial pressure gradient. Also, "ocular-cranial pressure gradient theory" has urged the glaucoma community to rethink and pursue a deeper understanding of the relationship between pressure factors and glaucoma (Fig. 4.3).

4.4 Summary

As the ophthalmology community is gaining a deeper and profounder understanding of glaucoma, the definition of primary glaucoma has undergone a series of transitions. We have achieved a great progress from defining glaucoma with only IOP values to realizing that the essence of glaucoma is the atrophy of optic nerve and the loss of retinal ganglion cells and their axons. However, current definition of glaucoma might still need further refinement for lack of clear etiology incorporated. As more and more researches on etiology, genetics, and molecular biology of glaucoma are being conducted or will be conducted, it is hopeful that the pathogenesis of glaucoma will be clarified thoroughly from the cellular and molecular level.

References

1. Quigley HA, Broman AT. The number of people with glaucoma worldwide in 2010 and 2020. Br J Ophthalmol. 2006;90(3):262–7.
2. Glaucoma Group Of Chinese Ophthalmological Society. The Preliminary Proposals for Early Diagnosis of Primary Glaucoma. Chin J Ophthalmol. 1987;23(2):127.
3. Glaucoma Group Of Chinese Ophthalmological Society. The Expert Consensuses on Diagnosis and Treatments of Primary Glaucoma in China (2008). Chin J Ophthalmol. 2008;44(9):862–3.
4. Glaucoma Group Of Chinese Ophthalmological Society. The Expert Consensuses on Diagnosis and Treatments of Primary Glaucoma in China. Chin J Ophthalmol. 2014;2014(5):382–3.
5. Lee PP. Understanding the new primary open-angle glaucoma preferred practice pattern. Int Ophthalmol Clin. 1998;38(3):93–9.
6. Prum BEJ, Rosenberg LF, Gedde SJ, et al. Primary Open-Angle Glaucoma Preferred Practice Pattern. Ophthalmology 2016;123(1):P41–111.
7. Prum BEJ, Lim MC, Mansberger SL, et al. Primary Open-Angle Glaucoma Suspect Preferred Practice Pattern. Ophthalmology 2016;123(1):P112–51.
8. Kass MA, Heuer DK, Higginbotham EJ, et al. The Ocular Hypertension Treatment Study: a randomized trial determines that topical ocular hypotensive medication delays or prevents the onset of primary open-angle glaucoma. Arch Ophthalmol. 2002;120(6):701–13. 829-30

9. European Glaucoma Society Terminology and Guidelines for Glaucoma. 4th Edition - Chapter 3: Treatment principles and options. Br J Ophthalmol. 2017;101(6):130–95.
10. Foster PJ, Buhrmann R, Quigley HA, Johnson GJ. The definition and classification of glaucoma in prevalence surveys. Brit J Ophthalmol. 2002;86(2):238–42.
11. Prum BEJ, Herndon LWJ, Moroi SE, et al. Primary Angle Closure Preferred Practice Pattern. Ophthalmology. 2016;123(1):1–40.
12. Wang N, Wu H, Fan Z. Primary angle closure glaucoma in Chinese and Western populations. Chin Med J. 2002;115(11):1706–15.
13. He M, Ge J. Primary angle closure--a new term in the definition of primary angle closure glaucoma? Chin J Ophthalmol. 2005;12:1061–4.
14. Foster PJ, Baasanhu J, Alsbirk PH, et al. Glaucoma in Mongolia. A population-based survey in Hovsgol province, northern Mongolia. Arch Ophthalmol. 1996;114(10):1235–41.
15. Foster PJ, Oen FT, Machin D, et al. The prevalence of glaucoma in Chinese residents of Singapore: a cross-sectional population survey of the Tanjong Pagar district. Arch Ophthalmol. 2000;118(8):1105–11.
16. Salmon JF, Mermoud A, Ivey A, et al. The prevalence of primary angle closure glaucoma and open angle glaucoma in Mamre, western Cape, South Africa. Arch Ophthalmol. 1993;111(9):1263–9.
17. Congdon NG, Quigley HA, Hung PT, et al. Screening techniques for angle-closure glaucoma in rural Taiwan. Acta Ophthalmol Scand. 1996;74(2):113–9.
18. Douglas GR, Drance SM, Schulzer M. The visual field and nerve head in angle-closure glaucoma. A comparison of the effects of acute and chronic angle closure. Arch Ophthalmol. 1975;93(6):409–11.
19. Dhillon B, Chew PT, Lim ASM. Field loss in primary angle-closure glaucoma. Asia-Pac J Ophthalmoly. 1990;2:85–7.
20. Ren Z. Devoting much attention to further understanding the definition of glaucoma. Chin J Ophthalmol. 2006;3:193–5.
21. Thomas R, Parikh R, Muliyil J, Kumar RS. Five-year risk of progression of primary angle closure to primary angle closure glaucoma: a population-based study. Acta Ophthalmol Scand. 2003;81(5):480–5.
22. Aung T, Friedman DS, Chew PT, et al. Long-term outcomes in Asians after acute primary angle closure. Ophthalmology. 2004;111(8):1464–9.
23. Ge J. Scientific controversy to push the progress of glaucoma practice—inspiration by the debate on the classification of primary angle closure glaucoma. Chin J Ophthalmol. 2006;11:964–6.
24. Lu D, Liu X, Wang C. Analysis of intraocular pressure, cup disc ration and systemic blood pressure for the prediction of prognosis of glaucoma patients. Eye Science. 1985;01:77–80.
25. Glaucoma Group Of Chinese Ophthalmological Society. The Consensuses and Suggestions on POAG Ocular-Cranial Pressure Gradient in China (2017). Chin J Ophthalmol. 2017;53(2):89–91.
26. Hou R, Zhang Z, Yang D, et al. Pressure balance and imbalance in the optic nerve chamber: The Beijing Intracranial and Intraocular Pressure (iCOP) Study. Sci China Life Sci. 2016;12:1413–22.
27. Berdahl JP, Fautsch MP, Stinnett SS, Allingham RR. Intracranial pressure in primary open angle glaucoma, normal tension glaucoma, and ocular hypertension: a case-control study. Invest Ophthalmol Vis Sci. 2008;49(12):5412–8.
28. Berdahl JP, Allingham RR, Johnson DH. Cerebrospinal fluid pressure is decreased in primary open-angle glaucoma. Ophthalmology. 2008;115(5):763–8.
29. Ren R, Jonas JB, Tian G, et al. Cerebrospinal fluid pressure in glaucoma: a prospective study. Ophthalmology. 2010;117(2):259–66.
30. Ren R, Wang N, Zhang X, et al. Trans-lamina cribrosa pressure difference correlated with neuroretinal rim area in glaucoma. Graefes Arch Clin Exp Ophthalmol. 2011;249(7):1057–63.
31. Jonas JB, Wang NL, Wang YX, et al. Estimated trans-lamina cribrosa pressure difference versus intraocular pressure as biomarker for open-angle glaucoma. The Beijing Eye Study 2011. Acta Ophthalmol. 2015;93(1):e7–13.
32. Yang D, Fu J, Hou R, et al. Optic neuropathy induced by experimentally reduced cerebrospinal fluid pressure in monkeys. Invest Ophthalmol Vis Sci. 2014;55(5):3067–73.
33. Zhang Z, Liu D, Jonas JB, et al. Axonal Transport in the Rat Optic Nerve Following Short-Term Reduction in Cerebrospinal Fluid Pressure or Elevation in Intraocular Pressure. Invest Ophthalmol Vis Sci. 2015;56(8):4257–66.
34. Hou R, Zhang Z, Yang D, et al. Intracranial pressure (ICP) and optic nerve subarachnoid space pressure (ONSP) correlation in the optic nerve chamber: the Beijing Intracranial and Intraocular Pressure (iCOP) study. Brain Res. 1635;2016:201–8.
35. Zhou J. Wang Ning-li: stand on the international rostrum. Int Stud. 2010;10:24–7.

5 Primary Open-Angle Glaucoma, Trans-Lamina Cribrosa Pressure Difference, and Central Nerve System

Ning Fan, Guo Liu, Xiaoguang Zhang, and Xuyang Liu

Primary open-angle glaucoma (POAG) is an optic nerve disease with elevated IOP as the main risk factor. In recent years, with the development of interdisciplinary in the ophthalmology and neurology, new questions about the essence of POAG have been raised. Is POAG just an ocular disease? Is it a disease which involves the eye first and then the whole visual pathway? Or sometimes is it an ocular manifestation of a particular central nervous system (CNS) disease? Recent experimental and clinical studies have suggested that POAG patients may have an abnormally low cerebrospinal fluid pressure (CSFP). It was thought that trans-lamina cribrosa pressure difference (TLPD) may be associated with pathogenesis of POAG, instead of either IOP or CSFP alone. These questions have caused controversy in the field of ophthalmology. Previous studies showed that POAG does not only involve the optic nerve damage but also affects the lateral geniculate body, the optic radiation, and the visual cortex. It is a multilevel syndrome throughout the visual pathway. The mechanism of glaucomatous lesion is complex, which involves transsynaptic damage, blood supply disorder of the visual pathway, and blood-brain barrier abnormalities. It was hypothesized that glaucoma might be recognized as a CNS disease.

POAG is the second leading cause of blindness in the world after cataract. The prevalence rate of POAG is 0.21–1.64%, and the prevalence rate of people over 40 years old is 1–2%. By 2020, the number of POAG patients worldwide will be approximately 80 million [1]. The retinal ganglion cell death is the major cause of retinal nerve fiber layer thinning and visual field defects in POAG, and reducing IOP is the main treatment proven to be effective. The progression of glaucomatous damage can also sometimes be delayed by reducing the IOP in patients with normal tension glaucoma (NTG). However, even if the IOP is well controlled in some patients with advanced glaucoma, the glaucomatous optic neuropathy is still progressing. Recent studies revealed that some CNS degenerative diseases were similar to glaucoma in the characteristics and mechanisms. Animal experiments and human studies showed that POAG was more like a syndrome of the entire visual pathway from the retina to the optic nerve, optic chiasm, optic tract, lateral geniculate body, visual radiation, and visual cortex. Morphological and functional changes existed in all parts above, leading to a fundamental change in the concept of glaucoma – is POAG a CNS disease?

5.1 The Relationship Between POAG and CNS Diseases

POAG is similar to many other CNS diseases such as Alzheimer's disease (AD), Parkinson's disease (PD), and muscular atrophic lateral sclerosis. In general, these diseases start with axonal transport abnormality and are then followed by chronic neuronal degeneration with apoptosis as a common pathway. The relationship and similarity between AD and glaucoma are some of the examples.

Tamura et al. [2] found that 41 (23.8%) of 172 AD patients suffered from POAG, which was significantly higher than that (9.9%) of 176 age-matched controls. It was also found that there was no significant difference in IOP between glaucoma patients and non-glaucoma patients in the Alzheimer's disease group. A retrospective study of 112 AD patients in Germany by Bayer et al. [3] found that 29 patients of them (25.9%) had glaucomatous visual field defects and/or the cup-to-disc ratio is greater than 0.8. This study showed that the morbidity rate of POAG in AD patients was ten times higher than that in patients with non-AD. Bayer et al. [4] also reported 12 cases (24.5%) with glaucoma visual field defection or disc ratio >0.8 out of 49 patients with AD, which was significantly higher than that in the normal control group (6.5%). The above studies suggest that patients with AD were more possibly to develop glaucoma. Hence some authors proposed that glaucoma was an ocular Alzheimer [5].

N. Fan · G. Liu · X. Zhang · X. Liu (✉)
Shenzhen Eye Hospital, Jinan University, Guangdong, China
e-mail: xliu1213@126.com

N. Wang (ed.), *Intraocular and Intracranial Pressure Gradient in Glaucoma*,
Advances in Visual Science and Eye Diseases 1, https://doi.org/10.1007/978-981-13-2137-5_5

This viewpoint was supported by more and more evidences recently. In 2017, Chiara Criscuolo et al. [6] reviewed the similarity between AD and POAG in terms of synaptic dysfunction. Pathologically, the two diseases form chronic neurological damage by characteristic synaptic dysfunction. Both of them have protein aggregates such as the beta amyloid (Aβ) and intracellular microtubule inclusions with hyperphosphorylated tau, which belongs to microtubule-associated protein family. During the early phase of degeneration, the two diseases are characterized by synaptic dysfunction and mitogen-activated protein kinase (MAPK) changes.

Aβ plays an important role in both diseases. Ambra Masuzzo et al. [7] reviewed the amyloidosis in retinal neurodegenerative diseases including age-related macular degeneration (AMD) and POAG comparing to AD. Among the neurodegenerative diseases, which are related to Aβ amyloidosis, AD is undoubtedly the best known and the most studied. Recently, it has been recognized that Aβ-related amyloidosis also exists in POAG and AMD. The Aβ-related amyloidopathies include the increase of intra- and/or extracellular Aβ accumulation and deposition, in the form of insoluble substances, such as amyloid plaques or drusens. Most neurodegenerative diseases are associated with amyloidopathies. The amount of Aβ that exceeds normal physiological level would produce cytotoxicity that might be related to the disorders of Aβ-associated modulation of synaptic excitability in physiological conditions [8]. In addition, Aβ is also thought to be associated with mitochondrial dysfunction and glial activation in both visual pathway and the whole CNS [7].

Li et al. [9] developed a therapy method targeting amyloid β which was used to be a target of AD to treat POAG. They demonstrated that targeting different components of the Aβ formation and aggregation pathway could effectively reduce glaucomatous RGC apoptosis in vivo, and finally, the combined triple treatments were more effective than monotherapy.

There are also some central nervous demyelinating lesions, such as PD, that may be associated with POAG. Bayer et al. [4] found that 9 out of 38 PD patients (23.7%) suffered from POAG, which was significantly higher than the prevalence of glaucoma in the general population, indicating that these two diseases may also have a certain correlation.

In 2015, Fani Tsolaki et al. [10] elucidated the putative association between various forms of dementia, POAG, and *Helicobacter pylori* (*H. pylori*) infection in all possible combinations. A total of 156 patients were recruited in this study. Then they were divided into a dementia group, a POAG group, and two control groups. All patients were tested by neuropsychological evaluation, POAG detection, and *H. pylori* diagnostic testing. After statistical analysis, their results suggested that there were positive correlations between *H. pylori* infection and dementia, as well as *H. pylori* infection and POAG. *H. pylori* infection was more popular in CNS disease (dementia) group and POAG group comparing to the control group (68.33% in patients with dementia vs. 45.16%, $p < 0.05$, 68.57% in patients with POAG vs. 45.16%, $p < 0.05$). Furthermore, there was a higher rate of POAG in patients with AD and PD (16.66% dementia vs 0% control), as well as higher frequency of dementia (AD and frontotemporal dementia, FTD) in patients with POAG (16.66% POAG vs. 0% control), comparing to the control group. They concluded that neurodegenerative diseases such as dementia and POAG were linked to each other and to *H. pylori* infection.

Besides the same pathogenesis factors which can support that CNS diseases and POAG may be a same kind of disease, the similar manifestations can also indicate that POAG is a type of CNS disease. Multiple sclerosis is a chronic, inflammatory, and demyelinating lesion of CNS. Its optic nerve changes are very similar to POAG. It was believed that both of them may share a similar pathogenesis, and both of them express high level of vasoconstrictor cytokines [11].

5.2 The Relationship Between POAG and TLPD

The two optic nerves are the only cranial nerves which pass through the three sealing containers with pressure. Firstly, the RGCs and its axons belong to the ocular container. Then, the axons are surrounded by cerebrospinal fluid along its pathway until into the third container, the intracranial container. The connection between the first two containers is called the lamina cribrosa, which is the part of the sclera tissue that is pierced by the axons. The intracranial container is a bony structure without space to expand. Therefore, the intracranial pressure change could severely impair the neuro structures. Meanwhile, the ocular container is constructed with compact fiber tissues, also with no space to expand.

Normally, the IOP is a little bit higher than the intracranial pressure, which is 5–11 mmHg. When the pressure changes either in the intracranial or intraocular container, the pressure gradient might impose a sheared force on the site where the two pressures meet. The backward indentation of the lamina cribrosa of sclera is related to the increased IOP. The low intracranial pressure may also show the similar effects. In addition, the changes of pressure and composition of cerebrospinal fluid might also be associated with the glaucomatous optic neuropathy [12].

A prospective iCOP study from the Ningli Wang and his colleagues revealed that patients with NTG and/or high-pressure glaucoma as well as patients with ocular hypertension received a neurological examination of a lumbar puncture wit

lumbar CSFP measurement. When compared to non-glaucomatous control group, the patients with NTG had significantly lower lumbar CSFP than those with high-pressure glaucoma or those in the control group. Consequently, the TLPD was significantly higher in both glaucoma groups than in the control group. Patients with ocular hypertension had significantly higher CSFP. It also confirmed that the glaucomatous optic nerve damage, evaluated by neuroretinal rim area and visual field defect, was related to the decrease of CSFP and the increase of TLPD [13].

Gallina et al. [14] investigated 22 patients with normal pressure hydrocephalus (NPH) who had undergone ventriculoperitoneal (VP) shunt placement. Interestingly, after more than 6 months follow-up, they found nine of them had NTG. The median follow-up time was 12.0 months in patients with NTG and 18.0 months in those without NTG. This study concluded that changes in the pressure gradient between intraocular and intracranial compartments at the lamina cribrosa level play a role in the pathogenesis of NTG. If this is true, the decreased pressure gradient should be beneficial to prevent the development and progression of NTG. The study from Sawada et al. [15] supported this hypothesis. One hundred and fifty-nine myopic eyes with glaucomatous VFD under treatment and follow-up for 7 years were studied. The results showed that in myopic eyes, there are specific patterns of LC defect, which can function as a pathway to balance the pressure between the IOP and ICP, suggesting an important role of the pressure gradient in the pathogenesis of NTG. Imbalance of the TLPD may play an important role in the pathogenesis of glaucomatous optic nerve damage and other intracranial and intraocular pressure-related diseases.

All these suggest the association between glaucoma and CNS diseases. It is very necessary to have further study in this field. In another chapter of this book, the theory of intracranial and intraocular pressure-related diseases is discussed in detail.

5.3 DBA/2 Mouse Model of Glaucoma

Calkins et al. [16] pointed out that the initial lesion of POAG was located in the midbrain instead of the eye. The DBA/2 glaucoma mouse was a rodent model which IOP increased along with age. When cholera toxin – cholera toxin B (CTB) – was injected into the vitreous cavity of DBA/2 mouse glaucoma model, by observing the uptake and transport of CTB by RGCs, the early axonal injury could be detected. It was thought that the first sign of glaucomatous damage should be found in the retina. However, the results were unexpected. The earliest site of injury was in the midbrain, where the end of optic nerve fibers project at. His main findings are described below.

5.3.1 Obstruction of Axoplasmic Transport in Glaucoma Was Developed from the Proximal to the Distal Axon

Some of the optic nerve fibers of the DBA/2 mouse model of glaucoma were projected to the second layer of the superior colliculus (SC) via the third layer of SC, and the others were projected to the optic nerve nucleus, lateral geniculate nucleus, and ovule dome. The transportation of 3-month-old DBA/2 mouse axons was normal, and ordinary CTB signals could be detected in the SC. When these mice grew to 12 months old, their IOPs increased significantly, with the CTB signal reduced in the SC. The CTB signals could not be detected in the SC in the 14 DBA/2 mice aged 10–12 months and could be observed in their lateral geniculate body (43%), optic tract (29%), and optic nerve (21%), respectively. These finds suggested that the early axoplasmic transport disorder and axonal malnutrition in DBA/2 glaucoma mice were in the SC – the area where the RGC cell fibers projected, not in the eye, and the lesion developed slowly from the distal end to the proximal end. This pathological process of peripheral axons is very similar to some CNS diseases, such as AD, PD, and amyotrophic lateral sclerosis [17–19].

5.3.2 Obstruction of Distal Axonal Transport in Glaucoma Owns Characteristics of Age–Dependent and Retinal Localization

Calkins et al. [16] found that the CTB signal in the SC in the 5-month-old DBA/2 mice and the C57BL/6 mice was almost at the same time, while that in the 8-month-old and 10-month-old DBA/2 mice was decreased by 25% and 88%, respectively. And the pattern of CTB signal decrease owned retinal localization. At the same time, the authors also analyzed the correlation between the age, the IOP, and the decrease of CTB signal in the SC. The results were summarized below. In DBA/2 mice aged from 3 to 10 months, the decrease of CTB signal in the SC was significantly correlated with age. Particularly, no significant IOP change was found in 3- to 5-month-old mice, and their CTB signal intensity showed almost no difference. However, in mice aged from 5 to 8 months, the increase of IOP was found to be the most obvious one. But there was no significant correlation between the IOP change and the CTB signal decrease. At last, it was found in 8- to 12-month-old mice that the increase of IOP was relatively slow, while the CTB signal expressed was decreased by 96%. The elevation of IOP in this period was significantly related to the CTB signal change. In order to confirm the relationship among age, IOP, and the axonal terminal transport disorder of ganglion cells, the polystyrene microspheres were injected into the anterior chambers of two groups of DBA/2

mice aged from 3 to 4 months and 7 to 9 months, respectively. The IOP of mice in both groups elevated about 45% drastically. Meanwhile the same volume of saline was injected into the anterior chambers of mice from their corresponding control groups; no IOP change was found. In CTB signal analysis, it was found that there was no obvious SC CTB signal decrease in the 3- to 4-month-old group after the IOP elevated, but in the 7- to 9-month-old group, the same CTB signal was significantly weakened while the IOP was increasing. These results indicated that the glaucomatous distal axonal transport deficits were age related. As a highly risk factor of glaucoma, elevated IOP was more likely to cause distal axonal transport deficits in the elder group, which also suggested that glaucoma was similar to the other age-related neurodegenerative diseases, such as AD and PD.

5.3.3 The Axonal Structure of RGC Cells in Glaucoma Is Still Preserved After the Obstruction of Axonal Transport

Calkins chose two specific antibodies to mark the estrogen-related receptor and the glutamate vesicle transporter 2, respectively. The former can show the fibers of the whole RGC, and the latter can specifically show the synapse of RGCs. The results showed that the number of distal axons and proximal axons in DBA/2 mice decreased with the increase of age and the number of distal axons always decreased more obviously, which indicated that axonal damage also developed from the distal end to the proximal end. In 18-month-old DBA/2 mice, distal axonal transport was impaired, and CTB signals were not seen in the SC, but the anti-ERR staining results showed that there was no significant difference comparing to the 3-month-old DBA/2 mice. Moreover, in those 17-month-old DBA/2 mice, some of them might not observe the SC CTB signal, but both the anti-ERR and anti-VGluT2 staining results of them showed almost 100% stained, which indicates that the structures of the RGCs axons are still present for a certain period of time after the axonal transport is impaired in glaucoma.

5.4 The Visual Pathway Damage Induced by POAG

The axons of the retinal ganglion cells converge into the brain and form the optic nerve. Ninety percent of the fibers reach the lateral geniculate body. And the optic radiation projects to the occipital visual cortex. The other 10% of the fibers project to the superior colliculus and the pretectal area. The DBAs/2 glaucoma first showed the axoplasmic transport barrier in the peripheral axles of RGC cells, which is a typical lesion of senile dementia and amyotrophic lateral sclerosis. According to the transsynaptic mechanism of nerve injury, the damage of neurons causes secondary degeneration of neurons that are anatomically or functionally linked to it; in other words, the retrogression of RGCs can lead to damage to the lateral geniculate body, visual radiation, and visual cortex; meanwhile degeneration also retrogrades damage to RGC cells. The mechanisms may be oxidative damage and glutamate excitatory toxicity. Yucel et al. [20] have observed the obvious protective effects of retinal ganglion cells and lateral geniculate cells on glaucoma model of rhesus monkey by blocking N-methyl-D-aspartate receptor.

5.4.1 The Damage of the Anterior Visual Pathway of POAG

Sasaoka et al. [21] used a monkey laser-induced high intraocular pressure (IOP) model and observed that the diameter of the optic nerve was reduced and the optic chiasm became thin after 16 weeks after laser. In human studies, Kashiwagi et al. [22] performed MRI examination on 31 POAG patients and 23 normal controls. It was found that the optic nerve diameter and the thickness of optic chiasm in glaucoma patients were significantly smaller than those in normal controls and were positively correlated with the degree of visual field defect and the enlargement of cup-disc ratio. Garaci et al. [23] used NMR diffusion tensor imaging (DTI) and showed that the partial anisotropy ratio of optic nerve in POAG patients was reduced, the average diffusion rate was increased, and the range of change was related to the course of POAG. In the autopsy of POAG patients, it was also found that the diameter of the optic nerve was significantly reduced, the intraorbital pial meninges of the optic nerve were thickened, and the number of subarachnoid meningeal cell nests was obviously increased [24, 25].

5.4.2 The Damage of Posterior Visual Pathway in POAG

The lateral geniculate body is an important transit point for the visual system. It is divided into six layers. The cross fibers from two eyes terminate in the first, fourth, and sixth layer of the opposite side, and the non-cross fibers end in the ipsilateral layer of second, third, and fifth. The monocular glaucoma models of crab monkey and rhesus monkey were both confirmed that the replacement neurons in layers 1, 4, and 6 of the contralateral geniculate body and the ipsilateral layers 2, 3, and 5 of the ipsilateral geniculate body were obviously reduced, the large cell neurons and small cell neurons were both involved, and the denaturation degree of small cell neurons was significantly higher than that of large cell neurons [26]. The degeneration of neurons was accompanied with the proliferation of glial cells [27]. Postmortem [23] and MRI

results [28] also verified that the lateral geniculate body of POAG patients was significantly smaller than that of age-matched normal persons. The decrease in the number and function of neurons in the lateral geniculate body caused by POAG is bound to correspond to the changes of visual radiation and the visual cortex. Chan et al. [29] found that the ratio of choline/creatine in the visual cortex metabolites of chronic glaucoma mice was significantly lower than that in the normal control group by using magnetic resonance spectroscopy. Choline was involved in the synthesis of some neurotransmitters and acetylcholine, and it was also involved in cell membrane synthesis and cell regeneration, which may be related to the decreased activity of visual cortex cells. The decrease of the ratio of choline/creatine may be related to the decrease in the activity of visual cortex cells. Magnetic resonance imaging (MRI) on human body showed that visual radiation and injury to the visual cortex were confirmed. By using magnetic resonance diffusion imaging, Garaci et al. [23] found the decreasing of the anisotropy ratio of visual radiation and the increasing of the average diffusion rate in POAG patients and then proved the damage of visual radiation fiber. At the same time, Kitsos et al. [30] found that the white matter of the cerebrum of alive patients with POAG was higher than that of the normal control group in MRI results. Magnetization transfer imaging showed that the magnetization transfer rate of gray matter and white matter in POAG patients was lower than that in normal controls. Human autopsy provides strong evidence too that comparing with normal people, POAG patients manifested an obvious atrophy – visual cortex gray matter was thinner, and cerebral gyrus was shallower [25].

5.4.3 Other Glaucomatous Damage in CNS

Chiquet et al. [31] found that in the mouse glaucoma model, except the damage of the whole optic pathway, damage of the suprachiasmatic nucleus, which is related to the synchronization of the circadian rhythm, also exists. This may be initiated from the synaptic damage caused by the death of the retinal ganglion cells in the nucleus. Animal experiments showed that both acute and chronic high IOP could damage the melanopsin-containing retinal ganglion cells which were related to the regulation of the circadian rhythm [32], indicating that glaucoma could also damage the non-shape sensitive conduction pathway.

5.5 Mechanism of Action (MOA) Study of CNS Damage in Glaucoma

Besides the damaged RGCs, high IOP which blocks the axonal transportation and the secondary demyelination of nerve fibers may also contribute to the glaucomatous damage and dysfunction of the optic nerve fiber. Downs et al. [33] using the three-dimensional tissue measurement techniques reconstructed the optic disc of the monkey glaucoma model. It was found that the nerve tube and the subarachnoid structure in the beginning of the optic disc were obviously deformed. The optic nerve is part of the CNS, but the anterior vessels of the optic nerve sieve do not have the function of the blood-brain barrier and thus lack the barrier to the harmful substances. In the glaucoma patients, the barrier function is more obvious, which may also be one of the causes of the optic nerve damage. The CNS lesion of POAG is closely related to extensive cerebral blood supply deficiency. In 15 cases of POAG, Siesky et al. [34] found that the visual acuity, contrast sensitivity, mean central visual field defect, and the amplitude of electroretinogram of these subjects were closely related to the mean blood flow rate of the middle cerebral artery.

Neuronal damage caused secondary degeneration of its anatomic or functional contacted neuron, which is known as transsynaptic damage and is a typical lesion of AD and amyotrophic lateral sclerosis. The lateral geniculate body and visual cortex damage caused by glaucoma belong to the category of transsynaptic damage. Both of the anterograde and retrograde cross-synaptic damages exist in this kind of lesion. The mechanism may be oxidative damage and excitatory toxicity of glutamate. Reactive oxygen species which accumulated in the oxidative stress state reacting with nitrous oxide formed pernitrite. Thereby the intracellular environment was altered, and cell death was conducted. Pernitrite can turn protein into nitrotyrosine, and it is a marker of various neurodegenerative diseases. Some researchers found nitrotyrosine in the lateral geniculate parenchyma and vascular endothelium of glaucomatous animal models which indicates the mechanism of oxidative damage in glaucoma. Glutamate excitatory toxicity is also one of the causes of many central degenerative diseases. Blocking the N-methyl-D-aspartate (NMDA) receptor can effectively protect the retinal ganglion cells and lateral geniculate bodies from lesion which is caused by glaucoma in *Macaca rhesus* [20]. Sposato et al. [35] found that the expression of nerve growth factor and its receptor in the lateral geniculate body and visual cortex is downregulated significantly in the glaucoma mouse model. It is considered that the regulation of cytokines and its receptors plays a very important role in glaucomatous damage. Neurochemical changes in the lateral geniculate nucleus and primary optic cortex were studied by Crawford et al. [36] in the glaucoma monkey model, which confirmed that the cytochrome oxidase activity in the lateral geniculate nucleus and the visual cortex was significantly reduced, suggesting that the cytochrome system also played a role in the pathogenesis of glaucoma. The ratio of choline/creatine in the visual cortex metabolites of mice with chronic glaucoma was significantly lower than that in the normal

control group by using magnetic resonance spectroscopy [25]. It was believed that the magnetic resonance spectroscopy technique has the potential to study the pathogenesis of glaucoma. The spectrum analysis of the ratio of choline/creatine in the cortex can be used to judge the central damage of glaucoma.

Interestingly, the possible MOA of that *Helicobacter pylori* infection increases the incidence rate of both CNS diseases such as AD, PD, etc., and POAG was discussed by some literatures. They may share same pathogenesis under the same *H. pylori* infection stress. Sergio C Sacca et al. [37] reviewed 152 literatures which related to the relationship between *H. pylori* infection and eye diseases, most of which were POAG from 1998 to 2014. In particular, the pathogenetic researches were focused on oxidative damage. *H. pylori* infection can accumulate the reactive oxygen species (ROS) production, and then, mitochondrial function declined, mitochondrial DNA mutations accumulated under this condition. The level of oxidative damage to DNA, proteins, and lipids increased, while the capacity to degrade oxidatively damaged proteins and other macromolecules decreased. At last, RGC apoptosis is initiated, and glaucoma is formed.

In CNS diseases, ROS increase after *H. pylori* infection also played a very important role. Giulia Nesi et al. [38] reviewed the relationship between ROS and AD. They showed that an increasing body of evidence reveals that both mitochondrial abnormalities and metal accumulations synergistically act as major producers of ROS, thus contributing to neuronal toxicity.

Additionally, more pathogenesis factors under other conditions such as microglia reaction were reported contributing to both of CNS diseases and POAG. Ana I. Ramirez et al. [39] reviewed the same role of microglial played in the AD, PD, and POAG. After the literature analysis, they found microglial activation had been reported in AD, PD, and POAG in relation to protein aggregates and degenerated neurons. The activated microglia could release pro-inflammatory cytokines which could aggravate and propagate neuroinflammation, thereby degenerating neurons and impairing brain as well as retinal function.

Furthermore, same therapy which works for both CNS disease and POAG can also indicate they are same kind of disease. Mead et al. [40] introduced a method of dental pulp stem cell therapy, which can repair CNS damage, including recent findings on RGC neuroprotection and regeneration in optic nerve injury and glaucoma.

It was proved that trans-lamina cribrosa pressure difference (TLPD) may be the pathogenesis for glaucoma, not the elevated IOP or the reduced CSFP alone. It is still hard to say whether increase of TLPD is the hypostasis for POAG or just a manifestation. Many results can be provoked beyond the mechanical environment change by an increased trans-lamina cribrosa pressure difference. For example, the increased TLPD may also increase the strain power of the laminar pore and change the ocular perfusion status; in addition, reduced CSF flow in the optic nerve subarachnoid space may cause accumulation of metabolites and conglutination between optic nerve and its sheath. Killer et al. [41] suggested compartment of subarachnoid space and showed CSF composition difference in POAG patients with normal IOP; it is still hard to say whether the lowering of CSFP or CSF flow in the optic nerve subarachnoid space happens first or the optic nerve sheath compartment happens first. In the future, it is important to explore the downstream pathophysiology of the increased trans-lamina cribrosa pressure difference in POAG to find the true hypostasis.

The orbital CSFP as counterpressure against IOP is a determinant of the TLPD and is important for the pathophysiology of the pressure-related diseases originating at the optic nerve head, such as glaucoma. Taking the physiological triangular relationships between IOP, CSFP, and BP into account, glaucoma may be described as a misbalance between IOP, CSFP, and BP, finally leading to an increase in TLPD.

Since the central retinal vein passes through the orbital CSF space, the orbital CSFP is of importance for the pressure in the retinal veins and potentially for the development of retinal vein occlusions. In a similar manner, since the retinal venous pressure influences the retinal capillary pressure, the orbital CSFP may influence the development and severity of diabetic retinopathy. Similarly, since the choroid drains through the vortex veins into the superior ophthalmic vein and cavernous sinus intracranial, higher CSFP may be associated with a thicker choroid. But it remains unexplored about the body position-dependent and time-dependent changes in TLPD. Some experimental studies suggested that dorsomedial and perifornical hypothalamic neurons may be involved in the regulation of both IOP and CSFP [13].

5.6 Summary

In summary, it is believed that POAG may be a special CNS disease, because it not only shares similarities with some degenerative diseases of the CNS but also exhibits the functional and structural changes of the whole optic pathway. Additionally, imbalance of the TLPD may play an important role in the pathogenesis of glaucomatous optic nerve damage and other intracranial and intraocular pressure-related diseases.

Therefore, POAG should not only be considered as an ocular disease but a CNS disease that begins with the dysfunction of the axonal transport of RGC cells. On the other hand, it should be pointed out that lowering IOP only is not enough to treat POAG; neuroprotective therapy is also very important, for not only protecting the optical nerve but also the optic pathway and, furthermore, the CNS.

References

1. Quigley HA, Broman AT. The number of people with glaucoma worldwide in 2010 and 2020. Br J Ophthalmol. 2006;90(3):262–7.
2. Tamura H, Kawakami H, Kanamoto T, Kato T, Yokoyama T, Sasaki K, Izumi Y, Matsumoto M, Mishima HK. High frequency of open-angle glaucoma in Japanese patients with Alzheimer's disease. J Neurol Sci. 2006;246(1–2):79–83.
3. Bayer AU, Ferrari F, Erb C. High occurrence rate of glaucoma among patients with Alzheimer's disease. Eur Neurol. 2002;47(3):165–8.
4. Bayer AU, Keller ON, Ferrari F, Maag KP. Association of glaucoma with neurodegenerative diseases with apoptotic cell death: Alzheimer's disease and Parkinson's disease. Am J Ophthalmol. 2002;133(1):135–7.
5. Mckinnon SJ. Glaucoma: ocular Alzheimer's disease? Front Biosci. 2003;8(1–3):s1140–56.
6. Criscuolo C, Fabiani C, Cerri E, Domenici L. Synaptic dysfunction in Alzheimer's disease and glaucoma: from common degenerative mechanisms toward neuroprotection. Front Cell Neurosci. 2017;111(53):1–7.
7. Masuzzo A, Dinet V, Cavanagh C, Mascarelli F, Krantic S. Amyloidosis in retinal neurodegenerative diseases. Front Neurol. 2016;7(127):1–17.
8. Kamenetz F, Tomita T, Hsieh H, Seabrook G, Borchelt D, Iwatsubo T, Sisodia S, Malinow R. APP processing and synaptic function. Neuron. 2003;37(6):925–37.
9. Guo L, Salt TE, Luong V, Wood N, Cheung W, Maass A, Ferrari G, Russo-Marie F, Sillito AM, Cheetham ME, Moss SE, Fitzke FW, Cordeiro MF. Targeting amyloid-β in glaucoma treatment. PNAS. 2007;104(33):13444–9.
10. Tsolaki F, Kountouras J, Topouzis F, Tsolaki M. Helicobacter pylori infection, dementia and primary open-angle glaucoma: are they connected? BMC Ophthalmol. 2015;15(1):24.
11. Jankowska-Lech I, Terelak-Borys B, Grabska-Liberek I, Palasik W. Glaucoma neuropathy and neuropathy in multiple sclerosis- -common elements of pathogenesis? Klin Oczna. 2007;109(7–9):317–20.
12. Ren R, Jonas JB, Tian G, Zhen Y, Ma K, Li S, Wang H, Li B, Zhang X, Wang N. Cerebrospinal fluid pressure in glaucoma: a prospective study. Ophthalmology. 2010;117(2):259–66.
13. Jonas JB, Wang N, Yang D, Ritch R, Panda-Jonas S. Facts and myths of cerebrospinal fluid pressure for the physiology of the eye. Prog Retin Eye Res. 2015;46(3):67–83.
14. Gallina P, Savastano A, Becattini E, Orlandini S, Scollato A, Rizzo S, Carreras G, Di Lorenzo N, Porfirio B. Glaucoma in patients with shunt-treated normal pressure hydrocephalus. J Neurosurg. 2017;17:1–7.
15. Sawada Y, Araie M, Kasuga H, Ishikawa M, Iwata T, Murata K, Yoshitomi T. Focal lamina cribrosa defect in myopic eyes with non-progressive glaucomatous visual field defect. Am J Ophthalmol. 2018;190:34–49.
16. Crish SD, Sappington RM, Inman DM, Horner PJ, Calkins DJ. Distal axonopathy with structural persistence in glaucomatous neurodegeneration. Proc Natl Acad Sci U S A. 2010;107(11):5196–201.
17. Fischer LR, Culver DG, Tennant P, Davis AA, Wang M, Castellanosanchez A, Khan J, Polak MA, Glass JD. Amyotrophic lateral sclerosis is a distal axonopathy: evidence in mice and man. Exp Neurol. 2004;185(2):232–40.
18. Stokin GB, Lillo C, Falzone TL, Brusch RG, Rockenstein E, Mount SL, Raman R, Davies P, Masliah E, Williams DS, Goldstein LS. Axonopathy and transport deficits early in the pathogenesis of Alzheimer's disease. Science. 2005;307(5713):1282.
19. Coleman M. Axon degeneration mechanisms: commonality amid diversity. Nat Rev Neurosci. 2005;6(11):889–98.
20. Yücel YH, Gupta N, Zhang Q, Mizisin AP, Kalichman MW, Weinreb RN. Memantine protects neurons from shrinkage in the lateral geniculate nucleus in experimental glaucoma. Arch Ophthalmol. 2006;124(2):217–27.
21. Sasaoka M, Nakamura K, Shimazawa M, Ito Y, Araie M, Hara H. Changes in visual fields and lateral geniculate nucleus in monkey laser-induced high intraocular pressure model. Exp Eye Res. 2008;86(5):770–82.
22. Kashiwagi K, Okubo T, Tsukahara S. Association of magnetic resonance imaging of anterior optic pathway with glaucomatous visual field damage and optic disc cupping. J Glaucoma. 2004;13(3):189–95.
23. Garaci FG, Bolacchi F, Cerulli A, Melis M, Spanò A, Cedrone C, Floris R, Simonetti G, Nucci C. Optic nerve and optic radiation neurodegeneration in patients with glaucoma: in vivo analysis with 3-T diffusion-tensor MR imaging. Radiology. 2009;252(2):496.
24. Pache M, Meyer P. Morphological changes of the retrobulbar optic nerve and its meningeal sheaths in glaucoma. Ophthalmologica. 2006;220(6):393–6.
25. Gupta N, Ang L, Tilly LND, Bidaisee L, Yücel YH. Human glaucoma and neural degeneration in intracranial optic nerve, lateral geniculate nucleus, and visual cortex. Br J Ophthalmol. 2006;90(6):674.
26. Yücel YH, Zhang Q, Weinreb RN, Kaufman PL, Gupta N. Effects of retinal ganglion cell loss on magno-, parvo-, koniocellular pathways in the lateral geniculate nucleus and visual cortex in glaucoma. Prog Retin Eye Res. 2003;22(4):465–81.
27. Zhang S, Wang H, Lu Q, Qing GP, Wang NL, Wang YD, Li SN, Yang DY, Yan FC. Detection of early neuron degeneration and accompanying glial responses in the visual pathway in a rat model of acute intraocular hypertension. Brain Res. 2009;1303:131–43.
28. Gupta N, Greenberg G, Noël de Tilly L, Gray B, Polemidiotis M, Yücel YH. Atrophy of the lateral geniculate nucleus in human glaucoma detected by magnetic resonance imaging. Br J Ophthalmol. 2009;93(1):56–60.
29. Chan KC, So KF, Wuabc EX. Proton magnetic resonance spectroscopy revealed choline reduction in the visual cortex in an experimental model of chronic glaucoma. Exp Eye Res. 2009;88(1):65–70.
30. Kitsos G, Zikou AK, Bagli E, Kosta P, Argyropoulou MI. Conventional MRI and magnetisation transfer imaging of the brain and optic pathway in primary open-angle glaucoma. Br J Radiol. 2009;82(983):896.
31. Chiquet C, Drouyer E, Woldemussie E, Ruiz G, Wheeler L, Denis P, Cooper H, Romanet JP. Consequences of glaucoma on circadian and central visual system. J Fr Ophtalmol. 2006;29(7):847–51.
32. Wang H, Lu Q, Wang N, Liu H, Zhang L, Zhan GL. Loss of melanopsin-containing retinal ganglion cells in a rat glaucoma model. Chin Med J (Engl). 2008;121(11):1015–9.
33. Downs JC, Yang H, Girkin C, Sakata L, Bellezza A, Thompson H, Burgoyne CF. Three-dimensional histomor-phometry of the normal and early glaucomatous monkey optic nerve head: neural canal and subarachnoid space architecture[J]. Invest Ophthalmol Vis Sci. 2007;48(7):3195–208.
34. Harris A, Siesky BD, Haine C, Catoira Y, Sines D, Mccranor L, Garzozi H. Relationship of cerebral blood flow and central visual function in primary open-angle glaucoma. J Glaucoma. 2007;16(1):159–63.
35. Sposato V, Parisi V, Manni L, et al. Glaucoma alters the expression of NGF and NGF receptors in visual cortex and geniculate nucleus of rats: effect of eye NGF application. Vision Res. 2009;49(1):54–63.
36. Crawford ML, Harwerth RS, Smith EL, Mills S, Ewing B. Experimental glaucoma in primates: changes in cytochrome oxidase blobs in V1 cortex. Invest Ophthalmol Vis Sci. 2001;42(2):358–64.

37. Sacca SC, Vagge A, Pulliero A, Izzotti A. Helicobacter pylori infection and eye diseases: a systematic review. Medicine. 2014;93(28):1–13.
38. Nesi G, Sestito S, Digiacomo M, Rapposelli S. Oxidative stress, mitochondrial abnormalities and proteins deposition: multitarget approaches in Alzheimer's disease. Curr Top Med Chem. 2017;17(27):3062–79.
39. Ramirez AI, de Hoz R, Salobrar-Garcia E, Salazar JJ, Rojas B, Ajoy D, López-Cuenca I, Rojas P, Triviño A, Ramírez JM. The role of microglia in retinal neurodegeneration: Alzheimer's disease, Parkinson, and glaucoma. Front Aging Neurosci. 2017;09(214):1–21.
40. Mead B, Logan A, Berry M, Leadbeater W, Scheven BA. Concise review: dental pulp stem cells: a novel cell therapy for retinal and central nervous system repair. Stem Cells. 2017;35(1):61–7.
41. Killer HE, Jaggi GP, Flammer J, Miller NR, Huber AR, Mironov A. Cerebrospinal fluid dynamics between the intracranial and the subarachnoid space of the optic nerve. Is it always bidirectional? Brain. 2007;130(Pt 2):514–20.

The Role of CSFP in Glaucoma: A View in Retrospect

6

David Fleischman and R. Rand Allingham

Glaucoma is well-recognized as a pressure-related disease. Intraocular pressure has been known as a major contributor to glaucomatous pathogenesis for over a century. Blood pressure and glaucoma have been investigated closely over several decades. More recent studies have reignited an interest in cerebrospinal fluid pressure as an important contributor.

Perhaps one of the most important risk factors for primary open-angle glaucoma (POAG) is the intraocular pressure. However, it is not uncommon for POAG patients to present with normal IOP at diagnosis. This has been reported by many investigators that have described that the prevalence of normal-tension glaucoma in some populations could be as high as 70–90% of open-angle glaucoma cases [1].

Blood pressure has been measured in population-based studies, with evidence supporting that reduced blood pressure may increase risk for POAG. Several studies have shown that lower diastolic perfusion pressure, in particular, increased risk for the development of POAG. This is still a topic of debate, however, since other population-based studies have found different relationships between systolic and diastolic blood pressure and its effect on the prevalence of open-angle glaucoma [2–6].

The lamina cribrosa is the anatomic landmark that separates two differentially pressurized circulating fluid compartments—the intraocular space and the subarachnoid space (Fig. 6.1). This is also the tissue through which the axons from the retinal ganglion cells exit the eye and have been implicated as the site of injury in glaucomatous optic neuropathy. However, it was believed that mechanistically there was an insufficient pressure difference between the two fluid compartments to elicit a net force across the lamina cribrosa.

Similar to today, in the early 1900s, intraocular pressure and blood pressure did not satisfy ophthalmologists to explain glaucoma, especially normal-tension glaucoma—whose existence as a form of glaucoma was questioned. In the quest to identify *what else*, one pioneering clinician-scientist began to think beyond the two obvious pressures. Kasmir Noishevsky, MD, an ophthalmologist of Polish origin, perhaps pondered some extreme cases in ophthalmology. For example, in the case of ocular hypotony, the optic nerve can become edematous. On the other hand, an increased intracranial pressure with normal intraocular pressures could result in a similar appearance to the nerve. Therefore, with these two examples, Professor Noishevsky must have suspected that the optic nerve head is a region subject to a push-and-pull between two pressurized compartments. The case of normal pressure glaucoma was particularly confusing, and therefore, a model such as this would explain how this condition could arise, and further, the reason why reduction of IOP even at low pressures could be beneficial. In a lecture to the Conference of the Military Medical Academy in St. Petersburg, on December 15, 1908, Professor Noishevsky raised the question:

> Could it be the cause of depression papilla of the optic nerve [is] a simple … difference between the pressure inside the eye and the inside of the skull, on the assumption that the intraocular pressure, remaining within the normal range, is still more than the intracranial pressure.

Noishevsky set out to investigate this. In the laboratory of Ivan Pavlov, on January 20, 1910, assistant professor B. P. Babkin performed a cranial trephination through the frontal bone in a large, black dog by the name of "Gypsy." One month later, the dog developed glaucomatous excavation of the optic nerves [7]. Noishevsky presented the histological sections at the Ophthalmological Society meeting in St. Petersburg on January 27, 1911. The leading ophthalmologists of the time were not particularly convinced as the prevailing theories pointed toward a vascular etiology for normal-pressure glaucoma. Noishevsky also hypothesized

D. Fleischman (✉)
Department of Ophthalmology, University of North Carolina at Chapel Hill, Chapel Hill, NC, USA

R. Rand Allingham
Duke University Eye Center, Durham, NC, USA

N. Wang (ed.), *Intraocular and Intracranial Pressure Gradient in Glaucoma*,
Advances in Visual Science and Eye Diseases 1, https://doi.org/10.1007/978-981-13-2137-5_6

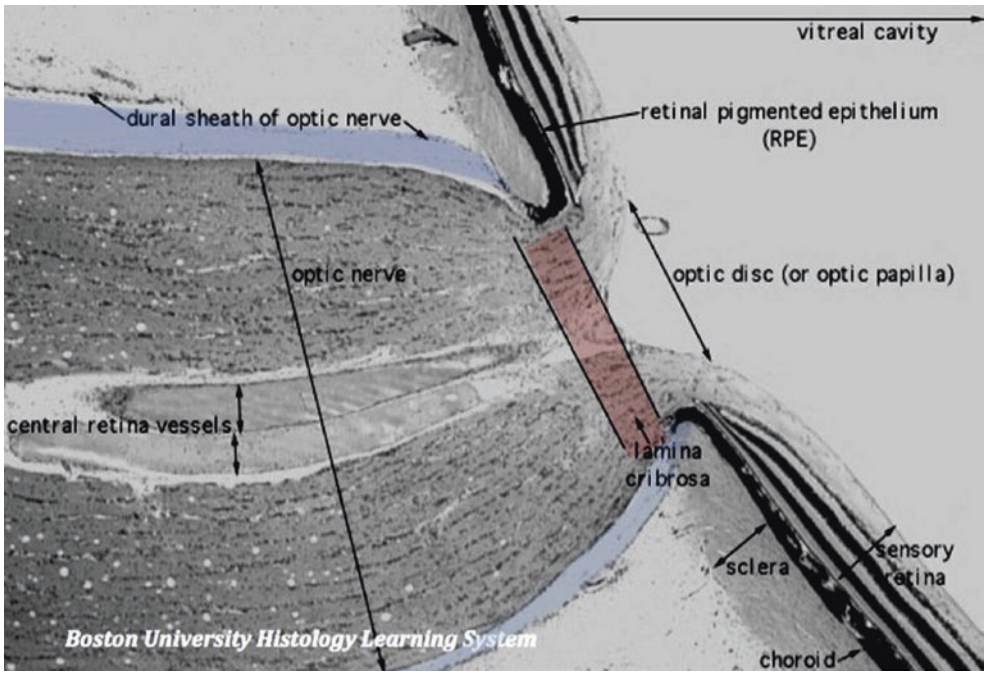

Fig. 6.1 Cross section of the optic nerve head, highlighting the lamina cribrosa (red) and the subarachnoid space (blue) (Reprinted with permission from Fleischman D, Allingham R R. The role of cerebrospinal fluid pressure in glaucoma and other ophthalmic diseases: A review [J]. Saudi Journal of Ophthalmology Official Journal of the Saudi Ophthalmological Society, 2013, 27(2):97)

that the pulsation of the retinal vessel is dependent on the relation of intraocular and intracranial pressure. His belief was that if the pressure in the eye was higher than the intracranial pressure, blood would only traverse the arteries during systole. He supposed that the venous pulse meant that the intracranial pressure was higher than the intraocular pressure.

Szymanski and Wladyczko, Polish doctors, carried out a similar experiment reported in 1925 [8]. They reported cupping of the optic nerves in a dog whose intracranial pressures were suddenly lowered. Noishevsky had, 2 years earlier, reformed the Polish Ophthalmological Society. Although we are unaware of the details of these meetings and its membership, it is probably not out of the realm of speculation that this investigation was possibly conceived from a discussion with Noishevsky. Regardless, 1 year later, Kirschmann in Germany was not able to confirm this finding in a repeat experiment performed on six dogs and followed for up to 9 months [9].

In 1940, the German ophthalmologist Klar would be the first to perform lumbar puncture in humans for the investigation of low-tension glaucoma [10]. His theory was that a low intracranial pressure might be expected to divert blood away from the optic nerve. Three cases revealed intracranial pressures in the lower end of normal. This satisfied his suspicion that carotid sclerosis was the cause of low-tension glaucoma. G. Miranda, in 1945, reviewed the few cases in the literature up to that point and presented one case of his own in which the CSFP was within normal limits in a normal-pressure glaucoma patient [11]. Matteuci, in 1949, reported that low intracranial pressure was not found in low-tension glaucoma [12, 13]. J. Stajduhar, in 1951, found a low cerebrospinal fluid pressure in one of two low-tension glaucoma patients [14]. John Primrose, in 1964, reported two cases of low-tension glaucoma with low intracranial pressures (85 [mm] H_2O and 95 [mm] H_2O [6.25 mm Hg and 6.99 mm Hg]) [15].

V. V. Volkov and students reintroduced the concept of the translaminar pressure difference as the potential etiology of normal-tension glaucoma [16]. Volkov was on faculty at the same institution where Noishevsky had presented much of his work nearly 55 years earlier. An important and oft-cited ARVO abstract from 1979, by Yablonski, Ritch, and Pokorny, discussed a cat model whose CSFP was lowered to −4 mm Hg [17]. One eye was cannulated to produce a pressure of 0 mm Hg, while the other eye was unchanged and maintained at a normal pressure. After 3 weeks, the uncannulated eye developed optic nerve damage consistent with glaucomatous optic neuropathy. The eye that was cannulated and maintained at a low pressure similar to the CSF pressure did not develop optic neuropathy. This study design, with an intereye comparison, strongly suggested the importance of the translaminar pressure differential in glaucoma. Many of these works were summarized by Ralph Z. Levene in his 1980 *Survey of Ophthalmology* review [18].

The next important series of studies regarding the translaminar pressure differential would not come about for another 15 years. William Morgan in 1995 produced the first of several landmark studies suggesting the importance of retrobulbar pressure compartments [19]. Morgan and his coworkers conducted experiments that demonstrated

posterior laminar movement using dog models [20]. This group, using a dog model, measured the pressure with a direct cannulation technique. They continuously measured pressure from the intraocular space (IOP) and then penetrated the lamina cribrosa using an intraocular approach and ultimately gained entry into the subarachnoid space to measure the CSF pressure. They reported that approximately 85% of the pressure drop occurred in the first 400 μm of the lamina cribrosa and concluded that the CSF pressure was the major determinant of post-laminar pressure and the biomechanical effect of CSF pressure variation on the lamina cribrosa was essentially equivalent to IOP. Further, he revealed that there is fluid conductivity between the cerebral ventricles and the perioptic subarachnoid space in the dog [19]. He characterized this in greater detail in a 1998 study that revealed that this conductivity met its limit when the intracranial pressures were lowered to −0.5 mm Hg [21]. Recently, Dr. Jonas showed that decrease in thickness of the lamina cribrosa was observed in patients with glaucoma and clearly stated that the lamina cribrosa separated these two pressurized compartments [22, 23].

In 2008, nearly 100 years after Noishevsky first proposed and tested this theory, Berdahl and colleagues carried out a retrospective study on the examination data of patients who had received a lumbar puncture and an eye exam at the Mayo Clinic [24]. The initial study reviewed 31,786 patients. Twenty-eight patients with primary open-angle glaucoma versus 49 control patients were analyzed. CSFP measured by lumbar puncture was significantly lower in POAG patients compared with non-glaucomatous controls (13.0 mmHg ± 4.2, vs. 9.2 mmHg ± 2.9, $p < 0.001$). A follow-up study encompassing a longer period of time identified more POAG patients, as well as normal-tension glaucoma, ocular hypertension, and a new control group [25]. Apart from confirming the prior study's POAG CSFP relationship, they reported that normal-tension glaucoma patients had lower CSFP than POAG with IOP greater than normal. Further they found that patients with CSFP in ocular hypertensive patients were higher than the control group. These data support the hypothesis that the translaminar pressure gradient difference is an important contributing factor mediating the risk for glaucomatous optic neuropathy. In an important investigation soon thereafter, Ren and colleagues performed the first controlled *prospective* studies and confirmed these findings [26, 27]. This validated the retrospective studies but importantly demonstrated that this relationship was conserved in two vastly different population groups—the largely European population of the Mayo Clinic and the Chinese Asian population.

This naturally raises the question, if CSFP is important in glaucoma, are there trends in CSFP that explain POAG risk? A study by Pasquale et al. showed that higher BMI was a protective factor for glaucoma in women but not in men [28]. A study from Asrani et al. revealed that patients with normal-tension glaucoma were thinner and had lower BMI [29]. A study on CSF pressure and BMI data from 4235 subjects in the Mayo dataset revealed a clear linear relationship between CSF pressure and BMI that was consistent with findings of Pasquale and Asrani [30–32].

It is well-known that the prevalence of POAG is low under the age of 40 and increases rapidly after age 50. Population-based studies support this observation in all races and ethnicities studied to date. In a study by Fleischman and coworkers, over 30,000 records from the Mayo Clinic of patients with a history of lumbar puncture were analyzed [32]. After accounting for all entry requirements, 12,118 were analyzed for age and CSF pressure trends. The results showed that the CSF pressure was consistent among patients up to age 50 years. After age 50 a steady reduction of CSF pressure to as low as 30% reduction was observed through age group 90–95 years. There were no significant trends of CSF pressure in diseases associated with glaucoma [33]. The observed reduction in CSF pressure (3–4 mmHg) was coincident with a similar increase in mean IOP increase that has been observed in patients with POAG and a rise in prevalence of glaucoma. As shown in the graph below, the age-related decrease in mean CSF pressure that is observed at about age 50 occurs at a similar time point with the rise in POAG prevalence (Fig. 6.2).

Hanspeter Killer has proposed that in addition to or instead of a biomechanical effect of the translaminar pressure differential on the axons within lamina cribrosa, there may be other factors that contribute to glaucomatous injury. Due to the small space afforded by the optic canal, the perioptic subarachnoid space may be compartmentalized in patients with glaucoma. Therefore, a lack of CSF flow may cause an increase in neurotoxic factors adjacent to the lamina that would otherwise be cleared from this region. According to Killer, the CSF pressure in this space, therefore, may not be important and quite possibly not even uniform as there may be differentially pressurized compartments within the trabeculations of the subarachnoid space surrounding the optic nerve itself [34–39].

The theory based on the translaminar pressure difference was recently reexamined as a function of papilledema and increased intracranial pressure. A few observations exist on cases of papilledema that were unmasked after IOP reduction induced by filtration surgery [40–42]. We suggested that perhaps an increase in IOP would result in suppression of edema of the optic nerve [43]. However, a retrospective study examining the translaminar pressure gradient in terms of papilledema severity did not find a statistically significant relationship [44]. There is clearly more at play than just intracranial pressure and intraocular pressure in papilledema and glaucoma. This is an exciting avenue for future research.

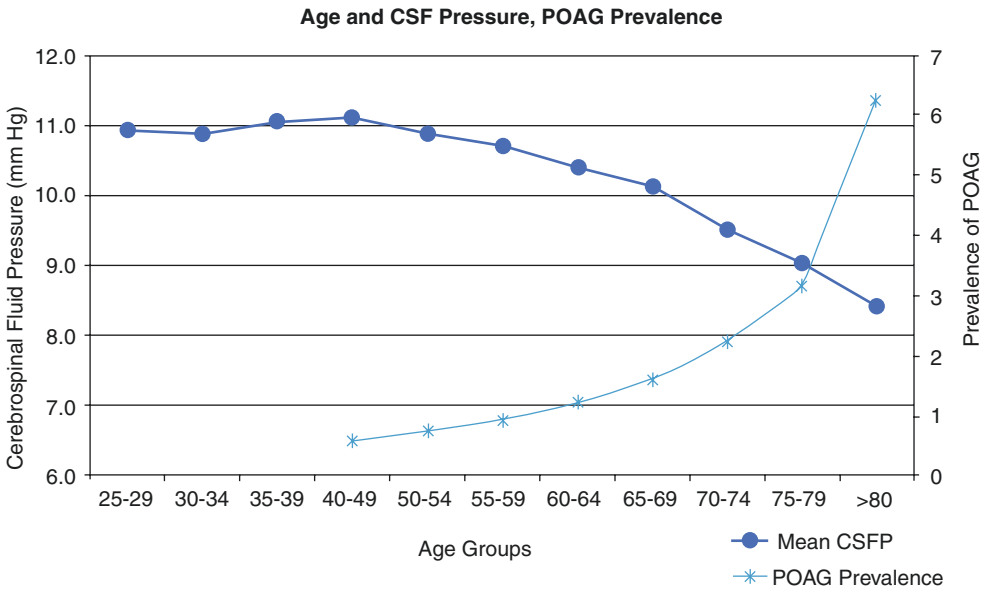

Fig. 6.2 Averaged data of Friedman's meta-analysis of prevalence studies of primary open-angle glaucoma in the United States, with the age-related decrease in cerebrospinal fluid pressure superimposed. Data shown are from Caucasian patients, which constitute the principal group contained within the Mayo Clinic population (Reprinted with permission from Fleischman D, Allingham R R. The role of cerebrospinal fluid pressure in glaucoma and other ophthalmic diseases: A review [J]. Saudi Journal of Ophthalmology Official Journal of the Saudi Ophthalmological Society, 2013, 27(2):97)

In summary, evidence derived from retrospective analysis of clinical databases supports the hypothesis that CSF pressure contributes to POAG risk. CSF pressure was lower in POAG and NTG and higher in patients with non-glaucomatous ocular hypertension. CSF pressure varies or is associated with BMI and age in some way which may lead to a change in POAG risk. These data also support the hypothesis that the translaminar pressure gradient is an important factor in the pathogenesis of glaucoma. In regard to retrospective studies, large EMR databases have proven to be very powerful. It had power to identify multiple factors related to disease pathology simultaneously. As EMR databases grow in patient numbers, test data, and inclusive of more diverse populations, we can anticipate a rapid rise in discovery. We have investigated the role of IOP and CSF pressure as well as their impact on optic nerve for patients with glaucoma. However, there remains an enormous amount of information for further exploration and identification.

Acknowledgments Much of the information, papers, and historical records pertaining to Professor Kasmir Noishevsky were provided by Vladimir Reituzuv, MD, of the Medical Military Institute in St. Petersburg, Russia. Edward Gamm, MD, from St. Petersburg, was instrumental in reintroducing the work of Professor Noishevsky.

References

1. Suzuki Y, Iwase A, Araie M, Yamamoto T, Abe H, Shirato S, et al. Risk factors for open-angle glaucoma in a Japanese population: the Tajimi study. Ophthalmology. 2006;113(9):1613–7.
2. Bonomi L, Marchini G, Marraffa M, Bernardi P, Morbio R, Varotto A. Vascular risk factors for primary open angle glaucoma: the Egna-Neumarkt study. Ophthalmology. 2000;107(7):1287–93.
3. Dielemans I, Vingerling JR, Algra D, Hofman A, Grobbee DE, de Jong PT. Primary open-angle glaucoma, intraocular pressure, and systemic blood pressure in the general elderly population. The Rotterdam Study. Ophthalmology. 1995;102(1):54–60.
4. Leske MC, Wu SY, Hennis A, Honkanen R, Nemesure B. Risk factors for incident open-angle glaucoma: the Barbados eye studies. Ophthalmology. 2008;115(1):85–93.
5. Leske MC, Wu SY, Nemesure B, Hennis A. Incident open-angle glaucoma and blood pressure. Archiv Ophthalmol (Chicago, Ill: 1960). 2002;120(7):954–9.
6. Leske MC, Wu SY, Nemesure B, Hennis A. Incident open-angle glaucoma and ocular perfusion pressure. Invest Ophthalmol Vis Sci. 2011;52(11):7943.
7. Noishevsky K. Glaucoma, its etiology and treatment. 1915.
8. Szymanski JW, S. Jaska prosta doswiadeczalna. Klin Ocz. 1925;3:145–50.
9. Kirschmann JS. Frage des aetiologie der glaukoms. Klin Monatshl Augenheilkd. 1926;77:256.
10. Klar J. Uber die entsehung des glaukom ohne hochdruck. Ber Dtsch Ophthalmol Gesell. 1940;52:162–5.

11. Miranda G. Glaucoma sin hipertension. Arch Soc Oftalmol Hisp-Am. 1945;5:579–99.
12. Matteuci P. Considerazioni sul glaucoma senza ipertensione. Atti 37 Con Soc Oftalmol Ital. 1948;10:168–9.
13. Matteuci PK, G. Dati clinicosperimentali sui rapporti tra escavazione glaucomatosa, ipertonia oculari e pressione liquorale. . Atti 37 Con Soc Oftalmol Ital. 1948;10:559.
14. Stajduhar J. Contribution to the aetiology of pseudo-glaucoma; pseudoglaucoma and hypotension of the intra-cranial fluid. Ophthalmol J Int. 1951;122(3):129–42.
15. Primrose J. Mechanism of production of papilloedema. Br J Ophthalmol. 1964;48:19–29.
16. Volkov V. Essential element of the glaucomatous process neglected in clinical practice. Oftalmol Zh. 1976;31:500–4.
17. Yablonsky MR, Pokorny KS. Effect of decreased intracranial pressure on optic disc. Invest Ophthalmol Vis Sci. 1979;18 [Suppl]:165.
18. Levene RZ. Low tension glaucoma: a critical review and new material. Surv Ophthalmol. 1980;24(6):621–64.
19. Morgan WH, Yu DY, Cooper RL, Alder VA, Cringle SJ, Constable IJ. The influence of cerebrospinal fluid pressure on the lamina cribrosa tissue pressure gradient. Invest Ophthalmol Vis Sci. 1995;36(6):1163–72.
20. Morgan WH, Chauhan BC, Yu DY, Cringle SJ, Alder VA, House PH. Optic disc movement with variations in intraocular and cerebrospinal fluid pressure. Invest Ophthalmol Vis Sci. 2002;43(10):3236–42.
21. Morgan WH, Yu DY, Alder VA, Cringle SJ, Cooper RL, House PH, et al. The correlation between cerebrospinal fluid pressure and retrolaminar tissue pressure. Invest Ophthalmol Vis Sci. 1998;39(8):1419–28.
22. Jonas JB, Berenshtein E, Holbach L. Anatomic relationship between lamina cribrosa, intraocular space, and cerebrospinal fluid space. Invest Ophthalmol Vis Sci. 2003;44(12):5189–95.
23. Jonas JB, Berenshtein E, Holbach L. Lamina cribrosa thickness and spatial relationships between intraocular space and cerebrospinal fluid space in highly myopic eyes. Invest Ophthalmol Vis Sci. 2004;45(8):2660–5.
24. Berdahl JP, Allingham RR, Johnson DH. Cerebrospinal fluid pressure is decreased in primary open-angle glaucoma. Ophthalmology. 2008;115(5):763–8.
25. Berdahl JP, Fautsch MP, Stinnett SS, Allingham RR. Intracranial pressure in primary open angle glaucoma, normal tension glaucoma, and ocular hypertension: a case-control study. Invest Ophthalmol Vis Sci. 2008;49(12):5412–8.
26. Ren R, Jonas JB, Tian G, Zhen Y, Ma K, Li S, et al. Cerebrospinal fluid pressure in glaucoma: a prospective study. Ophthalmology. 2010;117(2):259–66.
27. Ren R, Zhang X, Wang N, Li B, Tian G, Jonas JB. Cerebrospinal fluid pressure in ocular hypertension. Acta Ophthalmol. 2011;89(2):e142–8.
28. Pasquale LR, Willett WC, Rosner BA, Kang JH. Anthropometric measures and their relation to incident primary open-angle glaucoma. Ophthalmology. 2010;117(8):1521–9.
29. Asrani S, Samuels B, Thakur M, Santiago C, Kuchibhatla M. Clinical profiles of primary open angle glaucoma versus normal tension glaucoma patients: a pilot study. Curr Eye Res. 2011;36(5):429–35.
30. Berdahl JP, Fleischman D, Zaydlarova J, Stinnett S, Allingham RR, Fautsch MP. Body mass index has a linear relationship with cerebrospinal fluid pressure. Invest Ophthalmol Vis Sci. 2012;53(3):1422–7.
31. Fleischman D, Allingham RR, Berdahl J, Fautsch M. Body mass, spinal fluid, and glaucoma. Ophthalmology. 2011;118(6):1225–6. author reply 6
32. Fleischman D, Berdahl JP, Zaydlarova J, Stinnett S, Fautsch MP, Allingham RR. Cerebrospinal fluid pressure decreases with older age. PLoS One. 2012;7(12):e52664.
33. Fleischman D, Berdahl J, Stinnett SS, Fautsch MP, Allingham RR. Cerebrospinal fluid pressure trends in diseases associated with primary open-angle glaucoma. Acta Ophthalmol. 2015;93(3):e234–6.
34. Killer HE. Production and circulation of cerebrospinal fluid with respect to the subarachnoid space of the optic nerve. J Glaucoma. 2013;22(Suppl 5):S8–10.
35. Killer HE. Compartment syndromes of the optic nerve and open-angle glaucoma. J Glaucoma. 2013;22(Suppl 5):S19–20.
36. Killer HE, Jaggi GP, Miller NR. Optic nerve compartment syndrome. Acta ophthalmologica. 2011;89(5):e472; author reply e-3.
37. Killer HE, Jaggi GP, Miller NR, Huber AR, Landolt H, Mironov A, et al. Cerebrospinal fluid dynamics between the basal cisterns and the subarachnoid space of the optic nerve in patients with papilloedema. Br J Ophthalmol. 2011;95(6):822–7.
38. Killer HE, Miller NR, Flammer J, Meyer P, Weinreb RN, Remonda L, et al. Cerebrospinal fluid exchange in the optic nerve in normal-tension glaucoma. Br J Ophthalmol. 2012;96(4):544–8.
39. Killer HE, Subramanian PS. Compartmentalized cerebrospinal fluid. Int Ophthalmol Clin. 2014;54(1):95–102.
40. Abegg M, Fleischhauer J, Landau K. Unilateral papilledema after trabeculectomy in a patient with intracranial hypertension. Klinische Monatsblatter fur Augenheilkunde. 2008;225(5):441–2.
41. Greenfield DS, Wanichwecharungruang B, Liebmann JM, Ritch R. Pseudotumor cerebri appearing with unilateral papilledema after trabeculectomy. Archives of ophthalmology (Chicago, Ill : 1960). 1997;115(3):423–6.
42. Kawasaki A, Purvin V. Unilateral optic disc edema following trabeculectomy. J Neuro-ophthalmol. 1998;18(2):121–3.
43. Fleischman D, Berdahl JP, Fautsch MP, Chesnutt DA, Allingham RR. Increasing intraocular pressure as treatment for papilledema. Exp Eye Res. 2013;115:278.
44. Fleischman D, Perry JT, Rand Allingham R, Stinnett SS, Fleischman GM, Givre SJ, et al. Retrospective analysis of translaminar, demographic, and physiologic parameters in relation to papilledema severity. Canad J Ophthalmol. 2017;52(1):26–9.

Intracranial and Intraocular Pressure Gradient and Glaucoma: A Retrospective Point of View

7

Xiangxiang Liu, Diya Yang, and Ningli Wang

7.1 Introduction

Glaucoma is one of the most ancient diseases. It was first described as "glaykoseis" in the era of Hippocrates in the fourth century B. C. with the symptoms of the seawater-like "greenish gray" appearing in the eyes and no vision [1]. In China, the *Sheng Nong's Herbal Classic* recorded "green vision disorder" and "green vision impairment" back to Qin and Han dynasty [2]. However, doctors back then gave the diagnosis merely by judging the vision loss and change of the color of the eye; thus, other diseases, such as cataract, were also included, and the doctors could not distinguish them from glaucoma. In 1622, a British physician, Banister, recorded a patient whose vision wasn't improved after cataract removal and the eyeball showed a hard state, which was the first document to relate intraocular pressure (IOP) to glaucoma [3].

Nowadays, it is commonly known that glaucoma is a multifactorial disease, which results in progressive loss of retinal nerve ganglion cells (RGCs). However, the etiology of glaucoma remains unclear. Ischemia, abnormal immune response, and glial cell activation may all contribute to primary open-angle glaucoma (POAG) [4]. Various studies documented that the elevated IOP was a significant factor in the pathogenesis of glaucoma. However, as the optic nerve is surrounded by cerebrospinal fluid in the subarachnoid space, it is exposed to not only IOP but also intracranial pressure (ICP). Therefore, apart from the IOP and ICP, focusing on the relationship between IOP and ICP and how these two forces contribute to glaucomatous neuropathy by creating a trans-lamina cribrosa pressure difference (TLCPD) is very important. This article reviews the discovery and recent studies of the glaucoma-related pressures in order to better understand the pathology and progression of glaucoma.

7.2 Intracranial Pressure

7.2.1 Historical Perspective

The ventricles and cerebrospinal fluid (CSF) were first described by Edwin Smith in the seventeenth century. The Greek famous physician Galen described the anatomy of the ventricles and described CSF as a clear liquid based on the animal dissections [5]. In 1510, Leonardo da Vinci documented an accurate representation of human ventricular anatomy based on human dissection [6]. Though there were many different opinions about the anatomy and physiology of the CSF system, it was not until 1875 that the first definitive article was published. Ernst Key and Magnus Retzius proved that CSF was produced by the choroid plexus, flowed through the ventricular system, and was reabsorbed back into the venous system at the arachnoid granulations [7].

7.2.2 CSF Physiology

Approximately 400–600 mL volumes of CSF are produced by the choroid plexuses daily. While the extracellular fluid and cerebral capillaries also play a role in the CSF production as an extra-choroidal secretion, the circulating volume of the CSF is only 100–160 mL, with 25% in the ventricles and 75% in the subarachnoid spaces [8].

CSF is secreted into the lateral ventricles first, then flows to the third ventricle, then passes through the cerebral aqueduct to the forth ventricle, and finally runs into the cisterna magna, where the CSF pathway divides. It can circulate in the cranial subarachnoid space or in the spinal subarachnoid

X. Liu · D. Yang · N. Wang (✉)
Beijing Institute of Ophthalmology, Beijing Tongren Eye Center, Beijing Tongren Hospital, Capital Medical University, Beijing, China

Beijing Ophthalmology & Visual Sciences Key Laboratory, Beijing, China
e-mail: wningli@vip.163.com

N. Wang (ed.), *Intraocular and Intracranial Pressure Gradient in Glaucoma*,
Advances in Visual Science and Eye Diseases 1, https://doi.org/10.1007/978-981-13-2137-5_7

space or pass through the central canal of the spinal cord. Finally, the arachnoid granulations reabsorb CSF into the venous outflow system [8].

The brain weight reduced about 50 g for it is buoyant within the CSF. This may protect the brain from the blunt trauma for it buffers the acceleration. Besides, the CSF also plays an important role in metabolism. Some micronutrients including folate and vitamin C and hormones like thyroid hormones are transported from blood into CSF and taken up by brain cells, for they cannot enter the brain directly through the blood-brain barrier (BBB) like glucose and amino acids. Meanwhile the CSF also helps to transport waste products from the intercellular space to the systemic circulation [9].

7.2.3 CSF Pressure

Intracranial pressure (ICP) is the pressure within the skull vault, which recorded the tension on the brain by CSF and blood. CSF pressure (CSFP) is defined as the ICP in the horizontal position. It also represents the dynamic balance between secretion and absorption of the CSF. The value of the CSFP is measured by the manometer after a lumbar puncture. The normal CSFP is 70–180 mmH_2O, which equals 5.1–15 mmHg.

ICP fluctuates through the day, and it undergoes pulsatile with the cardiac and respiratory cycles. Some postures such as bending over and lying down, and certain maneuvers like sneezing and coughing, will influence the ICP. Besides, venous pressure also plays a role in the ICP fluctuation [9].

7.3 Intraocular Pressure

7.3.1 Discovery of Aqueous Dynamics

Aristotle first recorded the watery contents in the eyeball, which played an important role in the shape and function of the eye. It was not until the seventeenth century that attention was paid to the aqueous production and elimination when Anton Nuck discovered the inguinal "canal of Nuck" by injecting ducts and blood vessels with dyes. He believed there were two tubular systems for aqueous circulation, one for flowing into the eye and the other out. However, these were not confirmed by other researchers [1].

With the invention of the diagnostic instruments like ophthalmoscope, the ophthalmology began to flourish in the eighteenth century. Theodor Leber [10] measured the osmotic pressure, the manometric intraocular pressure (IOP), and the rate of aqueous flow [11]. Leber believed that the production and elimination of the aqueous were the result of filtration which was caused by the pressure differential. Later, with the advances in knowledge on the nature of cells, the Duke-Elder's dialysis theory proved that aqueous humor was secreted by the ciliary epithelium and then entered the posterior chamber. Meanwhile, three people were historically important to the outflow of aqueous who were Hans Virchow, Friedrich Schlemm, and Karl Ascher. Virchow described the structure of the trabecular meshwork, Schlemm discovered the drainage channel and named it by his name, and Ascher recorded the aqueous veins [1].

The abnormal symptom of "hardened eyeball" was recorded constantly in the entire eighteenth and nineteenth century. It was not until in 1832 Sir William Lawrence, for the first time, described the symptoms of glaucoma and defined this condition as "glaucoma" in his ophthalmic works. In 1864, Littell described the disease more accurately as "a condition of decreased vision similar to amaurosis, with greenish gray eyeball" and added "hardness of eyeball" to the description of the disease. McKenzie, a Scottish ophthalmologist, performed fluid drainage by puncturing at the eyeball to release IOP, which marked the beginning of glaucoma treatment [3].

7.3.2 Aqueous Humor and IOP

Aqueous humor circulation generates IOP. Aqueous humor is produced by an active secretion of the epithelial layer of the ciliary body and passes from the posterior chamber through the pupil into the anterior chamber [12]. The aqueous humor outflows via two pathways. In the trabecular outflow pathway, the aqueous humor flows through the trabecular meshwork, juxtacanalicular tissue (JCT), Schlemm's canal, and radial collector channels into the episcleral veins [13]. In the uveoscleral outflow pathway, aqueous humor passes through the interstitial spaces of the ciliary body into the capillaries of the ciliary body [14]. It's essential for a balance among the production, circulation, and drainage of aqueous humor to maintain a steady level of IOP. Besides, IOP fluctuates through the day, and habitual 24-h IOP can be changed by posture, circadian time, and glaucoma medications.

7.3.3 IOP and Glaucoma

Elevated intraocular pressure (IOP) has long been considered as the major risk factor for the development and progression of glaucoma [15]. However, in Handan Eye Study, statistics showed that about 80% of Chinese POAG patients identified in this population-based study had maximum IOPs of 21 mmHg or less over a 24-h period [16]. Meanwhile, the Ocular Hypertension Treatment Study Group (OHTS) found

only 9.5% of ocular hypertension patients would develop into glaucomatous optic neuropathy during 5-year follow-up [17]. Why would NTG patients still develop into glaucoma without high IOP? Are there factors other than IOP contributing to the pathogenesis of NTG as the role of IOP in the pathogenesis of POAG becomes vague and controversial?

7.4 Trans-lamina Cribrosa Pressure Difference (TLPD)

Intracranial and intraocular pressures are interrelated and relatively independent pressure systems; however, the forces of IOP and CSFP meet at the lamina cribrosa, which becomes a barrier between the posterior force of the IOP and the anterior force of the CSFP. Physiologically, IOP is slightly higher than intracranial pressure; therefore, the pressure difference is formed across the lamina cribrosa, also known as the TLPD (TLPD = IOP-CSFP). Many important structures that pass through the lamina cribrosa are influenced by these two pressures and the pressure difference, such as the retinal ganglion cell axons, the central retinal artery, and the central retinal vein. Increased TLPD could cause the deformation of the lamina cribrosa which may damage the optic nerve ganglion cells due to the mechanical efforts or ischemia as the vessels pass through the lamina cribrosa as well [18].

7.4.1 TLPD and Glaucoma

In 1976, Volkov VV first discussed about the effect of low CSF pressure on glaucoma [19]. Yablonski and colleagues then reported that CSFP may play a role in glaucomatous neuropathy. They lowered the CSFP to −4 mmHg in the cat model. One eye of the cat was cannulated to achieve 0 mmHg of pressure, while the other eye was the control. Three weeks later, the non-cannulated eye developed glaucomatous neuropathy. The fundus of the eye that has maintained a lower pressure as similar to the CSFP remained normal. This study strongly suggested the effect of the TLPD in glaucoma [20].

There was no related study regarding the TLPD until William Morgan and his co-workers performed several related studies suggesting the relationship between TLPD and pathogenies of glaucoma. His team used cannulation technique to measure the IOP and CSFP directly in the dog model and found that both IOP and CSFP variation had the equivalent effects on the TLPD and lamina cribrosa, which are also correlated with the optic disc surface movement [21, 22]. These studies have provided new views on the pathophysiology of the glaucoma and have opened new chapter of the research.

7.4.2 Clinical Studies

Berdahl and colleagues performed a retrospective study on clinical chart data analysis of patients who had received lumbar puncture CSFP measurement and eye exam at the Mayo Clinic [23]. Out of 31,789 patients, the author selected 28 POAG patients and 49 patients without glaucomatous optic neuropathy as the control group to analyze. It turned out that the lumbar CSFP was significantly lower in POAG patients than in the control group. And then a follow-up study showed that patients with NTG had lower CSFP than hypertension glaucoma patients. They also found that CSFP in ocular hypertensive patients was higher than that in the control group [24].

At the same time, the first controlled prospective study from Beijing iCOP study group observed NTG patients, high-pressure glaucoma patients, as well as ocular hypertension patients who underwent lumbar puncture for various reasons. Comparing with non-glaucomatous control group, they found that patients with NTG had significantly lower lumbar CSFP than those with high-pressure glaucoma or the control group and ocular hypertension patients had significantly higher CSFP. Consequently, in both glaucoma groups, the TLPD was significantly higher than in the control group. These studies support the hypothesis that TLPD is an important influence factor contributing to the glaucomatous optic neuropathy [25].

After that, much more attention paid on the role of TLPD in glaucoma; therefore, many clinical studies focusing on the relationship between TLPD and glaucoma-related parameters had been done. Beijing iCOP study group did some clinical observation studies and found that the TLPD as compared to the IOP was significantly better correlated with cup to disc ratio, rim width, and visual field loss [26]. This may provide some indirect evidence that the TLPD might play some role in the pathogenesis of glaucomatous optic neuropathy.

Considering the potential association between CSFP and glaucomatous optic neuropathy, one needs to emphasize that it is the orbital CSFP not the intracranial CSFP which determines the TLPD. However, it's difficult to measure the orbital CSFP directly or to perform lumbar puncture in every glaucoma patient. In order to noninvasively estimate orbital CSFP, Wang et al. from Beijing iCOP study group used MRI to measure the width of the orbital CSF space [27]. This group found that in NTG patients, the orbital CSF space was significantly narrower than in the hypertension glaucoma patients or control group. They also found the correlation between the orbital CSF space width and lumbar CSFP measurement, which revealed that the almost collapsed orbital CSF space was associated with an abnormally low CSFP in NTG patients [28]. The former studies reported that higher CSFP was associated with higher BMI, higher diastolic

blood pressure, and younger age [25, 29–31]. Therefore, this group developed an algorithm to obtain CSFP values based on these three parameters (estimated CSFP [mmHg] = 0.44 body mass index [kg/m^2] +0.16 × diastolic blood pressure [mmHg]−0.18 × age [years]−1.91) [28].

In a recent study, the same group reported an improved method to measure the area of the optic nerve subarachnoid space in patients with NTG, POAG, and controls. They used B-scan ultrasound to measure 3–7 mm posterior to the globe to obtain the "area of the optic nerve subarachnoid space," which was significantly reduced in NTG patients compared with the normal controls [32]. This study supports their prior work that optic nerve sheath was narrower in NTG patients. As a corollary, lower CSFP has been associated with NTG.

An optic nerve compartment syndrome had been proposed by Killer and colleagues [33]. They focused on the CSF dynamics around the optic nerve. Their study showed the compartmentalization was found in NTG patients. Reduced CSF turnover results in decreased CSF exchange between the orbital CSF space and basal intracranial cisterns which leads to accumulation of toxic substances and causes optic nerve damage. Although the mechanism leading to compartmentalization remains unknown, this theory adds more evidence for the role of CSF circulation and its toxicity effect on glaucomatous optic neuropathy.

However, there are some opposite results of TLPD in patients with NTG. Linda et al. published their study recently that NTG patients had normal ICP compared to the control group using a modified ICP monitor and measured the pressure in different body positions [34]. The authors measured the ICP at the auditory meatus and adjusted for hydrostatic gradients between the auditory meatus and the lamina cribrosa to get the TLPD. Getting the ICP at auditory meatus is preciser than that at lumbar level. Therefore, improving the measurement method may help us to understand the role of TLPD in glaucoma better.

7.4.3 Experimental Studies

Yang et al. from Beijing iCOP study group conducted a lower CSFP monkey model to explore the potential association between lower CSFP and glaucomatous neuropathy. In this study, nine monkeys underwent implantation of a lumbar-peritoneal CSF shunt. The shunts of four monkeys were opened to achieve approximately 40 mm H_2O of CSFP as the study group, while the shunt remained closed in the rest of the monkeys as the control group. Follow-up ophthalmological examinations including measurement of IOP and CSFP, optical coherence tomographic and photographic images of the optic nerve head, and retinal nerve fiber layer (RNFL) were performed. As the result, in the study group, four eyes of two monkeys had a continuous loss of RNFL, and one eye of the third monkey developed a splinter-like disc hemorrhage, while there was no change in the fourth monkey in the study group, nor was in the control group. It was concluded that experimental and chronic reduction in CSF led to optic neuropathy in some monkeys [35].

Jaggi and colleagues put a silicone band around one optic nerve of seven sheep and compressed to block the CSF flow around the optic nerve without compressing the optic nerve. After 4 or 21 days, all eyes with compression had loss of optic nerve fibers. The authors concluded that blocking the CSF flow in the orbital CSF space that led to severe optic nerve damage within 4 days revealed the severity of CSF flow and composition change on optic nerve damage [36].

Zhang et al. experimentally reduced CSFP and elevated IOP in rats to observe the change of axonal motor proteins in retinal ganglion cells. In this study, the authors found that short-term lowering of CSFP and short-term increasing of IOP were all associated with a disturbance of both the orthograde and retrograde axonal transport. Additionally, when the TLPD dramatically increased, an accumulation of dynein intermediate chain was noticed, while the kinesin heavy chain immunoreactivity reduced in the optic nerve fiber axons. They concluded that experimental models with acute CSFP reduction and an acute IOP elevation can cause the failure of axonal transport and show similar morphologic changes in the optic nerve fiber axons. It supports the hypothesis that these two changes of pressures may share similarities in the process of optic nerve damage [37].

Hou et al. analyzed the correlation between ICP and IOP in normal dog models and found three different stages of the ICP-IOP relationship. There is ICP-IOP dependent zone where ICP and IOP change in parallel, so the TLPD was unchanged. Right below the breakpoint, which is the second stage, there is also an ICP-IOP independent zone, where IOP changes are no longer parallel to ICP changes and lead to an increasing TLPD. Hou et al. proposed that the imbalanced relationship between ICP and IOP may play a role in the glaucomatous optic neuropathy in patients with lower ICP [38]. What's more, the optic nerve damage not only happened in the site of laminar cribrosa but all along the optic nerve, where pressure gradients exist. So the concept of "trans-lamina cribrosa pressure difference" may be changed into "optic nerve pressure gradient (ONPG)" to be more precise [38].

7.5 Conclusion

In conclusion, most evidence derived from retrospective and prospective studies of clinical databases and experimental studies of different emphasis supports the hypothesis that lower CSFP contributes to glaucomatous optic neuropathy. As a corollary, increased TLPD is an important influence

factor in the pathogenesis of glaucoma. However, all the related studies had small sample sizes and limited methods to measure the real orbital CSFP. Therefore, future studies should further develop noninvasive measurement of CSFP, and an international cooperative study covering different ethnic groups based on standard protocol would be of interest in the field.

References

1. Mark HH. Aqueous humor dynamics in historical perspective. Surv Ophthalmol. 2010;55(1):89–100.
2. Pi HT. History of glaucoma in traditional Chinese medicine. Chin Med J. 1962;81:403–16.
3. Wales H. A history of glaucoma. Trans Ophthalmol Soc N Z. 1978;30:71–2.
4. Yang Y, Yu M, Zhu J, Chen X, Liu X. Role of cerebrospinal fluid in glaucoma: pressure and beyond. Med Hypotheses. 2010;74(1):31–4.
5. Torack RM. Historical aspects of normal and abnormal brain fluids. I. Cerebrospinal fluid. Arch Neurol. 1982;39(4):197–201.
6. Gjerris F, Snorrason E. The history of hydrocephalus. J Hist Neurosci. 1992;1:285–312.
7. Aschoff A, Kremer P, Hashemi B, Kunze S. The scientific history of hydrocephalus and its treatment. Neurosurg Rev. 1999;22(2–3):67–93. discussion 4-5
8. Hirsch N. Cerebrospinal fluid and its physiology. Anaesth Intensive Care Med. 2013;14(9):379–80.
9. Puntis M, Reddy U, Hirsch N. Cerebrospinal fluid and its physiology. Anaesth Inten Care Med. 2016;17(12):611–2.
10. Jaeger W. The foundation of experimental ophthalmology by Theodor Leber. Doc Ophthalmol. 1988;68(1–2):71–7.
11. Grant WM. A tonographic method of measuring the facility and rate of aqueous flow in human eyes. Arch Ophthalmol. 1950;44:204–14.
12. Tamm ER. The role of the ciliary body in aqueous humor dynamics: structural aspects. Encyclop Eye. 2009:179–86.
13. Tamm ER. The trabecular meshwork outflow pathways: structural and functional aspects. Exp Eye Res. 2009;88(4):648–55.
14. Alm A, Nilsson SF. Uveoscleral outflow--a review. Exp Eye Res. 2009;88(4):760–8.
15. Leske MC, Heijl A, Hussein M, Bengtsson B, Hyman L, Komaroff E, et al. Factors for glaucoma progression and the effect of treatment: the early manifest glaucoma trial. Arch Ophthalmol. 2003;121(1):48–56.
16. Wang NL, Friedman DS, Zhou Q, Guo L, Zhu D, Peng Y, et al. A population-based assessment of 24-hour intraocular pressure among subjects with primary open-angle glaucoma: the handan eye study. Invest Ophthalmol Vis Sci. 2011;52(11):7817–21.
17. Kass MAHD, Higginbotham EJ, Johnson CA, Keltner JL, Miller JP, Parrish RK, Wilson MR, Gordon MO. The Ocular Hypertension Treatment Study: a randomized trial determines that topical ocular hypotensive medication delays or prevents the onset of primary open-angle glaucoma. Arch Ophthalmol. 2002;120(6):701–13.
18. Marek B, Harris A, Kanakamedala P, Lee E, Amireskandari A, Carichino L, et al. Cerebrospinal fluid pressure and glaucoma: regulation of trans-lamina cribrosa pressure. Br J Ophthalmol. 2014;98(6):721–5.
19. Volkov VV. Essential element of the glaucomatous process neglected in clinical practice. Oftalmol Zh. 1976;31:500–4.
20. Yablonski M, Ritch R, Pakorny K. Effect of decreased intracranial pressure on optic disc. Invest Ophthalmol Vis Sci. 1979;18(Suppl):165.
21. Morgan WH, Yu DY, Alder VA, Cringle SJ, Cooper RL, House PH, Constable IJ. The correlation between cerebrospinal fluid pressure and retrolaminar tissue pressure. Invest Opbthalmol Vis Set. 1998;39:l419–28.
22. Morgan WH, Yu DY, Balaratnasingam C. The role of cerebrospinal fluid pressure in glaucoma pathophysiology: the dark side of the optic disc. J Glaucoma. 2008;17:408–13.
23. Berdahl JP, Allingham RR, Johnson DH. Cerebrospinal fluid pressure is decreased in primary open-angle glaucoma. Ophthalmology. 2008;115(5):763–8.
24. Berdahl JP, Fautsch MP, Stinnett SS, Allingham RR. Intracranial pressure in primary open angle glaucoma, normal tension glaucoma, and ocular hypertension: a case-control study. Invest Ophthalmol Vis Sci. 2008;49(12):5412–8.
25. Ren R, Jonas JB, Tian G, Zhen Y, Ma K, Li S, et al. Cerebrospinal fluid pressure in glaucoma: a prospective study. Ophthalmology. 2010;117(2):259–66.
26. Ren R, Wang N, Zhang X, Cui T, Jonas JB. Trans-lamina cribrosa pressure difference correlated with neuroretinal rim area in glaucoma. Graefes Arch Clin Exp Ophthalmol. 2011;249(7):1057–63.
27. Wang N, Xie X, Yang D, Xian J, Li Y, Ren R, et al. Orbital cerebrospinal fluid space in glaucoma: the Beijing intracranial and intraocular pressure (iCOP) study. Ophthalmology. 2012;119(10):2065–73e1.
28. Xie X, Zhang X, Fu J, Wang H, Jonas JB, Peng X, et al. Noninvasive intracranial pressure estimation by orbital subarachnoid space measurement: the Beijing Intracranial and Intraocular Pressure (iCOP) study. Crit Care. 2013;17(4):R162.
29. Berdahl JP, Fleischman D, Zaydlarova J, Stinnett S, Allingham RR, Fautsch MP. Body mass index has a linear relationship with cerebrospinal fluid pressure. Investig Ophthalmol Vis Sci. 2012;53:1422e7.
30. Berdahl JP. Systemic parameters associated with cerebrospinal fluid pressure. J Glaucoma. 2013;22(Suppl 5):S17–8. https://doi.org/10.1097/IJG.0b013e31829349fc.
31. Ren R, Wang N, Zhang X, Tian G, Jonas JB. Cerebrospinal fluid pressure correlated with body mass index. Graefes Arch Clin Exp Ophthalmol. 2012;250(3):445–6.
32. Liu H, Yang D, Ma T, Shi W, Zhu Q, Kang J, et al. Measurement and Associations of the Optic Nerve Subarachnoid Space in Normal Tension and Primary Open-Angle Glaucoma. Am J Ophthalmol. 2018;186:128–37.
33. Killer HE. Compartment syndromes of the optic nerve and open-angle glaucoma. J Glaucoma. 2013;22(Suppl 5):S19–20.
34. Linden C, Qvarlander S, Johannesson G, Johansson E, Ostlund F, Malm J, et al. Normal-Tension Glaucoma Has Normal Intracranial Pressure: A Prospective Study of Intracranial Pressure and Intraocular Pressure in Different Body Positions. Ophthalmology. 2018;125(3):361–8.
35. Yang D, Fu J, Hou R, Liu K, Jonas JB, Wang H, et al. Optic neuropathy induced by experimentally reduced cerebrospinal fluid pressure in monkeys. Invest Ophthalmol Vis Sci. 2014;55(5):3067–73.
36. Jaggi GP, Harlev M, Ziegler U, Dotan S, Miller NR, Killer HE. Cerebrospinal fluid segregation optic neuropathy: an experimental model and a hypothesis. Br J Ophthalmol. 2010;94(8):1088–93.
37. Zhang Z, Wu S, Jonas JB, Zhang J, Liu K, Lu Q, et al. Dynein, kinesin and morphological changes in optic nerve axons in a rat model with cerebrospinal fluid pressure reduction: the Beijing Intracranial and Intraocular Pressure (iCOP) study. Acta Ophthalmol. 2016;94(3):266–75.
38. Hou R, Zhang Z, Yang D, Wang H, Chen W, Li Z, et al. Pressure balance and imbalance in the optic nerve chamber: The Beijing Intracranial and Intraocular Pressure (iCOP) Study. Sci China Life Sci. 2016;59(5):495–503.

Part II

Anatomy and Pathophysiology

Anatomy and Physiology of Optic Nerve Head

8

Xiaoxia Li and Ningli Wang

The optic nerve is a unique structure as it is only surrounded by cerebrospinal fluid in the nervous system (Fig. 8.1). The functions of cerebrospinal fluid (CSF) include nutrition supply, strength to intraocular pressure, taking away metabolic waste, etc. However, the functions and mechanism are not clear yet.

Optic nerve contains 1.2 million axons, in human which originate from retinal ganglion cells, goes through the lateral geniculate nucleus (LGN) or superior colliculus (SC), and ends at visual cortex.

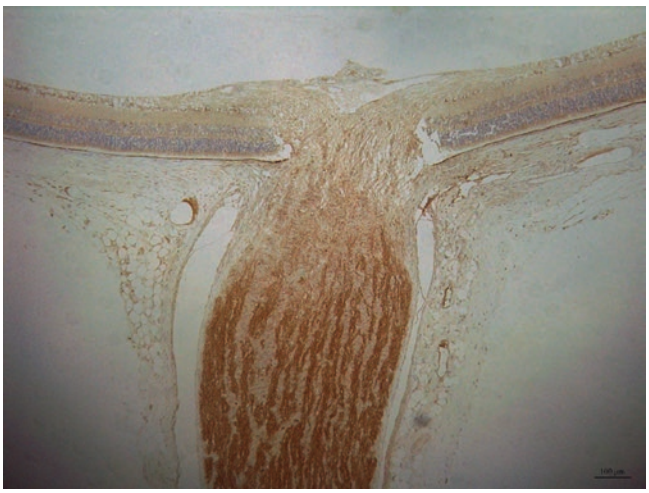

Fig. 8.1 In the glial lamina in rat, which is named optic nerve head (ONH) in human or primate animal, there are pre−/post-glial lamina tissue, glial lamina, optic nerve, and the subarachnoid space (SAS) in the retrobulbar optic nerve

X. Li · N. Wang (✉)
Beijing Institute of Ophthalmology, Beijing Tongren Eye Center, Beijing Tongren Hospital, Capital Medical University, Beijing, China

Beijing Ophthalmology & Visual Sciences Key Laboratory, Beijing, China
e-mail: wningli@vip.163.com

Human brain oxygen consumption accounts for 20% of the total, and the most is consumed in the retina. Except CSF surrounding the optic nerve (ON), the other tissues, such as the retinal ganglion cell axons, vessels, and glial cells, also present unique anatomic characteristics.

This chapter reviews the anatomy and physiology of the optic nerve head (ONH), the optic nerve (ON), and the CSF.

8.1 The Anatomy and Physiology of Retina

8.1.1 The Anatomy and Physiology of Ganglion Cells

The thickness of the retina is uneven, and the border of the optic nerve head is the thickest [1]. The diameters of retinal ganglion cell (RGC) axons vary in size at different regions with special varicosity morphology, even in peripapillary area and on the much thinner nerve fibers [2] (Fig. 8.2). There are plenty of mitochondria in these varicosities. Between axons, there is a mount of fibers (Fig. 8.2b) and the intercellular junctions in axon-axon and axon-glial cell. The exact functions of these junctions are unknown; thus, we proposed that they may be functional sites that are related to energy demand or signal transfer. Except that, the bulb whose constitution is not clear can be absorbed by axon through endocytosis (Fig. 8.2c).

8.1.1.1 Hypothesis: Varicosity-Like Morphology as a IOP Buffer System

In clinic, we can see that higher IOP will not cause branch retinal vein occlusion (BRVO) or central retinal artery occlusion (CRAO). Apart from the vessel's characteristics that resist the pressure, there may be other buffer system in the retina. We proposed that the intraretinal ganglion cell varicosities are mitochondria-rich as its special energy demand (Fig. 8.2b). Between the varicosities, the axon is

N. Wang (ed.), *Intraocular and Intracranial Pressure Gradient in Glaucoma*,
Advances in Visual Science and Eye Diseases 1, https://doi.org/10.1007/978-981-13-2137-5_8

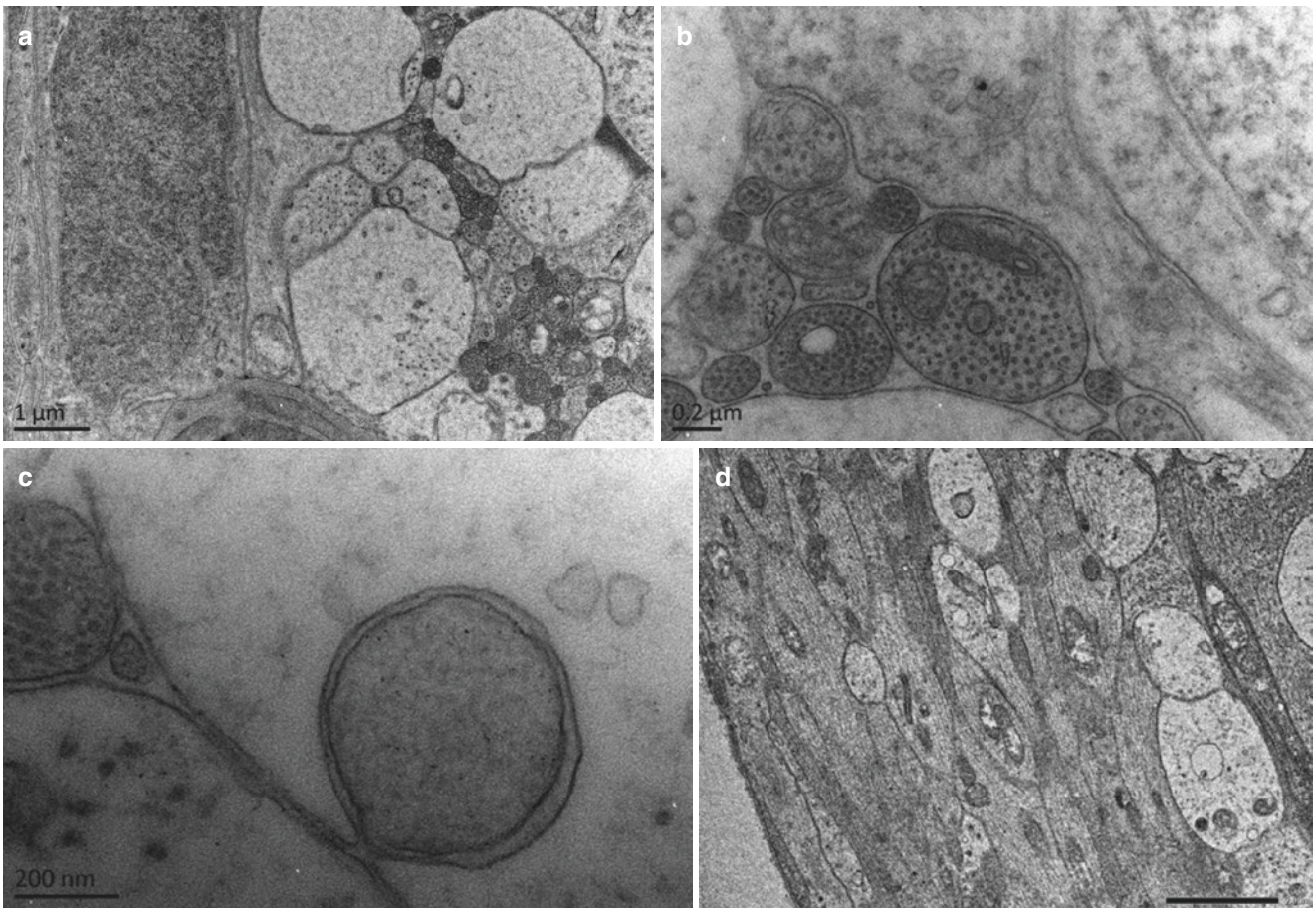

Fig. 8.2 The RGC axons in normal rat retina. (**a**) The diameters of intraretinal ganglion cell axons vary significantly between different axons. (**b**) The intercellular tight junction in axon-axon and axon-glial cells. (**c**) Axon absorbs extracellular bulb through endocytosis. (**d**) The ganglion cell varicosities are replaced by the strengthened glial cells processes

thinner; thus we propose this morphological structure maybe unique buffer system. If the IOP is elevated, mild, or moderate, this buffer system can resist the pressure until it returns to normal. Otherwise the varicosities diminish if the IOP elevation is severe and sustains for a long time and the varicosities are replaced by the strengthened glial cell processes (Fig. 8.2d).

8.1.1.2 Hypothesis: Neuron–Glial Cell Transcellular Transfer Theory

Intraretinal ganglion cell axons are predominantly varicose fibers in both human and nonhuman primates, and the varicosities are mitochondria-rich. Therefore, the varicosities can be considered as plenty energy demand sites and may take part in other functions. And we can see that there are glial cells around axons (Fig. 8.2b). It had been reported that neuron axon can release damaged mitochondria to transcellular degenerated by astrocytes in the RGC and brain [3]. More interestingly, astrocytes also can transfer health mitochondria to neurons after stroke which depends on CD38, Ca^{2+}, and cADPR [4]. The relationship between neuron and glial cells is very important; thus, we propose other cell components can also be transferred except mitochondria (Fig. 8.2c).

8.1.2 Muller Cells

The vertebrate retina contains four types of glial cells, and each exhibits distinct morphological, developmental, and molecular antigenic characteristics. Muller cells are the predominant, which compose 90% of all the glial cells, followed by astrocytes, microglial cells, and oligodendrocyte, which only exist in few species such as rabbit and are associated with myelinated ganglion cell axons.

Muller cells are radially oriented cells that transverse the retina from its inner border to the distal end of the outer nuclear layer (Fig. 8.3). Some research reported Muller cells are the last post-mitotic cells [5]. Muller cells involve many functions. For instance, it is supposed to be a scaffold which is rich in ion channels and which acts as the mechanosensors that maintain ion and water homeostasis in the retina.

Muller cells play a prominent role in the water handling in the retina and osmotically driving water flux to the vitre-

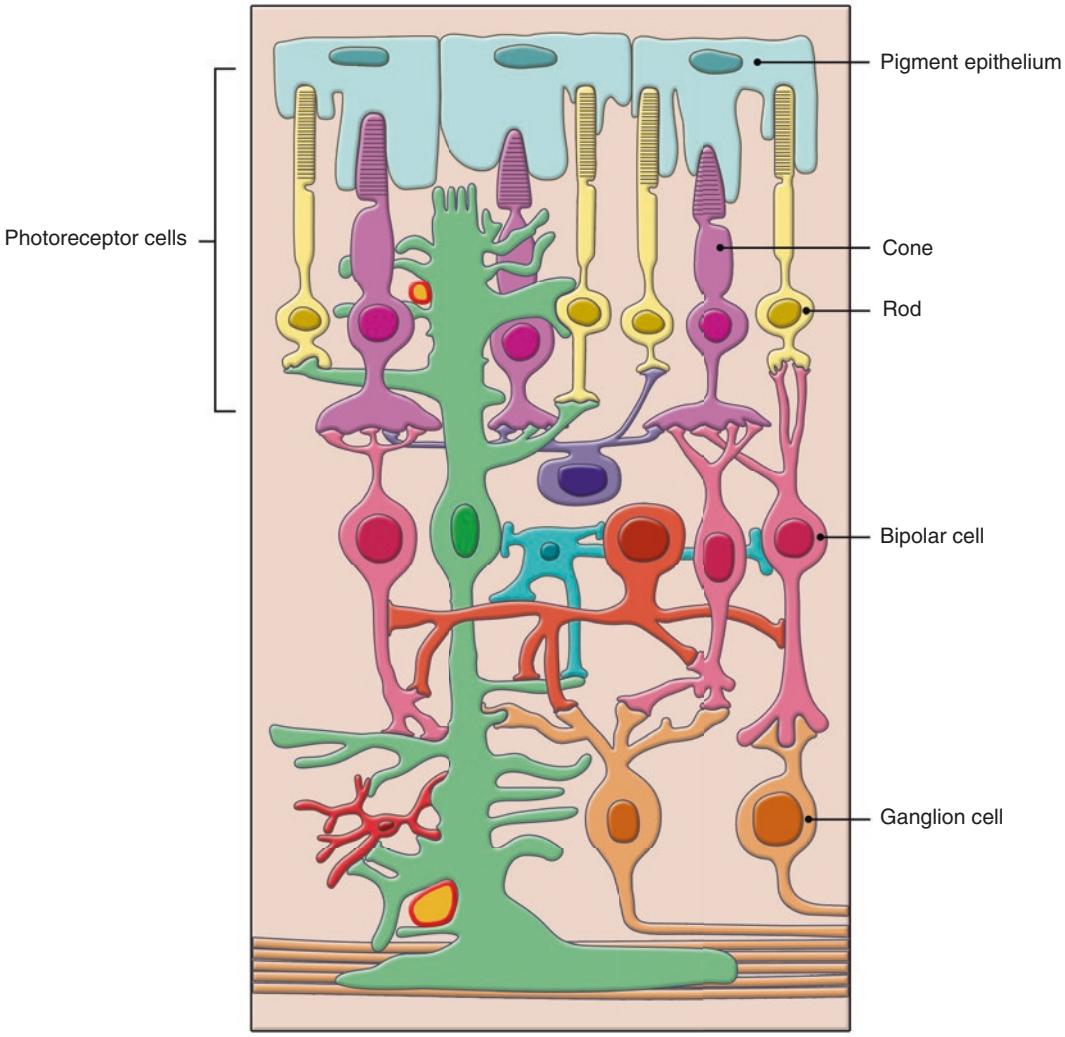

Fig. 8.3 Retina Muller cell

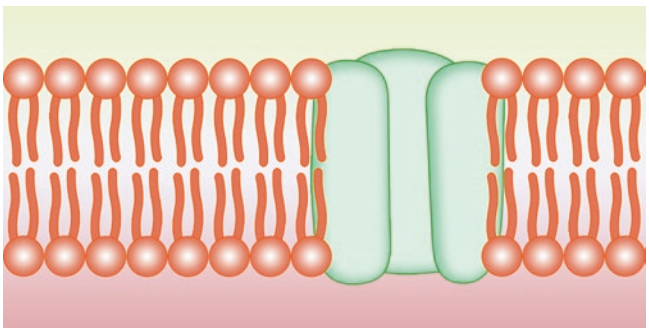

Fig. 8.4 The pattern diagram of aquaporin protein

ous body and vessels rather than to the subretinal space which may be because of its aquaporin (AQP) (Fig. 8.4), especially AQP4. The water flux through AQP4 is involved in the rapid volume regulation of the retina and maintains the water homeostasis in some diseases that induce retinal edema such as diabetes mellitus, glaucoma, and others. Muller cells also maintain the integrity of the blood-retina barrier and clear metabolic waste by regulating extracellular pH and K+ ions [6].

8.2 The Anatomy and Physiology of Optic Nerve Head

8.2.1 The Anatomy and Physiology of ONH

The morphology of rat ONH is quite unique, which is very different from human ONH that without lamina cribrosa (LC) instead of glial lamina [7], the RGC axons run through and which is also vulnerable. There are some buffer systems in ONH. We will discuss the morphological characteristics and underlying functions.

8.2.1.1 ONH Sheath

In rodent and primate animal, there are sheaths around the ONH surrounding, which may act as buffer system to the pressure change, increase or decrease (Fig. 8.5). In rat ONH, the vessels are in the basal of ONH, which is very different from primate's ONH in which the vessels including central artery/vein are in the ONH center (Fig. 8.5a). The sheath is mainly composed of collagen fibers and elastic fibers, which are hydrophilic as it is rich in proteoglycan (Fig. 8.5b) [8, 9].

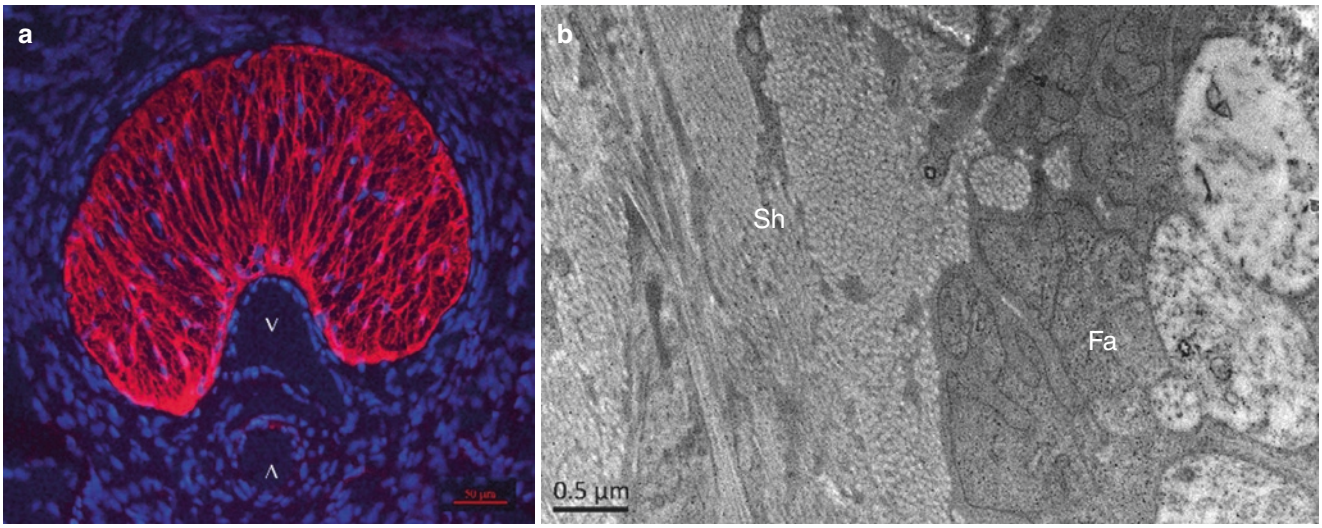

Fig. 8.5 The morphology of rat ONH. (**a**) The shape of rat ONH; the retinal central vein (V) and retinal central artery (A) are in the basal of ONH. The sheath wraps up the whole ONH (red: glial fibrillary acidic protein, GFAP). (**b**) The magnification photo of sheath, in which the main component is collagen fibers and elastic fibers. *Sh* sheath, *Fa* fortified astrocytes, *V* vessel, *A* artery

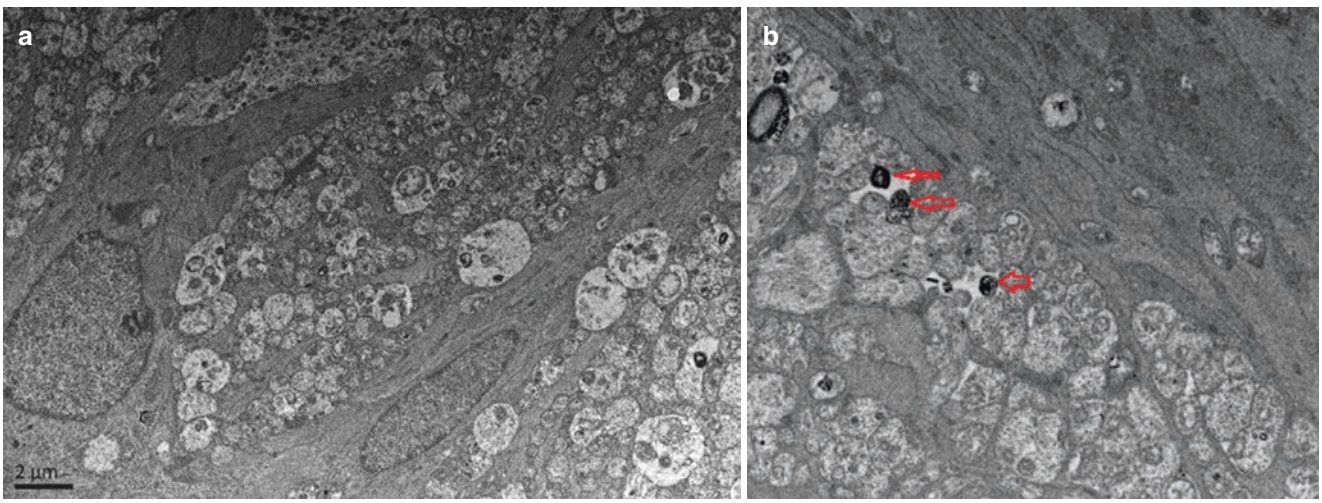

Fig. 8.6 (**a**) The ganglion cell axons in rat ONH and the axons of different sizes can be seen. (**b**) In 40 mmHg IOP 6 h acute IOP↑ rat model, the axon are destroyed and thus are diminishing, and the bare space can be seen. Arrow: destroyed axons

The sheath is surrounded by SAS which is filled with cerebrospinal fluid (CSF). CSF pressure fluctuation is consistent with the heartbeat and fluctuates over time. We propose the sheath is the first barrier to CSF pressure fluctuation and protects the axons.

8.2.1.2 Ganglion Cell Axons in ONH

In rat ONH, the ganglion cell axons have various shapes such as round, oval, or irregular which are close to each other (Fig. 8.6a). Between axons, there are a mount of astrocytes processes which separate axons and have important functions. If the axons are damaged, it will shrink and diminish which will be replaced by fibrous connective tissue. In acute higher IOP rat model, the axons are damaged and shrink with increased electron dense, and with the shrinking of axons, the bald spaces are left without scar tissue filling in (Fig. 8.6b).

Hypothesis: Ganglion Cell Axons in ONH

With the same circumference, round has the largest area. Some reported demonstrated axons are damaged earlier than ganglion cell body [10]. We proposed that, in some pathological conditions, the axons can swell and become much more round according to the morphologic characteristics without deterioration, even when the axons are arranged closely.

8.2.1.3 Fortified Astrocytes (FASTs)

There is a kind of special astrocytes in ONH named fortified astrocytes (FASTs); the FAST processes are scattered in axon intervals and closed tightly, of which functions we will discuss in the other chapter.

Geoffrey Raisman and his colleagues think FASTs have a close relationship with Muller cells or have the same origin with Muller cell (Fig. 8.7). In this conception, the FAST ventral side is cognate with Muller cell's outer part, and the dorsal surface is cognate with Muller cell end feet [11]. The dorsal side is vulnerable to damage and sensitive to pressure. When IOP is increased, the tiny feet from FAST dorsal part shrink and atrophy with bald space left (Fig. 8.7a, b). In our recent study, we found both the dorsal tiny feet and the ventral tiny feet are sensitive. We found the same phenomenon has occurred in the basal of FASTs.

Except that, we can see that in the tiny feet from FASTs, there are mount of pinocytotic vesicles (Fig. 8.7c) [11]. The particular functions of these pinocytotic vesicles are not clear. We proposed that these pinocytotic vesicles may maintain microenvironment stability through shallow water, metabolic waste, or other tissue fragments from all kinds of pressure.

8.3 The Anatomy and Physiology of Optic Nerve

8.3.1 ON Sheath

ON sheath is very similar to ONH sheath, which is mainly composed of a mount of elastic fibers and collagen fibers that wrap the sheath in different patterns such as vertically and horizontally. ON sheath is surrounded by CSF, and the elastic fibers and collagen fibers have good hydroscopicity. Therefore, the sheath may be able to keep ON in the balance of pressures and maintain tissue microenvironmental stabilization.

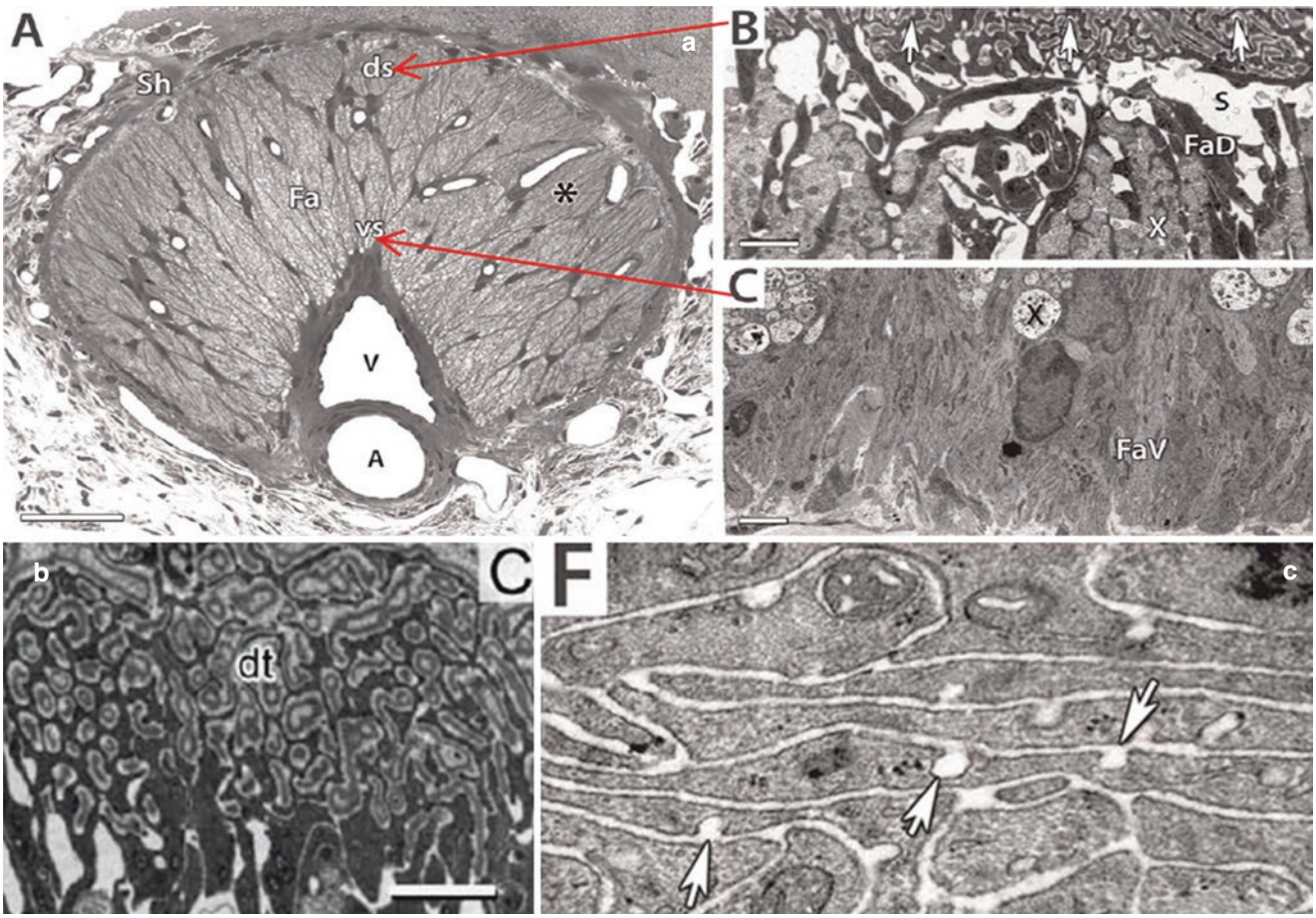

Fig. 8.7 (**a**) Rat morphology of ONH, the ventral and dorsal cleft of FASTs. (**b**) The tiny foot of FASTs dorsal. (**c**): The pinocytotic vesicles of FAST processes (arrow) (Reprinted with permission from Li Y, Li D, Ying X, et al. An energy theory of glaucoma[J]. (Reprinted with permission from Li Y, Li D, Ying X, et al. An energy theory of glaucoma[J]. Glia, 2015, 63(9):1537–1552). *Sh* sheath, *Fa* fortified astrocytes, *vs* ventral side, *ds* dorsal side, *V* vein, *A* artery, *FaD* Fa degenerating, *dt* dorsal terminal

8.3.2 Aquaporin 4 in ON Astrocytes

Similar to Muller cell, there are AQP4 located in ON astrocytes. AQP4 maintain the water balance between the outer and inner membrane. Astrocytes are scattered in ON to maintain the homeostasis.

8.4 Retro–ocular Buffer System: CSF

The translaminar pressure gradient (TLPD) is strongly correlated to the difference between IOP and CSFp [12–21]. The retro-ocular CSFp depends on the intracranial CSF [22]. Some research reported that under a key point, the CSFp in retro-ocular is little influenced by intracranial CSFp and is relatively stable to resist the forward pressure from IOP. If we destroy the anatomy in orbital, this relative stability to resist IOP will be destroyed, and the axon will degenerate gradually.

In our study we found after the acute reduction of CSFp, the retinal axon flow can be obstructed and the axon motor protein transport also blocked [19–21].

8.5 Vessels

8.5.1 Retinal Vessels

According to the mentioned above, we proposed that in these damaged vessels, elevated IOP is relatively higher than in other capillaries. When IOP is elevated, the vessel is compressed and returned with IOP decreased. If the pressure decreased rapidly and exceeded the limit of these vessel buffers, the capillaries will be destroyed and bleed. Thus, we usually see the clamp hemorrhage in glaucoma patients' posterior fundus with severe IOP elevation, without peripheral retina as capillary tension is relatively lower.

8.5.2 Hypothesis: Why the Central Retinal Artery/Vein Is Located in ON Center?

We are wondering why central retinal artery/vein is located in ON center in human and other mammalian or rodent animals. In human, the central retinal artery/vein is located in ONH center too but not in the rodents. We proposed that the central vessels are located in the core of tension balance from subarachnoid space (SAS), dura, and subarachnoid. According to this, we concluded that the CSF pressure influences ON indirectly. What's more, only the fluid produces pressure homogeneously. Maybe the pressure in the center of ON is zoned, and the pressure to the center vascular wall in 360° is quite balance.

8.5.3 Hypothesis—Why the Central Retinal Artery/Vein Enters into ON Tilted at a Certain

Comparing with posterior ciliary artery which vertically enters into tissue, the central retinal artery/vein gets into retro-ocular ON at a certain angle, and the artery angle is much bigger than the vein which is very different to the micro-small vessel especially posterior ciliary artery that vertically enters into ON for nutrition supply. We propose that the vessel pressures are the causes for these angles. The artery pressure is much bigger than the vein, so it can better resist the horizontal pressure from axon fluid dynamics. We further proposed that the axon microenvironment fluid flow including introgradient and retrograde brings some kind of pressure obviously.

8.5.4 Hypothesis: Why Does ONH Micro-Artery Return to ON with Axon?

It is very interesting that the retro-ocular ON blood supply is from the return branch of posterior ciliary artery (PCA) in ONH (Fig. 8.8). Except in this region, there is almost no other tissue blood supply like this. As the anatomic characteristics, we can see that there is a SAS chamber between the dura mater and retro-ocular ON, so it is impossible that the posterior ciliary artery (PCA) supplies ON directly.

Besides, maybe the forward axonal flow also influences the blood supply of ONH. We proposed that the IOP, SAS, or tissue pressure may also impede the backward blood supply which may accelerate tissue energy metabolism following

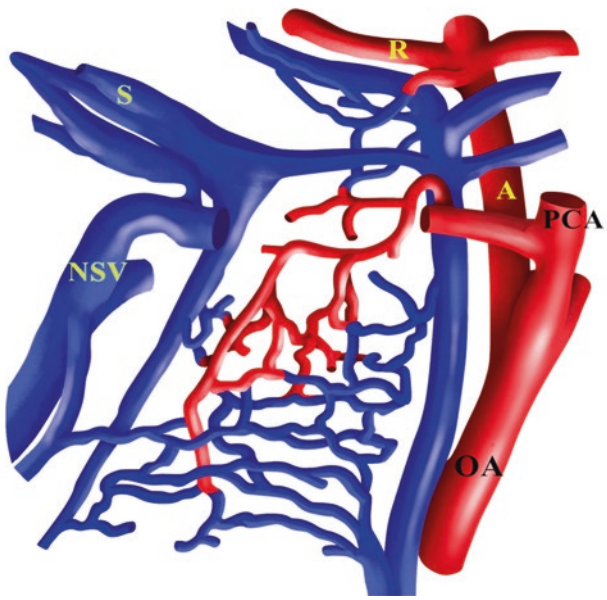

Fig. 8.8 Blood supply of ONH. *OA* ophthalmic artery, *PCA* posterior ciliary artery

axon transport. However, the hemodynamics of ONH will be devastated if the pressure balance is destroyed.

It may explain why the IOP returned to normal; however, the neuronal damage continued. We further proposed that the pressure in these damaged vessels because of IOP elevation is relatively higher than the capillary.

References

1. Gupta MP, Herzlich AA, Sauer T, et al. Retinal anatomy and pathology. Dev Ophthalmol. 2016;55:7–17.
2. Wang L, Dong J, Cull G, et al. Varicosities of intraretinal ganglion cell axons in human and nonhuman primates. Invest Ophthalmol Vis Sci. 2003;44(1):2–9.
3. Davis CH, Kim KY, Bushong EA, et al. Transcellular degradation of axonal mitochondria. Proc Natl Acad Sci U S A. 2014;111(26):9633–8.
4. Hayakawa K, Esposito E, Wang X, et al. Transfer of mitochondria from astrocytes to neurons after stroke. Nature. 2016;535(7613):551–5.
5. Altshuler D, Lo Turco JJ, Rush J, et al. Taurine promotes the differentiation of a vertebrate retinal cell type in vitro. Development. 1993;119(4):1317–28.
6. Vecino E, Rodriguez FD, Ruzafa N, et al. Glia-neuron interactions in the mammalian retina. Prog Retin Eye Res. 2016;51:1–40.
7. Schneider M, Fuchshofer R. The role of astrocytes in optic nerve head fibrosis in glaucoma. Exp Eye Res. 2016;142:49–55.
8. Dai C, Khaw PT, Yin ZQ, et al. Structural basis of glaucoma: the fortified astrocytes of the optic nerve head are the target of raised intraocular pressure. Glia. 2012;60(1):13–28.
9. Dai Y, Sun X, Yu X, et al. Astrocytic responses in the lateral geniculate nucleus of monkeys with experimental glaucoma. Vet Ophthalmol. 2012;15(1):23–30.
10. Howell GR, Libby RT, Jakobs TC, et al. Axons of retinal ganglion cells are insulted in the optic nerve early in DBA/2J glaucoma. J Cell Biol. 2007;179(7):1523–37.
11. Li Y, Li D, Ying X, et al. An energy theory of glaucoma. Glia. 2015;63(9):1537–52.
12. Ren R, Wang N, Li B, et al. Lamina cribrosa and peripapillary sclera histomorphometry in normal and advanced glaucomatous Chinese eyes with various axial length. Invest Ophthalmol Vis Sci. 2009;50(5):2175–84.
13. Zhang S, Wang H, Lu Q, et al. Detection of early neuron degeneration and accompanying glial responses in the visual pathway in a rat model of acute intraocular hypertension. Brain Res. 2009;1303:131–43.
14. Ren R, Jonas JB, Tian G, et al. Cerebrospinal fluid pressure in glaucoma: a prospective study. Ophthalmology. 2010;117(2):259–66.
15. Ren R, Li B, Gao F, et al. Central corneal thickness, lamina cribrosa and peripapillary scleral histomorphometry in non-glaucomatous Chinese eyes. Graefes Arch Clin Exp Ophthalmol. 2010;248(11):1579–85.
16. Liang YB, Friedman DS, Zhou Q, et al. Prevalence of primary open angle glaucoma in a rural adult Chinese population: the Handan eye study. Invest Ophthalmol Vis Sci. 2011;52(11):8250–7.
17. Ren R, Wang N, Zhang X, et al. Trans-lamina cribrosa pressure difference correlated with neuroretinal rim area in glaucoma. Graefes Arch Clin Exp Ophthalmol. 2011;249(7):1057–63.
18. Ren R, Zhang X, Wang N, et al. Cerebrospinal fluid pressure in ocular hypertension. Acta Ophthalmol. 2011;89(2):e142–8.
19. Zhang Z, Wu S, Jonas JB, et al. Dynein, kinesin and morphological changes in optic nerve axons in a rat model with cerebrospinal fluid pressure reduction: the Beijing intracranial and intraocular pressure (iCOP) study. Acta Ophthalmol, 2016;94(3):266-275.
20. Zhang Z, Liu D, Jonas JB, et al. Glaucoma and the role of cerebrospinal fluid dynamics. Invest Ophthalmol Vis Sci. 2015;56(11):6632.
21. Zhang Z, Liu D, Jonas JB, et al. Axonal transport in the rat optic nerve following short-term reduction in cerebrospinal fluid pressure or elevation in intraocular pressure. Invest Ophthalmol Vis Sci. 2015;56(8):4257–66.
22. Hou R, Zhang Z, Yang D, et al. Pressure balance and imbalance in the optic nerve chamber: the Beijing intracranial and intraocular pressure (iCOP) study. Sci China Life Sci. 2016;59(5):495–503.

The New Concepts of Cerebrospinal Fluid Physiology

9

Jiawei Wang and Ningli Wang

9.1 The History of Cerebrospinal Fluid

The description of cerebrospinal fluid first appeared in the 17th century BC [1]. An antique dealer named Edwin Smith bought a surgical papyrus which described the watery fluid around the brain. In 1747, Albrecht von Haller, a Swiss anatomist and physiologist, first described the existence of CSF systematically [2]. Subsequently, Cotugno, an Italian anatomist from Naples, observed the presence of water ("liquor cotunnii") around the ventricles and the spinal cord by conducting 20 autopsies [3]. Also, he found that the brain gets smaller in size and the volume of watery fluid around the ventricles and the spinal cord increases with age increase. His notable observations were published in Latin in 1764 in Naples and in English in 1775 in London. The term cerebrospinal fluid in published literature is "le liquid cérébrospinal" in a French document by Magendie in 1842 [4].

9.2 The Classical Concept of CSF Physiology

In 1875, Key published a very famous paper in which he demonstrated the CSF is absorbed by the arachnoid granulation or villi [5]. A long period of time after that, it is widely accepted that the CSF is absorbed by the arachnoid granulation or villi. Key's article has been cited by many classic textbooks. In 1913, Dandy published his extremely famous experiment in JAMA. He blocked the foramen of Monro of dogs, then excised the choroid plexus from the lateral ventricle, and preserved the choroid plexus from the contralateral lateral ventricle. The result of the experiment shows that ventricular dilatation does not occur in the choroid plexus excised side but occurs in the choroid plexus preserved side [6]. This experimental result demonstrated that the CSF is produced by choroid plexus. In 1926, Cushing, the American pioneering brain surgeon, introduced the concept of the "third circulation" which asserts CSF is produced by the choroid plexus and circulates unidirectional from the ventricles to the subarachnoid space to be absorbed by the arachnoid villi [7].

9.3 The New Concept of CSF Physiology

During 100 years, after Dany demonstrated that the choroid plexus is the site of CSF production, many scientists found that the CSF is also produced by structures other than the choroid plexus. Some articles sought out the brain itself as the site of CSF production [8], whereas others claimed CSF production from the cerebral superficial subarachnoid space [9], the perivascular system [10], or the pial artery [11]. Moreover, a study suggested its production by the spinal cord [12], and another has shown the presence of ependymal fluid secretion from the ependyma of the spinal cord central canal [13]. The hypothesis of Oreskovic and Klarica is the mostly accepted now. It asserts that the CSF is formed everywhere and resorbed everywhere in the brain [14]. Also it introduced the term of Virchow-Robin space (VRS), also known as the pericapillary space, in which the CSF was produced and resorbed.

In 1992, Agre discovered that red blood cells contain a membrane protein of high water permeability [15]. This protein, later called aquaporin-1 (AQP-1), turned out to be a member of a large family of water channel proteins that allow bidirectional transport of water across the phospholipid

J. Wang
Department of Neurology and Medical Research Center, Beijing Tongren Hospital, Capital Medical University, Beijing, China

N. Wang (✉)
Beijing Institute of Ophthalmology, Beijing Tongren Eye Center, Beijing Tongren Hospital, Capital Medical University, Beijing, China

Beijing Ophthalmology & Visual Sciences Key Laboratory, Beijing, China
e-mail: wningli@vip.163.com

N. Wang (ed.), *Intraocular and Intracranial Pressure Gradient in Glaucoma*,
Advances in Visual Science and Eye Diseases 1, https://doi.org/10.1007/978-981-13-2137-5_9

bilayer of the plasma membrane. In 2014, Nakada demonstrated that it was AQP-4 that regulated water influx into CSF [16]. In this experiment, he chose wild-type AQP-1 knockout and AQP-4 knockout mice. This experiment investigates water flux into CSF in wild-type AQP-1 knockout and AQP-4 knockout mice utilizing ^{17}O-labeled water and JJ vicuna coupling proton exchange (JJVCPE) MRI. This experiment supports the hypothesis that water movement within the Virchow-Robin space is critical for CSF volume. The result clearly demonstrated that water influx into CSF is regulated by AQP-4, known to be responsible for water homeostasis of the pericapillary space [17], and not by AQP-1 found in the choroid plexus. At the same time, this experiment strongly supports the Oreskovic and Klarica hypothesis.

The "third circulation," also known as the bulk flow theory of CSF introduced by Cushing in 1926, was recently replaced by the "cardiac cycle-dependent systolic-diastolic to-and-fro cranio-spinal CSF movements" [18]. This new concepts of CSF movement are based on three main factors. The first one is physiological oscillations of arterial and venous blood during cranio-spinal blood circulation. The second one is respiratory activity, and body activity and posture is the last one. The CSF movement hypothesis is now widely accepted benefits from the advancements in neuroimaging [19].

9.4 The Function of CSF

The CSF is very important for the brain to survive and function. The function of CSF includes five parts [20]:

1. Buoyancy: the CSF can provide partial buoyancy for the brain helping to prevent the brain from being impaired by its own weight. The actual mass of the human brain is about 1400 g. However, the net weight of the brain suspended in the CSF is about 25 g. The brain therefore exists in neutral buoyancy, which allows the brain to maintain its density without being impaired by its own weight, which would cut off blood supply and kill neurons in the lower sections without CSF.
2. Protection: when head hit occurs, the CSF may cushion the brain within the skull.
3. Chemical stability: the CSF exchanges components with interstitial fluid to maintain the chemical stability.
4. Prevention of brain ischemia: the CSF can act as a means to compensate for the changes in blood volume within the skull during the cardiac cycle.
5. Clearing waste: the CSF could take away the waste products from the brain.

9.5 Intracranial Hypertension

The normal intracranial pressure ranges from 5 to 15 mmHg (in the supine position) in adults. The signs of intracranial hypertension involve headache (diffuse and persistent, most severe in the morning), nausea and vomiting (typically in the morning−paroxysmal dry heaves), as well as papilledema. The common cause of intracranial hypertension includes (a) idiopathic intracranial hypertension, (b) intracranial mass lesion, (c) traumatic brain injury, (d) ischemic stroke, (e) nontraumatic intracranial hemorrhage, (f) intracranial infection, (g) hydrocephalus, (h) impaired venous outflow from the brain, (i) hypoxemia/hypercarbia (causes cerebral vasodilation), and (j) drugs and metabolic [21]. The classic radiologic findings of intracranial hypertension include empty sella, downward brain herniation, dilation of the optic nerve sheaths, flattening of the posterior globe, optic nerve head protrusion, and venous stenosis at the distal portion of the transverse sinuses.

9.6 Intracranial Hypotension

Intracranial hypotension refers to the intracranial pressure lower than 60 mmH_2O, and the clinical manifestations involve orthostatic headache, posterior neck pain, nausea, vomiting, photophobia, tinnitus, decreased level of consciousness, and coma. The CSF leakage through a dural defect is the main cause of this. The causes of CSF leakage vary from the secondary causes such as lumbar puncture, cranial or spinal surgery, head or spine trauma to the primary causes like actual or underlying dural defect, and connective disorders (meningeal diverticula, Frank holes, Marfan syndrome, etc.). The classic radiologic findings of intracranial hypotension include pachymeningeal enhancement, venous engorgement, dural thickening, pituitary fossa enlargement, and herniation of the hindbrain.

References

1. Deisenhammer F, Sellebjerg F, Teunissen CE, Tumani H (eds). Cerebrospinal fluid in clinical neurology, 2015; pp 3–6.
2. Matsumae M, Sato O, Hirayama A, et al. Research into the physiology of cerebrospinal fluid reaches a New Horizon: intimate exchange between cerebrospinal fluid and interstitial fluid may contribute to maintenance of homeostasis in the central nervous system[J]. Neurol Med Chir. 2016;56(7):416–41.
3. Di Ieva A, Yasargil MG. Liquor cotunnii: the history of cerebrospinal fluid in Domenico Cotugno's work[J]. Neurosurgery. 2008;63(2):352–8.
4. Magendie F. Recherches physiologiques et cliniques sur le liquide céphalo-rachidien ou cérébro-spinal[M]. Méquignon-Marvis fils. 1842.

5. Key A, Retzius G. Studien in der Anatomie des Nervensystemes[J]. Arch Mikrosk Anat. 1873;9(1):308–86.
6. Dandy WE, Blackfan KD. An experimental and clinical study of internal hydrocephalus[J]. J Am Med Assoc. 1913;61(25):2216–7.
7. Cushing H. Studies in intracranial physiology & surgery: the third circulation, the hypophysics, the gliomas [M]. H. Milford, Oxford University Press, 1926.
8. Bering EA. Cerebrospinal fluid production and its relationship to cerebral metabolism and cerebral blood flow[J]. American Journal of Physiology—Legacy Content. 1959;197(4):825–8.
9. Bering EA Jr, Sato O. Hydrocephalus: Changes in Formation and Absorption of Cerebrospinal Fluid Within the Cerebral Ventricles*[J]. J Neurosurg. 1963;20(12):1050–63.
10. Weed LH. Studies on cerebro-spinal fluid. No. IV: the dual source of cerebro-spinal fluid[J]. J Med Res. 1914;31(1):93.
11. Hassin GB. The morphology of the pial blood vessels and its bearing on the formation and absorption of the cerebrospinal fluid[J]. J Neuropathol Exp Neurol. 1948;7(4):432–8.
12. Sato O, Asai T, Amano Y, et al. Formation of cerebrospinal fluid in spinal subarachnoid space[J]. Nature. 1971;233:129–30.
13. Sonnenberg H, Solomon S, Frazier DT. Sodium and chloride movement into the central canal of cat spinal cord[J]. Exp Biol Med. 1967;124(4):1316–20.
14. Orešković D, Klarica M. The formation of cerebrospinal fluid: nearly a hundred years of interpretations and misinterpretations[J]. Brain Res Rev. 2010;64(2):241–62.
15. Preston GM, Agre P. Appearance of water channels in Xenopus oocytes expressing red cell CHIP28 protein[J]. Science. 1992;256(5055):385.
16. Igarashi H, Tsujita M, Kwee IL, et al. Water influx into cerebrospinal fluid is primarily controlled by aquaporin-4, not by aquaporin-1: 17O JJVCPE MRI study in knockout mice[J]. Neuroreport. 2014;25(1):39–43.
17. Brinker T, Stopa E, Morrison J, et al. A new look at cerebrospinal fluid circulation[J]. Fluids and Barriers of the CNS. 2014;11(1):1.
18. Orešković D, Klarica M. A new look at cerebrospinal fluid movement[J]. Fluids and Barriers of the CNS. 2014;11(1):1.
19. Yamada S, Kelly E. Cerebrospinal fluid dynamics and the pathophysiology of hydrocephalus: new concepts[C]. Semin Ultrasound, CT and MRI. WB Saunders. 2016;37(2): 84–91.
20. Hladky SB, Barrand MA. Mechanisms of fluid movement into, through and out of the brain: evaluation of the evidence[J]. Fluids and Barriers of the CNS. 2014;11(1):1.
21. Rangel-Castillo L, Gopinath S, Robertson CS. Management of intracranial hypertension[J]. Neurol Clin. 2008;26(2):521–41.

10 Cerebrospinal Fluid Pressure Dynamics and the Pulsatile Component of the Translaminar Pressure Gradient

Cynthia J. Roberts

Idiopathic intracranial hypertension (IIH) is a disease characterized by abnormal high intracranial pressure (ICP) with unknown etiology. Factors such as obesity and stenosis of the venous sinus are potentially linked. Symptoms mainly include persistent associated headache, pulsatile tinnitus, vomiting, cranial nerve palsies, and visual disturbances such as photophobia. Response to medical or surgical treatment is variable by patient.

Therefore, the research question is whether response to treatment can be predicted/customized by measuring cerebrospinal fluid pressure (CSFP) response to change in CSF volume during diagnostic lumbar puncture (LP). The first step is to characterize the relationship between CSFP and change in CSF volume. We prospectively enrolled 12 subjects who presented with signs and symptoms of IIH based on the modified Dandy criteria. Standard ophthalmic evaluation was done by an experienced neuro-ophthalmologist, including visual acuity, slit lamp exam, fundoscopy, and Humphrey visual fields. Intraocular pressure (IOP) and ocular pulse amplitude (OPA) were measured by Pascal dynamic contour tonometer (Ziemer Ophthalmic Systems, Port, Switzerland) in the clinic setting and a Model 30 Pneumatonometer (Reichert Technologies, Depew, New York, USA) during the LP. We used electronic measurement of CSFP during LP (Fig. 10.1) with ultrasound guidance (Fig. 10.2) for spinal needle placement. During the LP, CSFP waveforms were measured as CSF was incrementally drained (Fig. 10.3), and IOP and OPA were measured pre- and post-LP.

Figure 10.4 shows a series of CSFP signals, recorded from a single patient during the LP. The blue waveform on the top represents the opening pressure CSFP waveform with a mean value that was very high and a pulse amplitude that was also quite large. As CSF was drained, we measured the waveform at multiple discreet time points during the procedure. The CSFP was reduced gradually to the value of approximately 17 mmHg, with greatly reduced pulse amplitude with a morphology distinct from the waveforms recorded at high pressures.

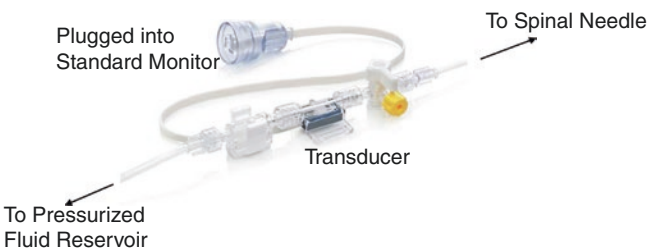

Fig. 10.1 Electronic transducer used to measure cerebrospinal fluid pressure during a lumbar puncture

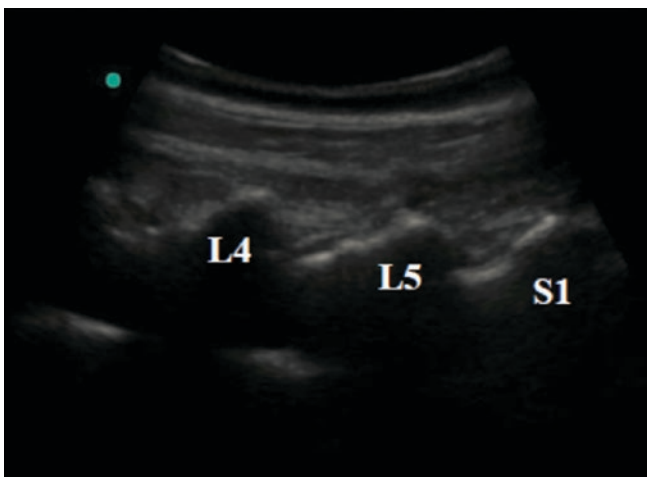

Fig. 10.2 Ultrasonic image of the spine showing lumbar vertebrae, L4 and L5, as well as sacrum, S1

Roberts Disclosures: Advisory Board to Optimeyes, Consultant to Ziemer Ophthalmic Systems AG, Consultant to Oculus Optikgerate GmbH, Travel support by Carl Zeiss Meditec

C. J. Roberts
Ophthalmology & Visual Science and Biomedical Engineering,
The Ohio State University, Columbus, OH, USA
e-mail: roberts.8@osu.edu

N. Wang (ed.), *Intraocular and Intracranial Pressure Gradient in Glaucoma*,
Advances in Visual Science and Eye Diseases 1, https://doi.org/10.1007/978-981-13-2137-5_10

All subjects showed a similar pattern of rapidly changing CSFP with fluid removal at higher pressures, followed by slower changing CSFP with fluid removal at lower pressures. This is shown in Fig. 10.5 for all 12 subjects.

Figure 10.6 shows the technique used for processing waveforms according to Löfgren [1]. Region 1 (blue line) is characterized by low compliance and high pressure, in which smaller changes in fluid volume cause larger changes in pressure. Region 2 (red line) is characterized by high compliance and low pressure, in which larger changes in volume cause smaller changes in pressure. The low pressure region may be associated with intracranial pressure (ICP) in glaucoma. Interestingly, fluid volume can be changed within a larger range, yet pressure is changed minimally.

Table 10.1 shows the significant reduction in CSFP and significant increase in both cerebrospinal pressure pulse amplitude (CPA) and cerebral perfusion pressure (CPP). The strong relationship between mean CSFP and CPA is illustrated in Fig. 10.7.

Interestingly, a very similar relationship was shown between the mean CSFP values and the CPA in all subjects. Through both the low compliance and the high compliance regions, we found a very strong linear relationship by individual patient with a characteristic slope. Therefore, each of the different colors represents a different subject. The R square of each regression was greater than 0.9 (Fig. 10.7).

A sample set of ocular pressure waveforms from one of the subjects is shown in Fig. 10.8. The pre-LP waveform is in red and the post-LP waveform is in blue. The reduction of IOP and OPA can be seen from the figure. The only difference between these two recordings was a relatively large reduction in CSFP. However, our n is too low to be conclusive. Therefore, it is clear that the interaction between intracranial pressure (ICP) and IOP is complex.

Consequently, we can conclude that it is feasible to measure the cerebrospinal system compliance in IIH during the diagnostic LP. High CSFP is associated with low compliance and high pulse amplitude. Furthermore, future studies will investigate the connections between cerebrospinal compliance and response to treatment in IIH.

Fig. 10.3 Monitor displaying both cerebrospinal fluid pressure waveform in white with mean value of 22 mmHg and pulse oximetry signal in green

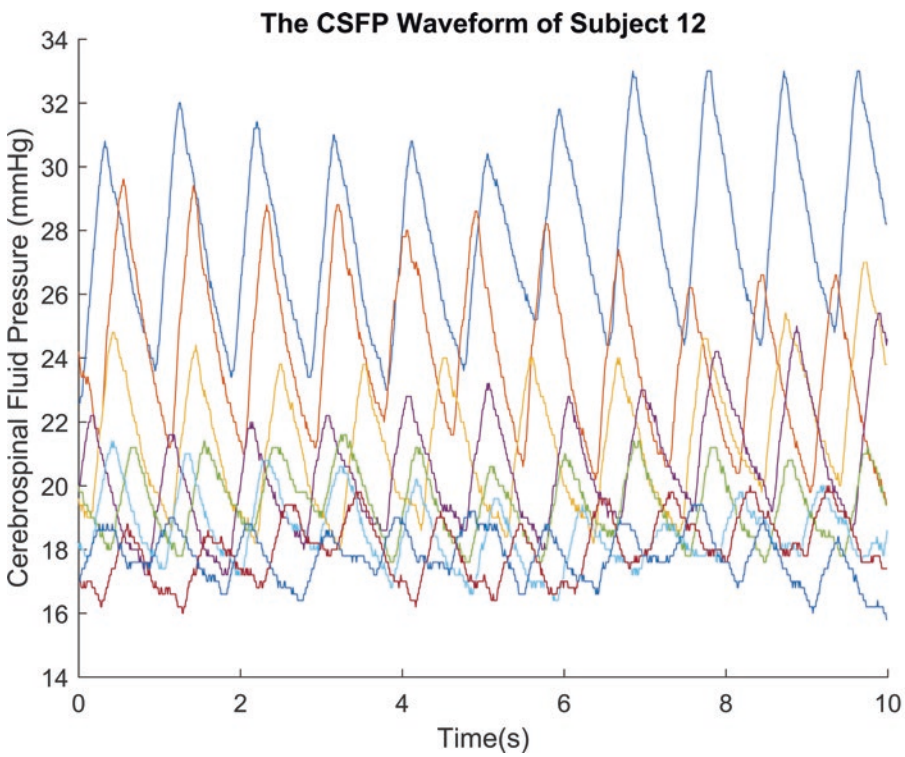

Fig. 10.4 Series of cerebrospinal fluid pressure waveforms recorded from a single subject as fluid was drained during a lumbar puncture

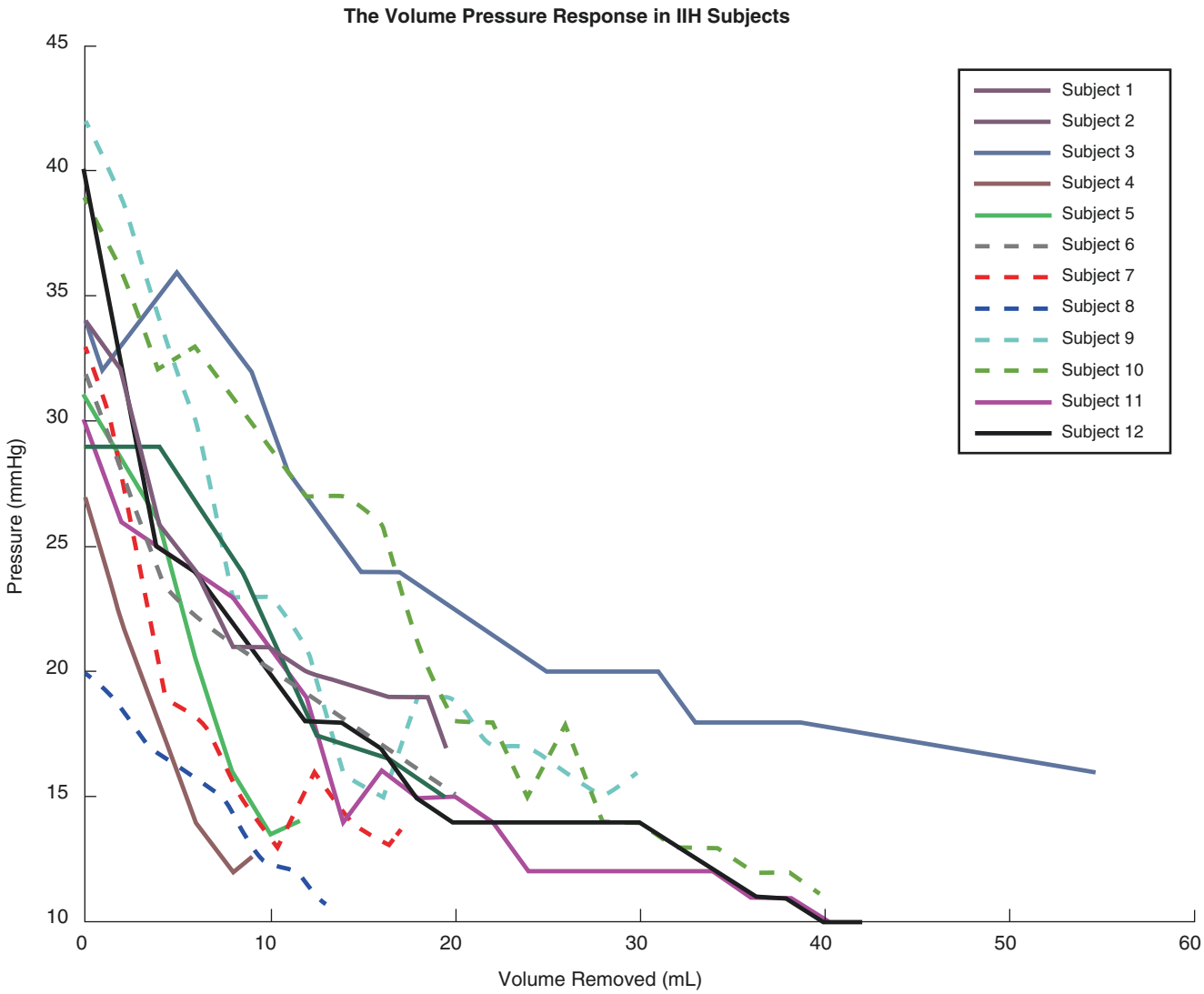

Fig. 10.5 Pressure-volume curves of 12 analyzed subjects

Based on our understanding of the relationship between mean CSFP and CPA from our study of IIH, as well as the relationship between CSFP and compliance, the translaminar pressure gradient (TLPG) in glaucoma is the next focus. As is known, both IOP and ICP are pulsatile in nature. It is important to also understand the spatial effect of IOP and ICP. IOP is distributed over the entire eye, so changes in volume/pressure will result in a change in the diameter of the eye with each pulsation. Also, IOP is measureable on the cornea. With each beat of the heart, the eyes become larger. If it is assumed that the heart rate is 60 bpm, this translates into over 31 million beats per year. Inevitably, across a lifetime, there is small magnitude and repetitive stretching of the eyes and the lamina cribrosa. ICP is present only behind and around the lamina cribrosa; thus it potentially buttresses the lamina and protects it from the action of the OPA (Fig. 10.9).

Therefore, since it was shown that normal to high intracranial pressure (ICP) leads to greater cerebral pulse amplitude (CPA), it is hypothesized that this buttresses the lamina cribrosa and protects it from the action of ocular pulse amplitude (OPA). Lower intracranial pressure and lower cerebral pulse amplitude in glaucoma make the lamina exposed to the action of ocular pulse.

This is consistent with the work reported from Dr. Lesk's laboratory, who explored the motion of fundus pulse amplitude (FPA). They found that there was no difference between normal and glaucoma eyes in the axial direction (Fig. 10.10). However, there was a significant difference in lateral motion between glaucoma and normal eyes (Fig. 10.10). Glaucomatous eyes showed greater motion in the nasal direction than the normal eyes [3].

We initially started our study to test this new hypothesis several years ago. The target is 120 subjects, including 30

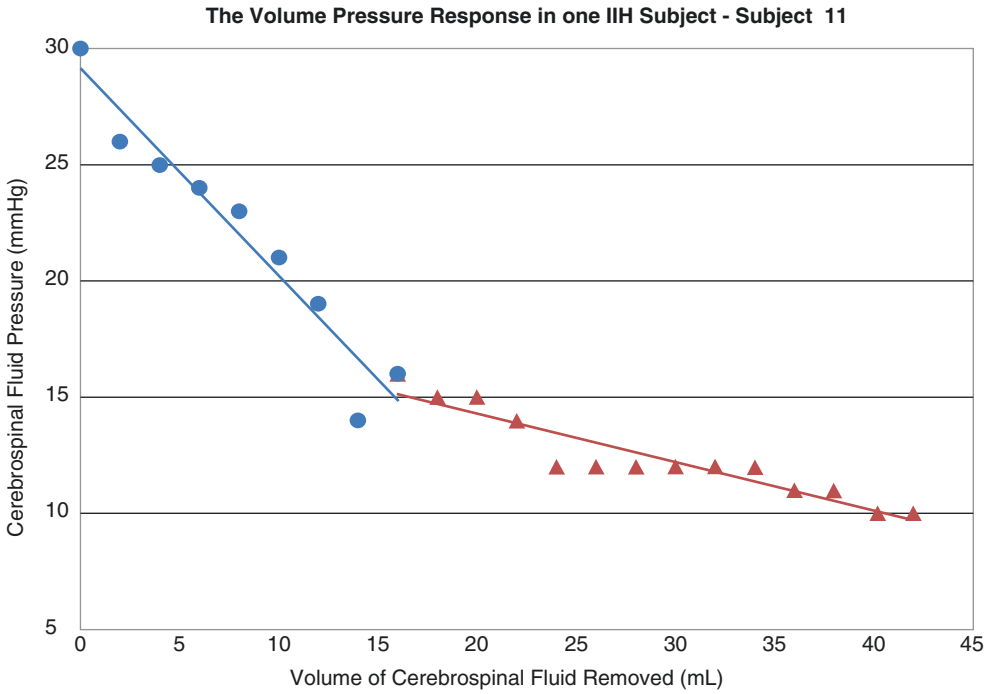

Fig. 10.6 Sample of how pressure-volume curves were analyzed to determine elastance (magnitude of slope of each line) and compliance (inverse of the magnitude of the slope of each line), such that higher pressure is associated with low compliance and lower pressure is associated with high compliance

Table 10.1 Pre and post-lumbar puncture measurements with compliance during LP

Measurement (pre−/post-LP)	**N**	**Pre-LP**	**Post-LP**	***P* value**
CSFP (mmHg)	$n = 12$	32.6 ± 6.0 (Range: 20–42)	13.4 ± 2.5 (Range: 10–17)	0.0001
CPA (mmHg)	$n = 6$	5.7 ± 3.2 (Range: 1.8–10.4)	1.3 ± 0.5 (Range: 0.79–1.79)	0.02
CPP (mmHg)	$n = 9$	50.7 ± 13.5 (Range: 30–65)	105 ± 10.8 (Range: 90–114)	4.7e–06
Measurement (during LP)	**N**	**(R1)**	**(R2)**	***P* value**
Compliance (mL/mmHg)	$n = 12$	0.8 ± 0.3 (Range: 0.43–1.3)	3.5 ± 2.0 (Range: 1.6–9.1)	0.0010

primary open-angle glaucoma (POAG), 15 ocular hypertension glaucoma (OHT), 15 normal tension glaucoma (NTG), and 60 normal subjects (NRM). Fifty-three subjects have been recruited thus far. The study is approved and monitored by the Institutional Review Board (IRB) and funded by the Ann Ellis Fund of the Columbus Foundation.

We measured IOP with multiple technologies. Goldmann applanation tonometry (GAT), as the most common device used for IOP estimation by ophthalmologists, will be used for comparison with other IOP measurements, despite the limitations in its accuracy [4]. Ocular response analyzer (ORA) produces a measurement of the viscoelastic corneal response to an air puff, which is referred to as corneal hysteresis (CH) and has been shown to correlate to glaucomatous damage. It also produces a more accurate assessment of IOP, known as corneal compensated IOP (IOPcc). We will also measure OPA using dynamic contour tonometry (DCT) in the sitting position and using pneumatonometry in the sitting, supine, and lateral decubitus position during a lumbar puncture (LP).

The CorVis ST is a new device, which measures corneal deformation characteristics. It functions by capturing high-speed images of the cornea deforming under an air puff, enabling measurement of deformation characteristics as indicators of the elastic properties of the cornea. We will compare IOP using multiple technologies and positions, to CSFP obtained during the LP. Blood pressure and heart rate were recorded with an automated sphygmomanometer.

For the anterior segment and optic nerve assessment, corneal tomography (Galilei or Pentacam anterior segment biometry) will be used for anterior chamber volume (ACV) and pachymetry. From ACV, IOP, and OPA, an estimate of ocular rigidity can be obtained. The cup-to-disk ratio from slit lamp examination is one of our structural estimates of glaucoma severity. This will be determined by our glaucoma specialists. The mean deviation (MD) from Humphrey visual fields will be used as a functional measurement of glaucoma severity.

Optical coherence tomography (OCT) provides a cross-sectional image of the nerve fiber layer thickness around the optic nerve head, which will serve as an additional structural indicator of glaucoma severity. The Heidelberg retinal tomography (HRT) provides a map of the surface topography of the nerve head, as well as a myriad of structural indices that relate to severity of glaucoma.

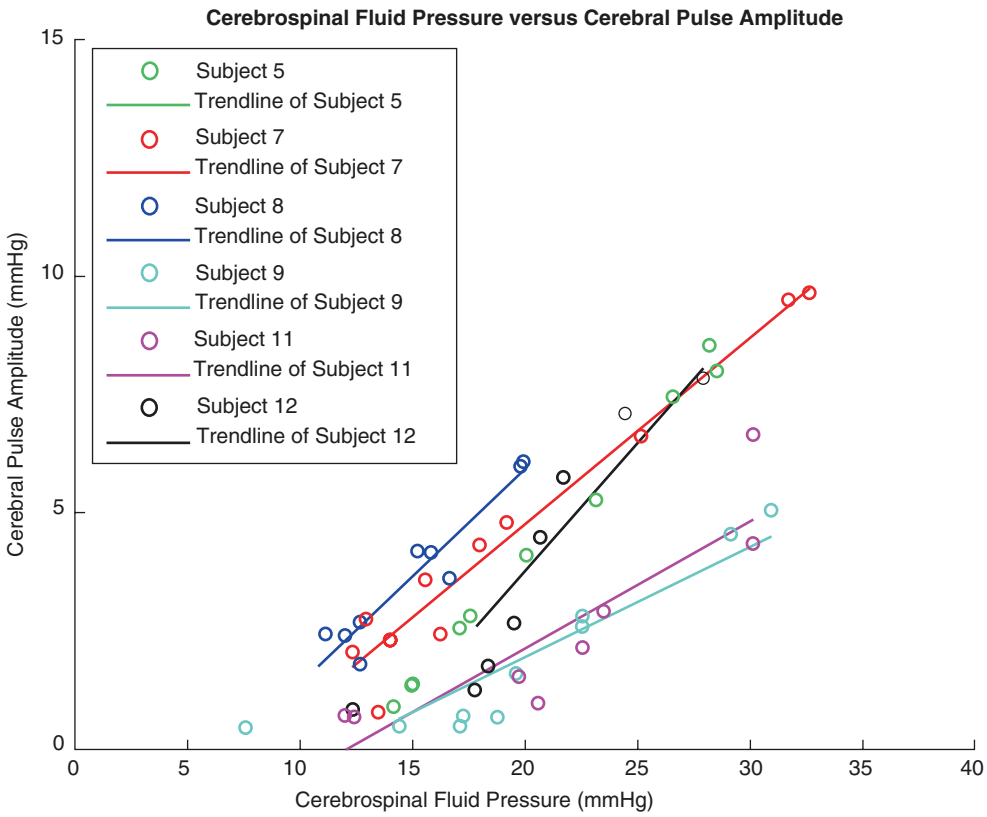

Fig. 10.7 Cerebrospinal fluid pressure versus cerebrospinal fluid pressure pulse amplitude

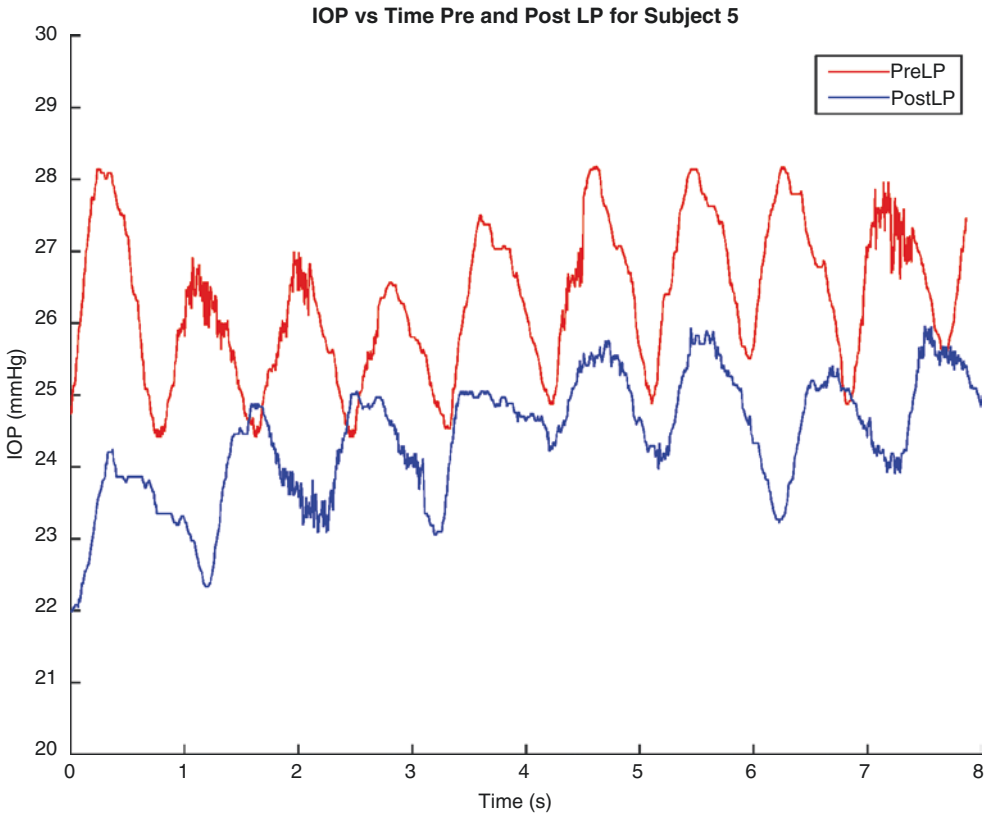

Fig. 10.8 Sample ocular pulse waveform immediately before the lumbar puncture (red) and immediately after lumbar puncture (blue)

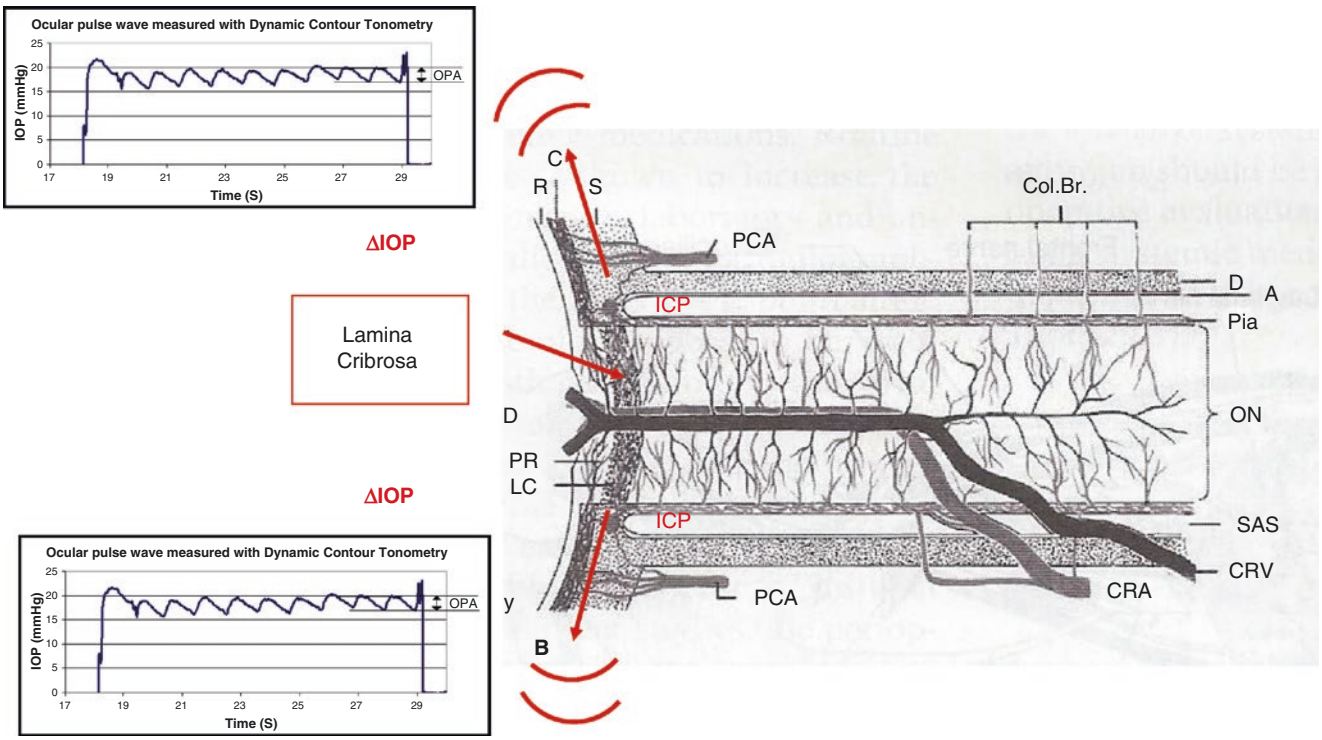

Fig. 10.9 Illustration of the repetitive action of the ocular pulse Adapted from Reference [2]

We use a newly developed technique for the LP. Specifically, electronic measurement of the CSFP waveform is recorded with a small needle gauge to minimize the risk of post-dural puncture headache and guided by ultrasound to minimize the risk of nerve injury. A 27-gauge needle can be used since it is not necessary to withdraw CSF. Also, a pencil point tip, rather than cutting tip commonly used for spinal needle, is used, and a single highly experienced anesthesiologist is approved by the IRB to perform this procedure for research purposes at OSU.

A standard monitor is used to record the electrocardiogram. The pulse oximetry waveform is also recorded. The ocular pressure waveform is recorded before the procedure, sitting and supine, as well as during the procedure using Reichert Model 30 Pneumatonometer, currently interfaced to patient monitor.

The study is ongoing. However, examples can be shown of data collected thus far. Figure 10.11 shows examples of recorded waveforms from two subjects, one normal subject (green signals) and one with glaucoma (red signals). The ocular pressure signals are shown within the globe on the left with quantitative relationships maintained between the two, and the CSFP signals are shown on the right within the space between the optic nerve and optic sheath, again with the quantitative relationships between the two maintained. The static translaminar pressure gradient is greater in the normal eye (green) than in the glaucomatous eye (red), but the difference in pulse amplitude is greater in the glaucomatous eye than the normal eye.

IOP and CSFP waveforms were measured simultaneously in a subset of subjects in our study. Figure 10.12 shows some sample waveforms to illustrate that the TLPG can either be pulsatile or relatively flat, depending on the pulse amplitudes of both the ocular pressure and CSFP waveforms, as well as any potential phase lag in between the two signals. The ocular pressure signal is measured transcorneally, and the CSFP is measured at the level of lumbar spine. Therefore, these signals do not represent the true phase lag or pulse amplitude experienced across the lamina cribrosa (LC). However, they are representative of the different morphologies that might be experienced by the LC. Different subjects have different IOP and ICP levels and different OPA and CPA. Therefore, the TLPG is also different by subjects, most of whom have positive TLPG.

Distinctly, the path length of pulsatile blood flow to ocular vessels is different from that of pulsatile blood flow to cerebral vessels, and therefore is likely a variable in different patients. However, it is not currently possible to measure pressures at the level of the lamina cribrosa in vivo.

An important question is whether pulsations are baffled by structures within the optic nerve sheath, such that ICP within the sheath is static. Padayachy L et al. used ultrasound to measure nerve sheath motion [5]. They found that when ICP was less than 20 cm H_2O, nerve sheath motion was asymmetric, and when ICP was more than 20 cm H_2O, nerve sheath motion became symmetric (Fig. 10.13). This

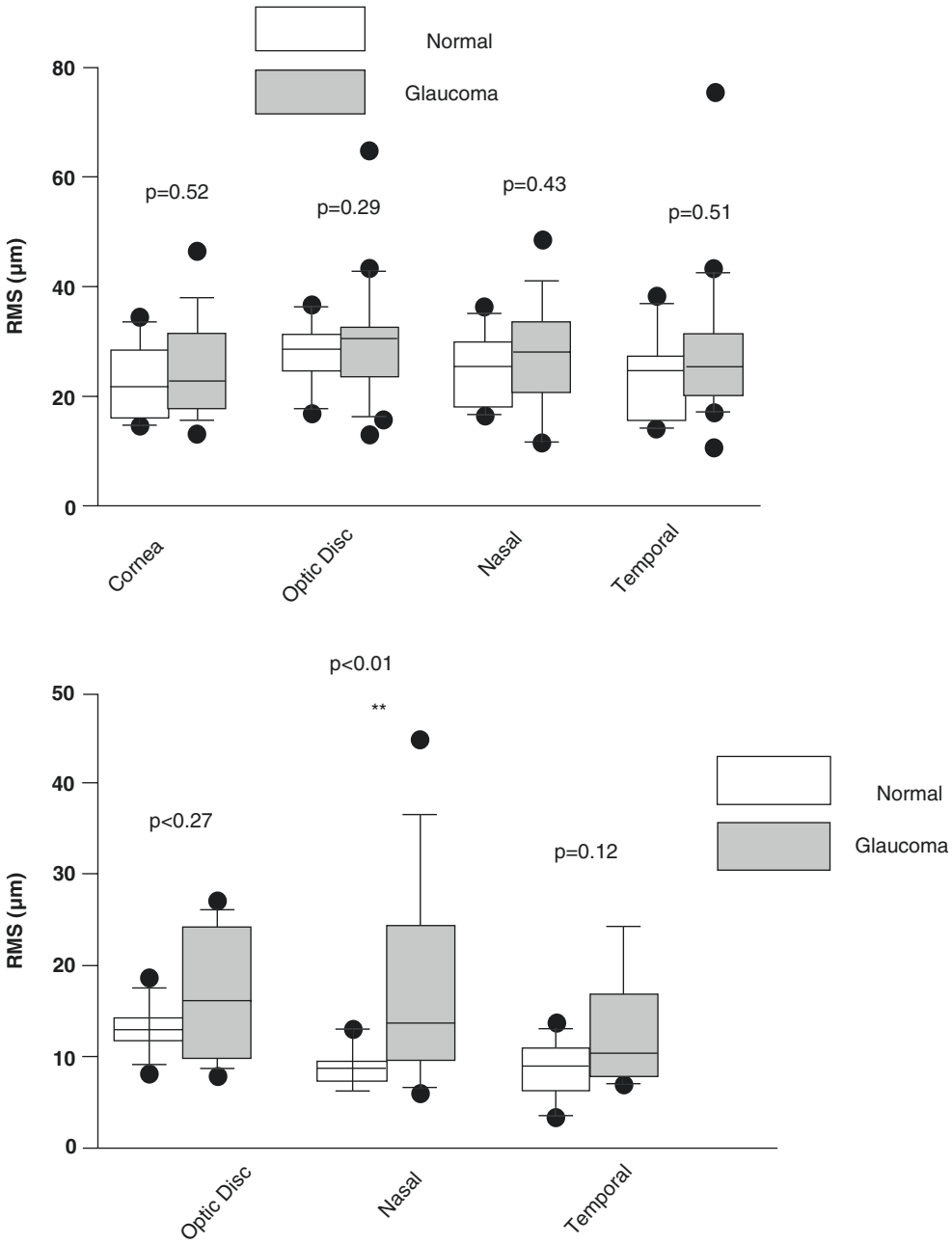

Fig. 10.10 Report of pulsatile fundus motion in normal and glaucomatous subjects, showing no difference in the axial direction (*TOP*) and a significant difference in the nasal direction with greater motion in glaucoma than normal subjects (*BOTTOM*). Figures are adapted with permission from Reference [3]. Copyright owned by ARVO

demonstrates that the pulsatile nature of the ICP is present within the nerve sheath, near the lamina cribrosa.

The effect of pulsations on the axons traversing the lamina cribrosa is repeated strain generated by the lamina cribrosa of varying patterns, depending on the microstructure. Thus the impact on the individual pores should be explored. Voorhees AP et al. revealed that the heterogeneous strain experienced by the neural tissue would be quite variable based on the microstructure of the lamina cribrosa (Fig. 10.14) [6].

Our research has some limitations. The CSFP is used to represent ICP but was measured in the lumbar region. Hou et al. showed a difference in lumbar CSFP, ICP, and pressure in the optic nerve sheath in dogs [7]. Hence, CSFP in the optic sheath may be lower than the actual measured value, and ICP may be greater than the actual measured value.

In conclusion, mean CSFP is strongly correlated with CPA in IIH patients [8]. It is likely that CSFP pulsations penetrate trabeculae within the nerve sheath to the lamina cribrosa, which is different by patient. The pulsatile component of the TLPD may be linked to glaucomatous damage.

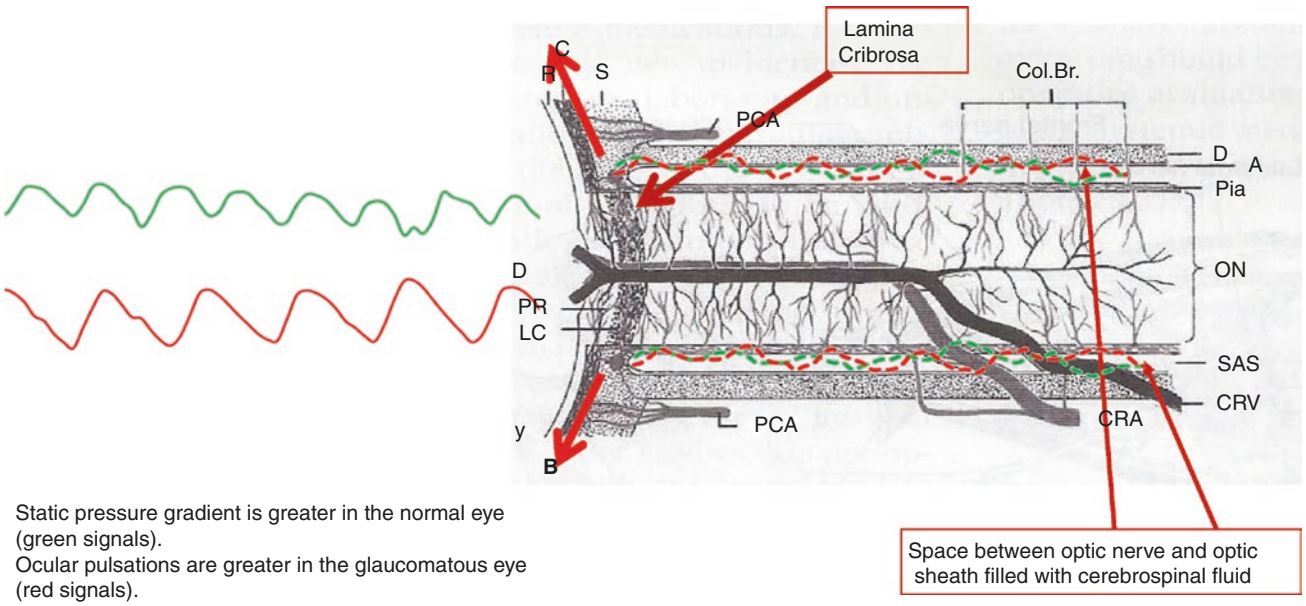

Fig. 10.11 Examples of ocular pressure waveforms in normal (solid green) and glaucomatous (solid red) subjects, compared to their similar cerebrospinal fluid waveforms (dotted red and dotted green). Adapted from Reference [2]

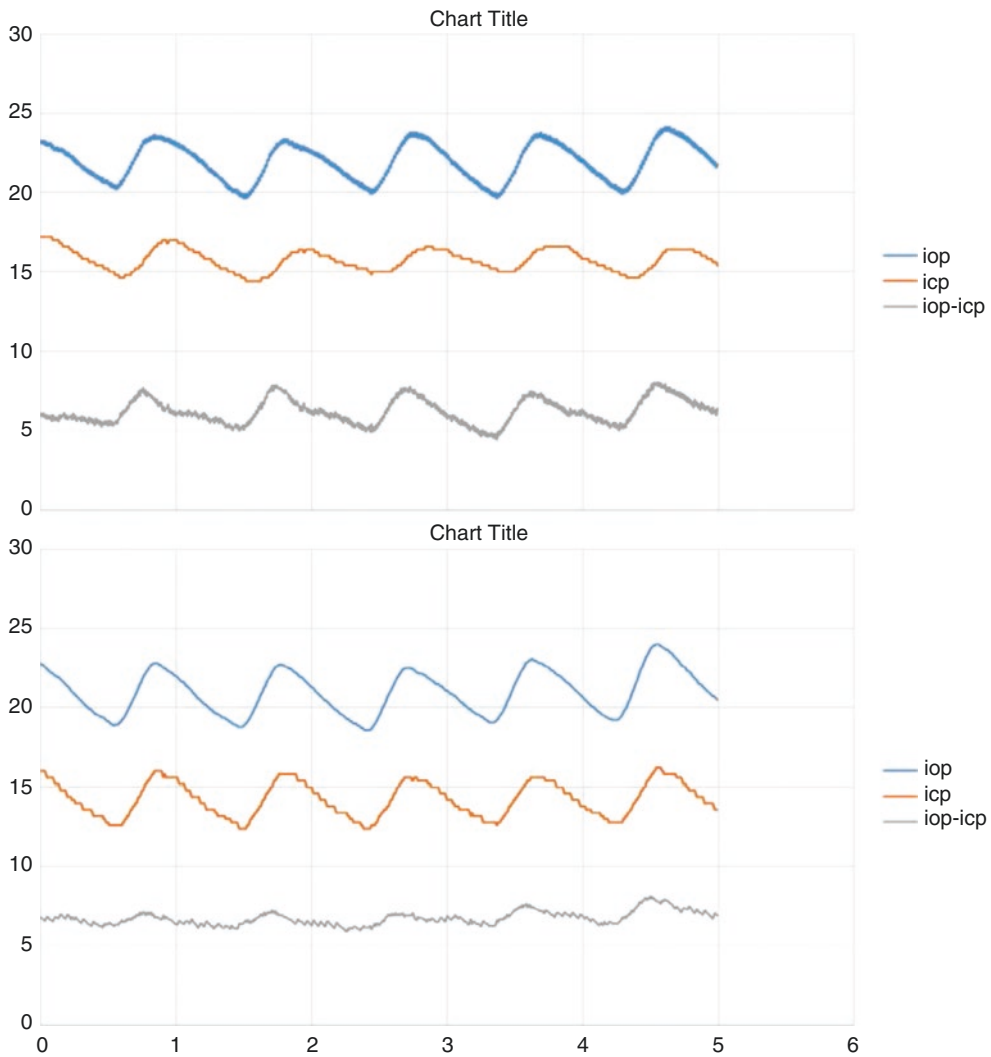

Fig. 10.12 Two example subjects in which the ocular pressure waveform (blue) was recorded simultaneously with the cerebrospinal fluid pressure waveform (orange) during a lumbar puncture. The translaminar pressure gradient waveform (gray) is generated by the subtraction, IOP minus CSFP. One subject showed larger pulse amplitude in the subtracted signal (*TOP*) than the other subject, where it was relatively flat (*BOTTOM*)

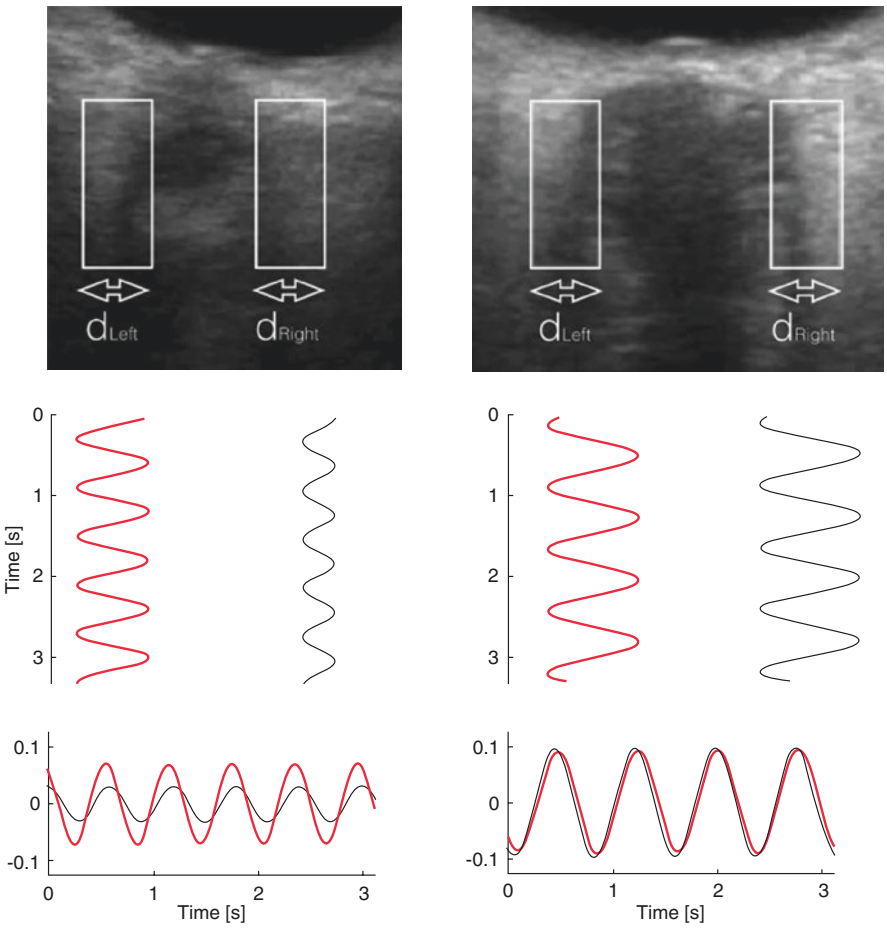

Fig. 10.13 Pulsations of the nerve sheath have been reported, with lower intracranial pressure showing asymmetric pulsations (LEFT) and higher intracranial pressure showing symmetric pulsations (RIGHT). Figure adapted with permission from Reference [4]

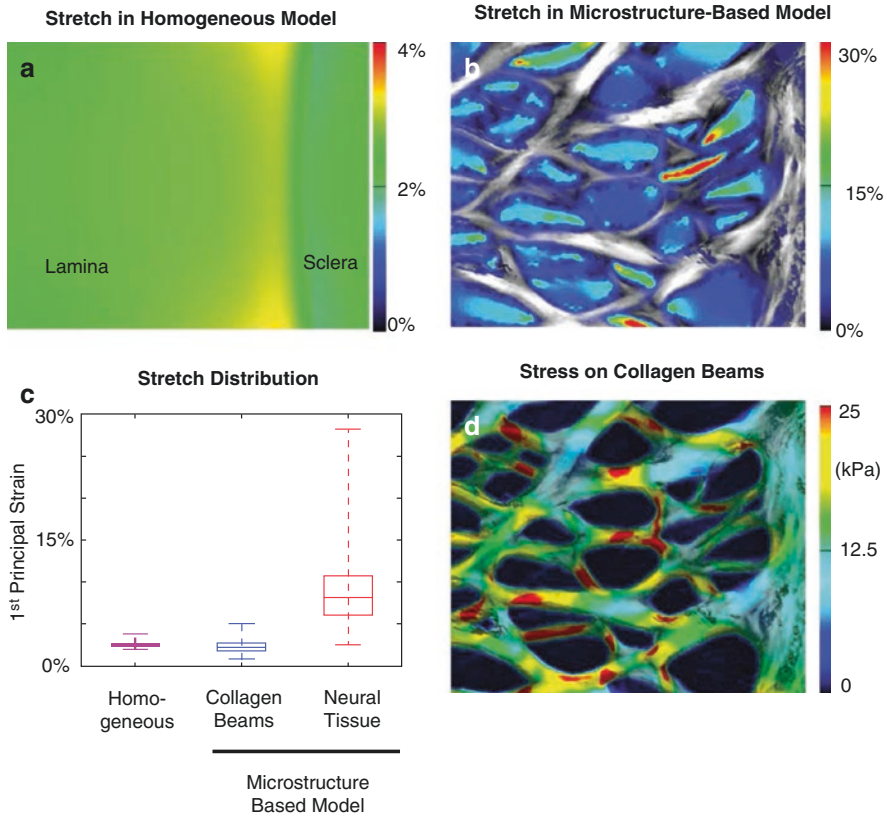

Fig. 10.14 Stretch (or strain) in the lamina cribrosa using a homogeneous model (**a**) and a microstructure-based model (**b**), with the associated stress distribution (**d**). The neural tissue experiences a large range of stretch (**c**), based on the microstructure of the lamina cribrosa. Figure adapted with permission from Reference [6]

Acknowledgments The author acknowledges the collaborative research contributions of Monica D. Okon; Ashraf M. Mahmoud; Andrew N. Springer, MD; Robert H. Small, MD; John M. McGregor, MD; and Steven E. Katz, MD.

References

1. Löfgren J, Essen CV, Zwetnow NN. The pressure-volume curve of the cerebrospinal fluid space in dogs. Acta Neurol Scand. 1973;49(4):557–74.
2. Mcalister AS. A review of the vascular anatomy of the optic nerve head and its clinical implications. Cureus. 2013;5(2):e98.
3. Singh K, Dion C, Godin AG, Lorghaba F, Descovich D, Wajszilber M, Ozaki T, Costantino S, Lesk MR. Pulsatile movement of the optic nerve head and the peripapillary retina in normal subjects and in glaucoma. Invest Ophthalmol Vis Sci. 2012;53:7819–24.
4. Liu J, Roberts CJ. Influence of corneal biomechanical properties on intraocular pressure measurement: Quantitative analysis. J Cataract Refract Surg. 2005;31(1):146–55.
5. Padayachy L, Brekken R, Fieggen G, Selbekk T. Pulsatile dynamics of the optic nerve sheath and intracranial pressure: an exploratory in vivo investigation. Neurosurgery. 2016;79:100–7.
6. Voorhees AP, Jan N-J, Flanagan JG, Sivak JM, Sigal IA. A microstructure based model of lamina cribrosa mechanical insult under IOP. Invest Ophthalmol Vis Sci. 2016;57:12.
7. Hou R, Zhang Z, Yang D, Wang H, Chen W, Li Z, Sang J, Liu S, Cao Y, Xie X, Ren R, Zhang Y, Sabel BA, Wang N. Intracranial pressure (ICP) and optic nerve subarachnoid space pressure (ONSP) correlation in the optic nerve chamber: the Beijing intracranial and intraocular pressure (iCOP) study. Brain Res. 2016;1635:201–8.
8. Okon MD, Roberts CJ, Mahmoud AM, Springer AN, Small RH, McGregor JM, Katz SE. Characterizing the cerebrospinal fluid pressure waveform and tissue compliance in idiopathic intracranial hypertension subjects. Fluids and Barriers of the CNS. 2018;15:21.

Pressure and Velocity: An Inseparable Couple

11

H. E. Killer

Pressure is probably the most frequent association with glaucoma. The effect of pressure—intraocular pressure (IOP)—however became under question when larger studies in patients with glaucomatous disc excavation and glaucomatous visual defects demonstrated that this clinical manifestations can also be present in patients with "normal" IOP. This is true for at least 30% of patients with primary open-angle glaucoma in the western hemisphere and for up to 90% of open-angle glaucoma patients in the Far East [1, 2]. Such observations stimulated the research for alternative mechanisms that could help to explain glaucomatous damage to the optic nerve. One direction of research focused on vascular dysregulation [3]. The current research topics are the concept of the translaminar pressure gradient defined as intraocular pressure (IOP)—intracranial pressure (ICP) [4–7]. The intraorbital optic nerve is located within the subarachnoid space (SAS) of the optic nerve (ON) and therefore completely surrounded with cerebrospinal fluid (CSF). The SAS itself is confined by the meninges (dura, arachnoid on one side, and the pia mater on the other side) (Fig. 11.1).

CSF enters the orbital SAS from the pituitary cistern via the optic canal and fills the SAS up to the lamina cribrosa. The lamina is therefore located between two pressure chambers, CSF pressure on one side and the intraocular pressure on the other side. According to the work of Morgan, [4] there is also a third force that needs to be taken into account, namely, the intraorbital tissue pressure (Figs. 11.2 and 11.3).

Pressure is defined as a scalar force over an area. $P = F/A$. In order for an accurate calculation to be done, the area and the force need to be known. CSF pressure is usually measured during lumbar puncture, a site quite remote from the region of interest, namely, the lamina cribrosa. IOP was measured in most studies with the Goldmann tonometer. There is no data of orbital tissue pressure in humans so far. The only data available was gathered during animal experiments [4]. The data available for ICP are pressures measured during lumbar puncture which serve as a surrogate for the SAS pressure in the SAS of the optic nerve. Due to technical difficulties, local measurements in the SAS of the ON are, to say the least, problematic. One possibility to get around this difficulty is to use the optic nerve sheath diameter (ONSD) as a surrogate for the local pressure [8]. A newly evolving technique is the noninvasive two-depth TCD device that is developed in Lithuania. First results seem to provide good results [9]. The system is currently evaluated in the neurosurgical department of Kantonsspital Aarau, Switzerland (private communication with Prof. Dr. J. Fandino).

In order to establish a model that is appropriate for the Bernoulli equation, there are some major problems in a

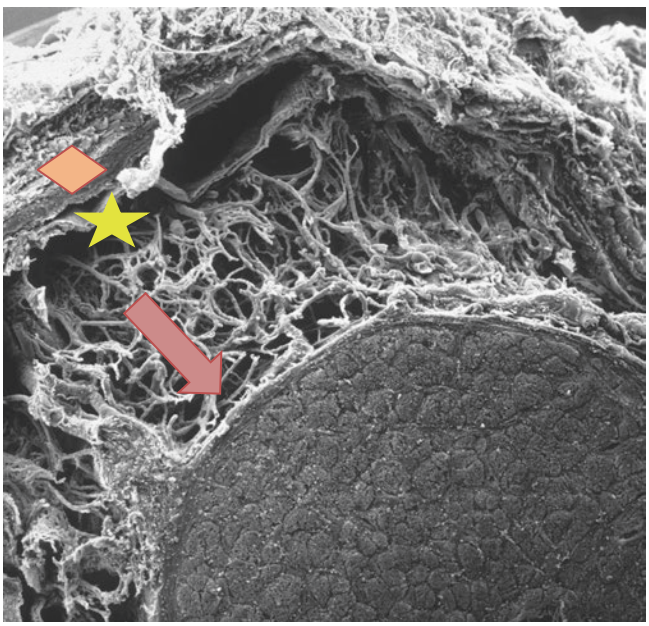

Fig. 11.1 Optic nerve with heavily trabeculated subarachnoid space. Pia mater (arrow), arachnoid layer (asterisk), and dura mater (diamond). Due to trabeculation CSF flow is in no way laminar

H. E. Killer (✉)
Department of Ophthalmology Kantonsspital Aarau, University of Basel, Basel, Switzerland
e-mail: killer@ksa.ch

N. Wang (ed.), *Intraocular and Intracranial Pressure Gradient in Glaucoma*,
Advances in Visual Science and Eye Diseases 1, https://doi.org/10.1007/978-981-13-2137-5_11

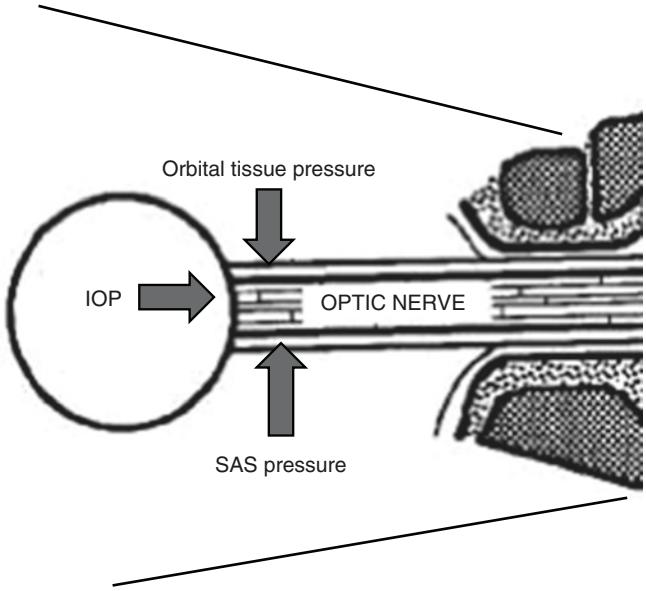

Fig. 11.2 Schematic picture of the orbit including the arrangement of all forces that influence the optic nerve and the lamina cribrosa

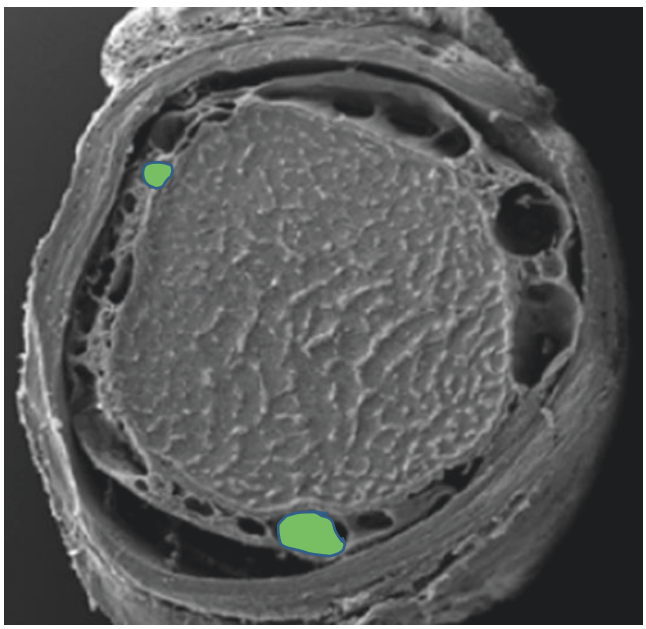

Fig. 11.3 Cross section through the optic nerve. Note that the subarachnoid space is segmented into many subunits. The area in question for the translaminar pressure is not the area of a circle but has an annular configuration

physiological setting. One of them is the composition of the fluid (CSF) as well as the nature of the subarachnoid space. Unlike a Bernoulli pipe, the SAS is not an empty but contains a complex system of trabeculae and septae that are suspended between the arachnoid and the pia layer (Fig. 11.1) [10]. This arrangement has a major effect onto the flow characteristics and flow dynamics of CSF. The bridging structures in the SAS divide the whole SAS into small units, each with their own volume, compliances, and flow behaviors. CSF as already noted is no homogenous frictionless Newtonian fluid. CSF sampling during optic nerve sheath fenestration demonstrated large concentration gradients of L-PGDS between lumbar CSF and CSF from the local SAS [11].

PGDS is the most frequent protein in CSF with a molecular weight of 29,000 Da. The concentration of this compound as well as of other proteins in CSF influences the viscosity of the fluid. This is expressed in the Navier-Stokes equation. $\rho(\partial v/\partial t + \nabla v) = -\nabla p + \nabla T + f$, where ρ represents viscosity. All the pathophysiological considerations in glaucoma so far were basically focused on the effect of pressure damage to intraocular retinal axons and ganglion cells by elevated IOP. As it becomes an evident form, the Bernoulli formula pressure however cannot be viewed in isolation if we want to apply it in a closed circuit system.

$P + phg + \frac{1}{2} pv^2 = c$. This equation shows that pressure and velocity are interdependently coupled. Isolating one term means a violation of a physical law. Changing one of them will affect the other. High pressure is therefore combined with low velocity and vice versa.

What are the consequences of this functional duality for the pathophysiology of glaucoma? CSF, just as blood, is a transport medium. It transports nutrition for neurons and axons within the central nervous system. It also works as a waste removal system that helps to maintain CNS functional. Accumulation of certain substances such as beta-amyloid, tau protein, and alpha-synuclein has been associated with the pathogenesis of neurodegenerative diseases such as Alzheimer's and Parkinson's disease [12–15].

Several studies propose that a reduced CSF turnover is associated with neurodegeneration via toxic agents in stagnant CSF [13].

Where now is the link to glaucoma? Unlike other cranial nerves, the optic nerve is not a mere nerve but a white matter tract of the brain located in the orbital socket. Another peculiarity of the optic "nerve" is its location within CSF on its entire length. CSF *is* the link that connects the brain and the optic nerve. Just as the brain (neuron, axons, and glial cells) depends on CSF cleaning, the ON (axons and glial cells) depends on it. CSF turnover in the brain is fairly well understood. While it is easy to see how CSF enters the SAS of the ON, it is far more complicated to understand how CSF can exit the SAS against the large-volume gradient that points from intracranial to the SAS of the ON. In the Navier-Stokes equation, this force is represented by $f\ (\rho(ut + (u,\nabla)u) = \eta\triangle u - \nabla p + f)$. So far three possible outflow routes have been described for the CSF surrounding the ON. A is the lymphatic system in the

dura, B is the meningothelial cells of the arachnoid and the pia mater, and C the glymphatic pathway [14, 16, 17].

$P + phg + \frac{1}{2} pv^2 = c$. The Bernoulli equation links pressure to velocity. The concept of the translaminar pressure so far only considers one part of this equation and neglects the consequences for the fluid dynamics that is related to fluid velocity. The translaminar pressure gradient concept so far focuses only on the mechanical force. Alzheimer's disease, the most common neurodegenerative disease however is not caused by simple mechanical forces but by a biochemical process mediated by toxic compounds. It therefore seems rational to postulate that at least a part of glaucomatous damage may be due to reduced CSF clearance in the SAS of the ON by reduced CSF velocity and turnover, thereby taking into account also the other part of Bernoulli's equation. In order to advance and improve the concept of the translaminar pressure, gradient reliable local pressure measurements (SAS of the ON) need to be advanced. VitaMed is such an option that demonstrated a high correlation between noninvasive and invasive ICP measurements (private conversation with Prof. Dr. J Fandino, head of neurosurgery Kantonsspital Aarau, Switzerland). As local measurements were not yet performed in larger series of patients with normal-tension glaucoma, the width of optic nerve sheath diameter could serve as a surrogate [8].

The results in different studies on the optic nerve sheath diameter however are not uniform. Some studies, most of them performed in Asia the ONSD was found to be narrow, while studies in Caucasians populations showed normal or enlarged ONSD [18, 19].

This difference might be based on genetic components between different populations as well as to different measuring techniques. The enlargement of the optic nerve sheath in the Caucasian group might be due to a higher local pressure similar to patients with elevated intracranial pressure.

Unlike in a normal population, CSF was found to be sequestered between the intracranial CSF spaces and the SAS of the ON (Killer). This finding may explain the conflict between a low CSF pressure at the lumbar site and elevated pressure in the SAS. Interesting enough a recent study demonstrated narrower optic canals in normal-tension glaucoma patients, a finding that helps to explain the formation of an optic nerve sheath compartment [20].

11.1 Conclusion

Normal-tension glaucoma is still a poorly understood entity. In addition to the intraocular pressure, the lamina cribrosa pressure gradient might play a role for the *mechanica*l component of optic nerve damage in these patients. Linked to pressure in a closed system is however the velocity of the fluid in question. As the pressure and velocity are constant according to Bernoulli's equation, they influence each other. Higher pressure results in lower velocity and therefore in a decreased CSF – dynamics and reduced CSF turnover. Considering that normal-tension glaucoma shares clear characteristics of a neurodegenerative disease, the link to Alzheimer's disease via reduced CSF clearance seems likely [21].

When researching the pathophysiology of normal-tension glaucoma, it is time to include the partner of pressure, the velocity.

References

1. Iwase A, Suzuki Y, Araie M. The prevalence of primary open-angle glaucoma in Japanese: The Tajimi study. Ophthalmology. 2004;111:1641–8.
2. Mi XS, Yuan TF, So KF. The current research status of normal tension glaucoma. Clin Interv Aging. 2014;9:1563–71.
3. Flammer J, Orgul S, Costa VP. The impact of ocular blood flow in glaucoma. Prog Retin Eye Res. 2002;21(4):359–93.
4. Morgan WH, Yu DY, Cooper RL. The influence of cerebrospinal fluid pressure on the lamina cribrosa tissue pressure gradient. Invest Ophthalmol Vis Sci. 1995;36:1163–72.
5. Jonas JB, Berenshtein E, Holbach L. Anatomic relationship between lamina cribrosa, intraocular space, and cerebrospinal fluid space. Invest Ophthalmol Vis Sci. 2003;44:5189–95.
6. Jonas JB, Wang N, Yang D. Facts and myths of cerebrospinal fluid pressure for the physiology of the eye. Prog Retin Eye Res. 2015;46:67–83.
7. Jonas JB, Wang N, Yang D. Translamina cribrosa pressure difference as potential element in the pathogenesis of glaucomatous optic neuropathy. Asia Pac J Ophthalmol. 2016;5:5–10.
8. Watanabe A, Kinouchi H, Horikoshi T. Effect of intracranial pressure on the diameter of the optic nerve sheath. J Neurosurg. 2008;109:255–8.
9. Siaudvytyte L, Januleviciene I, Ragauskas A, Bartusis L, Meiliuniene I, Siesky B, Harris A. The difference in translaminar pressure gradient and neuroretinal rim area in glaucoma and healthy subjects. J Ophthalmol. 2014, 2014:5. Article ID 937360
10. Killer HE, Hubert R, Laeng RH, Flammer J, Groscurth P. The arachnoid trabeculae and septae in the subarachnoid space of the human optic nerve: anatomy and clinical considerations. Br J Ophthalmol. 2003;87:777–81.
11. Killer HE, et al. The optic nerve: a new window into cerebrospinal fluid composition. Brain. 2006;129:1027–30.
12. Serot JM, Zmudka J, Jouanny P. A possible role for CSF turnover and choroid plexus in the pathogenesis of late onset Alzheimer's disease. J Alzheimers Dis. 2012;30:17–26.
13. Silverberg GD, Mayo M, Saul T. Alzheimer's disease, normal-pressure hydrocephalus, and senescent changes in CSF circulatory physiology: a hypothesis. Lancet Neurol. 2003;2:506–11.
14. Wostyn P, De Groot V, Van Dam D. The glymphatic system: a new player in ocular diseases? Invest Ophthalmol Vis Sci. 2016;57:5426–7.
15. Maesaka JK, Sodam B, Palaia T, Ragolia L. Prostaglandin D2 synthase: apoptotic factor in Alzheimer plasma, inducer of reactive oxygen species, inflammatory cytokines and dialysis dementia. J Nephropathol. 2013;2:166–80.

16. Killer HE, Laeng RH, Groscurth P. Lymphatic capillaries in the meninges of the human optic nerve. J Neuroophthalmol. 1999;19:222–8.
17. Fan B, Bordigari G, Flammer J. Meningothelial cells participate in immunological processes in the cerebrospinal fluid. J Neuroimmunol. 2012;244:45–50.
18. Wang N, Xie X, Yang D. Evaluation of optic nerve and optic nerve sheath diameter in primary open angle glaucoma with 3-tesla magnetic resonance imaging. Invest Ophthalmol Vis Sci. 2011;52:3963.
19. Jaggi GP, Miller NR, Flammer J, Weinreb R. Optic nerve sheath diameter in normal –tension glaucoma patients. J Ophthalmol. 2012;96:53–6.
20. Pircher A, Montali M, Berberat J. The optic canal: a bottleneck for cerebrospinal fluid dynamics in normal-tension glaucoma? Front Neurol. 2017;8:47.
21. Wostyn P, De Groot V, Van Dam D. The two faces of the translaminar pressure difference: the biomechanical one and the biochemical one. Clin Exp Optom. 2017;100:102–3.

Facts and Myths of Cerebrospinal Fluid Pressure for the Physiology of the Eye

12

Jost B. Jonas and Ningli Wang

In a strict sense, the term "optic nerve" is not correct, since the optic nerve is part of the central nervous system and is not similar to a peripheral nerve or other cranial nerves, such as the trigeminal nerve. As part of the central nervous system, the optic nerve is surrounded by the meninges and surrounded by cerebrospinal fluid (CSF). Since the optic nerve as a cerebral neural fascicle leaves the intracranial space, the CSF space extends from the intracranial compartment through the tiny optic canal into the orbit and ends anteriorly at the back of the globe. The tissue pressure in the orbital part of the optic nerve is therefore not equal to the tissue pressure in the orbit (about 2 mmHg [1, 2]) but is at least as high as the pressure in the orbital CSF space or the orbital CSF pressure (CSFP) [3–15]. These anatomic relationships may be of profound importance for the physiology and pathophysiology of the optic nerve head (optic disc), which acts as the pressure barrier between the intraocular compartment and the retrobulbar compartment.

The term "intraocular pressure" (IOP) is also a misnomer, since the IOP is really the transcorneal pressure difference, measured by corneal applanation or indentation [7] (Fig. 12.1). The physically true "intraocular pressure" is the pressure in the anterior chamber plus the pressure external to the eye, which usually equals the atmospheric pressure. It explains why the physical pressure in an eye with an "IOP" of 40 mmHg is just 2.5% higher than the physical pressure in an eye with an IOP of 20 mmHg. An IOP of 40 mmHg translates into a physical pressure of an external atmospheric pressure of 760 mmHg plus 40 mmHg (800 mmHg) compared to a physical pressure of 760 mmHg plus 20 mmHg (780 mmHg) in the eye with an IOP of 20 mmHg. Correspondingly, diving in water to a depth of 100 meters increases the physical pressure in the eye by a factor of 11 or about 11 times atmospheric pressure. Although the physical pressure in the intraocular compartment is markedly elevated, it does not lead to acute glaucoma situation, since the transcorneal pressure difference remains unchanged. As a corollary, an acute glaucoma attack due to intraocular reasons may be present in a patient on the top of Mount Everest, although the physical pressure in this eye is about only 50% of the pressure at sea level. Its transcorneal pressure difference (i.e., IOP), however, can be markedly elevated due to intraocular changes. The transcorneal pressure difference, or so-called IOP, is only of partial importance for the physiology and pathophysiology of the optic nerve head, since the latter forms the border between the intraocular space and the retrobulbar compartment. For the optic nerve head, the translamina cribrosa pressure difference (TLPD) plays a direct role, since the TLPD is the difference between the IOP and the retrobulbar pressure [7] (Fig. 12.1). The latter is either the optic nerve tissue pressure in the case of a very low orbital CSFP, or it is equal to the orbital CSFP, if the latter is higher than a threshold value of about 4 mmHg, as revealed by an experimental study in dogs [10]. The latter study had the limitation that dogs as compared to humans have a completely different body posture and thus a different relationship between height of the brain and height of the spine. The value of 4 mmHg may therefore be specific for dogs and may not directly be transferred onto the human situation. It generally shows however that the IOP as only one of the two determinants of the TLPD does not fully explain the pressure situation at the optic nerve head. Optic nerve diseases which originate at the optic nerve head and which are influenced by the pressure situation at the optic nerve head can theoretically thus be influenced by an abnormal IOP and/or by an

J. B. Jonas (✉)
Department of Ophthalmology, Medical Faculty Mannheim of the Ruprecht-Karls-University, Seegartenklinik Heidelberg, Heidelberg, Germany
e-mail: jonas@medma.uni-heidelberg.de

N. Wang
Beijing Institute of Ophthalmology, Beijing Tongren Eye Center, Beijing Tongren Hospital, Capital Medical University, Beijing, China

Beijing Ophthalmology & Visual Sciences Key Laboratory, Beijing, China
e-mail: wningli@vip.163.com

N. Wang (ed.), *Intraocular and Intracranial Pressure Gradient in Glaucoma*,
Advances in Visual Science and Eye Diseases 1, https://doi.org/10.1007/978-981-13-2137-5_12

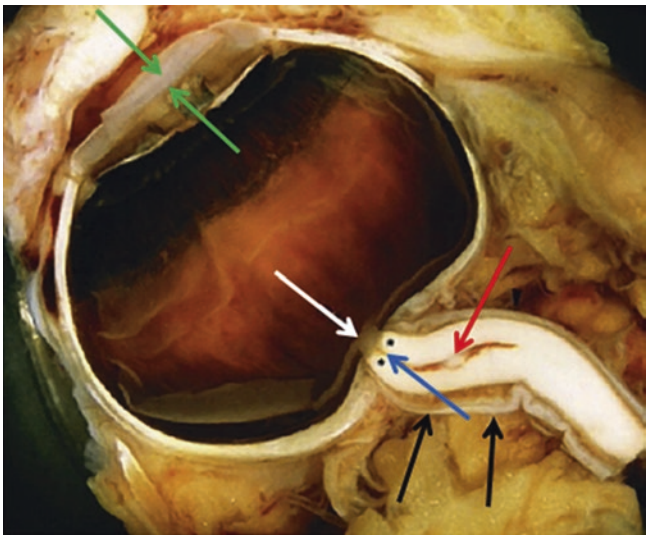

Fig. 12.1 A globe showing the transcorneal pressure relationship (green arrows), the trans-lamina cribrosa pressure relationship (between white arrow and blue arrow), the central retinal vessel trunk in the retrobulbar optic nerve (red arrow), and the orbital optic nerve dura mater (black arrows) with the adjacent orbital cerebrospinal fluid space

abnormal orbital CSFP. This anatomical and physiological fact was the basis for the theory that some patients with so called normal-pressure glaucoma (NPG) could have an abnormally low orbital CSFP leading to an abnormally high TLPD, analogous to the situation as if the IOP were to be slightly elevated and the orbital CSFP normal [7, 9–16].

Although the TLPD is the counter-pressure against the IOP, one has to take into account that, from a practical point of view, the TLPD is still also a misnomer, since studies addressing the TLPD have so far measured the CSFP only at the lumbar level and not in the orbital space. The TLPD has thus not yet been measured. What has partially been addressed so far is the CSFP taken during lumbar puncture, a site that is more than 100 cm away from the lamina cribrosa. The assumption that the pressure in this location equals the pressure behind the lamina cribrosa is speculative. A study by Lenfeldt and colleagues [17] compared the lumbar CSFP with the parenchymal brain pressure but not with the CSFP in the subarachnoid space of the optic nerve. Lenfeldt et al. included in their study patients with normal-tension hydrocephalus, but not normal subjects. They concluded that the CSFP in the lumbar region was the same as that in the brain given an open pathway for the CSF. It may clearly show that even if the lumbar CSFP equals the ventricular CSFP, the pressure in the orbital portion of the subarachnoid space will not be known.

In considering the orbital CSFP as counter-pressure against the IOP across the lamina cribrosa (LC), one must also take into account that the subarachnoid pressure behind the lamina cribrosa is not constant for various reasons. One of these are the pulse-synchronous changes of the intracranial CSFP, which will likely be forwarded through the open optic nerve canal into the orbital CSF space. Another reason for the orbital CSFP changes are movements of the optic nerve, which is almost constantly moving due to the movements of the globe. Since the changes in the orbital CSFP do not occur at the same time and for the same amount as the changes in IOP, the TLPD varies. The amount and exact timing of these TLPD changes have remained unexplored yet, however, may be of high importance for the physiology and pathophysiology of the optic nerve.

Besides the TLPD as the difference of IOP minus orbital CSFP, the CSFP may have additional importance for ocular physiology and pathophysiology, since the central retinal vein passes from the optic nerve head through the optic nerve and the orbital CSF space and then drains into the superior orbital vein, which eventually runs back into the intracranial compartment. One may postulate that the pressure in the central retinal vein should be at least as high as the orbital CSFP plus a pressure value due to a hypothetical trans-lamina cribrosa outflow resistance. A trans-lamina cribrosa outflow resistance may be defined as resistance to the passage of venous blood through the lamina cribrosa, perhaps in a parallel manner to the resistance to the passage of the orthograde axoplasmic flow across the lamina cribrosa, with the latter mechanism necessitating a higher IOP than orbital CSFP. The trans-lamina cribrosa outflow resistance to the venous efflux may be increased in eyes with glaucomatous optic neuropathy due to glaucoma-associated changes in the lamina cribrosa. These changes include thinning or condensation of the lamina cribrosa as shown histomorphometrically in human eyes with advanced glaucoma [18, 19]. The potentially increased trans-lamina cribrosa outflow resistance in glaucomatous eyes could explain the finding of decreased retinal artery diameters, but mostly unchanged retinal vein diameters in eyes with advanced glaucoma [8, 20, 21], and the observation of elevated retinal venous pressure as determined by ophthalmodynamometry [22]. The anatomic relationship between the retinal vein and the orbital CSFP space opens the possibility to estimate the CSFP by determination of the central retinal venous pressure with ophthalmodynamometry [23–29]. However, the ophthalmodynamometer as a potentially noninvasive CSFP measuring device has so far not found general approval nor has it generally been considered to be reliable.

Also, the choroidal blood drains through the vortex veins to the superior orbital vein and indirectly back into the intracranial compartment. Based on this anatomic fact, one may postulate that the venous blood pressure (BP) in the choroid may be influenced by intracranial CSFP [30].

In a similar manner, the episcleral veins, which take up the aqueous humor and which directly influence the IOP, drain through the superior orbital vein into the intracranial system. The episcleral vein pressure may thus depend on the intracranial CSFP [5].

Besides these considerations of the static aspects of the intracranial and orbital CSFP, the TLPD, and the IOP,

specifics of the dynamics of the CSFP and IOP may need to be taken into account [31] if their role in the physiology and pathophysiology of the eye in general and the optic nerve head in particular is discussed [31–34].

Finally, it may be taken into account that the CSF and aqueous humor share many similarities, as both are produced by carbonic anhydrase-catalyzed reactions, generally represent an ultrafiltrate of blood, and have nearly identical chemical composition, with more proteins and less ascorbate in the CSF than in the aqueous humor. Normal intracranial CSFP has generally been considered to be approximately 5–15 mmHg in healthy supine adults, 3–7 mmHg in children, and 1.5–6 mmHg in infants [35]. Physiologically, IOP and CSFP are dynamic parameters; both have circadian variations and similar response to changes in posture and intra-abdominal or intrathoracic pressures [36]. Correspondingly, studies have suggested a positive correlation between the CSFP and IOP [37, 38]. While the circadian cycle of IOP is quite well known [39], the circadian pattern of the CSFP is less clear, suggesting a nocturnal elevation in CSFP [40]. It is another similarity between IOP and CSFP, since both increase at night in the supine position.

12.1 Anatomy of the Optic Nerve Head and Orbital CSF Space

The optic nerve head or optic disc is the region located nasally close to the posterior pole and through which retinal ganglion cell axons and the central retinal vein exit and the central retinal artery enters. It simultaneously keeps the eye wall sufficiently watertight to prevent a major drop in IOP by a major outflow of intraocular fluid. For that purpose, the bottom of the optic nerve head is formed by the LC as a sievelike structure. The LC is the continuation of the peripapillary scleral flange which forms the anterior roof of the orbital CSF space and which is the continuation of the inner layer of the posterior sclera ([41, 42];) (Fig. 12.2). This inner scleral layer comprises approximately 50% of the posterior scleral thickness. The outer layer of the posterior sclera merges with the dura mater of the optic nerve. The LC is composed of several layers and shows pores of variable size [43]. The largest pores are located close to the inferior and superior poles of the optic disc. The pores of the layers of the LC are not completely congruent to each other but can deviate between the layers. This can lead to a splitting up of the retinal ganglion cell axon bundles during their passage through the LC.

Previous studies reported that the LC is not completely watertight but allows diffusion of fluid from the vitreous cavity into the retrobulbar CSF space [44–47]. This may be the reason for the clinical observation that after pars plana vitrectomy, pigment particles can settle at the bottom of the cup, with the LC potentially serving like a sieve. Similarly, it may be one reason why triamcinolone acetonide crystals accumulate close to the optic nerve head after a recent intravitreal injection (Fig. 12.3). The diffusion of intraocular fluid through the LC may also lead to a change in the composition of the orbital CSF. It has not yet been determined whether the trans-

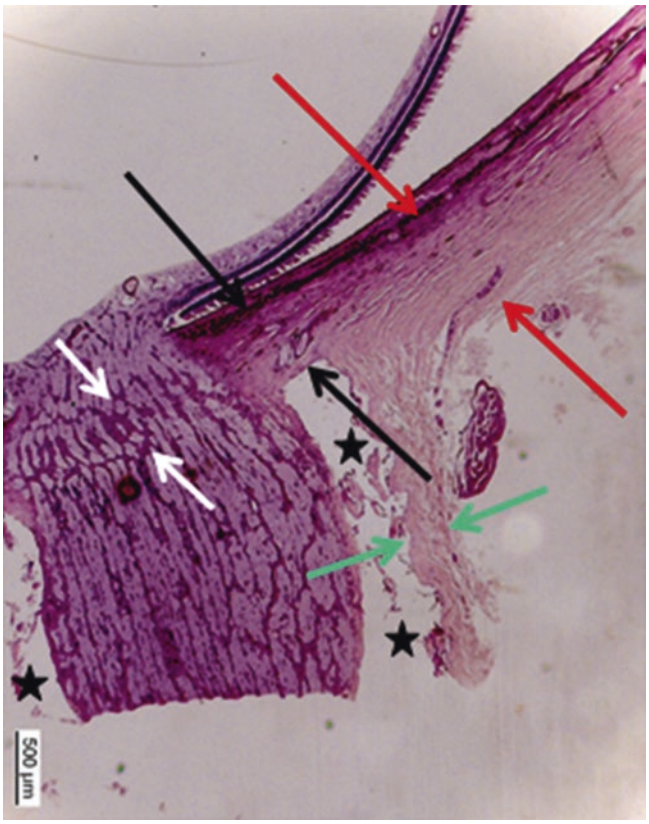

Fig. 12.2 Photohistograph of a normal optic nerve head, with the lamina cribrosa (white arrows), the peripapillary scleral flange (black arrows), the posterior sclera (red arrows), the dura mater of the optic nerve (green arrows), and the orbital cerebrospinal fluid space (black stars)

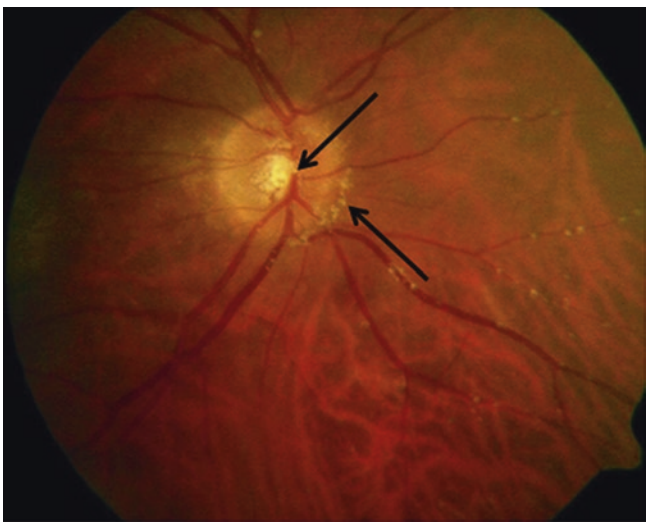

Fig. 12.3 Fundus photograph of an eye shortly after an intravitreal injection of crystalline triamcinolone acetonide, with the crystals (black arrows) accumulated at the optic nerve head

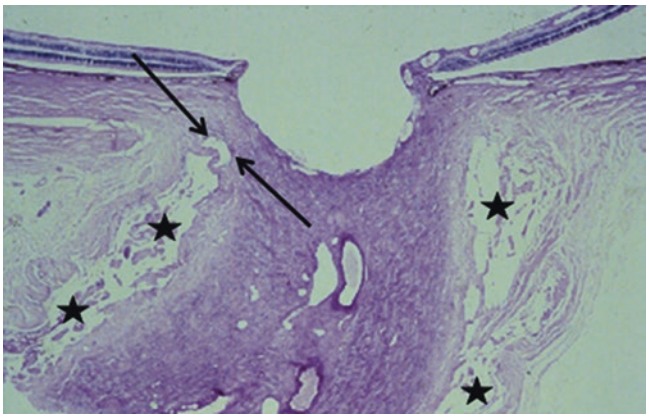

Fig. 12.4 Photohistograph of a glaucomatous optic nerve head. The peripheral posterior surface of the lamina cribrosa (between black arrows) is (no longer) covered by the solid optic nerve but, due to the shrinkage of the optic nerve, directly exposed to the retrobulbar cerebrospinal fluid space (black stars)

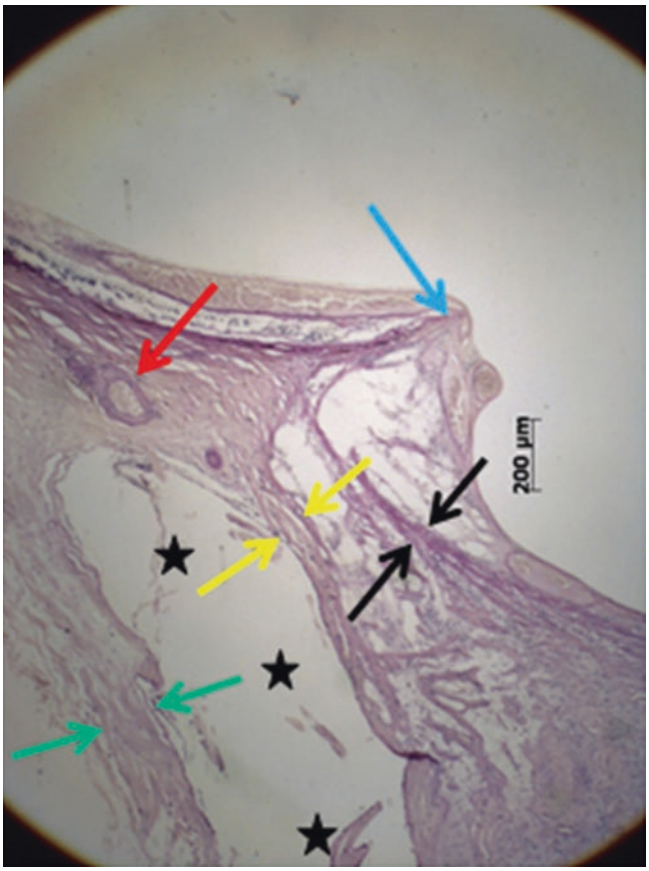

Fig. 12.5 Photohistograph of a glaucomatous optic nerve head, with the very thin lamina cribrosa (black arrows), the pia mater of the optic nerve (yellow arrows), the dura mater of the optic nerve (green arrows), the peripapillary arterial circle of Zinn-Haller (red arrow), the end of Bruch's membrane (blue arrow), and the orbital cerebrospinal fluid space (black stars)

lamina cribrosa fluid flow reduces IOP and by which factors it is influenced. Considerations based on anatomy and physiology may make one assume that a higher amount of trans-lamina cribrosa fluid flow may be related with a higher TLPD, a larger optic disc, a larger optic cup, a smaller neuroretinal rim, and a vitreous-free zone in the region of the optic nerve head to allow the fluid free access to the optic disc surface. A higher TLPD may be able to press more fluid through the optic nerve head into the orbital CSF space. A larger optic disc surface and a larger optic cup surface may give more space for the trans-lamina fluid flow. A smaller neuroretinal rim associated with a larger optic cup may lead to the same result. Finally, a vitreous-free zone in front of the optic disc may allow the fluid free access to the optic nerve head. Since the central part of the posterior LC surface continues into the trunk of the optic nerve, one may assume that the trans-lamina cribrosa fluid flow may take place predominantly through the peripheral region of the LC. It may in particular be the case if the peripheral posterior surface of the LC is not, or is no longer (as in the case of optic nerve atrophy) (Figs. 12.4 and 12.5), covered by the optic nerve tissue but directly exposed to the orbital CSF space [18, 19].

Besides the description of the laminar anatomy as it appears in enucleated fixed specimens, one should note that the LC in vivo is in continuous movement. Due to pulse-synchronous changes in the TLPD, the LC moves back and forth in a sagittal direction in a frequency synchronous with the pulse. The amplitude of these sagittal laminar movements may depend on the height of the TLPD, on the pulse-synchronous changes in the TLPD, and on biomechanical properties of the LC, the peripapillary scleral flange, and the optic nerve tissue. The optic nerve tissues buffer the backward movement of the LC and mechanically limit the movements of the LC.

In addition to the sagittal movements of the LC, the tissue in the vicinity of the LC, and possibly also in the LC, undergoes movements in the coronary plane, i.e., in the vertical and horizontal directions. About 80% to 90% of normal eyes spontaneously show pulsations of the central retinal vein [48]. The vein pulsations lead to a pulse-synchronous compression and decompression of the tissue in the coronary plane. The degree of these coronary movements may depend on the amplitude of the central retinal vein pulsation and again on the biomechanical properties of the LC and its adjacent tissues. It remains unclear how far the central retinal vein pulsations detectable upon ophthalmoscopy in the prelaminar region extend into the LC itself.

The physiological importance of the LC movements remains unclear. One may hypothesize that the movements are helpful to allow the orthograde axoplasmic flow to enter the eye and the retrograde axoplasmic flow to leave it [31, 33, 49, 50]. It may perhaps be a bit similar to a "massage" of the axons. Since the LC movements presumably are physiologically important, any factor changing them will have

pathophysiological meaning. Since the TLPD as external counter-pressure against the IOP influences the sagittal lamina cribrosa movements, and since the orbital CSFP determines the central retinal vein pressure and thus the amplitude of the spontaneous central retinal vein pulsations, the CSFP may be of indirect or direct importance for both types of LC movements.

12.2 Associations of CSFP and IOP and Dynamics of CSFP and IOP

12.2.1 Associations with IOP and Blood Pressure

Recent studies suggest a correlation between a higher CSFP and higher IOP in patients without major neurological abnormalities and without a markedly elevated IOP [13, 38, 51–54]. Sheeran and colleagues' study on 22 neurosurgical patients demonstrated a significant correlation between IOP and CSFP and simultaneously concluded that changes in IOP were a poor predictor of changes in CSFP. In other studies, a correlation between IOP and CSFP was not found [55–57]. The reason for the discrepancies between the studies may be that the association between IOP and CSFP is valid only under mostly physiological conditions. If IOP is markedly changed (such as in angle-closure glaucoma or ocular hypotony due to an overactive filtering bleb) or if CSFP is markedly changed (as in the case of cerebral tumors), the relationship between IOP and CSFP may no longer be valid. In addition, a significant variability in IOP and in CSFP may prevent a clinically valid use of IOP as surrogate for CSFP and vice versa [53].

An association between IOP and CSFP, which also share similarities in their composition, in their physiological pressure range, and in their response to changes of intraabdominal and intrathoracic pressure, has also been found experimentally (Fig. 12.6). In rhesus monkeys, acutely raised CSFP caused an acute increase in IOP, though it plateaued thereafter [58]. The authors explained the fast changes in IOP and CSFP by a probable alteration of intraocular and intracranial blood volumes. In another animal study, CSFP and IOP changed in parallel during respiratory acidosis and alkalosis [59]. The causes for a physiological association between IOP and CSFP have so far remained elusive. One may consider that the CSFP in a retrograde manner influences the pressure in the superior ophthalmic vein and thus in the episcleral vein, the pressure of which directly and linearly influences the IOP.

Interestingly, CSFP is related to BP (Fig. 12.6) [13, 60]. There is an association between higher BP and higher IOP [61, 62]. One may assume a physiological association between IOP, CSFP, BP, and IOP, potentially with the BP (and the heart) as the driving force. The mechanism behind such a triangular relationship has thus far remained unclear. In a recent experimental study, chemical stimulation of the

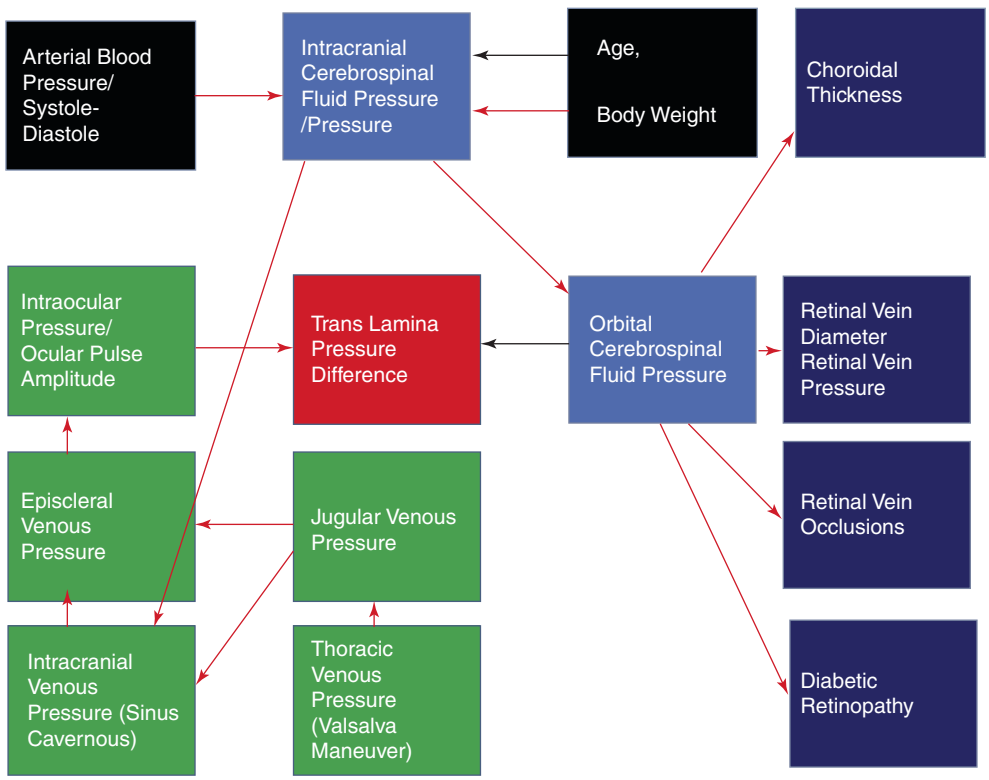

Fig. 12.6 Scheme illustrating the relationships between cerebrospinal fluid pressure, intraocular pressure, and other ocular and systemic parameters (red arrows, positive relationship; black arrows, negative relationship)

dorsomedial/perifornical hypothalamic region evoked substantial increases in IOP, CSFP, TLPD, heart rate, and mean arterial blood pressure in rats [63]. The authors postulated that the dorsomedial and perifornical hypothalamic neurons may be a key effector pathway for circadian regulation of the autonomic tone by the suprachiasmatic nucleus.

Morgan and colleagues have shown that the pressure wave starting at the heart at the beginning of systole arrives first in the brain and orbital CSF space before leading to a pulse-synchronous IOP increase [33, 64]. This means that the TLPD is not constant but fluctuates due to the difference in the arrival time first of the pressure wave in the orbital CSF and then the pressure wave in the intraocular compartment. During an early and brief period of the pulse phase, the orbital CSFP increases in relation to the IOP, so that the TLPD decreases. If, for this short fraction of the pulse phase, the orbital CSFP may actually become higher than the IOP, the TLPD could be briefly reversed. Whether the orbital CSFP may shortly get higher than the IOP is a matter of discussion and will depend on the body posture. A short period of higher orbital CSF pressure than intraocular pressure may occur after lying down when due to hydrostatic reasons, the CSFP is elevated at once after lying down; however, the IOP may need some more time to elevate. In a recent study by Jasien and colleagues (own data), the IOP in head-down yoga positions took about 1 minute to get elevated. The pulse-synchronous swinging of the TLPD may be physiologically important for retrograde axoplasmic flow, which would have difficulty entering the eye against an otherwise marked pressure gradient [31, 33]. If that is the case, any change in the timing of the arrival of the pressure wave in the orbital CSF space compared to the IOP compartment may result in an altered variation of the TLPD and thus in pathophysiological consequences for the axoplasmic flow. An impeded axoplasmic flow has been discussed in association with the pathogenesis of glaucomatous optic neuropathy.

In the discussion about the dynamics of the CSFP and IOP, one may also wonder how exactly the LC moves and how it is related to the biomechanical properties of the sclera and optic nerve head. One may imagine that the sagittal movements of the LC occur a bit similar to the door wings of a saloon, with the door hinge in the region of the peripapillary scleral flange. Histological studies have revealed that in eyes with an axial length greater than 26.5 mm, the peripapillary scleral flange markedly thins with increasing axial length. In highly myopic eyes, the flange can be increased to ten times its normal length and decreased to 10% of its normal thickness [65, 66]. One may infer that the sagittal movements of the lamina cribrosa differ markedly between highly myopic eyes and non-highly myopic eyes. An additional possibility can be that in highly myopic eyes, the very thin peripapillary scleral flange itself moves back and forth by the undulation of the pressure difference, since the peripapillary scleral flange is, similar to the lamina cribrosa, the border tissue between the intraocular compartment and the orbital CSF space.

Another question is what the basis is for the IOP fluctuations. In a study by Kaufmann and colleagues applying dynamic contour tonometry, higher ocular pulse readings were associated with higher IOP and shorter axial length [67]. The authors discussed that, according to a previous investigation by Wegner in 1930, systole-associated filling of the orbital vessels causes a pulsatile protrusion of the whole globe, allowing for pressure wave recordings even from enucleated eye sockets [68]. Real intraocular reasons for the ocular pulse are mostly the systole-associated filling of the choroidal vessels [69]. This could explain the positive association between the ocular pulse amplitude and IOP in Kaufmann's study. The negative correlation between the ocular pulse amplitude and longer axial length can be attributed to the larger intraocular volume of eyes with longer axial length so that a given inflow of blood represented a smaller relative volume change in myopic eyes than in hyperopic eyes [67, 70]. Another factor influencing the ocular pulse amplitude may be the expansibility of the ocular coats accommodating for the systole-associated increase in choroidal volume. Since myopia is associated with thinning of the sclera, with presumably less resistance to expansion in the posterior half of the globe, it may be another mechanism leading to lower ocular pulse amplitude in myopic eyes. Other parameters which may play a role are the relationship between blood pressure and pulse pressure amplitude and how this relation is dependent on intraocular volume or what in general is the relation between intraocular volume and IOP. Addressing the latter question, several population-based studies have revealed that IOP increases with longer axial length (Jonas et al. [71]).

In addition to the pulse-synchronous changes in CSFP, IOP, and TLPD, both IOP and CSFP also change in relationship to body position. In the supine position compared to the standing position, or even more marked in a headstand, both IOP and CSFP increase [72–81]. Questions remain as to whether body position-dependent changes in the pressure on both sides of the lamina cribrosa (i.e., IOP and orbital CSFP) occur at the same amount and at the same time, so that it remains unclear whether and how the TLPD depends on body position. One may assume that, due to hydrostatic reasons and the principle of communicating tubes assumedly present in the circulatory system of the CSF, the CSFP rapidly changes with any change in body position. In contrast, the IOP, which is not directly associated with hydrostatic body position-dependent changes, may take longer to adapt to new body positions. This adaptation may occur through changes in the episcleral venous pressure, choroidal blood pressure, and other factors. The time lag between an immediate adaptation of the CSFP and a later occurring adaptation

of the IOP on new body positions leads to body position-dependent changes in the TLPD. If these TLPD changes are prolonged, optic nerve damage may result. As an example, if a person lies down to sleep, the CSFP increases immediately, and the IOP lags behind. In the first minutes after lying down, the TLPD is reduced. If the person gets up, the CSFP drops immediately, while the reaction of the IOP again lags behind. It leads to an increase in the TLPD. If this high-TLPD phase takes longer than physiologically allowed, optic nerve damage will develop, even if IOP, CSFP, and TLPD would be normal at measurements performed during daytime or during sleeping.

The changes in pressure occurring in both the intraocular compartment (i.e., IOP) and the orbital CSF compartment (i.e., orbital CSFP) are supplemented by changes in the orbital CSFP due to the continuous movements of the optic nerve. It remains unclear how much this unilateral change in pressure (i.e., only the orbital CSFP) affects the TLPD. In that context one may additionally argue that any movement of the globe also leads to changes in IOP, due to the pull on the external ocular muscles and the pressure thus exerted onto the globe.

12.2.2 Associations with Changes in Thoracic Pressure

Besides changes in body position, changes in thoracic pressure influence CSFP and IOP [82]. IOP increases during horn blowing [83]. In players of high-resistance instruments, Schuman and colleagues observed an IOP elevation dependent on the force of blowing and uveal thickening associated with IOP elevation. The magnitude of IOP elevation was dependent on the amount of expiratory resistance provided by the particular instrument. Schuman and colleagues concluded that high- and low-resistance wind musicians experienced a transient rise in their IOP while playing their instruments as a result least in part of uveal engorgement. They also observed that cumulative lifetime hours of high-resistance wind instrument playing had a marginally significant ($P = 0.03$) relationship to visual field loss and corrected pattern standard deviation (CPSD) scores ($P = 0.007$) in univariate logistic regression and univariate linear regression, respectively. One may also argue that the rise in IOP observed in Schuman's study was due to an elevation of the episcleral venous pressure, which increased due to an increase in CSFP, which increased due to the elevation in jugular venous pressure. In a similar manner, the potential increase in CSFP might have caused choroidal thickening, which then was an additional factor for the increase in IOP. An association between subfoveal choroidal thickness and estimated CSFP has been discussed in a recent study [30]. It remains unclear whether the timing of the horn blowing-associated rise in IOP differs from the timing of the rise in CSFP, so that the TLPD may be changed. It may be of importance in counseling glaucoma patients playing high-resistance wind instruments.

Finally, if changes in body position are not associated with changes in IOP and CSFP, as in the case of astronauts spending several months in space, the TLPD is markedly changed for a long period of time. Recent studies have suggested that the majority of astronauts spending more than 6 months in the space laboratory develop optic disc edema with retinal nerve fiber layer loss [84–86]. Investigations are ongoing on how the optic nerve damage due to the zero gravity-induced change in the relationship of IOP to CSFP can be prevented. It may perhaps be a possibility yet unexplored whether an induced rise in IOP by topical applications of steroids could counteract the indirect rise in orbital CSFP caused by the zero gravity.

12.3 Methods for Estimating or Measuring CSFP

CSFP has usually been measured by direct lumbar puncture or, more recently, by a pressure sensor implanted into the cerebral ventricles or spinal canal [17, 87, 88]. Since these direct methods are invasive and harbor the risk of infections and lesions to the brain and spine [89, 90], noninvasive technologies are needed. Methods applied for noninvasive estimation of CSFP have been transcranial Doppler ultrasonography, tympanic membrane displacement, ophthalmodynamometry, measurement of the orbital CSFP space around the optic nerve, two-depth transcranial Doppler technology, and others [23, 91–100].

Transcranial Doppler ultrasonography measures blood flow velocity in the middle cerebral artery. Klingerhofer and coworkers described that the flow patterns in the middle cerebral artery measured by transcranial Doppler ultrasonography were related to changes in CSFP [101]. These were findings of a pilot study on patients with dissociated brain death and may thus not be very helpful to measure CSFP under normal conditions. Other investigators reported that the pulsatility index (difference between systolic and diastolic flow velocities, divided by mean flow velocity) of the middle cerebral artery was associated with CSFP [102]. Others, however, did not find a significant relationship between the pulsatility index and CSFP [103–105]. Reasons may have been the intra-observer and interobserver variation of the technique that the method cannot be applied in about 10–15% of patients and that the pulsatility index depends on a multitude of parameters including arterial pressure pulsatility, pulse, cerebral perfusion pressure, arterial carbon dioxide concentration, and others [106].

Estimation of CSFP by tympanic membrane displacement technique requires a patent cochlear aqueduct, normal middle ear pressure, and an intact stapedial reflex. According to studies by Reid, Lang, and others, stimulation of the stapedial reflex causes movement of the tympanic membrane, the amplitude of which correlates with CSFP [107, 108]. Shimbles and collaborators reported on an association between the CSFP measured by the tympanic membrane displacement method and direct lumbar CSFP measurements [109]. Due to a high intersubject variability, however, the diagnostic precision was too low for a practical and valid use. In addition, the perilymphatic duct becomes permeable with older age, further decreasing the practicality in elderly individuals.

Ophthalmodynamometry is a noninvasive technique to estimate the BP in the central retinal artery and central retinal vein [5, 6, 22–24, 110–115]. The application of ophthalmodynamometry for the estimation of CSFP is based on the anatomic consideration that the central retinal vein passes through the optic nerve head and the first 10 mm of the anterior portion of the optic nerve before it pierces through the orbital CSF space and the optic nerve meninges. The pressure in the central retinal vein on the surface of the optic nerve head should therefore be at least as high as the orbital CSFP, plus a hypothetical pressure caused by trans-lamina cribrosa outflow resistance [25–27]. In a first step, the optic nerve head is examined ophthalmoscopically with a noncontact ophthalmoscopic lens. In 80 to 90% of all normal subjects, a spontaneous pulsation of the central retinal vein can be observed [48, 116]. If there is no spontaneous vein pulsation, a Goldmann contact lens with a pressure sensor in its holding grip is put onto the cornea, and a slight pressure is applied until the vein (or the artery) shows early pulsations. At that point, the pressure applied onto the contact lens plus the IOP at baseline gives the diastolic central retinal vein (and artery) pressure. In studies by Motschmann and Firsching and colleagues, the pressure measured by ophthalmodynamometry correlated linearly with the CSFP [24, 117, 118]. Firsching and collaborators reported that an increased pressure of the central retinal vein indicated an elevated CSFP in 84% of patients with increased intracranial pressure, whereas a normal pressure of the central retinal vein indicated a normal CSFP in 93% of subjects with normal brain pressure [24]. Ophthalmodynamometry can thus be a valid and noninvasive tool to estimate elevated CSFP. It is, however, usually not possible to detect an abnormally low CSFP, since the technique can be applied only if there are no spontaneous pulsations of the central retinal vein. In addition, glaucomatous changes of the lamina cribrosa may increase the trans-lamina cribrosa outflow resistance so that the central retinal vein pressure is no longer directly correlated with the orbital CSFP [18, 19]. It remains unclear whether and how much an increased trans-lamina cribrosa outflow resistance, caused by glaucomatous changes in the LC, such as thinning and condensation of the LC tissue, influences the central retinal vein pressure.

Assuming free communication of fluid between the intracranial compartment and the orbit through the optic nerve canal, the width of the orbital CSFP space has been considered to correlate with the lumbar CSFP. Correspondingly, sonographic studies revealed that an enlarged optic nerve sheath diameter as measured by ultrasound correlated with elevated CSFP [91, 119–127]. Using sonography, Pinto et al. did not detect a significant difference in optic nerve sheath diameter between patients with NPG, patients with high-pressure glaucoma, and healthy controls [128]. That finding contradicted the hypothesis of an abnormally low CSFP in some patients with NPG. Besides a relatively poor reliability of the sonographic measurement of the optic nerve sheath diameter [127], a major limiting factor of the technique is that the diameter of the optic nerve influences the optic nerve sheath diameter. In patients with optic atrophy and a reduced optic nerve diameter, a normal sheath diameter could be associated with an elevated CSFP. Using computerized tomography, Jaggi et al. measured the widest intraorbital optic nerve sheath diameter in 18 patients with NPG and 17 age- and gender-matched patients without optic nerve or intracranial disease [129]. They found that patients with NPG as compared with the individuals of the control group had a significantly ($P < 0.001$) larger optic nerve sheath diameter (right side, 7.9 ± 0.9 mm; left, 8.0 ± 1.1 mm, versus right side, 6.3 ± 0.5 mm; left side, 6.1 ± 0.6 mm). Although mentioning that an increased optic nerve sheath diameter is generally considered to be associated with an increased CSFP, Jaggi and Killer concluded that the increased optic nerve sheath diameter in the patients with NPG might have been due to an optic nerve sheath compartmentation or due to the thinning of the optic nerve in the study with group with NPG [129]. These examples show that there may be other features which are not currently understood concerning optic nerve sheath dimensions and CSFP.

Magnetic resonance imaging (MRI) may overcome the limitations of sonography and computed tomography with respect to the dependence of the optic nerve sheath diameter on the optic nerve diameter. Using MRI, Wang and colleagues measured the orbital subarachnoid space width by subtracting the optic nerve diameter from the optic nerve sheath diameter, with both diameters measured on the MRI images [16]. They found significantly smaller measurements of the orbital cerebrospinal fluid compartment width in Chinese patients with NPG compared to Chinese patients with high-pressure glaucoma or normal Chinese subjects. In another study, Xie et al. showed a linear relationship between the orbital CSF space width determined by MRI and direct lumbar CSFP measurements [99].

Using the data obtained in Xie et al.'s study [99], Jonas and colleagues from the same study team calculated a formula to estimate the CSFP of a normal population [130]. Xie's study included 74 patients with a mean age of 42.0 ± 13.4 years and a CSFP of 12.6 ± 4.8 mm Hg. The final diagnosis of the patients included diseases such as peripheral neuropathy, multiple sclerosis, unilateral ischemic optic neuropathy, and unilateral optic neuritis, in which it was unlikely that the neurological disease was associated with an abnormal CSFP. Out of the total group, a training group was randomly formed consisting of 32 patients and a testing group including the remaining 42 patients. Due to randomization, the training group and testing group did not differ significantly in age, gender, body height and weight, body mass index, intraocular pressure, retinal nerve fiber layer thickness, and arterial blood pressure (all $P > 0.10$). Performing a multivariate analysis in the training group with the lumbar CSFP measurements as dependent variable and age, body mass index, and blood pressure as independent variables revealed that estimated CSFP was best described by the formula of estimated CSFP [mmHg] = 0.44 x body mass index [kg/m^2] + 0.16 x diastolic blood pressure [mmHg] – 0.18 x age [years] - 1.91. The correlation coefficient was r = 0.55. The association between higher CSFP and younger age, higher body mass index, and higher blood pressure had also been found in other previous investigations [131, 132]. The calculated formula was then tested in the testing group. In this testing group, the measured lumbar CSFP (12.6 ± 4.8 mm Hg) did not differ significantly ($P = 0.29$) from the calculated CSFP (13.3 ± 3.2 mm Hg). The coefficient for the correlation between the calculated CSFP value and the measured lumbar CSFP was r = 0.59. The Durbin-Watson value was 2.08. Durbin-Watson values falling into the acceptable range of 1.5 to 2.5 indicated a nonsignificant autocorrelation for the residuals in the multiple regression models. The intra-class correlation coefficient was 0.71. The Bland-Altman analysis revealed that 36 out of 42 measurements were within the 95% limits of agreement, which were +/– 4.98 mmHg. This value of 4.98 mmHg was the 1.96-fold of the standard deviation of the mean absolute error for prediction (2.54 mmHg). Since the algorithm for the estimation of CSFP was based on largely normal (non-ophthalmic condition affected) patients, the algorithm cannot be applied to patients with CSFP-altering diseases or patients with intraocular pressure-altering diseases.

The two-depth transcranial Doppler technology uses the ophthalmic artery as a natural intracranial pressure sensor [95, 96]. The method measures simultaneously the blood flow velocities in the intracranial segments and extracranial segments of the ophthalmic artery. The principle is based on the idea of noninvasive arterial BP measurement, where externally applied pressure to a segment of an artery is used to find a balance point when the external pressure is equal to the arterial pressure measure of interest. Blood flow parameters in both segments of the ophthalmic artery are simultaneously monitored, and the two-depth transcranial Doppler technology device is used as an indicator of the pressure balance point, at which the CSFP is equal to the pressure externally applied to the non-compressible tissues of the orbit surrounding the extracranial segment of the ophthalmic artery. The pressure balance point is reached when the blood flow velocity pulsations in both segments of the ophthalmic artery are approximately equal. In a study with 57 simultaneous invasive and noninvasive CSFP measurements (with a CSFP range from 3 to 37 mmHg), the Bland-Altman plot of the differences between simultaneous invasive and noninvasive CSFP measurements showed a mean difference of 0.94 mmHg with a standard deviation of 6.2 mmHg. In a study of 62 neurologic patients by the same study team, good accuracy for the noninvasive method was found, as indicated by a confidence level of 0.80 mmHg of the absolute error delta in the Bland-Altman analysis. Mean CSFP measured with noninvasive two-depth TCD transcranial Doppler technology was 12.8 ± 3.3 mmHg (range 4.0–23.7 mmHg) compared to the mean direct CSFP measurement of 13.2 ± 3.0 mmHg (range 4.4–24.3 mmHg). The 95% limit of agreement was +/– 4 mmHg [96]. In another study, the two-depth transcranial Doppler technology compared to the sonographic measurement of the optic nerve sheath diameter showed a higher reliability in determining the CSFP in neurological patients [97]. Ragauskas and colleagues described the two-depth transcranial Doppler technology as suitable for 96% or more of patients with normal ophthalmic artery anatomy (i.e., the ophthalmic artery is a branch of internal carotid artery and has an intracranial segment which is influenced by the intracranial CSFP). The technique additionally depends on a free communication between the intracranial compartment to the orbital portion of the CSF space. The method may thus not be applicable if the optic nerve canal is blocked, e.g., due to a parasellar tumor obstructing the inner aperture of the optic nerve canal, due to adhesions after tuberculous basal meningitis, or due to an intracanalicular ophthalmic artery aneurysm.

12.4 CSFP, TLPD, and IOP in Relationship to Glaucomatous Optic Neuropathy

12.4.1 Morphological Particularities of Glaucomatous Optic Neuropathy Versus Vascular Optic Nerve Neuropathy

In the discussion of a potential role of low CSFP in the pathogenesis of glaucomatous optic neuropathy, one may differentiate between anatomical facts and hypothetical speculations. The anatomical facts are:

(1) A loss of neuroretinal rim as is typical for glaucoma can also be found only in eyes after giant cell arteritis-induced anterior ischemic optic neuropathy [133]. All other vascular optic neuropathies do not develop loss of rim or deepening of the optic cup [134, 135].
(2) Parapapillary atrophy can be differentiated into four zones [8, 65, 66, 136]. Alpha zone is characterized by irregular pigmentation and is present in almost all eyes. Its histologic equivalent consists of irregular structured retinal pigment epithelium cells resting on Bruch's membrane. Beta zone shows ophthalmoscopically a visible sclera and visible large choroidal vessels and is histologically characterized by complete loss of retinal pigment epithelium cells and a present but superficially denuded Bruch's membrane. Gamma zone represents a region in which Bruch's membrane is not present. Delta zone is an elongated gamma zone in highly myopic eyes with a stretched and thinned peripapillary scleral flange. Histologic and clinical studies have revealed that beta zone correlates mostly with glaucoma but not with axial myopia, while gamma zone is associated mostly with axial myopia but not with glaucoma [136, 137]. Presence and enlargement of beta zone is almost pathognomonic for glaucoma and is not associated with any vascular optic neuropathy [138–142].
(3) Glaucomatous optic neuropathy is associated with the thinning of the retinal arteries, and at a first glance, it has been assumed that this could be evidence for a vascular pathogenesis of glaucomatous optic nerve damage [8, 21]. However, thinning of retinal arteries can be found in eyes with any optic nerve damage, so that the finding is not pathognomonic for glaucoma and is at least partially secondary to loss of retinal tissue and thus less blood demand in the retina [8, 143]. A recent longitudinal evaluation of the Blue Mountain Eye Study however reported that retinal arteriolar narrowing, quantitatively measured from retinal photographs, was associated with long-term risk of open-angle glaucoma [144]. It supported the concept that early vascular changes were involved in the pathogenesis of optic nerve damage in open-angle glaucoma.
(4) Localized retinal nerve fiber layer defects which formerly were thought to be typical for NPG in contrast to high-pressure glaucoma can be found in both groups, so that both groups do not differ in this prominent defect [145].
(5) Eyes with either high-pressure glaucoma or NPG can have a strikingly similar optic nerve head appearance, both groups showing deepening of the optic cup, loss of neuroretinal rim, and increased prevalence and enlargement of the beta zone of parapapillary atrophy [134]. In both high-pressure glaucoma and NPG, a segmental deepening of the optic cup is associated with a spatially correlated greater loss of visual field [146]. These examples show that eyes with both NPG and high-pressure glaucoma, despite marked differences in IOP, do not profoundly differ in optic nerve head morphology. One has also to take into account that the finding of morphological similarities between high-pressure glaucoma and NPG could also be taken as an argument that not only NPG but also high-pressure glaucoma is generally to a large degree pressure-independent and that increased IOP could be an epiphenomenon. An argument against this hypothesis would be that IOP-lowering therapy has been proven to be helpful to prevent or slow down the progression of glaucomatous optic neuropathy in patients with high-pressure glaucoma as well as with NPG.
(6) Correspondingly, studies on monkeys with experimental high-pressure glaucoma revealed loss of rim, deepening of the optic cup, development of parapapillary beta zone, and occurrence of localized retinal nerve fiber layer defects as is found in patients with both NPG and high-pressure glaucoma [147, 148]. In contrast, monkeys with typical vascular optic nerve damage due to temporary clamping of the retrobulbar central retinal artery did not develop optic disc upping or parapapillary beta zone [149–151]. Similar observations have been made in patients with typical vascular optic nerve damage, such as in diabetic retinopathy, after non-arteritic anterior ischemic optic neuropathy or after a central retinal artery occlusion [152].

12.4.2 Clinical Studies

Discussions about the importance of the CSFP for the optic nerve head and in particular about its potential role in the pathogenesis of glaucomatous optic neuropathy started over four decades ago with studies by Volkov [14], Hayreh [153, 154], Morgan et al. [9–12, 33, 155], and others [4, 7, 13, 43, 77, 156–165].

In dependence on the body posture [78, 79], the average IOP is physiologically higher than the average ICP, resulting in a posteriorly directed trans-lamina cribrosa difference [166]. Normal IOP combined with low CSFP leads to the same pressure differential across the LC as elevated IOP in combination with normal CSFP [167]. The pressure gradient across the LC can then be defined as the pressure difference in relation to the distance between the intraocular compartment and the retrobulbar compartment, i.e., the thickness of the LC [18, 19]. It was reported that the LC is thinner in axially highly myopic eyes than in emmetropic eyes and that the LC gets thinner in eyes with glaucomatous optic nerve damage [19]. The thinner LC determines a higher or steeper trans-lamina cribrosa pressure gradient that may have an influence of the orthograde and retrograde axoplasmic flow.

Interestingly, experimental studies revealed that the LC thickens at an early stage of glaucoma [168]. Changes in the TLPD may lead to abnormal function and optic nerve damage due to changes in axonal transportation, deformation of the LC, altered blood flow, or a combination thereof.

Berdahl and colleagues performed a retrospective clinical chart analysis on patients who had undergone lumbar CSFP measurements for a variety of reasons [169, 170]. Out of more than 30,000 charts of patients who had undergone lumbar puncture for a variety of reasons, the authors selected the charts of patients with primary open-angle glaucoma and with no glaucomatous optic neuropathy. The lumbar CSFP was highly significantly lower in the glaucoma group than in the non-glaucomatous group. As a corollary, patients with ocular hypertension had significantly higher lumbar CSFP measurements than the control group and the glaucoma group. Although the study had limitations such as the design as a retrospective investigation selecting a small proportion of patients out of a very large number of patients, it was inferred that NPG may be associated with low CSFP, while ocular hypertension was associated with high CSFP [169, 170].

In a prospective study from the iCOP study group, patients with NPG and patients with high-pressure glaucoma as well as patients with ocular hypertension underwent for various reasons a neurological examination including a lumbar puncture with lumbar CSFP measurement [13, 159, 160]. They were compared with individuals of a non-glaucomatous control group. For all study participants, the final neurological diagnosis made it unlikely that the clinical symptoms leading to the examination had influenced the CSFP [13, 132, 159, 160]. The patients with NPG had significantly lower lumbar CSFP measurements than those with high-pressure glaucoma or those in the control group. Consequently, the TLPD was significantly higher in both glaucoma groups than in the control group. Patients with ocular hypertension had significantly higher CSFP. It was also shown that the amount of glaucomatous optic nerve damage as measured by neuroretinal rim area and visual field defect correlated with lower CSFP and with higher TLPD.

Interestingly in the control group, higher CSFP was relatively strongly correlated with higher IOP as well as with higher diastolic BP, higher BMI, and younger age [13, 132]. The association between CSFP and IOP confirmed previous studies by Lashutka et al., Li et al., Sajjadi et al., Spentzas et al., and others [38, 51, 52, 54].

In an attempt to estimate orbital CSFP noninvasively, Wang and colleagues from the iCOP study group then measured the width of the orbital CSF space by MRI [16]. After adjusting the amount of optic nerve damage as determined by perimetry or measurement of neuroretinal rim area, they found that the orbital CSF space width was significantly narrower in patients with NPG than in patients with high-pressure glaucoma or normal subjects. In another study, the same group showed that the orbital CSF space width correlated with lumbar CSFP measurements [99]. It strengthened the notion that the almost collapsed orbital CSF space in the patients with NPG was associated with an abnormally low predicted CSFP.

The studies described above had shown that higher CSFP in the individuals of the control groups was associated with higher diastolic BP, higher BMI, and younger age [13, 60, 131, 132]. One then divided the study population into a subgroup to calculate an algorithm for determination of the CSFP based on the three parameters of diastolic BP, BMI, and age and then tested the formula in the remaining second subgroup of individuals by comparing the calculated CSFP values with the direct CSFP measurements. *We applied the formula (estimated CSFP [mmHg] = 0.44 × body mass index [kg/m2] + 0.16 × diastolic blood pressure [mmHg]–0.18 × age [years]–1.91)* [99].

The formula was then used by the iCOP study group to calculate the CSFP and the TLPD for the participants of three population-based studies, the Beijing Eye Study, the Handan Eye Study, and the Central India Eye and Medical Study [30, 37, 130, 171–174]. All three study populations, although markedly differing in geography, educational level, socioeconomic background, BMI, and lifestyle, showed a Gaussian distribution of predicted CSFP and predicted TLPD and that the predicted CSFP was correlated with IOP. This finding concurred with the results of the clinical study in which higher measured CSFP was correlated with higher IOP. In addition, prevalence and amount of glaucomatous optic nerve damage in patients with open-angle glaucoma were more strongly correlated with TLPD than with IOP. In contrast, optic nerve damage in patients with angle-closure glaucoma was associated with IOP but not with TLPD [171, 174]. Also, individuals with ocular hypertension had significantly higher estimated CSFP values than normal individuals [130]. These findings supported the notion of an abnormally low CSFP playing a role in the pathogenesis of NPG. The potential association between a low CSFP and glaucomatous optic neuropathy is further corroborated by indirect findings. In the Beijing Eye Study and in the Central India Eye and Medical Study, smaller neuroretinal rim area was associated with lower BMI [175, 176]. Taking the BMI as a surrogate for CSFP, these findings support the notion of an association between a low CSFP and a small neuroretinal rim.

In a clinical study on more than 500 patients with parasellar, intrasellar, or suprasellar benign tumors, glaucoma-like optic discs with abnormally thin neuroretinal rim and abnormally large beta zone of parapapillary atrophy were abnormally frequent suggesting that slowly growing tumors in this location may have an association with a glaucoma-like disc cupping and parapapillary beta zone [177, 178]. It supported the speculation that these tumors, in addition to compressing the optic nerve and leading to non-glaucomatous optic nerve

damage, might have obstructed the internal opening of the optic nerve canal so that the CSF might no longer have had access to the orbital CSF space. It would reduce the orbital CSFP and increase the TLPD.

Taking into account the physiological associations between higher BP, higher CSFP, and higher IOP, glaucoma may be described as a misbalance between IOP, CSFP, and BP. Either IOP is elevated (as in angle-closure glaucoma), while CSFP and BP are normal, the cause is intraocular. Or, IOP is normal, and BP and intracranial CSFP are normal; however, the orbital CSFP is abnormally low, e.g., due to obstruction of the optic nerve canal by a parasellar meningioma occluding the inner aperture of the optic nerve canal, due to an intracanalicular ophthalmic artery aneurysm, or due to circular adhesions in the optic nerve canal after basal meningitis. In that situation, TLPD is elevated, although IOP, BP, and intracranial CSFP are normal. Or, patients have low BP, and due to the association between BP and CSFP and between BP and IOP, they also have low CSFP and low IOP. If unfortunately, the low BP-induced reduction in CSFP is more marked than the low BP-induced reduction in IOP, the TLPD increases, leading to barotraumatic damage to the optic nerve. One may hypothesize that the latter situation may be valid in some patients with NPG, typically women in their 40s or 50s, who are slim and jogging, and with low blood pressure, cold hands and feet, and decreased thirst, showing vasospastic symptoms [179].

The relatively low BMI may be another hint for a low CSFP, due to the correlation between CSFP and BMI. This hypothesis fits with the observation of a higher prevalence of NPG in Japan than in the USA [180, 181]. Japanese patients with NPG are not only elderly (as one of the factors for a low CSFP), but they are, in contrast to patients in North America, additionally rather slim (as another factor for a low CSFP). The hypothesis also fits with the observation of the occurrence of NPG in patients with chronic intracranial hypotension [182, 183]. If a low BMI is confirmed as a risk factor for NPG, it might be useful to recommend patients (moderately) increasing in weight. Additionally, systemically applied carbonic anhydrase inhibitors may be avoided, since they lower the pressure on both sides of the LC. The involvement of the carbonic anhydrase in the production of aqueous humor as well as CSF shows another similarity between IOP and CSFP.

In the considerations of a potential association between CSFP and glaucomatous optic neuropathy, it has to be taken into account that it is the orbital, not the intracranial, CSFP which determines the TLPD. It has remained unclear whether the lumbar CSFP is directly related to the orbital CSFP. The orbital CSF communicates with the intracranial CSF at the site of the chiasmatic cistern [184]. Any obliteration in that region or in the region of the optic nerve canal or any space occupying lesion in the CSF compartment could limit the free flow of CSF. Jaggi and colleagues reported a patient with an optic nerve sheath meningioma, unilateral optic disc swelling, and a difference in the CSF composition between the lumbar CSF and the orbital CSF (as aspirated from the subarachnoid space of the affected optic nerve) [185]. They suggested an optic nerve sheath compartment syndrome with a marked concentration gradient of albumin, immune globulin G, and beta-trace proteins between the CSF in the orbital CSF space of the affected optic nerve and the CSF in the spinal canal. In a separate study, Jaggi and colleagues detected that the optic nerve sheath diameter as measured by computerized tomography was significantly ($P < 0.001$) larger in patients with NPG than in individuals of a control group [129]. They assumed that the increased optic nerve sheath diameter in the patients with NPG might have been due to an optic nerve sheath compartmentation or due to the thinning of the optic nerve in the study with group with NPG. An optic nerve compartment syndrome had previously been described by Killer and associates [186]. Killer also described that the CSF turnover in the orbital CSF space of the optic nerve was reduced in patients with papilledema from various causes and that the composition of the CSF differed between the spinal CSF and the orbital CSF [187]. It has remained unclear whether an optic nerve compartment syndrome may also be associated with a difference in orbital CSFP and intracranial CSFP or lumbar CSFP. Moreover, the termination of the orbital CSF space around the optic nerve contains atypical meningeal tissue with lymphoid characteristics [188, 189]. Meningothelial cells have been discussed to be associated with the drainage of the CSF and to react under exposure to elevated pressure under experimental conditions with a significant cellular proliferation and a marked decrease in endocytotic activity. In a similar manner, mild oxidative stress reduced the endocytosis of meningothelial cells [190].

In an experimental study by Jaggi and colleagues, a silicone band was placed around one optic nerve of seven sheep to compress the subarachnoid space surrounding the nerve, thus blocking the flow of CSF without compressing the optic nerve itself [191]. After 4 or 21 days, all treated optic nerves showed a marked loss of optic nerve fibers, destruction of myelin, and swelling of meningoepithelial cells, most pronounced in the proximal optic nerve adjacent to the globe at the location most distant to the ligature. There was no significant difference in histological findings between the optic nerves that were ligated for 4 days and those with 21 days of ligature. The authors concluded that segregation of CSF in the orbital CSF space by blocking the orbital CSF space led within 4 days to severe optic nerve damage. The finding that the severity of these changes increased with a longer distance from the site of the ligature was considered to argue against a simple pressure- or microperfusion-dependent effect and to support the hypothesis that interruption of CSF flow in the

subarachnoidal space of the optic nerve could produce optic nerve damage due to a change of CSF flow and composition. Another or an additional mechanism could have been that the CSFP just behind the globe, distant to the site of the orbital CSF space compression, was low leading to an increased TLPD. It has remained unclear whether the CSF once in the orbital CSF space completely returns to the intracranial compartment or whether it is partially absorbed in the orbit [182–184]. In the latter case, the composition of the CSF could be different in the orbital compartment compared to the intracranial compartment or the compartment of the spine. Killer and colleagues discussed whether there may be reduced CSF exchange between the basal intracranial cisterns and the orbital CSF space in patients with NPG, leading to reduced CSF turnover in the CSF space of the optic nerve in these patients [155, 192–195]. A lower intracranial CSFP in patients with NPG could explain the reduced density of the contrast-loaded CSF in the orbital CSF space [195]. Interestingly, experimental studies showed that the orbital CSFP was identical to the intracranial CSFP at the same vertical level [196, 197].

12.4.3 Experimental Studies

Yang et al. conducted an experimental investigation in monkeys to further explore a potential association between an abnormally low CSFP and glaucomatous optic nerve damage [198]. Four monkeys received a lumbar-peritoneal shunt to reduce the CSFP, while five control monkeys underwent the same procedure but with the shunt remaining closed. Follow-up examinations included regular measurements of IOP and CSFP, confocal laser scanning tomography of the optic nerve head and retinal nerve fiber layer, and fundus photography. Four eyes of two study-group monkeys developed a continuous loss of retinal nerve fiber layer, and one eye of a third monkey showed a splinter-like disc hemorrhage during the follow-up. The other three eyes of the study group and all eyes of the monkeys of the control group remained unchanged. It was concluded that the chronic reduction of CSFP led to an optic nerve damage in some monkeys with experimental and chronic reduction in CSFP. It remained unclear whether the optic nerve damage was glaucoma-like.

12.5 CSFP in Relationship to Retinal Vein Pressure and Retinal Vein Occlusions

Since the central retinal vein passes through the optic nerve head, the retrobulbar optic nerve, and the orbital CSF space before it joins the superior ophthalmic vein and drains into the intracranial cavernous sinus, the pressure in the central retinal vein should be at least as high as is the orbital or intracranial CSFP (Fig. 12.6). This relationship has been used in ophthalmodynamometry to estimate the CSFP by measuring the central retinal vein pressure. Subsequently, one may postulate that the diameter of the retinal veins depends on the CSFP and, potentially, that retinal vein occlusions may be correlated with a higher CSFP.

Estimating the CSFP in the longitudinal Beijing Eye Study and assessing the 10-year incidence of retinal vein occlusions showed that higher estimated CSFP was associated with a higher incidence of CRVOs ($P = 0.004$) in a multivariate analysis [199]. In a similar manner, a higher incidence of retinal vein occlusions in general or a higher incidence of CRVOs together with a higher incidence of branch retinal vein occlusions originating at the optic nerve head was significantly associated with higher estimated CSFP ($P = 0.002$) after adjusting for older age. It supported the notion that the CSFP may have an influence on the retinal vein pressure and thus on the occurrence of retinal vein occlusions (originating at the optic nerve head). This hypothesis was further supported by other findings. The amount of macular edema in patients with retinal vein occlusions shows diurnal changes with thicker values at 7 am than at 7 pm, as has also been described for choroidal thickness [200–205]. Since both, the central retinal vein and the vortex veins with the choroidal blood partially drain via the superior orbital vein into the brain, the findings of diurnal changes in macular edema in patients with retinal vein occlusions and in choroidal thickness point to a potential role, the CSFP may play for retinal vein occlusions and potentially other conditions. Due to postural and hydrostatic reasons, the CSFP is higher at night and in the early morning than during daytime. Correspondingly, also for choroidal thickness, a positive association with CSFP has been found [30]. It has to be taken into account, however, that the superior orbital vein also has anastomotic connections to the angular vein which drains to the surface of the face. Also, the superior orbital vein does not drain into the brain tissue proper. It has therefore remained elusive whether the posture-dependent increase in macula edema in eyes with retinal vein occlusions is due to a posture-associated increase in CSFP or a posture-related general increase in the venous pressure in the head. One may therefore not categorically state that elevated CSFP definitely increases the superior orbital venous pressure, particularly in individuals who may have predominantly an anterior outflow into the angular vein.

In the discussion of the application of the formula for the estimation of CSFP, one has to take into account the limitations of this approach, in particular from the point of view of the explanatory parameters which the formula relies upon, namely, body mass index, blood pressure, and age. Since these three parameters taken separately are also associated with the prevalence of retinal vein occlusions, hypertensive retinopathy, and diabetic retinopathy and with choroidal

thickness, they may potentially be statistical confounders when the algorithm including all of them is correlated against the other parameters such as diabetic retinopathy and hypertensive retinopathy. Future studies may therefore address whether the observed associations between the estimated CSFP and diseases such as retinal vein occlusions mean that retinal vein occlusions are associated with higher blood pressure (in the algorithm) and/or with the degree of obesity and how one could separate those two factors from CSFP, to cite an example.

12.6 CSFP in Relationship to Hypertensive Retinopathy

Since retinal microvascular abnormalities associated with hypertensive retinopathy include widening of retinal veins and an increase in the retinal vein-to-artery diameter ratio, it has been assessed whether the widening of the retinal veins in arterial hypertensive patients is related to CSFP (Fig. 12.6) [172]. In a multivariate analysis in the Beijing Eye Study, larger retinal vein diameters and higher vein-to-artery diameter ratios were significantly associated with higher estimated CSFP ($P = 0.001$). In contrast, retinal arterial diameters were not significantly associated with estimated CSFP nor were other microvascular abnormalities such as arteriovenous crossing signs. In a reverse manner, higher estimated CSFP was correlated with wider retinal veins and higher vein-to-artery diameter ratio, but not with retinal artery diameters or other retinal microvascular abnormalities. Before including the CSFP into the consideration on the pathogenesis of hypertensive retinopathy, it had been difficult to explain why a pressure elevation on the arterial side could lead to a wider retinal vein diameter, in particular since the retinal arterial diameter decreased. Including however the CSFP into the considerations and taking into account the dependence of the CSFP ion, the arterial BP then explained that elevated arterial BP, through the deviation of an increased CSFP, could indirectly lead to a widening of the retinal vein diameters.

12.7 CSFP in Relationship to Diabetic Retinopathy

In the Beijing Eye Study, a higher 10-year incidence of diabetic retinopathy was significantly associated with higher estimated CSFP ($P = 0.04$; odds ratio, 1.10; 95% CI, 1.01, 1.22) after adjusting for a higher HbA1c value, longer duration of diabetes mellitus, higher serum concentration of creatinine, lower educational level, and shorter axial length (Fig. 12.6) (Jon asset al. 2014d). Correspondingly, the Wisconsin Epidemiologic Study of Diabetic Retinopathy revealed that independently of the severity level of diabetic retinopathy, glycemic control, and other factors, widening of retinal venular caliber but not of arteriolar diameter was associated with subsequent incidence and progression of diabetic retinopathy [206–208]. The reason for these associations may be that an elevated retinal venous pressure in patients with higher CSFP may be associated with a higher retinal capillary blood pressure, potentially explaining the increased incidence and prevalence of retinal hemorrhages, edema, and lipid exudates as part of diabetic retinopathy.

As recently suggested by Stodtmeister and colleagues, an elevated retinal venous pressure due to an increased CSFP may additionally decrease the ocular perfusion pressure defined as the difference between the retinal arterial BP and the retinal venous BP [113, 209]. A decrease in the ocular perfusion pressure leads to an increase in the risk for ischemic retinopathies such as diabetic retinopathy. If the association between higher CSFP and diabetic retinopathy is further examined in future studies, one may address the question whether lowering of CSFP by drugs such as systemic carbonic anhydrase inhibitors may have a therapeutically positive effect on the development of diabetic retinopathy. A therapeutic effect systemically administered acetazolamide has been discussed as early as in 1988 [210]. The association between higher estimated CSFP and diabetic retinopathy may also explain the dilatation of retinal veins and their increased tortuosity as hallmarks of diabetic retinopathy. An increased arterial BP alone may not explain why on the venous side of the vascular bed the vessels get wider.

It remains unclear whether diabetes mellitus in general is associated with an elevated CSFP, independently of the association of CSFP with blood pressure and body mass index. Some studies suggested that diabetic ketoacidosis can be associated with increased CSFP [211–214].

12.8 CSFP and Choroidal Thickness

Thicker subfoveal choroidal thickness was associated with higher estimated CSFP ($P = 0.009$) after adjusting for lower age, shorter axial length, lower BMI, and higher corneal curvature radius [37]. In univariate analysis, subfoveal choroidal thickness increased by 9.2 µm (95% confidence interval, 8.3, 10.1) for each mmHg increase in estimated CSFP. In a reverse manner, estimated CSFP was significantly associated with thicker subfoveal choroidal thickness ($P < 0.001$) in a multivariate analysis.

12.9 Future Directions

Future studies may further develop techniques for noninvasive measurement of CSFP, including studies on the associations of CSFP with other parameters, so that refined formulas may be

used to estimate the CSFP in neurologically normal subjects. Future investigations may also address the dynamic aspects of CSFP, such as pulse-synchronous changes and daytime-associated changes of the CSFP, in addition to the dependence of the CSFP on body posture. The latter may also be of importance for yoga performance, since it remains undetermined whether a headstand-associated increase in IOP is fully compensated by an increase in CSFP so that the TLPD may or may not be affected. A direct consequence would be whether yoga can or cannot be recommended for patients with glaucoma. Examinations of dynamic aspects of the relationship of CSFP to IOP include investigations whether a change in IOP due to a change in the body position takes longer or shorter than the corresponding change in CSFP. It could have importance for glaucoma. Let us assume that after lying down, the rise in IOP takes longer time to occur than the immediate, hydrostatically explained rise in CSFP; the first minutes (or longer) after lying down would result in a lower TLPD and could, theoretically, be helpful for the glaucomatous optic nerve. If, however, after rising from a supine position, the drop in CSFP occurred much earlier than the drop in IOP, rising out of a supine position would result in an increase in TLPD and could thus be of risk for glaucomatous damage.

Future studies may examine the physiological flow of CSF from the brain to the orbit and questionably back to the brain. These studies indirectly address the questions whether the composition of the CSF differs between various regions of the central nervous system. If, in the example given, the composition of the orbital CSF may be important for susceptibility to NPG, patients with the disease could be recommended to maintain body positions in which likely the composition of the orbital CSF would be altered or unaltered. Similar questions may be addressed whether patients with glaucoma should sleep with their head elevated or flat or in a downward position, depending on studies which examined the changes in IOP and in CSFP associated with a change in body position and with reflection on the TLPD. It would be desirable to summarize the relationship between the orbital CSFP and the IOP in a mathematical formula; however, the data accumulated so far may not yet be sufficient for a clear mathematical model. Issues, which have not been sufficiently addressed, are among others whether the decrease in pressure across the lamina cribrosa occurs continuously or in a stepwise manner; whether the differences in the timing of the pulse-synchronous pressure wave in the CSF space and the intraocular compartment lead to pulse-synchronous changes in the TLPD; whether anatomical parameters such as thickness and length of the lamina cribrosa and its anchoring in the peripapillary scleral flange influence the parameters of the TLPD; and whether the amount of optic nerve damage and shrinkage, leading to an enlarged area of the posterior lamina cribrosa surface directly exposed to the orbital CSF space, are of importance for the TLPD.

Other points are quantitative data on the relationship between intracranial CSFP and orbital CSFP (and also lumbar CSFP), the relationship with the body posture, and the timing of changes in CSFP and in IOP in relationship to changes of body posture and associated changes in blood pressure. Some of these issues are now going to be examined in astronauts spending several months in orbit [84–86]. It has also remained unclear whether CSFP has an impact on the retinal arterial blood pressure, a parameter which would additionally influence a mathematical formulation of the association between CSF, IOP, TLPD, and arterial and venous blood pressure in the retina (and optic nerve head). If more hints were gathered that a low orbital CSFP is associated with glaucomatous optic neuropathy, therapeutic modalities may be developed to increase the CSFP, not only by elevating arterial BP or by avoiding systemic carbonic anhydrase inhibitors, but by drugs specifically increasing the CSF production or decreasing the CSF absorption from the central nervous system.

12.10 Conclusions

The orbital CSFP as counter-pressure against IOP is a determinant of the TLPD and is important for the physiology and pathophysiology of the optic nerve head and pressure-related diseases originating at the optic nerve head, such as glaucomatous optic neuropathy. Taking into account the physiological triangular relationships between IOP, CSFP, and BP, glaucoma may be described as a misbalance between IOP, CSFP, and BP, finally leading to an increase in TLPD. Potentially, since the central retinal vein passes through the orbital CSF space, the orbital CSFP is of importance for the pressure in the retinal veins, for their diameters, and potentially for the development of retinal vein occlusions. Since the retinal venous pressure influences the retinal capillary pressure, the orbital CSFP may have an influence on the development and severity of signs of diabetic retinopathy. In a similar manner, the retinal perfusion pressure may be reduced in patients with an increased orbital CSFP and secondarily increased retinal venous pressure. Since the choroid drains through the vortex veins into the superior ophthalmic vein and cavernous sinus intracranial, higher CSFP may be associated with a thicker choroid, fitting with the observation of a thicker choroid in the morning than in the evening. Changes in body position influence, potentially, in different amount and in a different time frame, IOP, CSFP, and regional BP. Resulting body position-dependent and time-dependent changes in TLPD remain unexplored. Experimental studies have suggested that dorsomedial and perifornical hypothalamic neurons may be involved in the regulation of both IOP and CSFP.

Acknowledgments The text and figures of this manuscript have appeared previously in a Progress in Retinal and Eye Research review of our work: *Jonas JB, Wang N, Yang D, Ritch R, Panda-Jonas S. Facts and myths of cerebrospinal fluid pressure for the physiology of the eye. Prog Retin Eye Res. 2015;46:67–83* [215]. They have been used with permission and edited for this chapter.

References

1. Møller PM. Tissue pressure in the orbit. Acta Ophthalmol. 1954;32:597–604.
2. Moller PM. The pressure in the orbit. Acta Ophthalmol. 1955;(Suppl 43):1–100.
3. Balaratnasingam C, Morgan WH, Johnstone V, Pandav SS, Cringle SJ, Yu DY. Histomorphometric measurements in human and dog optic nerve and an estimation of optic nerve pressure gradients in human. Exp Eye Res. 2009;89:618–28.
4. Burgoyne CF, Downs JC, Bellezza AJ, Suh JK, Hart RT. The optic nerve head as biomechanical structure: a new paradigm for understanding the role of IOP-related stress and strain in the pathophysiology of glaucomatous optic nerve head damage. Prog Retin Eye Res. 2005;24:39–73.
5. Jonas JB. Ophthalmodynamometry in eyes with dilated episcleral veins. J Glaucoma. 2003a;12:285–7.
6. Jonas JB. Ophthalmodynamometric determination of the central retinal vessel collapse pressure correlated with systemic blood pressure. Br J Ophthalmol. 2004;88:501–4.
7. Jonas JB. Role of cerebrospinal fluid pressure in the pathogenesis of glaucoma. Acta Ophthalmol. 2011;89:505–14.
8. Jonas JB, Fernández MC, Naumann GO. Parapapillary atrophy and retinal vessel diameter in nonglaucomatous optic nerve damage. Invest Ophthalmol Vis Sci. 1991a;32:2942–7.
9. Morgan WH, Yu DY, Cooper RL, Alder VA, Cringle SJ, Constable IJ. The influence of cerebrospinal fluid pressure on the lamina cribrosa tissue pressure gradient. Invest Ophthalmol Vis Sci. 1995;36:1163–72.
10. Morgan WH, Yu DY, Alder VA. The correlation between cerebrospinal fluid pressure and retrolaminar tissue pressure. Invest Ophthalmol Vis Sci. 1998;39:1419–28.
11. Morgan WH, Chauhan BC, Yu DY. Optic disc movement with variations in intraocular and cerebrospinal fluid pressure. Invest Ophthalmol Vis Sci. 2002;43:3236–42.
12. Morgan WH, Yu DY, Balaratnasingam C. The role of cerebrospinal fluid pressure in glaucoma pathophysiology: the dark side of the optic disc. J Glaucoma. 2008a;17:408–13.
13. Ren R, Jonas JB, Tian G, Zhen Y, Ma K, Li S, Wang H, Li B, Zhang X, Wang N. Cerebrospinal fluid pressure in glaucoma. A prospective study. Ophthalmology. 2010;117:259–66.
14. Volkov VV. Essential element of the glaucomatous process neglected in clinical practice. Oftalmol Zh. 1976;31:500–4.
15. Yablonsky M, Ritch R, Pokorny KS. Effect of decreased intracranial pressure on optic disc. Invest Ophthalmol Vis Sci. 1979;18(Suppl):165.
16. Wang N, Xie X, Yang D, Xian J, Li Y, Ren R, Wang H, Zhang S, Kang Z, Peng X, Sang J, Zhang Z, Jonas JB, Weinreb RN. Orbital cerebrospinal fluid space in glaucoma. Ophthalmology. 2012;119:2065–2073.e1.
17. Lenfeldt N, Koskinen LO, Bergenheim AT, Malm J, Eklund A. CSF pressure assessed by lumbar puncture agrees with intracranial pressure. Neurology. 2007;68:155–8.
18. Jonas JB, Berenshtein E, Holbach L. Anatomic relationship between lamina cribrosa, intraocular space and cerebrospinal fluid space. Invest Ophthalmol Vis Sci. 2003;44:5189–95.
19. Jonas JB, Berenshtein E, Holbach L. Lamina cribrosa thickness and spatial relationship between intraocular space and cerebrospinal fluid space in highly myopic eyes. Invest Ophthalmol Vis Sci. 2004;48:2660–5.
20. Jonas JB, Naumann GOH. Parapapillary retinal vessel diameter in normal and glaucoma eyes. II. Correlations. Invest Ophthalmol Vis Sci. 1989;30:1604–11.
21. Jonas JB, Nguyen XN, Naumann GO. Parapapillary retinal vessel diameter in normal and glaucoma eyes. I. Morphometric data. Invest Ophthalmol Vis Sci. 1989;30:1599–603.
22. Jonas JB. Central retinal artery and vein pressure in patients with chronic open-angle glaucoma. Br J Ophthalmol. 2003c;87:949–51.
23. Firsching R, Schütze M, Motschmann M, Behrens-Baumann W. Venous opthalmodynamometry: a noninvasive method for assessment of intracranial pressure. J Neurosurg. 2000;93:33–6.
24. Firsching R, Müller C, Pauli SU, Voellger B, Röhl FW, Behrens-Baumann W. Noninvasive assessment of intracranial pressure with venous ophthalmodynamometry. J Neurosurg. 2011;115:371–4.
25. Jonas JB, Groden C. Spontaneous carotid-cavernous sinus fistula diagnosed by ophthalmodynamometry. Acta Ophthalmol. 2003;81:419–20.
26. Jonas JB, Harder B. Ophthalmodynamometric estimation of cerebrospinal fluid pressure in pseudotumor cerebri. Br J Ophthalmol. 2003;87:361–2.
27. Jonas JB, Hennerici M. Ophthalmodynamometry for diagnosis of dissection of internal carotid artery. Graefes Arch Clin Exp Ophthalmol. 2006;244:129–30.
28. Jonas JB, Pfeil K, Chatzikonstantinou A, Rensch F. Ophthalmodynamometric measurement of central retinal vein pressure as surrogate of intracranial pressure in idiopathic intracranial hypertension. Graefes Arch Clin Ophthalmol. 2008;246:1059–60.
29. Morgan WH, Yu DY, Cooper RL, Alder VA, Cringle SJ, Constable IJ. Retinal artery and vein pressures in the dog and their relationship to aortic, intraocular, and cerebrospinal fluid pressures. Microvasc Res. 1997;53:211–21.
30. Jonas JB, Wang N, Wang YX, You QS, Xie XB, Yang D, Xu L. Subfoveal choroidal thickness and cerebrospinal fluid pressure. The Beijing Eye Study 2011. Invest Ophthalmol Vis Sci. 2014b;55:1292–8.
31. Jonas JB, Wang N, Yang D. Retinal vein pulsation is in phase with intracranial pressure and not intraocular pressure. Invest Ophthalmol Vis Sci. 2012a;53:6045.
32. Kain S, Morgan WH, Yu DY. New observations concerning the nature of central retinal vein pulsation. Br J Ophthalmol. 2010;94:854–7.
33. Morgan WH, Lind CR, Kain S, Fatehee N, Bala A, Yu DY. Retinal vein pulsation is in phase with intracranial pressure and not intraocular pressure. Invest Ophthalmol Vis Sci. 2012a;53:4676–81.
34. Morgan WH, Lind CR, Kain S, Fatehee N, Bala A, Yu DY. Author response: retinal vein pulsation is in phase with intracranial pressure and not intraocular pressure. Invest Ophthalmol Vis Sci. 2012b;53:6880.
35. Albeck MJ, Borgesen SE, Gjerris F, Schmidt JF, Sørensen PS. Intracranial pressure and cerebrospinal fluid outflow conductance in healthy subjects. J Neurosurg. 1991;74(4):597–600.
36. Dickerman RD, Smith GH, Langham-Roof L. Intra-ocular pressure changes during maximal isometric contraction: does this reflect intra-cranial pressure or retinal venous pressure? Neurol Res. 1999;21:243–6.
37. Jonas JB, Wang N, Wang YX, You QS, Xie XB, Yang D, Xu L. Body height, estimated cerebrospinal fluid pressure, and open-angle glaucoma. The Beijing Eye Study 2011. PLoS One. 2014a;9:e86678.
38. Li Z, Yang Y, Lu Y, Liu D, Xu E, Jia J, Yang D, Zhang X, Yang H, Ma D, Wang N. Intraocular pressure vs intracranial pressure in disease conditions: A prospective cohort study (Beijing iCOP study). BMC Neurol. 2012;12:66.

39. Mansouri K, Liu JH, Weinreb RN, Tafreshi A, Medeiros FA. Analysis of continuous 24-hour intraocular pressure patterns in glaucoma. Invest Ophthalmol Vis Sci. 2012;53:8050–6.
40. Maurel D, Ixart G, Barbanel G. Effects of acute tilt from orthostatic to headdown antiorthostatic restraint and of sustained restraint on the intra-cerebroventricular pressure in rats. Brain Res. 1996;736:165–73.
41. Jonas JB, Holbach L, Panda-Jonas S. Peripapillary ring: Histology and correlations. Acta Ophthalmol. 2014i;92:e273–9.
42. Ren R, Wang N, Li B, Li L, Gao F, Xu X, Jonas JB. Lamina cribrosa and peripapillary sclera histomorphometry in normal and advanced glaucomatous Chinese eyes with normal and elongated axial length. Invest Ophthalmol Vis Sci. 2009;50:2175–84.
43. Jonas JB, Mardin CY, Schlötzer-Schrehardt U, Naumann GOH. Morphometry of the human lamina cribrosa surface. Invest Ophthalmol Vis Sci. 1991b;32:401–5.
44. Hayreh SS. Fluids in the anterior part of the optic nerve in health and disease. Surv Ophthalmol. 1978;23:1–25.
45. Peyman GA, Apple D. Peroxidase diffusion processes in the optic nerve. Arch Ophthalmol. 1972;88:650–4.
46. Rodriguez-Peralta LA. Hematic and fluid barriers in the optic nerve. J Comp Neurol. 1966;126:109–21.
47. Tsukahara I, Yamashita H. An electron microscopic study on the blood-optic nerve and fluid-optic nerve barrier. Albrecht Von Graefes Arch Klin Exp Ophthalmol. 1975;196:239–46.
48. Harder B, Jonas JB. Frequency of spontaneous pulsations of the central retinal vein in normal eyes. Br J Ophthamol. 2007;91:401–2.
49. Minckler DS, Tso MOM, Zimmermann LE. A light microscopic, autoradiographic study of axonal transport in the optic nerve head during ocular hypotony, increased intraocular pressure, and papilledema. Am J Ophthalmol. 1976;82:741–57.
50. Quigley HA, Anderson DR. The dynamics and location of axonal transport blockade by acute intraocular pressure elevation in primate optic nerve. Invest Ophthalmol Vis Sci. 1976;15:606–16.
51. Lashutka MK, Chandra A, Murray HN, Philipps GS, Hiestand BC. The relationship of intraocular pressure to intracranial pressure. Ann Emerg Med. 2004;43:585–91.
52. Sajjadi SA, Harirchian MH, Sheikhbahaei N, Mohebbi MR, Malekmadani MH, Saberi H. The relation between intracranial and intraocular pressures: study of 50 patients. Ann Neurol. 2006;59:867–70.
53. Sheeran P, Bland JM, Hall GM. Intra ocular pressure changes and alterations in intra cranial pressure. Lancet. 2000;355:899.
54. Spentzas T, Henricksen J, Patters AB, Chaum E. Correlation of intraocular pressure with intracranial pressure in children with severe head injuries. Pediatr Crit Care Med. 2010;11:593–8.
55. Czarnik T, Gawda R, Latka D, Kolodzej W, Sznajd-Weron K, Weron R. Noninvasive measurement of intracranial pressure: is it possible? J Trauma. 2007;62(1):207–11.
56. Han Y, McCulley TJ, Horton JC. No correlation between intraocular pressure and intracranial pressure. Ann Neurol. 2008;64:221–4.
57. Kirk T, Jones K, Miller S, Corbett J. Measurement of intraocular and intracranial pressure: is there a relationship? Ann Neurol. 2011;70:323–6.
58. Hayreh SS, Edwards J. Ophthalmic arterial and venous pressures. Effects of acute intracranial hypertension. Br J Ophthalmol. 1971;55:649–63.
59. Cullen LK, Steffey EP, Bailey CS, Kortz G, da Silva Curiel J, Bellhorn RW, Woliner MJ, Elliott AR, Jarvis KA. Effect of high PaCO2 and time on cerebrospinal fluid and intraocular pressure in halothane-anesthetized horses. Am J Vet Res. 1990;51:300–4.
60. Berdahl JP. Systemic parameters associated with cerebrospinal fluid pressure. J Glaucoma. 2013;22(Suppl 5):S17–8.
61. Mitchell P, Lee AJ, Wang JJ, Rochtchina E. Intraocular pressure over the clinical range of blood pressure: blue mountains eye study findings. Am J Ophthalmol. 2005;140:131–2.
62. Xu L, Wang H, Wang Y, Jonas JB. Intraocular pressure correlated with arterial blood pressure. The Beijing Eye Study. Am J Ophthalmol. 2007a;144:461–2.
63. Samuels BC, Hammes NM, Johnson PL, Shekhar A, McKinnon SJ, Allingham RR. Dorsomedial/Perifornical hypothalamic stimulation increases intraocular pressure, intracranial pressure, and the translaminar pressure gradient. Invest Ophthalmol Vis Sci. 2012;53:7328–35.
64. Balaratnasingam C, Morgan WH, Hazelton ML, House PH, Barry CJ, Chan H, Cringle SJ, Yu DY. Value of retinal vein pulsation characteristics in predicting increased optic disc excavation. Br J Ophthalmol. 2007;91:441–4.
65. Jonas JB, Jonas SB, Jonas RA, Holbach L, Panda-Jonas S. Histology of the parapapillary region in high myopia. Am J Ophthalmol. 2011a;152:1021–9.
66. Jonas JB, Nangia V, Matin A, Sinha A, Kulkarni M, Bhojwani K. Intraocular pressure and associated factors. The Central India Eye and Medical Study. J Glaucoma. 2011b;20:405–9.
67. Kaufmann C, Bachmann LM, Robert YC, Thiel MA. Ocular pulse amplitude in healthy subjects as measured by dynamic contour tonometry. Arch Ophthalmol. 2006;124:1104–8.
68. Wegner W. Neue Ergebnisse über die pulsatorischen Schwankungen des menschlichen Bulbus und seiner Hüllen. Arch Augenheilkd. 1930;102:1–32.
69. Silver DM, Geyer O. Pressure-volume relation for the living human eye. Curr Eye Res. 2000;20:115–20.
70. James CB, Trew DR, Clark K, Smith SE. Factors influencing the ocular pulse—axial length. Graefes Arch Clin Exp Ophthalmol. 1991;229:341–4.
71. Wang YX, Jonas JB, Wang N, You QS, Yang D, Xie XB, Xu L. Intraocular pressure and estimated cerebrospinal fluid pressure. The Beijing eye study 2011. PLoS One. 2014;9:e104267.
72. Anderson DR, Grant WM. The influence of position on intraocular pressure. Investig Ophthalmol. 1973;12:204–12.
73. Baskaran M, Raman K, Ramani KK, Roy J, Vijaya L, Badrinath SS. Intraocular pressure changes and ocular biometry during Sirsasana (headstand posture) in yoga practitioners. Ophthalmology. 2006;113:1327–32.
74. Carlson KH, McLaren JW, Topper JE, Brubaker RF. Effect of body position on intraocular pressure and aqueous flow. Invest Ophthalmol Vis Sci. 1987;28:1346–52.
75. Gallardo MJ, Aggarwal N, Cavanagh HD, Whitson JT. Progression of glaucoma associated with the Sirsasana (headstand) yoga posture. Adv Ther. 2006;23:921–5.
76. Hirooka K, Shiraga F. Relationship between postural change of the intraocular pressure and visual field loss in primary open-angle glaucoma. J Glaucoma. 2003;12:379–82.
77. Jonas JB. Intraocular pressure during headstand. Ophthalmology. 2007;114:1791; author reply 1791
78. Magnaes B. Body position and cerebrospinal fluid pressure. Part 1: clinical studies on the effect of rapid postural changes. J Neurosurg. 1976a;44:687–97.
79. Magnaes B. Body position and cerebrospinal fluid pressure. Part 2: clinical studies on orthostatic pressure and the hydrostatic indifferent point. J Neurosurg. 1976b;44:698–705.
80. Tarkkanen A, Leikola J. Postural variations of the intraocular pressure as measured with the Mackay-Marg tonometer. Acta Ophthalmol. 1967;45:569–75.
81. Weinreb RN, Cook J, Friberg TR. Effect of inverted body position on intraocular pressure. Am J Ophthalmol. 1984;98:784–7.
82. Zhang Z, Wang X, Jonas JB, Wang H, Zhang X, Peng X, Ritch R, Tian G, Yang D, Li L, Li J, Wang N. Valsalva manoeuver, intraocular pressure, cerebrospinal fluid pressure, optic disc topography: Beijing Intracranial and Intraocular Pressure Study. Acta Ophthalmol. 2014;92:e475–80.
83. Schuman JS, Massicotte EC, Connolly S, Hertzmark E, Mukherji B, Kunen MZ. Increased intraocular pressure and visual field

defects in high resistance wind instrument players. Ophthalmology. 2000;107:127–33.
84. Kramer LA, Sargsyan AE, Hasan KM, Polk JD, Hamilton DR. Orbital and intracranial effects of microgravity: findings at 3-T MR imaging. Radiology. 2012;263:819–27.
85. Mader TH, Gibson CR, Pass AF, Kramer LA, Lee AG, Fogarty J, Tarver WJ, Dervay JP, Hamilton DR, Sargsyan A, Phillips JL, Tran D, Lipsky W, Choi J, Stern C, Kuyumjian R, Polk JD. Optic disc edema, globe flattening, choroidal folds, and hyperopic shifts observed in astronauts after long-duration space flight. Ophthalmology. 2011;118:2058–69.
86. Mader TH, Gibson CR, Pass AF, Lee AG, Killer HE, Hansen HC, Dervay JP, Barratt MR, Tarver WJ, Sargsyan AE, Kramer LA, Riascos R, Bedi DG, Pettit DR. Optic disc edema in an astronaut after repeat long-duration space flight. J Neuroophthalmol. 2013;33:249–55.
87. Salman MS. Can intracranial pressure be measured non-invasively? Lancet. 1997;350:1367.
88. Siaudvytyte L, Januleviciene I, Ragauskas A, Bartusis L, Siesky B, Harris A. Update in intracranial pressure evaluation methods and translaminar pressure gradient role in glaucoma. Acta Ophthalmol. 2014;93(1):9–15. https://doi.org/10.1111/aos.12502. [Epub ahead of print]
89. Hawthorne C, Piper I. Monitoring of intracranial pressure in patients with traumatic brain injury. Front Neurol. 2014;5:121.
90. Zeng T, Gao L. Management of patients with severe traumatic brain injury guided by intraventricular intracranial pressure monitoring: a report of 136 cases. Chin J Traumatol. 2010;13:146–51.
91. Bauerle J, Nedelmann M. Sonographic assessment of the optic nerve sheath in idiopathic hypertension. J Neurol. 2011;258:2014–9.
92. Bellner J, Romner B, Reinstrup P, Kristiansson KA, Ryding E, Brandt Ll. Transcranial Doppler sonography pulsatility index (PI) reflects intracranial pressure (ICP). Surg Neurol. 2004;62:45–51.
93. Chacón M, Pardo C, Puppo C, Curilem M, Landerretche J. Non-invasive intracranial pressure estimation using support vector machine. Conf Proc IEEE Eng Med Biol Soc. 2010;2010:996–9.
94. Potgieter DW, Kippin A, Ngu F, McKean C. Can accurate ultrasonographic measurement of the optic nerve sheath diameter (a non-invasive measure of intracranial pressure) be taught to novice operators in a single training session? Anaesth Intensive Care. 2011;39:95–100.
95. Ragauskas A, Daubaris G, Dziugys A, Azelis V, Gedrimas V. Innovative non-invasive method for absolute intracranial pressure measurement without calibration. Acta Neurochir Suppl. 2005;95:357–61.
96. Ragauskas A, Matijosaitis V, Zakelis R, Petrikonis K, Rastenyte D, Piper I, Daubaris G. Clinical assessment of noninvasive intracranial pressure absolute value measurement method. Neurology. 2012;78:1684–91.
97. Ragauskas A, Bartusis L, Piper I, Zakelis R, Matijosaitis V, Petrikonis K, Rastenyte D. Improved diagnostic value of a TCD-based non-invasive ICP measurement method compared with the sonographic ONSD method for detecting elevated intracranial pressure. Neurol Res. 2014;36:607–14.
98. Tain RW, Alperin N. Noninvasive intracranial compliance from MRI-based measurements of transcranial blood and CSF flows: indirect versus direct approach. IEEE Trans Biomed Eng. 2009;56:544–51.
99. Xie XB, Zhang XJ, Fu J, Wang H, Jonas JB, Peng X, Tian G, Xian J, Ritch R, Li L, Kang Z, Zhang S, Yang D, Wang N. Beijing iCOP Study Group: Intracranial pressure estimation by orbital subarachnoid space measurement. Crit Care. 2013;17:R162.
100. Xu P, Kasprowicz M, Bergsneider M, Hu X. Improved noninvasive intracranial pressure assessment with nonlinear kernel regression. IEEE Trans Inf Technol Biomed. 2010;14:971–8.
101. Klingerhofer J, Conrad B, Benecke R, Sander D. Intracranial flow patterns at increasing intracranial pressure. Klin Wochenschr. 1987;65:542–5.
102. Voulgaris SG, Partheni M, Kaliora H, Haftouras N, Pessach IS, Polyzoidis KS. Early cerebral monitoring using the transcranial Doppler pulsatility index in patients with severe brain trauma. Med Sci Monit. 2005;11:CR49–52.
103. Behrens N, Lenfeldt N, Ambarki K, Siesjo P, Peter JC. Transcranial Doppler pulsatility index: not an accurate method to assess intracranial pressure. Neurosurgery. 2010;66:1050–7.
104. Brandi G, Béchir M, Sailer S, Haberthür C, Stocker R, Stover JF. Transcranial color-coded duplex sonography allows to assess cerebral perfusion pressure noninvasively following severe traumatic brain injury. Acta Neurochir. 2010;152:965–72.
105. Figaji AA, Zwane E, Fieggen AG, Siesjo P, Peter JC. Transcranial Doppler pulsatility index is not a reliable indicator of intracranial pressure in children with severe traumatic brain injury. Surg Neurol. 2009;72:389–94.
106. Czonsnyka M. Pulsatility index. J Neurosurg. 2001;94:685–6.
107. Lang EW, Paulat K, Witte C, Zolondz J, Mehdorn HM. Noninvasive intracranial compliance monitoring: technical note and clinical results. J Neurosurg. 2003;98:214–8.
108. Reid A, Marchbanks RJ, Burge DM, Martin AM, Bateman DE, Pickard JD, Brightwell AP. The relationship between intracranial pressure and tympanic membrane displacement. Br J Audiol. 1990;24:123–9.
109. Shimbles S, Dodd C, Banister K, Mendelow AD, Chambers IR. Clinical comparison of tympanic membrane displacement with invasive ICP measurements. Acta Neurochir Suppl. 2005;95:197–9.
110. Jonas JB. Reproducibility of ophthalmodynamometric measurements of the central retinal artery and vein collapse pressure. Br J Ophthalmol. 2003b;87:577–9.
111. Jonas JB. Ophthalmodynamometric assessment of the central retinal vein collapse pressure in eyes with retinal vein stasis or occlusion. Graefes Arch Clin Exp Ophthalmol. 2003d;241:367–70.
112. Morgan WH, Hazelton ML, Balaratnasingam C, Chan H, House PH, Barry CJ, Cringle SJ, Yu DY. The association between retinal vein ophthalmodynamometric force change and optic disc excavation. Br J Ophthalmol. 2009;93:594–6.
113. Pillunat KR, Ventzke S, Spoerl E, Furashova O, Stodtmeister R, Pillunat LE. Central retinal venous pulsation pressure in different stages of primary open-angle glaucoma. Br J Ophthalmol. 2014;98:1374–8.
114. Stodtmeister R, Oppitz T, Spoerl E, Haustein M, Boehm AG. Contact lens dynamometry: the influence of age. Invest Ophthalmol Vis Sci. 2010;51:6620–4.
115. Stodtmeister R, Ventzke S, Spoerl E, Boehm AG, Terai N, Haustein M, Pillunat LE. Enhanced pressure in the central retinal vein decreases the perfusion pressure in the prelaminar region of the optic nerve head. Invest Ophthalmol Vis Sci. 2013;54:4698–704.
116. Morgan WH, Hazelton ML, Azar SL, House PH, Yu DY, Cringle SJ, Balaratnasingam C. Retinal venous pulsation in glaucoma and glaucoma suspects. Ophthalmology. 2004;111:1489–94.
117. Motschmann M, Muller C, Kuchenbecker J. Ophthalmodynamometry: a reliable method for measuring intracranial pressure. Strabismus. 2001;9:13–6.
118. Querfurth H, Lieberman P, Arms S, Mundell S, Bennett M, van Horne C. Ophthalmodynamometry for ICP prediction and pilot test on the Mt. Everest. BMC Neurol. 2010;10:106.
119. Dubourg J, Javouhey E, Geeraerts T, Messerer M, Kassai B. Ultrasonography of optic nerve sheath diameter for detection of raised intracranial pressure: a systematic review and meta-analysis. Intensive Care Med. 2011;37:1059–68.
120. Dubourg J, Messerer M, Karakitsos D, Rajajee V, Antonsen E, Javouhey E, Cammarata A, Cotton M, Daniel RT, Denaro

C, Douzinas E, Dubost C, Berhouma M, Kassai B, Rabilloud M, Gullo A, Hamlat A, Kouraklis G, Mannanici G, Marill K, Merceron S, Poularas J, Ristagno G, Noble V, Shah S, Kimberly H, Cammarata G, Moretti R, Geeraerts T. Individual patient data systematic review and meta-analysis of optic nerve sheath diameter ultrasonography for detecting raised intracranial pressure: protocol of the ONSD research group. Syst Rev. 2013;2:62.
121. Geeraerts T, Launey Y, Martin L, Pottecher J, Vigué B, Duranteau J, Benhamou D. Ultrasonography of the optic nerve sheath may be useful for detecting raised intracranial pressure after severe brain injury. Intensive Care Med. 2007;33:1704–11.
122. Kimberly HH, Shah S, Marill K, Noble V. Correlation of optic nerve sheath diameter with direct measurement of intracranial pressure. Acad Emerg Med. 2008;15:201–4.
123. Le A, Hoehn ME, Smith ME, Spentzas T, Schlappy D, Pershad J. Bedside sonographic measurement of optic nerve sheath diameter as a predictor of increased intracranial pressure in children. Ann Emerg. 2009;53:785–91.
124. Moretti R, Pizzi B. Optic nerve ultrasound for detection of intracranial hypertension in intracranial hemorrhage patients: confirmation of previous findings in a different patient population. J Neurosurg Anesthesiol. 2009;21:16–20.
125. Moretti R, Pizzi B, Cassini F, Vivaldi N. Reliability of optic nerve ultrasound for the evaluation of patients with spontaneous intracranial hemorrhage. Neurocrit Care. 2009;11:406–10.
126. Soldatos T, Karakitsos D, Chatzimichail K, Papathanasiou M, Gouliamos A, Karabinis A. Optic nerve sonography in the diagnostic evaluation of adult brain injury. Crit Care. 2008; 12:R67.
127. Strumwasser A, Kwan RO, Yeung L, Miraflor E, Ereso A, Castro-Moure F, Patel A, Sadjadi J, Victorino GP. Sonographic optic nerve sheath diameter as an estimate of intracranial pressure in adult trauma. J Surg Res. 2011;170:265–71.
128. Pinto LA, Vanderwalle E, Pronk A, Stalmans I. Intraocular pressure correlates with optic nerve sheath diameter in patients with normal tension glaucoma. Graefes Arch Clin Exp Ophthalmol. 2012;250:1075–80.
129. Jaggi GP, Miller NR, Flammer J, Weinreb RN, Remonda L, Killer HE. Optic nerve sheath diameter in normal-tension glaucoma patients. Br J Ophthalmol. 2012;96:53–6.
130. Jonas JB, Wang N, Wang YX, You QS, Yang D, Xu L. Ocular Hypertension: General characteristics and estimated cerebrospinal fluid pressure. The Beijing Eye Study 2011. PLoS One. 2014e;9:e100533.
131. Berdahl JP, Fleischman D, Zaydlarova J, Stinnett S, Allingham RR, Fautsch MP. Body mass index has a linear relationship with cerebrospinal fluid pressure. Invest Ophthalmol Vis Sci. 2012;53:1422–7.
132. Ren R, Wang N, Zhang X, Tian G, Jonas JB. Cerebrospinal fluid pressure correlated with body mass index. Graefes Arch Clin Exp Ophthalmol. 2012;250:445–6.
133. Hayreh SS, Jonas JB. Optic disc morphology after arteritic anterior ischemic optic neuropathy. Ophthalmology. 2001;108: 1586–94.
134. Jonas JB, Budde WM. Diagnosis and pathogenesis of glaucomatous optic neuropathy: morphological aspects. Prog Retin Eye Res. 2000;19:1–40.
135. Jonas JB, Xu L. Optic disc morphology in eyes after nonarteritic anterior ischemic optic neuropathy. Invest Ophthalmol Vis Sci. 1993;34:2260–5.
136. Jonas JB, Jonas SB, Jonas RA, Holbach L, Dai Y, Sun X, Panda-Jonas S. Parapapillary atrophy: Histological gamma zone and delta zone. PLoS One. 2012b;7:e47237.
137. Dai Y, Jonas JB, Huang H, Wang M, Sun X. Microstructure of parapapillary atrophy: Beta zone and gamma zone. Invest Ophthalmol Vis Sci. 2013;54:2013–8.
138. De Moraes CG, Ketner S, Teng CC, Ehrlich JR, Raza AS, Liebmann JM, Ritch R, Hood DC. Beta-zone parapapillary atrophy and multifocal visual evoked potentials in eyes with glaucomatous optic neuropathy. Doc Ophthalmol. 2011a; 123:43–50.
139. De Moraes CG, Juthani VJ, Liebmann JM, Teng CC, Tello C, Susanna R Jr, Ritch R. Risk factors for visual field progression in treated glaucoma. Arch Ophthalmol. 2011b;129:562–8.
140. Teng CC, De Moraes CG, Prata TS, Tello C, Ritch R, Liebmann JM. Beta-Zone parapapillary atrophy and the velocity of glaucoma progression. Ophthalmology. 2010;117:909–15.
141. Teng CC, De Moraes CG, Prata TS, Liebmann CA, Tello C, Ritch R, Liebmann JM. The region of largest β-zone parapapillary atrophy area predicts the location of most rapid visual field progression. Ophthalmology. 2011;118:2409–13.
142. Xu L, Wang Y, Yang H, Jonas JB. Differences in parapapillary atrophy between glaucomatous and normal eyes: The Beijing Eye Study. Am J Ophthalmol. 2007b;144:541–6.
143. Frisén L, Claesson M. Narrowing of the retinal arterioles in descending optic atrophy. A quantitative clinical study. Ophthalmology. 1984;91:1342–6.
144. Kawasaki R, Wang JJ, Rochtchina E, Lee AJ, Wong TY, Mitchell P. Retinal vessel caliber is associated with the 10-year incidence of glaucoma: the Blue Mountains Eye Study. Ophthalmology. 2013;120:84–90.
145. Jonas JB, Schiro D. Localized retinal nerve fiber layer defects in nonglaucomatous optic nerve atrophy. (Brief Report). Graefes Arch Clin Exp Ophthalmol. 1994;232:759.
146. Jonas JB, Budde WM. Optic cup deepening spatially correlated with optic nerve damage in focal normal-pressure glaucoma. J Glaucoma. 1999;8:227–31.
147. Jonas JB, Hayreh SS. Optic disc morphology in experimental central retinal artery occlusion in rhesus monkeys. Am J Ophthalmol. 1999a;127:523–30.
148. Jonas JB, Hayreh SS. Localized retinal nerve fiber layer defects in chronic high-pressure experimental glaucoma in rhesus monkeys. Br J Ophthalmol. 1999b;83:1291–5.
149. Hayreh SS, Jonas JB. Optic disc and retinal nerve fiber layer damage following transient central retinal artery occlusion. An experimental study in rhesus monkeys. Am J Ophthalmol. 2000a;129:786–95.
150. Hayreh SS, Jonas JB. Appearance of the optic disk and retinal nerve fiber layer in atherosclerosis and arterial hypertension: an experimental study in rhesus monkeys. Am J Ophthalmol. 2000b;130:91–6.
151. Hayreh SS, Jonas JB, Zimmerman MB. Parapapillary chorioretinal atrophy in chronic high-pressure experimental glaucoma in rhesus monkeys. Invest Ophthalmol Vis Sci. 1998;39: 2296–303.
152. Jonas JB, Nguyen NX, Naumann GOH. Optic disc morphometry in "simple" optic nerve atrophy. Acta Ophthalmol. 1989c;67:199–203.
153. Hayreh SS. Optic disc edema in raised intracranial pressure. V Pathogenesis. Arch Ophthalmol. 1977;95:1553–65.
154. Hayreh SS. Cerebrospinal fluid pressure and glaucomatous optic disc cupping. Graefes Arch Clin Exp Ophthalmol. 2009;247:721–4.
155. Morgan WH, Cringle SJ, Balaratnasingam C, Yu DY. Impaired cerebrospinal fluid circulation and its relationship to glaucoma. Clin Exp Ophthalmol. 2008b;36:802–3.
156. Burgoyne CF, Morrison JC. The anatomy and pathophysiology of the optic nerve head in glaucoma. J Glaucoma. 2001;10(5 Suppl 1):S16–8.
157. Fleischman D, Berdahl J, Stinnett SS, Fautsch MP, Allingham RR. Cerebrospinal fluid pressure (CSFP) trends in diseases associated with primary open angle glaucoma (POAG). Acta

Ophthalmol. 2015;33(3):e234–6. https://doi.org/10.1111/aos.12551. [Epub ahead of print]
158. Jonas JB. Intraocular pressure during weight lifting. Arch Ophthalmol. 2008;126:287–8. Comment on Arch Ophthalmol. 2006; 124:1251-1254
159. Ren R, Zhang X, Wang N, Li B, Tian G, Jonas JB. Cerebrospinal fluid pressure in ocular hypertension. Acta Ophthalmol. 2011a;89:e142–8.
160. Ren R, Wang N, Zhang X, Cui T, Jonas JB. Trans-lamina cribrosa pressure difference correlated with neuroretinal rim area in glaucoma. Graefes Arch Clin Exp Ophthalmol. 2011b;249:1057–63.
161. Shin DH. Influence of cerebrospinal fluid pressure on the lamina cribrosa tissue pressure gradient. Invest Ophthalmol Vis Sci. 1995;36:2163–4.
162. Wostyn P, Audenaert K, De Deyn PP. High occurrence rate of glaucoma among patients with normal pressure hydrocephalus. J Glaucoma. 2010;19:225–6.
163. Wostyn P, De Groot V, Van Dam D, Audenaert K, De Deyn PP. Senescent changes in cerebrospinal fluid circulatory physiology and their role in the pathogenesis of normal-tension glaucoma. Am J Ophthalmol. 2013;156:5–14.e2.
164. Wostyn P, De Groot V, Van Dam D, Audenaert K, De Deyn PP. The role of low intracranial pressure in the development of glaucoma in patients with Alzheimer's disease. Prog Retin Eye Res. 2014;39:107–8.
165. Wostyn P, De Groot V, Van Dam D, Audenaert K, De Deyn PP. Intracranial pressure fluctuations: a potential risk factor for glaucoma? Acta Ophthalmol. 2015;93(1):e83–4. [Epub ahead of print]
166. Gilland O. Normal cerebrospinal-fluid pressure. N Engl J Med. 1969;280:904–5.
167. Greenfield DS, Wanichwecharungruang B, Liebmann JM, Ritch R. Pseudotumor cerebri appearing with unilateral papilledema after trabeculectomy. Arch Ophthalmol. 1997;115:423–6.
168. Yang H, Downs JC, Bellezza A, Thompson H, Burgoyne CF. 3-D histomorphometry of the normal and early glaucomatous monkey optic nerve head: prelaminar neural tissues and cupping. Invest Ophthalmol Vis Sci. 2007;48:5068–84.
169. Berdahl JP, Allingham RR, Johnson DH. Cerebrospinal fluid pressure is decreased in primary open-angle glaucoma. Ophthalmology. 2008a;115:763–8.
170. Berdahl JP, Fautsch MP, Stinnett SS, Allingham RR. Intracranial pressure in primary open angle glaucoma, normal tension glaucoma, and ocular hypertension: a case-control study. Invest Ophthalmol Vis Sci. 2008b;49:5412–8.
171. Jonas JB, Nangia V, Wang N, Bhate K, Nangia P, Nangia P, Yang D, Xie X, Panda-Jonas S. Trans-lamina cribrosa pressure difference and open-angle glaucoma: The Central India Eye and Medical Study. PLoS One. 2013;8:e82284.
172. Jonas JB, Wang N, Wang S, Wang YX, You QS, Yang D, Wei WB, Xu L. Retinal vessel diameter and estimated cerebrospinal fluid pressure in arterial hypertension. The Beijing Eye Study. Am J Hypertens. 2014c;27:1170–8.
173. Jonas JB, Wang N, Xu J, Wang YX, You QS, Yang D, Xie XB, Xu L. Diabetic retinopathy and estimated cerebrospinal fluid pressure. The Beijing Eye Study 2011. PLoS One. 2014d;9:e96273.
174. Jonas JB, Wang N, Wang YX, You QS, Xie XB, Yang D, Xu L. Estimated trans-lamina cribrosa pressure difference versus intraocular pressure as biomarker for open-angle glaucoma: The Beijing Eye Study 2011. Acta Ophthalmol. 2014f; https://doi.org/10.1111/aos.12480. [Epub ahead of print]
175. Jonas JB, Nangia V, Gupta R, Agarwal S, Matin A, Khare A, Bhate K, Sinha A, Bhojwani K, Kulkarni M, Panda-Jonas S. Retinal nerve fibre layer cross-sectional area, neuroretinal rim area and body mass index. Acta Ophthalmol. 2014g;92:e194–9.
176. Xu L, Wang YX, Wang S, Jonas JB. Neuroretinal rim area and body mass index. PLoS One. 2012;7:e30104.
177. Qu Y, Wang YX, Xu L, Zhang L, Zhang J, Zhang J, Wang L, Yang L, Yang A, Wang J, Jonas JB. Glaucoma-like optic neuropathy in patients with intracranial tumors. Acta Ophthalmol. 2011;89:E428–33.
178. Wang YX, Xu L, Lu W, Liu FJ, Qu YZ, Wang J, Jonas JB. Parapapillary atrophy in patients with intracranial tumors. Acta Ophthalmol. 2013;91:521–5.
179. Flammer J, Orgül S, Costa VP, Orzalesi N, Krieglstein GK, Serra LM, Renard JP, Stefánsson E. The impact of ocular blood flow in glaucoma. Prog Retin Eye Res. 2002;21:359–93.
180. Iwase A, Suzuki Y, Araie M, Yamamoto T, Abe H, Shirato S, Kuwayama Y, Mishima HK, Shimizu H, Tomita G, Inoue Y, Kitazawa Y, Tajimi Study Group, Japan Glaucoma Society. The prevalence of primary open-angle glaucoma in Japanese: the Tajimi Study. Ophthalmology. 2004;111:1641–8.
181. Shiose Y, Kitazawa Y, Tsukahara S, Akamatsu T, Mizokami K, Futa R, Katsushima H, Kosaki H. Epidemiology of glaucoma in Japan--a nationwide glaucoma survey. Jpn J Ophthalmol. 1991;35:133–55.
182. Li J, Fang L, Killer HE, Flammer J, Meyer P, Neutzner A. Meningothelial cells as part of the central nervous system host defence. Biol Cell. 2013a;105:304–15.
183. Li Z, Yang DY, Lu Y, Liu DC, Jia JP, Jonas JB, Wang NL. Intracranial hypotension and co-existent normal-pressure glaucoma: the Beijing intracranial and intraocular pressure study. Chin Med J. 2013b;126:1588–9.
184. Killer HE. Production and circulation of cerebrospinal fluid with respect to the subarachnoid space of the optic nerve. J Glaucoma. 2013a;22(Suppl 5):S8–10.
185. Jaggi GP, Mironov A, Huber AR, Killer HE. Optic nerve compartment syndrome in a patient with optic nerve sheath meningioma. Eur J Ophthalmol. 2007;17:454–8.
186. Killer HE. Compartment syndromes of the optic nerve and open-angle glaucoma. J Glaucoma. 2013b;22(Suppl 5):S19–20.
187. Killer HE, Jaggi GP, Miller NR, Huber AR, Landolt H, Mironov A, Meyer P, Remonda L. Cerebrospinal fluid dynamics between the basal cisterns and the subarachnoid space of the optic nerve in patients with papilloedema. Br J Ophthalmol. 2011;95:822–7.
188. Killer HE, Laeng HR, Groscurth P. Lymphatic capillaries in the meninges of the human optic nerve. J Neuroophthalmol. 1999;19:222–8.
189. Killer HE, Jaggi G, Miller NR, Flammer J, Meyer P. Does immunohistochemistry allow easy detection of lymphatics in the optic nerve sheath? J Histochem Cytochem. 2008a;56:1087–92.
190. Xin X, Fan B, Flammer J, Miller NR, Jaggi GP, Killer HE, Meyer P, Neutzner A. Meningothelial cells react to elevated pressure and oxidative stress. PLoS One. 2011;6:e20142.
191. Jaggi GP, Harlev M, Ziegler U, Dotan S, Miller NR, Killer HE. Cerebrospinal fluid segregation optic neuropathy: an experimental model and a hypothesis. Br J Ophthalmol. 2010;94:1088–93.
192. Killer HE, Jaggi GP, Flammer J, Miller NR, Huber AR. The optic nerve: a new window into cerebrospinal fluid composition? Brain. 2006;129:1027–30.
193. Killer HE, Jaggi GP, Flammer J, Miller NR, Huber AR, Mironov A. Cerebrospinal fluid dynamics between the intracranial and the subarachnoid space of the optic nerve. Is it always bidirectional? Brain. 2007;130:514–20.
194. Killer HE, Jaggi GP, Flammer J, Miller NR. Is open-angle glaucoma caused by impaired cerebrospinal fluid circulation: around the optic nerve? Clin Exp Ophthalmol. 2008b;36:308–11.
195. Killer HE, Miller NR, Flammer J, Meyer P, Weinreb RN, Remonda L, Jaggi GP. Cerebrospinal fluid exchange in the optic nerve in normal-tension glaucoma. Br J Ophthalmol. 2012;96:544–8.

196. Hedges TR, Zaren HA. The relationship of optic nerve tissue pressure to intracranial and systemic arterial pressure. Am J Ophthalmol. 1973;75:90–8.
197. Rios-Montenegro EN, Anderson DR, Noble JD. Intracranial pressure and ocular hemodynamics. Arch Ophthalmol. 1973;89:52–8.
198. Yang D, Fu J, Hou R, Liu K, Jonas JB, Wang H, Chen WW, Li Z, Sang J, Zhang Z, Liu S, Cao Y, Xie X, Ren R, Lu Q, Weinreb RN, Wang N. Optic neuropathy induced by experimentally reduced cerebrospinal fluid pressure in monkeys. Invest Ophthalmol Vis Sci. 2014;55:3067–73.
199. Jonas JB, Wang N, Wang YX, You QS, Yang D, Xie XB, Xu L. Incident retinal vein occlusions and estimated cerebrospinal fluid pressure. The Beijing Eye Study. Acta Ophthalmol. 2015b;93(7):e522–6.
200. Gupta A, Raman R, Mohana K, Kulothungan V, Sharma T. Communications between intraretinal and subretinal space on optical coherence tomography of neurosensory retinal detachment in diabetic macular edema. Oman J Ophthalmol. 2013;6:183–8.
201. Gupta A, Raman R, Kulothungan V, Sharma T. Association of systemic and ocular risk factors with neurosensory retinal detachment in diabetic macular edema: a case-control study. BMC Ophthalmol. 2014a;14:47.
202. Gupta P, Sidhartha E, Girard MJ, Mari JM, Wong TY, Cheng CY. A simplified method to measure choroidal thickness using adaptive compensation in enhanced depth imaging optical coherence tomography. PLoS One. 2014b;9:e96661.
203. Paques M, Massin P, Sahel JA, Gaudric A, Bergmann JF, Azancot S, Lévy BI, Vicaut E. Circadian fluctuations of macular edema in patients with morning vision blurring: correlation with arterial pressure and effect of light deprivation. Invest Ophthalmol Vis Sci. 2005;46:4707–11.
204. Tan CS, Ouyang Y, Ruiz H, Sadda SR. Diurnal variation of choroidal thickness in normal, healthy subjects measured by spectral domain optical coherence tomography. Invest Ophthalmol Vis Sci. 2012;53:261–6.
205. Toyokawa N, Kimura H, Fukomoto A, Kuroda S. Difference in morning and evening choroidal thickness in Japanese subjects with no chorioretinal disease. Ophthalmic Surg Lasers Imaging. 2012;43:109–14.
206. Klein R, Klein BE, Moss SE, Wong TY, Hubbard L, Cruickshanks KJ, Palta M. The relation of retinal vessel caliber to the incidence and progression of diabetic retinopathy: XIX: the Wisconsin Epidemiologic Study of Diabetic Retinopathy. Arch Ophthalmol. 2004;122:76–83.
207. Klein R, Klein BE, Moss SE, Wong TY, Sharrett AR. Retinal vascular caliber in persons with type 2 diabetes: the Wisconsin Epidemiological Study of Diabetic Retinopathy: XX. Ophthalmology. 2006;113:1488–98.
208. Klein R, Klein BE, Moss SE, Wong TY. Retinal vessel caliber and microvascular and macrovascular disease in type 2 diabetes: XXI: the Wisconsin Epidemiologic Study of Diabetic Retinopathy. Ophthalmology. 2007;114:1884–92.
209. Stodtmeister R. The pulsation and the pressure of the central retinal vein and their relation to glaucoma damage and therapy. Klin Monatsbl Augenheilkd. 2008;225:632–6.
210. Cox SN, Hay E, Bird AC. Treatment of chronic macular edema with acetazolamide. Arch Ophthalmol. 1988;106:1190–5.
211. Rosenbloom AL. Intracerebral crises during treatment of diabetic ketoacidosis. Diabetes Care. 1990;13:22–33.
212. Srinivasan S, Benneyworth B, Garton HJ, Hervey-Jumper SL, Raimer PL, Odetola FO, Han YY. Intracranial pressure/cerebral perfusion pressure-targeted management of life-threatening intracranial hypertension complicating diabetic ketoacidosis-associated cerebral edema: a case report. Pediatr Emerg Care. 2012;28:696–8.
213. Van der Meulen JA, Klip A, Grinstein S. Possible mechanism for cerebral oedema in diabetic ketoacidosis. Lancet. 1987;2(8554):306–8.
214. Wood EG, Go-Wingkun J, Luisiri A, Aceto T Jr. Symptomatic cerebral swelling complicating diabetic ketoacidosis documented by intraventricular pressure monitoring: survival without neurologic sequela. Pediatr Emerg Care. 1990;6:285–8.
215. Jonas JB, Wang N, Yang D, Ritch R, Panda-Jonas S. Facts and myths of cerebrospinal fluid pressure for the physiology of the eye. Prog Retin Eye Res. 2015;46:67–83.

Energy Theory of Glaucoma

13

Xiaoxia Li and Ningli Wang

Glaucoma is the leading cause of irreversible blindness [1], and it is a major public health issue. The pathological mechanism of glaucoma is not fully understood yet. In this chapter, we mainly focus on the glia cells which take part in the underlying mechanism of glaucoma.

Glia cells tile throughout the whole central nervous system (CNS). Glia cells are at least equal to or exceed neurons in numbers, and 20–40% of total glia cells in mammalian brains cells are specialized glia cells named astrocytes [2]. But the studies of astrocytes functions are lagged relatively. Unlike the brain, the main retinal glial cell is Müller cell, which is composed of 90% total retinal glia cells, followed by astrocytes and microglial cells. In most rodent optic nerve head (ONH), a very important region that has to deal with continuous intraocular pressure (IOP) and cerebrospinal fluid pressure (CSFp) fluctuation, the glial lamina is formed by a kind of special astrocytes named fortified astrocytes (FASTs) which occupies 50% in volume.

Glia cells play important roles in neuronal development, in microenvironmental stability, and especially in neuronal circuit function [3]. Glia cells have two opposite effects on neurons; in normal condition, astrocytes or other glial cells protect neurons and maintain their functions, but in pathological condition, they may damage neurons by releasing deteriorate factors.

Mitochondria play an important role in the intracellular core function for energy supply and viability. In recent research, Nicholas Marsh-Armstrong reported that neurons can transcellularly release damaged mitochondria to astrocytes for disposal and recycling at ONH [4, 5]. Interestingly, Lo Eng H. demonstrated that in cerebral ischemia model, neuroglial may transcellularly transfer healthy mitochondrial particles from astrocytes to damaged neurons after stroke through CD38 and cADPR which are Ca^{2+} dependent in supporting cell viability and recovery [6] (Fig. 13.1). We proposed this phenomenon as "astrocytes-mitochondria-neuron circle."

In the following part, we will explore the potential cross talk between neuron, mitochondria, and glia cells in ONH of high-IOP rat model.

13.1 Morphology of Astrocytes in ONH

In ONH, there is a special type of astrocytes named FASTs; they account for almost 50% astrocytes in volume as its special functions. In human and nonhuman primates, the ONH is traversed by a dense meshwork of tough connective tissue which transfers damaging mechanical forces to the ganglion axons. Here, we mainly discuss the glial cells reaction in rat ONH. It is well known unlike human lamina cribrosa (LC), most of rodent animals lack of LC, instead of glial lamina formed by a mount of FASTs.

In rat ONH, the very tiny processes of FASTs are scattered in the intervals of axons and tightly close to axons (Fig. 13.2a). These axons are circled completely, and some axons are half circled by FASTs tiny processes.

The FASTs and axons bind together to avoid relative motion and further sustain the pressure fluctuation from IOP and CSF. For another reason, the close relationship between axons and FASTs makes it easy for nutrients and metabolic waste exchange. What's more, except these small materials, the much more bigger organelle can also be transcellularly disposed and recycled in ONH [4, 5].

In pathological conditions, tiny processes from FASTs shrink or diminish, accompanied by axon shrinking or diminishing (Fig. 13.2b), and it is hard to verify which one is influenced at first. But it is clear that, in the early stage of damage, the diminished axons and processes left bald space and the glial lamina is much more vulnerable. At the last stage, the bald space is filled by scar connective tissue.

X. Li · N. Wang (✉)
Beijing Institute of Ophthalmology, Beijing Tongren Eye Center, Beijing Tongren Hosptial, Capital Medical University, Beijing, China

Beijing Ophthalmology & Visual Sciences Key Laboratory, Beijing, China
e-mail: wningli@vip.163.com

N. Wang (ed.), *Intraocular and Intracranial Pressure Gradient in Glaucoma*,
Advances in Visual Science and Eye Diseases 1, https://doi.org/10.1007/978-981-13-2137-5_13

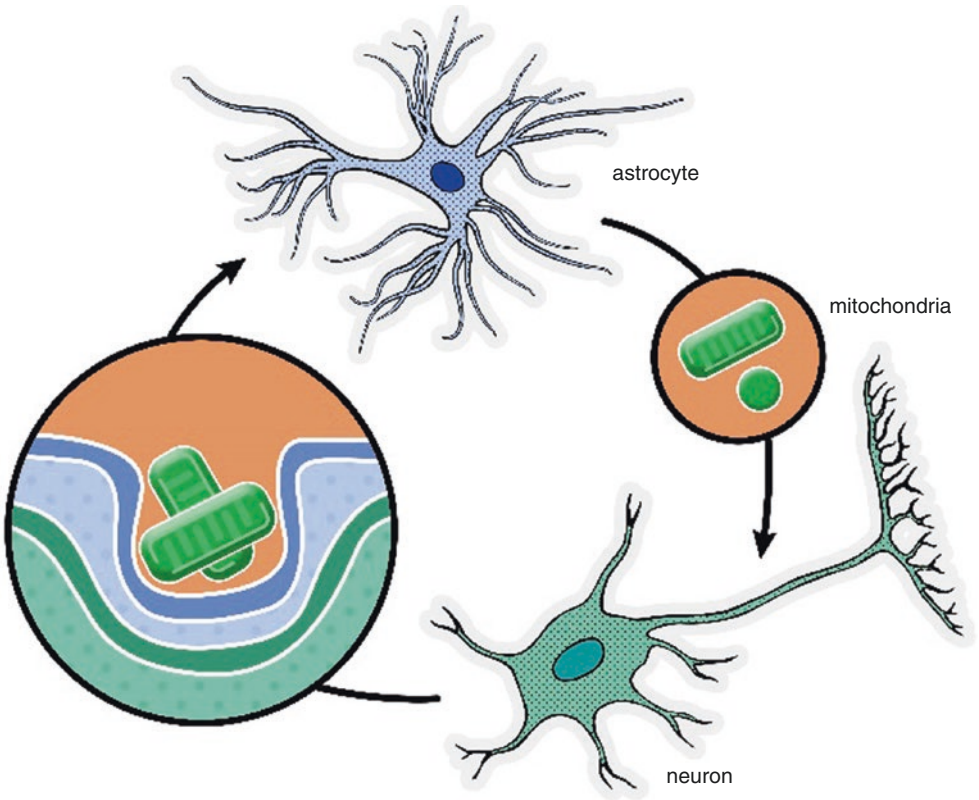

Fig. 13.1 In ONH the axon mitochondria can be transcellularly disposed and recycled by astrocytes, and astrocytes may release healthy mitochondrial particles to damaged neurons for its recovery

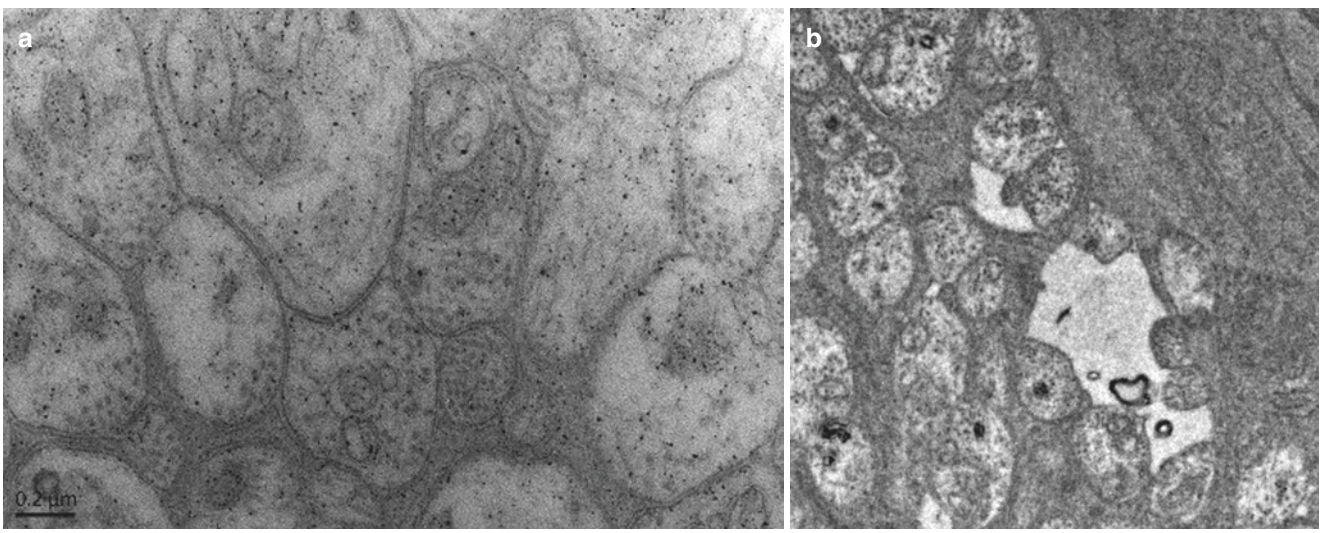

Fig. 13.2 (**a**) Axons and FASTs tiny processes in ONH; (**b**) the bald space formed as axons and tiny processes diminished

13.2 Energy Theory of High–IOP Model

It is quite different with retina that there is a complete absence of aquaporins from the ONH [7]. It is well known in the retina the differential distribution of aquaporin-4(AQP4) along the radial axis of the Müller cell membranes, and transport water away from the subretinal space toward the vitreous or vessels.

In research report, there are a lot of pinocytotic vesicles in the FASTs tiny processes. Davis et al. proposed that these pinocytotic vesicles may take part in the origin of glaucomatous process, when the maintained high IOP outstrip the energy needed to maintain the extracellular fluid buffer in the rim of the ONH [4, 5]. Raisman and his colleague proposed that the initial damage occurred in the peripheral of

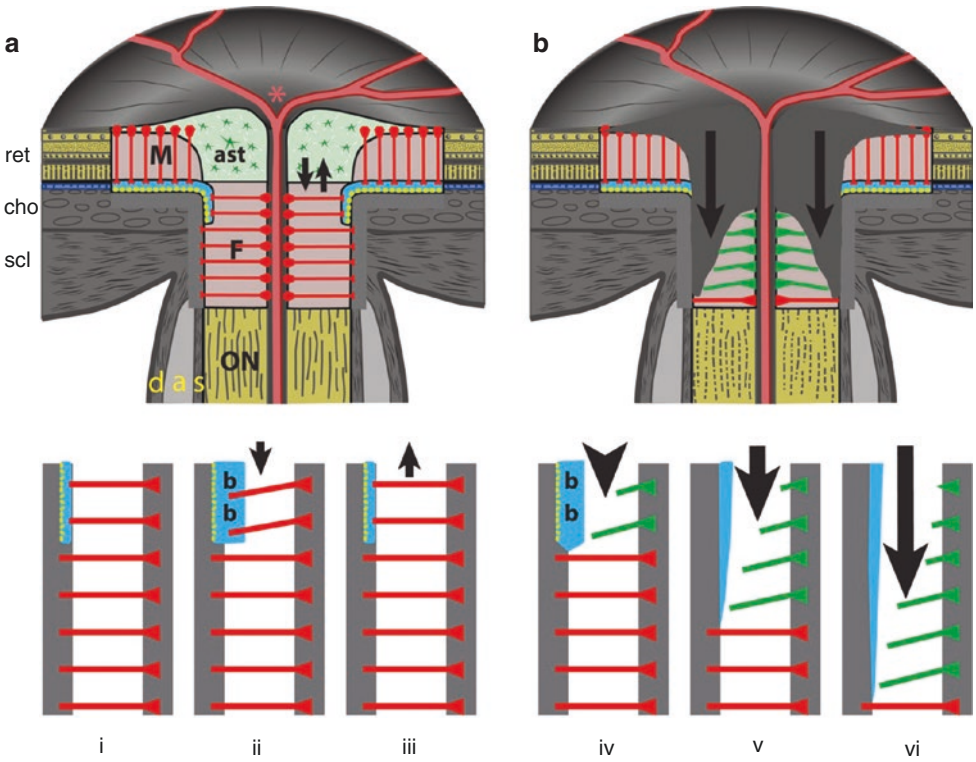

Fig. 13.3 The energy theory of glaucoma: overload water in ONH (Reprinted with permission from [8]) *M* muller cell; *F* fortified astrocyte; *ast* astrocytes; *d* dura mater; *a* subarachnoid space; *s* sheath; *b* bubles; *ret* retinal; *cho* choroid; *scl* sclera

ONH and the glial lamina is gradually destroyed, until it deformed significantly with motion (Fig. 13.3).

However, in our recent acute high-IOP rat model, we also found the peripheral of ONH is vulnerable which is similar to the above research. However, we found these axons of half circled or un-circled by FASTs processes is vulnerable too, even if it is not in the peripheral of ONHs. After the recue stem cell was injected in ONH, the axons are survival (Fig. 13.4) [9]. We propose that except the pressure, there are other factors involved.

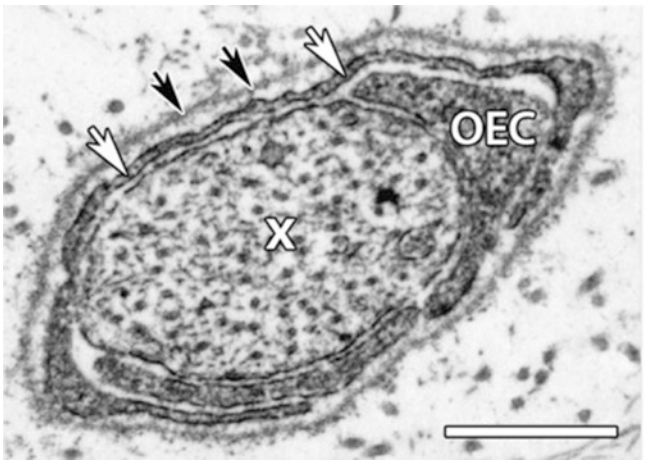

Fig. 13.4 Olfactory ensheathing cells (OEC) rescue dying axon (come from [9]). (Reprinted with permission from [8])

13.3 Astrocytes-Mitochondria-Axons Circle

13.3.1 Transcellular Disposal of Astrocytes Degrading Mitochondria by Transmitophagy

In the recent report, in ONH, astrocytes can transcellularly dispose damaged or unhealthy axonal mitochondria, and this procedure can be seen as a kind of natural mitophagy [4, 5]. And mitochondria are the only energy supply organelle, which is very important for cell survival and development. The retinal ganglion cells (RGC) axons, from RGC bodies afferent to lateral geniculate nucleus (LGN) or superior colliculus (SC). Little is known about how neurons with long axons degrade mitochondria. Degrading mitochondria can be transcellularly disposed by astrocytes in ONH and can be transmitophagy by cerebral cortex in young wild-type mice, although at a relative lower density than at ONH [5]. This ability to exchange mitochondria may represent a potential mode of cell-to-cell signaling in the central nervous system and peripheral optic nerve system. Except that, research has reported that bone marrow-derived astrocytes may transfer mitochondria into pulmonary alveoli to rescue acute lung injury [10].

13.3.2 Astrocytes May Release Healthy Mitochondrial Particles to Damaged Neurons

Although the damage/injury signals that initiate mitochondrial transfer have yet to be identified, it is plausible that the intracellular energy storage condition may play an important role in directing one cell to transfer mitochondria to another. It had been proved that this procedure is highly sensitive to cytosolic Ca2+, cADPR, and sometimes to CD38 [6, 11]. This transcellular mitochondria transfer is mainly focused on mesenchymal stem cell, and there is no research that had been reported in optic nerve system yet.

Similar to high IOP, our recent study demonstrated selective glial reactivity in visual system in reduced cerebrospinal fluid pressure, which accompanied with damaged neurons (data not shown).

References

1. Quigley HA, Broman AT. The number of people with glaucoma worldwide in 2010 and 2020. Br J Ophthalmol. 2006;90:262–7.
2. Herculano-Houzel S. The glia/neuron ratio: how it varies uniformly across brain structures and species and what that means for brain physiology and evolution. Glia. 2014;62:1377–91.
3. Khakh BS, Sofroniew MV. Diversity of astrocyte functions and phenotypes in neural circuits. Nat Neurosci. 2015;18:942–52.
4. Davis CH, Kim KY, Bushong EA, et al. Transcellular degradation of axonal mitochondria. Proc Natl Acad Sci U S A. 2014;111:9633–8.
5. Davis CH, Marsh-Armstrong N. Discovery and implications of transcellular mitophagy. Autophagy. 2014;10:2383–4.
6. Hayakawa K, Esposito E, Wang X, et al. Transfer of mitochondria from astrocytes to neurons after stroke. Nature. 2016;535:551–5.
7. Nagelhus EA, Veruki ML, Torp R, et al. Aquaporin-4 water channel protein in the rat retina and optic nerve: polarized expression in Muller cells and fibrous astrocytes. J Neurosci. 1998;18:2506–19.
8. Li Y, Li D, Ying X, et al. An energy theory of glaucoma. Glia. 2015;63(9):1537–52.
9. Dai C, Khaw PT, Yin ZQ, Li D, Raisman G, Li Y. Olfactory ensheathing cells rescue optic nerve fibers in a rat glaucoma model. Transl Vis Sci Technol. 2012;1:3.
10. Islam MN, Das SR, Emin MT, et al. Mitochondrial transfer from bone-marrow-derived stromal cells to pulmonary alveoli protects against acute lung injury. Nat Med. 2012;18:759–65.
11. Spees JL, Lee RH, Gregory CA. Mechanisms of mesenchymal stem/stromal cell function. Stem Cell Res Ther. 2016;7:125.

Part III

Methodology

Techniques in Measuring Intraocular and Intracranial Pressure Gradients

14

Xiaobin Xie, April Peszel, Feras Kamel Rizeq, Chenyu Sun, Diya Yang, and Ningli Wang

14.1 Background

As a part of the central nervous system, the optic nerve goes through the comparatively independent intraocular and retrobulbar pressurized cerebrospinal fluid cavity. Additionally, the central retinal vein and artery pass from the optic nerve head through the optic nerve and the orbital cerebrospinal fluid (CSF) space. The CSF pressure, as the counter pressure against intraocular pressure (IOP) from the opposite side of the lamina cribrosa, may have pathophysiologic importance for several intracranial and intraocular pressure gradient-related ophthalmic disorders, such as glaucomatous optic neuropathy associated with CSF pressure dysregulation [1–12], optic neuropathy secondary to idiopathic intracranial hypertension [13–19], visual impairment syndrome in space [20–22], and retinal vein occlusion [23].

The role of intracranial and intraocular gradients in the pathogenesis of glaucoma is increasingly drawing the attention of scholars. Techniques of IOP measurement are now relatively mature. Till now, continuous IOP measurements can be realized in a habitual posture over a 24-h period with commercial devices in clinical practice [24]. The advancements in measurements of intracranial pressure (ICP), which is the pressure of the cerebrospinal fluid and also an important component of intracranial and intraocular gradients, will be discussed in detail in this chapter.

14.2 Advances in ICP Monitoring Techniques

There are several different ICP monitoring techniques. These methods have gone from being an invasive procedure to more of a noninvasive approach. While there are several things to consider, the most important initial task is to address the central considerations of this technology.

First and foremost, the most fundamental issue for doctors to address is precision. The ANSI/AAMI has set a certain criterion for ICP monitoring devices. Based on their standards for this technology, the ICP monitoring equipment's scope of pressure must be between 0 and 100 mmHg. It must also have a reliability of at least 2 mmHg in the scope of 0–20 mmHg, while the highest inaccuracy should not vary more than 10% between the values from 20 to 100 mmHg. Secondly, compared with transient ICP monitoring, continuous monitoring divulges the complete array of ICP fluctuations during a state of awareness, various sleep stages, changes in the position of the patient, and other activities. Thirdly, problems can occur during the procedure and hinder the analysis. Some of these complications that can possibly alter the analysis include but are not limited to bleeding, contamination, sensor malfunction, drift, and imprecise arrangement of the device. These hindrances not only affect the ICP readings but also may cause further harm to the patient's brain. Another key factor needing to be addressed is the cost of this technology and infrastructure which should be evaluated. Last but not the least, portability and field deployability should be considered [25].

X. Xie
Eye Hospital, China Academy of Chinese Medical Sciences, Beijing, China

A. Peszel · C. Sun
The First Affiliated Hospital of Anhui Medical University, Hefei, China

F. Kamel Rizeq
Avalon University School of Medicine, Willemstad, Curacao

D. Yang · N. Wang (✉)
Beijing Institute of Ophthalmology, Beijing Tongren Eye Center, Beijing Tongren Hospital, Capital Medical University, Beijing, China

Beijing Ophthalmology & Visual Sciences Key Laboratory, Beijing, China
e-mail: wningli@vip.163.com

N. Wang (ed.), *Intraocular and Intracranial Pressure Gradient in Glaucoma*,
Advances in Visual Science and Eye Diseases 1, https://doi.org/10.1007/978-981-13-2137-5_14

14.2.1 Direct or Invasive ICP Monitoring

Direct or invasive ICP monitoring provides direct signals from distinctive intracranial structural positions, namely, intraventricular, intraparenchymal, epidural, subdural, and subarachnoidal spaces. Furthermore, lumbar punctures may assist in measuring the ICP in patients that have communicating CSF pathways. Invasive ICP measurement via a brain ventriculostomy, intraparenchymal systems, or by lumbar puncture in patients with free CSF circulation is the most reliable method for ICP measurement [26–28].

14.2.1.1 External Ventricular Drain (EVD) Placement

EVD is also known as an intraventricular catheter or ventriculostomy. ICP monitoring by EVD was described in the report by Guillaume and Janny in 1951 [29]. Moreover, EVD is a very common neurosurgical procedure in the emergency room and intensive care unit. The EVD technique is the most accurate system for ICP measurements, hence why it is the preferred method by the American Brain Trauma Foundation and remains the gold standard [27, 28, 30].

Fluid-filled tubing is used to attach an intraventricular catheter to an external pressure transducer. The most common entry points are Kocher's point and the forehead (Fig. 14.1) [31]. Placement of the intraventricular catheter requires its penetration through the skull, dura mater, and brain in such a way that the ventricle of the brain is accessed.

By far, EVD, a safe and effective method, is considered to be the "gold standard" of ICP measurement. This method of measuring global ICP has advantages in the following aspects: in vivo calibration at a relatively low cost, therapeutic drainage of cerebrospinal fluid, and administration of drugs, all the while keeping measurements uninfluenced by eventual pressure gradients in the brain parenchyma. Generally, the complication rate of EVD is approximately 16.1%, with an infection rate of 10.2%, catheter malalignment rate of 2.2%, and a bleeding rate of 3.6%. The degree of severity of the complications is contingent upon the abilities of the surgeon [32]. The other disadvantages include inaccuracies of the pressure measurements when the fluid column gets obstructed or leaks and the necessity to maintain the transducer at a fixed reference point relative to the patient's head, etc.

Neuronavigation techniques using computed tomography, magnetic resonance imaging, stereotaxy, endoscopy, or ultrasound for catheter placements are superior to freehand techniques. An efficient image-guidance system may improve patient safety and the surgeon's ability to successfully target the ventricles [33, 34].

It is necessary for EVDs to be zero-balanced consistently to ensure precision. This is due to the fact that they can become obstructed by cerebral tissues or clots in the blood.

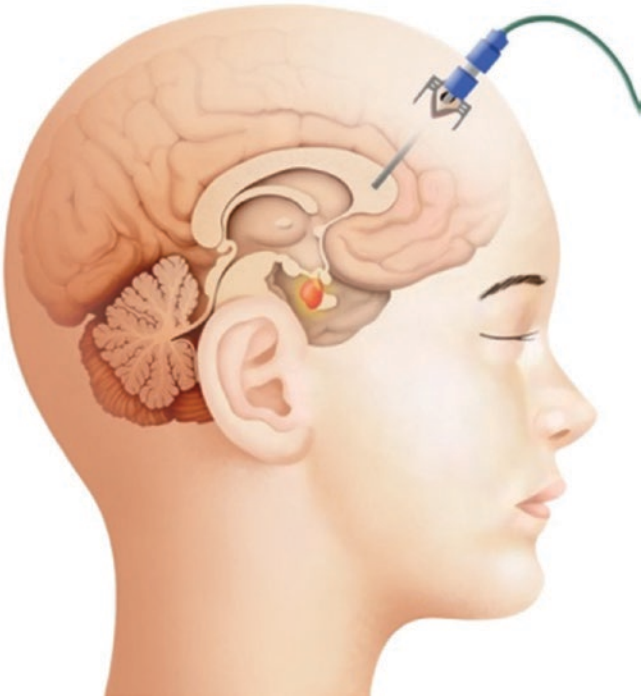

Fig. 14.1 External ventricular drain placement at the entry points of forehead

This can happen whenever a patient becomes repositioned, any changes in the drain level, or if the reading does not correspond to the patient's clinical situation.

14.2.1.2 Implantable Microtransducer ICP Monitoring Devices

The implantable microtransducer ICP monitoring devices allow measurement of absolute ICP levels and identification and analysis of high-resolution ICP waveforms. As with EVDs, microtransducers can reduce the infection rate and the risk of hemorrhages. The devices can be classified as fiber optic devices, piezoelectric strain gauge devices, and pneumatic sensors.

Types of Implantable Microtransducer ICP Monitoring

Fiber optic devices enable light to be transferred by cables to a displaceable mirror. The mirror becomes displaced by variations in ICP, and thus the changes of light refraction are deciphered into an ICP value. As an example, Camino ICP Monitor (Camino Laboratories, San Diego, California, USA) can provide a continuous display of the ICP waveform [35]. A continuous record of mean pressure over the most recent 24-h period is stored in memory. Intraventricular or intraparenchymal Camino sensors have shown an average drift of up to 3.2 mmHg per day [36]. Epidural Camino sensor considerably overestimated ICP with a mean of about 9 mmHg but extending to almost 30 mmHg [37]. Mechanical compli-

cations included breakage of the optical fiber, dislocations of the fixation screw or the probe, and failure of ICP recording for unknown reasons [38]. Fiber optic monitors have a lower risk of infection, ranging from 0% to 1.7%.

Piezoelectric strain gauge devices have a miniaturized strain gauge located on the side of the catheter near the distal tip. Changes in the position of the diaphragm cause changes in the electrical resistance that is recorded and transformed, and ICP values can be calculated. The Codman MicroSensor (Codman, Johnson & Johnson, Raynham, MA, USA) [39], the Raumedic Neurovent-P ICP sensor (Raumedic AG + CO, Raumedic, Germany) [40], and the Pressio sensor (Sophysa Ltd., Orsay, France) [41] are piezoelectric strain gauge devices.

Pneumatic sensors recognize variations in pressure with small balloons located at the far end of the catheter. The measured ICP is conveyed through the delicate pouch, which is partitioned to the volume of air in the pouch. An electric signal is produced by converting the signal by a pressure transducer. The ICP monitor zeroes automatically once per hour. The Spiegelberg Air-Pouch System is a kind of low-cost pneumatic device. In a clinical study, the Spiegelberg 3-PN sensor (Spiegelberg KG, Hamburg, Germany) was inserted into five patients. The patients' intraventricular pressure was analyzed concurrently and compared to either the intraparenchymal or subdural Spiegelberg 3-PN pressure. The contrasts between the Spiegelberg reading were fewer than ±3 mmHg in 99.6% and fewer than ±2 mmHg in 91.3% of interpretations [42].

Location of devices

The microtransducer systems can be positioned directly in the intraventricular, intraparenchymal, epidural, subdural, or subarachnoid cavity, as shown in the Fig. 14.2. The microtransducers' ideal placement is determined by incorporating key aspects, such as the interval or length of monitoring, a satisfactory drift, accuracy within the limits, and any benefits that the patient may receive. Taking accuracy into consideration, the ideal placement of the microtransducer probe in descending order is firstly intraventricular, followed by intraparenchymal, then subarachnoid, and finally epidural. There are other options apart from ventricular catheters in cases where patients have severe brain damage that leads to swelling. Some of the other options, which could be considered, are alternatives such as epidural and subdural catheters and subarachnoid bolts which are all surface monitors. The downside to these surface monitors is that they are error prone and can be misplaced, and a baseline drift can occur during uninterrupted usage over the span of a few days [43–45]. ICP tends to be underestimated with the use of subarachnoid screws, bolts, or catheters [43, 46]. The opposite is true of epidural methods which overestimate ICP values [37]. Although epidural monitoring is not a reliable method

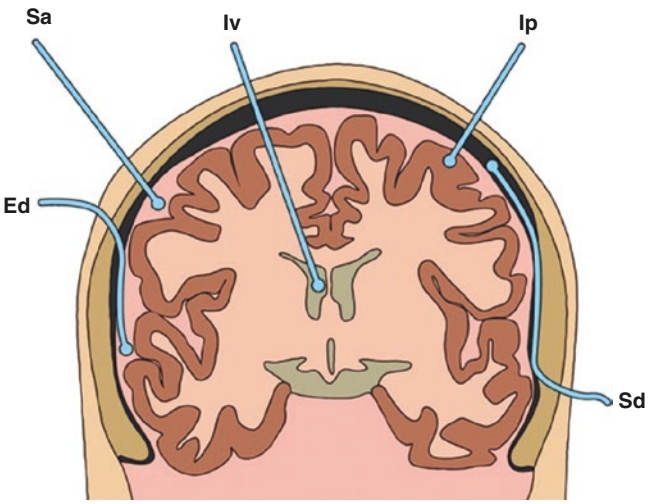

Fig. 14.2 Sites for intracranial pressure measurement. *Ed* epidural, *Sa* subarachnoid space, *Iv* intraventricular, *Ip* intraparenchymal, *Sd* subdural

to evaluate ICP, it can be used in other areas such as defining waveform parameters seen in the amplitude of pulse pressures and the mean amplitudes of the ICP wave [47]. The reason behind this discrepancy is due to the relatively inelasticity of the dura tissues which get relayed from the CSF to the sensor [27]. Due to these inaccuracies, intraparenchymal probes are seen as a paramount substitute.

The microtransducer sensors are a type of robust ICP measuring technology. They can be placed directly in several intracranial locations and have lower complication rates than EVD, such as lower risk of infection and hemorrhage rate [48, 49]. They also do not require any adjustments of the patient's position and can be easily transported. However, all surgical procedures are associated with a risk of hemorrhage. The degree of hemorrhage differs based on the type of technology used. Monitors that are placed subdurally are linked with nearly a 5% rate of hemorrhage; however lower risks of 4% and 1.1% are seen with intraparenchymal and ventricular catheters, correspondingly [46]. The microtransducer systems that measure ICP are possibly not the best representation of global pressure, as transtentorial and interhemispheric pressure gradients may be present. High costs are associated with an ICP sensor's implantation procedure. The high cost is reflected by the need for a monitor which costs thousands of dollars and a transducers which costs at least $400–$600 a piece, not to mention the ongoing costs of preserving and changing out broken parts [50]. Technical malfunctions can lead to inaccurate readings, for example, fiber optic transducers can be easily marred by unwarranted twisting or folding [46]. The absence of constant calibration can produce an inaccurate ICP reading. Considerable zero drift can sometimes occur in long-term monitoring and when in vivo recalibration is not possible [51].

14.2.1.3 Lumbar Cerebrospinal Fluid Pressure Measurement

Following certain conditions, lumbar punctures are another route where ICP can be measured, as long as the cerebral spinal fluid is free of any blockages that may hinder the flow of fluid. This is a precise method to establish ICP in patients with communicating cerebral spinal fluid systems. A clinical study conducted by Lenfeldt N and colleagues showed that lumbar cerebrospinal fluid pressure correlated exceptionally to ICP in brain tissue, which was determined by a mean difference in measurement of 10 mm H_2O (0.75 mmHg) and a regression coefficient of 0.98 [26]. Lumbar cerebrospinal fluid pressure amplitude measurement is an alternative to ICP recording. Intracranial pulsations measurement via lumbar puncture in an alternative clinical analysis had marginally dampened amplitudes. These amplitude values should be understood as raised amplitudes that require correction [52].

Lumbar punctures require a sterile setting. The needle is inserted into the subarachnoid space, most commonly between the third and fourth lumbar vertebrae in order to circumvent the spinal cord. Cerebral spinal fluid is then removed with the needle and analyzed.

In the event where increased intracranial pressure is questioned, a lumbar puncture should certainly not be done due to dangerous consequences such as brain herniation and consequently death. Some circumstances may be due to conditions such as a cancerous growth or a brain hemorrhage. Approximately 1/3 of patients experiences a headache following a lumbar puncture [53].

Generally, direct or invasive methods of ICP monitoring are the most accurate ways to measure ICP by far. The most reliable methods of ICP monitoring are the use of ventricular catheters; closely followed by microtransducers, which measure ICP almost just as accurately; and then lumbar puncture under certain circumstances with non-obstructed pathways of cerebral spinal fluid flow.

However, in practice, direct or invasive ICP monitoring is not widely performed in many patients because of the following reasons: first, the invasiveness of the monitoring methods adds risk of intracranial infection, hemorrhage, or even cerebral herniation [46, 48]. Second, the insertion of a catheter or transducer is traditionally done only by trained personnel, i.e., a neurosurgeon, in a specialized facility. Third, economically, the high price of microtransducers prevents many clinical centers from using this microtransducer-based ICP monitor [50, 54].

14.2.2 Noninvasive ICP Monitoring

Since the use of invasive ICP measuring techniques has many limitations, noninvasive methods have been developed and proposed to evaluate ICP via related physiological variables [55]. In this chapter we will focus on the most common noninvasive techniques available [56]. The predominant methodologies to assess noninvasive ICP ground their basis on the knowledge that the anatomical structures play an intricate part of the physiology that governs ICP.

14.2.2.1 Methods that Infer ICP from Intracranial Structures

Ultrasound Time-of-Flight Techniques

Ultrasound "time-of-flight" method can be used for noninvasive ICP assessment and is predominantly constructed on a theory that fluctuations in ICP can change the physical dimensions and/or acoustic properties of the intracranial structure components, including CSF, brain parenchyma tissue, and blood [57, 58]. As shown in Fig. 14.3, the changes of signal's oscillation period and time of flight are seen to be linear under the physiologically limited volume changes in the intracranial component (i.e., 8 mL) [58]. The changes of time of light and oscillation period range from 6 to 20 ns and 0.12 to 0.5 ns, respectively, per 8 mL changes of craniospinal volume [59]. The increased craniospinal volume led by the volume changes of ±8 ml intracranial components can cause ICP to raise to the critical level of 25 mmHg [58].

The disadvantage to this method is that it singly measures relative variations of ICP. The variations are compared to an absolute baseline measurement of ICP. To obtain an accurate reading, ultrasounds should be calibrated between patients and compared to invasive techniques. Another area that remains uncharted is how intracranial masses can change the measurements. Consequently, for clinical practice, this method may not be sufficiently precise [56].

Transcranial Doppler Ultrasonography (TCD)

ICP can be continuously estimated from the TCD measurements because some TCD-derived parameters change during an increase of ICP, such as the form of cerebral blood flow velocity pulse waveform or pulsatility index. Techniques have been categorized and established on the basis of the following categories: TCD pulsatility index, noninvasive approximation of intracranial perfusion pressure, and model-based methods. The extrapolation of TCD velocity to zero flow velocity [60], the brain biomechanics coupled with TCD [61], and using TCD spectral waveform properties [62] are all new methods to estimate ICP according to TCD. Previously published studies presented with dissimilar accuracies, more specifically with prediction capabilities for recognizing ICP ≥20 mmHg ranging from 0.62 to 0.92 [63].

TCD consists of many of the beneficial factors that are shared with noninvasive ICP techniques, namely, uninterrupted monitoring, comparatively low expense, free from complications, straightforwardly accessible, transportable, high temporal resolution, ability to be duplicated, and

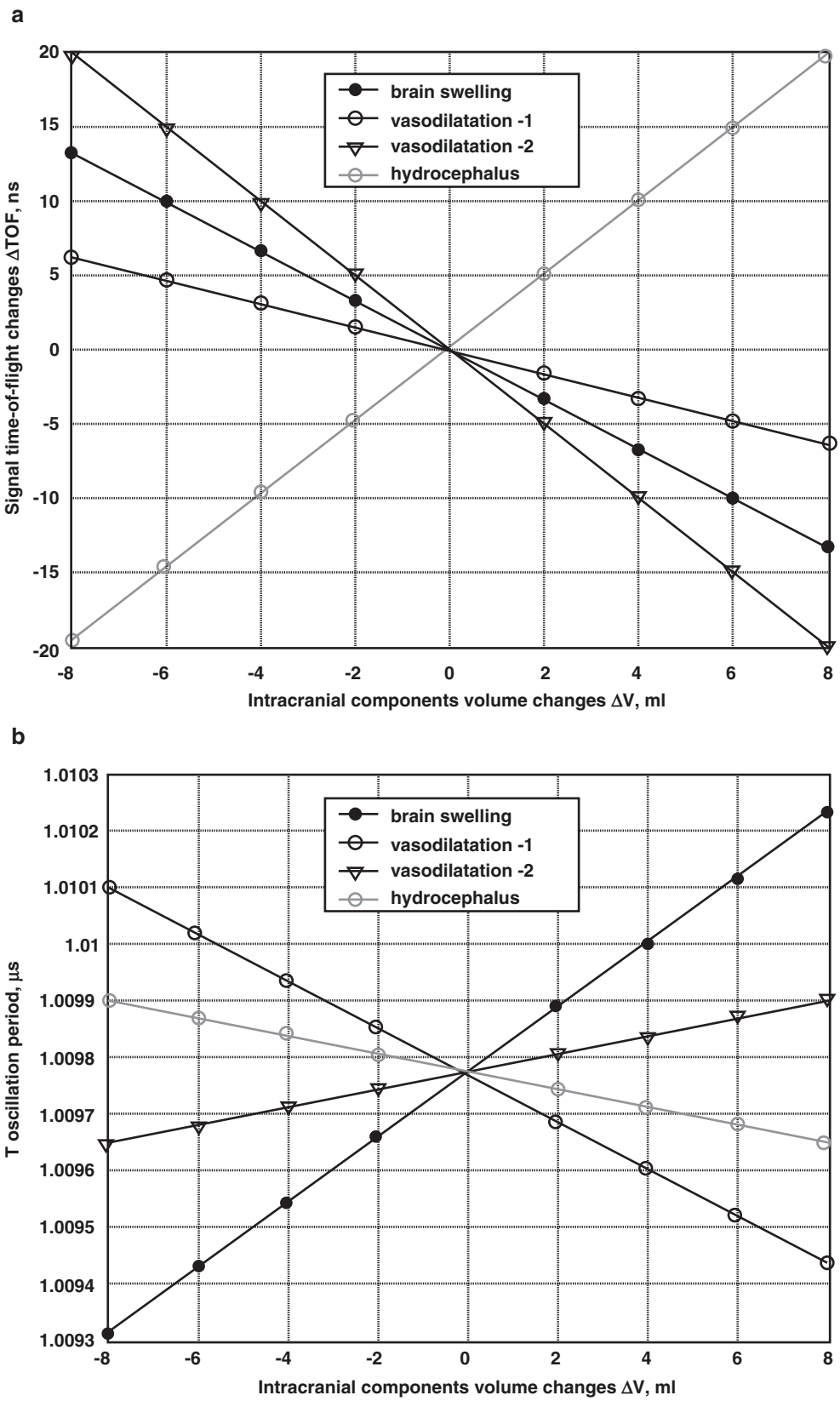

Fig. 14.3 The time-of-flight changes (**a**) and oscillation period changes (**b**) of a simulated ultrasound signal passed through the head in different physiological phenomena. (Reprinted with permission from [58])

appropriate in the emergency and ambulatory settings. Still though, TCD presents some inherent drawbacks, which can adversely impact its accuracy. Some of the drawbacks are mostly characterized by signal conduction attenuation transmitted through the cranial bones. Additionally, TCD measurements may be specifically challenging in an undeniable proportion of the population (up to 8%). Unfortunately, this does not present an acceptable acoustic window for artery insonation [63, 64].

Pulsed Phase Lock Loop (PPLL) Technique

PPLL was originally invented to accurately measure bolt tensioning for critical applications by the National Aeronautics and Space Administration [65, 66]. The PPLL device records skull movement associated with ICP pulsations. Briefly, a 500-kHz ultrasonic wave is transmitted by the PPLL device, and it passes through the cranium by a transducer placed on the temporal area. The ultrasonic tone burst passes through the brain, reflects off the inner surface of cranium, and is received by the same transducer.

Once locating the inner surface of the cranium, the ultrasonic phases between emitted and received signals are compared using PPLL device. A change of cranial diameter leads to a phase shift between these two signals, and then the output voltage of PPLL is changed in proportion to the cranial pulsation diameter. Only approximately 0.5 ms is needed for this ultrasonic distance measurement to be complete. Therefore, the recording of cranial diameter pulsation is continuously provided via the measurement of PPLL output voltage. PPLL output represents ICP waveforms in both frequency and time domains. PPLL technology allows for the noninvasive assessment of ICP dynamics in vivo and can obtain uninterrupted ICP waveforms during spaceflight since it is both inherently compact and noninvasive [67].

Electroencephalography (EEG)

An EEG is often used to record the spontaneous electrical activity of the cerebral cortex according to the electrodes placed on the scalp. Recently, Chen et al. reported the use of the EEG power spectrum analysis as a novel technique [68]. A power spectral analysis over time allows for a graphical representation of an EEG reading. The intracranial pressure index (IPI) is obtained through the power spectrum analysis of the EEG, and this is then associated with the measurements of ICP. Meanwhile, a correlation between ICP and IPI was also proposed.

Unsatisfactorily, it is still too early to apply an EEG power spectrum analysis to clinical ICP measurements as EEGs are affected by many factors except for ICP, including disease itself, acid-base and electrolyte imbalances, temperature, and drugs that affect brain activity. Furthermore, additional studies also confirmed this clinical utility, and this method has been improved with a wireless and portable EEG system [68].

Near-Infrared Spectroscopy (NIRS)

Transcranial NIRS is a well-known method to assess the regional changes in cerebral blood flow, regional oxygen saturation index (rSO2) of cerebral blood, and cerebral blood volume (CBV) [69]. The infrared spectrum of light, 700–1000 nm, has the property of low absorption which permits it to penetrate through the skin and bone easily and permeate to the deep tissue. Thus, this infrared spectrum of light is chosen as the NIRS work wavelength, and it can be scattered and absorbed when it passes through the brain tissue. Different objects have various absorption properties of the infrared light; thus the changes in oxyhemoglobin and deoxyhemoglobin concentration can be detected. The rSO2 values were significantly different in severe traumatic brain injury (TBI) patients with raised and normal ICP [70]. The cerebral oxygenation changes are well correlated with ICP slow waves in TBI and CSF infusion studies [71]. NIRS has been used to calculate certain indices that are related with the pressure reactivity of the cerebrovascular system in TBI patients [72]. However, NIRS does not provide an absolute ICP estimation [73]. Besides, the use of NIRS is limited by the specialized equipment, and the required indices also take extended time to be obtained [72].

Fontanometry for Infants

In infants, ICP is commonly assessed using pneumatic applanation fontanometer [74, 75], which consists of a tambour placed on the anterior fontanelle. Before declining, the pulsation increases to its maximum with the increases of external pressure applied in a tambour. The pulsation amplitude is up to the peak when the pressure of the tambour is equal to the pressure inside the cranium. Noninvasive anterior fontanometry can satisfactorily reflect the changes in ICP using a variety of sensors on the baby and newborn whose anterior fontanel is not closed. This method is of great significance in the diagnosis of early intracranial hypertension. But noninvasive technologies can only reflect the ICP indirectly and are vulnerable to extracranial factors and other physiological factors. Flattening of the anterior fontanelle reduces the cranial cavity volume to a certain extent, resulting in a higher measured ICP, which is a limitation for accurate ICP measurements.

Impedance Mismatch [76]

The impedance mismatches between cerebral vessels and carotid arteries can be detected through the carotid pressure waveform reflection using a pressure sensor placed on the palpable carotid artery. The ICP can be calculated according to the analysis of this reflection, and then the result will be compared with the previous reported cerebral vasculature data [77].

The arterial pulse is commonly palpated on the common carotid arteries in the neck, which are the main vessels supplying blood for the brain. The pressure waves of the carotid

arteries are transferred to the brain and are reflected by striking the smaller diameter to a certain extent. The carotid pressure waveform shape is influenced by this reflection. An increase of ICP in the brain can lead to compressed cerebral vasculature and a decrease in the compliance of these vessels. Afterward, the impedance mismatch between the cerebral vessels and carotid arteries is increased owing to this reduction of cerebral vascular compliance. The impedance mismatch extent between cerebral vascular bed and carotid arteries is manifested by the waveform strength of carotid pressure contributed by the reflection of pressure wave [78].

However, as the physiological and pathological states of the brain are different with time, the physiological states corresponding to the impedance of each frequency are also different. This feature affects the accuracy of ICP measurements and is not conducive to continuous real-time ICP monitoring.

14.2.2.2 Methods that Infer ICP from Extracranial Structures

Optic Nerve Sheath Diameter (ONSD)/Orbital Subarachnoid Space Width (OSASW)

From an embryological perspective, the optic nerve originates from the central nervous system and is bordered by each of the meningeal tissue layers (dura, arachnoid, and pia mater). A connection exists within the orbital subarachnoid space that surrounds the optic nerve with the cranial subarachnoid space. The pressure that exists in this space is associated with the ICP [79]. A strong connection between the changes of optic nerve sheath diameter (ONSD) and ICP has been demonstrated by several previous studies [80–84]. The breadth of the optic nerve sheath has been associated with being a reliable predictor of raised intracranial pressure [85]. The cutoff value of ONSD is suggested to range from 4.1 to 5.9 mm in an adult, and an increase of ICP is delimited to vary from 14.7 to 30 mmHg [83]. The changes of ONSD can be visualized on a magnetic transorbital ultrasound (Fig. 14.4), CT scan, and resonance imaging (MRI).

The advantages of sonographic ONSD assessment include allowing for bedside assessment, avoidance of patient transport for imaging, transportability of equipment, speed of implementation, reasonably low price, and circumvention of ionizing radiation. In order to obtain a defined location for the optic nerve sheath borders, smaller footprint ultrasound probes and higher frequencies are adopted during ONSD measurements [86]. However, this method still has its drawbacks, mainly including inter-rater variability, hyperechoic artifacts, different cutoff values of the optic nerve sheath, submillimetric measurements, and the heterogeneity of patient population.

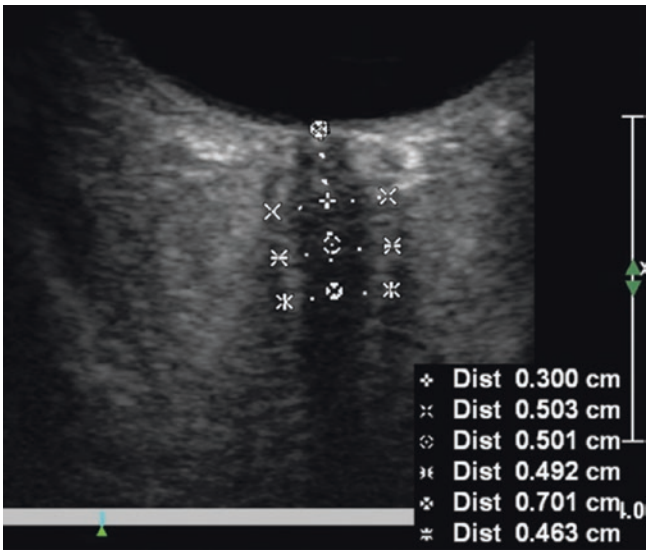

Fig. 14.4 Transorbital ultrasound sonography of the optic nerve sheath taken with a 13 MHz linear probe (Philips iU22 L12-5) from a normal person. (Reprinted with permission from Liu H, Yang D, Ma T, Shi W, Zhu Q, Kang J, et al. Measurement and Associations of the Optic Nerve Subarachnoid Space in Normal Tension and Primary Open-Angle Glaucoma. Am J Ophthalmol. 2018;186:128–37)

The main disadvantage of the CT remains that a better image quality needs a higher dose of ionizing radiation. The radiation that it emits may be harmful and is therefore not recommended, especially for pregnant women.

An image of the orbital subarachnoid space of the optic nerve can be demonstrated by incorporating the use of a T2-weighted MRI with a fat-suppressed sequence [87, 88] (Fig. 14.5). The main advantages of MRI scans are as follows: advantageousness for displaying soft tissues; they have a higher spatial resolution and thus can provide good cerebrospinal fluid imaging; they can image the entire stretch of optic nerve in the orbit; they have shown acceptable scan-rescan reproducibility and acceptable observer agreement; because there is no radiation emitted, susceptible subjects, like women who are pregnant and small children, can safely use these machines. However, MRIs can be costly, time-consuming, improper for the patients with claustrophobia, and affected by movement, and it does not allow for bedside assessments.

Because the optic nerve diameter can be affected by the change of the ICP similar to ONSD [89], orbital subarachnoid space width of the optic nerve (optic nerve sheath diameter minus optic nerve diameter) is considered to be a more reliable parameter which can reflect ICP. As for the noninvasive ICP assessment based on MRI-measured OSASW, Xie et al. [88] have carried out the preliminary exploration and application (this is described in detail in Sect. 14.4).

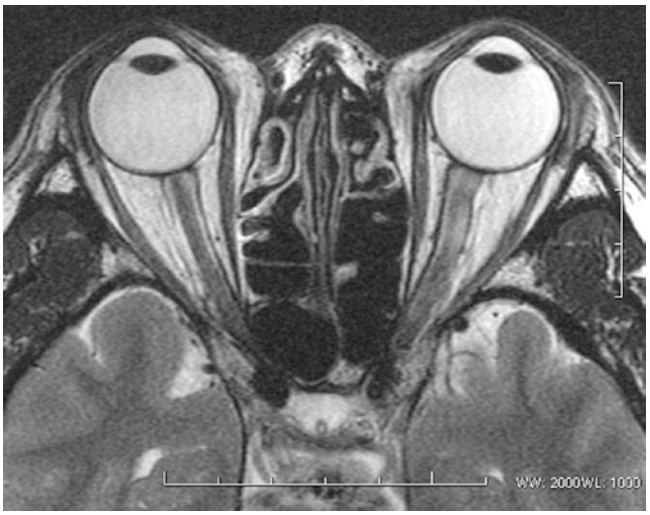

Fig. 14.5 Transversal section of 3.0 Tesla MRI scan of the whole length of optic nerve in the orbit with T2-weighted MRI with a fat-suppressed sequence (digital field of view = 8, window width = 2000, window level = 1000). (Signa HDx; General Electric Medical System, Milwaukee, WI, USA)

ONSD/OSASW measurement is considered to be one of the promising means to evaluate ICP. However, continuous monitoring can't be achieved by this method.

Venous Ophthalmodynamometry

Under normal physiological circumstances, the pressure in the central retinal vein is equal to or higher than the ICP. This is due to the fact that the cerebrospinal fluid passes by the optic nerve sheath prior to emptying into the cavernous sinus. The venous ophthalmodynamometry method is utilized to assess ICP by manually increasing intraocular tension (IOT) above the baseline IOP, until a collapse is observed in central retinal vein [90–93]. The venous outflow pressure of the central retinal vein is made up from this outside pressure that is added to the baseline IOP. The resulting value is correlated to the ICP [92]. The value of ICP is obtained from a linear transformation for the applied force (gms) to the change of IOT (mm Hg) using the published nomogram or based on the calibrated patient data. The venous outflow pressure detected using venous ophthalmodynamometry has a linear relationship with ICP ($r = 0.87$ based on the Pearson's coefficient of linear correlation) according to a previous study that reported ICP predictability using this method [94].

Ophthalmodynamometry is advantageous for transitory ICP evaluations as it is simple to repeat and can be adopted whenever an elevated ICP is suspected in hydrocephalus and brain tumors or after a head injury [90, 92]. However, the downfall of this method could be that it may only be applied in the patients with elevated ICP without papilledema [95]. It is not suitable for continuous ICP monitoring [90, 92].

Flash Visual Evoked Potential (F-VEP)

In the early 1980s, York et al. identified a strong relationship between the second latency of negative-going latency (N2) in F-VEP and ICP in young adults with head trauma and children with hydrocephalus [96, 97]. The correlation between a latency period of prolonged N2 and raised ICP values has also been demonstrated in children [98]. However, F-VEP has a wide range of latency, amplitude, and waveforms across normal subjects. A high intersubject variability, demonstrated in a recent study, might limit the ability to reliably predict ICP [99].

Papilledema

Identification of papilledema on fundoscopy is a useful method to detect increased ICP [100]. There is a positive correlation between the volume and height of the optic nerve head with ICP [101]. Spectral domain OCT (SD-OCT) provides high-quality imaging, which can reliably and reproducibly demonstrate alterations in the optic nerve head and the retinal nerve fiber layer (RNFL) in patients with idiopathic intracranial hypertension (IIH) [102–105].

However, restrictions exist for it in clinical medicine. This method can only screen increased ICP or half quantitative judge elevated ICP but cannot quantitatively and reliably estimate the ICP of a wider range: during severe disc edema, collapse of systematized algorithms, and decreases in the RNFL thickness. Although papilledema does not essentially characterize progress in the reduction of edema, it can on the other hand characterize deterioration of the optic nerve [102, 106].

Tympanic Membrane Displacement (TMD)

Vibrations in the form of sound are transferred via the tympanic membrane to the cochlea across the ossicles in the middle ear. The contraction of tensor tympani muscles and stapedius is known to be followed by a quite small but measurable displacement of tympanic membrane from its original position. Because the CSF and perilymph communicate through the cochlear aqueduct, an increase of ICP is directly transmitted to the stapes footplate, causing magnitude and directional changes of the TMD.

The tympanic membrane movement caused by the stimulation of the stapedial reflex is influenced by raised ICP, and the movement in turn indicates the change of ICP, namely, inward displacement manifests high ICP while outward displacement manifests low or normal ICP [107]. However, the assessment of TMD is only used for detecting an increase of ICP to provide qualitative ICP data owing to its limited accuracy [108, 109]. The TMD is usually influenced and limited by other factors, including the cochlear aqueduct patency, tympanic membrane integrity and acoustic reflex strength, and poor intersubject reproducibility [110].

14.2.2.3 Some Other Noninvasive ICP Monitoring Methods

Recent publications on the recognition of intracranial hypertension propose that measuring IOP may have a clinical advantage in the recognition of intracranial hypertension [111, 112]; conversely, preceding studies fail to support it [113–115]. According to the results of our own study, a highly significant positive association between ICP and the IOP has been revealed ($P < 0.001$). However, while using IOP as a measurement to envisage the ICP, the accuracy was 65.4% [116]. This means that IOP is a poor predictor of ICP.

Recently, Jonas et al. generated a regression model (ICP was calculated as ICP [mmHg] = 0.44 × body mass index [kg/m(²)] + 0.16 × diastolic blood pressure [mmHg] − 0.18 × age [years] − 1.91) and attempted to use it to estimate ICP in different large-scale population [23, 117, 118]. This model was derived from the same dataset from which another weighting function of noninvasive ICP evaluation is mainly based on. This is the manner in which the orbital subarachnoid space width was developed (This is described in detail in Sect. 14.4) [88]. While body mass index and diastolic blood pressure indeed contribute to the ICP evaluation, the whole weighting function can only explain about 80% of the ICP variation. Both body mass index and diastolic blood pressure only account for about 30%, and the orbital subarachnoid space width accounts for about 50% [119]. Therefore, the regression model derived from body mass index and diastolic blood pressure may be insufficient to predict a reliable ICP value.

To sum up, procedures that are noninvasive are advantageous in terms of entirely circumventing the complications that are frequently seen with the more invasive methods. However, at present, none of the abovementioned methods are accurate enough to replace the invasive techniques.

14.2.3 Continuous ICP Monitoring

Compared with transient ICP monitoring, uninterrupted monitoring discloses the complete range in variations of ICP throughout attentiveness, slumber, changes in bodily positions, and movements. Recently, implantation of a wireless IOP transducer in the human eye was reported [120, 121]. For patients suffering from the intracranial and intraocular pressure gradient-related ophthalmic disorders, continuous ICP monitoring is significantly more meaningful.

Currently, some implantable, wireless methods for long-term monitoring of ICP can be realized by installing a microtransducer ICP monitoring device in the brain.

In a prospective study, the ICP value of 22 patients was continually monitored with the intraparenchymal Codman MicroSensor system and ventriculostomy simultaneously on average 7.2 ± 0.4 days per patient. A positive association was seen amid ICP measured by using the Codman MicroSensor system and by the ventriculostomy ($P < 0.0001$, $r = 0.79$). The average ICP that was measured with the ventriculostomy was 18.3 ± 0.3 mmHg, while the average ICP with the Codman MicroSensor system was 19.0 ± 0.2 mmHg. The drift from zero was 0.9 ± 0.2 mmHg. There were few complications. Scarcely, some small hematomas were recognized. Infections were not straightforwardly associated to the devices used [122].

An electronic implant was designed for eventual use in humans, containing a Codman MicroSensor system located in the ventricles, a two-axis acceleration sensor, a microcontroller, a communication chip, and a battery for the energy source. ICP dynamics and 2D acceleration data were concurrently documented in five pigs for approximately 2 weeks. The acceleration, compared to amplitudes, frequently had a larger effect on the physiological ICP features [123].

A new telemetric ICP measurement device, Raumedic's NEUROVENT(®) P-Tel/S-Tel, was evaluated over periods of up to 12 months in nine minipigs and proved to provide reliable data [124, 125]. Intraparenchymal placement was more favored [124].

Installing a microtransducer ICP monitoring device in the brain is less invasive; however, it is still a surgical procedure.

14.3 The Phase Relationship Between the Circadian Rhythms of ICP and IOP in Glaucoma

Every healthy individual has his own 24-h circadian fluctuation in IOP [126–128]. In general, there are three IOP circadian patterns, nocturnal peak pattern (52%), diurnal peak pattern (17%), and no evident pattern (31%) [129]. It is widely accepted that the circadian pattern of IOP plays an important role in the pathophysiology of glaucoma [130–132]. Lowering IOP and controlling its fluctuation are still the only available option for treating patients with glaucoma [133].

It is worth noting that the circadian fluctuation pattern of a 24-h ICP reading and its phase relationship with IOP should be seen as an independent risk factor and be taken into consideration for the pathogenesis of glaucoma [134]. Research on the phase relationship of circadian fluctuation patterns between the ICP and IOP might be of vital significance to explore the relationship of the intracranial and intraocular pressure gradient fluctuations in glaucoma. This may also be potentially useful to find a new target of treatment. We hypothesize that, when the phase relationship between the circadian fluctuation of IOP and ICP is in an inconsistent state, especially when heterodromous directions of the ICP and IOP circadian pattern exist, the enlarged intracranial and

intraocular pressure disparity possibly plays a role in the development of glaucomatous optic neuropathy. For example, Fig. 14.6 shows the aforementioned idea in the condition of nocturnal peak pattern of IOP circadian fluctuation.

Till now, the variations throughout the nychthemeron (the full 24-h period of a night and a day) of IOP can be measured continuously in a habitual posture over a 24-h time frame with implantable devices as well as a 24-h contact lens sensor [24]. The continuous ICP monitoring technology is recommended to guide the exploring of the pathogenesis of primary open angle glaucoma, therapeutic interventions, and prognosis assessment.

14.4 Estimation of ICP and Translaminar Cribrosa Pressure Difference in Tongren Eye Center

In close collaboration with the departments of neurology, radiology, and biostatistics, we explored a noninvasive quantitative assessment method of ICP and translaminar cribrosa pressure difference by MRI-assisted orbital subarachnoid space width (OSASW), which has primarily been applied in the clinic in Tongren Eye Center [88].

14.4.1 Standard Operation Procedure

14.4.1.1 Measurement of IOP

IOP is measured using a calibrated Goldmann applanation tonometer in the sitting position within 1 hour before the orbital MRI examination.

14.4.1.2 Orbital MRI Examination [88]

The ideal method to visualize optic nerve sheath, more specifically, the orbital segment, is in the supine position using a Tesla MRI 3.0 full-length 8-channel phased-array head coil (Signa HDx; General Electric Medical System, Milwaukee, WI, USA). The subject's eye is positioned to fixate on an object that is directly in the primary line of sight and the MRI machine's gantry in order to circumvent any inaccuracies caused by eye movement. Both the subject's eyes are examined with the same method.

A fast recovery fast spin echo sequence (FRFSE) is used to obtain an accurate measurement of the optic nerve/sheath complex. The ideal placement of the head was optimized by the use of transverse and oblique sagittal plane scout images. Quantification relies on oblique coronal scout scans. Two rudimentary FRFSE sequences are employed:

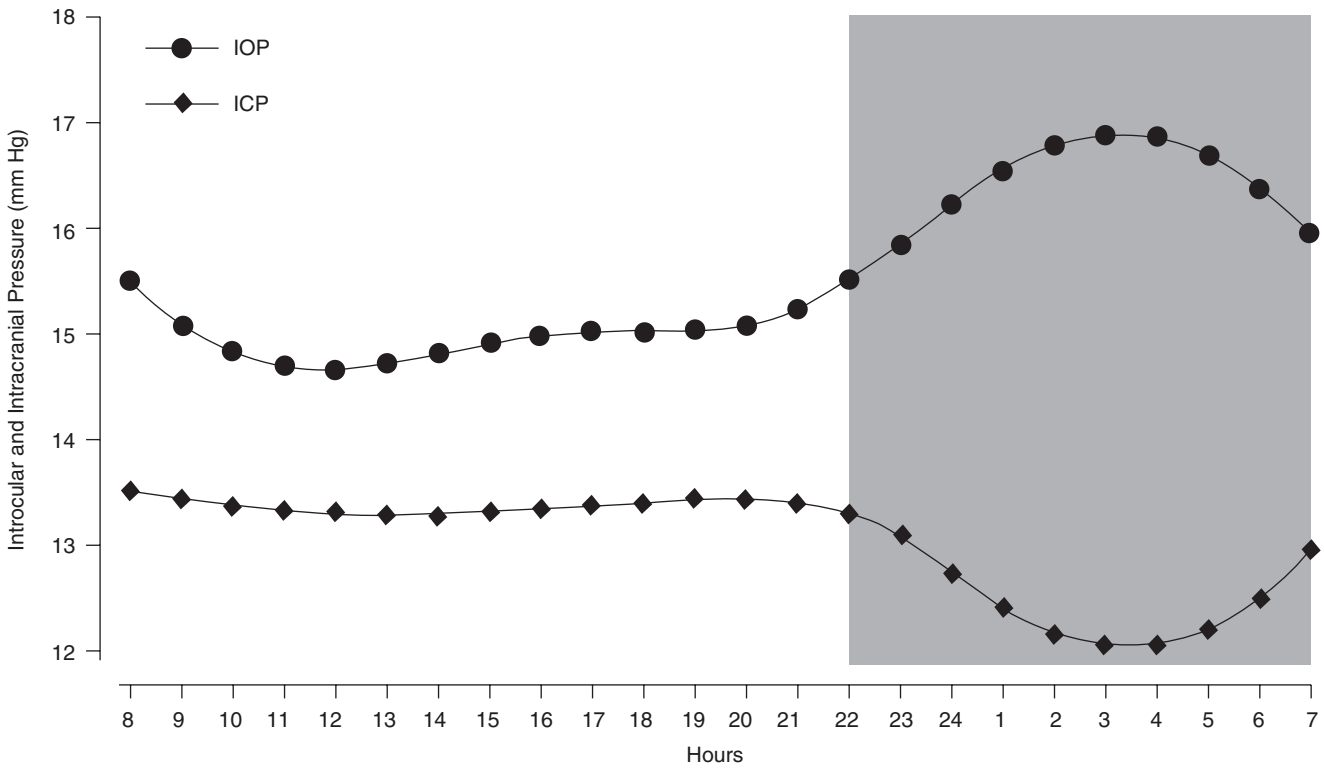

Fig. 14.6 Schematic diagram shows the heterodromous against direction of the ICP against IOP nocturnal peak pattern

- One being a T2-weighted fast recovery fast spin echo sequence (T2WI-FRFSE). This sequence is done due to the detailed distinction of soft tissues and other morphological features (TR = 2760 ms; TE = 120 ms; number of excitations = 2; echo train length = 18; bandwidth = 41.67 Hz/pixel; field of view = 16 cm × 16 cm; matrix = 512 × 256; slice thickness = 3 mm; slice gap = 0.3 mm; leading to a nominal spatial resolution of 0.2 mm × 0.2 mm) [88]. This specific series undergoes two rounds with 12 adjacent slices in each sagittal and transverse direction (Fig. 14.7).

- The second is a T2WI-FRFSE with fat suppression. This technique enhances morphological quantification (TR = 6000 ms; TE = 245 ms; number of excitations = 2; echo train length = 60; bandwidth = 20.83 Hz/pixel; field of view = 16 cm × 16 cm; matrix = 320 × 320; nominal spatial resolution = 0.5 mm × 0.5 mm; slice thickness = 3 mm; slice gap = 0) [88].

14.4.1.3 Measurement of Optic Nerve/Sheath Complex [88]

To obtain a better quality of the image, the T2WI-FRFSE scans are interposed to a superior size of 1024 × 1024 matrices, creating a pixel dimension of 0.16 mm × 0.16 mm. Seven oblique coronal MR images of uninterrupted pictures are taken at a right angle in relation to the optic nerve. The initial slice is subsequent to the globe. Measurements are taken for each eye individually (Fig. 14.7). Looking at the resulting oblique coronal scans, the CSF is seen as an intense white signal while the optic nerve parenchyma is portrayed as a dark black signal (Fig. 14.8). Three oblique coronal slices at a right angle to the optic nerve are captured at the positions of 3, 9, and 15 mm posterior to the globe. These slices are analyzed using Image J 1.46r software (National Institutes of Health, USA; available at https://imagej.nih.gov/ij/). These images are then zoomed to 300×. An electronic caliper is used to gauge the horizontal and vertical spans of the optic nerve including the optic nerve sheath. The mean is then taken from these measurements and computed. Another calculation is done of the orbital subarachnoid space width (OSASW). It is assessed by subtracting the dimensions of the mean optic nerve value from the dimensions of the mean optic nerve sheath value and dividing that number by 2.

14.4.1.4 Acquisition Anthropometric Data

Body mass index (BMI) is a well-known calculation, measured by taking the subject's weight (in kilograms) and dividing it by the height squared (in meters). Mean arterial blood pressure (MAP) is calculated by taking the systolic and diastolic blood pressures while the patient is laying supine and calculating it by adding 1/3 of the systolic blood pressure to 2/3 of the diastolic blood pressure.

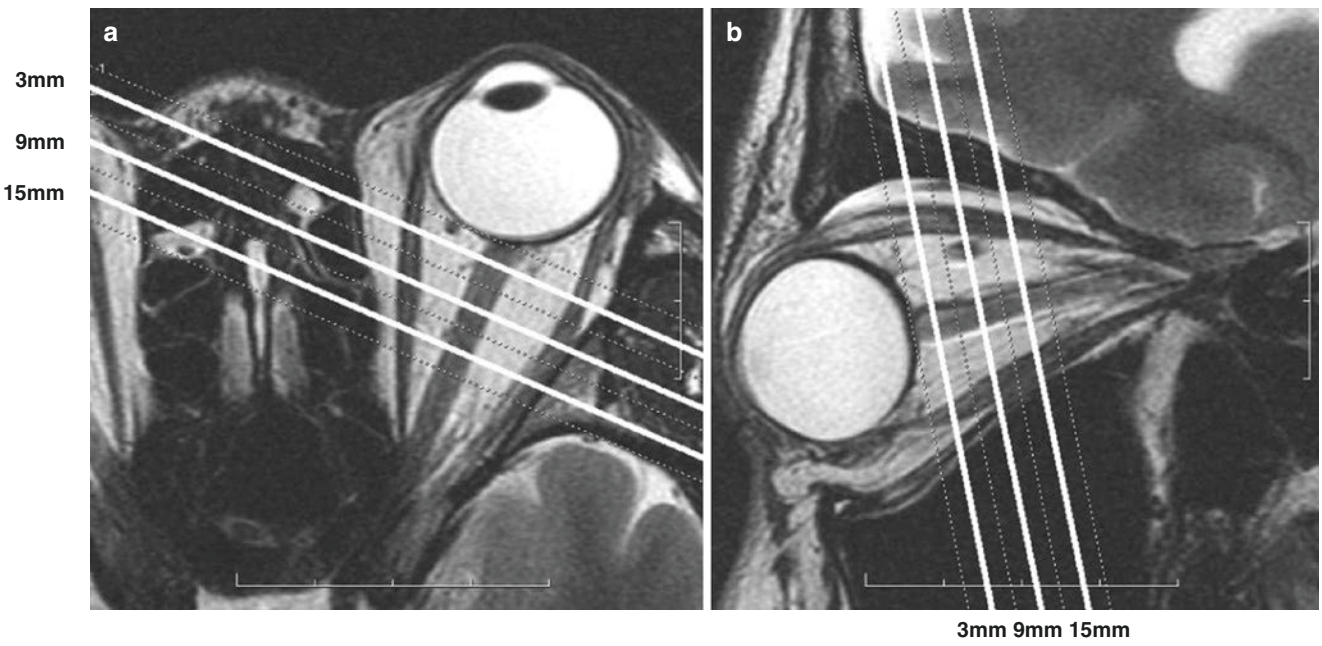

Fig. 14.7 Example of MRI scan of the retrobulbar optic nerve ([**a**] transversal section and [**b**] oblique sagittal section) T2WI-FRFSE of the retrobulbar optic nerve (digital field of view = 8, window width = 2000, window level = 1000). These images were used to plan the position of three slices at 3, 9, and 15 mm behind the globe of T2WI-FRFSE fat-suppressed sequences to measure the optic nerve diameter, optic nerve sheath diameter, and width of the orbital subarachnoid space at 3, 9, and 15 mm behind the globe. (Reprinted with permission from [88])

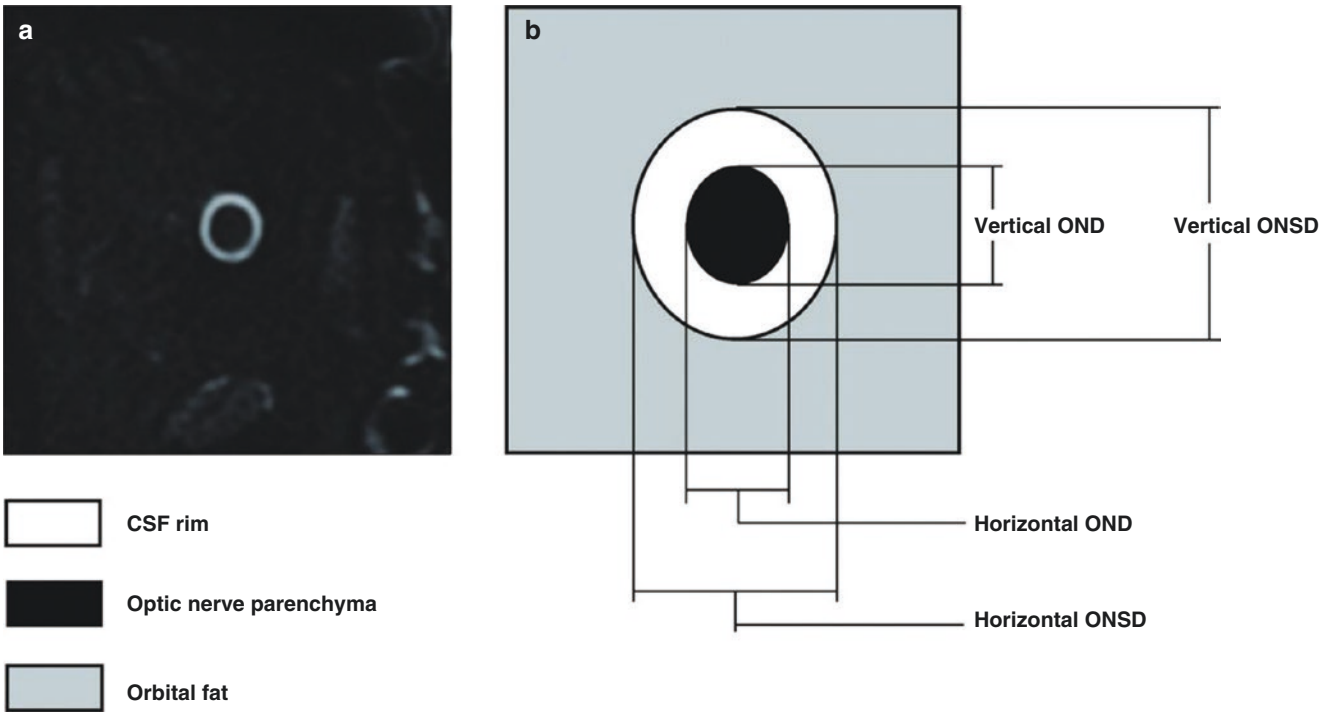

Fig. 14.8 Scheme to demonstrate the optic nerve/sheath complex. (**a**) Oblique coronal T2-weighted fast recovery fast spin echo sequence (T2WI-FRFSE) image with fat suppression for demonstrating the optic nerve/sheath complex taken at 3 mm behind the globe perpendicular to the optic nerve axis (digital field of view = 4, window width = 2000, window level = 1000). (**b**) Schematic drawing of the optic nerve/sheath complex including the optic nerve (the black area represents optic nerve), surrounding cerebrospinal fluid space (white rim area), and the optic nerve sheath (at the conjunction of the cerebrospinal fluid space rim and the orbital fat). *OND* optic nerve diameter, *ONSD* optic nerve sheath diameter (Reprinted with permission from [88])

14.4.1.5 Calculation of ICP and Translaminar Cribrosa Pressure Difference

Estimated ICP [mmHg] = 16.95 × OSASW (in mm at 9 mm behind the globe) + 0.39 × BMI [kg/m^2] + 0.14 × MAP [mmHg]—20.90.

Estimated translaminar cribrosa pressure difference (mmHg) = IOP—estimated ICP. The following is an example of a report sheet of noninvasive quantitative ICP and translaminar cribrosa pressure difference (Fig. 14.9):

When the noninvasive OSASW-assisted method of ICP assessment was applied, it revealed that patients with normal-pressure glaucoma had an atypically narrow orbital subarachnoid space width when examined by MRI as compared with patients with high-pressure glaucoma and normal control subjects [135]. We noninvasively compared the OSASW and estimated ICP derived from OSASW in ocular hypertensive subjects and controls. The result showed that the mean OSASW was significantly wider in ocular hypertensive subjects than in the controls and the MRI-derived ICP value in ocular hypertension was considerably greater than in the normal group (our own data has been recently submitted and is under review) (Fig. 14.10).

14.5 Conclusion

In conclusion, the latest research has shown that an abnormal intracranial and intraocular gradient could lead to glaucomatous damage and other intracranial and intraocular pressure gradient-related disorders. If the detection of the ICP's biological rhythm and volatility can be realized in the same manner as a "Holter monitor," when combined with IOP, it may shed light on the pathogenesis, disease process, and drawing up of individualized therapeutic plans. Therefore, the development of such ICP monitoring techniques represents a promising direction for future research.

a

Medical and Health Organization: _____

Noninvasive cerebrospinal Fluid Pressure and Translaminar Pressure Difference based on MRI

Patient name: Gender: Age: Medical record No:

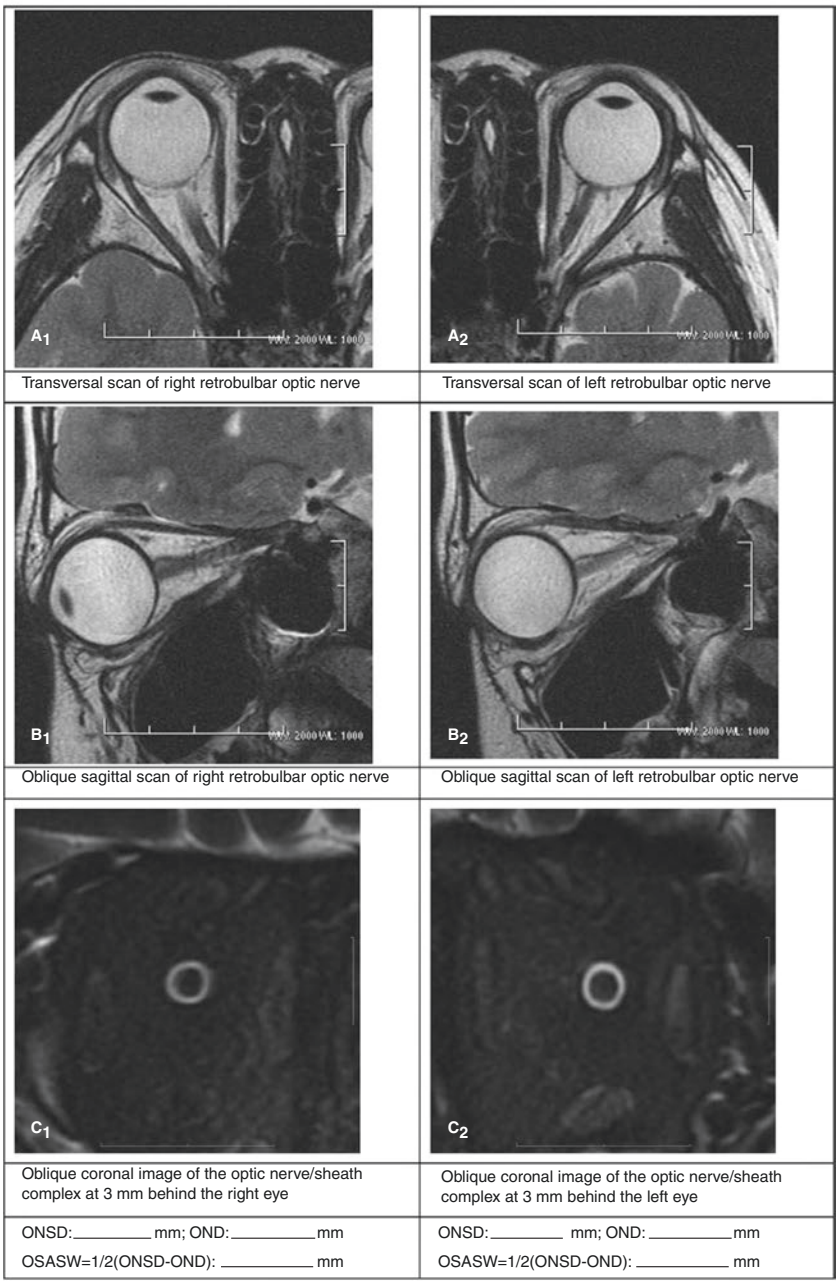

Fig. 14.9 (**a**) Report sheet example of noninvasive quantitative ICP and translaminar cribrosa pressure difference assessment by MRI-assisted orbital subarachnoid space width [A_1, A_2] transversal and [B_1, B_2] oblique sagittal T2WI-FRFSE scan of the right and left retrobulbar optic nerve. [C_1, C_2] Oblique coronal T2-weighted fast recovery fast spin echo sequence (T2WI-FRFSE) image with fat suppression for demonstrating the right and left optic nerve/sheath complex taken at 3 mm behind the globe perpendicular to the optic nerve axis. (**b**) Report sheet example of noninvasive quantitative ICP and translaminar cribrosa pressure difference assessment by MRI-assisted orbital subarachnoid space width [D_1, D_2] Oblique coronal T2-weighted fast recovery fast spin echo sequence (T2WI-FRFSE) image with fat suppression for demonstrating the right and left optic nerve/sheath complex taken at 9 mm behind the globe perpendicular to the optic nerve axis. [E_1, E_2] Oblique coronal T2-weighted fast recovery fast spin echo sequence (T2WI-FRFSE) image with fat suppression for demonstrating the right and left optic nerve/sheath complex taken at 15 mm behind the globe perpendicular to the optic nerve axis. (**c**) Report sheet example of noninvasive quantitative ICP and translaminar cribrosa pressure difference assessment by MRI-assisted orbital subarachnoid space width. The conversion relationship among the MRI-assisted orbital subarachnoid space width (OSASW), estimated ICP, and disease categories are shown, the same as the normal reference value of optic nerve/sheath complex at 3, 9, and 15 mm behind the globe

b Medical and Health Organization: _____

Noninvasive Cerebrospinal Fluid Pressure and Translaminar Pressure Difference based on MRI

Patient name: Gender: Age: Medical record No:

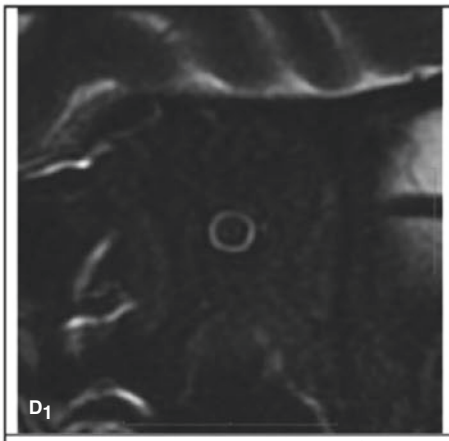

Oblique coronal image of the optic nerve/sheath complex at 9 mm behind the right eye

ONSD:_____ mm ; OND: _____mm

OSASW=1/2(ONSD-OND): _____ mm

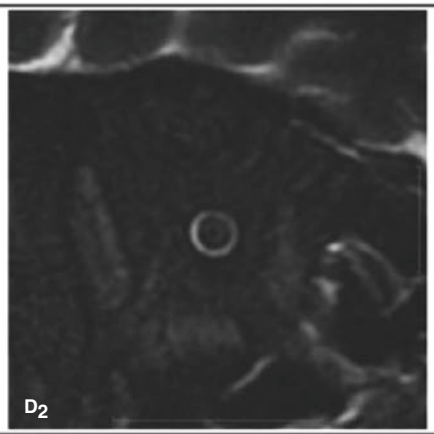

Oblique coronal image of the optic nerve/sheath complex at 9 mm behind the left eye

ONSD:_____ mm ; OND: _____mm

OSASW=1/2(ONSD-OND): _____ mm

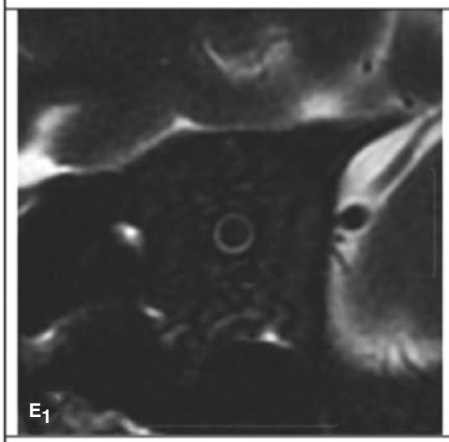

Oblique coronal image of the optic nerve/sheath complex at 15 mm behind the right eye

ONSD:_____ mm ; OND: _____ mm

OSASW=1/2(ONSD-OND): _____ mm

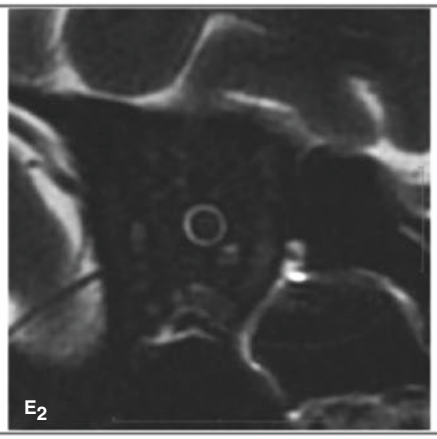

Oblique coronal image of the optic nerve/sheath complex at 15 mm behind the left eye

ONSD:_____ mm ; OND: _____mm

OSASW=1/2(ONSD-OND): _____ mm

IOP= _____ mm Hg

Non-invasive CSF-P = 16.95 x SASW9+0.39 x BMI+0.14MAP-20.90= _____ mm Hg

(_____ mm H2O) (1 mm Hg = 13.6 mm H2O)

Non-invasive TLPD = IOP-Non-invasive CSF-P=_____ mm Hg

Fig. 14.9 (continued)

c

Medical and Health Organization: _____

Noninvasive Cerebrospinal Fluid Pressure and Translaminar Pressure Difference based on MRI

Patient name: Gender: Age: Medical record No:

Table 1 Conversion Table of Cerebrospinal Fluid Space Width and Cerebrospinal Fluid Pressure

	Very High	High	Moderate High	Middle	Moderate Low	Low	Very Low
OSASW3	>1.85	1.85~1.46	1.46~1.07	1.07~0.83	0.83~0.77	0.77~0.51	<0.51
OSASW9	>1.38	1.38~0.92	0.92~0.76	0.76~0.64	0.64~0.62	0.62~0.46	<0.46
ONSASW15	>1.23	1.23~0.79	0.79~0.73	0.73~0.63	0.63~0.47	0.47~0.39	<0.39
CSF-P mmH_2O	>355	355~225	225~195	195~160	160~140	140~100	<100
CSF-P mmHg	>26.1	26.1~16.5	16.5~14.3	14.3~11.8	11.8~10.3	10.3~7.4	<7.4

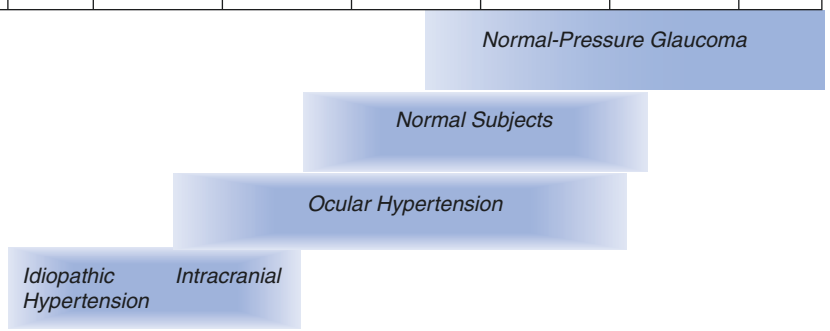

table 2 Reference value of oblique coronal scan of the normal optic nerve/sheath complex

Measurement index	3mm behind the globe	9mm behind the globe	15mm behind the globe
ONSD (mm)	3.29 ± 0.31	2.89 ± 0.21	2.67 ± 0.17
OND (mm)	5.03 ± 0.35	4.22 ± 0.22	3.89 ± 0.26
OSASW (mm)	0.87 ± 0.15	0.67 ± 0.07	0.61 ± 0.07

Annotation

Non-invasive CSF-P: Non-invasive Cerebralspinal Fluid Pressure
ONSD 3-5: the optic nerve sheath diameter at 3 mm, 9 mm and 15 mm behind the globe
OND 3-5: the optic nerve diameter at 3 mm, 9 mm and 15 mm behind the globe
OSASW 3-5: the orbital subarachnoid space width at 3 mm, 9 mm and 15 mm behind the globe
MAP: Mean arterial blood pressure
BMI: Body mass index
Non-invasive CSFP: Non-invasive cerebrospinal fluid pressure
Non-invasive TLPD: Non-invasive trans-laminar pressure difference

Patient name: _____ Report time: _____

Fig. 14.9 (continued)

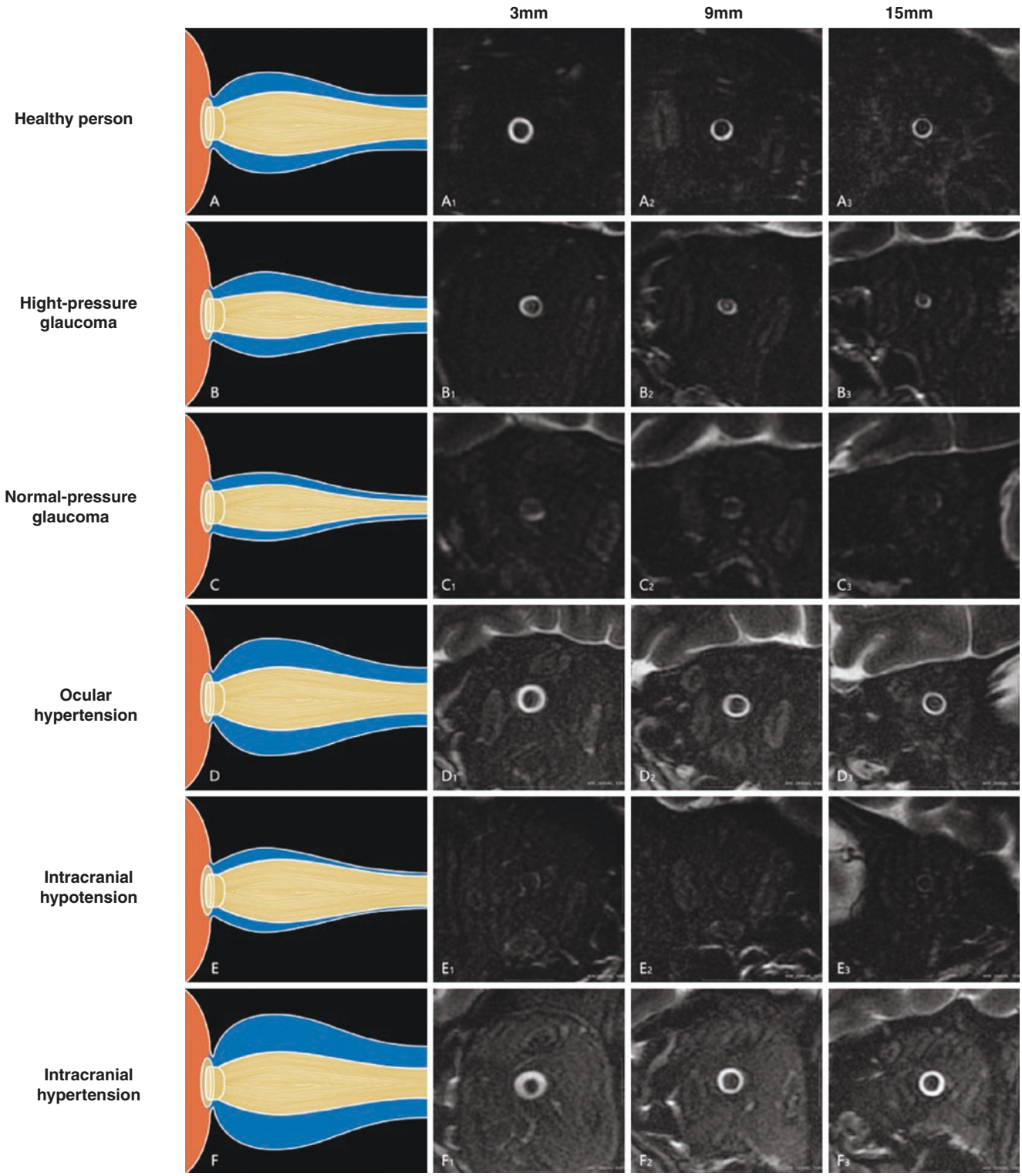

Fig. 14.10 Oblique magnetic resonance coronal T2WI-FRFSE image with fat suppression for demonstrating the optic nerve/sheath complex, taken at 3 mm (A1–F1), at 9 mm (A2–F2), and at 15 mm (A3–F3) behind the globe. (**a**) A1–A3 Healthy person. Note: optic nerve subarachnoid space width relatively wide and bright. (**b**) B1–B3: High-pressure glaucoma. Note: though optic nerve diameter narrower than healthy person in A1–A3, optic nerve subarachnoid space width is similar with healthy person. (**c**) C1–C3: Normal tension glaucoma. Note: orbital subarachnoid space is relatively narrow and faint. (**d**) D1–D3: Ocular hypertension. Note: orbital subarachnoid space is comparatively wide and bright. (**e**) E1–E3: A patient with spontaneous intracranial hypotension; lumbar cerebrospinal fluid opening pressure is 3.7 mmHg. (**f**) F1–F3: A patient with benign intracranial hypertension; lumbar cerebrospinal fluid opening pressure is 24.3 mmHg

Acknowledgments We would like to thank Ning Tian for drawing diagrams for this chapter. Ning Tian, designer at Beijing Tianming Ophthalmological Novel Technology Development Corporation, 17 Hougou Lane, Chongwenmen, Beijing, 100005, China.

References

1. Ren R, Jonas JB, Tian G, et al. Cerebrospinal fluid pressure in glaucoma: a prospective study. Ophthalmology. 2010;117(2):259–66.
2. Berdahl JP, Allingham RR, Johnson DH. Cerebrospinal fluid pressure is decreased in primary open-angle glaucoma. Ophthalmology. 2008;115(5):763–8.
3. Wang N, Xie X, Yang D, et al. Orbital cerebrospinal fluid space in glaucoma: the Beijing iCOP study. Ophthalmology. 2012;
4. Berdahl JP, Fautsch MP, Stinnett SS, Allingham RR. Intracranial pressure in primary open angle glaucoma, normal tension glaucoma, and ocular hypertension: a case-control study. Invest Ophthalmol Vis Sci. 2008;49(12):5412–8.
5. Ren R, Wang N, Zhang X, Cui T, Jonas JB. Trans-lamina cribrosa pressure difference correlated with neuroretinal rim area in glaucoma. Graefes Arch Clin Exp Ophthalmol. 2011;249(7):1057–63.
6. Jonas JB, Wang NL, Wang YX, et al. Estimated trans-lamina cribrosa pressure difference versus intraocular pressure as biomarker for open-angle glaucoma. The Beijing Eye Study. Acta Ophthalmol. 2011;93(1):e7–e13.
7. Jonas JB, Wang N, Wang YX, You QS, Yang D, Xu L. Ocular hypertension: general characteristics and estimated cerebrospinal fluid pressure. The Beijing Eye Study. PLoS One. 2011;9(7):e100533.
8. Ren R, Zhang X, Wang N, Li B, Tian G, Jonas JB. Cerebrospinal fluid pressure in ocular hypertension. Acta Ophthalmol. 2011;89(2):e142–8.
9. Bayer AU, Ferrari F, Erb C. High occurrence rate of glaucoma among patients with Alzheimer's disease. Eur Neurol. 2002;47(3):165–8.
10. Wostyn P, Audenaert K, De Deyn PP. More advanced Alzheimer's disease may be associated with a decrease in cerebrospinal fluid pressure. Cerebrospinal Fluid Res. 2009;6:14.
11. Tamura H, Kawakami H, Kanamoto T, et al. High frequency of open-angle glaucoma in Japanese patients with Alzheimer's disease. J Neurol Sci. 2006;246(1-2):79–83.
12. Wostyn P, De Groot V, Van Dam D, Audenaert K, De Deyn PP. Senescent changes in cerebrospinal fluid circulatory physiology and their role in the pathogenesis of normal-tension glaucoma. Am J Ophthalmol. 2013;156(1):5–14 e12.
13. Tso MO, Hayreh SS. Optic disc edema in raised intracranial pressure. IV. Axoplasmic transport in experimental papilledema. Arch Ophthalmol. 1977;95(8):1458–62.
14. Hayreh MS, Hayreh SS. Optic disc edema in raised intracranial pressure. I. Evolution and resolution. Arch Ophthalmol. 1977;95(7):1237–44.
15. Hayreh SS, Hayreh MS. Optic disc edema in raised intracranial pressure. II. Early detection with fluorescein fundus angiography and stereoscopic color photography. Arch Ophthalmol. 1977;95(7):1245–54.
16. Tso MO, Hayreh SS. Optic disc edema in raised intracranial pressure. III. A pathologic study of experimental papilledema. Arch Ophthalmol. 1977;95(8):1448–57.
17. Hayreh SS. Optic disc edema in raised intracranial pressure. V. Pathogenesis. Arch Ophthalmol. 1977;95(9):1553–65.
18. Hayreh SS. Optic disc edema in raised intracranial pressure. VI. Associated visual disturbances and their pathogenesis. Arch Ophthalmol. 1977;95(9):1566–79.
19. Laemmer R, Heckmann JG, Mardin CY, Schwab S, Laemmer AB. Detection of nerve fiber atrophy in apparently effectively treated papilledema in idiopathic intracranial hypertension. Graefes Arch Clin Exp Ophthalmol. 2010;248(12):1787–93.
20. Zhang LF, Hargens AR. Intraocular/Intracranial pressure mismatch hypothesis for visual impairment syndrome in space. Aviat Space Environ Med. 2014;85(1):78–80.
21. Mader TH, Gibson CR, Pass AF, et al. Optic disc edema in an astronaut after repeat long-duration space flight. J Neuroophthalmol. 2013;33(3):249–55.
22. Mader TH, Gibson CR, Pass AF, et al. Optic disc edema, globe flattening, choroidal folds, and hyperopic shifts observed in astronauts after long-duration space flight. Ophthalmology. 2011;118(10):2058–69.
23. Jonas JB, Wang N, Wang YX, et al. Incident retinal vein occlusions and estimated cerebrospinal fluid pressure. The Beijing Eye Study. Acta Ophthalmol. 2015;93(7):e522–6.
24. Mansouri K, Weinreb RN. Ambulatory 24-h intraocular pressure monitoring in the management of glaucoma. Curr Opin Ophthalmol. 2015;26(3):214–20.
25. Kawoos U, McCarron RM, Auker CR, Chavko M. Advances in intracranial pressure monitoring and its significance in managing traumatic brain injury. Int J Mol Sci. 2015;16(12):28979–97.
26. Lenfeldt N, Koskinen LO, Bergenheim AT, Malm J, Eklund A. CSF pressure assessed by lumbar puncture agrees with intracranial pressure. Neurology. 2007;68(2):155–8.
27. Zhong J, Dujovny M, Park HK, Perez E, Perlin AR, Diaz FG. Advances in ICP monitoring techniques. Neurol Res. 2003;25(4):339–50.
28. Bhatia A, Gupta AK. Neuromonitoring in the intensive care unit. I. Intracranial pressure and cerebral blood flow monitoring. Intensive Care Med. 2007;33(7):1263–71.
29. Guillaume J, Janny P. Continuous intracranial manometry; importance of the method and first results. Rev Neurol (Paris). 1951;84(2):131–42.
30. Kakarla UK, Kim LJ, Chang SW, Theodore N, Spetzler RF. Safety and accuracy of bedside external ventricular drain placement. Neurosurgery. 2008;63(1 Suppl 1):ONS162–6; discussion ONS166–167.
31. Park YG, Woo HJ, Kim E, Park J. Accuracy and safety of bedside external ventricular drain placement at two different cranial sites : Kocher's point versus forehead. J Korean Neurosurg Soc. 2011;50(4):317–21.
32. Woernle CM, Burkhardt JK, Bellut D, Krayenbuehl N, Bertalanffy H. Do iatrogenic factors bias the placement of external ventricular catheters?—a single institute experience and review of the literature. Neurol Med Chir (Tokyo). 2011;51(3):180–6.
33. Patil V, Gupta R, San Jose Estepar R, et al. Smart stylet: the development and use of a bedside external ventricular drain image-guidance system. Stereotact Funct Neurosurg. 2015;93(1):50–8.
34. Sarrafzadeh A, Smoll N, Schaller K. Guided (VENTRI-GUIDE) versus freehand ventriculostomy: study protocol for a randomized controlled trial. Trials. 2014;15:478.
35. Munch E, Weigel R, Schmiedek P, Schurer L. The Camino intracranial pressure device in clinical practice: reliability, handling characteristics and complications. Acta Neurochir. 1998;140(11):1113–9; discussion 1119–1120.
36. Chambers KR, Kane PJ, Choksey MS, Mendelow AD. An evaluation of the camino ventricular bolt system in clinical practice. Neurosurgery. 1993;33(5):866–8.
37. Bruder N, N'Zoghe P, Graziani N, Pelissier D, Grisoli F, Francois G. A comparison of extradural and intraparenchymatous intracranial pressures in head injured patients. Intensive Care Med. 1995;21(10):850–2.
38. Gelabert-Gonzalez M, Ginesta-Galan V, Sernamito-Garcia R, Allut AG, Bandin-Dieguez J, Rumbo RM. The Camino intracra-

nial pressure device in clinical practice. Assessment in a 1000 cases. Acta Neurochir. 2006;148(4):435–41.
39. Piper IR, Miller JD. The evaluation of the wave-form analysis capability of a new strain-gauge intracranial pressure MicroSensor. Neurosurgery. 1995;36(6):1142–4; discussion 1144–1145.
40. Citerio G, Piper I, Cormio M, et al. Bench test assessment of the new Raumedic Neurovent-P ICP sensor: a technical report by the BrainIT group. Acta Neurochir. 2004;146(11):1221–6.
41. Allin D, Czosnyka M, Czosnyka Z. Laboratory testing of the Pressio intracranial pressure monitor. Neurosurgery. 2008;62(5):1158–61; discussion 1161.
42. Lang JM, Beck J, Zimmermann M, Seifert V, Raabe A. Clinical evaluation of intraparenchymal Spiegelberg pressure sensor. Neurosurgery. 2003;52(6):1455–9; discussion 1459
43. Ghajar J. Intracranial pressure monitoring techniques. New Horiz. 1995;3(3):395–9.
44. Raabe A, Totzauer R, Meyer O, Stockel R, Hohrein D, Schoche J. Reliability of epidural pressure measurement in clinical practice: behavior of three modern sensors during simultaneous ipsilateral intraventricular or intraparenchymal pressure measurement. Neurosurgery. 1998;43(2):306–11.
45. Miller JD, Bobo H, Kapp JP. Inaccurate pressure readings for subarachnoid bolts. Neurosurgery. 1986;19(2):253–5.
46. Raboel PH, Bartek J Jr, Andresen M, Bellander BM, Romner B. Intracranial pressure monitoring: invasive versus non-invasive methods-a review. Crit Care Res Prac. 2012;2012:950393.
47. Eide PK. Comparison of simultaneous continuous intracranial pressure (ICP) signals from ICP sensors placed within the brain parenchyma and the epidural space. Med Eng Phys. 2008;30(1):34–40.
48. Guyot LL, Dowling C, Diaz FG, Michael DB. Cerebral monitoring devices: analysis of complications. Acta Neurochir Suppl. 1998;71:47–9.
49. Martinez-Manas RM, Santamarta D, de Campos JM, Ferrer E. Camino intracranial pressure monitor: prospective study of accuracy and complications. J Neurol Neurosurg Psychiatry. 2000;69(1):82–6.
50. Brain Trauma F, American Association of Neurological S, Congress of Neurological S, et al. Guidelines for the management of severe traumatic brain injury. VII. Intracranial pressure monitoring technology. J Neurotrauma. 2007;24(Suppl 1):S45–54.
51. Steiner LA, Andrews PJ. Monitoring the injured brain: ICP and CBF. Br J Anaesth. 2006;97(1):26–38.
52. Behrens A, Lenfeldt N, Qvarlander S, Koskinen LO, Malm J, Eklund A. Are intracranial pressure wave amplitudes measurable through lumbar puncture? Acta Neurol Scand. 2013;127(4):233–41.
53. Colledge NR, Walker BR, Ralston SH, editors. Davidson's principles and practice of medicine. 21st ed. Edinburgh: Churchill Livingstone/Elsevier; 2010. p. 1147–8. ISBN 978-0-7020-3084-0.
54. March K. Intracranial pressure monitoring: why monitor? AACN Clin Issues. 2005;16(4):456–75.
55. Hanlo P, Peters R, Gooskens R, et al. Monitoring intracranial dynamics by transcranial Doppler—a new Doppler index: trans systolic time. Ultrasound Med Biol. 1995;21(5):613–21.
56. Popovic D, Khoo M, Lee S. Noninvasive monitoring of intracranial pressure. Recent Patents on Biomedical Engineering. 2009;2(3):165–79.
57. Petkus V, Ragauskas A, Jurkonis R. Investigation of intracranial media ultrasonic monitoring model. Ultrasonics. 2002;40(1):829–33.
58. Ragauskas A, Daubaris G, Ragaisis V, Petkus V. Implementation of non-invasive brain physiological monitoring concepts. Med Eng Phys. 2003;25(8):667–78.
59. Ragauskas A DG, Inventor. Method and apparatus for non-invasively deriving and indicating of dynamic characteristics of the human and animal intracranial media. US patent 5,388,5831995.
60. Buhre W, Heinzel F, Grund S, Sonntag H, Weyland A. Extrapolation to zero-flow pressure in cerebral arteries to estimate intracranial pressure. Br J Anaesth. 2003;90(3):291–5.
61. Ursino M, Ter Minassian A, Lodi C, Beydon L. Cerebral hemodynamics during arterial and CO2 pressure changes: in vivo prediction by a mathematical model. Am J Phys Heart Circ Phys. 2000;279(5):H2439–55.
62. Miao J, Benkeser PJ, Nichols FT. A computer-based statistical pattern recognition for doppler spectral waveforms of intracranial blood flow. Comput Biol Med. 1996;26(1):53–63.
63. Cardim D, Robba C, Bohdanowicz M, et al. Non-invasive monitoring of intracranial pressure using transcranial doppler ultrasonography: is it possible? Neurocrit Care. 2016;25(3):473–91.
64. Maeda H, Matsumoto M, Handa N, et al. Reactivity of cerebral blood flow to carbon dioxide in various types of ischemic cerebrovascular disease: evaluation by the transcranial doppler method. Stroke. 1993;24(5):670–5.
65. Yost WT, Cantrell JH, Kushnick PW. Fundamental aspects of pulse phase-locked loop technology-based methods for measurement of ultrasonic velocity. J Acoust Soc Am. 1992;91(3):1456–68.
66. Ueno T, Macias BR, Yost WT, Hargens AR. Noninvasive assessment of intracranial pressure waveforms by using pulsed phase lock loop technology. Technical note. J Neurosurg. 2005;103(2):361–7.
67. Ueno T, Macias BR, Yost WT, Hargens AR. Pulsed phase lock loop device for monitoring intracranial pressure during space flight. J Gravit Physiol. 2003;10:117–8.
68. Chen H, Wang J, Mao S, Dong W, Yang H. A new method of intracranial pressure monitoring by EEG power spectrum analysis. Can J Neurol Sci. 2012;39(04):483–7.
69. Ghosh A, Elwell C, Smith M. Cerebral near-infrared spectroscopy in adults: a work in progress. Anesth Analg. 2012;115(6):1373–83.
70. Kampfl A, Pfausler B, Denchev D, Jaring H, Schmutzhard E. Near infrared spectroscopy (NIRS) in patients with severe brain injury and elevated intracranial pressure. Acta Neurochir Suppl. 1997;70:112–4.
71. Weerakkody RA, Czosnyka M, Zweifel C, et al. Near infrared spectroscopy as possible non-invasive monitor of slow vasogenic ICP waves. Acta Neurochir Suppl. 2012;114:181–5.
72. Zweifel C, Castellani G, Czosnyka M, et al. Continuous assessment of cerebral autoregulation with near-infrared spectroscopy in adults after subarachnoid hemorrhage. Stroke. 2010;41(9):1963–8.
73. Kristiansson H, Nissborg E, Bartek J Jr, Andresen M, Reinstrup P, Romner B. Measuring elevated intracranial pressure through noninvasive methods: a review of the literature. J Neurosurg Anesthesiol. 2013;25(4):372–85.
74. Purin V. Measurement of intracranial pressure in children without puncture (new method). Pediatriia. 1964;43:82.
75. Wealthall S, Smallwood R. Methods of measuring intracranial pressure via the fontanelle without puncture. J Neurol Neurosurg Psychiatry. 1974;37(1):88–96.
76. Singh D, Cronin DS. Investigation of cavitation using a modified Hopkinson apparatus. Dynam Behav Mat. 2015;1:177–83.
77. Swoboda M, Hochman MG, Fritz FJ, Inventor. Non-invasive intracranial pressure sensor. 2008.
78. Nichols WW, McDonald DA, O'Rourke MF. McDonald's blood flow in arteries: theoretical, experimental and clinical principles. Abingdon: Taylor & Francis; 2005. p. 570.
79. Liu D, Kahn M. Measurement and relationship of subarachnoid pressure of the optic nerve to intracranial pressures in fresh cadavers. Am J Ophthalmol. 1993;116(5):548–56.
80. Geeraerts T, Duranteau J, Benhamou D. Ocular sonography in patients with raised intracranial pressure: the papilloedema revisited. Crit Care. 2008;12(3):150.
81. Gibby W, Cohen M, Goldberg H, Sergott R. Pseudotumor cerebri: CT findings and correlation with vision loss. AJR Am J Roentgenol. 1993;160(1):143–6.

82. Soldatos T, Karakitsos D, Chatzimichail K, Papathanasiou M, Gouliamos A, Karabinis A. Optic nerve sonography in the diagnostic evaluation of adult brain injury. Crit Care. 2008;12(3):1.
83. Kimberly HH, Shah S, Marill K, Noble V. Correlation of optic nerve sheath diameter with direct measurement of intracranial pressure. Acad Emerg Med. 2008;15(2):201–4.
84. Rajajee V, Vanaman M, Fletcher JJ, Jacobs TL. Optic nerve ultrasound for the detection of raised intracranial pressure. Neurocrit Care. 2011;15(3):506–15.
85. Dubourg J, Javouhey E, Geeraerts T, Messerer M, Kassai B. Ultrasonography of optic nerve sheath diameter for detection of raised intracranial pressure: a systematic review and meta-analysis. Intensive Care Med. 2011;37(7):1059–68.
86. Steinborn M, Friedmann M, Makowski C, Hahn H, Hapfelmeier A, Juenger H. High resolution transbulbar sonography in children with suspicion of increased intracranial pressure. Childs Nerv Syst. 2016;32(4):655–60.
87. Weigel M, Lagreze WA, Lazzaro A, Hennig J, Bley TA. Fast and quantitative high-resolution magnetic resonance imaging of the optic nerve at 3.0 tesla. Investig Radiol. 2006;41(2):83–6.
88. Xie X, Zhang X, Fu J, et al. Noninvasive intracranial pressure estimation by orbital subarachnoid space measurement: the Beijing Intracranial and Intraocular Pressure (iCOP) study. Crit Care. 2013;17(4):R162.
89. Geeraerts T, Newcombe VF, Coles JP, et al. Use of T2-weighted magnetic resonance imaging of the optic nerve sheath to detect raised intracranial pressure. Crit Care. 2008;12(5):R114.
90. Querfurth HW, Arms SW, Lichy CM, Irwin WT, Steiner T. Prediction of intracranial pressure from noninvasive transocular venous and arterial hemodynamic measurements: a pilot study. Neurocrit Care. 2004;1(2):183–94.
91. Querfurth HW, Lieberman P, Arms S, Mundell S, Bennett M, van Horne C. Ophthalmodynamometry for ICP prediction and pilot test on Mt. Everest. BMC Neurol. 2010;10:106.
92. Motschmann M, Muller C, Kuchenbecker J, et al. Ophthalmodynamometry: a reliable method for measuring intracranial pressure. Strabismus. 2001;9(1):13–6.
93. Firsching R, Schutze M, Motschmann M, Behrens-Baumann W. Venous opthalmodynamometry: a noninvasive method for assessment of intracranial pressure. J Neurosurg. 2000;93(1):33–6.
94. Querfurth HW, Arms SW, Lichy CM, Irwin WT, Steiner T. Prediction of intracranial pressure from noninvasive transocular venous and arterial hemodynamic measurements. Neurocrit Care. 2004;1(2):183–94.
95. Jonas JB, Pfeil K, Chatzikonstantinou A, Rensch F. Ophthalmodynamometric measurement of central retinal vein pressure as surrogate of intracranial pressure in idiopathic intracranial hypertension. Graefes Arch Clin Exp Ophthalmol. 2008;246(7):1059–60.
96. York DH, Pulliam MW, Rosenfeld JG, Watts C. Relationship between visual evoked potentials and intracranial pressure. J Neurosurg. 1981;55(6):909–16.
97. York D, Legan M, Benner S, Watts C. Further studies with a noninvasive method of intracranial pressure estimation. Neurosurgery. 1984;14(4):456–61.
98. Desch LW. Longitudinal stability of visual evoked potentials in children and adolescents with hydrocephalus. Dev Med Child Neurol. 2001;43(02):113–7.
99. Andersson L, Sjolund J, Nilsson J. Flash visual evoked potentials are unreliable as markers of ICP due to high variability in normal subjects. Acta Neurochir. 2012;154(1):121–7.
100. Echegaray S, Zamora G, Yu H, Luo W, Soliz P, Kardon R. Automated analysis of optic nerve images for detection and staging of papilledema. Invest Ophthalmol Vis Sci. 2011;52(10):7470–8.
101. Heckmann JG, Weber M, Junemann AG, Neundorfer B, Mardin CY. Laser scanning tomography of the optic nerve vs CSF opening pressure in idiopathic intracranial hypertension. Neurology. 2004;62(7):1221–3.
102. Rebolleda G, Munoz-Negrete FJ. Follow-up of mild papilledema in idiopathic intracranial hypertension with optical coherence tomography. Invest Ophthalmol Vis Sci. 2009;50(11):5197–200.
103. Group OCTS-SCfNIIHS, Auinger P, Durbin M, et al. Baseline OCT measurements in the idiopathic intracranial hypertension treatment trial, part I: quality control, comparisons, and variability. Invest Ophthalmol Vis Sci. 2014;55(12):8180–8.
104. Group OCTS-SCfNIIHS, Auinger P, Durbin M, et al. Baseline OCT measurements in the idiopathic intracranial hypertension treatment trial, part II: correlations and relationship to clinical features. Invest Ophthalmol Vis Sci. 2014;55(12):8173–9.
105. Optical Coherence Tomography Substudy C, Group NIIHS. Papilledema outcomes from the optical coherence tomography substudy of the idiopathic intracranial hypertension treatment trial. Ophthalmology. 2015;122(9):1939–1945.e1932.
106. Kupersmith MJ, Sibony P, Mandel G, et al. Optical coherence tomography of the swollen optic nerve head: deformation of the peripapillary retinal pigment epithelium layer in papilledema. Invest Ophthalmol Vis Sci. 2011;52(9):6558.
107. Reid A, Marchbanks RJ, Burge DM, et al. The relationship between intracranial pressure and tympanic membrane displacement. Br J Audiol. 1990;24(2):123–9.
108. Samuel M, Burge DM, Marchbanks RJ. Quantitative assessment of intracranial pressure by the tympanic membrane displacement audiometric technique in children with shunted hydrocephalus. Eur J Pediatr Surg. 1998;8(4):200–7.
109. Gwer S, Sheward V, Birch A, et al. The tympanic membrane displacement analyser for monitoring intracranial pressure in children. Childs Nerv Syst. 2013;29(6):927–33.
110. Silverman CA, Linstrom CJ. How to measure cerebrospinal fluid pressure invasively and noninvasively. J Glaucoma. 2013;22(Suppl 5):S26–8.
111. Yavin D, Luu J, James MT, et al. Diagnostic accuracy of intraocular pressure measurement for the detection of raised intracranial pressure: meta-analysis: a systematic review. J Neurosurg. 2014;121(3):680–7.
112. Lashutka MK, Chandra A, Murray HN, Phillips GS, Hiestand BC. The relationship of intraocular pressure to intracranial pressure. Ann Emerg Med. 2004;43(5):585–91.
113. Sheeran P, Bland JM, Hall GM. Intraocular pressure changes and alterations in intracranial pressure. Lancet. 2000;355(9207):899.
114. Han Y, McCulley TJ, Horton JC. No correlation between intraocular pressure and intracranial pressure. Ann Neurol. 2008;64(2):221–4.
115. Czarnik T, Gawda R, Latka D, Kolodziej W, Sznajd-Weron K, Weron R. Noninvasive measurement of intracranial pressure: is it possible? J Trauma. 2007;62(1):207–11.
116. Li Z, Yang Y, Lu Y, et al. Intraocular pressure vs intracranial pressure in disease conditions: a prospective cohort study (Beijing iCOP study). BMC Neurol. 2012;12:66.
117. Jonas JB, Wang N, Wang YX, et al. Body height, estimated cerebrospinal fluid pressure and open-angle glaucoma. The beijing eye study. PLoS One. 2011;9(1):e86678.
118. Jonas JB, Nangia V, Wang N, et al. Trans-lamina cribrosa pressure difference and open-angle glaucoma. The central India eye and medical study. PLoS One. 2013;8(12):e82284.
119. Asrani S, Samuels B, Thakur M, Santiago C, Kuchibhatla M. Clinical profiles of primary open angle glaucoma versus normal tension glaucoma patients: a pilot study. Curr Eye Res. 2011;36(5):429–35.

120. Melki S, Todani A, Cherfan G. An implantable intraocular pressure transducer: initial safety outcomes. JAMA Ophthalmol. 2014;132(10):1221–5.
121. Koutsonas A, Walter P, Roessler G, Plange N. Implantation of a novel telemetric intraocular pressure sensor in patients with glaucoma (ARGOS study): 1-year results. Invest Ophthalmol Vis Sci. 2015;56(2):1063–9.
122. Koskinen LO, Olivecrona M. Clinical experience with the intraparenchymal intracranial pressure monitoring Codman MicroSensor system. Neurosurgery. 2005;56(4):693–8; discussion 693–698.
123. Jetzki S, Weinzierl M, Krause I, et al. A multisensor implant for continuous monitoring of intracranial pressure dynamics. IEEE Trans Biomed Circuits Syst. 2012;6(4):356–65.
124. Schmitt M, Eymann R, Antes S, Kiefer M. Subdural or intraparenchymal placement of long-term telemetric intracranial pressure measurement devices? Acta Neurochir Suppl. 2012;113:109–13.
125. Orakcioglu B, Beynon C, Kentar MM, Eymann R, Kiefer M, Sakowitz OW. Intracranial pressure telemetry: first experience of an experimental in vivo study using a new device. Acta Neurochir Suppl. 2012;114:105–10.
126. Liu JH, Kripke DF, Hoffman RE, et al. Nocturnal elevation of intraocular pressure in young adults. Invest Ophthalmol Vis Sci. 1998;39(13):2707–12.
127. Liu JH, Kripke DF, Twa MD, et al. Twenty-four-hour pattern of intraocular pressure in the aging population. Invest Ophthalmol Vis Sci. 1999;40(12):2912–7.
128. Hao J, Zhen Y, Wang H, Yang D, Wang N. The effect of lateral decubitus position on nocturnal intraocular pressure over a habitual 24-hour period in healthy adults. PLoS One. 2014;9(11):e113590.
129. Wang NL, Hao J, Zhen Y, et al. A population-based investigation of circadian rhythm of intraocular pressure in habitual position among healthy subjects: the handan eye study. J Glaucoma. 2016;25(7):584–9.
130. Tsukahara S, Sasaki T. Postural change of IOP in normal persons and in patients with primary wide open-angle glaucoma and low-tension glaucoma. Br J Ophthalmol. 1984;68(6):389–92.
131. Renard E, Palombi K, Gronfier C, et al. Twenty-four hour (Nyctohemeral) rhythm of intraocular pressure and ocular perfusion pressure in normal-tension glaucoma. Invest Ophthalmol Vis Sci. 2010;51(2):882–9.
132. Lee YR, Kook MS, Joe SG, et al. Circadian (24-hour) pattern of intraocular pressure and visual field damage in eyes with normal-tension glaucoma. Invest Ophthalmol Vis Sci. 2012;53(2):881–7.
133. Weinreb RN, Khaw PT. Primary open-angle glaucoma. Lancet. 2004;363(9422):1711–20.
134. Wostyn P, De Groot V, Audenaert K, De Deyn PP. Are intracranial pressure fluctuations important in glaucoma? Med Hypotheses. 2011;77(4):598–600.
135. Wang N, Xie X, Yang D, et al. Orbital cerebrospinal fluid space in glaucoma: the Beijing intracranial and intraocular pressure (iCOP) study. Ophthalmology. 2012;119(10):2065–2073.e2061.

Which MRI Sequence Shows Subarachnoid Space of the Optic Nerve Better?

15

Junfang Xian and Ningli Wang

Glaucoma is a worldwide leading cause of irreversible vision loss, with primary open-angle glaucoma (POAG) as its most common form. Although the pathogenesis of POAG is still not fully understood, it has been highlighted over the past few years that increased trans-lamina cribrosa pressure (TLCP) can lead to POAG [1]. As low cerebrospinal fluid pressure (CSF-P) is responsible for TLCP decrease, it is necessary to find a proper way to measure CSF-P of POAG patients. Lumbar puncture is the conventional method for CSF-P measurement. However, the adoption of invasive method for glaucoma screening is not acceptable. Currently, calculated CSF-P with detected ONSASW by MRI is gradually becoming a substitute for the conventional method [2].

Prior studies imply that the width of optic nerve subarachnoid space (ONSAS) is an important parameter to evaluate the CSF-P [3]. T2-weighted imaging (T2WI) has an advantage in cerebrospinal fluid imaging; however, routine T2WI without fat suppression is not the appropriate choice because of its low spatial resolution and chemical shift artifact. Thus, we employed fast recovery fast spin echo T2-weighted imaging (FRFSE T2WI) sequence, three-dimensional fast spin echo (3D-FSE-Cube) T2WI, and single-shot fast spin echo (SSFSE) T2WI to detect the ONSAS, in order to find the best way for ONSAS measurement.

Magnetic resonance imaging data was acquired using a GE Signa HDxt 3.0 T MRI scanner (General Electric Medical Systems, Milwaukee, WI, USA). For the scans, subjects were instructed simply to rest with their eyes closed, to relax but not to fall asleep. Head movements were prevented by a custom-built head holder. T2WI with fat suppression was used to separate the ONSAS and surrounding fat. As 2D images and 3D images have their own edges, both 2D T2WI and 3D T2WI were employed. To measure the width of ONSAS, the images which were vertical to the optic nerve at 3 mm, 9 mm, and 15 mm behind the globe were selected (Figs. 15.1 and 15.2).

15.1 FRFSE T2WI

After scanning the axial and oblique sagittal images of orbit, the oblique coronal images were positioned. The parameters of FRFSE T2WI were as follows: TR = 6000 ms, TE = 245 ms, and spatial resolution = 0.2 × 0.2 mm.

FRFSE T2WI could show the edge of ONSAS clearly, providing great support in increasing the accuracy and repeatability of ONSAS measurement. However, it also has its drawbacks. As the location of vertical sections of optic nerve was determined by fixed slice space (Fig. 15.1), when the optic nerve was tortuous, the sections were inaccurate (Fig. 15.3a). Besides, FRFSE T2WI took about 1 min and 18 s, so that some patients found it difficult to control their eye movement. In addition, obvious motion artifact severely impacted the accuracy of measurement (Fig. 15.3b).

15.2 3D Cube T2WI

3D cube was less influenced by the morphology of optic nerve. Once scanned, the data could be reconstructed in any direction (Figs. 15.4 and 15.5); therefore, it was less influenced by tortuous optic nerve. The parameters were as follows: TR = 3000 ms, TE = min, slice thickness = 1 mm, and spatial resolution = 0.7 × 0.7 mm.

Compared with FRFSE T2WI, the resolution of reconstructed image of 3D cube was lower, and the edge of ONSAS was more obscure. Besides, 3D cube took more than 6 min. Hence, it was neither clear enough nor fast enough.

J. Xian
Department of Radiology, Beijing Tongren Hospital, Capital Medical University, Beijing, China

N. Wang (✉)
Beijing Institute of Ophthalmology, Beijing Tongren Eye Center, Beijing Tongren Hosptial, Capital Medical University, Beijing, China

Beijing Ophthalmology & Visual Sciences Key Laboratory, Beijing, China
e-mail: wningli@vip.163.com

N. Wang (ed.), *Intraocular and Intracranial Pressure Gradient in Glaucoma*,
Advances in Visual Science and Eye Diseases 1, https://doi.org/10.1007/978-981-13-2137-5_15

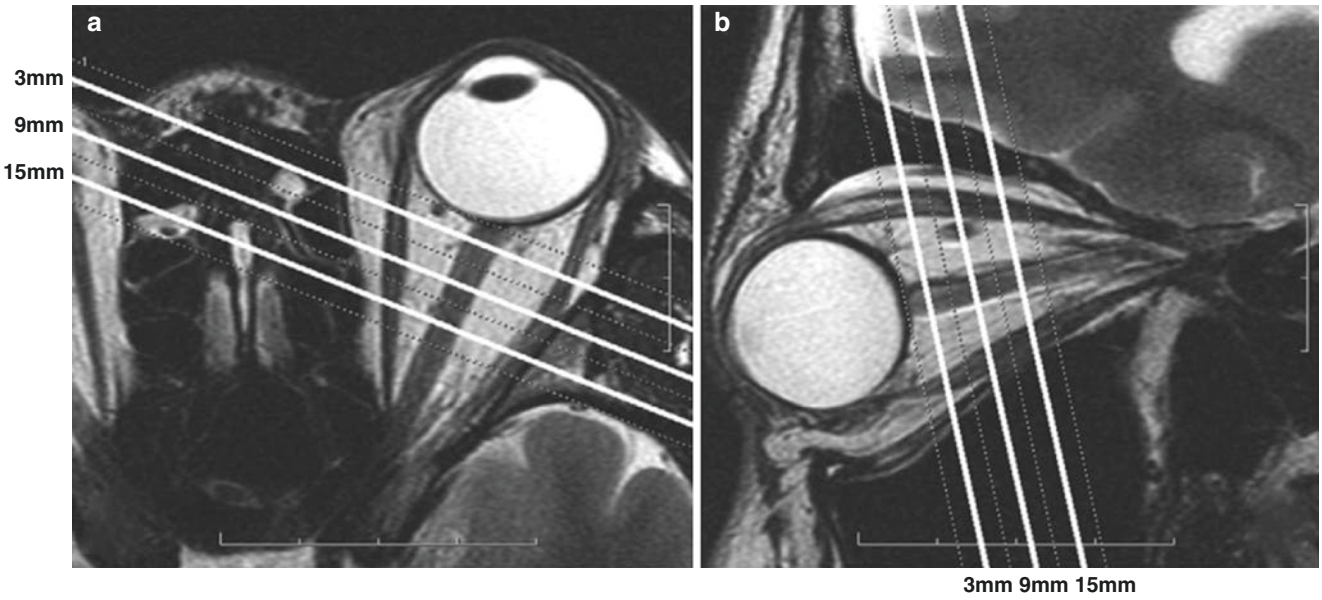

Fig. 15.1 Location images of FRFSE T2WI. (**a**, **b**) showed that the scanning baseline was vertical to the optic nerve and the oblique coronal planes which were used for ONSAS measurement were located at 3, 9, and 15 mm after the eyeball (Reprinted with permission from [2])

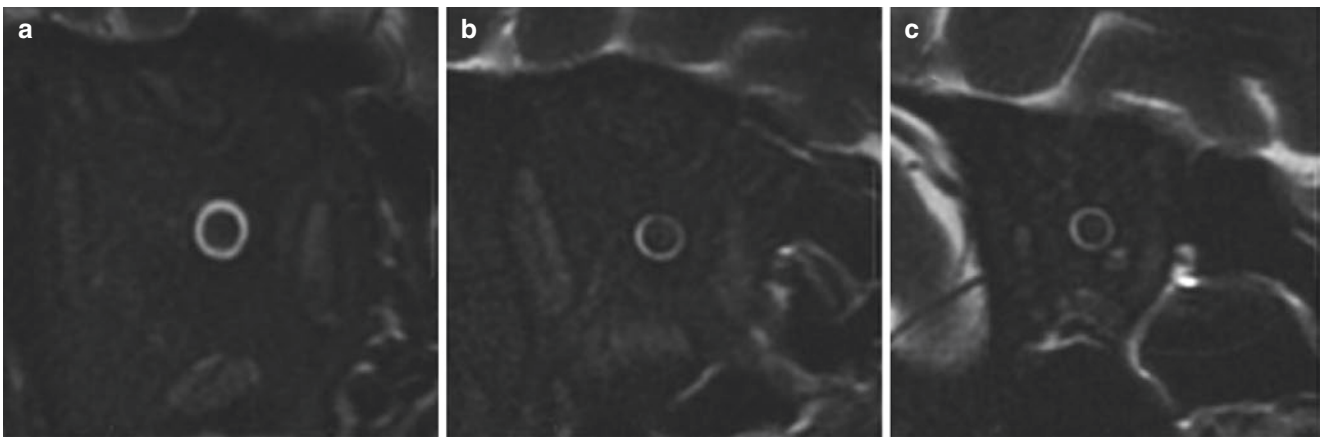

Fig. 15.2 (**a**–**c**) showed the cross sections of ONSAS at 3, 9, and 15 mm after the eyeball. The white ring was ONSAS. The spatial resolution was 0.16 × 0.16 mm (Reprinted with permission from [2])

15.3 SSFSE T2WI

SSFSE T2WI can solve some problems of FRFSE T2WI and 3D cube. It is not only faster but more clear with less artifact. Before SSFSE T2WI, we scanned axial plane and oblique sagittal plane of orbit for localization (Fig. 15.6). On the basis of these images, we positioned SSFSE T2WI. It had only two slices, with one slice set at the posterior pole of eyeball and the other set at 3 mm, 9 mm, and 15 mm, respectively (Fig. 15.7). It took only 2 s for each slice. The parameters were as follows: TR = 4000 ms, TE = 250 ms, slice thickness = 3 mm, and spatial resolution = 0.35 × 0.4 mm.

In conclusion, TCPD is important for normal-tension glaucoma. The ONSASW could be a surrogate for lumbar puncture, and the measurement of ONSASW based on MRI could provide clinical evidence for POAG diagnosis. The resolution of FRFSE T2WI and SSFSE T2WI is better than 3D cube, and SSFSE T2WI takes less time than FRFSE T2WI. Therefore, it is obvious that SSFSE T2WI is the best sequence to measure ONSAS. Nowadays, many researchers have posited that POAG is a neurodegenerative disease. Is increased ONSASW an effective parameter for neurodegenerative diseases or brain alteration? Larger sample study is still needed to verify the value of MRI.

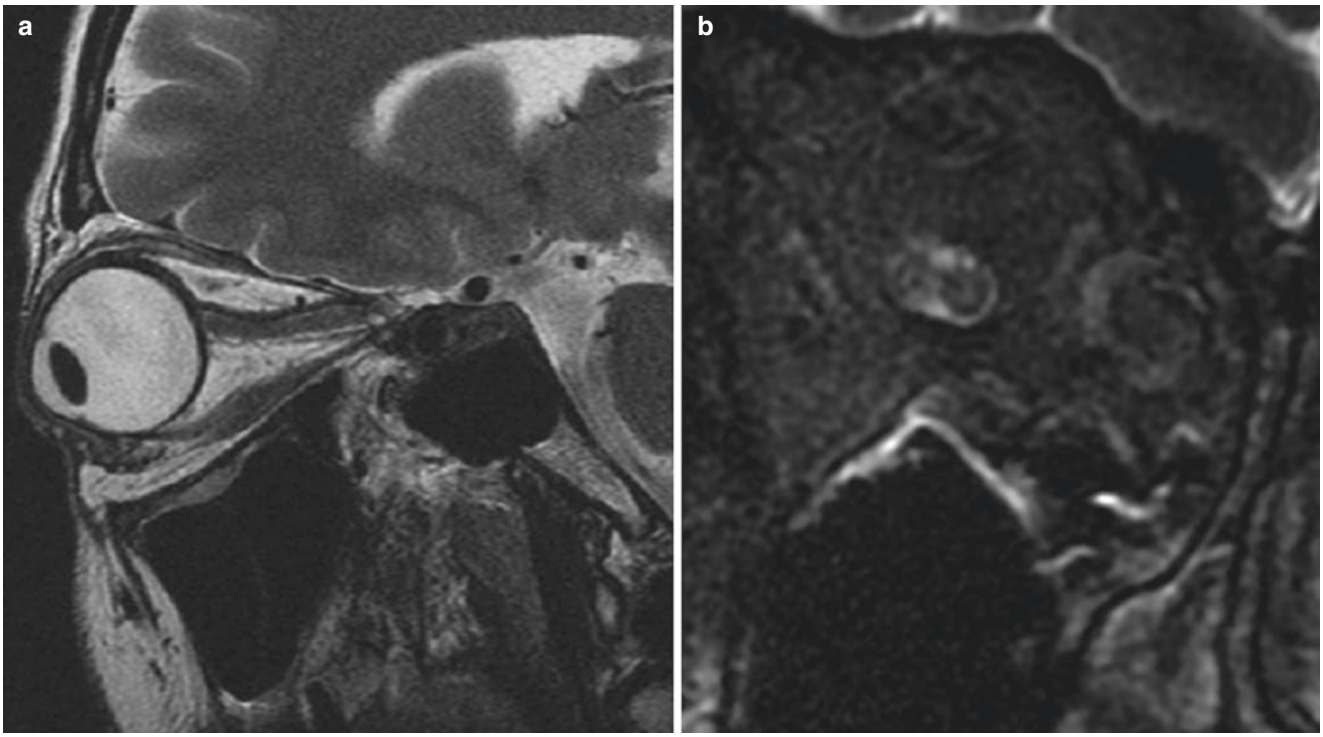

Fig. 15.3 (**a**) was a patient with tortuous optic nerve. It was difficult to localize the vertical sections of optic nerve. (**b**) showed the motion artifact

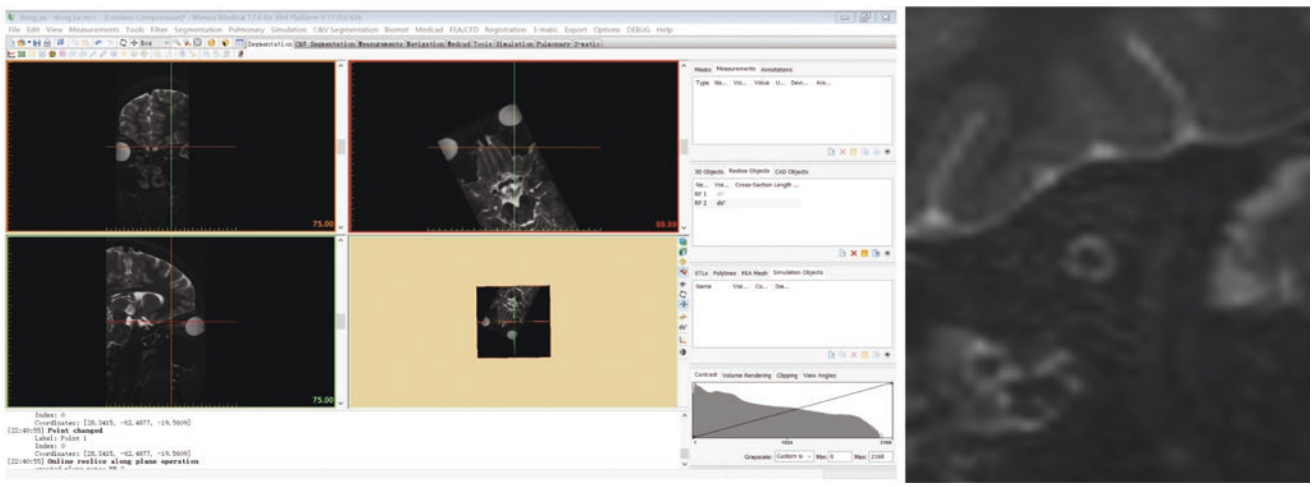

Fig. 15.4 3D cube images and reconstruction of optic nerve

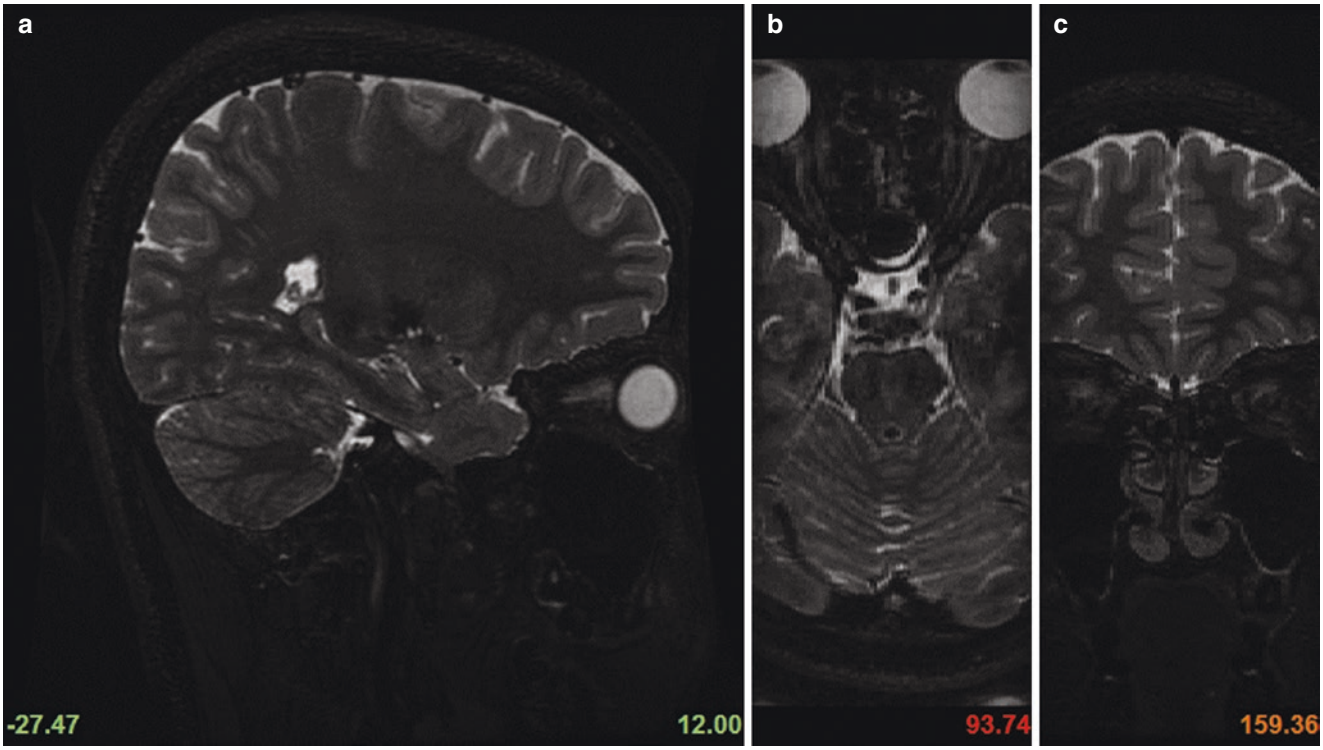

Fig. 15.5 (**a**–**c**) showed the reconstruction images of optic nerves

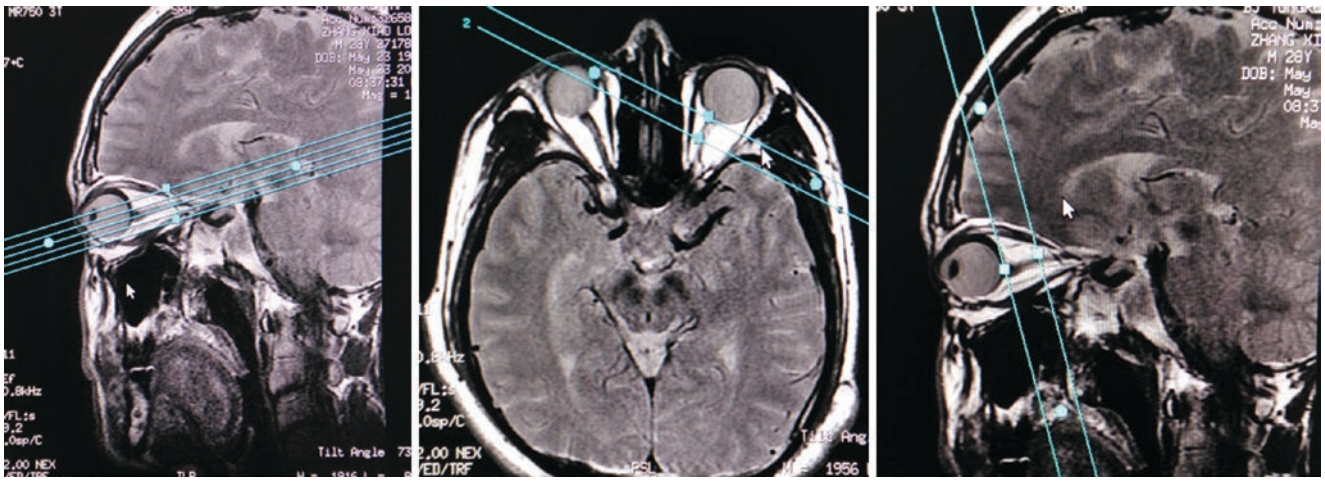

Fig. 15.6 Location images of SSFSE T2WI

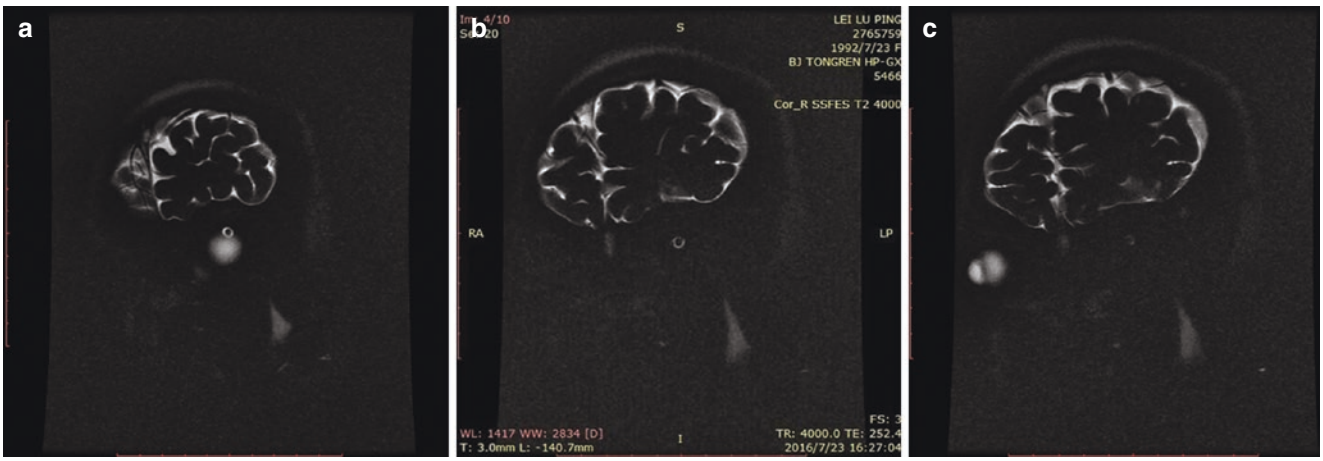

Fig. 15.7 (**a**–**c**) shows the cross sections of ONSAS at 3, 9, and 15 mm after the eyeball

References

1. Ren R, Wang N, Zhang X, Cui T, Jonas JB. Trans-lamina cribrosa pressure difference correlated with neuroretinal rim area in glaucoma. Graefes Arch Clin Exp Ophthalmol. 2011;249:1057–63.
2. Wang N, Xie X, Yang D, Xian J, Li Y, Ren R, Peng X, Jonas JB, Weinreb RN. Orbital cerebrospinal fluid space in glaucoma: the Beijing intracranial and intraocular pressure (iCOP) study. Ophthalmology. 2012;119:2065–2073 e2061.
3. Xie X, Zhang X, Fu J, Wang H, Jonas JB, Peng X, Tian G, Xian J, Ritch R, Li L, Kang Z, Zhang S, Yang D, Wang N, Beijing i COPSG. Noninvasive intracranial pressure estimation by orbital subarachnoid space measurement: the Beijing Intracranial and Intraocular Pressure (iCOP) study. Crit Care. 2013;17:R162.

16 B-Ultrasound Imaging of Optic Nerve Subarachnoid Space: A More Portable Way?

Hanruo Liu, Diya Yang, Teng Ma, Wenyuan Shi, Zhu Qiang, and Ningli Wang

Glaucoma is an important irreversible blinding eye disease [1]. For primary open-angle glaucoma (POAG), intraocular pressure (IOP) is a known pathogenic factor. Other factors are also associated with morbidity, including low body mass index (BMI), ocular perfusion pressure, migraine, cardiovascular disease, and vasospastic disorders [2–6]. Intracranial pressure (ICP) has been receiving attention in recent years [7], especially in normal pressure glaucoma. At present, it is believed that the trans-lamina cribrosa pressure difference (TLCPD) of normal-tension glaucoma (NTG) is affected by the low cerebrospinal fluid pressure (CSFP) in the subarachnoid space.

In order to study the role of ICP in normal pressure glaucoma, it needs to be measured, but currently there is a lack of available noninvasive measurement method of CSFP, especially in the optic nerve subarachnoid space (ONSAS). Lumbar puncture is a common method of CSFP measurement, but it is an invasive examination, and it is not measuring the CSFP in the optic nerve subarachnoid space [8]. There is a need for new CSFP noninvasive measurement techniques for glaucoma studies. Studies have found that increased orbital CSFP leads to an increase in the ONSAS [9, 10]. The literature of neurosurgical also reported that increased ICP leads to widening of the ONSAS and that intracranial hypotension is associated with decreased ONSAS [10]. Moreover, Wang and colleagues proposed measuring the mean width of ONSAS at 3, 9, and 15 mm behind the globe on magnetic resonance images and found the mean width of ONSAS (ONSASW) in the NTG group was smaller than in control groups or primary open-angle glaucoma patient groups [11].

We believed that measuring the area of the ONSASA is a more powerful surrogate measure than measuring the width in three different locations. If the cerebrospinal fluid pressure is lower in NTG and the optic nerve subarachnoid space is an alternative for the CSFP, then the optic nerve subarachnoid space should be smaller in normal-tension glaucoma as compared to POAG and controls. In order to test this hypothesis, we compared the measurements of the ONSASA in normal-tension glaucoma group with primary open-angle glaucoma group and the control group and studied its associations.

The study protocol was approved by the Medical Ethics Committee of the Beijing Tongren Hospital. The study was a randomized, double-masked, controlled clinical trial, conducted according to the Declaration of Helsinki. All subjects signed a written informed consent. The study was registered at http://www.chictr.org.cn (Study No. ChiCTR-INR-16010398).

The study participants were divided into three groups: 40 patients with NTG, 42 patients with POAG, and 45 healthy control subjects. All glaucoma patients were selected from the glaucoma clinic at Beijing Tongren Eye Center. The control group included healthy subjects recruited from local communities through advertisements. The ages of the control group and the study group were required to match.

The diagnosis of open-angle glaucoma patients was based on the presence of glaucomatous abnormalities of the optic nerve head, visual field defects in glaucoma, and an open angle on gonioscopy. Complete ophthalmic examinations were performed in both groups of glaucoma patients, including refraction, best-corrected visual acuity, slit-lamp biomicroscopy, applanation tonometry, gonioscopy using anterior segment optical coherence tomography (Casia ss-1000; Tomey Corporation, Nagoya, Japan), dilated optic disc and fundus examination, measurement of central corneal thickness, automated perimetry (central 30-2 full-threshold program; Humphrey Field Analyzer; Zeiss Meditec AG, Jena, Germany), photography of the optic nerve head and fundus (fundus camera EOS D60; Canon Co, Utsunomiyashi, Tochigiken, Japan), and spectral-domain optical coherence tomography (Spectralis; Heidelberg Engineering GmbH,

H. Liu · D. Yang · T. Ma · W. Shi · Z. Qiang · N. Wang (✉)
Beijing Institute of Ophthalmology, Beijing Tongren Eye Center, Beijing Tongren Hospital, Capital Medical University, Beijing, China

Beijing Ophthalmology & Visual Sciences Key Laboratory, Beijing, China
e-mail: wningli@vip.163.com

N. Wang (ed.), *Intraocular and Intracranial Pressure Gradient in Glaucoma*,
Advances in Visual Science and Eye Diseases 1, https://doi.org/10.1007/978-981-13-2137-5_16

Heidelberg, Germany). All optic disc photographs were independently examined in a masked manner by two glaucoma experts (N.W. and H.W.). If the two experts have different opinions, the patient will be excluded. NTG and POAG were distinguished by IOP. All subjects in both groups used the Goldmann applanation tonometer to measure intraocular pressure at 2 a.m., 6 a.m., 8 a.m., 10 a.m., 2 p.m., 6 p.m., and 10 p.m. Subjects with at least two IOP measurements >21 mmHg were included in the POAG group, and subjects with each untreated IOP measurement <21 mmHg were included in the NTG group. Patients with NTG must have never used antiglaucomatous medication or have stopped taking any antiglaucomatous medication at least 6 weeks prior to inclusion in the study. In POAG subjects, the IOP was controlled within the normal range at the time of ultrasound examination.

The control group received the same examination as the glaucoma patients. Two glaucoma experts examined the optic disc and fundus to confirm that there was no evidence of glaucoma or other ocular diseases. Patients with a family history of glaucoma, patients with an IOP > 21 mmHg, and other subjects who met the exclusion criteria were excluded.

Exclusion criteria for all participants included those with refractive error of >8 diopters, participants with any history or discovery of eye disease other than glaucoma that may affect IOP or vision, participants with any neurological disease that may affect intracranial pressure, those with a history of brain surgery or traumatic brain injury, patients with drugs such as carbonic anhydrase inhibitors, and those who had undergone a lumbar puncture previously at any time.

The collection of experimental data includes ultrasound data and other parameters. Ultrasound data collection used a 12.5-MHz linear array probe (L15-7io; Philips, Bothell, Washington, USA). An experienced investigator (T.M.) used the ultrasound probe to acquire ultrasound images of all participants' eyes. Ultrasound provides a transverse view of the globe and the structures in the retrobulbar area (Fig. 16.1). After the image was stored, it was analyzed off-line by two experienced observers (Y.C. and J.D.) in a masked manner. The patient was required to lie supine during data collection. A clear barrier covered the lid of the eye being examined while the fellow eye focused on a fixation target. The eyelid is covered with coupling gel, and the ultrasound probe was placed over the upper eyelid in an axial plane.

The acquired ultrasound photographs can be used to measure the axial length and establish ONSASA. The axial length can be measured by measuring the optic nerve diameter (OND) and optic nerve sheath diameter (ONSD) at 1, 3, 5, and 7 mm from the optic nerve head. ONASW (width of both sides of the ONSAS) at these positions can be obtained by calculating ONSD and OND. The establishment of ONSASA requires the ImageJ 1.51e analysis software

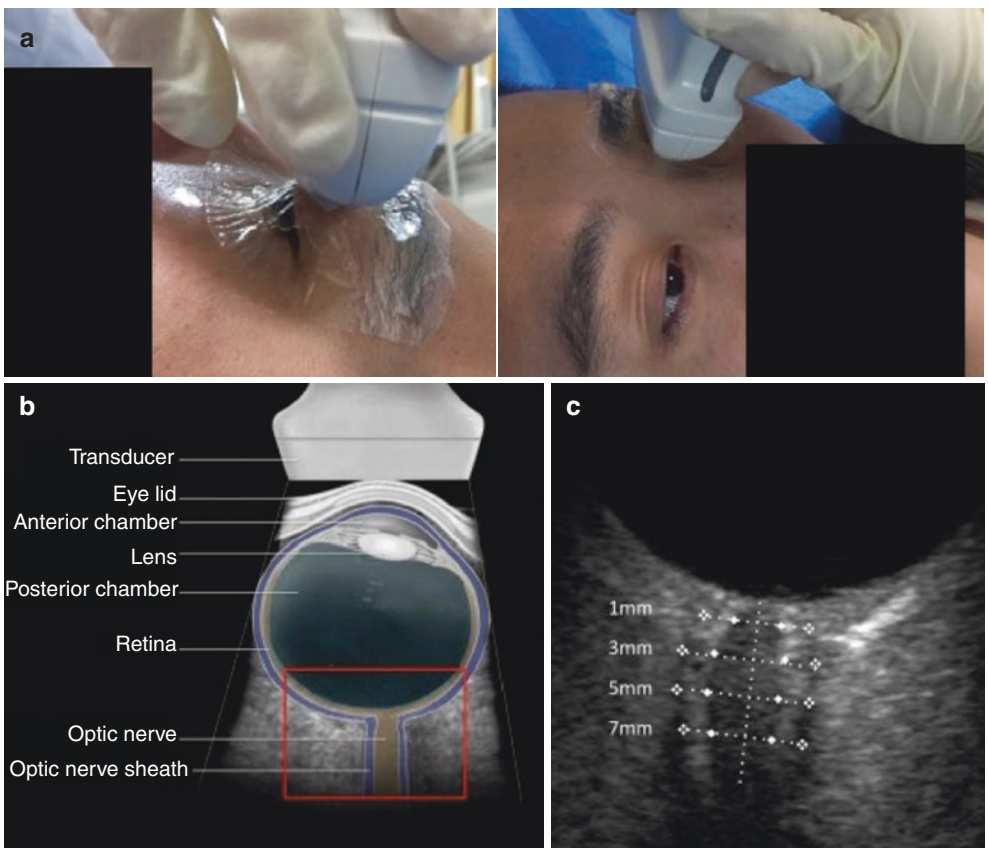

Fig. 16.1 Ultrasound measurements. A clear barrier was placed over the patient's eyelid, followed by application of ultrasound gel (**a**). The fellow eye focused on a distant point (**b**). The optic nerve complex is seen as a sharply defined hypoechoic stripe in the echogenic retrobulbar fat (**c**). The optic nerve sheath was measured at a depth of 1, 3, 5, and 7 mm behind the orbit in the zoom mode (Reprinted with permission from Liu H, Yang D, Ma T, Shi W, Zhu Q, Kang J, et al. Measurement and Associations of the Optic Nerve Subarachnoid Space in Normal Tension and Primary Open-Angle Glaucoma. Am J Ophthalmol. 2018;186:128–37)

(available in the public domain at http://rsbweb.nih.gov/ij/) [12]. We can use this software to sketch and measure the entire ONSAS between 3 and 7 mm. If needed, an average width can be calculated as the determined ONSASA/axial length of the captured region, which in this case is 4 mm. In all cases, images were captured when the ONSAS width was maximal. For each ultrasound photograph, we can calibrate the measurement using the scale at the base of the photograph that comes with the ultrasound system. The study calculated interobserver and intra-observer reliability. In order to assess intra-observer reliability, all images were remeasured after 1 month.

Other parameters collected included gender, age, height, weight, BMI, waist circumference, head circumference, and mean arterial pressure (MABP). Mean arterial blood pressure (MABP) was calculated as 1/3 × systolic pressure + 2/3 × diastolic pressure. Systolic blood pressure (SBP) and diastolic blood pressure (DBP) measurements were taken using a standardized mercury sphygmomanometer after the subject assumed a sitting position for 5 min.

Statistical testing in this study was all performed using SPSS (SPSS for Mac, v. 24.0; IBM-SPSS, Chicago, Illinois, USA). Data are presented as mean values ± standard deviation. Homogeneity of the variance was checked with the Levene test, and normal distribution of data was checked with the Shapiro-Wilk W test. Weight and BMI did not show homogeneity of variance, whereas the diastolic and systolic blood pressure, sex, and refractive error were not normally distributed. These parameters between the three groups which the variables are not conforming to the normal distribution are compared using the Kruskal-Wallis test with post hoc Dunn multiple comparisons. One-way analysis of variance with post hoc least significant difference analysis was performed to assess significant differences between diagnostic groups with the variables conforming to the normal distribution. ONSD, OND, and ONSASW were analyzed using two-way repeated measure ANOVA with three groups as the between-subject factor and the different location as within-subject factor.

Comparing the mean deviation between the NTG and POAG groups can be applied to t-tests for analysis of unpaired samples. Correlation between variables was studied using Spearman correlation. Significance tests were two-sided, and $P < 0.05$ was considered statistically significant.

A linear regression analysis was performed to assess the association between ONSASA and mean IOP in NTG group. The inter- and intra-observer reliability was assessed by the internal correlation coefficient (ICC).

The results of the study showed that demographic parameters were not statistically different among the three groups of the study population. The average and highest IOP were significantly lower in normal-tension glaucoma group and control group than in primary open-angle glaucoma group.

From the results obtained by the ultrasound examination, both OND and ONSD were similar in the three groups at 1 mm behind the globe. At 3, 5, and 7 mm behind the globe, the OND was similar in the two glaucoma groups but significantly smaller than in the control group. The ONSD of NTG group was significantly smaller than that of POAG group. The ONSD of both glaucoma groups was smaller than that of control group. At 1 mm behind the globe, the ONSASW was also similar in the three groups. At 3, 5, and 7 mm behind the globe, the ONSASW of NTG group was significantly smaller than that of POAG group and control group, and there was no difference between POAG group and control group (Fig. 16.2).

The ONSASA between 3 and 7 mm in normal-tension glaucoma group was less than in primary open-angle

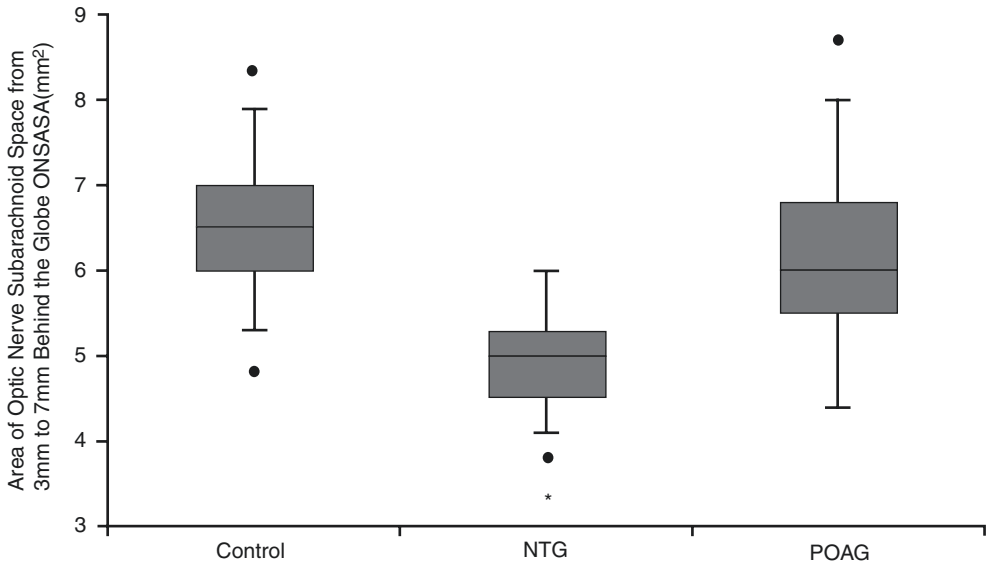

Fig. 16.2 Box plots showing the differences in ONSASA measured from 3 to 7 mm behind the globe (Reprinted with permission from Liu H, Yang D, Ma T, Shi W, Zhu Q, Kang J, et al. Measurement and Associations of the Optic Nerve Subarachnoid Space in Normal Tension and Primary Open-Angle Glaucoma. Am J Ophthalmol. 2018;186:128–37)

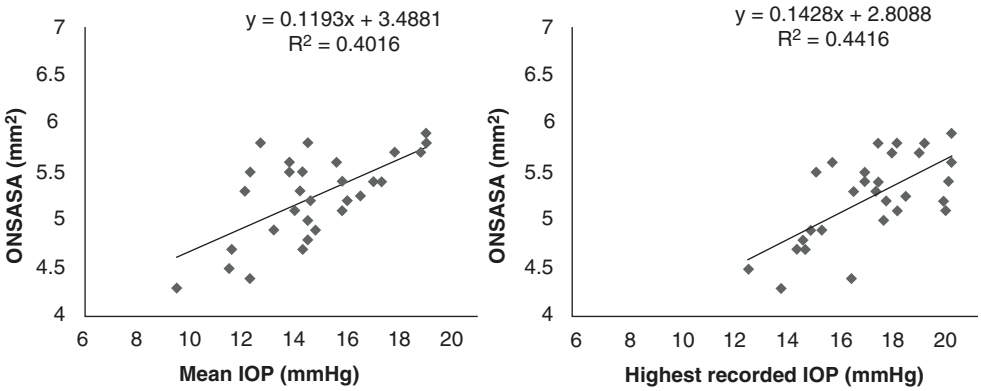

Fig. 16.3 Scatterplot showing the relationship between the mean IOP and ONSASA in NTG group (Reprinted with permission from Liu H, Yang D, Ma T, Shi W, Zhu Q, Kang J, et al. Measurement and Associations of the Optic Nerve Subarachnoid Space in Normal Tension and Primary Open-Angle Glaucoma. Am J Ophthalmol. 2018;186:128–37.)

glaucoma group. The ONSASA was similar in primary open-angle glaucoma group and control group. In normal-tension glaucoma group, there was a positive correlation between the mean IOP and normal-tension glaucoma. Other parameters were not associated with ONSASA in any of the groups (Fig. 16.3).

Assessing whether the optic nerve subarachnoid space measurement in glaucoma subjects is an appropriate indirect tool for predicting ICP and determining how this correlates with clinical observations in these subjects are the main purpose of this study. We found that indirect measurement of CSFP using the ONSD ultrasound-based assessment at 3 mm behind the globe is an effective way to predict ICP [13, 14]. The subarachnoid space of NTG subjects was significantly smaller than that of POAG subjects. The main limiting factor of this technique is the change of the optic nerve diameter in some cases. For example, patients with optic atrophy present a reduced optic nerve diameter, but their sheath diameter is similar to healthy individuals [15]. This may affect ONSD.

The progress of ultrasound technology has helped this study. We used a 12.5-MHz probe to generate high-resolution images of the optic nerve subarachnoid space and use it to measure the optic nerve sheath diameter and optic nerve diameter in more detail. This improves the reliability of image capture and measurements with the subarachnoid space and consequently increased power to predict ICP. It will overcome differences that may occur owing to individual anatomy and pathologic influence. However, there are still some factors that we need to consider, for example, changes of ICP can cause changes in shear stress on the optic nerve sheath wall, altered distribution of cerebrospinal fluid, the nonlinear properties of optic nerve sheath stiffness, abnormal responses to external stimuli, and/or even a different retrobulbar remodeling in NTG patients [16]. Therefore, we need to reduce the impact of deformation on the prediction of ICP, obtain measurements at multiple points rather than a single site, create more robust anatomical images, and reduce abnormalities. In this study, we used ONSAS as a substitute for the optic nerve subarachnoid space volume. This design helps offset the errors caused by the deformation and provides a more reflective assessment of ONSAS changes under different clinical scenarios. The estimated ONSAS volume can be derived from ONSASA data, but the two would always correlate and would not account for asymmetric deformations. Capturing images in multiple planes and performing 3D modeling can further enhance prediction capabilities. However, at present, the method of this study is an improvement over existing methods. ONSASA is an effective substitute to the volume change of ONSAS.

ONSASA is a cross-sectional two-dimensional area of a single ultrasound image calculated between 3 and 7 mm behind the globe. The selection of this range has a reliable theoretical basis. Because the thickness of the dura of ONS is 0.35–0.5 mm, with its thickest section close to the sclera, there was no difference between any groups at the 1 mm measurement point [17]. And the optic nerve sheath edge was difficult to identify at the 9 mm measurement point (data not shown). Between 3 and 7 mm positions posterior to the globe, the optic nerve sheath structure may expand more easily. At this point, expansion owing to ICP would cause an increase in sheath thickness in that retrobulbar segment of the optic nerve. Measuring the optic nerve sheath between 3 and 7 mm posterior to the globe is the best choice for predicting ICP. This view was supported by some studies using the cadaveric optic nerves as an experimental model [18]. The findings from these studies suggested that after gelatin-induced subarachnoid expansion, the mean diameter increased by 60% at 3 mm posterior to the globe but only by 35% at 10 mm posterior to the globe. In addition, previous studies using ultrasound to measure ONSDs have commonly used a site 3 mm behind the globe as a reference point to make correlations with ICP [19, 20].

In our study, the ONSASW in the NTG group was narrow, indicating that normal-tension glaucoma is associated with abnormally low CSFP, consistent with previous experimental and clinical studies (Fig. 16.4) [21–24]. Previous ONSD-related studies have also supported this result [11]. There have been also studies showing a good correlation between ultrasound and magnetic resonance imaging of the ONS [25]. However, there have been still different results reported

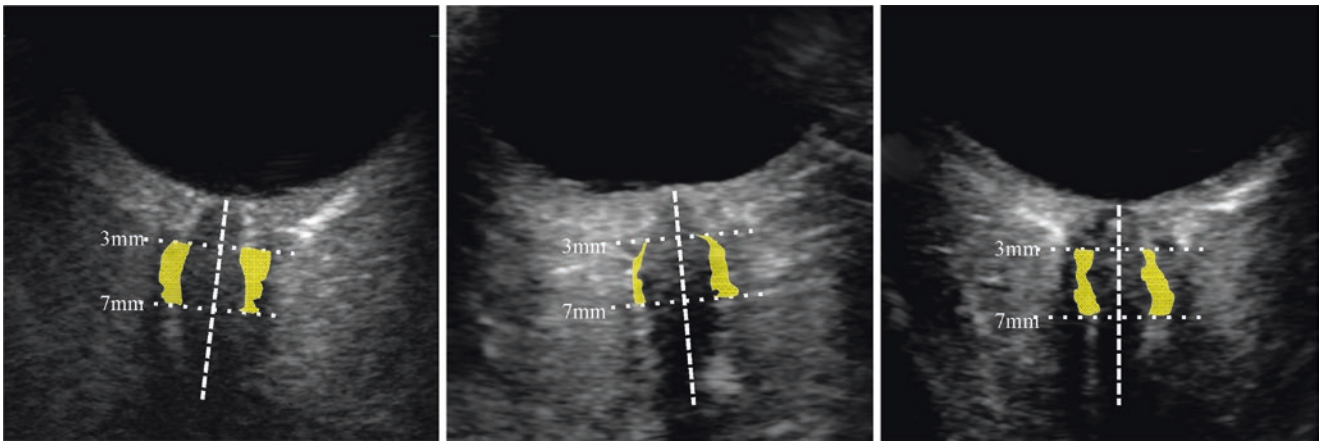

Fig. 16.4 The representative example of area of optic nerve subarachnoid space (ONSASA) sonography of healthy, NTG, and POAG (Reprinted with permission from Liu H, Yang D, Ma T, Shi W, Zhu Q, Kang J, et al. Measurement and Associations of the Optic Nerve Subarachnoid Space in Normal Tension and Primary Open-Angle Glaucoma. Am J Ophthalmol. 2018;186:128–37)

with ONSD-related studies using computed tomography [26] and ultrasound [27]. Jaggi and colleagues [26] found that the ONSD in NTG patients was higher than in the control group, whereas Abegago Pinto and colleagues [27] found no difference in ONSD between these groups. The reason why the results of these studies differ from ours may be due to a variety of factors.

The study of Jaggi and colleagues. First, their sample size is smaller than our study [26]. More subjects can reduce individual differences and improve statistical power. Second, the current study established measurements at defined distances behind the globe, while Jaggi and colleagues [26] measured the maximum diameter of the optic nerve sheath. In addition, Jaggi and colleagues [26] capture image in a prone position. In our study, patients were in a supine position. It has been confirmed that the prone position affects the distribution of CSF in the central nervous system and allows the effects of gravity to be considered.

The study of Abegao Pinto and colleagues [27]. First, they used a 7.5 MHz B-scan ultrasound probe (Antares ecograph device; Siemens, Munich, Germany). The resolution of this probe was lower than the 12.5 MHz probe used in our study; it may also cause artifacts that affect the accuracy of the optic nerve sheath diameter measurement. The transbulbar sound direction and the incidence of the ultrasound beam on the lamina cribrosa [28] or the dura mater may produce acoustic shadows behind the globe. These artifacts are more likely to occur for probes with frequency <7.5 MHz. The 12.5 MHz probe in our study can reduce these artifacts. Second, the refractive state of the patient may introduce bias because their properties of the sclera are different from hyperopic to myopic patients.

It is also important to point out that the difference in optic nerve diameter between the study groups may affect the calculation of the optic nerve subarachnoid space, especially because of glaucomatous loss of optic nerve fibers or optic nerve atrophy caused by glaucoma. The data shows that in the current study, the optic nerve diameters in the NTG group and the POAG group were significantly smaller than the control group at 3, 5, and 7 mm posterior to the globe. Correspondingly, the optic nerve sheath diameters at 3, 5, and 7 mm posterior to the globe in the two glaucoma groups were significantly smaller than those of the healthy group. These phenomena need to be explained by the optic nerve subarachnoid space anatomy and sheath ultrastructure. The optic nerve sheath has a unique tissue structure consisting of flexible dural tissue and radially oriented trabecular fibers that pass through the subarachnoid space and connect the pia mater of the nerve with the innermost arachnoid layer of the sheath [29, 30]. The trabecular fibers and the sheath collagen structure are the main structures that maintain the stability of the spatial structure. Moreover, there was no significant difference in optic nerve diameter between the two groups of glaucoma patients. The amount of glaucomatous mean defect and RNFL thickness also showed no significant difference between the two glaucoma groups. Therefore, we can exclude glaucoma-related differences in optic nerve diameter as a component for the calculation of the subarachnoid space. In addition, a multivariate analysis adjusting the ONSASA for optic nerve diameter and visual field defect showed that ONSAS reduction was associated with the NTG group and was not related to the severity of visual field defects.

There is also a very interesting finding that the ONSASA measurement is positively correlated with the mean IOP of subjects with NTG; but this is not present in the healthy control group. Similar results have also appeared in the study of Abegao Pinto and associates [27]. This may be because the intraocular pressure measured by Goldmann applanation tonometer does not affect the forces acting in the retrolamina cribrosa space, but the forces may affect IOP, which we believe is related to aqueous humor drainage. ICP may

affect ocular venous drainage of the eye to influence aqueous humor drainage [31]. As the volume of cerebrospinal fluid changes, intracranial blood volume also changes, so a change in the volume of cerebrospinal fluid may affect the intracranial venous sinus flow and influence the drainage of the superior ophthalmic veins. The superior ophthalmic veins are responsible for the anterior ciliary vein drainage, thus affecting the aqueous humor drainage [32]. Because of this, ICP changes will affect the intraocular pressure. Therefore, any unknown structural defect or changes in the NTG patient's drainage pathway just mentioned would weaken the buffer capacity, resulting in changes in aqueous humor drainage. There is evidence that for NTG patients, their peripheral blood vessels differ in diameter and stiffness, and the prevalence of spontaneous venous phenomena is reduced. In future studies, the potential mechanism and the degree of the impact of this vascular venous dysregulation on IOP will become a hot issue. One hypothesis is that if there is a greater upstream obstruction in the trabecular meshwork or other drainage pathway components of a POAG patient, it may interfere with the superior ophthalmic vein drainage, explaining why this ONSD would not have correlated with IOP.

Our study still has some limitations. First, although the differences between the study groups are statistically significant, the number of patients was still relatively small. More research is needed, and a more extensive and comprehensive study of each group will be conducted, to further evaluate the correlation between NTG and ONSAS. Second, the control subjects did not perform a comprehensive neurological examination, and patients with undiagnosed neurological disease in the control group could not be ruled out.

In a word, in patients with normal open-angle glaucoma, the optic nerve subarachnoid space is narrower than that in high-pressure patients, indicating that normal-tension glaucoma patients have lower orbital CSFP. Ultrasound-based noninvasive ONSD assessment may provide further insights into the forces acting behind the lamina cribrosa. The interesting relationship between ICP and optic nerve still needs more research, whose significance may be of particular importance in NTG patients and have clinical and pathologic importance, implying that the trans-lamina cribrosa pressure difference might be abnormally higher in the NTG group than in controls.

References

1. Quigley HA, Broman AT. The number of people with glaucoma worldwide in 2010 and 2020. Br J Ophthalmol. 2006;90(3):262–7.
2. Bonomi L, Babighian S, Bonadimani M, et al. Correlation between glaucoma and vascular factors, and circumstances leading to the diagnosis of glaucoma. Acta Ophthalmol Scand Suppl. 2000;232:34–5.
3. Leske MC, Wu SY, Hennis A, Honkanen R, Nemesure B, Group BES. Risk factors for incident open-angle glaucoma: the Barbados Eye Studies. Ophthalmology. 2008;115(1):85–93.
4. Cherecheanu AP, Garhofer G, Schmidl D, Werkmeister R, Schmetterer L. Ocular perfusion pressure and ocular blood flow in glaucoma. Curr Opin Pharmacol. 2013;13(1):36–42.
5. Ren R, Wang N, Zhang X, Tian G, Jonas JB. Cerebrospinal fluid pressure correlated with body mass index. Graefes Arch Clin Exp Ophthalmol. 2012;250(3):445–6.
6. Abegao Pinto L, Willekens K, Van Keer K, et al. Ocular blood flow in glaucoma—the Leuven Eye Study. Acta Ophthalmol. 2016;94(6):592–8.
7. Jonas JB. Role of cerebrospinal fluid pressure in the pathogenesis of glaucoma. Acta Ophthalmol. 2011;89(6):505–14.
8. Hou R, Zhang Z, Yang D, et al. Intracranial pressure (ICP) and optic nerve subarachnoid space pressure (ONSP) correlation in the optic nerve chamber: the Beijing Intracranial and Intraocular Pressure (iCOP) study. Brain Res. 1635;2016:201–8.
9. Watanabe A, Kinouchi H, Horikoshi T, Uchida M, Ishigame K. Effect of intracranial pressure on the diameter of the optic nerve sheath. J Neurosurg. 2008;109(2):255–8.
10. Geeraerts T, Newcombe VF, Coles JP, et al. Use of T2-weighted magnetic resonance imaging of the optic nerve sheath to detect raised intracranial pressure. Crit Care. 2008;12(5):R114.
11. Wang N, Xie X, Yang D, et al. Orbital cerebrospinal fluid space in glaucoma: the Beijing intracranial and intraocular pressure (iCOP) study. Ophthalmology. 2012;119(10):2065–73. e2061
12. Schneider CA, Rasband WS, Eliceiri KW. NIH Image to ImageJ: 25 years of image analysis. Nat Methods. 2012;9(7):671–5.
13. Soldatos T, Chatzimichail K, Papathanasiou M, Gouliamos A. Optic nerve sonography: a new window for the non-invasive evaluation of intracranial pressure in brain injury. Emerg Med J. 2009;26(9):630–4.
14. Moretti R, Pizzi B, Cassini F, Vivaldi N. Reliability of optic nerve ultrasound for the evaluation of patients with spontaneous intracranial hemorrhage. Neurocrit Care. 2009;11(3):406–10.
15. Jonas JB, Wang N, Yang D, Ritch R, Panda-Jonas S. Facts and myths of cerebrospinal fluid pressure for the physiology of the eye. Prog Retin Eye Res. 2015;46:67–83.
16. Killer HE, Miller NR, Flammer J, et al. Cerebrospinal fluid exchange in the optic nerve in normal-tension glaucoma. Br J Ophthalmol. 2012;96(4):544–8.
17. Francois P, Lescanne E, Velut S. The dural sheath of the optic nerve: descriptive anatomy and surgical applications. Adv Tech Stand Neurosurg. 2011;36:187–98.
18. Helmke K, Hansen HC. Fundamentals of transorbital sonographic evaluation of optic nerve sheath expansion under intracranial hypertension I. Experimental study. Pediatr Radiol. 1996;26(10):701–5.
19. Tayal VS, Neulander M, Norton HJ, Foster T, Saunders T, Blaivas M. Emergency department sonographic measurement of optic nerve sheath diameter to detect findings of increased intracranial pressure in adult head injury patients. Ann Emerg Med. 2007;49(4):508–14.
20. Beare NA, Kampondeni S, Glover SJ, et al. Detection of raised intracranial pressure by ultrasound measurement of optic nerve sheath diameter in African children. Trop Med Int Health. 2008;13(11):1400–4.
21. Berdahl JP, Allingham RR, Johnson DH. Cerebrospinal fluid pressure is decreased in primary open-angle glaucoma. Ophthalmology. 2008;115(5):763–8.
22. Yablonski E, Rafalski K. Effect of time of administration of food supplement amino acids on protein utilization and the body composition of rats. Vopr Pitan. 1979;5:17–21.
23. Berdahl JP, Fautsch MP, Stinnett SS, Allingham RR. Intracranial pressure in primary open angle glaucoma, normal tension glaucoma, and ocular hypertension: a case-control study. Invest Ophthalmol Vis Sci. 2008;49(12):5412–8.
24. Ren R, Jonas JB, Tian G, et al. Cerebrospinal fluid pressure in glaucoma: a prospective study. Ophthalmology. 2010;117(2):259–66.

25. Bauerle J, Schuchardt F, Schroeder L, Egger K, Weigel M, Harloff A. Reproducibility and accuracy of optic nerve sheath diameter assessment using ultrasound compared to magnetic resonance imaging. BMC Neurol. 2013;13:187.
26. Jaggi GP, Miller NR, Flammer J, Weinreb RN, Remonda L, Killer HE. Optic nerve sheath diameter in normal-tension glaucoma patients. Br J Ophthalmol. 2012;96(1):53–6.
27. Abegao Pinto L, Vandewalle E, Pronk A, Stalmans I. Intraocular pressure correlates with optic nerve sheath diameter in patients with normal tension glaucoma. Graefes Arch Clin Exp Ophthalmol. 2012;250(7):1075–80.
28. Copetti R, Cattarossi L. Optic nerve ultrasound: artifacts and real images. Intensive Care Med. 2009;35(8):1488–9. author reply 1490-1481
29. Raspanti M, Marchini M, Della Pasqua V, Strocchi R, Ruggeri A. Ultrastructure of the extracellular matrix of bovine dura mater, optic nerve sheath and sclera. J Anat. 1992;181(Pt 2):181–7.
30. Liu D, Kahn M. Measurement and relationship of subarachnoid pressure of the optic nerve to intracranial pressures in fresh cadavers. Am J Ophthalmol. 1993;116(5):548–56.
31. Spentzas T, Henricksen J, Patters AB, Chaum E. Correlation of intraocular pressure with intracranial pressure in children with severe head injuries. Pediatr Crit Care Med. 2010;11(5):593–8.
32. Lirng JF, Fuh JL, Wu ZA, Lu SR, Wang SJ. Diameter of the superior ophthalmic vein in relation to intracranial pressure. AJNR Am J Neuroradiol. 2003;24(4):700–3.

Translamina Cribrosa Pressure Difference-Related Animal Models

17

Jing Li and Ningli Wang

17.1 Introduction

Glaucoma is a progressive optic neuropathy that leads to structural changes in retinal nerve fiber layer (RNFL) and optic nerve head (ONH), as well as characterized changes in the visual field (VF) which may result in irreversible visual impairment and blindness [1]. Intraocular pressure (IOP) is always thought to be a major factor in the pathogenesis of glaucoma. Animal model, as a vital method, plays an irreplaceable part in studying the mechanisms of disease progression and developing therapeutic strategies to control the progression of various kinds of diseases including glaucoma. Over the years, high IOP animal models have been established by many researchers, in order to study the etiology, pathogenesis, diagnosis, treatment, and prognosis of glaucoma. Recently, more and more researchers have found that low orbital cerebrospinal fluid pressure (CSFP) may have a role similar to an elevated IOP in the pathogenesis of glaucomatous optic neuropathy [2–5]. The concept of translamina cribrosa pressure difference, which means the difference between IOP and ICP, has recently been accepted. Thus, not only high/low IOP but also high/low CSFP animal models were more frequently studied in recent years.

Besides rodent and mammal animal models which are commonly used, the nonhuman primate (NHP) experimental glaucoma (EG) model has been well established for more than 40 years. As we all know, NHP is the optimal choice for animal model. First, NHP's anatomy of whole visual pathway is quite similar to that of human beings. Second, the NHP model provides a way of investigating the earliest visual pathway responses to the change of IOP/ICP. However, NHP has some limitations when used for animal models, including the high cost, large number of animals needed, and rare spontaneous glaucoma.

The purpose of this article is to summarize the current research progress in translamina cribrosa pressure difference-related animal models with different methods and shed a light on the future research directions.

17.2 IOP-Related Animal Models

Over the years, high IOP animal models of rodent animals and NHPs have been established by many researchers, in order to investigate the mechanisms, diagnosis, and treatment (such as laser photocoagulation, anterior chamber injection, and episcleral vein cauterization) of glaucomatous optic neuropathy.

17.2.1 Rodent Animal Models

Glaucoma is a series of chronic neurodegenerative conditions with unclear pathogenesis and insufficient therapeutic strategies. Therefore, inexpensive, effective, repeatable, available, and relatively low-cost animal models are needed urgently, including mice and rats. The methods of establishing glaucoma models are various, including spontaneous animal models, episcleral vein injection of hypertonic saline, laser photocoagulation, episcleral vein cauterization, and anterior chamber injection. Every method has its own strengths and weaknesses.

17.2.1.1 Spontaneous Animal Models

Till now, various kinds of transgenic models have been established to change the structure of anterior segment or RGC of the eye in order to investigate the characteristics of glaucomatous optic neuropathy. Myocilin (MYOC/GLC1A) and opti-

J. Li · N. Wang (✉)
Beijing Institute of Ophthalmology, Beijing Tongren Eye Center, Beijing Tongren Hospital, Capital Medical University, Beijing, China

Beijing Ophthalmology & Visual Sciences Key Laboratory, Beijing, China
e-mail: wningli@vip.163.com

N. Wang (ed.), *Intraocular and Intracranial Pressure Gradient in Glaucoma*,
Advances in Visual Science and Eye Diseases 1, https://doi.org/10.1007/978-981-13-2137-5_17

neurin (OPTN/GLC1E) are found to be related to the pathogenesis of primary open-angle glaucoma (POAG) [6–8].

DBA/2J mouse is another vital and popular secondary glaucoma model in establishing chronic IOP elevation model, which has two mutational genes including Tyrp1 and Gpnmb. These mice presented defects of iris with pigment blocking the outflow of aqueous and eventually resulting in high level of IOP. However, high individual variability and the difficulty of introducing genetic mutations limit their application and popularization. Wilson et al. found this kind of mouse model of glaucoma before IOP elevation or axonal degeneration showed early pro-inflammatory cytokine elevations [9].

17.2.1.2 Episcleral Vein Injection of Hypertonic Saline

Some researchers induced ocular hypertension in rodent animals by means of injecting a hypertonic saline solution into the episcleral veins, which results in the sclerosis of the trabecular meshwork. This method can induce relatively long ocular hypertension and can also lead to both progressive RGC loss and optic nerve degeneration. Jia L et al. studied the patterns of IOP elevation of this model and found that IOP was most likely increased during the dark phase than the light, which can be explained by the circadian rhythm of aqueous humor production [10]. Tezel et al. found that inflammatory responses of astrocytes in this model included upregulation of TNF-α/TNFR signaling, nuclear factor kappa-B (NF-κB) activation, autophagy regulation, and inflammasome assembly, supporting the astrocyte-related treatment strategy for glaucoma [11]. However, IOP varies significantly in different animals, and repeated injections are required if IOP stops increasing after the first injection.

17.2.1.3 Laser Photocoagulation

Laser photocoagulation of the trabecular meshwork is the most common method of inducing IOP elevation, RGC loss, and eventually glaucomatous optic neuropathy. Salinas-Navarro M et al. found that laser photocoagulation-induced ocular hypertension leads to a lack of retrograde axonal transport in most RGCs in albino Swiss mice [12]. However, all of these laser-induced models showed inflammation in the anterior chamber and large interanimal variability.

17.2.1.4 Episcleral Vein Cauterization

Another method commonly used to elevate IOP is cauterizing the episcleral vein to affect the drainage of aqueous humor. The level of IOP mainly depends on the number of episcleral veins that are cauterized. This method constitutes a reliable, economic, and reproducible animal model [13]. One study found that Akt was activated via insulin/IGF-1 receptor in the retina of Sprague-Dawley rats with episcleral vein cauterization [14].

17.2.1.5 Intraocular Injection

Intraocular injection is a common method to establish acute IOP elevation animal model, which mainly include anterior chamber injection and vitreous cavity injection. Various materials have been used, including methyl cellulose, normal saline, sodium hyaluronate, α-chymotrypsin, etc. [15–18]. Repeated injection is needed to maintain the high IOP level. Experimenter should pay attention to the control of the concentration of drugs, site, angle, and dose of injection.

Recently, Ito et al. established a novel method of using magnetic microbead to induce ocular hypertension-dependent glaucoma in mice. They injected magnetic microbeads into the anterior chamber by a modified microneedle with a facetted bevel, which led to a steady high level of intraocular pressure and then the loss of retinal ganglion cells. Therefore, they concluded this method as a powerful tool to research on the progression of glaucoma [19].

17.2.2 Nonhuman Primate (NHP) Animal Models

Compared to the rodent animals, NHPs share almost the same ocular structures as human beings, for which NHP is the most ideal animal to establish animal models. However, the price of NHP is very high, which is still a main limitation.

17.2.2.1 Laser Photocoagulation

In 1974, Gasterland and Kupfer first reported a model of chronic, laser-induced IOP elevation, which has become the most commonly used method of establishing the primate glaucoma model to mimic human glaucoma [20]. Ocular blood flow of optic nerve head is decreased to variable extents depending on the different level of IOP [21]. Repeated laser photocoagulation is often needed to obtain a sustained IOP.

Retinal nerve fiber layer (RNFL) degeneration and apoptosis of retinal ganglion cells (RGCs) in this model have been corroborated by optical coherence tomography (OCT) and histological examination. However, the features of cone function on long-duration elevated IOP in the primate model are unclear. Kegao Liu et al. recently studied full-field cone ERG responses in chronic ocular hypertension monkeys induced by laser to verify the hypothesis that long-duration elevated IOP caused cone response dysfunction and found that mean amplitude of the photopic negative response (PhNR) and mean R-cone were obviously lower in the lasered eye, and no difference of S-cone were found between the two eyes. Therefore, they made a conclusion that long-duration ocular hypertension induced by laser photocoagulation affects the function of cone photoreceptor in monkeys [22].

17.2.2.2 Anterior Chamber Injection

Till now, many kinds of agents were adopted to inject into the anterior chamber of NHPs to induce acute experimental glaucoma including alpha-chymotrypsin and red blood cells [23, 24]. However, all were abandoned because IOP elevated by these methods is all hard to control and sustains only shortly and usually influences the observation of fundus.

17.3 Intracranial Pressure (ICP)-Related Animal Models

Recent researches have showed that low orbital cerebrospinal fluid pressure (CSFP) may have an important part in the pathogenesis of glaucomatous optic neuropathy. Thus, both low and high CSFP animal models gained popularity rapidly in recent years.

17.3.1 Rodent Animal Models

Dr. Zheng Zhang and coauthors of Beijing iCOP study group recently reported the experimental rat models with an acute CSFP reduction. In details, transparent dura mater was firstly exposed, and then a taper glass capillary tube was inserted into the cisterna magna to aspirate the cerebrospinal fluid from the cistern magna (Fig. 17.1). Then, they tested the efficiency of the acute low CSFP model by using a 1.6F pressure catheter (Scisense Inc., London, Canada) which was inserted into the brain parenchyma and measured the CSFP using BIOPAC Systems MP150 workstation (BIOPAC Systems, Gleeta, CA, USA) [5].

Interestingly and illuminatingly, Zheng Zhang et al. found that experimental models with an acute IOP elevation or CSFP reduction showed similar morphologic changes in the axons of RGCs and similar immunohistochemical features in the axonal motor proteins including both kinesin HC and dynein IC, indicating they share similarities in the disturbance of both the orthograde and retrograde axonal transport and supporting the hypothesis of the relationship between low CSFP and glaucomatous optic neuropathy [5].

17.3.2 Nonhuman Primate (NHP) Animal Models

Dr. Yang and coauthors of Beijing iCOP study group recently reported that they established a chronic CSF reduction monkey model by the method of lumbar-peritoneal shunt. The CSFP was measured by the cerebral microsensor to make sure that the CSFP was lowered to the target pressure. The ICP of four monkeys was successfully lowered from the normal level of 8–9 mmHg to the level of 3 mmHg for more than 5 years (Fig. 17.2) [4].

The result was that two of the four NHPs showed diffuse RNFL and optic nerve rim thinning. A third NHP developed a single nerve fiber hemorrhage, without other changes. The model was very vital and creative because the hypothesis that primary CSF reduction was an important risk factor for RGC axon loss and glaucoma-like optic neuropathy was

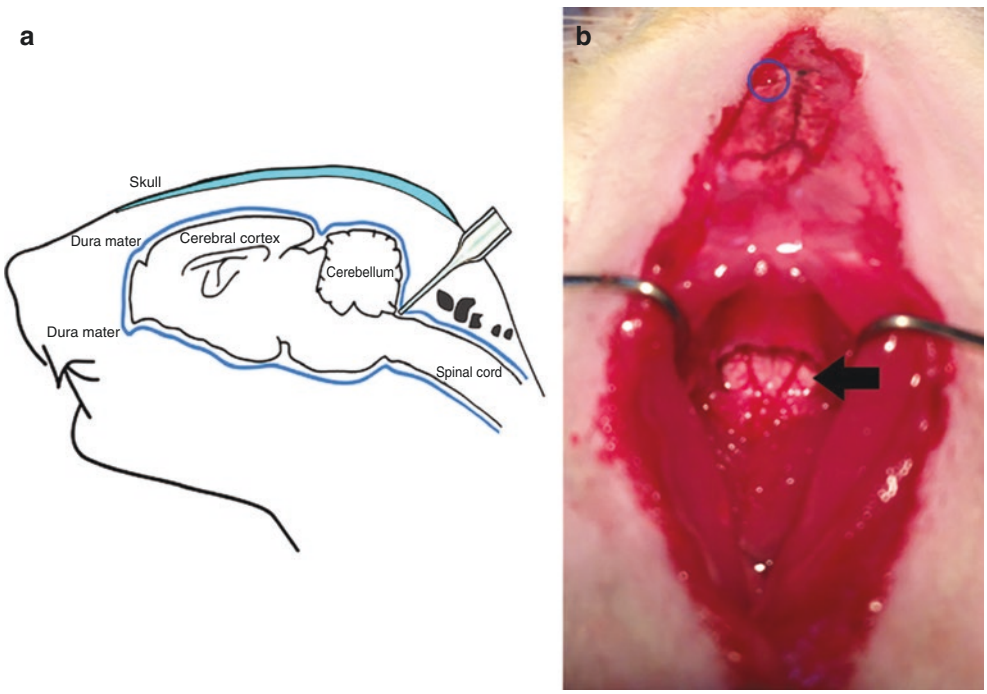

Fig. 17.1 Preparation of the cerebrospinal fluid fistulation. (**a**) A taper glass capillary tube was inserted into the cisterna magna. (**b**) After measuring the baseline CSFP by the burr hole 0.8 mm caudal and 1.5 mm lateral to the bregma (blue circle), cerebrospinal fluid was drained from cisterna magna (arrow) (Reprinted with permission from Zhang et al. [5])

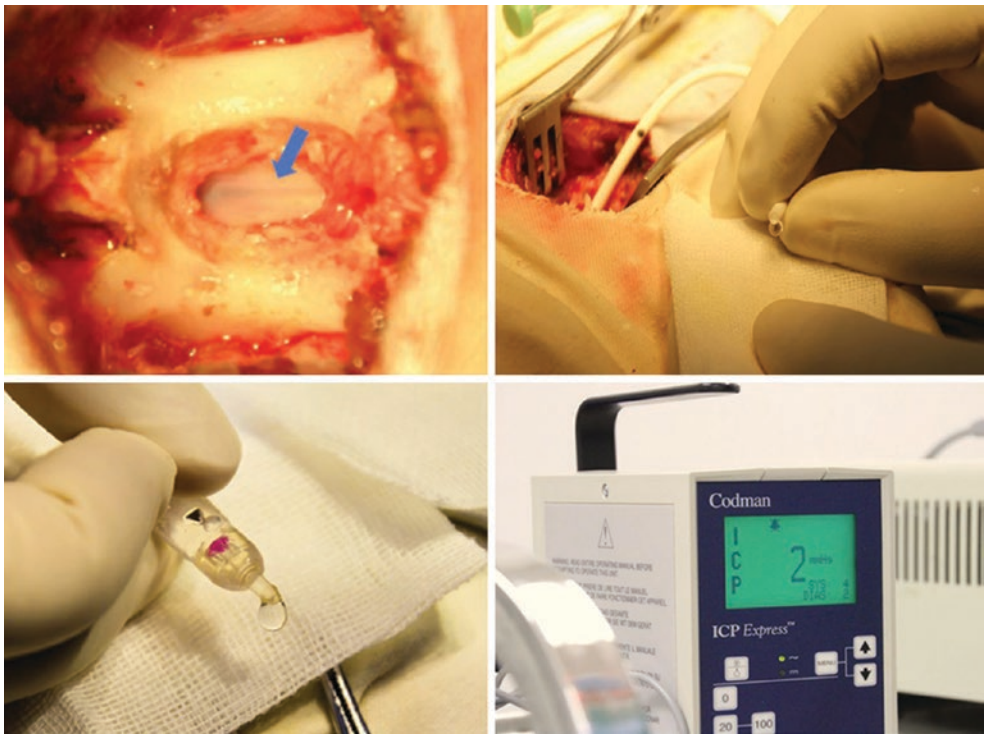

Fig. 17.2 Photographs showing the method of preparation and insertion of cerebrospinal fluid pressure-measuring sensor (Reprinted with permission from Yang et al. [4])

confirmed for the first time in NHP eyes. It also further proved that translaminar cribrosa pressure difference may be a true risk factor for glaucoma [4].

Bang V. Bui from University of Melbourne recently created a new method to change the level of CSFP. Intracranial pressure was measured by a custom-made dual cannula inserted into the lateral ventricle on the side ipsilateral to the eye cannula (Fig. 17.3). To make sure accurate ICP control over a long time, a dual-lumen needle cannula was developed, which infuses saline via a syringe pump (Model 22, Harvard Apparatus, Holliston, MA) and measures pressure in the same lateral ventricle at the same time. Infusion pressure and ICP were continuously measured by two precalibrated pressure transducers (Fig. 17.3a, Transpac, Abbott Critical Care System, Iligo, IRE) connected to a Powerlab system (Bridge Amp ML110, Amplifier ML 785, Powerlab/8SP, ADInstruments, Colorado Springs, Colorado) and recorded on LabChartTM (Lab Chart 7, ADInstruments) [25].

17.4 Future Directions

17.4.1 Development of New Experimental Animals

Tree shrew owns a perfect visual system, with cone cells accounting for 96% of photosensory cells. Our country is rich in resources of tree shrew, which is proved to be ideal for animal model studying ocular diseases by comparative medicine. Some researches have found that optic nerves of tree shrews aged between 4 weeks and 5 years were similar in many aspects including cellular morphology, extracellular matrix, and especially the structure of lamina cribrosa [26]. Therefore, tree shrews would be a good choice for research on the pathogenesis of glaucoma.

Besides tree shrew, zebrafish is becoming another popular option for animal model by virtue of its small size, strong breeding ability, and fast-growing characteristic. In addition, it has gained wide attention because of high gene conservation and similarity in the eye. Link et al. established the method of measuring IOP of zebrafish and found that IOP varied in obvious genetic zebrafish, which provided a benchmark of IOP to measure the mutants of zebrafish [27]. Therefore, zebrafish is a good choice to study the mechanisms of glaucoma in genetic perspective. However, the research on zebrafish is urgently needed to be standardized.

17.4.2 Establishment of Mild IOP Elevation Animal Model

Establishment of mild IOP elevation animal model was important for us to further study the relationship between CSFP and glaucoma. However, so far, no literature has reported the successful establishment of mild IOP elevation animal model.

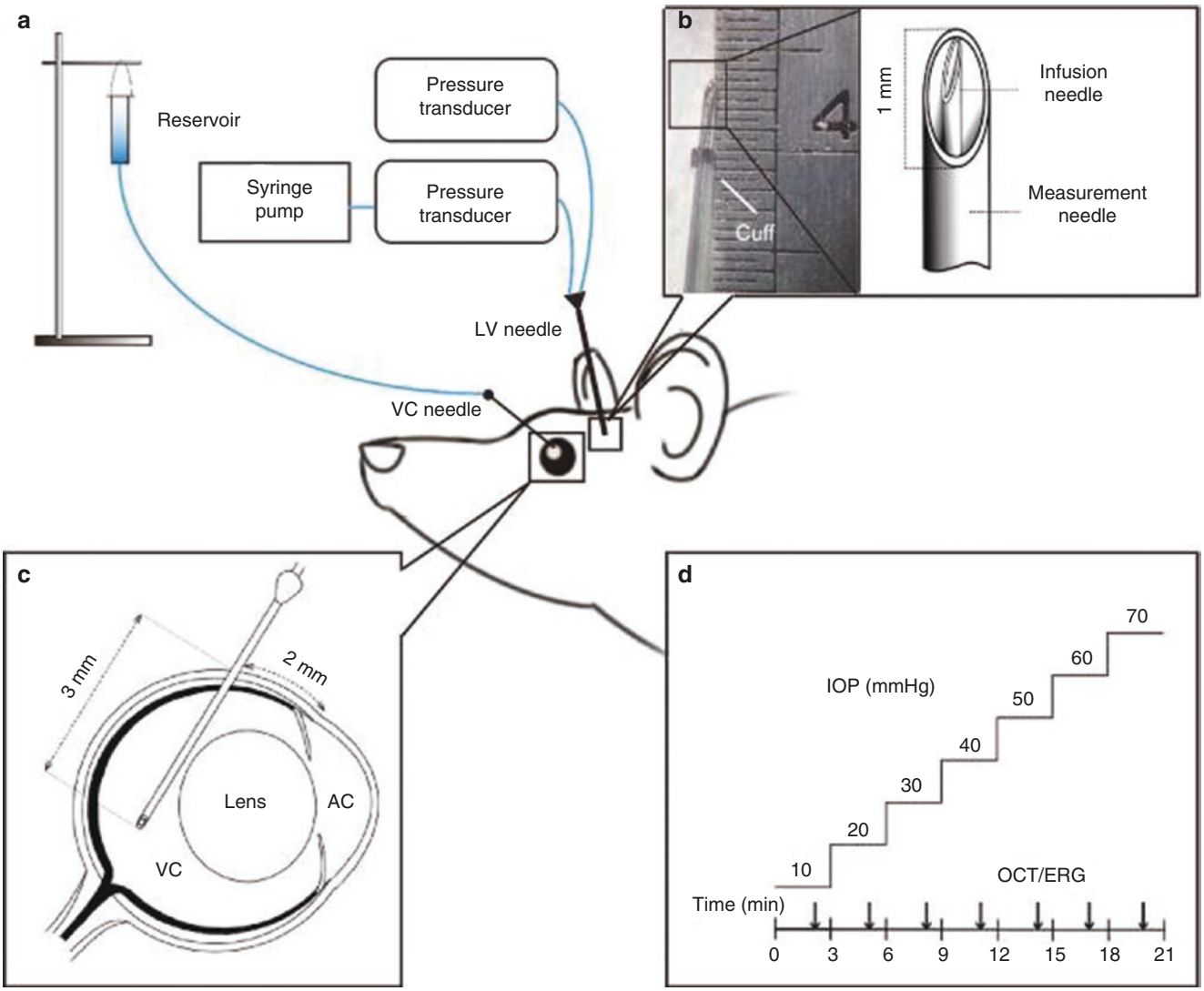

Fig. 17.3 Intraocular and intracranial pressure elevation methodology. (**a**) IOP and ICP elevation was achieved by inserting a needle to the vitreous chamber (VC) and a dual-lumen needle to the ipsilateral lateral ventricle (LV). A saline reservoir was connected to the vitreous chamber needle, whereas a syringe pump was connected to the lateral ventricle cannula. (**b**) A custom-made dual-lumen needle with infusion (inner needle) and measurement ports (outer needle) was used in order to elevate the ICP. (**c**) Vitreous chamber cannulation employed a 27G needle inserted 2 mm behind the limbus at a 45° angle. (**d**) At each ICP level, IOP was elevated from 10 to 70 mmHg in 10 mmHg steps each lasting 3 min. Optical coherence tomography (OCT) or electroretinography (ERG) was analyzed at each IOP and ICP level (Reprinted with permission from Zhao et al. [25])

References

1. Weinreb RN, Aung T, Medeiros FA. The pathophysiology and treatment of glaucoma: a review. JAMA. 2014;311(18):1901–11.
2. Hou R, Zhang Z, Yang D, Wang H, Chen W, Li Z, Sang J, Liu S, Cao Y, Xie X, Ren R, Zhang Y, Sabel BA, Wang N. Intracranial pressure (ICP) and optic nerve subarachnoid space pressure (ONSP) correlation in the optic nerve chamber: the Beijing Intracranial and Intraocular Pressure (iCOP) study. Brain Res. 2016;1635:201–8.
3. Ren R, Jonas JB, Tian G, Zhen Y, Ma K, Li S, Wang H, Li B, Zhang X, Wang N. Cerebrospinal fluid pressure in glaucoma: a prospective study. Ophthalmology. 2010;117(2):259–66.
4. Yang D, Fu J, Hou R, Liu K, Jonas JB, Wang H, Chen W, Li Z, Sang J, Zhang Z, Liu S, Cao Y, Xie X, Ren R, Lu Q, Weinreb RN, Wang N. Optic neuropathy induced by experimentally reduced cerebrospinal fluid pressure in monkeys. Invest Ophthalmol Vis Sci. 2014;55(5):3067–73.
5. Zhang Z, Wu S, Jonas JB, Zhang J, Liu K, Lu Q, Wang N. Dynein, kinesin and morphological changes in optic nerve axons in a rat model with cerebrospinal fluid pressure reduction: the Beijing Intracranial and Intraocular Pressure (iCOP) study. Acta Ophthalmol. 2016;94(3):266–75.
6. Resch ZT, Fautsch MP. Glaucoma-associated myocilin: a better understanding but much more to learn. Exp Eye Res. 2009;88(4):704–12.
7. Senatorov V, Malyukova I, Fariss R, Wawrousek EF, Swaminathan S, Sharan SK, Tomarev S. Expression of mutated mouse myocilin induces open-angle glaucoma in transgenic mice. J Neurosci. 2006;26(46):11903–14.

8. Tseng HC, Riday TT, McKee C, Braine CE, Bomze H, Barak I, Marean-Reardon C, John SW, Philpot BD, Ehlers MD. Visual impairment in an optineurin mouse model of primary open-angle glaucoma. Neurobiol Aging. 2015;36(6):2201–12.
9. Wilson GN, Inman DM, Dengler Crish CM, Smith MA, Crish SD. Early pro-inflammatory cytokine elevations in the DBA/2J mouse model of glaucoma. J Neuroinflammation. 2015;12:176.
10. Jia L, Cepurna WO, Johnson EC, Morrison JC. Patterns of intraocular pressure elevation after aqueous humor outflow obstruction in rats. Invest Ophthalmol Vis Sci. 2000;41(6):1380–5.
11. Tezel G, Yang X, Luo C, Cai J, Powell DW. An astrocyte-specific proteomic approach to inflammatory responses in experimental rat glaucoma. Invest Ophthalmol Vis Sci. 2012;53(7):4220–33.
12. Salinas-Navarro M, Alarcón-Martínez L, Valiente-Soriano FJ, Jiménez-López M, Mayor-Torroglosa S, Avilés-Trigueros M, Villegas-Pérez MP, Vidal-Sanz M. Ocular hypertension impairs optic nerve axonal transport leading to progressive retinal ganglion cell degeneration. Exp Eye Res. 2010;90(1):168–83.
13. Bai Y, Zhu Y, Chen Q, Xu J, Sarunic MV, Saragovi UH, Zhuo Y. Validation of glaucoma-like features in the rat episcleral vein cauterization model. Chin Med J (Engl). 2014;127(2):359–64.
14. Kanamori N. M, Nakanishi Y, Nagai A, Mukuno H, Yamada Y, Negi A. Akt is activated via insulin/IGF-1 receptor in rat retina with episcleral vein cauterization. Brain Res. 2004;1022(1-2):195–204.
15. Urcola JH, Hernández M, Vecino E. Three experimental glaucoma models in rats: comparison of the effects of intraocular pressure elevation on retinal ganglion cell size and death. Exp Eye Res. 2006;83(2):429–37.
16. Lentschener C, Fredi-Reygrobellet D, Bouaziz H, Mazoit JX, Niessen F, Benhamou D. Effect of CO(2) pneumoperitoneum on early cellular markers of retinal ischemia in rabbits with alpha-chymotrypsin-induced glaucoma. Surg Endosc. 2000;14(11):1057–61.
17. Matsumoto Y, Kanamori A, Nakamura M, Negi A. Rat chronic glaucoma model induced by intracameral injection of microbeads suspended in sodium sulfate-sodium hyaluronate. Jpn J Ophthalmol. 2014;58(3):290–7.
18. Manni G, Lambiase A, Centofanti M, Mattei E, De Gregorio A, Aloe L, de Feo G. Histopathological evaluation of retinal damage during intraocular hypertension in rabbit: involvement of ganglion cells and nerve fiber layer. Graefes Arch Clin Exp Ophthalmol. 1996;234(Suppl1):S209–13.
19. Ito YA, Belforte N, Cueva Vargas JL, Di Polo AA. Magnetic microbead occlusion model to induce ocular hypertension-dependent glaucoma in mice. J Vis Exp. 2016;(109):e53731.
20. Gaasterland D, Kupfer C. Experimental glaucoma in the rhesus monkey. Invest Ophthalmol. 1974;13:455–7.
21. Brooks DE, Kallberg ME, Komaromy AM, Ollivier FJ, Lambrou GN. Optic nerve head neuroretinal rim blood flow differences in monkeys with laser-induced glaucoma. Vet Ophthalmol. 2005;8(2):113–9.
22. Liu K, Wang N, Peng X, Yang D, Wang C, Zeng H. Long-term effect of laser-induced ocular hypertension on the cone electroretinogram and central macular thickness in monkeys. Photomed Laser Surg. 2014;32(7):371–8.
23. Lessell S, Kuwabara T. Experimental alpha-chymotrypsin glaucoma. Arch Ophthalmol. 1969;81:853–64.
24. Quigley HA, Addicks EM. Chronic experimental glaucoma in primates. I. Production of elevated intraocular pressure by anterior chamber injection of autologous ghost red blood cells. Invest Ophthalmol Vis Sci. 1980;19:126–36.
25. Zhao D, He Z, Vingrys AJ, Bui BV, Nguyen CT. The effect of intraocular and intracranial pressure on retinal structure and function in rats. Physiol Rep. 2015;3(8):pii: e12507.
26. Albon J, Farrant S, Akhtar S, Young R, Boulton ME, Smith G, Taylor M, Guggenheim J, Morgan JE. Connective tissue structure of the tree shrew optic nerve and associated ageing changes. Invest Ophthalmol Vis Sci. 2007;48(5):2134–44.
27. Link BA, Gray MP, Smith RS, John SW. Intraocular pressure in zebrafish: comparison of inbred strains and identification of a reduced melanin mutant with raised IOP. Invest Ophthalmol Vis Sci. 2004;45(12):4415–22.

18 Outlook on Therapeutic Strategies for Primary Open-Angle Glaucoma Based on the Theory of Translamina-Pressure Difference

Weiwei Chen and Ningli Wang

Glaucoma is a group of optic nerve lesions characterized by progressive loss of retinal ganglion cells (RGCs) and their axons and primarily manifested by progressive optic nerve damage, atrophy, and visual field defects, with increased intraocular pressure (IOP) being the main risk factor [1]. Generally, glaucoma is classified into two types: primary angle-closure glaucoma (PACG) and primary open-angle glaucoma (POAG). PACG is mainly a result of optic nerve damage caused by blockage of aqueous humor outflow and elevated intraocular pressure due to mechanical angle closure, and its pathogenesis has been clearly known. Along with the economic development and lifestyle changes in the country, the disease profiles have changed greatly. Currently, primary open-angle glaucoma (POAG) has become the most common irreversible eye disease that results in blindness and disability, accounting for 74% of the patients with glaucoma, with its pathogenesis yet remaining unknown so far [2].

It is traditionally believed that high intraocular pressure (IOP) is a high-risk factor for optic nerve damage associated with glaucoma. However, in the Handan Eye Study, we discovered that about 83% of patients with POAG suffered normal-tension glaucoma (NTG) [3]. Clinically, we also observed that the majority of patients with POAG were NTG patients. Why would NTG patients with intraocular pressure levels within the normal range suffer IOP-related optic nerve damage like patients with high-tension glaucoma?

W. Chen · N. Wang (✉)
Beijing Institute of Ophthalmology, Beijing Tongren Eye Center, Beijing Tongren Hospital, Capital Medical University, Beijing, China

Beijing Ophthalmology & Visual Sciences Key Laboratory, Beijing, China
e-mail: wningli@vip.163.com

18.1 Establishment of the Theory of Increased Translamina-Pressure Difference Leading to POAG

For these clinical questions, we conducted analysis from the anatomical structure of the lamina: the laminar anterior tissue bears the action of intraocular pressure (IOP), which produces a backward force on the lamina, while the laminar posterior tissue bears the action of cerebrospinal fluid pressure in the subarachnoid space of the optic nerve, which produces a forward force on the lamina; a difference exists between the laminar anterior IOP and the cerebrospinal fluid pressure in the subarachnoid space of the optic nerve, and this difference is called "translamina-pressure difference" (TLPD). Would TLPD be a direct cause of POAG if IOP is not?

With this question, the research team of professor Wang Ningli with Beijing Institute of Ophthalmology conducted retrospective and prospective clinical studies, finding that patients with normal-tension glaucoma (NTG) had lower intracranial pressure values than patients with high-tension glaucoma and healthy subjects in the control group. Meanwhile, the research team also found that patients with NTG had an obviously narrow subarachnoid space of the optic nerve than patients with high-tension glaucoma and the non-glaucoma control group [4], which also has proved that the cerebrospinal fluid pressure measured by lumbar puncture (LP) is consistent to cerebrospinal fluid pressure in the subarachnoid space of the optic nerve. Therefore, we conjectured that this relatively low intracranial pressure in NTG patients may result in decreased cerebrospinal fluid pressure in the subarachnoid space of the optic nerve, causing relatively high anterior IOP of the lamina and increased translamina-pressure difference, thus resulting in IOP-related optic nerve damage in glaucoma. On this basis, macaque models of chronic low intracranial pressure with increased translamina-pressure difference were constructed for observation on optic nerve lesions in the

N. Wang (ed.), *Intraocular and Intracranial Pressure Gradient in Glaucoma*,
Advances in Visual Science and Eye Diseases 1, https://doi.org/10.1007/978-981-13-2137-5_18

macaques. The results showed that during 3–8 months after successful induction of chronic low intracranial pressure, the macaques developed signs of glaucomatous optic nerve damage, including expansion of optic cup, narrowing of disk edges, thinning of retinal nerve fiber layer, and bleeding along the disk edges. This study demonstrated from the perspective of large animal model that increased translamina-pressure difference associated with low intracranial pressure has a causal relationship with optic nerve damage.

Then, it comes the question "Why would increased translamina-pressure difference result in glaucomatous optic nerve damage?" Currently, the mainstream theories on how primary open-angle glaucoma (POAG) causes optic nerve damage are "mechanical damage theory" [5, 6] and "vascular ischemia theory" [7]. However, neither of the theories can fully and thoroughly explain how increased translamina-pressure difference causes glaucomatous optic nerve damage. Recently, Band [8] and other scholars performed mathematical modeling for translamina-pressure difference and optic axons, in which the values of various parameters of the eyeball (including radius of axon, radius of optic nerve, axoplasmic coefficient of viscosity, axon length, etc.) were all determined depending on actual conditions. Upon calculation, the authors concluded that pressure difference between IOP and intracranial pressure would cause fluids outside the axon to permeate into the axon to form one passive neuronal intracellular fluid flux (PNIFF), which, when large enough, will wash away ATP gathering around the axon to produce an ATP flow void effect. Hence, we conjectured that this ATP deficiency would result in local energy deficiency to interfere with normal transport of axoplasmic flow and ultimately causes apoptosis of RGCs because the axons are unable to maintain mass and information transfer between RGCs and their axon terminals.

In the rat models of acute intracranial pressure decrease established using cerebrospinal fluid drainage, Wang Ningli's research team used RITC intravitreal injection to detect the transport of forward axoplasmic flow in rats in the low intracranial pressure group, and fluoro-gold (FG) (Biotium Inc., Hayward, CA, USA) injected into the superior colliculus as the tracer to detect the transport of reverse axoplasmic flow in rats in the low intracranial pressure group, and made comparisons with the high IOP group. The study results showed that both acute intracranial pressure decrease and acute IOP elevation would affect the transport of forward and reverse axoplasmic flows in RGCs. Therefore, we conjecture that axoplasmic flow transport disorder is one of the important causes of POAG caused by translamina-pressure difference (TLPD) [9].

18.2 Outlook on Treatment of POAG Based on the Theory of Translamina–Pressure Difference

It was previously believed that the only effective approach to the treatment of POAG is IOP-lowering therapy. The establishment and improvement of the theory of POAG caused by translamina-pressure difference provide more possibilities for POAG treatment.

18.3 Strategy of Increasing Intracranial Pressure Within the Safe Range

18.3.1 Belly Band Compression

Research shows that intracranial pressure is positively correlated with intra-abdominal venous pressure, probably because a high abdominal pressure causes the intra-abdominal venous pressure to increase, resulting in a relatively high intracranial pressure [10]. A relatively high intracranial pressure makes it more difficult for increased translamina-pressure difference to happen. Based on the above ground, we conjectured that the strategy of increasing abdominal pressure to a certain degree by compressing the abdomen with belly band to increase intra-abdominal venous pressure and ultimately the intracranial pressure may possibly produce a therapeutic effect on POAG. However, intra-abdominal pressure could be a double-edged sword for the elevation of intracranial pressure in a way that a too high intra-abdominal pressure may cause irreversible damage to the blood-brain barrier [11]. Therefore, how to perform belly band compression appropriately yet requires further study.

18.3.2 Treatment with Drugs That Increase Intracranial Pressure

Some drugs that may elevate intracranial pressure may also be effective in the treatment of POAG, such as glucocorticoids [12], vitamin A, etc. [13–15], but further exploration is still required regarding dose control of the drugs to ensure elevation of intracranial pressure within the safe range.

18.3.3 Dietary adjustment to increase BMI

Body mass index (BMI) is a protective factor for glaucoma. People with a high BMI are not susceptible to POAG, and we certainly do not recommend increasing BMI for all patients with POAG. However, for patients with a relatively low

BMI, particularly patients with normal-tension glaucoma, appropriate dietary adjustment to increase the BMI is conducive to the treatment of the disease from the perspective of TLPD theory [16–18].

18.4 Neuroprotective Drugs for Axoplasmic Flow Transport Function

Optic nerve protection therapy for glaucoma has always remained the focus of glaucoma research, but currently there are no commercially available drugs with recognized efficacy. In either the previous theory of increased intraocular pressure causing glaucoma or the recent theory of increased translamina-pressure difference causing glaucoma, axoplasmic flow transport disorder of the optic nerve is the core factor. Therefore, we conjecture that the development of drugs able to regulate the axoplasmic flow transport function might be an important direction toward research on optic nerve protection in glaucoma.

18.5 Summary

To sum up, considering glaucoma as a disorder of axoplasmic flow transport associated with translamina-pressure difference opens a new gate to the treatment of this disease. For the treatment of glaucoma in future, we should also pay attention to changes of intracranial pressure and maintenance of normal axoplasmic flow transport function while using the conventional IOP-lowering therapy.

References

1. Kwon YH, Fingert JH, Kuehn MH, Alward WL. Primary open-angle glaucoma. N Engl J Med. 2009;360(11):1113–24.
2. Quigley HA, Broman AT. The number of people with glaucoma worldwide in 2010 and 2020. Br J Ophthalmol. 2006;90(3):262–7.
3. Shields MB. Normal-tension glaucoma: is it different from primary open-angle glaucoma? Curr Opin Ophthalmol. 2008;19(2):85–8.
4. Wang N, Xie X, Yang D, Xian J, Li Y, Ren R, Peng X, Jonas JB, Weinreb RN. Orbital cerebrospinal fluid space in glaucoma: the Beijing intracranial and intraocular pressure (iCOP) study. Ophthalmology. 2012;119(10):2065–73. e2061
5. Burgoyne CF, Downs JC. Premise and prediction-how optic nerve head biomechanics underlies the susceptibility and clinical behavior of the aged optic nerve head. J Glaucoma. 2008;17(4):318–28.
6. Fechtner RD, Weinreb RN. Mechanisms of optic nerve damage in primary open angle glaucoma. Surv Ophthalmol. 1994;39(1):23–42.
7. Yamamoto T, Kitazawa Y. Vascular pathogenesis of normal-tension glaucoma: a possible pathogenetic factor, other than intraocular pressure, of glaucomatous optic neuropathy. Prog Retin Eye Res. 1998;17(1):127–43.
8. Band LR, Hall CL, Richardson G, Jensen OE, Siggers JH, Foss AJ. Intracellular flow in optic nerve axons: a mechanism for cell death in glaucoma. Invest Ophthalmol Vis Sci. 2009;50(8):3750–8.
9. Zhang Z, Wang X, Jonas JB, Wang H, Zhang X, Peng X, Ritch R, Tian G, Yang D, Li L, et al. Valsalva manoeuver, intra-ocular pressure, cerebrospinal fluid pressure, optic disc topography: Beijing intracranial and intra-ocular pressure study. Acta Ophthalmol. 2013;
10. Sakka SG. The patient with intra-abdominal hypertension. Anasthesiol Intensivmed Notfallmed Schmerzther. 2016;51(1):8–16.
11. Youssef AM, Hamidian Jahromi A, Vijay CG, Granger DN, Alexander JS. Intra-abdominal hypertension causes reversible blood-brain barrier disruption. J Trauma Acute Care Surg. 2012;72(1):183–8.
12. Sinclair AJ, Walker EA, Burdon MA, van Beek AP, Kema IP, Hughes BA, Murray PI, Nightingale PG, Stewart PM, Rauz S, Tomlinson JW. Cerebrospinal fluid corticosteroid levels and cortisol metabolism in patients with idiopathic intracranial hypertension: a link between 11beta-HSD1 and intracranial pressure regulation? J Clin Endocrinol Metab. 2010;95(12):5348–56.
13. Jacobson DM, Wall IM, Digre KB, Corbett J. Serum vitamin A concentrate is elevated in idiopathic intracranial hypertension. Neurology. 1999;53:1114–8.
14. Warner JEA, Bernstein PS, Yemelyanov A, Alder SC, Farnsworth ST, Digre KB. Vitamin A in the cerebrospinal fluid of patients with and without idiopathic intracranial hypertension. Ann Neurol. 2002;52:647–50.
15. Selhorst J, Kulkantrakorn K, Corbett JJ, Leira EC, Chung SM. Retinol- binding protein in idiopathic intracranial hypertension (IIH). J Neuroophthalmol. 2000;20:250–2.
16. Wang YX, Jonas JB, Wang N, You QS, Yang D, Xie XB, Xu L. Intraocular pressure and estimated cerebrospinal fluid pressure. The Beijing Eye Study 2011. PLoS One. 2014;9(8):e104267.
17. Xu L, Wang YX, Wang S, Jonas JB. Neuroretinal rim area and body mass index. PLoS One. 2012;7(1):e30104.
18. Ren R, Wang N, Zhang X, Tian G, Jonas JB. Cerebrospinal fluid pressure correlated with body mass index. Graefes Arch Clin Exp Ophthalmol. 2012;250(3):445–6.

Part IV

Basic Experiment and Hypothesis

Fortified Astrocyte: The Target of Pathological Intraocular Hypertension

19

Chao Dai, Geoffrey Raisman, and Ying Li

19.1 Gross Anatomy of Rat Optic Nerve Head

The rat optic nerve head (ONH) is a segment about 250 μm in length extending from the funnel-shaped region where the optic nerve fibres (retinal ganglion cell axons, RGC) converge on the optic disc rostrally to the transition to the optic nerve (ON) caudally (Fig. 19.1a). The ONH has a characteristic kidney shape, some 500 μm wide and 300 μm dorsoventrally, with the 'hilus' of the kidney always at the midventral pole and occupied by two large vessels, the ophthalmic vein dorsally and the ophthalmic artery ventral to this (Fig. 19.1b). For complete orientation of the cross sections in space, therefore, it is only necessary to mark the medial and lateral edges at the time when the tissue is removed. The rat ONH contains only three tissue components—totally unmyelinated RGC axons, specialised astrocytes, and the endothelial cells of the microvessels which penetrate from the ventral to the dorsal surfaces (Fig. 19.1d, f, g). Unlike the human lamina cribrosa, there is no connective tissue, collagenous strengthening of the perivascular spaces. Since raised intraocular pressure causes RGC axon damage in the ONH of the rat, this indicates that the injurious effects of pressure transduction can be exerted in the absence of a connective tissue lamina cribrosa (Fig. 19.1c). Both structural integrity and function of axon are supported by astrocytes and microvessels. Astrocytes play the key role in the interactions of axons and microvessels. Rat ONH is a good model to understand the relationship of axon, astrocyte and microvessel in human lamina cribrosa (Fig. 19.1).

19.2 Fortified Astrocytes

The organisation of the ONH consists of a simple radiating array of astrocytes with stout end feet anchored around the midventral, 'hilar' surface facing the ophthalmic vessels (Fig. 19.2a, b). As the astrocytic processes radiate out towards the overarching cap of the dorsal surface, they break up into finer and finer processes, which are either closely apposed to each other or separated by longitudinal channels containing unmyelinated RGC axons (Fig. 19.2a, f, g). The radial processes ultimately terminate in complex delicate branches at the dorsal surface. As they approach the dorsal circumference the radial processes converge into an axon free pre-terminal layer where they branch into fine parallel segments devoid of cytoskeleton and with a tendency to separate (Fig. 19.2c, d).The perinuclear regions of the cell bodies generally lie more or less midway along this trajectory. Longitudinal sections show that the perikarya are packed immediately adjacent to each other in longitudinal rows.

Morphologically the radial astrocytes of the ONH are a unimodal population, the direct descendants of the radial glia of the developing optic stalk. Their ventral, end foot surface is the former pial surface of the optic stalk, and their expanded dorsal circumference is the former ventricular surface which, as in the case of the retina itself, becomes massively expanded. Unlike the retina, however, this former ventricular surface is not fused with an overlying pigment cell layer but is totally denuded of optic stalk cells and apposed directly to a collagen-containing extracellular space. It shows the continuity between this surface and the pigment cell layer of the retina, with the pigment cells ceasing as the ONH is reached.

The ONH astrocytes have a unique cellular composition. In marked contrast to the highly pale cytoplasm of

C. Dai (✉)
Southwest Eye Hospital, Southwest Hospital, Third Military Medical University, Chongqing, China

G. Raisman · Y. Li
UCL Department of Cell and Developmental Biology and Spinal Repair Unit, Department of Brain Repair and Rehabilitation, UCL Institute of Neurology, London, UK

N. Wang (ed.), *Intraocular and Intracranial Pressure Gradient in Glaucoma*,
Advances in Visual Science and Eye Diseases 1, https://doi.org/10.1007/978-981-13-2137-5_19

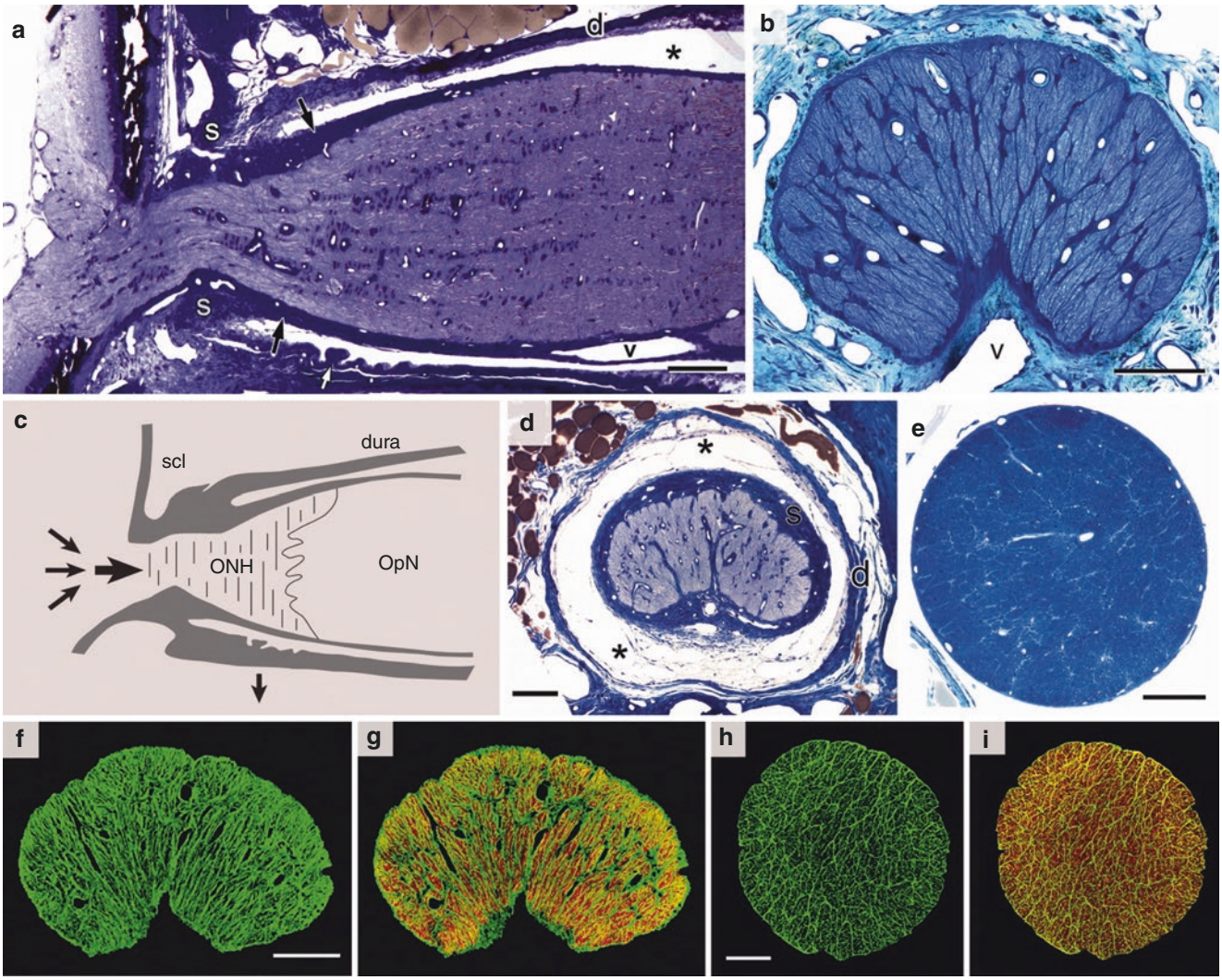

Fig. 19.1 (**a**) Longitudinal section across the ONH from the retina to the junction with the OpN, showing the characteristic longitudinal rows of astrocytic cell bodies. The thick sheath of the ONH (black arrows) is continuous rostrally with the sclera (s) and caudally with the dural sheath of the optic nerve (d). Asterisk, CSF containing subarachnoid space; v, ophthalmic vein; white arrow, arachnoid villus. (**b**) Cross section of ONH showing radial astrocytes and associated microvessels. Stout astrocytic basal processes (stained dark) are anchored on the mid-ventral surface, which is invaginated by the ophthalmic vein (v). (**c**) Line drawing (based on A) showing how the attachments of the thick sheath of the ONH to the sclera (scl) and the dura concentrate the force of raised IOP (arrows) into the ONH at right angles to its radial array of astrocytes. The arachnoid villus (white arrow in Fig. 19.1a above) acts as a drain that would lower the local CSF pressure (down arrow), thus increasing the pressure gradient across the ONH. OpN, optic nerve. (**d**) Cross section showing the thick sheath (s) of the ONH separated by the CSF containing subarachnoid space (*) from the dural sheath (d) of the optic nerve. (**e**–**i**) Cross sections contrasting the ONH (**d**, **f**, **g**) with the OpN (**e**, **h**, i). The ONH has a thick vascular outer sheath and is traversed by darkly stained "fortified" astrocytes that are anchored by thick bases to the deep ventromedian indentation and which radiate out to terminate in thin processes attached to the overarching dorsal surface. The OpN has random arrangement of pale astrocytes and no connective tissue sheath, and the circular outline is not indented. Resin sections (1.5 μm thick) stained with methylene blue and Azur II (**a**, **b**, **d**, **e**). Cryostat sections: GFAP (green) for astrocytes (**f**, **h**), combined with TUJ (red) for axons (**g**, **i**). Scale bars: 100 μm (Reproduced with permission from [1]

astrocytes in virtually every other location (including the retina and the ON) (Fig. 19.2e), the cytoplasm of the ONH astrocytes is highly and uniformly electron dense throughout all the cell processes (Fig. 19.2a, b, i, f). The striking feature of the astrocytic processes is their massive 'strengthening' of longitudinal massed filaments and tubules. We consider this the structural basis of the pressure transduction which gives the ONH its mechanical strength and makes it vulnerable to the distorting effects of raised intraocular pressure (IOP and probably raised CSF pressure). This opinion is supported by our finding that the first effect of raised IOP is a localised tearing away of the fine astrocytic branches from the overlying circumferential surface of the dorsal dome of the ONH. For this reason we refer to these uniquely specialised cells as 'fortified astrocytes (Fig. 19.2).'

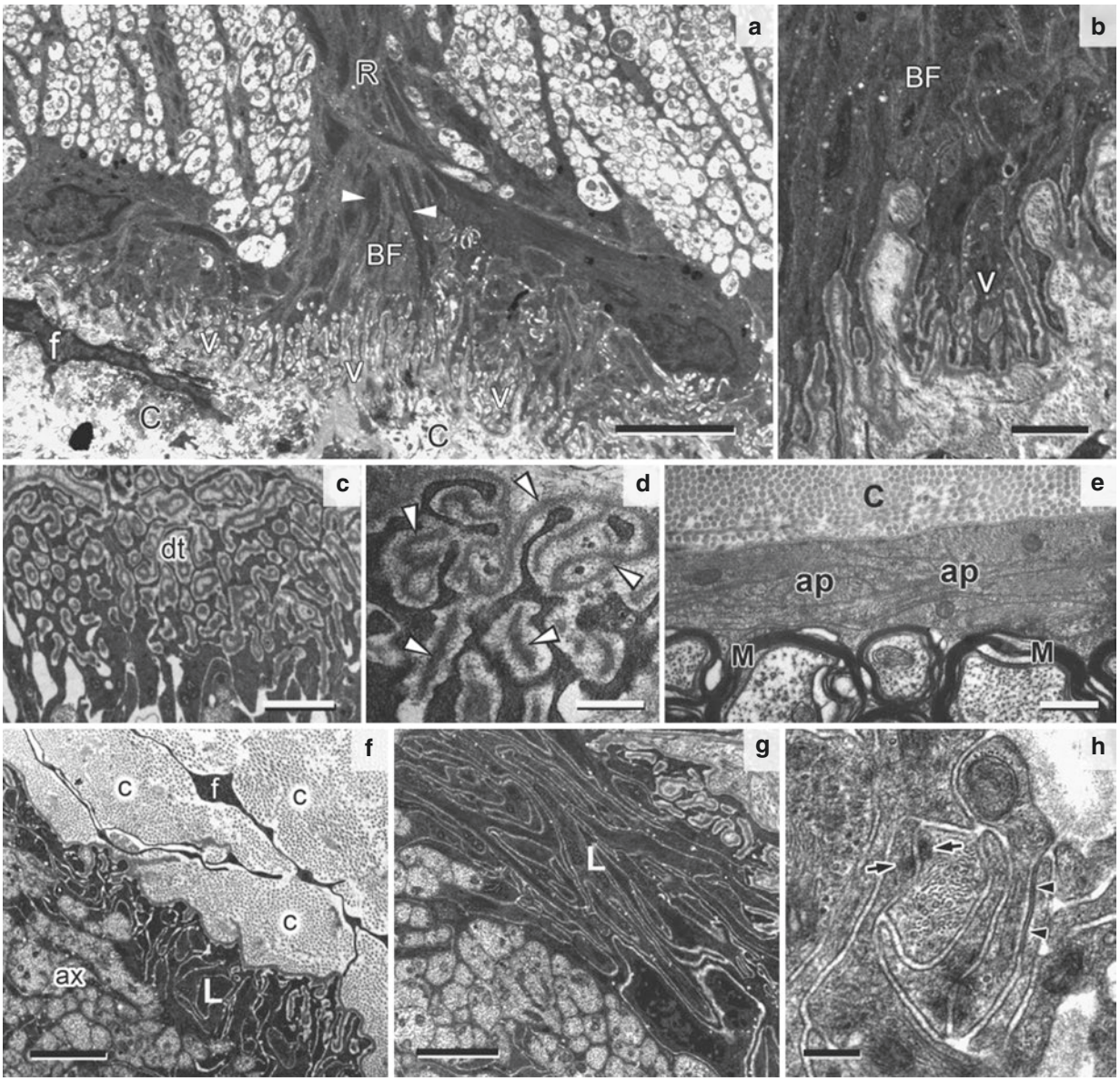

Fig. 19.2 Electron micrographs: (**a**) stout basal foot (BF) of a fortified ONH astrocyte firmly anchored into the collagenous sheath (**c**) by fine, straight villus projections (v) deeply invaginated into the cell cytoplasm. White arrow heads, cytoplasmic swirls of strengthening cytoskeletal filaments and tubules. R, radial processes separated by channels filled with RGC axons; f, fibroblast. (**b**) Enlarged view of astrocytic basal end foot (BF) with straight villi (v) invested with thickened basal lamina. (**c**) Enlarged in (**d**) dorsal terminations of radial glial processes (dt) in a massive cap of complex, interdigitating curved villous processes invested with thickened basal lamina (white arrow heads). (**e**) Segment of the surface of the OpN. In contrast to the ONH where the surface consists of a mass of electron dense villous processes, the surface of the OpN consists of a simple overlay of electron pale astrocytic processes (ap), devoid of villi, and forming the same glia-pial array as found at surface of the rest of the CNS. C, collagen of sheath; M, myelinated RGC axons. (**f**, **g**) The lateral surface of the ONH showing the axon-free region occupied by the electron dense, directly apposed, interweaving preterminal processes (L). Another field at high power in G. ax, axons; collagen (c) and fibroblast (f) of sheath. (**h**) High-power view to show astrocytic junctions: symmetrical desmosome-like (arrows) and gap junction (arrow heads). (**i**) Radial glial process showing aligned cytoskeletal core (f) and fine processes (arrows) arising from the periphery and interweaving among the RGC axons (x). (**j**) Parallel radial array of directly apposed branches of the radial astrocytic process. (**k**) Parallel circumferential array of fibroblasts in the dense collagenous sheath of the ONH. (**l**) Segment of endothelial cell surface from an ONH microvessel, showing the typical array of pinocytotic vesicles on the abluminal surface. In contrast to the OpN (panel M), the endothelial cell is separated from the astrocytic processes (out of the field) by a wide perivascular space containing a fibroblast (fbl) and collagen fibrils. Note that a permeable blood–brain barrier is present in the ONH and absent in the OpN. (**m**) Segment of the surface of an endothelial cell (E) from an OpN microvessel. Note the absence of pinocytotic vesicles and the narrow and uniform apposition (arrows) of the astrocyte (nucleus, n), an anatomical configuration found in regions with a blood–brain barrier. L, lumen. (**n**) Enlarged view of the closely apposed preterminal astrocytic processes (as in **f**, **g**) showing the rich array of pinocytotic vesicles (which may represent a local mechanism to counteract fluid accumulation and close up the spaces during reversible stage of distortion due to mild rises in IOP). See also visible at low power in panels B and J. Scale bars: 5 μm (**a**), 3 μm (**c**), 2.5 μm (**k**), 2 μm (**f**, **g**), 1 μm (**b**, **j**, **m**), 0.5 μm (**d**, **i**, **l**, **n**), 0.2 μm (**e**, **h**) (Reproduced with permission from [1]

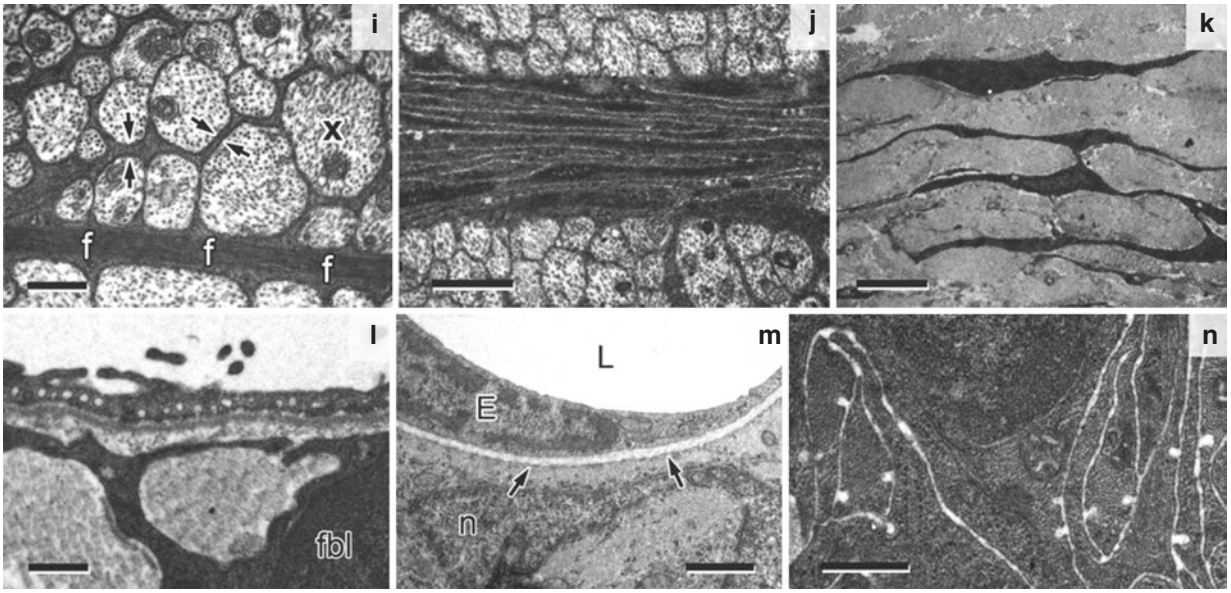

Fig. 19.2 (continued)

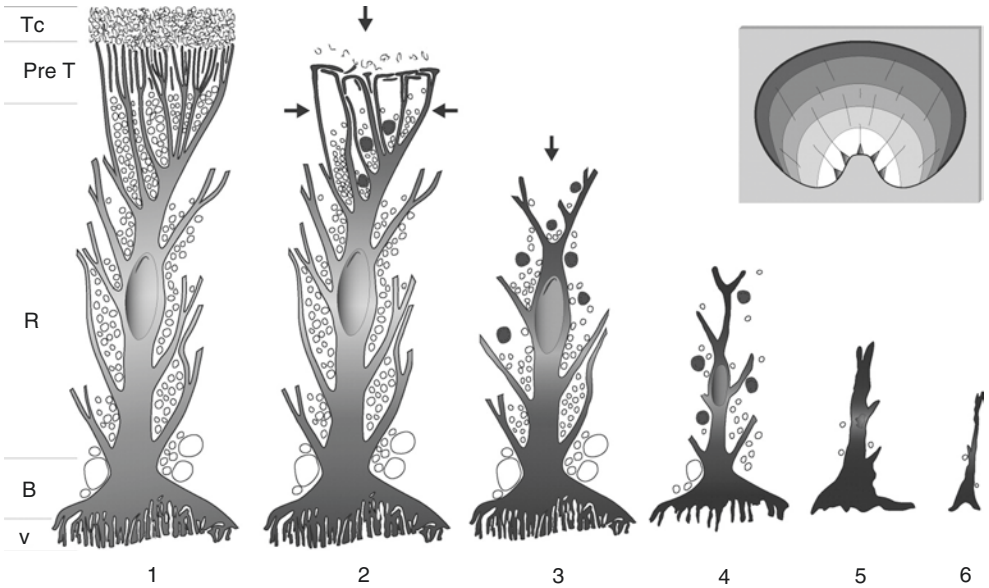

Fig. 19.3 Schematic representation of the changes occurring during damage by raised IOP. (1) Normal structure of a fortified radial astrocyte of the ONH. The enlarged basal end foot (B) is firmly anchored by long, straight villous processes (v) into the collagenous sheath at the ventral median indentation of the ONH. R, radial process branching to enclose separate territories of RGC axons. In the preterminal region (PreT), the finest branches come together in direct apposition to each other and excluding all axons. The terminal cap (TC) is made up of a thick layer of interdigitating curled endings invested with basal lamina. (2) The first stage of damage by raised IOP begins along the dorsal circumference. The preterminal processes become separated by massive spaces of tissue fluid (horizontal arrows). Their terminals are pulled away from the collagenous sheath and collapse (vertical arrow) into reduplicated layers on the dorsal surface. RGC axons spill out into the spaces; degenerating axons (grey-filled circles). The loss of axons is already considerable at this stage. (3)The axon terminals are entirely pulled away (arrow) from the dorsal surface. We suggest this represents the irreversible stage of damage. The space they previously occupied is filled with cellular debris. Axon loss is severe. (4–6) Final stages of degradation leading to loss of all axons and total degeneration of the radial astrocytes. Inset: Isobar representation of stress gradient across the ONH (Reproduced with permission from [1]

19.3 Glial Isomerisation in ONH

At the dorsal surface of the ONH, the radial astrocytic processes branch progressively and lose their cytoskeletal cores of filaments and tubules. This narrow, preterminal region of the ONH (about 1–2 μm deep) is devoid of axons, so that the radial processes converge into direct contact with each other in fine, parallel, electron dense arrays. The preterminal region just under the dorsal surface of the ONH shows a degree of loosening, with spaces filled with extracellular fluid separating the preterminal astrocytic processes (Figs. 19.2c and 19.3), although we have not found any degenerating axons in preterminal area in normal rats with electromicroscopy. The size of space in preterminal region is different in rats and eyeballs with semi-thin sections under light microscopy. Figure 19.4 shows the quite different space in both eyes of one normal rat (Figs. 19.3 and 19.4). There is vulnerable region in the dorsal of ONH. This vulnerable region is isomerisation in bilateral eyes and different rats. The size of space might be related to some vulnerable property. In experimental intraocular hypertension rat, the earliest sign of damage was always seen at the region of the preterminal astrocytic segments just under the dorsal circumferential margin of the ONH (Fig. 19.3).

Glaucoma is the most important cause of irreversible blindness worldwide [2]. A key question in the pathogenesis of glaucoma is to identify the mechanism by pathological high intraocular pressure (IOP). Intraocular hypertension does not always lead to glaucoma. Pathological intraocular hypertension is defined as IOP which could result in glaucoma, even if the IOP is normal. The increased IOP [3–9] or translamina pressure difference (TLPD) [10–14] damages the RGC. What is the first event of the damage procedure? Fortified astrocytes in ONH formed the main supportive structure of glial lamina cribrosa in normal rat. Astrocytes are arranged as a fan-like radial array, firmly attached ventrally to the sheath of the lamina cribrosa by thick basal processes but

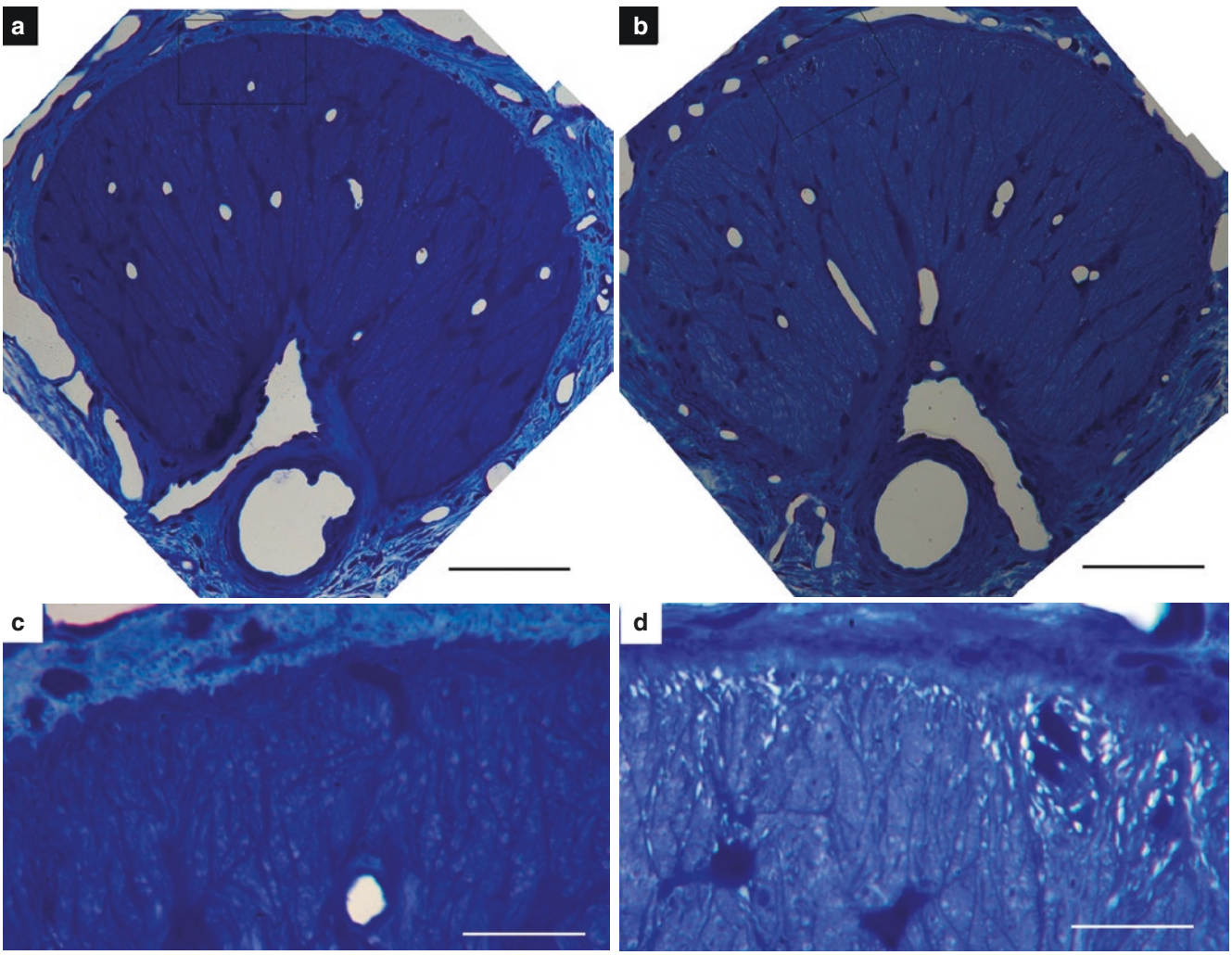

Fig. 19.4 Bilateral ONH of one normal rat. A and C. right ONH, the pre-terminal region is solitary. B and D. left ONH, the pre-terminal region is loosening with obvious space. Scale bars: A-B, 100μm, C-D, 20μm

dividing dorsally into progressively more slender processes with only delicate attachments to the sheath. These fortified astrocytes form ventral stout basal end feet, radial array, and axon-free preterminal layer before terminating in a complex layer of fine interdigitating delicate branches at the dorsal. Fortified astrocyte is highly and uniformly electron dense throughout all the cell processes. An equally striking feature of the astrocytic processes is their massive cytoskeletal 'strengthening' of longitudinal massed filaments and tubules. Especially, cytoskeletal cores form 'scaffold' of astrocytes. There is vulnerable region in the dorsal of glial lamina cribrosa [1, 15]. This vulnerable region is isomerisation in bilateral eyes and different rats. It is hard to test there is also glial isomerisation in human lamina cribrosa. If glial isomerisation also happens in human lamina cribrosa, individual difference of glaucomatous damage may be coincident with glial isomerisation in lamina cribrosa. The deformation of astrocytes in lamina cribrosa could be the 'first event' in glaucomatous optic nerve damage. It hints that glial isomerisation in lamina cribrosa is the mechanism of glaucomatous damage to the optic nerve. With some like solitary preterminal region in lamina cribrosa, intraocular hypertension would not result in RGC damage. On the contrary, with special loosening preterminal region in lamina cribrosa, normal IOP would lead to glaucomatous damage. With increased TLPD or pathological ocular hypertension, the processes of astrocytes withdraw and separate from microvessels, not only focal atrophy will happen, but also blood–brain barrier will be broken. Glaucomatous damage (including optic disc bleeding, immune reaction, ischemia and axon loss of RGC) procedure is set up. With glial isomerisation in ONH, it might throw light on a new hypothesis to understand the mechanism of glaucomatous neuropathy, including mechanical, microcirculatory, immunological, biochemistrical factors. It is owing to the first event of glaucoma, withdrawing processes of fortify astrocytes, which triggers glaucomatous damage.

Acknowledgments The text and figures of this manuscript have appeared previously in our own work: *Dai C, Khaw PT, Yin ZQ, Li D, Raisman G, Li Y. Structural basis of glaucoma: the fortified astrocytes of the optic nerve head are the target of raised intraocular pressure. Glia. 2012;60(1):13–28* [1]. They have been used with permission and edited for this chapter.

References

1. Dai C, Khaw PT, Yin ZQ, Li D, Raisman G, Li Y. Structural basis of glaucoma: the fortified astrocytes of the optic nerve head are the target of raised intraocular pressure. Glia. 2012;60:13–28.
2. Quigley HA, Broman AT. The number of people with glaucoma worldwide in 2010 and 2020. Br J Ophthalmol. 2006;90:262–7.
3. Hernandez MR, Miao H, Lukas T. Astrocytes in glaucomatous optic neuropathy. Prog Brain Res. 2008;173:353–73.
4. Morrison JC, Cepurna Ying Guo WO, Johnson EC. Pathophysiology of human glaucomatous optic nerve damage: insights from rodent models of glaucoma. Exp Eye Res. 2011;93:156–64.
5. Morrison JC, Johnson EC, Cepurna W, Jia L. Understanding mechanisms of pressure-induced optic nerve damage. Prog Retin Eye Res. 2005;24:217–40.
6. Quigley HA, Addicks EM. Regional differences in the structure of the lamina cribrosa and their relation to glaucomatous optic nerve damage. Arch Ophthalmol. 1981;99:137–43.
7. Quigley HA, Addicks EM, Green WR. Optic nerve damage in human glaucoma. III. Quantitative correlation of nerve fiber loss and visual field defect in glaucoma, ischemic neuropathy, papilledema, and toxic neuropathy. Arch Ophthalmol. 1982;100:135–46.
8. Quigley HA, Addicks EM, Green WR, Maumenee AE. Optic nerve damage in human glaucoma. II. The site of injury and susceptibility to damage. Arch Ophthalmol. 1981;99:635–49.
9. Soto I, Oglesby E, Buckingham BP, Son JL, Roberson ED, Steele MR, et al. Retinal ganglion cells downregulate gene expression and lose their axons within the optic nerve head in a mouse glaucoma model. J Neurosci. 2008;28:548–61.
10. Jonas JB, Wang N, Nangia V. Ocular perfusion pressure vs estimated trans-lamina cribrosa pressure difference in glaucoma: The Central India Eye and Medical Study (An American Ophthalmological Society Thesis). Trans Am Ophthalmol Soc. 2015;113:T61–T613.
11. Jonas JB, Wang N, Wang YX, You QS, Yang D, Xie X, et al. Subfoveal choroidal thickness and cerebrospinal fluid pressure: the Beijing Eye Study 2011. Invest Ophthalmol Vis Sci. 2014;55:1292–8.
12. Jonas JB, Wang N, Yang D. Translamina cribrosa pressure difference as potential element in the pathogenesis of glaucomatous optic neuropathy. Asia-Pacific J Ophthalmol. 2016;5:5–10.
13. Zhang Z, Liu D, Jonas JB, Wu S, Kwong JM, Zhang J, et al. Axonal transport in the rat optic nerve following short-term reduction in cerebrospinal fluid pressure or elevation in intraocular pressure. Invest Ophthalmol Vis Sci. 2015;56:4257–66.
14. Zhang Z, Wu S, Jonas JB, Zhang J, Liu K, Lu Q, et al. Dynein, kinesin and morphological changes in optic nerve axons in a rat model with cerebrospinal fluid pressure reduction: the Beijing Intracranial and Intraocular Pressure (iCOP) study. Acta Ophthalmol. 2016;94:266–75.
15. Dai C, Li DQ, Li Y, Raisman G, Yin ZQ. [Studies on glial isomerization of lamina cribrosa in rat], [Zhonghua yan ke za zhi]. Chinese J Ophthalmol. 2013;49:723–8.

Lymphatic Drainage from the Eye: Is Cerebrospinal Fluid Involved?

20

Neeru Gupta and Yeni Yucel

Lowering intraocular pressure (IOP) is known to slow the rate of glaucoma injury. Aqueous humor is produced by the ciliary epithelium and drains out of the eye via the well-established trabecular meshwork route and uveoscleral outflow pathways. It is helpful to remember that most of our body tissues are bathed in lymph, which drains fluid, waste, and pathogens from the interstitium, pumping as much as 3 L of fluid per day. In the absence of a pump such as the heart, capillary walls act as one-way valves in which endothelial cells overlap allowing fluid to enter, while preventing fluid from exiting. Once fluid enters the lymphatics, the valves allow flow toward the node, preventing backflow. Small capillaries merge to form larger vessels, passing through lymph nodes, and eventually lymphatic trunks merge until the lymph enters the right lymphatic duct and thoracic ducts at the base of the neck where they are returned to the venous circulation.

20.1 Do Lymphatics Exist in the Human Eye?

Lymphatics are well known to be found in most tissues except for hair and nails. Whether lymphatics exist in the eye has been questioned for the past centuries.

20.2 Lymphatics in Human Ciliary Muscle

Research advances have identified specific markers for lymphatics that include podoplanin, a transmembrane mucin-type glycoprotein, and lymphatic vessel endothelial hyaluronan receptor-1 (LYVE-1). In the human ciliary body, lymphatic channels were identified by immunofluorescence with D2-40 antibody for podoplanin and LYVE-1 antibody. Lymphatic channels had a distinct lumen and were negative for CD34, a blood vessel endothelial cell marker, surrounded by discontinuous or no collagen IV-positive basement membrane. Electron microscopy confirmed D2-40 immunoreactivity in lymphatic endothelium in the human ciliary body [1] (Fig. 20.1).

20.3 Does Aqueous Flow Through Lymphatics?

If lymphatics absorb fluid from the aqueous humor, radioactive protein tracer should appear along the lymphatic drainage routes within lymph nodes. Ethical approval for

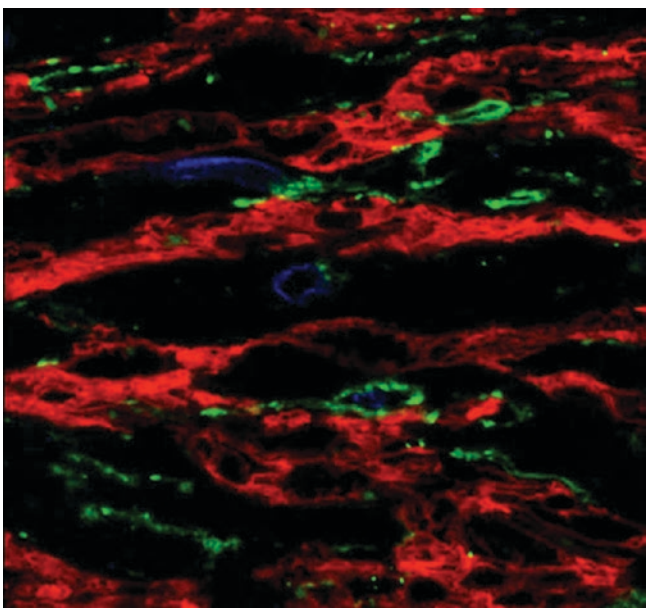

Fig. 20.1 Immunofluorescence—triple labeling. D2-40—antibody to podoplanin specific for lymphatic endothelial cells (green channel). SMA—smooth muscle actin (red channel), CD34—blood vessels (blue channel). (Reprinted with permission from [1])

N. Gupta (✉)
Department of Ophthalmology and Vision Sciences, University of Toronto, Toronto, ON, Canada
e-mail: guptan@smh.ca

Y. Yucel
Department of Ophthalmology and Vision Sciences, Laboratory Medicine and Pathobiology, Keenan Research Centre for Biomedical Science, Li Ka Shing Knowledge Institute of St. Michael's Hospital, University of Toronto, Toronto, ON, Canada

N. Wang (ed.), *Intraocular and Intracranial Pressure Gradient in Glaucoma*,
Advances in Visual Science and Eye Diseases 1, https://doi.org/10.1007/978-981-13-2137-5_20

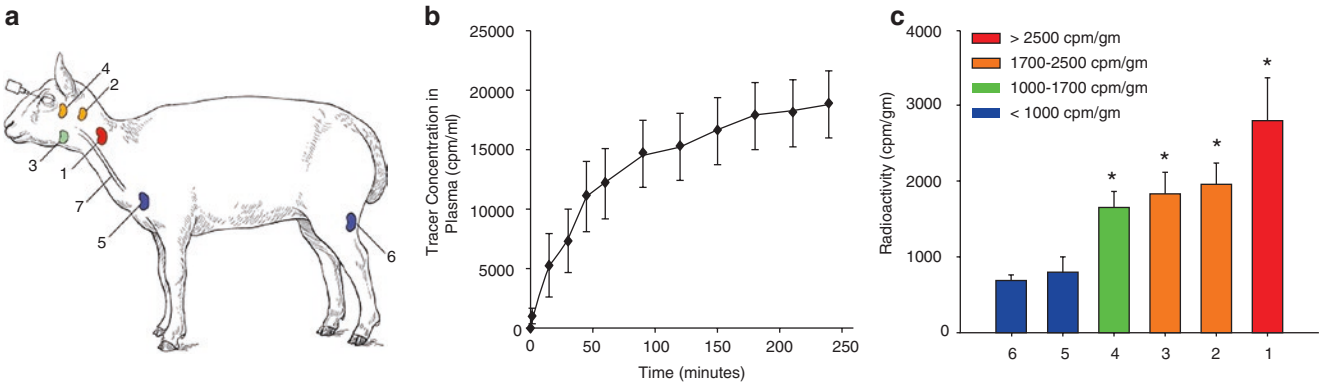

Fig. 20.2 (**a**) Drawing of color-coded regional lymph nodes 4 h after intracameral injection of ^{125}I human serum albumin shows cervical (#1), retropharyngeal (#2), submandibular (#3), and preauricular (#4) nodes with high tracer counts compared to prescapular (#5) and popliteal (#6) lymph nodes. A catheter inserted into the jugular vein (#7) allowed plasma sampling for tracer concentrations at various time points (**b**). The histogram shows radioactivity counts in regional lymph nodes compared to the reference popliteal site. (**c**) There were significant differences in radioactivity counts in submandibular, retropharyngeal, preauricular, and cervical nodes compared to popliteal site by one-way repeated ANOVA measures followed by single degree of freedom contrasts for each site ($P < 0.05$). The numbers along the x-axis of C indicate the lymph node locations as seen in A (Reprinted with permission from [1].)

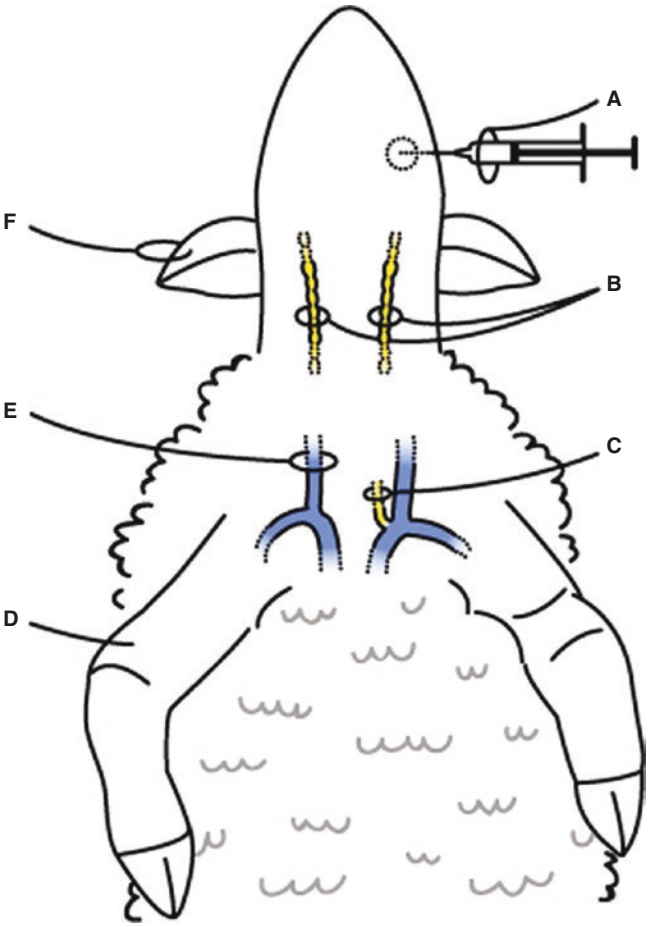

Fig. 20.3 Experimental preparation in a dorsal recumbent position: cannulation of left and right cervical lymphatic vessels (**b**) and of thoracic lymphatic duct (**c**) for continuous collection of lymph, and placement of catheter in the right jugular vein for sampling of blood (**d**) and pulse oximeter (**e**) IV line for fluids (**f**). After that, the sheep was placed in a sternal recumbent position with their head on a stand and chin resting on the bar, and 125I-BSA was injected into the anterior chamber of each eye (**a**) (Reprinted with permission from [2].)

studies was provided by the institution in keeping with ARVO's guidelines on use of animals in research. Fluorescent nanospheres injected into the sheep anterior chamber were seen in LYVE-1-positive channels of the ciliary body 15, 30, and 45 min following injection. Iodine-125 radiolabeled human serum albumin injected into the sheep eye ($n = 5$) drained preferentially into cervical, retropharyngeal, submandibular, and preauricular lymph nodes in the head and neck region compared to reference popliteal lymph nodes ($P < 0.05$). Collectively, these findings along with the presence of distinct lymphatic channels in the human ciliary body suggest that fluid and solutes flow at least partially through this system [1] (Fig. 20.2).

20.4 Can Lymphatic Drainage Be Measured?

A quantitative method to assess lymphatic drainage was developed using a sheep model, which also assessed trabecular meshwork™ and uveoscleral (UVS) outflow [2] (Fig. 20.3).

Over a 3–5-hour period, lymph was collected from cannulated cervical lymphatic vessels and the thoracic lymphatic duct after injecting ^{125}I-bovine serum albumin (BSA) into the eye. Blood samples were also collected every 15 min. Lymphatic and TM drainage were measured in lymph and plasma, respectively. In addition, radioactivity was measured in uvea, sclera (UVS) and other ocular tissue, as well as periocular tissue harvested after injection. ^{125}I-BSA recovered from different fluid and tissue compartments was expressed as a percentage of total recovered tracers. Three hours after injection, the percentage of tracer recovered in lymph and plasma was

1.64% ± 0.89% and 68.86% ± 9.27%, respectively ($n = 8$). The percentage of tracer in UVS and other ocular and periocular tissues was 19.87% ± 5.59%, 4.30% ± 3.31%, and 5.32% ± 2.46%, respectively. At 5 h after injection ($n = 2$), lymphatic drainage was increased (6.40% and 4.96% vs. 1.64%). On the other hand, the percentage of tracer recovered from UVS and other ocular tissue decreased, and that of periocular tissue showed no change. Lymphatic drainage increased steadily over the 3-h postinjection period, compared to rapid increase in TM drainage, reaching a plateau at 30 min.

This sheep model enabled quantitative assessment of relative contributions of lymphatic drainage and TM and UVS outflow and may be relevant to understanding effects of various glaucoma agents on outflow pathways.

20.4.1 A Mouse Model to Assess Lymphatic Drainage

We injected quantum dots into the left anterior chamber of the mouse eye and performed whole-body hyperspectral fluorescence imaging prior to injection and 5, 20, 40, and 70 min and 2, 6, and 24 h after injection. Postinjection at 6 h, a quantum dot signal was observed in the left neck region. Immunofluorescence-labeled sections showed quantum dot signal in the left submandibular lymph node using confocal microscopy – the first direct evidence of lymphatic drainage from the mouse eye. The approach described using quantum dots to visualize the lymphatic pathway in vivo is novel and may be used as a tool to explore new treatments aimed at reducing intraocular pressure to prevent blindness from glaucoma [3] (Fig. 20.4).

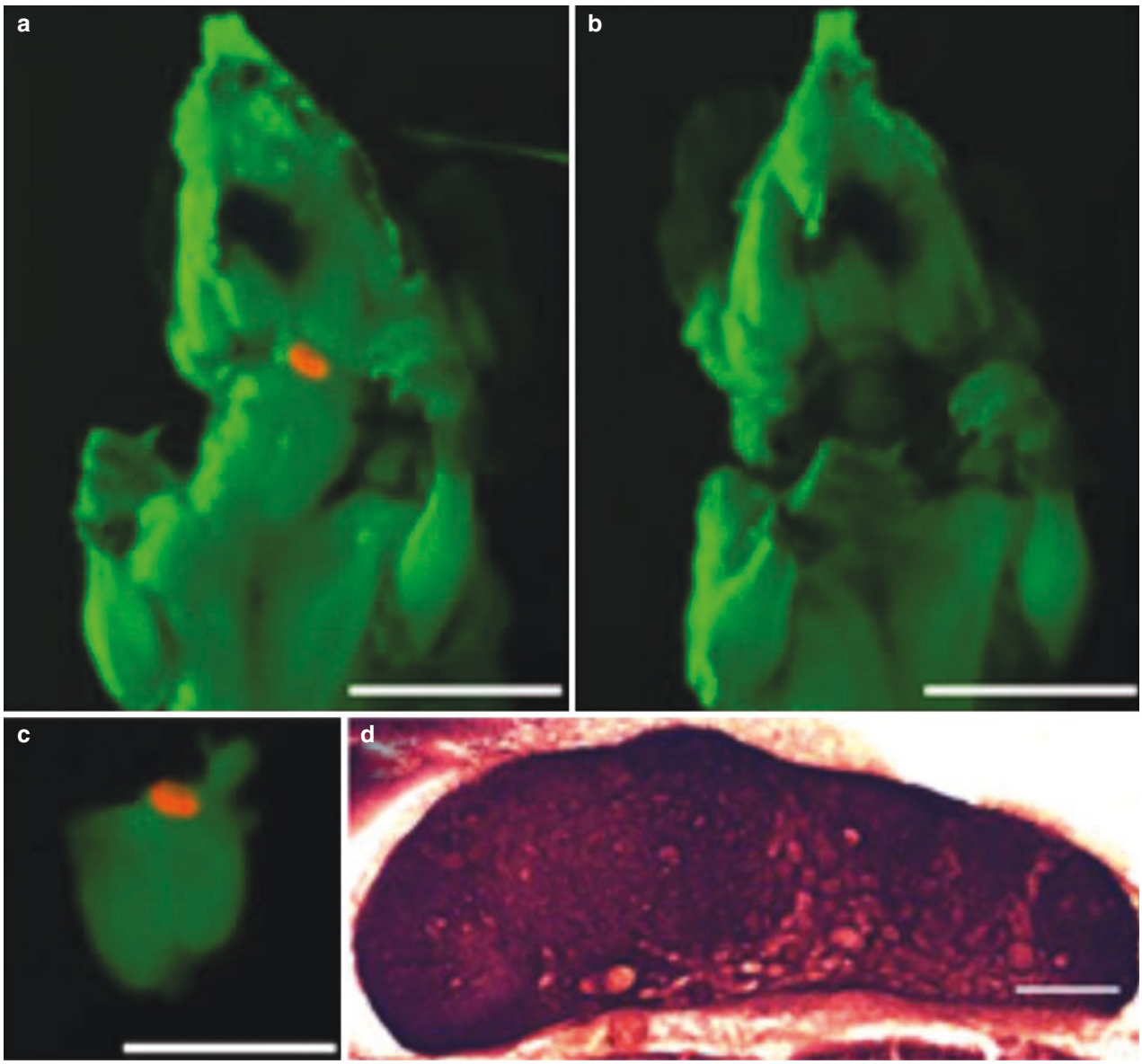

Fig. 20.4 Neck tissue containing QD signals (red) (**a**) was harvested (**b**) and isolated (**c**). Hematoxylin- and eosin-stained section shows a lymph node (**d**). Scale = 10 mm (**a**–**c**) and 250 μm (**d**) (Reprinted with permission from [3].)

20.4.2 Can Lymphatic Drainage Be Manipulated?

Whether lymphatic outflow can be stimulated by pharmacological agents is unknown. Latanoprost is a prostaglandin F2 alpha analog used to lower IOP to treat glaucoma [4]. Lymphatic drainage in mice was assessed in vivo following quantum dot drainage into the eye using hyperspectral imaging at multiple times. Lymphatic drainage rate into the submandibular lymph node was increased in the latanoprost group compared to controls (1.23 ± 1.06 h^{-1} vs. 0.30 ± 0.17 h^{-1}, mean ± SD, $P < 0.02$). Quantum dot signal intensity in the submandibular lymph node was also greater in the latanoprost-treated group compared to controls (10.55 ± 1.12 vs. 9.48 ± 1.24, log scale, $P < 0.05$). Latanoprost appears to increase lymphatic drainage from the eye, and this finding may be relevant to intraocular pressure lowering treatments in glaucoma [5] (Figs. 20.5 and 20.6).

20.4.3 Role of Cerebrospinal Fluid?

In the field of glaucoma research, there is a growing interest in the relationship between IOP and pressure in the tissues behind the eye, including cerebrospinal fluid (CSF). As CSF drainage in mouse is not well characterized, we combined quantum dot fluorescent nanoparticles with hyperspectral imaging. Quantum dots were injected into the CSF of the cisterna magna and visualized by in vivo hyperspectral imaging at various time points up to 6 h after injection. Quantum dots applied directly onto intact dura mater covering the cisterna magna served as controls. Post imaging, neck lymph nodes were removed and histological analysis was performed. Quantum dots injected into the CSF were detected in vivo in submandibular lymph nodes as early as 20 min, with none in controls (Fig. 20.7).

20.4.4 Is There a Communication Between The Eye and the CSF?

Aqueous humor drains into the submandibular node. CSF drains into the submandibular node. Is there a communication between the eye and the CSF? To answer this, we used a mouse model in which male 129SVE mice were injected with 3 μL of a fluorescent nanoparticle tracer into the left anterior chamber. A noninvasive imaging system called Maestro (Cambridge Research & Instrumentation, Inc., Hopkinton, MA) was then used to conduct in vivo hyperspectral imaging to monitor tracer drainage from the eye. What this does is incrementally excite the specimen (in this case a mouse under general anesthesia) over a designated range of wavelengths. The captured images can then be unmixed using algorithms to separate the signal of

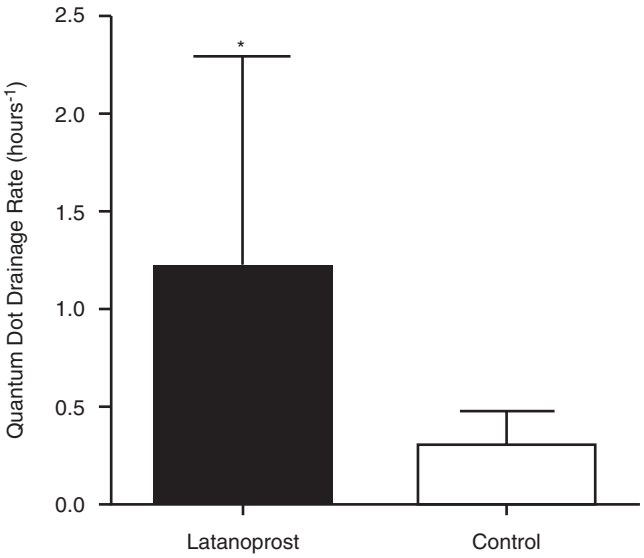

Fig. 20.5 Histogram shows mean and SD of QD drainage rate ($hours^{-1}$) for latanoprost-treated (black) and control (white) groups. *$P < 0.05$ (Reproduced with permission from [4])

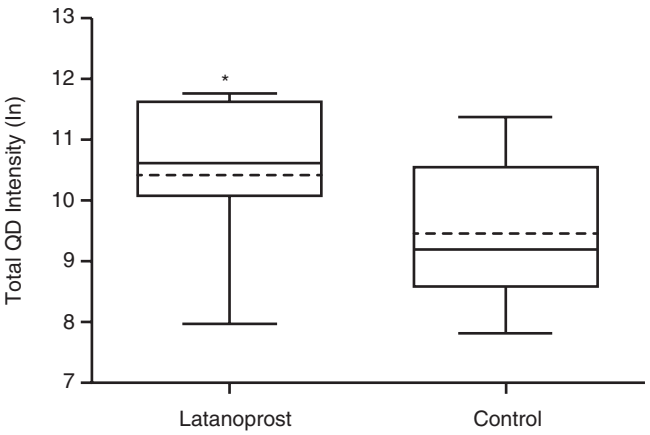

Fig. 20.6 Total QD intensities in the left submandibular node in latanoprost-treated and control groups are displayed. Box plots show the mean (dotted line), median (solid line), 25th and 75th percentiles (solid line box), and the minimum and maximum intensity (whiskers) for the natural log-transformed total QD intensity gray value measured. *$P < 0.05$ (Reproduced with permission from [4])

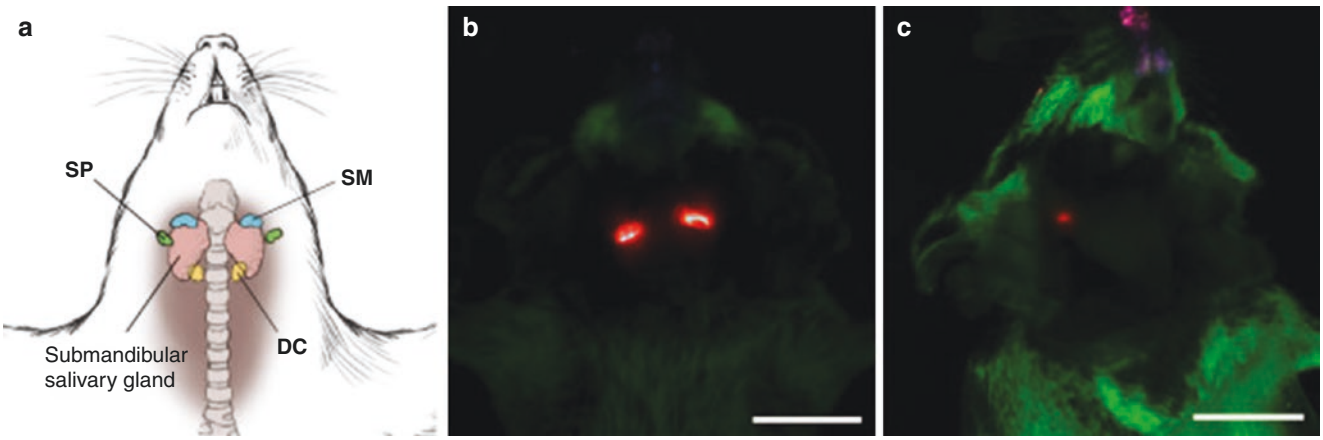

Fig. 20.7 (**a**) Diagram of murine lymph nodes in the neck showing locations for the submandibular (SM; blue), superficial parotid (SP; green), and deep cervical (DC; yellow) lymph nodes. (**b**) Ventral view of the upper body and head showing intense QD signal (red) in left and right submandibular region 6 h after QD injection into CSF. (**c**) Right latero-ventral view of the head and neck of a control mouse showing weak QD signal (red) in the right superficial parotid lymph node 6 h after QD application onto the dura mater overlying the cisterna magna. Tissue autofluorescence is shown in green. Scale = 1 cm (Reprinted with permission from [6].)

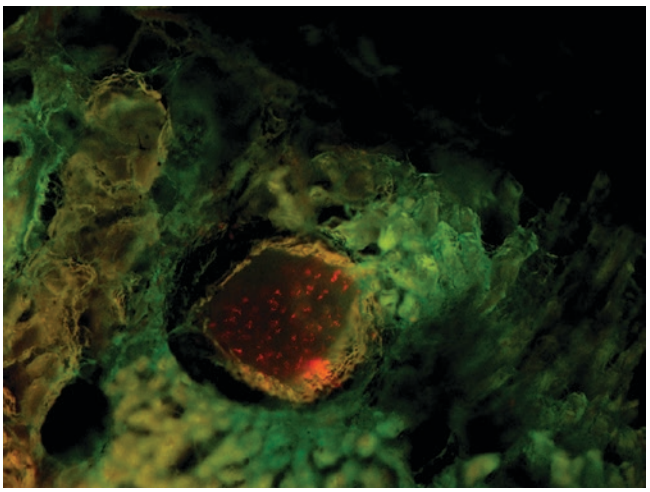

Fig. 20.8 QDs were found concentrated within the optic nerve head, while largely absent from the surrounding retinal tissue. (Reproduced with permission from [7])

interest from autofluorescence in the skin and fur. Moving on to the results, if we first look at the tracer distribution at the back of the eye, we can find that QD was found concentrated within the optic nerve head, while largely absent from the surrounding tissue (Fig. 20.8).

Acknowledgement This work was supported by the Canadian Institutes of Health Research, Canada Foundation of Innovation, Glaucoma Research Society of Canada, Dorothy Pitts Chair and Henry Farrugia Research Fund.

References

1. Yücel YH, Johnston MG, Ly T, Patel M, Drake B, Gumus E, Fraenkl SA, Moore S, Tobbia D, Armstrong D, et al. Identification of lymphatics in the ciliary body of the human eye: a novel "uveolymphatic" outflow pathway. Exp Eye Res. 2009;89(5):810–9.
2. Kim M, Johnston MG, Gupta N, Moore S, Yucel YH. A model to measure lymphatic drainage from the eye. Exp Eye Res. 2011;93(5):586–91.
3. Tam AL, Gupta N, Zhang Z, Yucel YH. Quantum dots trace lymphatic drainage from the mouse eye. Nanotechnology. 2011;22(42):425101.
4. Tam AL, Gupta N, Zhang Z, Yucel YH. Latanoprost stimulates ocular lymphatic drainage: an in vivo Nanotracer study. Transl Vis Sci Technol. 2013;2(5):3.
5. Zarbin MA. A new target for Glaucoma therapy. JAMA Ophthalmol. 2013;131(10):E1.
6. Mathieu E, Gupta N, Macdonald RL, et al. In vivo imaging of lymphatic drainage of cerebrospinal fluid in mouse [J]. Cerebrospinal Fluid Res. 10(1):35.
7. Mathieu E, Islam F, Gupta N, Tam ALC, Yucel Y. Quantum dots travel from the anterior chamber of the eye into the optic nerve and this is enhanced by latanoprost. In: 2014 International Society for Eye Research (ISER) XXI Biennial Meeting, San Francisco, California, July 22, 2014
8. Mathieu E, Gupta N, Macdonald RL, Ai J, Yücel YH. In vivo imaging of lymphatic drainage of cerebrospinal fluid in mouse. Fluids Barriers CNS. 2013;10:35. https://doi.org/10.1186/2045-8118-10-35.

Response of the Rat Optic Nerve to Acute Intraocular and Intracranial Pressure Changes

21

Da Zhao, Zheng He, Anna Van Koeverden, Algis J. Vingrys, Vickie H. Y. Wong, Jeremiah K. H. Lim, Christine T. O. Nguyen, and Bang V. Bui

21.1 Introduction

Glaucoma is a neurodegenerative disease, characterized by the progressive death of retinal ganglion cells. Elevated intraocular pressure (IOP) is known to be an important risk factor for glaucoma; however, it is not the only force acting on the optic nerve. Intracranial pressure (ICP) also exerts an effect on the optic nerve head, effectively opposing the force applied by IOP. Indeed, this balance of forces creates a pressure gradient (or the translaminar pressure gradient) across the optic nerve head [1]. Increasingly it is thought that the pressure difference between IOP and ICP, the translaminar pressure (TLP), may be critical for the integrity of the retina and optic nerve [2], and thus ICP may be an important risk factor for glaucoma [2–6].

Morgan and colleagues [7] used scanning laser ophthalmoscopy to study the deformation of the optic nerve head surface in canine eyes. They found that posterior and anterior displacement of the optic nerve surface could be produced by increasing IOP and ICP, respectively [7]. Thus acute changes in translaminar pressure have measureable effects on structure of the optic nerve. Whether such structural changes will occur in species whose optic nerve lacks a substantive lamina cribrosa, such as the rat, is not known. Importantly, whether these structural changes lead to deficits in retinal and ganglion cell function has yet to be studied.

In this study we employ spectral domain optical coherence tomography (OCT) to quantify the response of the rat optic nerve to a wide range of IOP and ICP levels. We assess the effect optic nerve pressure difference on surface deformation as well as retinal thickness. We relate these changes to the full-field electroretinogram (ERG) to determine the relationship between optic nerve structure and function. By studying the rat optic nerve, we hope to show that this species, which has become a widely used model of IOP-related injury, may also have utility for studies of ICP modification [8].

21.2 Methodology

All experimental procedures were in compliance with the National Health and Medical Research Council Australian Code of Practice for the care and use of animals for scientific purposes. Prior to commencement, animal ethics approval was obtained from the Howard Florey Institute Animal Experimentation Ethics Committee (13-044-UM).

As described in detail in our study [8], we employ adult male Long-Evans rats (n = 5–9 each group). All experiments were conducted under anesthesia induced using ketamine and xylazine (60:5 mg/kg). Body temperature was maintained at 37.5 ± 0.5 °C; pupils were dilated prior to imaging.

21.3 Optic Nerve Pressure Gradient Manipulation

21.3.1 Intraocular Pressure Control

IOP control was achieved by vitreous chamber cannulation using a 27G needle [9], which was connected to a saline reservoir (Fig. 21.1). IOP level was increased from 10 to 90 mmHg in steps of 10 mmHg each lasting 3 min. Each animal underwent the IOP step protocol twice at two randomly chosen ICP levels (0, 5, 15, 25, or 30 mmHg). Each IOP/ICP run was separated by 21 min. OCT and ERG measurements were conducted in two parallel cohorts of animals (n = 6–7, OCT; n = 5–9, ERG). OCT or ERG assessment was conducted at each IOP step.

D. Zhao · Z. He · A. Van Koeverden · A. J. Vingrys · V. H. Y. Wong
J. K. H. Lim · C. T. O. Nguyen · B. V. Bui (✉)
Department of Optometry and Vision Sciences,
University of Melbourne, Parkville, VIC, Australia
e-mail: bvb@unimelb.edu.au

N. Wang (ed.), *Intraocular and Intracranial Pressure Gradient in Glaucoma*,
Advances in Visual Science and Eye Diseases 1, https://doi.org/10.1007/978-981-13-2137-5_21

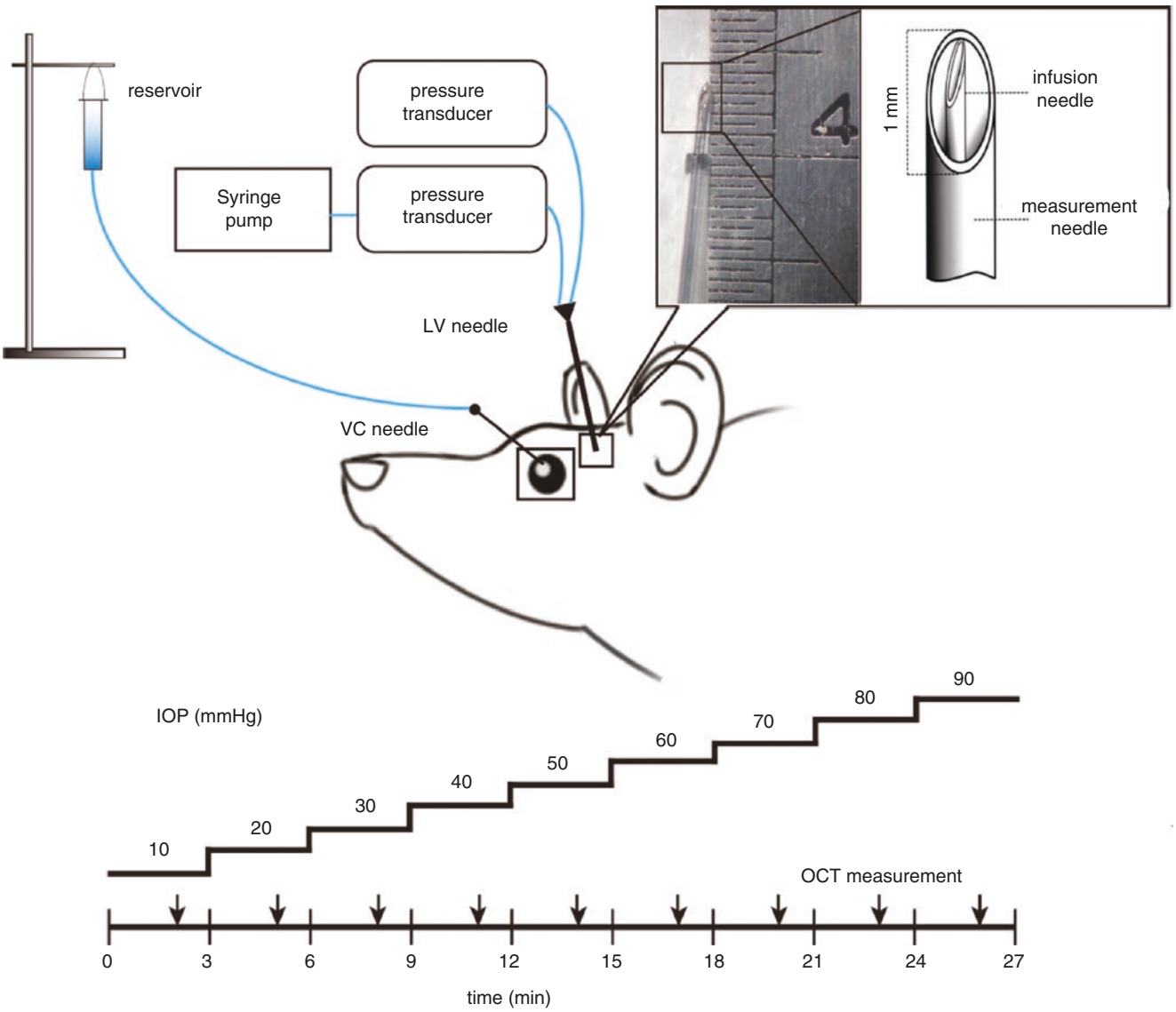

Fig. 21.1 Modifying intracranial pressure and intraocular pressure. A: a cannula is placed into the vitreous chamber. This is connected to a saline reservoir to allow IOP to be controlled, in this case from 10 to 90 mmHg in steps of 10 mmHg. A double lumen needle is inserted into the lateral ventricle. The inner lumen is connected to a syringe pump for intracranial pressure control. The outer lumen is connected to a pressure transducer for ICP monitoring. Once ICP had stabilized (0, 5, 15, 25, 30 mmHg), optical coherence tomography (OCT) or electroretinograms (ERG) were measured at each IOP level [8] (Reprinted with permission from Da Z, Zheng H, Vingrys A J, et al. The effect of intraocular and intracranial pressure on retinal structure and function in rats [J]. Physiological Reports, 2015, 3(8):2904–6)

21.3.2 Intracranial

Pressure (ICP) control: Intracranial pressure was manipulated via a custom-made dual cannula placed into the lateral ventricle on the side ipsilateral to the eye cannula. The needle was inserted to a depth of 3.5 mm at coordinates of 1.5 mm caudal to bregma, and 2 mm lateral to midline.

21.4 Outcome Measures

Functional assessment using the electroretinogram: Retinal function was assessed using the full-field electroretinogram (ERG). As described previously [10], custom-made silver-chloride active and reference electrodes were placed on the central cornea and sclera (ring shaped), respectively. Dim light levels were used to probe inner retinal function. For

electroretinogram (ERG) recordings, rats were dark-adapted overnight (12 h). All preparation was undertaken only with light from a dim red light emitting diode to maintain retinal sensitivity for scotopic threshold response (STR) measurements [10].

Structural assessment using optical coherence tomography: Spectral domain optical coherence tomography (OCT) was utilized to investigate the deformation of the optic nerve head (ONH) and thickness changes in the retina (Image-Guided 830 nm OCT, Phoenix Research Laboratories, Pleasanton, CA, USA). A line scan through the optic nerve was measured and analyzed for anterior surface position at 200 μm from the center of the optic nerve. Retinal thickness was measured as the perpendicular distance Bruch's membrane to the anterior surface of the retina. RNFL thickness was also measured at fixed locations from the center of the optic nerve.

21.5 Results

21.5.1 Structural Changes in Response to IOP and ICP Modification

Figure 21.2 shows that with increasing IOP elevation for a fixed ICP level of 5 mmHg, there is progressively more deformation of the anterior retinal surface.

Figure 21.3 shows that in comparison to an ICP of 5 mmHg, when ICP is raised to 25 mmHg, there is less IOP-induced tissue deformation of the rat optic nerve. This is summarized in Fig. 21.4, where for a fixed IOP level of 70 mmHg, the effect of ICP modification becomes readily apparent. In particular, when ICP is higher, there is less surface deformation (15, 25, and 30 mmHg), whereas when ICP is lower (−5 mmHg), we observed more surface deformation. Similarly, Fig. 21.5 shows that higher ICP attenuates

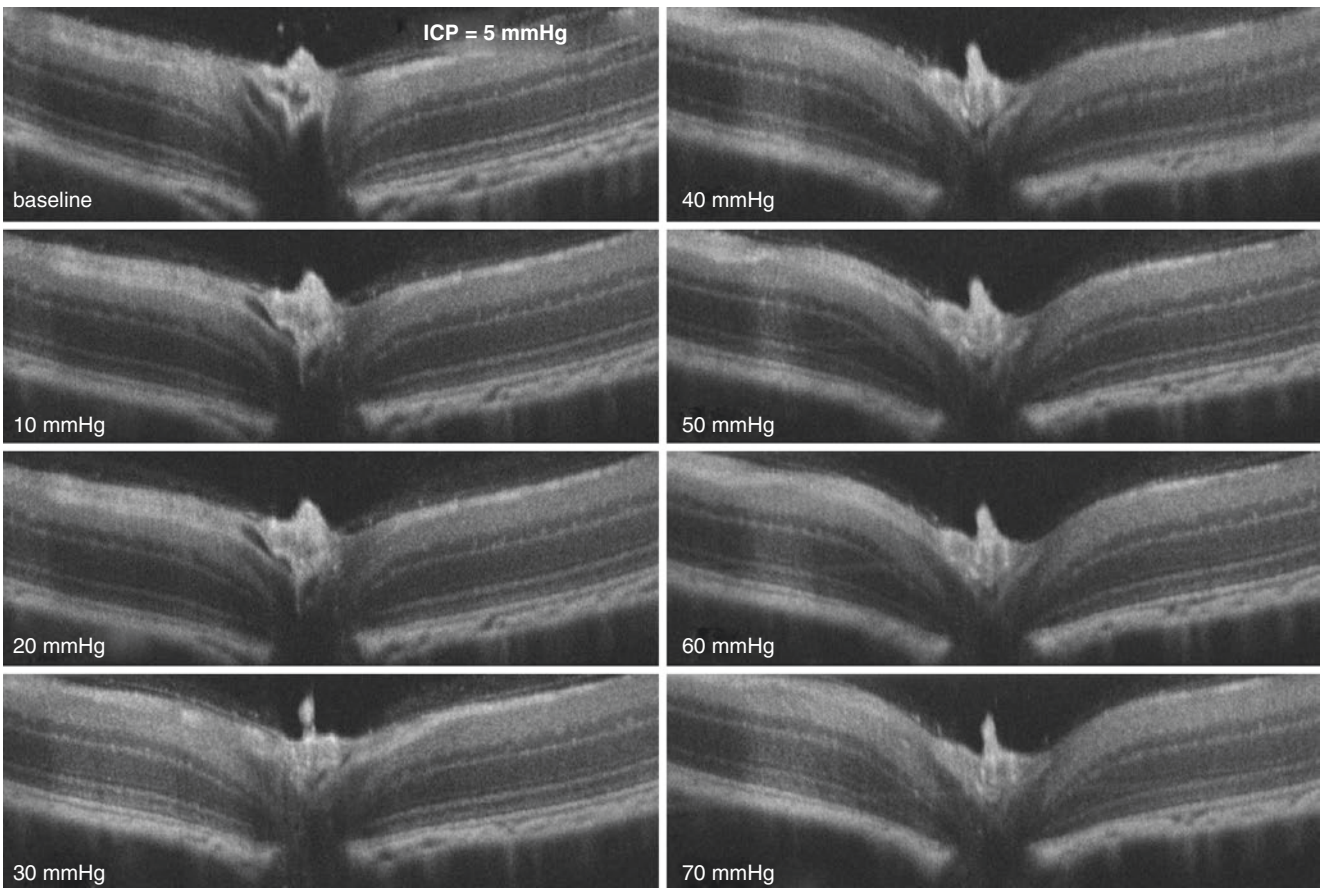

Fig. 21.2 Tissue deformation at the rodent optic nerve head at various levels of IOP levels from 10 to 70 mmHg. Intracranial pressure was marinated at 5 mmHg through the IOP procedure [8]

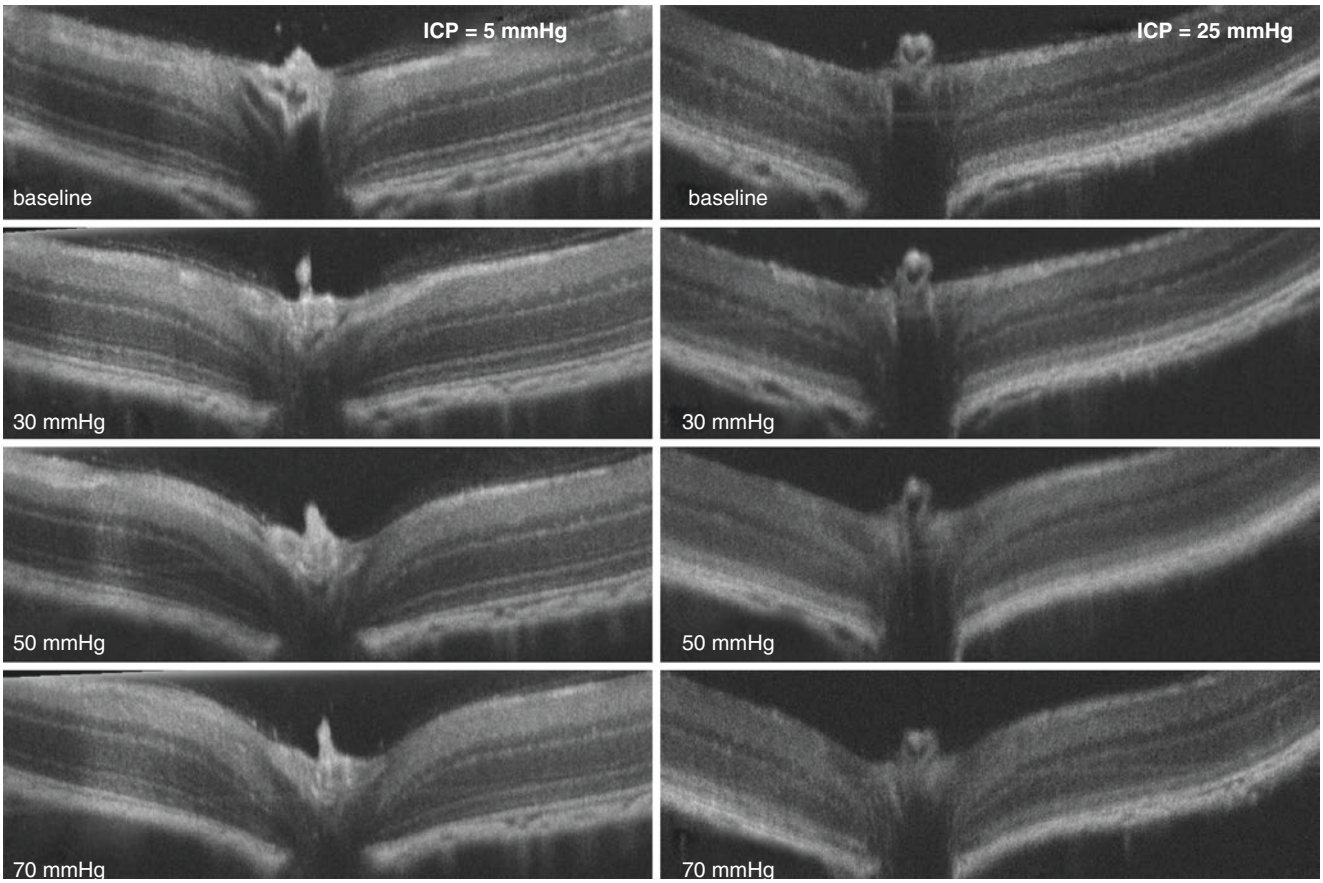

Fig. 21.3 Effect of ICP on the response of the rat optic nerve to IOP elevation. At selected IOP levels, it is clear that when ICP is raised, there is less deformation of the anterior surface of the optic nerve [8]

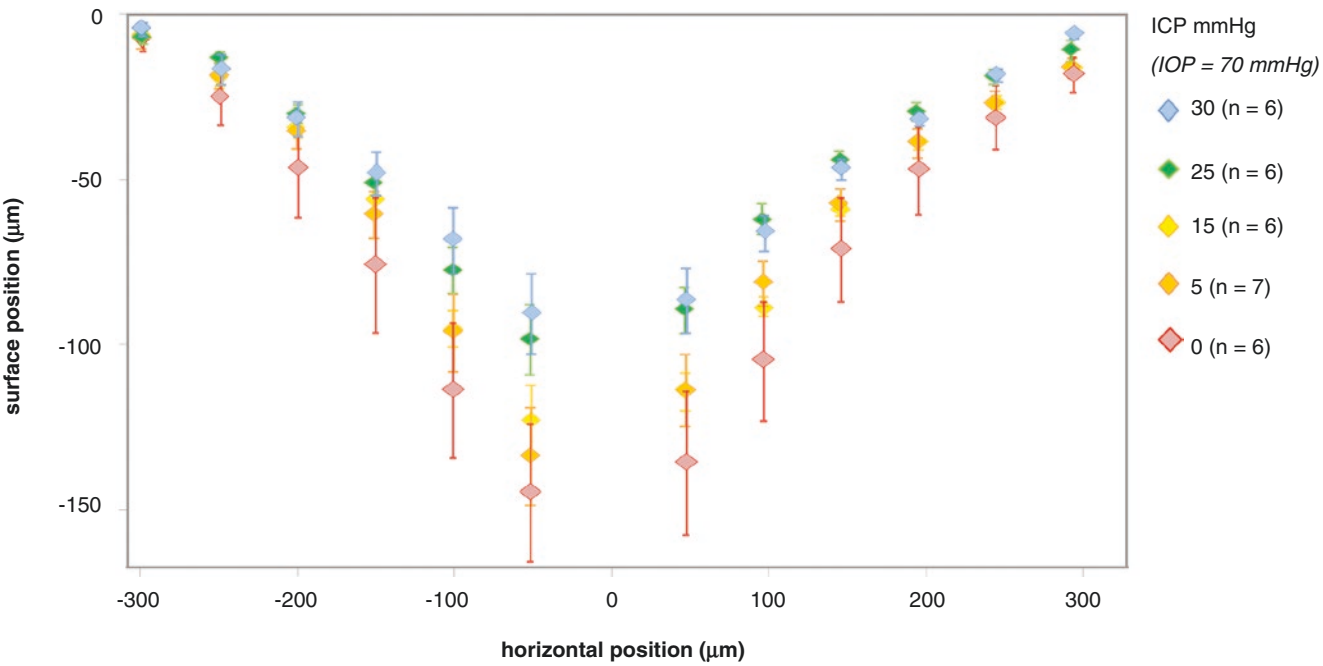

Fig. 21.4 Summary of effect of IOP elevation (70 mmHg) on the anterior retina surface at a range of ICP levels. Relative retinal surface position (±SEM) measured at a range of locations on either side of the optic nerve. Deformation is greater nearer the center of the optic nerve. Deformation seen with IOP elevation is increased at lower ICP and reduced at higher ICP [8]

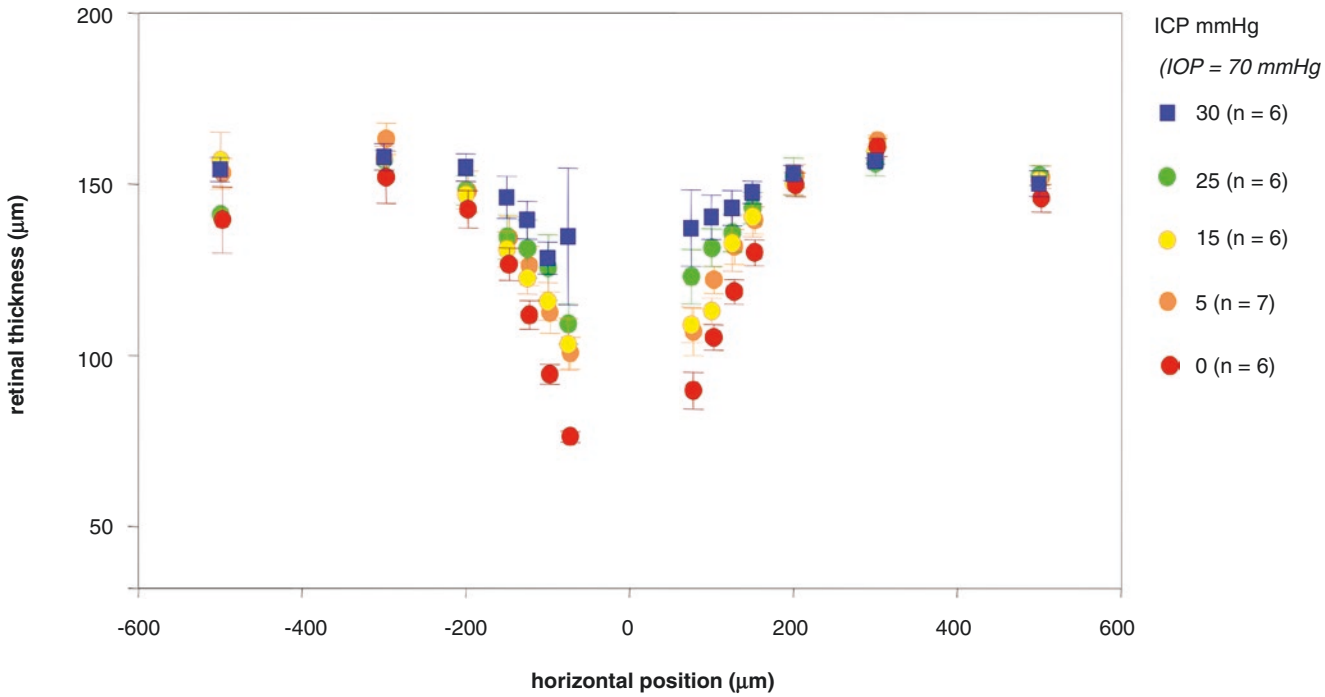

Fig. 21.5 Summary of effect of IOP elevation (70 mmHg) on retinal thickness at a range of ICP levels. Retinal thickness (±SEM) measured at a range of locations on either side of the optic nerve. Retinal compression is greater nearer the center of the optic nerve. Retinal compression seen with IOP elevation is increased at lower ICP and reduced at higher ICP [8]

retinal compressions caused by IOP elevation, whereas low ICP exacerbates the retinal compression.

21.6 Functional Changes in Response to IOP and ICP Modification

Figures 21.6 and 21.7 clearly demonstrate that there is a functional correlate of the structural changes shown in the preceding figures. In particular, it is clear that in response to IOP elevation retinal function gradually declines. At an IOP of 70 mmHg, the ERG is less than half of its original size. This is the case for animals with ICP of 5 mmHg. In comparison, when ICP is elevated to 25 mmHg, retinal function is less affected by IOP elevation. In contrast, when ICP is lowered to 0 mmHg, there is increased function susceptibility to IOP elevation. These outcomes are summarized in Fig. 21.7.

21.7 Discussion

The above data show that the rat optic nerve shows robust responses to both IOP and ICP modification. This response was measurable in terms of structural change (deformation and compression), and for the first time, we show that there is a clear functional correlate.

We show that when ICP is high, the optic nerve tissue shows less IOP-induced deformation and compression, which correlate with reduced functional susceptibility. The converse is true when ICP is low. There were more structural changes and greater functional susceptibility to IOP elevation.

Few studies have investigated the effect that both ICP and IOP modification have on optic nerve tissues. Morgan et al. [7] assessed the effect of acute pressure manipulation on the canine optic nerve and concluded that the optic nerve pressure gradient was the major determinant of optic nerve head surface position. In fact, the authors suggested that intracranial pressure might have slightly greater effect than IOP on modifying optic nerve structure. This is in accordance with the current findings in the rats. Both our study and that of Morgan et al. [7] are qualitatively in agreement with Yang et al. [11]. This study showed that 12 months of chronic ICP lowering in nonhuman primates leads to posterior deformation of the optic nerve head and peripapillary retina. These laboratory studies provide evidence that ICP is an important determinant of optic nerve health.

Evidence is mounting in favor of ICP as a risk factor glaucoma development. A number of studies have reported that

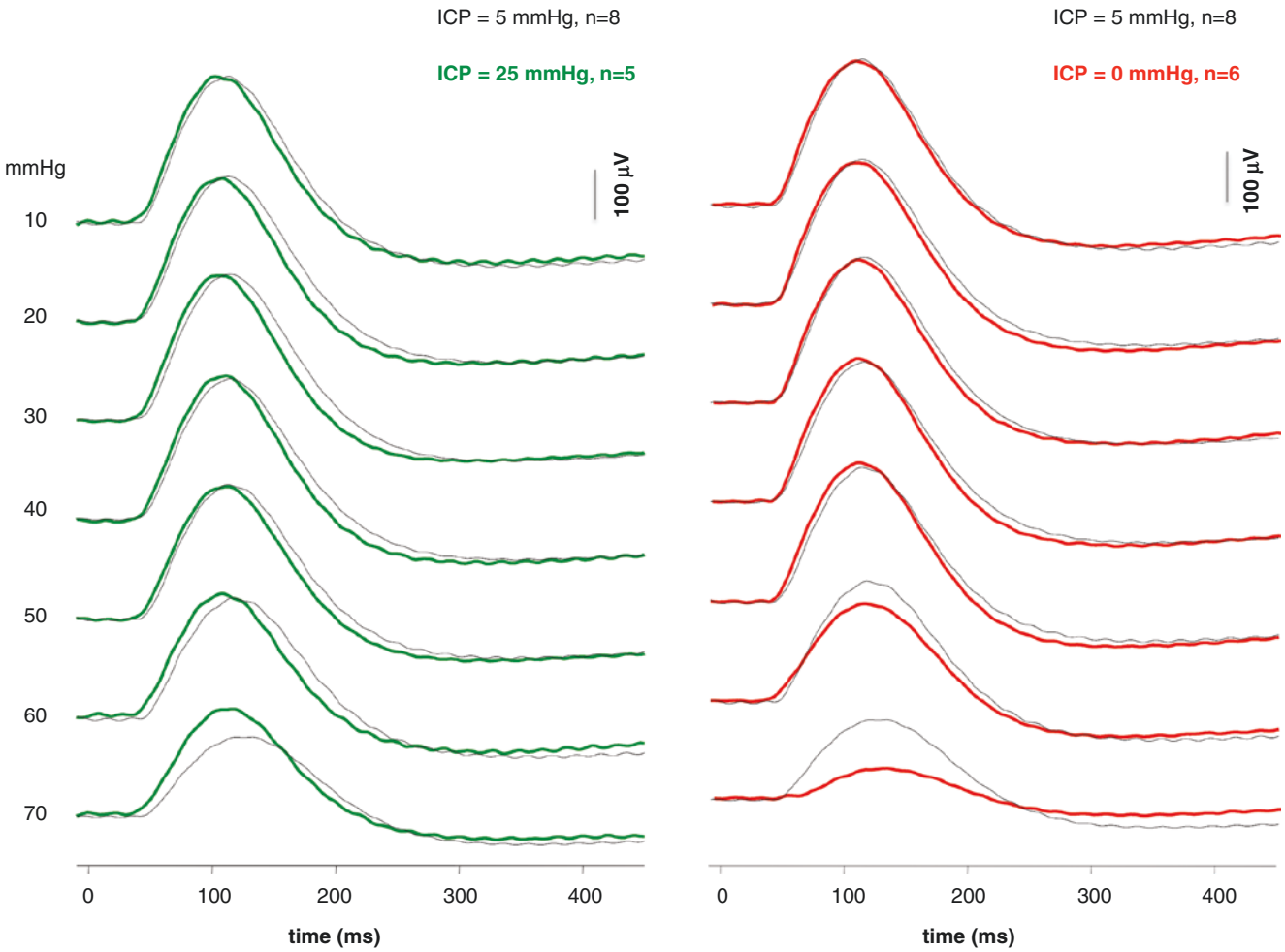

Fig. 21.6 Functional susceptibility to IOP elevation is influenced by the ICP level. ERG responses are measured at each IOP level in animals with normal (black traces), high (green traces), or low (red traces) intracranial pressure [8]

ICP is lower in glaucoma patients, which results in higher translaminar pressure gradients [12–16]. Models such as these may help us better understand how high pressure gradient might lead to ganglion cell injury in glaucoma.

21.8 Summary

1. The influence that ICP has on the optic nerve and how this might influence the risk of glaucoma are an area of interest.
2. We show for the first time that acute ICP and IOP modification affect both structure and function of the retina and optic nerve head.
3. Although the rat optic nerve lacks a well-developed connective tissue lamina cribrosa, these data suggest that rats are a good model, as IOP, ICP, and blood pressure can all be monitored and controlled during imaging for electroretinography assessment.

21.9 Future Directions

1. Relating retinal function with blood flow and optic nerve structure will move us toward a better understanding of vascular and biomechanical determinates of retinal health.
2. Studies in older animals can help us understand how aging influences the response of the optic nerve to pressure gradient modification.
3. Development of a rodent model of chronic ICP modification can help us better understand longer-term adaptive changes in the optic nerve head.

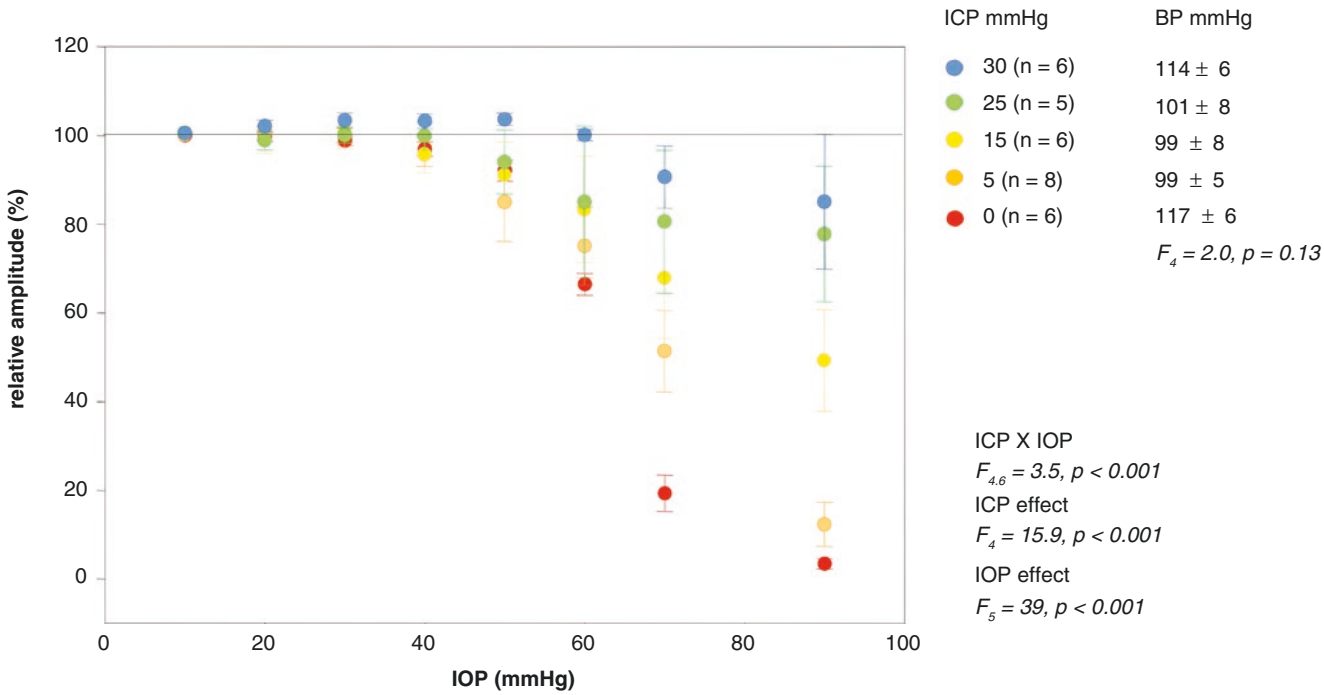

Fig. 21.7 Functional susceptibility to IOP elevation is influenced by the ICP level. ERG amplitude is expressed relative to baseline at 10 mmHg (%). Group averaged (±SEM) data for a range of ICP levels [8]

Acknowledgement Research Collaboration Grant 501098, University of Melbourne (CTON, BVB, ZH, AJV). National Health and Medical Research Council (NHMRC) Grants 1046203 (BVB, AJV), Melbourne Neuroscience Institute Fellowship (CTON).

References

1. Morgan WH, et al. The correlation between cerebrospinal fluid pressure and retrolaminar tissue pressure. Invest Ophthalmol Vis Sci. 1998;39:1419.
2. Berdahl JP, Allingham RR. Intracranial pressure and glaucoma. Curr Opin Ophthalmol. 2010;21:106.
3. Jonas JB, et al. Intracranial pressure and glaucoma. J Glaucoma. 2013;22(Suppl 5):S13.
4. Pasquale LR. Low intracranial pressure: a tipping point in our understanding of primary open-angle glaucoma? Ophthalmology. 2008;115:761.
5. Siaudvytyte L, et al. Update in intracranial pressure evaluation methods and translaminar pressure gradient role in glaucoma. Acta Ophthalmol. 2015;93:9.
6. Wostyn P, et al. Are intracranial pressure fluctuations important in glaucoma? Med Hypotheses. 2011;77:598.
7. Morgan WH, et al. Optic disc movement with variations in intraocular and cerebrospinal fluid pressure. Invest Ophthalmol Vis Sci. 2002;43:3236.
8. Zhao D, et al. The effect of intraocular and intracranial pressure on retinal structure and function in rats. Physiol Rep. 2015;3(8):2904–6.
9. He Z, et al. Blood pressure modifies retinal susceptibility to intraocular pressure elevation. PLoS One. 2012;7:e31104.
10. Bui BV, Fortune B. Ganglion cell contributions to the rat full-field electroretinogram. J Physiol. 2004;555:153.
11. Yang D, et al. Optic neuropathy induced by experimentally reduced cerebrospinal fluid pressure in monkeys. Invest Ophthalmol Vis Sci. 2014;55:3067.
12. Berdahl JP, et al. Cerebrospinal fluid pressure is decreased in primary open-angle glaucoma. Ophthalmology. 2008;115:763.
13. Ren R, et al. Cerebrospinal fluid pressure in glaucoma: a prospective study. Ophthalmology. 2010;117:259.
14. Wang N, et al. Orbital cerebrospinal fluid space in glaucoma: the Beijing intracranial and intraocular pressure (iCOP) study. Ophthalmology. 2012;119:2065.
15. Ren R, et al. Cerebrospinal fluid pressure in ocular hypertension. Acta Ophthalmol. 2011;89:e142.
16. Ren R, et al. Trans-lamina cribrosa pressure difference correlated with neuroretinal rim area in glaucoma. Graefes Arch Clin Exp Ophthalmol. 2011;249:1057.

The Optic Nerve Chamber Syndrome

22

Ruowu Hou and Ningli Wang

The main cause of glaucoma has been complex and not very clear until now. The higher intraocular pressure (IOP) is generally regarded as the high risk factor, whereas recently more and more researches have found that intracranial pressure (ICP) was also a danger factor in the pathogenesis of glaucoma, especially for "normal tension glaucoma" (NTG) in which IOP is at normal levels, but patients also suffer from progressing disk cupping and defect of visual field [1, 2]. Therefore, the elevated IOP alone cannot explain the neuropathology of NTG, and it is not clear what kind of role the ICP play. The contribution of intraocular pressure (IOP) in glaucoma has been studied for many years, but the effectiveness of the intracranial pressure (ICP) is still unknown. Furthermore, the exact correlation between ICP and IOP also remains unclear, specifically the relationship between ICP and the optic nerve subarachnoid space pressure (ONSP) [3–6].

If we want to understand the role of ICP in the glaucoma, first of all we should gain a better understanding of the cerebrospinal fluid (CSF) circulating around the optic nerve. Thus, concerning the optic neuropathy, the CSF in the optic nerve SAS and the pressure in it (ONSP) are the key point for this.

22.1 What Is the Optic Nerve Chamber Syndrome?

The optic nerve is different from the other cranial nerves such as olfactory nerve and oculomotor nerve, which is part of the tissue of the brain. In other words, it is like the myelinopathy and surrounded by CSF. Why do we want to use the concept of the optic nerve chamber syndrome to explain some phenomenons involving the optic nerve? It is because the optic nerve subarachnoid space (ONSAS) can be considered as a water pond, just like a chamber. The CSF flows from the intracranial SAS into ONSAS and then flows out from it, drained by lymphatic system, paravascular system, and meningothelial cells. The communication of the optic nerve subarachnoid space (ONSAS), "water pond," with the intracranial subarachnoid space (ISAS) is vital and essential to sustain the normal function of the optic nerve.

Under free communicative situation, we could not call it "chamber syndrome" because the CSF circulates around ONSAS, brings nutrition to it, and then takes toxic substances away from it, which is fundamental to keep the optic nerve health. It could be called "live water pond." In contrast, if the CSF could not flow from the ISAS into the ONSAS or if the CSF volume in the ONSAS is reduced for some reasons such as tumor, inflammation, trauma, and so forth, the optic nerve would not get enough nutrition from the CSF and excrete metabolic waste through the CSF drainage. To put it another way, there is decreasing or no communication between the ISAS and the ONSAS, and the "water pond" will change from living to dying: the "live water pond" turns into the "dead water pond." So, we call it the optic nerve chamber syndrome.

R. Hou
Department of Neurosurgery, Beijing Tongren Hospital,
Capital Medical University,
Beijing, China

N. Wang (✉)
Beijing Institute of Ophthalmology, Beijing Tongren Eye Center,
Beijing Tongren Hospital, Capital Medical University,
Beijing, China

Beijing Ophthalmology &Visual Sciences Key Laboratory,
Beijing, China
e-mail: wningli@vip.163.com

N. Wang (ed.), *Intraocular and Intracranial Pressure Gradient in Glaucoma*,
Advances in Visual Science and Eye Diseases 1, https://doi.org/10.1007/978-981-13-2137-5_22

22.2 How to Explain the Optic Nerve Chamber Syndrome?

Here, using the "dead water pond" explains the optic nerve chamber syndrome. Figure 22.1 shows three cavities and the correlation among pressures: CSF flows from the intracranial part via the ONSAS into the orbital part. It can be seen that there is an ICP-dependent zone (ICP 70–100%; ONSP 40–60%), in which ICP is powerful to push CSF flows from the ISAS into the ONSAS. In contrast, it is obvious that in the ICP-independent zone (when ICP < 70%), ONSP keeps relatively stationary, at about 40%, in spite of ICP declining, i.e., ICP is not sufficient to maintain CSF flowing via the optic canal. Apparently, there is a certain optic canal resistance (OCR) in the optic canal, about 30%. Furthermore, it can be found that the outflow resistance consequently is about 40%. The "dead pond theory" shows that a free CSF flowing is necessary for the optic nerve not only to receive nutrients but also to get rid of toxic wastes in the optic nerve chamber. If ICP is lower than a critical point, about 70% in normal conditions, CSF cannot inflow and outflow from the ONSAS; that is, a healthy "CSF pond" turns into a dead "CSF pond," causing the chamber syndrome with optic nerve damage.

22.3 CSF Dynamics in the Optic Nerve Chamber Syndrome

In order to explain these pressure dynamics, it is necessary to understand the anatomical structure of the optic nerve. From the perspective of anatomy, the optic nerve (ON) originates in the intracranial cavity, via ONSAS, and reaches the orbital cavities: the intraocular cavity, the intra-orbital cavity, and the intracranial cavity. Each of them owns distinctive pressure conditions: IOP, ONSP, and ICP.

Because the optic nerve is surrounded by cerebrospinal fluid, it was long assumed that ONSP is as much as ICP. But we have now shown the pressure relations are, in fact, more complex, with IOP >ICP >LCP >ONSP. There are two pressure gradients among them: one is the TLPG between the IOP and ONSP and the other is the trans-optic canal pressure gradient (TCPG) between ICP and ONSP [3, 7].

Due to CSF flowing from ISAS to the ONSAS via the optic canal, ICP is considered to influence the ONSP. The normal anatomy should be carefully studied to understand the correlation between the ICP and the ONSP. As there are three different parts on the optic nerve (Fig. 22.2) and CSF

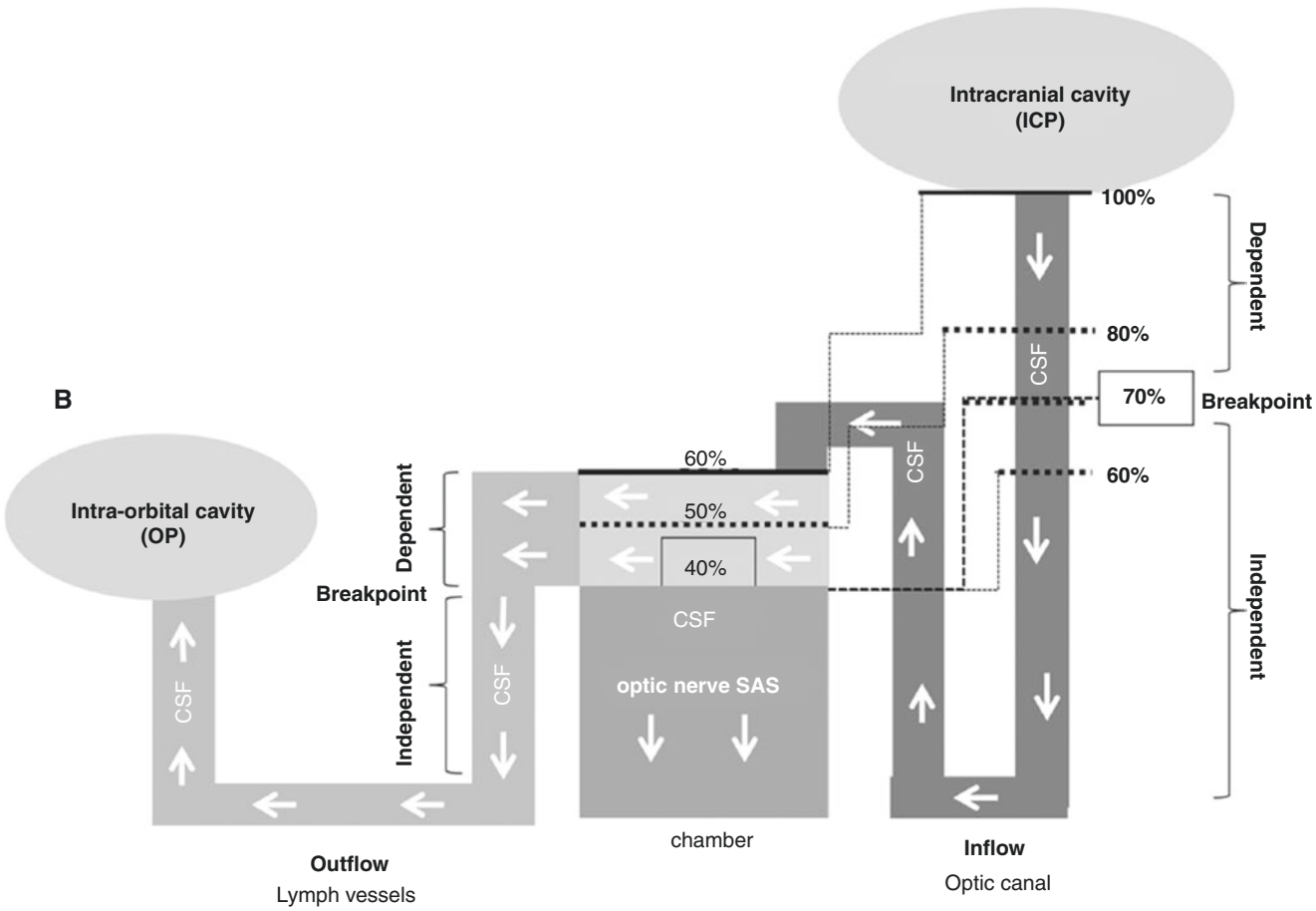

Fig. 22.1 The "dead water pond" of the optic nerve chamber syndrome (Reprinted with permission from [7])

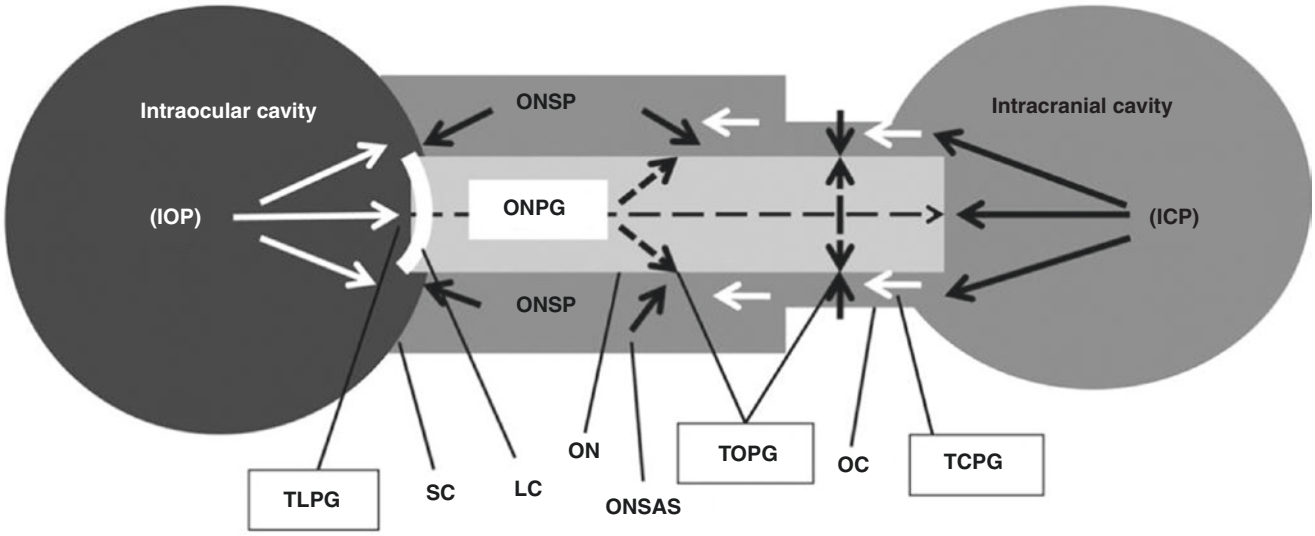

Fig. 22.2 The scheme of the pressures around the optic nerve (Reprinted with permission from [3])

flowing through them, it is better to recognize the correlation between ICP and ONSP on the basis of the dynamics of CSF.

CSF flows from the ISAS, via ONSAS, and drains into the orbit. It was considered that ONSP = ICP. However, from our studies, the pressures are, in fact, not equal in the different cavities, and the relationship is ICP > LCP > ONSP. Namely, the ONSP is lower than the ICP. Because these pressures are not the same, the optic nerve is under the influence of two pressure gradients. One is TLPG between the IOP and ONSP, and according to the results, TLPG was highest by IOP-ONSP and then IOP-LCP and lowest by IOP-ICP. The other is the trans-optic canal pressure gradient (TCPG), because CSF flows from ISAS to ONSAS and ICP directly influences ONSP. However, when ICP is below a critical point, CSF flow will stop, and ICP cannot control ONSP further.

Regarding the CSF circulation as the third circulation, in addition to the vascular circulation and lymphatic circulation, it is a special fluid circulation through the SAS. As the optic nerve is a white trace and surrounded by the pia mater, arachnoid, and dura, the ISAS extends as ONSAS. By this I mean the intracranial SAS turn into the optic nerve SAS; that is, the third circulation, CSF circulation, also plays an important role in the optic nerve. As we know, the blood supply is important and necessary for the optic nerve to gain nutrition and excrete toxics, but that is not enough for the optic nerve. The latest studies show that the CSF circulation around the optic nerve is more important than we thought [8–12].

22.4 Optic Canal Resistance in the Optic Nerve Chamber Syndrome

What causes this resistance in the optic nerve canal? To begin with, there is a critical breakpoint, and the correlations between ICP and ONSP above and below it are different. In some pathological situations causing an increase of the breakpoint such as obstructions because of traumatic or inflammatory diseases, optic canal bone thickening induced by fibrous dysplasia, and optic nerve sheath meningioma, CSF cannot flow from the ISAS to ONSAS even though ICP is in the normal range, resulting in the optic nerve chamber syndrome. A lower CSF flow would be thought of as deficiency of nutrition supply and reducing clearance of toxic substances, finally causing the optic nerve damage over time. It may be the cause in some patients of NTG although they have the normal ICP. The critical "breakpoint," therefore, could also be a possible pathological marker reflecting the CSF dynamic status in ONSAS. Hence, optic neuropathy may be a consequence of CSF pressure—ICP and ONSP—asymmetries in the optic nerve chamber. Either IOP is higher or ICP is lower could be the risk factor in the mechanism in NTG. Therefore, glaucoma, a kind of "eye disease," may actually also be a kind of "brain disease."

Given that most research is focusing on the effect of IOP on the lamina cribrosa in glaucoma, it is still unknown what is the correlation between ICP and ONSP. In fact, we also do not exactly know the CSF dynamics in the optic nerve subarachnoid space.

There are three features of the ICP-ONSP relationship in the experiment on dogs: an ICP-dependent zone, a breakpoint, and an ICP-independent zone. On the other hand, it also shows that the relationship between ICP and ONSP is not linear; in ICP-dependent zone, ONSP drops linearly with ICP decreasing, but this linear correlation no longer exists after the ICP drops to or below a certain breakpoint as ONSP keeps stable in spite of further ICP decline, which is called ICP-independent zone. Thus, the ICP-independent zone is a special area, which causes the occurrence and development of "optic nerve chamber syndrome." In other words, if the

ICP is below the critical point, CSF cannot flow from the ISAS into the ONSAS and flow out from the ONSAS. In the previous studies [13, 14], the researchers performed on sheep and studied patients with optic nerve sheath meningioma in clinic, and they also found CSF segregation by interruption of CSF flow from the ISAS into the ONSAS would lead to optic nerve chamber syndrome and optic nerve damage.

We compared our findings of the two zones: ICP-independent zone and ICP-dependent zone with the proposals by Morgan [15, 16] who have done the experiment in dogs about 20 years ago and found linear correlation between ICP and ONSP. His findings indicate that the ONSP and ICP decline together. Obviously, it is true in normal dogs, but only in ICP-dependent zone. However, in ICP-independent zone, i.e., at lower ICP levels—below the "breakpoint"—ICP and ONSP are uncoupled.

22.5 CSF Outflowing in the Optic Nerve Chamber Syndrome

CSF exchange in ONSAS involves a sufficient *inflow* as well as unobstructed *outflow*. If outflow is obstructed, the pressure in the optic nerve chamber, ONSP, increases, and a higher ICP will be needed to maintain free CSF flowing. Therefore, the critical point is determined both by the optic canal resistance and by outflow resistance. Hence, understanding the fate of the CSF may also help explain the "dead pond" phenomenon.

At present, the exact mechanism of outflow from ONSAS to the orbit part is still unclear as the end of ONSAS is cul-de-sac. Because ONSP is lower than ICP, CSF cannot flow back into the ISAS. Several animal models [17, 18] found that the possible passways of CSF flowing out include the olfactory cribriform plate, nasal submucosa, and cervical lymphatics. Other researches [19, 20] have shown that CSF could drain through the lymphatic system. There are sort of pore-like openings in a thin neuroepithelial layer along the optic nerve extending into the lymphatic system. The new study shows that in the brain, the lymphatic system exists [21]. These findings support that CSF could drain into the intra-orbital cavity via the lymphatic system. Whatever the drainage mechanism may be, we firmly believe that the critical point would always be a function of the outflow pressure. Therefore, CSF flows into the ONSAS, depending on the absolute ICP, the optic canal resistance, and the outflow pressure.

22.6 The Correlation Between ICP and ONSP in the Optic Nerve Chamber Syndrome

Regardless of what causes the CSF inflow stagnation, we strongly deem that these complex pressure dysregulations are the cause of the optic nerve chamber "dead pond" syndrome. Several authors have already proposed that the optic nerve chamber syndrome is the possible mechanism of optic nerve damage in NTG [22, 23]. They, however, did not specify the correlation between ICP and ONSP. The dog experiment shows that the chamber syndrome is a balance and imbalance process. At the balance status, these pressures, at least including ICP and ONSP, keep CSF free flowing into and out of the optic nerve chamber. At the imbalance status, such as either a physical obstruction in the optic canal or a blockage of CSF drainage, the greater the TCPG is, the greater the outflow pressure is. If CSF flow stagnates, it is like a "dead pond" that has no water inflow or outflow.

Another resistant force is outflow resistance that may be caused by the lymphatic system around the optic nerve. When ONSP is higher than outflow resistance, the CSF flows out enough, and the optic nerve is kept in a healthy state (provided that inflow is sufficient).

Further studies should be conducted to identify pathological conditions that may raise the breakpoint in glaucoma or optic neuropathy and whether it is an obstruction on CSF flowing into ONSAS and/or on CSF outflowing from ONSAS. In any event, it seems clear that ICP is an essential factor in glaucoma especially NTG and optic neuropathy. The "dead pond theory" may be able to explain the chamber syndrome, guide the search for underlying mechanisms, and facilitate the discovery of new therapeutic approaches.

22.7 Conclusion

Both a higher ICP and lower ICP can cause the optic nerve damage: the former is the reason of idiopathic intracranial hypertension, and the latter is a possible cause of NTG. It is fundamental to understand the mechanism CSF in ONSAS. Therefore, the correlation between ICP and ONSP gives more evidence to CSF circulation in the optic nerve chamber and identifies the possible mechanism of the optic nerve damage, especially in glaucoma.

The pressures around the optic nerve include ICP, ONSP, and IOP. The highest is IOP and then ICP, the lowest is ONSP. Thus, there are two pressure gradients among the three pressures as they are different: TLPG and TCPG. Using diverse method to calculate TLPG is different: IOP-ONSP is the highest, followed by IOP-LCP, and IOP-ICP is the lowest.

The correlation between ICP and ONSP is not always linear. There are two zones: ICP-dependent zone and ICP-independent zone. There is a critical point between the two zones. When ICP is above the critical point, ICP and ONSP are coupled, and ONSP changed linearly. When ICP is below the critical point, ONSP remained constant in spite of the further ICP decline, i.e., they are uncoupled. This is a sign of stop of CSF free flowing from ISAS to ONSAS. Either optic canal resistance or outflowing resistance can obstacle CSF inflowing through the optic canal or outflowing into the intra-orbital cavity.

The optic nerve chamber is just like a pond. In the healthy pond, the CSF flow is balance, and the optic nerve can get enough nutrients and excrete toxic wastes. By contrast, as described by "dead pond theory," this CSF exchange arrest leads to malnutrition, accumulation of toxic substances, and, subsequently, optic nerve damage, resulting in the optic nerve chamber syndrome.

References

1. Abegao Pinto L, et al. Intraocular pressure correlates with optic nerve sheath diameter in patients with normal tension glaucoma. Graefes Arch Clin Exp Ophthalmol. 2012;250(7):1075–80.
2. Berdahl JP, et al. Intracranial pressure in primary open angle glaucoma, normal tension glaucoma, and ocular hypertension: a case-control study. Invest Ophthalmol Vis Sci. 2008;49(12):5412–8.
3. Hou R, et al. Pressure balance and imbalance in the optic nerve chamber: The Beijing Intracranial and Intraocular Pressure (iCOP) Study. Sci China Life Sci. 2016;59(5):495–503.
4. Yavin D, et al. Diagnostic accuracy of intraocular pressure measurement for the detection of raised intracranial pressure: meta-analysis: a systematic review. J Neurosurg. 2014;121(3):680–7.
5. Li Z, et al. Intraocular pressure vs intracranial pressure in disease conditions: a prospective cohort study (Beijing iCOP study). BMC Neurol. 2012;12(1):66.
6. Kirk T, et al. Measurement of intraocular and intracranial pressure: is there a relationship? Ann Neurol. 2011;70(2):323–6.
7. Hou R, et al. Intracranial pressure (ICP) and optic nerve subarachnoid space pressure (ONSP) correlation in the optic nerve chamber: the Beijing Intracranial and Intraocular Pressure (iCOP) study. Brain Res. 2016;1635:201–8.
8. Tokuda T, Kida S. erebrospinal fluid: reconsiderations and revisions of an unquestioningly accepted dogma of 100 years. Brain Nerve. 2015;67(5):617–26.
9. Kasprowicz M, et al. Intracranial pressure, its components and cerebrospinal fluid pressure-volume compensation. Acta Neurol Scand. 2015;134(3):168–80.
10. Yamada S. Cerebrospinal fluid physiology: visualization of cerebrospinal fluid dynamics using the magnetic resonance imaging Time-Spatial Inversion Pulse method. Croat Med J. 2014;55(4):337–46.
11. Killer HE. Production and circulation of cerebrospinal fluid with respect to the subarachnoid space of the optic nerve. J Glaucoma. 2013;22(Suppl 5):S8–10.
12. Sakka L, Coll G, Chazal J. Anatomy and physiology of cerebrospinal fluid. Eur Ann Otorhinolaryngol Head Neck Dis. 2011;128(6):309–16.
13. Jaggi GP, Mironov A, Huber AR, Killer HE. Optic nerve compartment syndrome in a patient with optic nerve sheath meningioma. Eur J Ophthalmol. 2007;17:454–8.
14. Jaggi GP, Harlev M, Ziegler U, Dotan S, Miller NR, Killer HE. Cerebrospinal fluid segregation optic neuropathy: an experimental model and a hypothesis. Br J Ophthalmol. 2010;94:1088–93.
15. Morgan WH, Yu DY, Cooper RL, Alder VA, Cringle SJ, Constable IJ. The influence of cerebrospinal fluid pressure on the lamina cribrosa tissue pressure gradient. Invest Ophthalmol Vis Sci. 1995;36:1163–72.
16. Morgan WH, Yu DY, Alder VA, et al. The correlation between cerebrospinal fluid pressure and retrolaminar tissue pressure. Invest Ophthalmol Vis Sci. 1998;39:1419–28.
17. Murtha LA, Yang Q, Parsons MW, et al. Cerebrospinal fluid is drained primarily via the spinal canal and olfactory route in young and aged spontaneously hypertensive rats. Fluids Barriers CNS. 2014;11:12.
18. Liu H, Ni Z, Chen Y, et al. Olfactory route for cerebrospinal fluid drainage into the cervical lymphatic system in a rabbit experimental model. Neural Regen Res. 2012;7:766–71.
19. Brinker T, Ludemann W, Berens von Rautenfeld D, Samii M. Dynamic properties of lymphatic pathways for the absorption of cerebrospinal fluid. Acta Neuropathol. 1997;94:493–8.
20. Ludemann W, Berens von Rautenfeld D, Samii M, Brinker T. Ultrastructure of the cerebrospinal fluid outflow along the optic nerve into the lymphatic system. Childs Nerv Syst. 2005;21:96–103.
21. Louveau A, Smirnov I, Keyes TJ, et al. Structural and functional features of central nervous system lymphatic vessels. Nature. 2015;523:337–41.
22. Orgul S. Compartment syndrome in the optic nerve: a new hypothesis in the pathogenesis of glaucoma. Acta Ophthalmol. 2012;90:686–9.
23. Killer HE. Compartment syndromes of the optic nerve and open-angle glaucoma. J Glaucoma. 2013;22(Suppl 5):S19–20.

The Molecular Basis of Retinal Ganglion Cell Death in Glaucoma

23

Zheng Zhang and Ningli Wang

23.1 The Role of Mitochondria

All biochemical activities accompany with energy exchange [1]. Fabulously, the oxygen consumption per tissue weight in the retina is one of the highest in the human body. Therefore, retinal tissue is heavily dependent on mitochondria for energy supplement. Retinal ganglion cells (RGCs) have been estimated to have more mitochondria than any other neurons in the central nervous system (CNS).

23.2 Mitochondrial and Mitochondrial Enzyme Distribution in the RGC

Mitochondria concentrate on regions of high energy consumption. Retinal ganglion cell axons are unmyelinated within the ocular globe, and there are many varicosities, which are rich in mitochondria in that region. The mitochondria-enriched axon varicosities with local high-energy concentration are particularly relevant for maintaining normal signal transmission. In the myelinated regions of the ganglion cell axons outside the globe, the number of mitochondria is much fewer except in the nodes of Ranvier where energy is needed for the continuous propagation of action potentials. Thus there is an asymmetrical distribution of mitochondria along the ganglion cell axons, with the unmyelinated regions within the globe (highly energy demanding) containing an enriched population of mitochondria and the myelinated regions behind the laminar cribrosa (less energy demanding) having less mitochondria. The number of mitochondria in each ganglion cell axon also varies depending on the ganglion cell axon lengths, which is determined by the localization of their somata in relation to the optic nerve head [2, 3] (Fig. 23.1).

Cytochrome c oxidase in one of the oldest enzymes known, and it accounts for more than 90% of oxygen consumption by living organisms. An increase in cytochrome c oxidase expression reflects vibrant mitochondrial activity, while a decrease in cytochrome c oxidase expression is represented as a mark of neurodegeneration. Histochemical staining shows that mitochondrial enzymes are predominantly located in the non-myelinated axons in the retina and optic nerve head and have a less expression in the optic nerve. Presumably, an alteration in the functional status of mitochondria will influence nerve axon survival in a disease like glaucoma.

23.3 Dynamics of Mitochondria

As the intracellular diffusion of ATP is restricted, changes in regional energy demands mainly depend on mitochondrial motility. Mitochondria move toward regions of high energy requirements and away from regions of low energy requirements. Mitochondria are transported bidirectionally by the anterograde and retrograde axonal transport.

Z. Zhang · N. Wang (✉)
Beijing Institute of Ophthalmology, Beijing Tongren Eye Center, Beijing Tongren Hospital, Capital Medical University, Beijing, China

Beijing Ophthalmology & Visual Sciences Key Laboratory, Beijing, China
e-mail: wningli@vip.163.com

N. Wang (ed.), *Intraocular and Intracranial Pressure Gradient in Glaucoma*,
Advances in Visual Science and Eye Diseases 1, https://doi.org/10.1007/978-981-13-2137-5_23

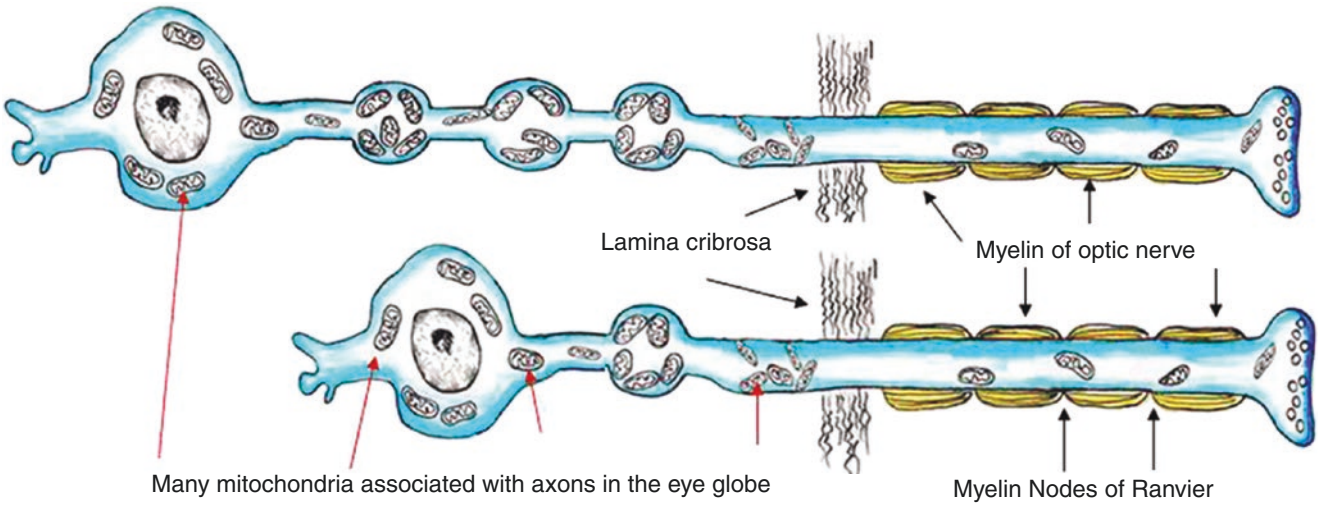

Fig. 23.1 Diagrammatic view of two ganglion cells having different axon lengths within the eye globe. The supplement of mitochondria for each ganglion cell axon varies depending on their axonal length. Ganglion cell axons in the myelinated optic nerve have few mitochondria except at the nodes of Ranvier and in the unmyelinated regions have enriched population of mitochondria (Reprinted with permission from [2])

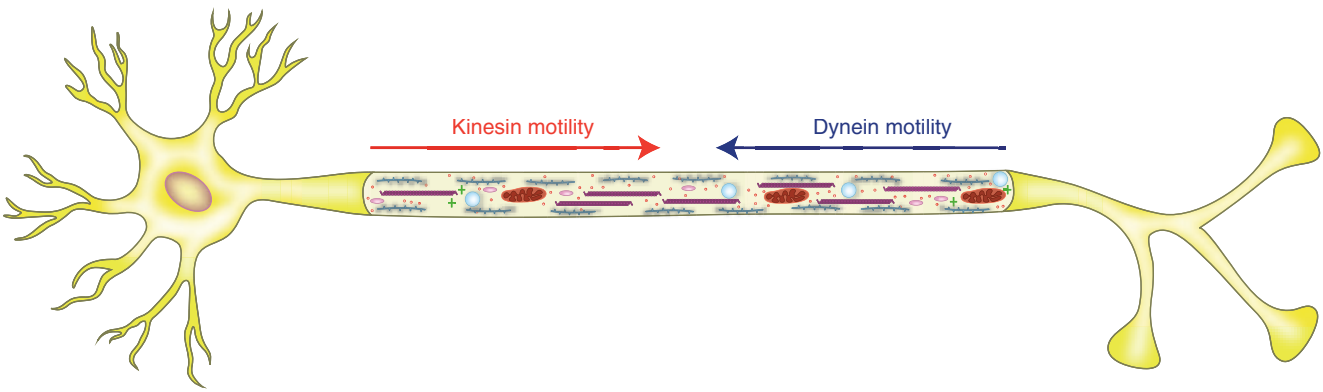

Fig. 23.2 Diagrammatic view of axonal transport

The long-distance movement along microtubules (MTs) is supported by kinesin motor proteins, for anterograde transport, and by dynein motor proteins for retrograde transport. Translocation along actin filaments is assumable driven by myosin V. However, the proteins that mediate mitochondria docking remain unknown.

Mitochondria vary in shape and size caused by fission and fusion event, which usually retains a dynamic balance. Interruption of mitochondrial fission activity will lead to the formation of large elongated organelles caused by ongoing fusion events, while breaking of the fusion activity will result in the generation of multiple small organelles. Large dynamin-related GTPases and proteins such as Opa1 are the core element for mitochondrial network maintenance, so the abnormal expression of those proteins can lead to excessive fission and cell death.

23.4 Importance of Axonal Transport

An abnormal accumulation of proteins in the optic nerve head is the earliest indication of RGC damage. Axonal transport refers to the process whereby vesicles are transported along microtubules by the dynein and kinesin motor proteins. The dynein and kinesin motor proteins gain energy by hydrolyzing ATP (adenosine triphosphate), which is mainly produced by the mitochondria. Axonal transport is vital to ensure communication between the cell body and synapse, so interruption of axonal transport is potentially fatal to the cells. Orthograde axonal transport is mainly in charge of transporting the translated proteins from the cell body to the synapse. Retrograde transport is mainly in charge of transporting neurotrophic factor from the synapse to the cell body [4] (Fig. 23.2).

23.5 Mitochondrial Dysfunction

Mitochondrial dysfunction has been reported to have an important role in RGC death in glaucoma [5, 6]. Changes in the optic nerve head, including disruption in blood flow dynamics and ischemia during glaucomatous damage, might impair mitochondrial function and weaken RGC viability [2]. RGCs have numerous mitochondria in their soma and axons, which reflect their high metabolic activity and energy demand [7, 8]. A recent study demonstrated that the ATP content in the mouse optic nerve dropped with age and that the rate of ATP reduction was positive related to increased intraocular pressure in glaucomatous DBA/2 J mice [9]. Another study by Ju found that the optic nerve degeneration that occurs in DBA/2 J mice with elevated IOP includes changes of COX reduction, mitochondrial fission, and abnormal mitochondrial cristae depletion and alterations of OPA1 and Dnm1 expression [10]. These findings suggest that mitochondrial dysfunction contributes to the pressure-related RGC axon degeneration in glaucomatous optic neuropathy. Also, the lack of energy supply due to reduced ATP availability could have a negative impact on RGC function because it disables Na^+/K^+ ion pumps, which play an important role in transduction of action potentials along RGC axons. Of interest, a mathematic model established by Band revealed that abnormal TLPD can disrupt the diffusion of ATP along the axoplasm and result in the blockage of axonal transport, which finally leads to cell death [11].

23.6 Axonal Transport Failure

Disruption of the axonal transport in the retinal ganglion cell axons impacts the viability of the retinal ganglion cells by reducing the supply of neurotrophic factors. The bottleneck of the orthograde and retrograde axonal transport in the visual afference is the lamina cribrosa of the optic nerve head with its trans-lamina pressure difference (TLPD) between the intraocular compartment (i.e., the IOP) and the subarachnoid compartment behind the lamina cribrosa (i.e., the CSFP). Previous studies have showed that an experimentally elevated IOP can lead to the impediment of both the orthograde and the retrograde axonal transport in animals. By including the CSFP as one of the two determinants of TLPD into the discussion of the pathogenic mechanism of glaucomatous optic neuropathy, we designed our study to inspect whether an abnormally low CSFP is associated with the disturbance of the axonal transport, similar to the situation with an elevated IOP. We injected rhodamine-ß-isothiocyanate (RITC) into the vitreous and examined the distribution of RITC within optic nerve axons to assess the change of the orthograde axonal transport in the low-CSFP rat model. We injected fluorogold into the superior colliculi and examined the retinal fluorogold fluorescence to assess the retrograde axonal transport in the same model.

The results of the study showed that fluorogold fluorescence of RITC in the retina was significantly ($P < 0.05$) lower in the low-CSFP group than in the control group at 24 h after baseline. At 6 h after the fluorogold injection, fluorogold intensity in the retina was significantly lower in the IOP40-group, the PP25-group, and the low-CSFP group than in the control groups, and the attenuation of retinal fluorogold fluorescence in the low-CSFP group was continued to 24 h after fluorogold injection. Our experimental study revealed that in both groups either with elevated IOP or with reduced CSFP, the orthograde axonal transport and the retrograde axonal transport in the retinal ganglion cell axons were all retardant, and the impediment of axonal transport may play an important role in the pathogenesis of glaucomatous optic neuropathy [12].

The PNIFF theory proposed by Band explains our findings well. The theory hypothesize that (1) the elevation of TLPD causes fluid to permeate the axon's membranes, creating a passive neuronal intracellular fluid flux (PNIFF) within the axoplasm. (2) If the PNIFF is strong enough, it interrupts the normal diffusive ATP transport, causing sporadic washout zones in which ATP is depleted. (3) The ATP deficiency leads to short of energy that disrupts axonal transport. The communication between the cell body and the synapse will be disrupted, which could lead to cell death (Figs. 23.3 and 23.4).

Our study also found that the RGC axons in both the high-IOP group and the low-CSFP group as compared to the control group became abnormally dilated and accumulated with vesicles. Both high TLPD groups as compared to the control group showed an accumulation of dynein motor protein at the optic nerve head and retina and a reduction of kinesin motor protein in the optic nerve, which also verified that the lamina is a bottleneck for axonal transport during the change of TLPD [13].

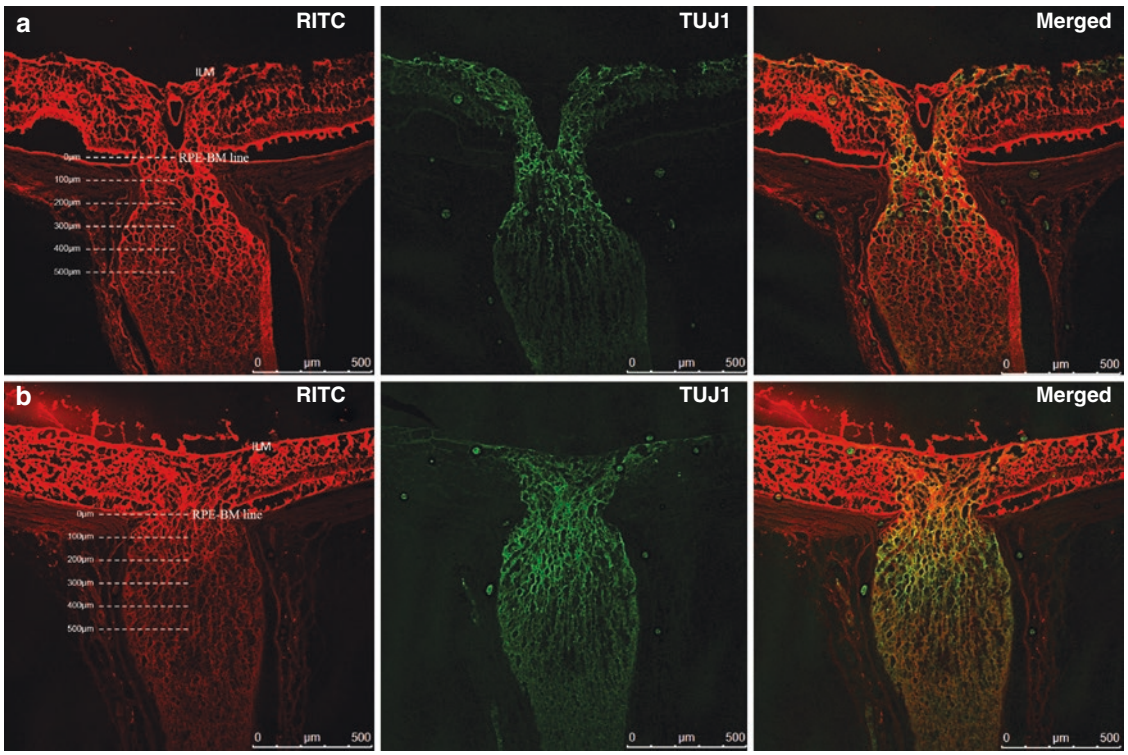

Fig. 23.3 Orthograde axonal transport of rhodamine isothiocyanate (RITC) in the optic nerve of rats of the control group (**a**) and in the optic nerve of rats with a short-term (6 h) reduction in cerebrospinal fluid pressure (**b**), imaged at 1 day after surgery. Note: RITC transported deeper into the optic nerve in the eye of the control group (**a**) than in the eye with low cerebrospinal fluid pressure (**b**). Scale bars: 500 μm (Reprinted with permission from [12])

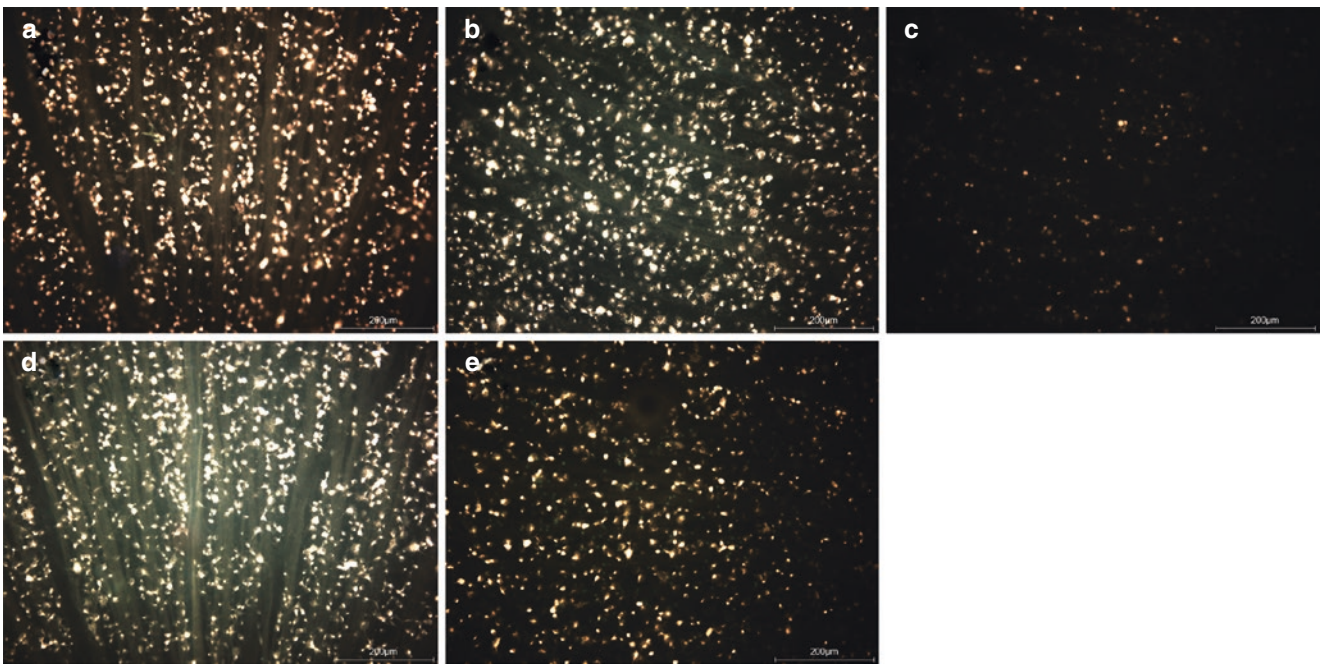

Fig. 23.4 Fluorogold fluorescence on retinal flat mounts after injection of fluorogold in rats of the control group (**a**), in rats with a short-term (6 h) elevation of intraocular pressure to 40 mmHg (**b**), in rats with a short-term (6 h) reduction of the ocular perfusion pressure to 25 mmHg (**c**), in rats of a sham control group (**d**), and in rats with an experimental short-term (6 h) reduction in cerebrospinal fluid pressure (**e**), imaged at 24 h after surgery; (**f**): quantitative analysis of the retrograde axonal transport assay. Error bars: standard deviation; *significant at $P < 0.05$ when low-ocular perfusion pressure group was compared with the control group; **significant at $P < 0.05$ when low cerebrospinal fluid pressure group was compared with the sham control group; n = six retinal flat mounts per group. Scale bars: (**a**–**e**) 200 μm (Reprinted with permission from [12])

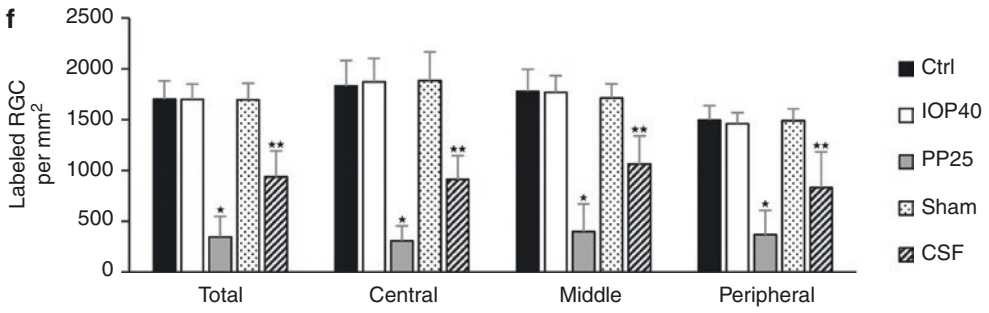

Fig. 23.4 (continued)

References

1. Coyle JT, Puttfarcken P. Oxidative stress, glutamate, and neurodegenerative disorders. Science. 1993;262(5134):689–95.
2. Osborne NN. Mitochondria: their role in ganglion cell death and survival in primary open angle glaucoma. Exp Eye Res. 2010;90(6):750–7.
3. Osborne NN, del Olmo-Aguado S. Maintenance of retinal ganglion cell mitochondrial functions as a neuroprotective strategy in glaucoma. Curr Opin Pharmacol. 2013;13(1):16–22.
4. Morgan JE. Circulation and axonal transport in the optic nerve. Eye (Lond). 2004;18(11):1089–95.
5. Kong GY, Van Bergen NJ, Trounce IA, Crowston JG. Mitochondrial dysfunction and glaucoma. J Glaucoma. 2009;18(2):93–100.
6. Lee S, Van Bergen NJ, Kong GY, Chrysostomou V, Waugh HS, O'Neill EC, Crowston JG, Trounce IA. Mitochondrial dysfunction in glaucoma and emerging bioenergetic therapies. Exp Eye Res. 2011;93(2):204–12.
7. Hollander H, Makarov F, Stefani FH, Stone J. Evidence of constriction of optic nerve axons at the lamina cribrosa in the normotensive eye in humans and other mammals. Ophthalmic Res. 1995;27(5):296–309.
8. Wang L, Dong J, Cull G, Fortune B, Cioffi GA. Varicosities of intraretinal ganglion cell axons in human and nonhuman primates. Invest Ophthalmol Vis Sci. 2003;44(1):2–9.
9. Baltan S, Inman DM, Danilov CA, Morrison RS, Calkins DJ, Horner PJ. Metabolic vulnerability disposes retinal ganglion cell axons to dysfunction in a model of glaucomatous degeneration. J Neurosci. 2010;30(16):5644–52.
10. Ju WK, Kim KY, Lindsey JD, Angert M, Duong-Polk KX, Scott RT, Kim JJ, Kukhmazov I, Ellisman MH, Perkins GA, et al. Intraocular pressure elevation induces mitochondrial fission and triggers OPA1 release in glaucomatous optic nerve. Invest Ophthalmol Vis Sci. 2008;49(11):4903–11.
11. Band LR, Hall CL, Richardson G, Jensen OE, Siggers JH, Foss AJ. Intracellular flow in optic nerve axons: a mechanism for cell death in glaucoma. Invest Ophthalmol Vis Sci. 2009;50(8):3750–8.
12. Zhang Z, Liu D, Jonas JB, Wu S, Kwong JM, Zhang J, Liu Q, Li L, Lu Q, Yang D, et al. Axonal transport in the rat optic nerve following short-term reduction in cerebrospinal fluid pressure or elevation in intraocular pressure. Invest Ophthalmol Vis Sci. 2015;56(8):4257–66.
13. Zhang Z, Wu S, Jonas JB, Zhang J, Liu K, Lu Q, Wang N. Dynein, kinesin and morphological changes in optic nerve axons in a rat model with cerebrospinal fluid pressure reduction: the Beijing Intracranial and Intraocular Pressure (iCOP) study. Acta Ophthalmol. 2015;94(3):266–75.

24 Trans-lamina Cribrosa Pressure Difference Activates Mechanical Stress Signal Transduction to Induce Glaucomatous Optic Neuropathy: A Hypothesis

Jingxue Zhang, Shen Wu, and Ningli Wang

24.1 Background

Glaucoma is the leading cause of irreversible blindness in the world. According to a recent meta-analysis, the global prevalence of glaucoma has reached 3.54%, and the number of people with glaucoma worldwide would increase to 110 million in 2040. Glaucoma, as one of the most common eye conditions resulting in blindness, has been recognized as a major public health challenge [1].

Glaucoma is a group of optic nerve degenerative disorders characterized by progressive loss of retinal ganglion cells (RGCs) and their axons, resulting in progressive optic neuropathy and visual field loss [2]. Glaucoma can be roughly divided into two main categories: primary angle-closure glaucoma (PACG) and primary open-angle glaucoma (POAG). In China, the proportion of POAG in all glaucoma cases has gradually increased from 47.5 to 70.4–76.4%, and POAG is becoming the most common cause of irreversible blindness [3]. As the etiology of POAG remains unknown, there is still a lack of effective treatment strategies, leading to a high incidence rate of blindness. Therefore, it is imperative to clarify the pathogenesis of POAG to seek for effective targets and interventions.

At present, the proposed mechanisms of POAG-induced optic neuropathy mainly include "mechanical hypothesis," [4, 5] "vascular hypothesis," [6] and "mixed mechanical-vascular hypothesis." Elevated intraocular pressure (IOP) is a known risk factor for optic neuropathy [2]. According to the mechanical hypothesis, IOP elevation induces posterior deformation of the optic disk and the lamina cribrosa, resulting in distortion of the optic nerve passing through these structures, blockage of axoplasmic flow, destruction of axonal functions, apoptosis of RGCs, and thus the occurrence of pressure-related optic neuropathy. It is postulated in ischemic injury hypothesis that in an environment with elevated IOP, the self-regulatory function of blood circulation in the optic disk area may become decompensated, leading to a cascade of optic neuropathies.

Although these hypotheses explain the possible pathogenesis of optic neuropathy in a subset of glaucomatous patients, some clinical phenomena still remain inexplicable. For example, why do up to 83% of patients with normal tension glaucoma (NTG) still suffer from glaucomatous optic neuropathy in China [7]? Why does glaucomatous optic neuropathy only occur in a subset of patients with ocular hypertension (OHT) [2]? Why does optic neuropathy continues to progress in some glaucomatous patients despite well-controlled IOP? All of these cannot be explained by the current hypotheses, indicating that some other unknown mechanisms may underlie the pathogenesis of glaucoma.

Together with Prof. Allingham and his colleagues from Duke University, we conducted a series of clinical studies and found that about 70–80% of patients with NTG had a lower intracranial pressure (ICP) compared with that of OHT patients and normal controls, with significantly enlarged IOP-ICP difference [8–11]. In OHT patients without optic neuropathy despite their increased IOP, increased ICP was also observed, and the IOP-ICP difference remained generally unchanged [12]. A further meta-analysis showed that no single factor—either IOP or ICP—could account for the occurrence of glaucomatous optic neuropathy; it might be caused by the changes in trans-lamina cribrosa pressure difference (TLPD) (Fig. 24.1) [13].

The pre-laminar tissue is exposed to intraocular pressure (IOP), while the post-laminar optic nerve is subjected to cerebrospinal fluid (CSF) pressure in the subarachnoid space; thus, trans-lamina cribrosa pressure difference

J. Zhang · S. Wu · N. Wang (✉)
Beijing Institute of Ophthalmology, Beijing Tongren Eye Center, Beijing Tongren Hospital, Capital Medical University, Beijing, China

Beijing Ophthalmology & Visual Sciences Key Laboratory, Beijing, China
e-mail: wningli@vip.163.com

N. Wang (ed.), *Intraocular and Intracranial Pressure Gradient in Glaucoma*,
Advances in Visual Science and Eye Diseases 1, https://doi.org/10.1007/978-981-13-2137-5_24

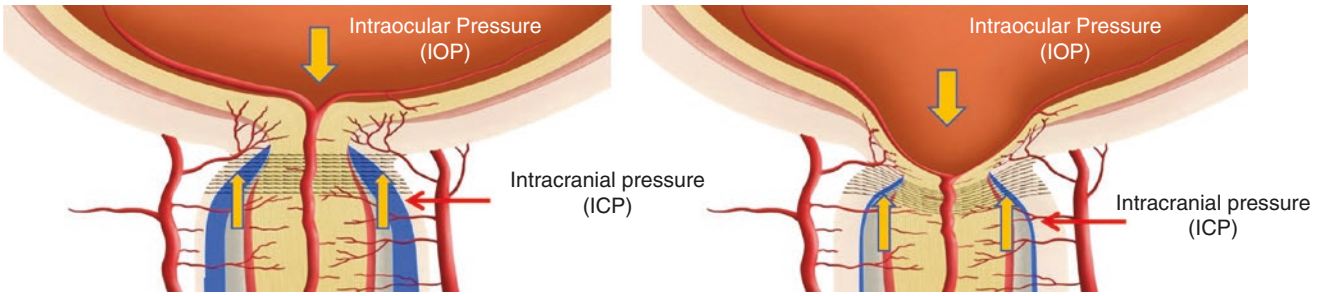

Fig. 24.1 Diagram of trans-lamina cribrosa pressure difference

Table 24.1 TLPD changes due to different causes may exert different biological effects to induce optic neuropathy

	Direct damage to RGCs	Laminar deformation	Impaired axoplasmic transport	Microenvironmental changes
TLPD elevation (glaucoma with higher IOP)	√	√	√	Ischemia, glia activation, inflammation
TLPD reduction (POAG or lower ICP)	×	×	√	Undefined

Notes: TLPD elevation (PACG or higher IOP) may induce direct damage to RGCs and laminar deformation to cause optic neuropathy, while TLPD reduction (POAG or lower ICP) mainly induces mechanical microenvironmental changes and impaired axoplasmic transport

(TLPD) is formed between the pre-laminar IOP and the post-laminar CSF pressure. In normal conditions, a relatively stable TLPD is maintained between IOP and CSF pressure (A); however, the TLPD becomes larger in the case of increased IOP or decreased CSF pressure, leading to optic neuropathy.

Although the eyeball and the cranial cavity are two anatomically separate chambers, ICP and IOP are interrelated via the optic nerve and its surrounding CSF-containing spaces. It is essential to maintain a stable TLPD, namely, the mechanical microenvironment balance between ICP and IOP. In the presence of ICP-IOP imbalance, the mechanical microenvironment related to the optic nerve is disturbed, which may be responsible for the occurrence of glaucomatous optic neuropathy.

However, we noted that a large TLPD resulted from low ICP or high IOP might induce somewhat different forms of optic neuropathies. In primate animal models with a large TLPD due to ICP reduction, laminar deformation associated with OHT was not observed, indicating that the cause of optic neuropathy might be independent of laminar deformation or squeezing postulated in the "mechanical hypothesis" [14]. In rat models without laminar structures, a large TLPD due to ICP reduction could also result in glaucomatous optic neuropathy in the absence of lamina cribrosa. It is assumed that these damages may be mainly caused by impaired axoplasmic transport and mitochondrial deformation or loss of RGCs, which are closely related with changes in the mechanical microenvironment [15].

These findings indicate that the pathogenic mechanism of optic neuropathy may vary with the cause of TLPD changes (Table 24.1). IOP elevation may exert strong biomechanical effects; although impaired axoplasmic transport may also exist due to mechanical microenvironmental changes, the main contributor to optic neuropathy is posterior laminar deformation, leading to distortion or extrusion of the optic nerve passing through the lamina cribrosa and damages to RGCs, which supports the traditional "mechanical hypothesis." Compared with IOP elevation, ICP reduction tends to produce weaker mechanical effects on RGCs and optic nerve; mitochondrial injury and impaired axoplasmic transport due to mechanical microenvironmental changes may mainly account for the occurrence of glaucomatous optic neuropathy. It is important to clarify the molecular mechanisms underlying optic neuropathy, which may provide novel insights into the clinical management of POAG.

In order to elucidate the pathogenesis of glaucomatous optic neuropathy, we need to define the mechanical microenvironment surrounding RGCs and optic nerve. In the eyeball, the RGCs and optic nerve are exposed to IOP, which generates two dimensions of forces. On the one hand, as IOP is generally higher than the inherent pressure of the retina and optic nerve tissues, an inside-to-outside hydrostatic pressure force is exerted perpendicularly (F1). On the other hand, a surface tension force is produced on the peripheral optic disk (F2), particularly when the optic disk bears the maximum force [16–18] (Fig. 24.2). As for the intracanalicular segment of the optic nerve, it is subjected to CSF pressure in the subarachnoid space, which generates a forward hydrostatic pressure force on the optic disk. All of these forces, belonging to the category of mechanical stress, form the stress microenvironment surrounding the retina and optic nerve, which is

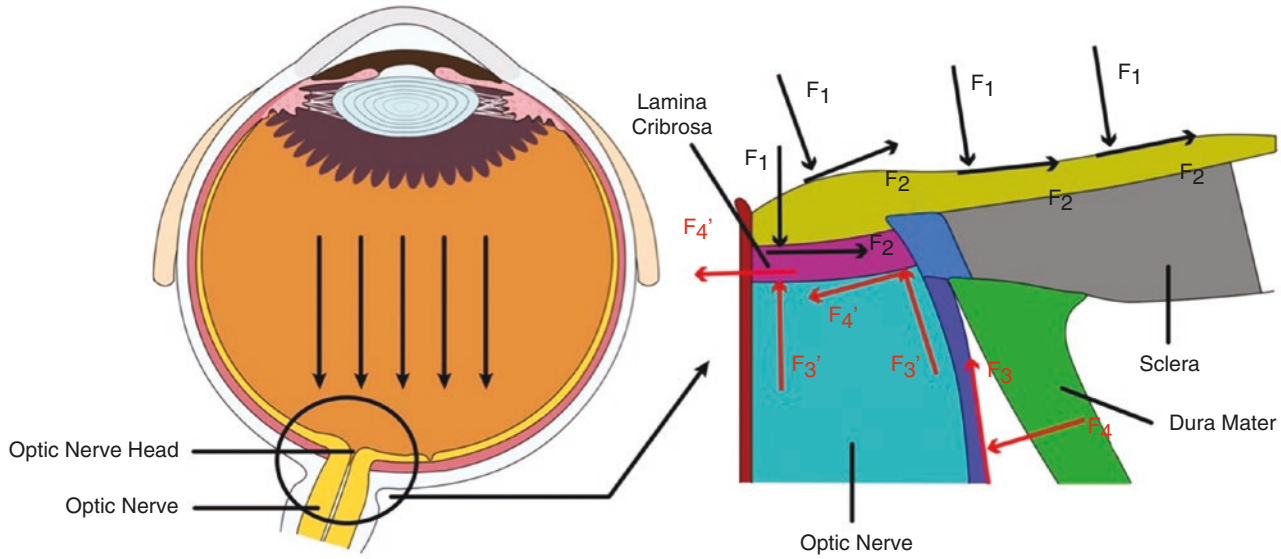

Fig. 24.2 Mechanical analysis of the optic nerve

maintained stable and balanced in normal conditions. Any stress variations in this microenvironment would induce pressure-related biological changes.

24.2 Unsolved Question

But how do RGCs and their surrounding gliocytes sense these stress variations and convert them into biochemical signals and finally produce a biological response? This is a key question in this field that remains to be answered.

Prior cardiovascular and orthopedic studies have found stress-sensitive receptors on the cell surface, and these receptors could sense and transmit mechanical signals to different intracellular structural components via specific molecular channels on the cell surface, so as to realize mechanochemical transformation and regulate cellular physiological functions; such receptors mainly include integrins and ion channels [19]. Under mechanical stress, the integrin receptors on the surface of cardiovascular endothelial cells and osteoblasts can bind to transmembrane adhesion proteins such as extracellular matrix (ECM) to form a ECM—focal adhesion complex—cytoskeleton network system, through which mechanobiological signal transduction is achieved both extracellularly and intracellularly to play a role in regulating cell movement, adhesion, proliferation, and apoptosis as well as mitochondrial dysfunction via Rho, MAPK, JAK-SATA, and other signaling pathways [20–22]. On the other hand, integrins are connected to the cytoskeleton, providing a physical approach for stress transfer [23]. Through this approach, the cell nucleus is able to directly respond to the changes in ECM adhesiveness and mechanical stress to modulate gene transcription [24] and also directly stimulate calcium release from the intracellular calcium pool [25, 26]. In addition to integrin receptors, mechanical stress can also stimulate the opening of ion channels on the cell surface, disturb the intracellular calcium homeostasis, and induce mitochondrial dysfunctions such as decreased mitochondrial membrane potential, abnormal ROS metabolism, and reduced ATP production, which may finally lead to cell death [27, 28].

It has been shown in recent studies that integrin and ion channel receptors generally exist in RGCs and gliocytes, and both of them play a role in modulating cellular biochemical reactions. The integrin-FAK signaling pathway mediates the cytoskeletal rearrangement of astrocytes in the optic nerve head [29] and regulates the apoptosis of RGCs [30]. In vitro cell experiments found that ion channel receptors such as TRPV could mediate the increase in intracellular calcium concentration of RGCs [31, 32], resulting in inflammatory response and cell apoptosis. But it still remains unknown whether the mechanical stress signaling mediated by integrins and ion channels plays a role in glaucomatous optic neuropathy due to a large TLPD.

24.3 Our Hypothesis

Based on these findings, we propose a hypothesis that (Fig. 24.3) optic neuropathy due to a large TLPD may be mediated by stress signaling pathways, which could perceive the changes in the mechanical microenvironment; modulate gene transcription via integrin-FAK, integrin-cytoskeleton, or ion channel pathways; and induce abnormal cytoskeletal

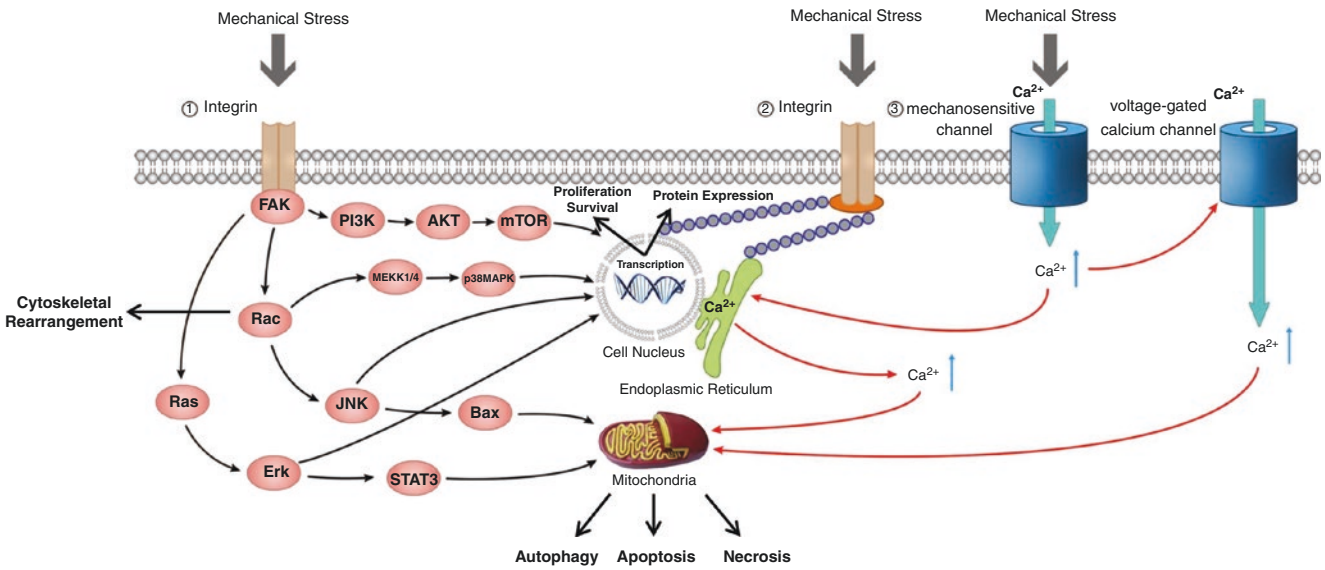

Fig. 24.3 Stimulated by pressure gradient changes, mechanical stress signaling pathways modulate RGC-related life activities

remodeling, abnormal intracellular ion concentrations, and impaired mitochondrial functions, which finally result in damages to the RGCs and optic neuropathy.

The mechanosensitive receptors on the surface of RGCs and astrocytes can be roughly divided into integrins and ion channels. Integrins are an important family of enzyme-activated receptors on the cell surface that bind to transmembrane adhesion proteins such as ECM to form a ECM—focal adhesion complex—cytoskeleton network system, through which mechanobiological signal transduction is achieved both extracellularly and intracellularly. There are three major approaches: (1) through integrin-FAK-MAPK (JNK/Erk/p38MAPK) and integrin-FAK-PI3K/AKT-mTOR pathways, integrins modulate gene transcription to get involved in important cell life activities such as cell movement, adhesion, proliferation and apoptosis; (2) through integrin-FAK-STAT3 and JNK pathways, integrins induce mitochondrial dysfunctions to trigger mitochondria apoptosis pathway; and (3) through integrin-cytoskeleton-nucleus pathways, integrins mediate the direct response of the cell nucleus and endoplasmic reticulum to mechanical stress and modulate gene transcription and intracellular calcium homeostasis. Ion channels mainly regulate the homeostasis of multiple ions inside and outside the cell. Under mechanical stress, increase in intracellular calcium concentration is one of the earliest events. In response to mechanical stimulation, the mechanosensitive channels (MCs) on the cell surface are activated to trigger rapid calcium influx. This can effectively stimulate calcium release from the intracellular calcium pool, and meanwhile cell membrane depolarization is induced to activate the voltage-gated calcium channels at the cell membrane, facilitating the influx of more extracellular calcium ions into the cell and thereby resulting in a further increase in intracellular calcium concentration. An intracellular calcium concentration that exceeds the threshold of mitochondrial metabolism would induce decreased mitochondrial membrane potential, reduced ATP production, and abnormal ROS metabolism and thus trigger mitochondria apoptosis pathway.

It is important to investigate the effect of integrin and ion channel signal transduction on cytoskeleton pathways and mitochondrial functions in RGCs and their surrounding gliocytes in the presence of mechanical microenvironmental changes. We believe that these efforts would provide a novel theoretical basis for understanding the pathogenesis of optic neuropathy in patients with POAG and also offer valuable insights into the molecular mechanism underlying mechanical stress-related long axon-type neuron injuries. Moreover, potential molecular targets for intervention may be identified to enhance the ability of RGCs to fight against pressure gradient: we may clarify whether mitochondria is a common target of mechanical injuries in different subtypes of glaucoma, so as to look for common interventions based on mitochondria-related pathways; meanwhile, we may also elucidate the specific molecular signaling pathways of different subtypes of glaucomatous optic neuropathy, which may aid in the design of target-specific interventions for glaucoma optic neuroprotection.

References

1. Tham YC, Li X, Wong TY, et al. Global prevalence of glaucoma and projections of glaucoma burden through 2040: a systematic review and meta-analysis. Ophthalmology. 2014;121(11):2081–90.
2. De Moraes CG, Demirel S, Gardiner SK, et al. Effect of treatment on the rate of visual field change in the ocular hypertension treatment study observation group. Investig Ophthalmol Vis Sci. 2012;53(4):1704–9.
3. Quigley HA, Broman AT. The number of people with glaucoma worldwide in 2010 and 2020. Br J Ophthalmol. 2006;90(3):262–7.
4. Fechtner RD, Weinreb RN. Mechanisms of optic nerve damage in primary open angle glaucoma. Surv Ophthalmol. 1994;39(1):23–42.
5. Burgoyne CF, Downs JC. Premise and prediction-how optic nerve head biomechanics underlies the susceptibility and clinical behavior of the aged optic nerve head. J Glaucoma. 2008;17(4):318–28.
6. Yamamoto T, Kitazawa Y. Vascular pathogenesis of normal-tension glaucoma: a possible pathogenetic factor, other than intraocular pressure, of glaucomatous optic neuropathy. Prog Retin Eye Res. 1998;17(1):127–43.
7. Liang YB, Friedman DS, Zhou Q, et al. Prevalence of primary open angle glaucoma in a rural adult Chinese population: the Handan eye study. Investig Ophthalmol Visual Sci. 2011;52(11):8250–7.
8. Ren R, Jonas JB, Tian G, et al. Cerebrospinal fluid pressure in glaucoma: a prospective study. Ophthalmology. 2010;117(2):259–26.
9. Berdahl JP, Allingham RR, Johnson DH. Cerebrospinal fluid pressure is decreased in primary open-angle glaucoma. Ophthalmology. 2008;115(5):763–8.
10. Berdahl JP, Fautsch MP, Stinnett SS, et al. Intracranial pressure in primary open angle glaucoma, normal tension glaucoma, and ocular hypertension: a case-control study. Invest Ophthalmol Vis Sci. 2008;49(12):5412–8.
11. Wostyn P, De Groot V, Van Dam D, et al. Fast circulation of cerebrospinal fluid: an alternative perspective on the protective role of high intracranial pressure in ocular hypertension. Clin Exp Optom. 2016;99(3):213–8.
12. Ren R, Zhang X, Wang N, et al. Cerebrospinal fluid pressure in ocular hypertension. Acta Ophthalmol. 2011;89(2):e142–8.
13. Siaudvytyte L, Januleviciene I, Daveckaite A, et al. Literature review and meta-analysis of translaminar pressure difference in open-angle glaucoma. Eye. 2015;29(10):1242–50.
14. Yang D, Fu J, Hou R, et al. Optic neuropathy induced by experimentally reduced cerebrospinal fluid pressure in monkeys. Invest Ophthalmol Vis Sci. 2014;55(5):3067–73.
15. Zhang Z, Wu S, Jonas JB, et al. Dynein, kinesin and morphological changes in optic nerve axons in a rat model with cerebrospinal fluid pressure reduction: the Beijing Intracranial and Intraocular Pressure (iCOP) study. Acta Ophthalmol. 2016;94(3):266–75.
16. Hernandez MR, Igoe F, Neufeld AH. Extracellular matrix of the human optic nerve head. Am J Ophthalmol. 1986;102(2):139–48.
17. Morrison JC, Jerdan JA, L'Hernault NL, et al. The extracellular matrix composition of the monkey optic nerve head. Invest Ophthalmol Vis Sci. 1988;29(7):1141–50.
18. Hernandez MR, Igoe F, Neufeld AH. Cell culture of the human lamina cribrosa. Invest Ophthalmol Vis Sci. 1988;29(1):78–89.
19. Ingber DE. Tensegrity: the architectural basis of cellular mechanotransduction[J]. Annu Rev Physiol. 2003;59(1):575–99.
20. Visavadiya NP, Keasey MP, Razskazovskiy V, et al. Integrin-FAK signaling rapidly and potently promotes mitochondrial function through STAT3. Cell Commun Signal. 2016;14(1):32.
21. Clark EA, Brugge JS. Integrins and signal transduction pathways: the road taken. Science. 1995;268(5208):233–9.
22. Cabodi S, Di Stefano P, Leal Mdel P, et al. Integrins and signal transduction. Adv Exp Med Biol. 2010;674:43–54.
23. Martins RP, Finan JD, Guilak F, et al. Mechanical regulation of nuclear structure and function. Annu Rev Biomed Eng. 2012;14:431–55.
24. Tajik A, Zhang Y, Wei F, et al. Transcription upregulation via force-induced direct stretching of chromatin. Nat Mater. Dec 2016;15(12):1287–96.
25. George CH, Higgs GV, Lai FA. Ryanodine receptor mutations associated with stress-induced ventricular tachycardia mediate increased calcium release in stimulated cardiomyocytes. Circ Res. 2003;93(6):531–40.
26. Liu B, Lu S, Zheng S, et al. Two distinct phases of calcium signalling under flow. Cardiovasc Res. 2011;91(1):124–33.
27. Bhosale G, Sharpe JA, Sundier SY, et al. Calcium signaling as a mediator of cell energy demand and a trigger to cell death. Ann N Y Acad Sci. 2015;1350:107–16.
28. Zou H, Lifshitz LM, Tuft RA, et al. Visualization of Ca2+ entry through single stretch-activated cation channels. Proc Natl Acad Sci USA. 2002;99(9):6404–9.
29. Tehrani S, Davis L, Cepurna WO, et al. Astrocyte structural and molecular response to elevated intraocular pressure occurs rapidly and precedes axonal tubulin rearrangement within the optic nerve head in a rat model. PLoS One. 2016;11(11):e0167364.
30. Santos AR, Corredor RG, Obeso BA, et al. beta1 integrin-focal adhesion kinase (FAK) signaling modulates retinal ganglion cell (RGC) survival. PLoS One. 2012;7(10):e48332.
31. Ryskamp DA, Witkovsky P, Barabas P, et al. The polymodal ion channel transient receptor potential vanilloid 4 modulates calcium flux, spiking rate, and apoptosis of mouse retinal ganglion cells. J Neurosci. 2011;31(19):7089–101.
32. Krizaj D, Ryskamp DA, Tian N, et al. From mechanosensitivity to inflammatory responses: new players in the pathology of glaucoma. Curr Eye Res. 2014;39(2):105–19.

Retinal Vessels Changes During the Low Cerebrospinal Fluid Situation

25

Lu Liu, Caixia Lin, and Ningli Wang

Glaucoma is an optic neuropathy characterized by optic disc cupping and visual field loss. Its pathogenesis mainly involves mechanical and vascular factors, the mechanical theory claims that high intraocular pressure (IOP) causes a deformation of the optic nerve head (ONH), and the vascular theory claims that glaucomatous optic neuropathy is the consequence of insufficient blood supply due to IOP elevation and other risk factors. Up to now, IOP is the only modifiable risk factor for glaucoma. Nevertheless, in some glaucoma patients, the progression of disease continues despite IOP reduction, indicating that vascular disturbance may play a more important role in the development of glaucoma in these patients.

In addition to IOP, elevated trans-lamina cribrosa pressure difference (TLPD) induced by elevated IOP or decreased cerebrospinal fluid pressure (CSFp) may be a further risk factor for glaucoma or glaucoma-like optic neuropathy [1–7]. The pre-lamina tissue is influenced by IOP, and the tissue behind the laminar cribrosa (LC) is under the influence of CSFp in the subarachnoid space of the optic nerve.

Furthermore, previous studies suggested that low CSFp had some effect on glaucomatous disease progression such as optic disc hemorrhage and visual field (VF) loss [8]. Recently we also found that in animal model, low CSFp caused disturbance of both the orthograde and retrograde axonal transport in retinal ganglion cell like high IOP [9].

Besides, some clinical researches showed a decrease in retinal blood flow and velocity when IOP was increased [10]. Latterly, an animal model demonstrated that after continuous IOP elevation for 7 weeks, the caliber of the retinal vessels was significantly lowered [11]. Since both high IOP and low CSFp could induce axonal transport disturbance in retinal ganglion cell, whether low CSFp could also cause retinal vessel diameter changes as high IOP is still unknown.

For investigating the influence of CSFp reduction on retinal vessels, we carried out an animal experiment at first. The CSFp was reduced by draining at cisterna magna in rat successfully. Then we obtained the fundus photographs of the rat's right eye at pre and post day 1, day 4, and day 7, respectively. The results showed that the mean diameters of retinal arteries and veins became narrower over time gradually (Fig. 25.1).

Compared to pre-operation, the mean diameters of both arteries and veins after CSFp reduction decreased. What effect does CSFp reduction have on the human retinal vessel? Does it have the same effect on the retinal vessel as in the rat? To answer these questions, we did a clinical trial on human. In this trial, we observed the diameter changes of retinal vessel trunks after lumber puncture (LP) drainage in patients who needed to have an LP examination (Fig. 25.2). Those with systemic or ocular diseases that may influence retinal vessels were excluded. We found that about half of the eyes' retinal artery trunk diameters narrowed and the rest dilated at both 15 min and 6 h after LP. However, the mean diameter of the retinal artery trunk remained relatively stable at the two time points. For retinal vein, the mean diameter of the venous trunk dilated at 15 min and 6 h after LP, but there was no significantly statistical difference.

From the above, we found that CSFp reduction could cause the retinal vessel diameter became thinner in rat but not in human. There are several possible reasons for this difference. Firstly, the ocular blood supply is different in rodents and human (Fig. 25.3). The rat central retinal artery (CRA) and peripapillary choroid are supplied by posterior ciliary artery (PCA) which travels in the CSF and along the inferior side of optic nerve (ON) without giving off any branch until optic nerve head (ONH) [12]. In human, the

L. Liu · C. Lin · N. Wang (✉)
Beijing Institute of Ophthalmology, Beijing Tongren Eye Center, Beijing Tongren Hospital, Capital Medical University, Beijing, China

Beijing Ophthalmology & Visual Sciences Key Laboratory, Beijing, China
e-mail: wningli@vip.163.com

N. Wang (ed.), *Intraocular and Intracranial Pressure Gradient in Glaucoma*,
Advances in Visual Science and Eye Diseases 1, https://doi.org/10.1007/978-981-13-2137-5_25

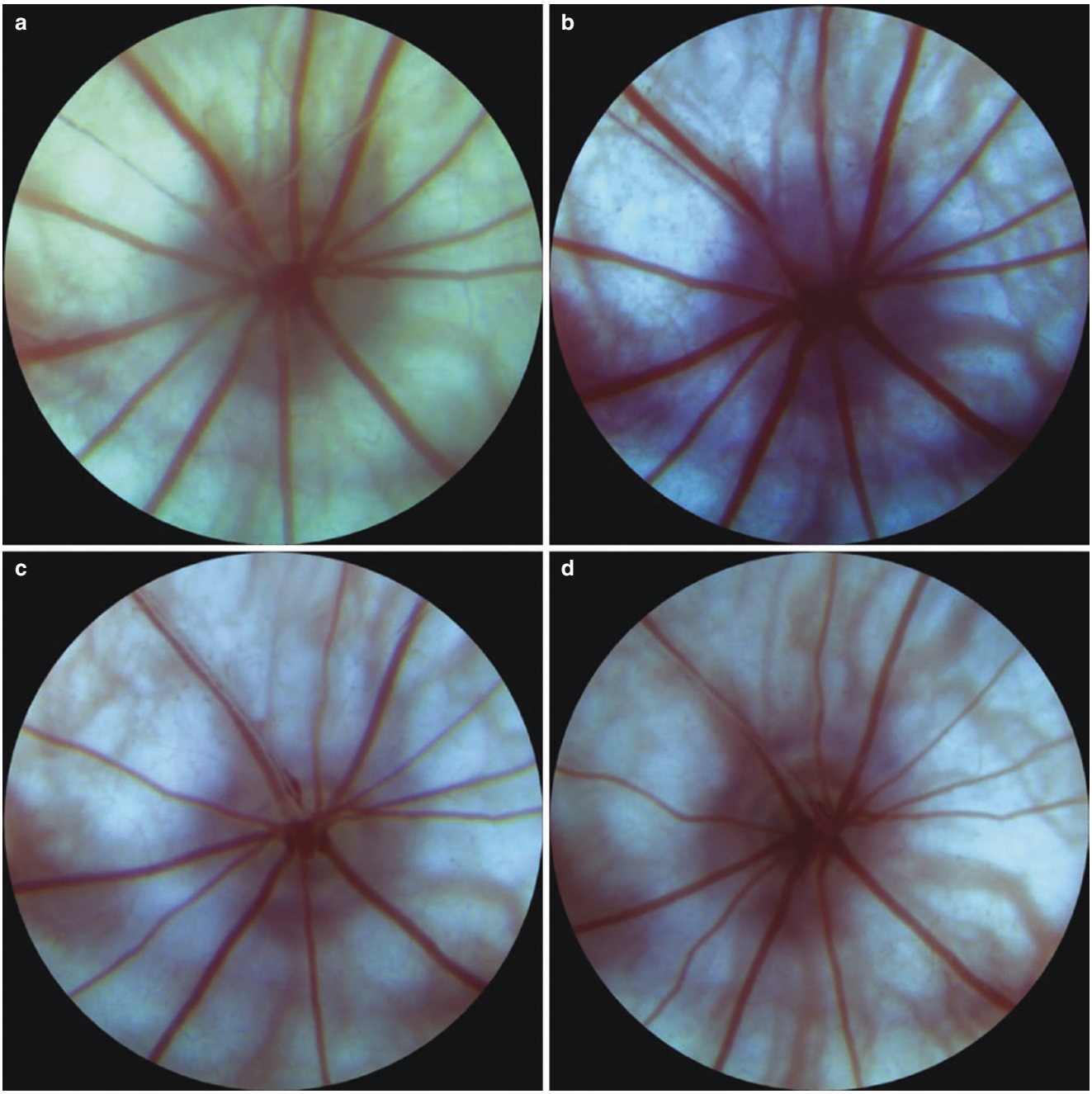

Fig. 25.1 Diameter changes of retinal blood vessels in rat at different time points. Pre-operation, post day 1, post day 4, and post day 7

CRA branches out from ophthalmic artery and trans-through in the ON center [13]. The vessels of rat CRA and choroid may be more affected by CSFp as its unique and simple angioarchitecture compared with human. Secondly, the extent of CSFp reduction in rat was much greater than that in human (54.7–86.1% vs. 10–36%). The last but not the least, the CSFp kept at a low level in the rat during the whole experiment process, while the CSFp increased slowly in human after CSFp reduction. As a result, the diameter of the rat's retinal vessel became narrow after CSFp reduction, while the diameter of the human's retinal vessel trunk kept relatively stable.

The retinal vessel became narrow after CSFp reduction in the rat, which may occur as the retinal artery is in fact a branch of PCA and PCA is directly influenced by surrounding CSF. A drop in CSFp can lead to a drop in extravascular and intravascular pressure, as an adaption to the lower surrounding pressure.

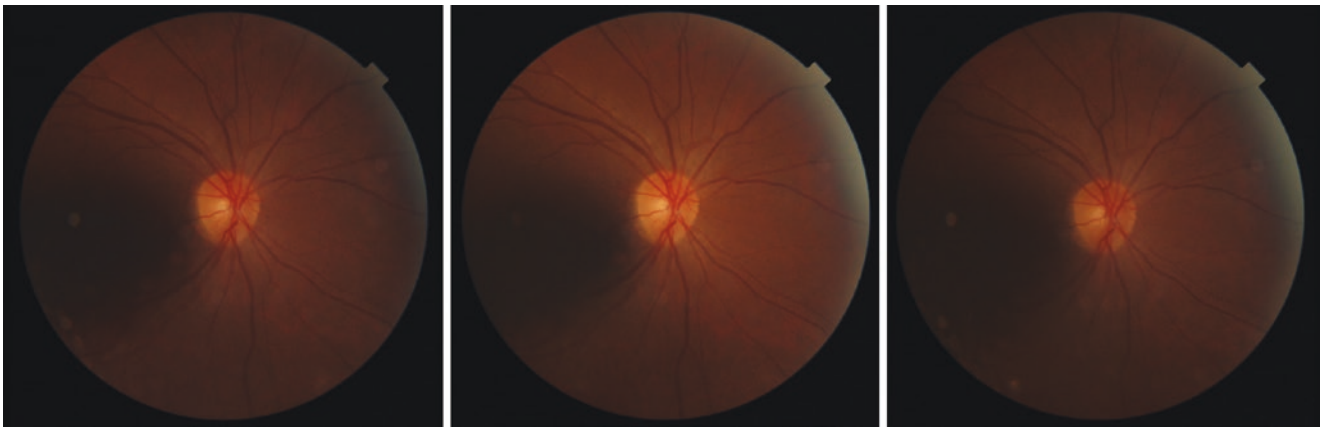

Fig. 25.2 Diameter changes of retinal blood vessels in human at different time points. Before LP, 15 min, and 6 h after LP

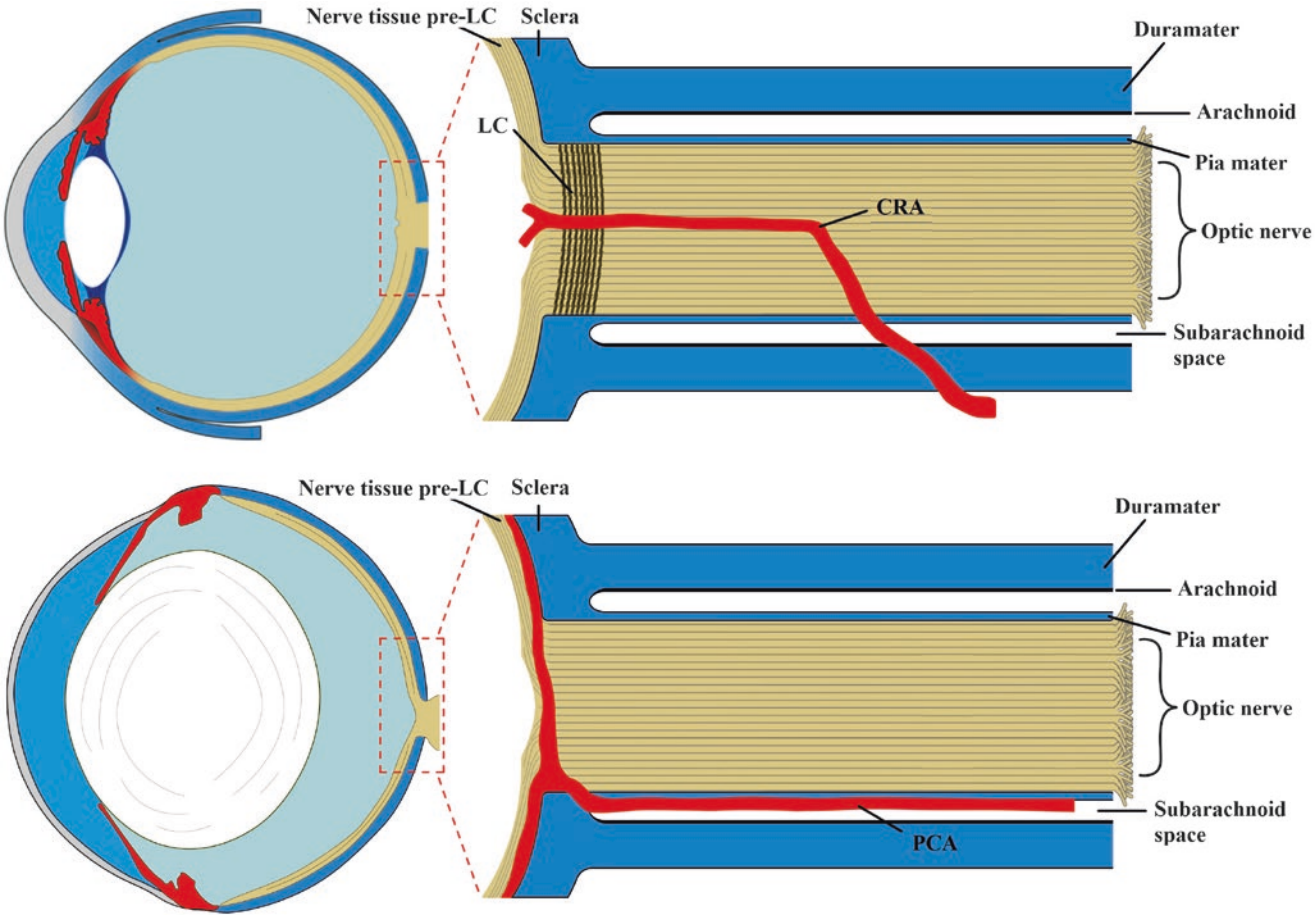

Fig. 25.3 Diagrams of central retinal artery of human and posterior ciliary artery of rat

What's more, the dynamics of rat CSF in the optic nerve subarachnoid space (ONSAS) may be quite different from that in human. The pressure and components of CSF were much more stable as the ONSAS was divided by a complex system of arachnoid trabeculae and septa which may act as a buffer system in human [14, 15]. The ONSAS pressure could keep stable even when the lateral ventricular CSFp is reduced by a large extent [16–18]. Compared with human, retro-ocular CSFp in rat may be more dependent on the lateral ventricular CSFp, which further influences the diameter of vessel.

The anatomy of rat's ONH is also different from that in human. In human, the lamina cribrosa (LC) is derived from the sclera, and the posterior border of LC is aligned with the outer border of sclera. However, the posterior portion of rat

ONH is coated by pia mater and surrounded by CSF [19]. We concluded that the diameter of the vessels may therefore be influenced by CSFp directly, as the PCA does not branch off until the ONH level.

These differences in anatomy between rat and human may cause a different response of retinal vessel to CSFp reduction.

Some clinical studies [20, 21] have found that the retinal diameter of glaucoma patients is relatively narrow, and the site of retinal vascular stenosis corresponds to the site of optic disc stenosis and the retinal nerve fiber layer (RNFL) thinning. Most published researches demonstrated that the mean vessel diameter in RNFL defects was significantly smaller. This might be explained by a reduced demand for oxygen in normal-tension glaucoma (NTG) patient [22]. Even the blood flow velocities in the ophthalmic artery, CRA, lateral ciliary arteries, and medium ciliary arteries were demonstrated to be reduced in patients with POAG [23]. Further studies showed that a narrow central retinal artery equivalent (CRAE) was strongly associated with higher long-term risk for developing open-angle glaucoma (OAG). However, the reason for narrowing of retinal vessel needs to be explored further.

In conclusion, CSFp reduction could cause thinning of retinal vessels in rats. And the influence of changes in the retinal vessel diameter on the ocular tissue and the optic nerve blood supply needs further investigation. However, in human, the change of the retinal vascular diameter after CSFp reduction is negligible. For the number of the patients in our study is small, we need to increase the number of the patients and analyze furthermore. In addition, we will use optical coherence tomography angiography to observe the retinal vessel change before and after LP in patients, so that we could further understand how the retinal vessel changes after CSFp reduction. Through these preliminary results, we could see that both low CSFp and high IOP influence not only the axonal transport of the retinal ganglion cell but also the ocular blood vessels. In the future, we need to further explore the relationship between retinal vessel change and the pathogenesis of glaucoma.

References

1. Volkov VV. Essential element of the glaucomatous process neglected in clinical practice. Oftalmol Zh. 1976;31(7):500–4.
2. Morgan WH, Yu DY, Cooper RL, Alder VA, Cringle SJ, Constable IJ. The influence of cerebrospinal fluid pressure on the lamina cribrosa tissue pressure gradient. Invest Ophthalmol Vis Sci. 1995;36(11):2163–4.
3. Berdahl JP, Allingham RR, Johnson DH. Cerebrospinal fluid pressure is decreased in primary open-angle glaucoma. Ophthalmology. 2008;115(5):763.
4. Ren R, Jonas JB, Tian G, Zhen Y, Ma K, Li S, Wang H, Li B, Zhang X, Wang N. Cerebrospinal fluid pressure in glaucoma : a prospective study. Ophthalmology. 2010;117(2):259–66.
5. Ren R, Wang N, Zhang X, Cui T, Jonas JB. Trans-lamina cribrosa pressure difference correlated with neuroretinal rim area in glaucoma. Graefes Arch Clin Exp Ophthalmol. 2011;249(7):1057.
6. Jonas JB, Wang N, Yang D, Ritch R, Panda-Jonas S. Facts and myths of cerebrospinal fluid pressure for the physiology of the eye. Prog Retin Eye Res. 2015;46:67–83.
7. Dongqi H, Zeqin R. A biomathematical model for pressure-dependent lamina cribrosa behavior. J Biomech. 1999;32(6):579–84.
8. Chen BH, Drucker MD, Louis KM, Richards DW. Progression of normal-tension glaucoma after ventriculoperitoneal shunt to decrease cerebrospinal fluid pressure. J Glaucoma. 2016;25(1):e50–2.
9. Zhang Z, Liu D, Jonas JB, Wu S, Kwong JM, Zhang J, Liu Q, Li L, Lu Q, Yang D, Wang J, Wang N. Axonal transport in the rat optic nerve following short-term reduction in cerebrospinal fluid pressure or elevation in intraocular pressure. Invest Ophthalmol Vis Sci. 2015;56(8):4257–66.
10. Guidoboni G, Harris A, Cassani S, Arciero J, Siesky B, Amireskandari A, Tobe L, Egan P, Januleviciene I, Park J. Intraocular pressure, blood pressure, and retinal blood flow autoregulation: a mathematical model to clarify their relationship and clinical relevance. Invest Ophthalmol Vis Sci. 2014;55(7):4105–18.
11. Mann C, Anders F, Liu H, et al. Morphological and quantitative changes in retinal and optic nerve vessels in experimental glaucoma model with elevated IOP for 7 weeks. Klin Monbl Augenheilkd. 2018; https://doi.org/10.1055/s-0044-101617.
12. Sugiyama K, Gu Z, Sugiyama K, Gu Z, Yamamoto CT, Kitazawa Y. Optic nerve and peripapillary choroidal microvasculature of the rat eye. Invest Ophthalmol Vis Sci. 1999;40(13):3084.
13. Flammer J, Orgul S, Costa VP, Orzalesi N, Krieglstein GK, Serra LM, Renard JP, Stefansson E. The impact of ocular blood flow in glaucoma. Prog Retin Eye Res. 2002;21(4):359–93.
14. Killer HE, Laeng HR, Flammer J, Groscurth P. Architecture of arachnoid trabeculae, pillars, and septa in the subarachnoid space of the human optic nerve: anatomy and clinical considerations. Br J Ophthalmol. 2003;87(6):777–81.
15. Killer HE, Jaggi GP, Flammer J, Miller NR, Huber AR. The optic nerve: a new window into cerebrospinal fluid composition? Am J Ophthalmol. 2006;142(3):1027–30.
16. Morgan WH, Yu DY, Alder VA, Cringle SJ, Cooper RL, House PH, Constable IJ. The correlation between cerebrospinal fluid pressure and retrolaminar tissue pressure. Invest Ophthalmol Vis Sci. 1998;39(8):1419–28.
17. Jaggi GP, Harlev M, Ziegler U, Dotan S, Miller NR, Killer HE. Cerebrospinal fluid segregation optic neuropathy: an experimental model and a hypothesis. Br J Ophthalmol. 2010;94(8):1088–93.
18. Hou R, Zhang Z, Yang D, Wang H, Chen W, Li Z, Sang J, Liu S, Cao Y, Xie X, Ren R, Zhang Y, Sabel BA, Wang N. Intracranial pressure (ICP) and optic nerve subarachnoid space pressure (ONSP) correlation in the optic nerve chamber: the Beijing Intracranial and Intraocular Pressure (iCOP) study. Brain Res. 2016;1635:201–8.
19. Sugiyama K, Cioffi GA, Bacon DR, Van Buskirk EM. Optic nerve and peripapillary choroidal microvasculature in the primate. J Glaucoma. 1994;3(Suppl 1):S45–54.
20. Amerasinghe N, Aung T, Cheung N, Fong CW, Wang JJ, Mitchell P, Saw SM, Wong TY. Evidence of retinal vascular narrowing in glaucomatous eyes in an Asian population. Invest Ophthalmol Vis Sci. 2008;49(12):5397–402.
21. Mitchell P, Leung H, Wang JJ, Rochtchina E, Lee AJ, Wong TY, Klein R. Retinal vessel diameter and open-angle glaucoma: the Blue Mountains Eye Study. Ophthalmology. 2005;112(2):245–50.
22. Kim JM, Sae Kim M, Jang HJ, Ho Park K, Caprioli J. The association between retinal vessel diameter and retinal nerve fiber layer thickness in asymmetric normal tension glaucoma patients. Invest Ophthalmol Vis Sci. 2012;53(9):5609–14.
23. Kaiser HJ, Schoetzau A, Stumpfig D, Flammer J. Blood-flow velocities of the extraocular vessels in patients with high-tension and normal-tension primary open-angle glaucoma. Am J Ophthalmol. 1997;123(3):320–7.

Part V

Clinical Studies and Cases

Impact of Intraocular Pressure on Optic Nerve Head Deformation

26

Christopher Leung

Glaucoma is a form of chronic optic neuropathy characterized by progressive thinning of the retinal nerve fiber layer (RNFL), narrowing of the neuroretinal rim, and deformation of the optic nerve head (ONH). Deciphering the temporal sequence of the structural changes of the RNFL, neuroretinal rim, and ONH and their associations with the decline in visual function and change in intraocular pressure (IOP) levels has major implications in the clinical management of glaucoma patients. In a previous study following 90 glaucoma patients with confocal scanning laser ophthalmoscopy (CSLO) imaging of the ONH surface and optical coherence tomography (OCT) imaging of the RNFL at 4-month intervals over 4 years [1], we showed that among patients demonstrating both progressive RNFL thinning and posterior deformation of the ONH, 82.6% of eyes had posterior deformation of the ONH before progressive RNFL thinning, and the median lag time was approximately 16 months (Fig. 26.1). Whereas 7% of eyes had progressive RNFL thinning at the onset of posterior deformation of the ONH, about 46% had posterior deformation of the ONH at the onset of progressive RNFL thinning. This finding suggests posterior deformation of the ONH may occur before progressive RNFL thinning in many patients with glaucoma, and a therapeutic time window may exist upon detection of posterior deformation of the ONH before irreversible loss of the RNFL.

The advent of Fourier domain OCT has greatly facilitated examination of the ONH as well as the lamina cribrosa (LC) surfaces (Fig. 26.2). Using the Spectralis OCT (Heidelberg Engineering, Heidelberg, Germany) which allows image registration for studying progressive changes of the ONH surface depth and anterior lamina cribrosa surface depth with reference to the Bruch's membrane opening, we investigated the association between IOP during follow-up and the deformation of ONH and LC surfaces in 88 glaucoma patients who were monitored every 4 months for a mean of 5.3 years [2]. Linear mixed modeling showed that for each mmHg increase in the mean IOP during follow-up, the ONH surface and the anterior laminar surface deformed posteriorly by 1.6 and 2.0 μm, respectively. In a follow-up study, we further demonstrated that a higher IOP is connected to a faster rate of posterior deformation of the ONH/LC surfaces and that eyes with a faster rate of posterior deformation of the ONH/LC surfaces have a higher risk of development of visual field progression (Table 26.1) [3]. In other words, identifying fast progressors of posterior deformation of the ONH/LC surfaces would be relevant to the management of glaucoma patients as they carry a higher risk of visual field progression. Studying the interaction between IOP levels and changes in ONH/LC surface depths of an individual glaucoma patient is a promising paradigm shift to help determine the risk of functional loss and guide the intensity of IOP lowering treatment.

C. Leung (✉)
Department of Ophthalmology and Visual Sciences,
The Chinese University of Hong Kong, Hong Kong, China
e-mail: cksleung@cuhk.edu.hk

N. Wang (ed.), *Intraocular and Intracranial Pressure Gradient in Glaucoma*,
Advances in Visual Science and Eye Diseases 1, https://doi.org/10.1007/978-981-13-2137-5_26

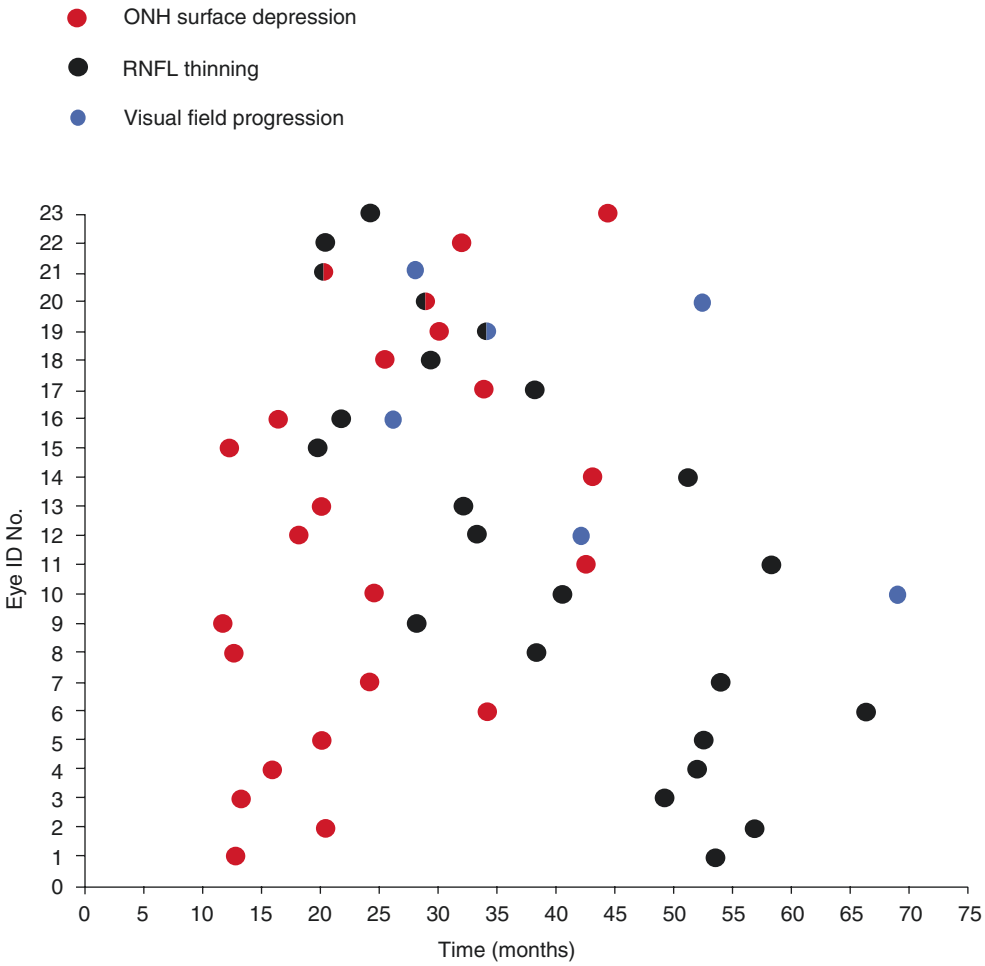

Fig. 26.1 The temporal relationship between posterior deformation of the optic nerve head (ONH) surface (red dots) and progressive retinal nerve fiber layer (RNFL) thinning (black dots) in 23 glaucomatous eyes detected with both posterior deformation of the ONH and progressive RNFL thinning at the latest study visit (Reprinted with permission from Xu G, Weinreb R N, Leung C K S. Optic Nerve Head Deformation in Glaucoma: The Temporal Relationship between Optic Nerve Head Surface Depression and Retinal Nerve Fiber Layer Thinning[J]. Ophthalmology, 2014, 121(12):2362–2370)

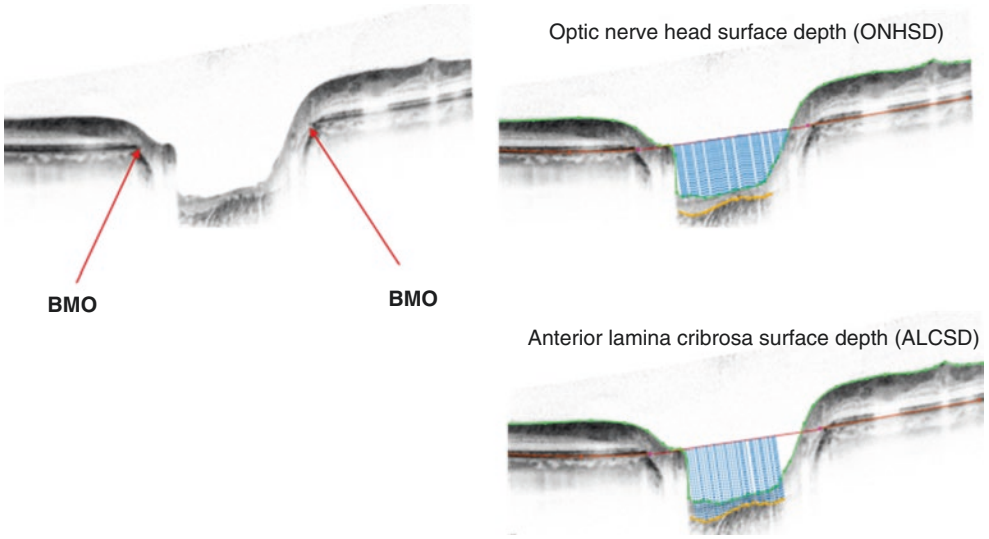

Fig. 26.2 An optical coherence tomography (OCT) B-scan demonstrating the measurements of the optic nerve head surface depth (ONHSD) and the anterior lamina cribrosa surface depth (ALCSD) after detection of Bruch's membrane opening (BMO), internal limiting membrane, ONH surface, and anterior LC surface. The reference line (pink) is a line joining the BMO. The ONHSD represents the perpendicular distances from the reference line to the ONH surface. The ALCSD represents the perpendicular distances from the reference line to the anterior LC surface. The retinal pigment epithelium/Bruch's membrane is highlighted in red (Reprinted with permission from [2].)

Table 26.1 Hazard ratios of the rates of change of ALCSD and ONHSD measured from the BMO and the covariates for development of visual field progression analyzed with joint longitudinal and survival models (Reproduced with permission from [3])

	$ALCSD_{BMO}$		$ONHSD_{BMO}$	
Longitudinal sub-model	Coefficient (95% CI)	*P*	Coefficient (95% CI)	*P*
Time (year)	7.09 (1.98–12.2)	0.007	4.98 (1.46–8.51)	0.006
Baseline age (year)	−0.76 (−1.85 to 0.34)	0.178	0.02 (−0.94 to 0.98)	0.974
1OP (mmHg)	−0.45 (−0.86 to −0.04)	0.033	0.05 (−0.26 to 0.37)	0.733
Baseline VF MD (dB)	−1.05 (−2.84 to 0.74)	0.252	−0.76 (−2.33 to 0.08)	0.338
Time × Baseline age	−0.18 (−0.26 to −0.09)	<0.001	−0.11 (−0.17 to −0.06)	<0.001
Time × 1OP	0.18 (0.07–0.29)	0.002	0.12 (0.03–0.2)	0.008
Time × Baseline VF MD	0.13 (0.00–0.27)	0.048	0.09 (0–0.18)	0.059
Intercept (baseline $ALCSD_{BMO}$/$ONHSD_{BMO}$)	488.61 (428.56–548.65)	<0.001	2.37.14 (184.8–289.49)	<0.001
Survival sub-model	Hazard ratio (95% CI)	*P*	Hazard ratio (95% CI)	*P*
Rate of change of $ALCSD_{BMO}$/$ONHSD_{BMO}$ (each μm/year)	1.064 (1.009–1.122)	0.023	1.109 (1.015–1.212)	0.022
Baseline age (year)	1.011 (0.971–1.053)	0.595	1.012 (0.972–1.054)	0.569
1OP (mmHg)	1.026 (0.89–1.181)	0.727	1.019 (0.882–1.176)	0.801
Baseline VF MD (dB)	1.031 (0.959–1.108)	0.414	1.029 (0.957–1.107)	0.435
Intercept (baseline $ALCSD_{BMO}$/$ONHSD_{BMO}$)	0.998 (0.992–1.004)	0.537	0.997 (0.991–1.004)	0.479

ALCD anterior lamina cribrosa surface death, *ONHSD* optic nerve head surface depth, *CI* confidence interval, *VF* visual field, *MD* mean deviation, *IOP* intraocular pressure

References

1. Xu G, Weinreb RN, Leung CK. Optic nerve head deformation in glaucoma: the temporal relationship between optic nerve head surface depression and retinal nerve fiber layer thinning. Ophthalmology. 2014;121:2362–70.
2. Wu Z, Xu G, Weinreb RN, Yu M, Leung CK. Optic nerve head deformation in glaucoma: a prospective analysis of optic nerve head surface and lamina Cribrosa surface displacement. Ophthalmology. 2015;122:1317–29.
3. Wu Z, Lin XC, Crowther M, Mak H, Yu M, Leung CK. Impact of rates of change of lamina cribrosa and ONH surface depths on visual field progression in glaucoma. Invest Ophthalmol Vis Sci. 2017;58(3):1825–33.

Push Me Pull You

27

Nancy J. Newman

This is a case of an 80-year-old woman who was referred for neuro-ophthalmologic assessment because of 11 months of disc swelling and progressive vision loss in the left eye.

Her medical history was unremarkable, and she had a family history of primary open-angle glaucoma in her father. Her ocular history was notable for uncomplicated cataract surgeries with intraocular lens placements, as well as advanced POAG with 0.9 cupping in both eyes. She underwent trabeculectomy in both eyes, and the pressure reduced significantly, especially in the left eye more than the right eye.

Eleven months prior to referral, the patient was incidentally noted to have left optic disc edema that persisted without overt symptoms of elevated intracranial pressure.

The patient's vision in the left eye slowly progressively worsened first by peripheral visual field constriction and then by visual acuity from 20/40 to 20/100 over the course of 11 months. Her intraocular pressures in the left eye remained in the range of 5–6 mmHg.

On examination 11 months after her disc edema in the left eye was discovered, she was 20/20 in the right eye and 20/80 in the left eye. Her IOP was 15 mmHg on the right and 5 mmHg on the left, with a + 0.9 log unit left relative afferent pupillary defect.

Funduscopic examination showed a typical glaucomatous optic nerve with vertical cupping and an inferior notch on the right and chronic disc swelling with atrophy on the left (Fig. 27.1). Visual fields showed a superior arcuate defect in the right eye and severe constriction to approximately 5 degrees in the left eye (Fig. 27.2).

MRI of the brain and orbits with and without contrast was normal except for a 2.2 × 2 cm mass at the right cerebellopontine angle which was consistent with a meningioma (Fig. 27.3). The mass was compressing the patient's right lateral venous sinus, which, in this case, was the dominant lateral sinus. There was no evidence of any optic nerve abnormality. Lumbar puncture demonstrated a moderately elevated intracranial pressure of 24 cm of water and normal cerebrospinal fluid contents.

Although the differential diagnosis for her left optic disc edema included hypotony and infectious/inflammatory/vascular optic neuropathies, the "Push Me Pull You" hypothesis is that in her right eye, the elevated intracranial pressure was countered by the normal intraocular pressure, whereas in the left eye, the intraocular pressure was lower, allowing the elevated intracranial pressure to manifest with left eye disc swelling [1, 2].

To conclude, the primary cause of the visual loss of her left eye was papilledema due to raised intracranial pressure secondary to venous hypertension from her dominant transverse venous sinus compression, and the right optic nerve head was "protected" by its higher intraocular pressure [3–7].

In this case, as in a few other cases in the literature, the disc edema and visual loss are unilateral because of the difference in intraocular pressures between the two eyes. Indeed, sudden unilateral disc edema has been reported in patients with idiopathic intracranial hypertension who underwent trabeculectomy for their glaucoma. Conversely, glaucomatous optic neuropathy after CSF shunting for normal pressure hydrocephalus has been reported, and there even are a few cases in which a patient developed glaucomatous optic neuropathy after optic nerve sheath fenestration locally reduced the CSF pressure immediately behind the globe. Rather than low intracranial pressure contributing to glaucomatous optic neuropathy, in our case low intraocular pressure allowed for progressive optic nerve damage from elevated intracranial pressure and papilledema.

Considering this gradient across the lamina cribrosa, several questions must be resolved. First, can the gradient across the lamina serve as a marker of intracranial pressure and/or of

N. J. Newman
Department of Ophthalmology, Neurology and Neurological Surgery, Emory University School of Medicine, Atlanta, GA, USA
e-mail: ophtnjn@emory.edu

N. Wang (ed.), *Intraocular and Intracranial Pressure Gradient in Glaucoma*,
Advances in Visual Science and Eye Diseases 1, https://doi.org/10.1007/978-981-13-2137-5_27

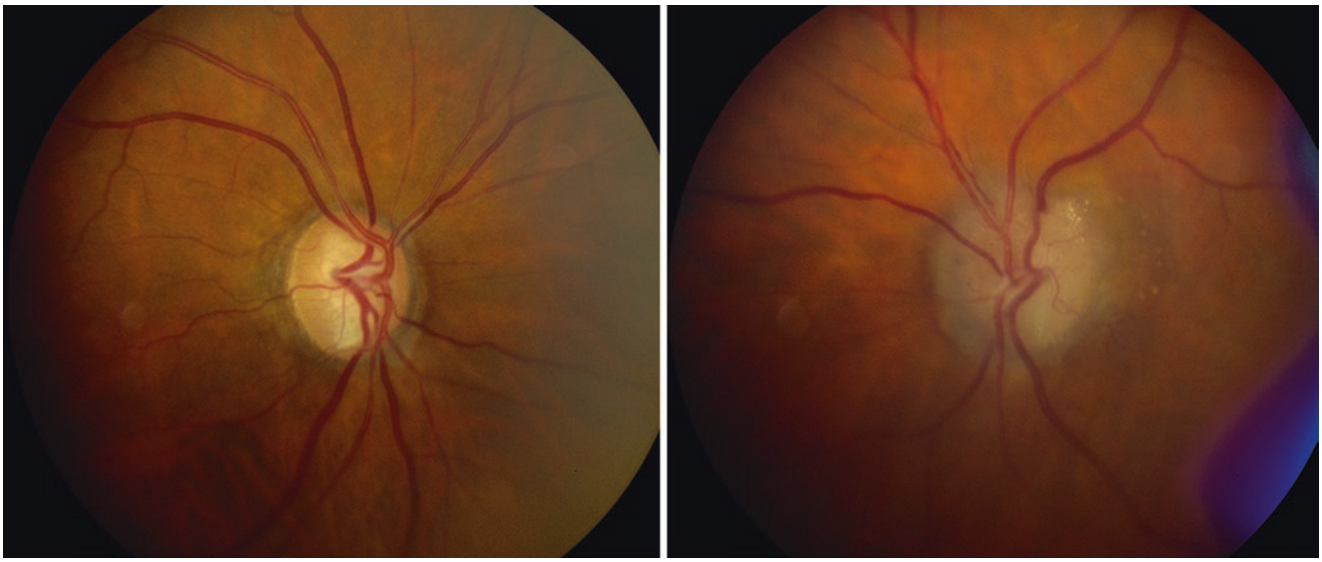

Fig. 27.1 Funduscopic appearance of the optic nerves: in the right eye, there is a typicla glaucomatous optic nerve with vertical cupping and an inferior notch; in the left eye, chronic disc swelling with atrophy can be observed

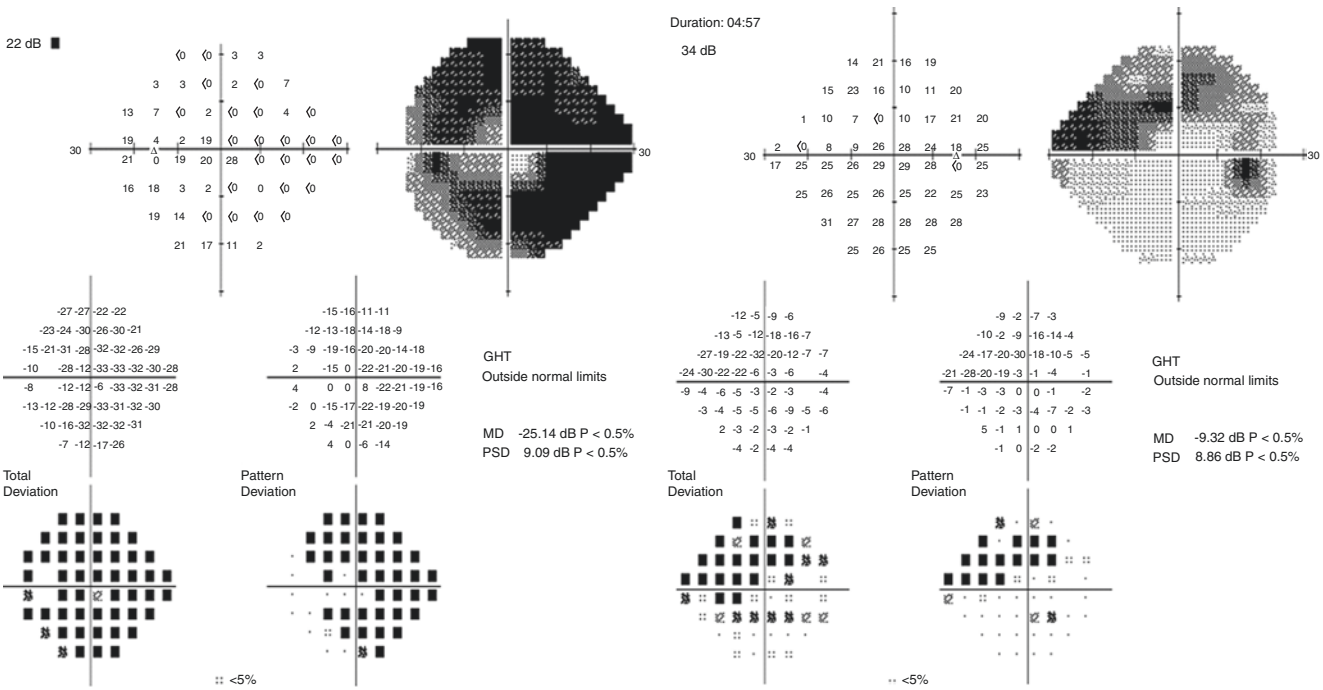

Fig. 27.2 Visual fields show in the right eye a superior arcuate defect that corresponds well with the inferior glaucomatous cupping; in the left eye, there is severe constriction to approximately 5 degrees corresponding to the chronic atrophic disc edema

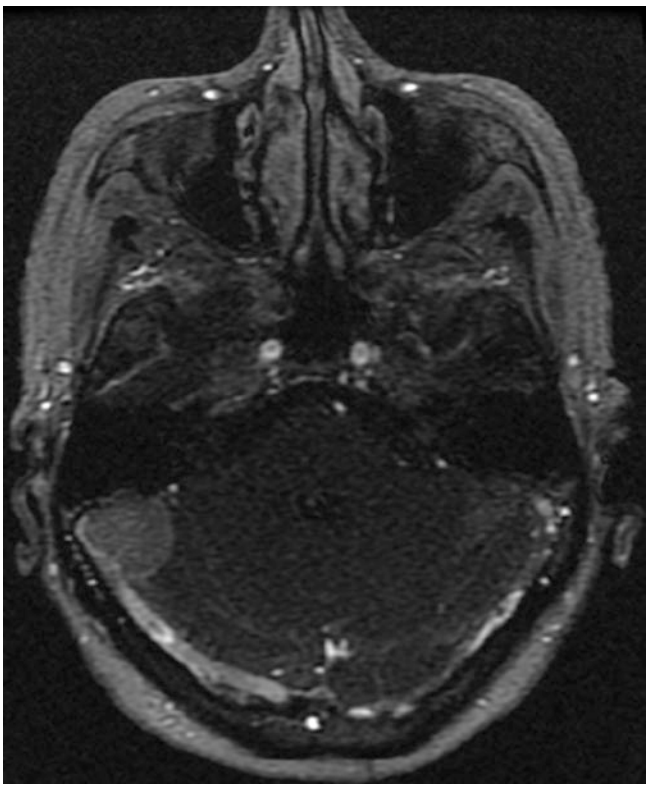

Fig. 27.3 MRI of the brain showed a 2.2 × 2 cm mass at the right cerebellopontine angle, which was consistent with a meningioma compressing the patient's dominant right lateral venous sinus

intraocular pressure? Is this gradient the key to the pathophysiology of glaucoma? Finally, is this pressure gradient the key to our understanding the pathophysiology of visual loss from disc edema in idiopathic intracranial hypertension and other disorders of elevated intracranial pressure? This case report illustrates what previous human and animal studies of the trans-laminar pressure gradient have already suggested.

References

1. McCulley TJ, Chang JR, Piluek J. Intracranial pressure and glaucoma. J Neuroophthalmol. 2015;35:S38–44.
2. Jonas JB, Yang D, Wang N. Intracranial pressure and glaucoma. J Glaucoma. 2013;22:S13–4.
3. Lee EJ, Kim TW, Weinreb RN, et al. Reversal of lamina cribrosa displacement after intraocular pressure reduction in open angle glaucoma. Ophthalmology. 2013;120:553–9.
4. Perez-Lopez M, Ting DS, Clarke L. Lamina cribrosa displacement after optic nerve sheath fenestration in idiopathic intracranial hypertension: a new tool for monitoring changes in intracranial pressure? Br J Ophthalmol. 2014;98:1603–4.
5. Lawlor M, Zhang MG, Virgo J, Plant GT. Asymmetrical intraocular pressures and asymmetrical papilloedema in pseudotumor cerebri syndrome. Neuro-Ophthalmology. 2016;40:292–6.
6. Bokhari RF, Baeesa SS. Does the treatment of normal pressure hydrocephalus put the retinal ganglion cells at risk? A brief literature review and novel hypothesis. Med Hypotheses. 2013;81:686–9.
7. Abegg M, Fleischhauer J, Landau K. Unilateral papilledema after trabeculectomy in a patient with intracranial hypertension. Klin Monatsbl Augenheilkd. 2008;225:441–2.

Optic Nerve Sheath Fenestration: A Way to Balance the Trans-Laminar Cribrosa Pressure Difference?

28

Zhen Li, Xuxiang Zhang, Dachuan Liu, and Ningli Wang

Papilledema is defined as a secondary edema of the optic disc caused by the increased intracranial pressure [1]. A variety of intracranial diseases will lead to increased intracranial pressure, such as intracranial space-occupying lesion, various forms of hydrocephalus, intracranial infection, cerebral venous sinus thrombosis, and idiopathic intracranial hypertension (IIH) (Fig. 28.1).

There are many theories about the pathogenesis of papilledema. Currently, the most widely accepted one is axoplasmic flow block theory [2, 3]. The transport of the axoplasmic flow depends on the physiological pressure difference between the intraocular pressure (IOP) and the internal pressure of the optic nerve. When the intracranial pressure (ICP) is increased, the increased intracranial pressure is transferred to the subarachnoid space around the optic nerve (ONSAS) through the cerebrospinal fluid circulation, which will block the anterograde axoplasmic flow and then lead to the swelling of the nerve fibers. On the other hand, due to the expansion and leakage of capillaries in the optic disc and interstitial fluid absorption disorder, resulting in an increase in interstitial fluid retention and interstitial pressure, further increase the optic nerve pressure. This is a vicious circle. Long-term axonal swelling can lead to neurons necrosis and optic nerve atrophy, and ultimately the patient's visual function is severely impaired.

Based on the mechanism of the papilledema, we proposed the hypothesis that surgical reduction of cerebrospinal fluid pressure in the ONSAS may be a protective factor for the optic nerve.

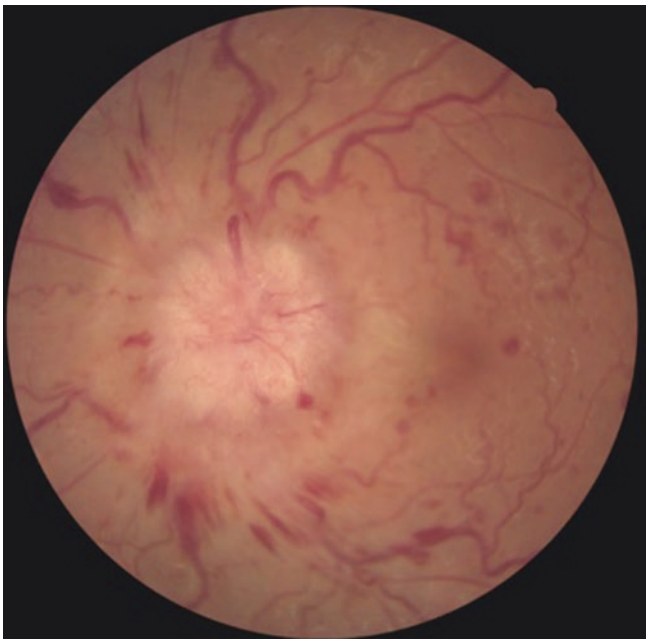

Fig. 28.1 Fundus photography shows papilledema in patient with intracranial hypertension

In order to verify the hypothesis, a prospective study was conducted in Xuanwu Hospital. Patients with papilledema due to intracranial hypertension caused by intracranial venous sinus thrombosis were recruited in this study. All the patients had significant visual impairment and increased cerebrospinal fluid pressure (measured by lumbar puncture). After all the neurological and ophthalmological examination, a surgery of optic nerve sheath fenestration was conducted.

The surgery of optic nerve sheath fenestration was conducted through the conjunctival approach. After a window of about 2 × 3 mm in size in the optic nerve sheath at 3 mm

Z. Li · X. Zhang · D. Liu
Department of Ophthalmology, Xuanwu Hospital, Capital Medical University, Beijing, China

N. Wang (✉)
Beijing Institute of Ophthalmology, Beijing Tongren Eye Center, Beijing Tongren Hospital, Capital Medical University, Beijing, China

Beijing Ophthalmology & Visual Sciences Key Laboratory, Beijing, China
e-mail: wningli@vip.163.com

N. Wang (ed.), *Intraocular and Intracranial Pressure Gradient in Glaucoma*,
Advances in Visual Science and Eye Diseases 1, https://doi.org/10.1007/978-981-13-2137-5_28

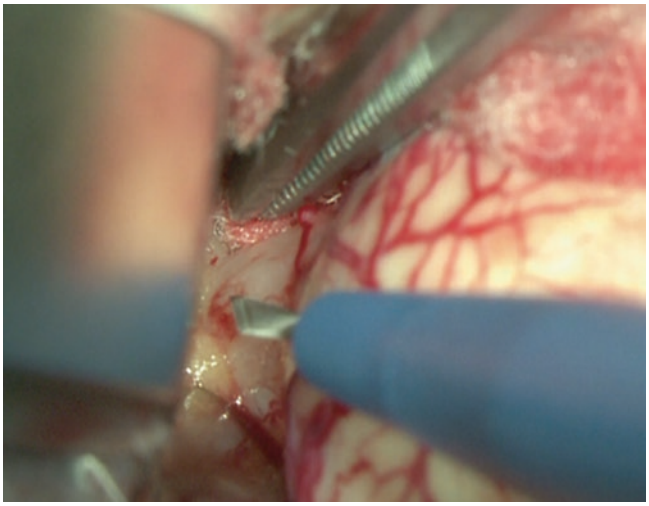

Fig. 28.2 The surgeon cut the optic nerve sheath at 3 mm behind the eyeball

behind the eyeball was opened, some clear CSF flowing out from the ONSAS was observed (Fig. 28.2).

Our results showed that papilledema in most of the eyes that received optic nerve sheath fenestration operation faded in 1 week. The visual acuity and visual field gradually recovered after operation, with the peak of recovery appearing at about 90–180 days after operation.

Cerebral venous sinus thrombosis is one of main causes of intracranial hypertension. At present, the main treatment is anticoagulant therapy [4]. Normally, the duration of anticoagulation therapy is about 6–12 months [5]. Therefore, patients with papilledema caused by cerebral venous sinus thrombosis would suffer from intracranial hypertension for a relative long time. However, without effective protective treatment, long-term high intraocular pressure would lead to optic nerve atrophy.

The surgery of optic nerve sheath fenestration drains out some of the cerebrospinal fluid by opening a window in the retrobulbar optic nerve sheath and decreases the pressure in the ONSAS directly.

Our study showed that patients with optic nerve injury caused by intracranial hypertension due to cerebral venous sinus thrombosis experienced obvious improvement of visual function after optic nerve sheath fenestration operation.

Overall, we draw the conclusion that the surgery of optic nerve sheath fenestration does have protective effect on patients with optic nerve injury caused by intracranial hypertension due to cerebral venous sinus thrombosis.

28.1 Typical Case

A 35-year-old woman complained of unrelenting headaches for 3 months and began to suffer from blurred vision 1 month ago, and her vision loss continued to progress.

The ophthalmological examination revealed a best corrected visual acuity of counting fingers in both eyes and a normal anterior ocular segment. IOP was 14 mmHg in the right eye and 13 mmHg in the left eye. The ophthalmoscopy showed optic disc edema and hemorrhage in both optic nerve heads, with OCT, correspondingly, showing optic disc edema in both eyes and B-scan ultrasound revealing an enlarged optic nerve sheath diameter. Neurological examination found CSF pressure was over 300 mmH_2O (measured by lumbar puncture). Neuroimaging findings were consistent with intracranial hypertension syndrome. MRV revealed intracranial cavernous sinus thrombosis (Fig. 28.3).

The surgery of optic nerve sheath fenestration was performed on both eyes, respectively. Alleviation of optic disc edema was observed on the first day after operation, and the patient's visual acuity increased to 0.2 in both eyes after 1 month. And the optic disc edema subsided (Fig. 28.4).

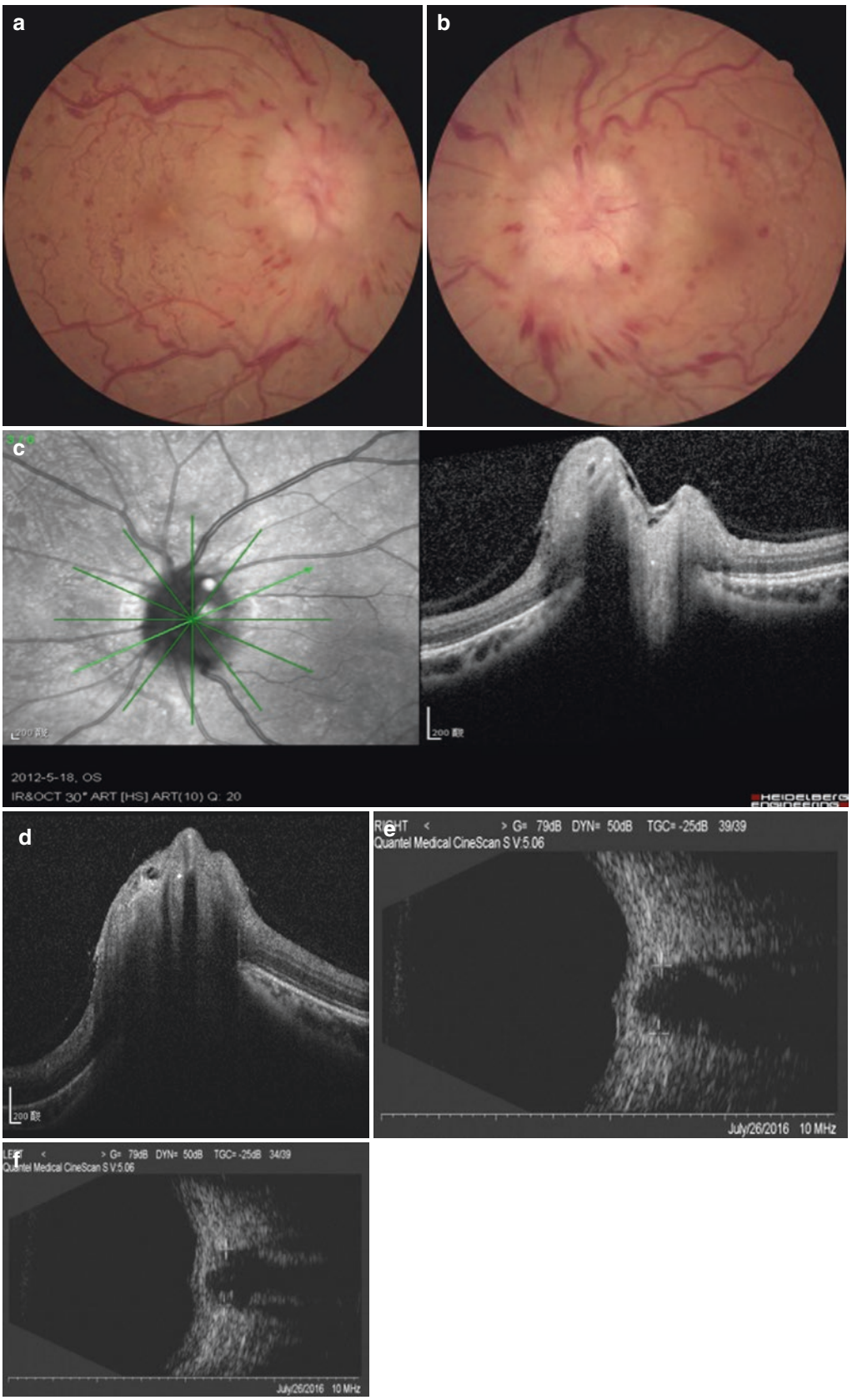

Fig. 28.3 The ophthalmological examination results before surgery. (**a**) and (**b**) were the patient's fundus photography, which showed optic disc edema and hemorrhage. (**c**) and (**d**) were optic head scan by OCT, which revealed an optic disc edema. (**e**) and (**f**) were the B-scan ultrasound, which showed an enlarged optic nerve sheath diameter

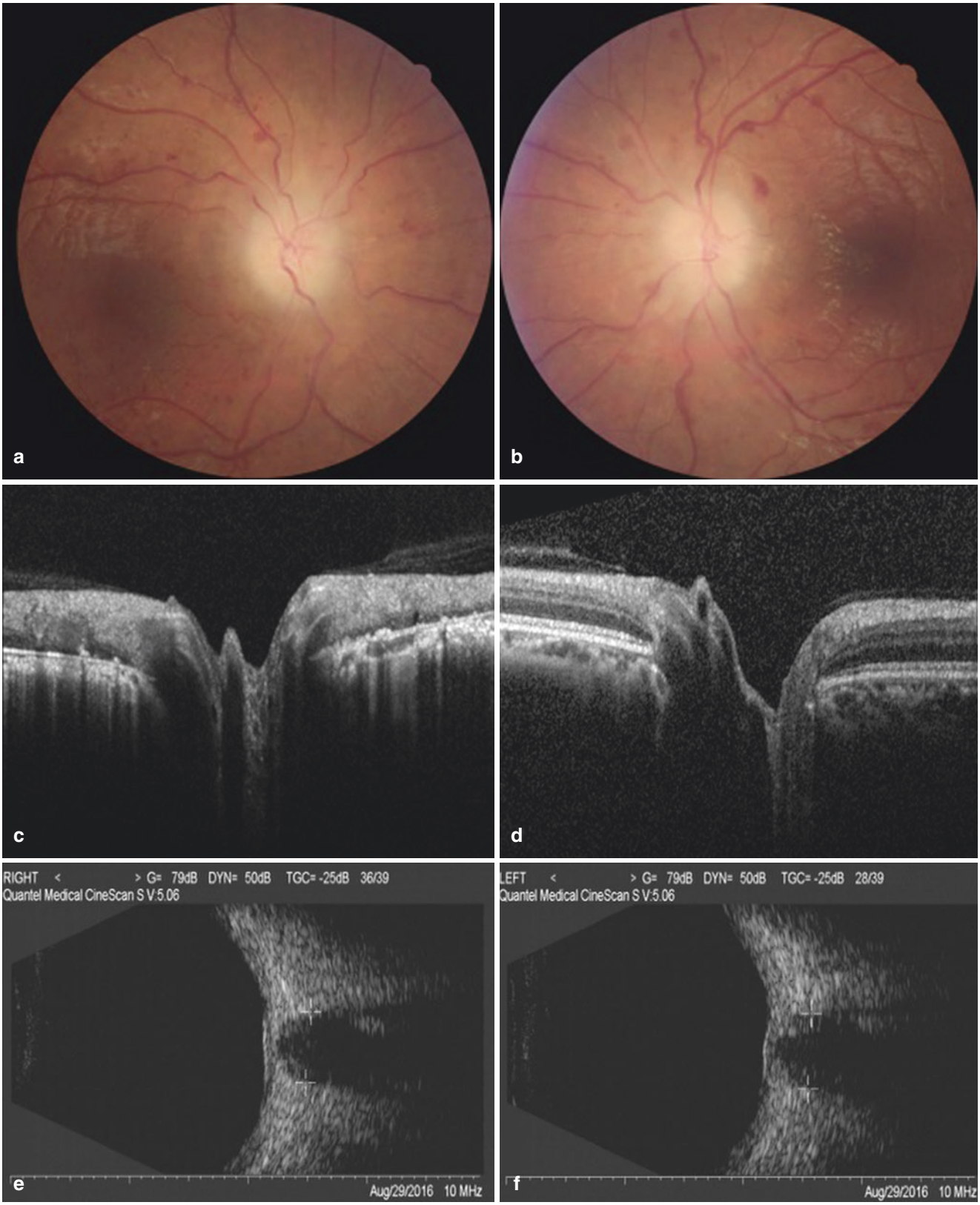

Fig. 28.4 The ophthalmological examination results after surgery. (**a**) and (**b**) were the patient's fundus photography, showing faded optic disc edema and absorbed optic disc hemorrhage. (**c**) and (**d**) were optic head scan by OCT, revealing reappeared optic cup. (**e**) and (**f**) were the B-scan ultrasound, showing a decreased optic nerve sheath diameter.

References

1. Whiting AS, Johnson LN. Papilledema: clinical clues and differential diagnosis. Am Fam Physician. 1992;45(3):1125–34.
2. Tso MO, Hayreh SS. Optic disc edema in raised intracranial pressure. III. A pathologic study of experimental papilledema. Arch Ophthalmol. 1977;95(8):1448–57.
3. Wirtschafter JD, Rizzo FJ, Smiley BC. Optic nerve axoplasm and papilledema. Surv Ophthalmol. 1975;20(3):157–89.
4. Luo Y, Tian X, Wang X. Diagnosis and treatment of cerebral venous thrombosis: a review. Front Aging Neurosci. 2018;10:2.
5. Coutinho JM, Stam J. A rare cause of thunderclap headache. BMJ. 2011;341:c6054.

Aging Effect on Lamina Cribrosa Depth in Ocular Hypertension and Glaucoma

29

Ruojin Ren, Hongli Yang, Stuart Gardiner, Christy Hardin, Shaban Demirel, and Claude F. Burgoyne

In clinic, "deep" vs. "shallow" cupping is well established in human glaucoma. Our central hypothesis is that the "shallow" or senile sclerotic cupping of aged eyes is a manifestation of their stiffer connective tissues. We predicted that there are age-related differences in structure/function relationships. The relationship between the magnitude of laminar deformation and visual field loss will be different in *young* ("compliant") eyes compared to *old* ("stiff") eyes.

Our purpose is to characterize optic nerve head (ONH) structure within study admission spectral domain optical coherence tomography (SDOCT) images from patients with ocular hypertension and glaucoma and then to assess the effect of age on laminar depth while controlling for visual field loss and retinal nerve fiber layer thickness (RNFLT).

Participants were taken from P3 study, Portland Progression Project (NIH/NEI R01-EY-019674 (PI: Shaban Demirel) 10/1/09-9/30/14), a longitudinal study of the course and risk factors for glaucomatous progression. All subjects were considered to have either high-risk ocular hypertension or primary open-angle glaucoma (POAG).

Eligibility criteria for the involved patients have been defined in previous series of publication as follows: (1) untreated intraocular pressure (IOP) ≥ 22 mmHg in both eyes and (2) one of the following additional risk factors, vertical cup-to-disc ratio ≥0.6 in at least one eye and/or an interocular cup-to-disc ratio asymmetry ≥0.2 between the two eyes; positive family history of glaucoma; personal history of migraine, Raynaud syndrome, or vasospasm; African American ancestry; and age >70 years.

This cross-sectional analysis was performed on 221 participants. The participants underwent a standardized ophthalmologic examination including automated perimetry (Humphrey 24-2, SITA Standard) and SDOCT test on the same day. Data were used from the first visit at which testing was carried out and reliable results were obtained. Demographic data and IOP were also recorded. Data from only one eye of each participant was included. The eye with the best qualitative SDOCT laminar visualization was chosen unless SDOCT laminar visualization was qualitatively similar in both eyes in which case one eye was randomly selected.

SDOCT imaging was performed using a standard Spectralis unit (Heidelberg Engineering, GmbH, Heidelberg, Germany) with an 870-nm source. A radial scanning pattern visually centered on the ONH by the technician was used to obtain 48 high-resolution radial B-scans over a 15° area (768 A-scans per B-scan), as seen in Fig. 29.1. 24 of 48 radial B-scans which were manually delineated. Bruch's membrane opening (BMO) reference plane was applied in each optic nerve head data.

For this study, anterior lamina cribrosa surface depth (ALCSD) was measured relative to Bruch's membrane opening (BMO) reference plane (Fig. 29.2).

To ensure that we were making comparisons between the most posterior portions of the anterior lamina cribrosa surface within all study eyes, we calculated three additional ALCSD parameters for each study eye. $ALCSD_{max1}$ was defined as the mean ALCSD value from the top 10% of all ALCSD values; $ALCSD_{max2}$ was defined as the mean ALCSD value from those BMO sectors containing the top 5% of all ALCSD values; and $ALCSD_{central}$ was defined as the mean ALCSD values from the center-most third of the projected anterior lamina cribrosa surface sectors.

RNFLT was measured between the internal limiting membrane and posterior surface of retinal nerve fiber layer at 1700 eccentricity from the centroid within the 24 delineated B-scans of each ONH (Fig. 29.3). The average of all RNFLT data of each optic nerve was reported.

Therefore 221 eyes were included for analysis. The characteristics of the participants were described in Table 29.1.

There was no significant univariate relationship between ALCSD and age (P = 0.50) and between ALCSD and IOP (P = 0.22) (Table 29.2). However, interestingly, the

R. Ren · H. Yang · S. Gardiner · C. Hardin · S. Demirel
C. F. Burgoyne (✉)
Devers Eye Institute, Optic Nerve Head Research Laboratory, Legacy Research Institute, Portland, OR, USA

N. Wang (ed.), *Intraocular and Intracranial Pressure Gradient in Glaucoma*,
Advances in Visual Science and Eye Diseases 1, https://doi.org/10.1007/978-981-13-2137-5_29

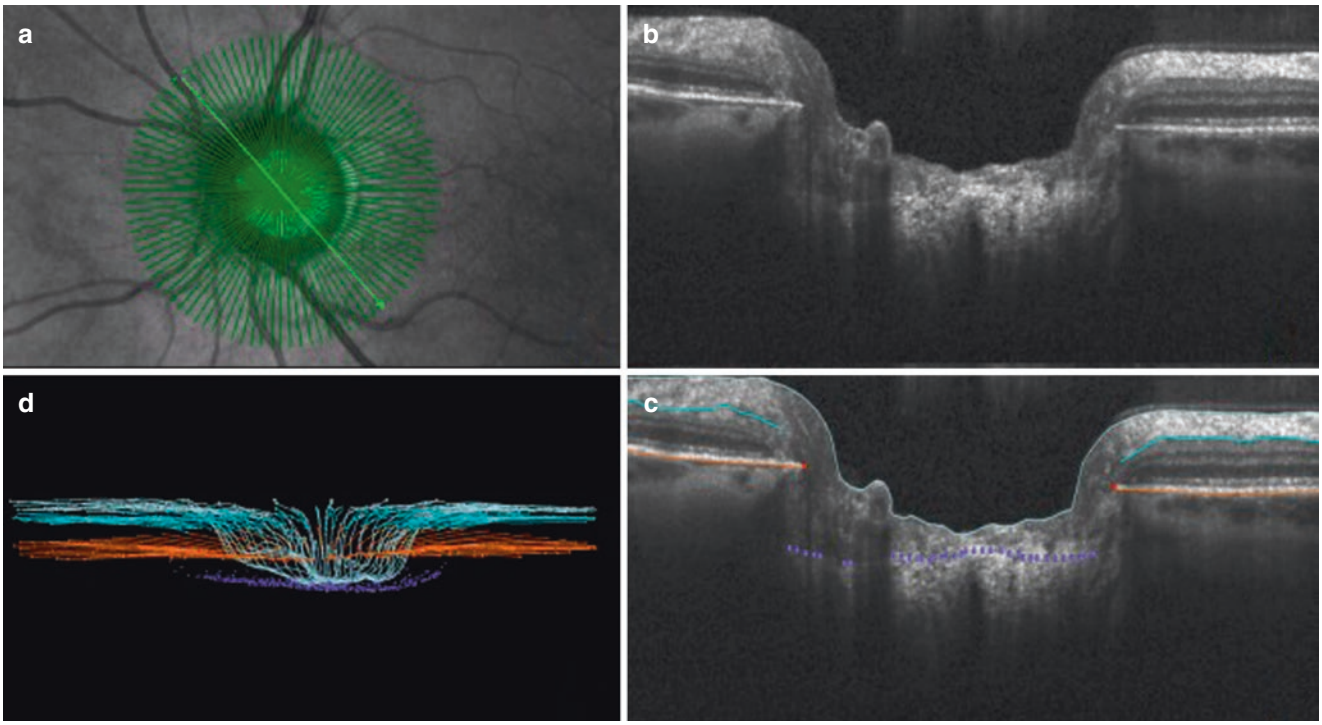

Fig. 29.1 Settings were 15° scan, 48 radial B-scans, 768 A-scans/B-scan, and each B-scan was the average of $n = 9$ repetitions. (**a**) IR image shows 48 radial B-scan pattern overlays. (**b**) Representative B-scan as described in the legend to (**a**). (**c**) Delineated B-scan shown in (**b**). *Light blue lines* indicate the ILM, *turquoise lines* the posterior surface of the RNFL, *orange lines* are the posterior surface of the BM/RPE complex, *red points* are the BMO, and *purple points* are the ALCS. (**d**) Point cloud of delineated points from the 24 radial B-scans that were delineated as a subset (Reproduced with permission from [1])

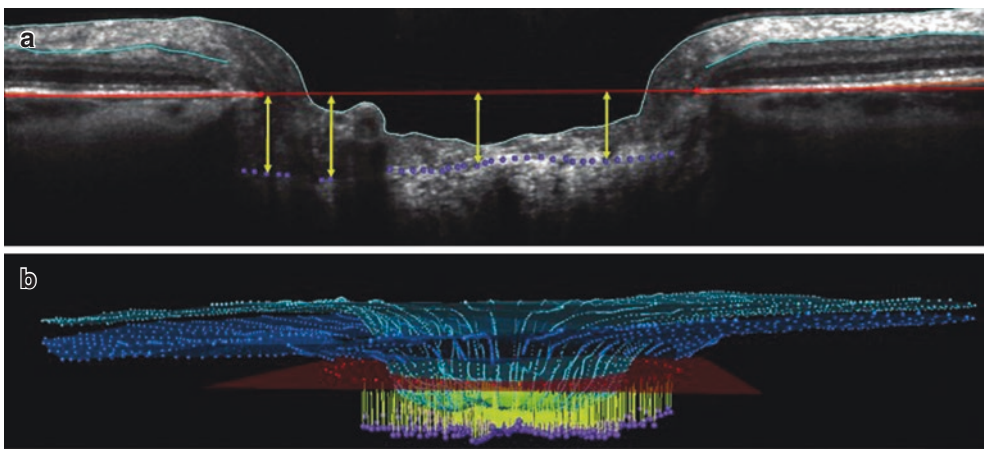

Fig. 29.2 ALCSD measurement is shown. (**a**) ALCSD (*yellow arrows*) was quantified as the perpendicular distance from each delineated ALCS point to BMO reference plane (seen in cross section as a *red line*). (**b**) Mean ALCSD was the average of all ALCSD measurements (*yellow*) in 3D space for the 24 radial B-scans that were delineated for each ONH. The ILM (*light blue*) and outer RNFL (*turquoise*) are also shown (Reproduced with permission from [1])

association between ALCSD and mean deviation (MD) was age-dependent.

Figure 29.4 plots ALCSD against age, with points shaded according to their MD. Left is ALCSD related to BMO zero reference plane at the top. In this graph, ALCSD increases its value away from the BMO zero reference plane. There are 221 patients' data points representing the magnitude of MD as shown on the right. The darker points indicate the worse MD. Even though the overall plots look like horizontal, a majority of the sequence are with worse MD. To the right is the older eye, and to the top meant with a shallow ALCSD. We used a linear regression model to generate a mathematic equation for ALCSD: ALCSD = 407.68–67.13 × MD − 0.08 × Age + 0.89 × MD × Age. Whereas both the MD ($P = 0.001$) and the MD × Age ($P = 0.004$) terms achieved significance, the age term did not ($P = 0.921$).

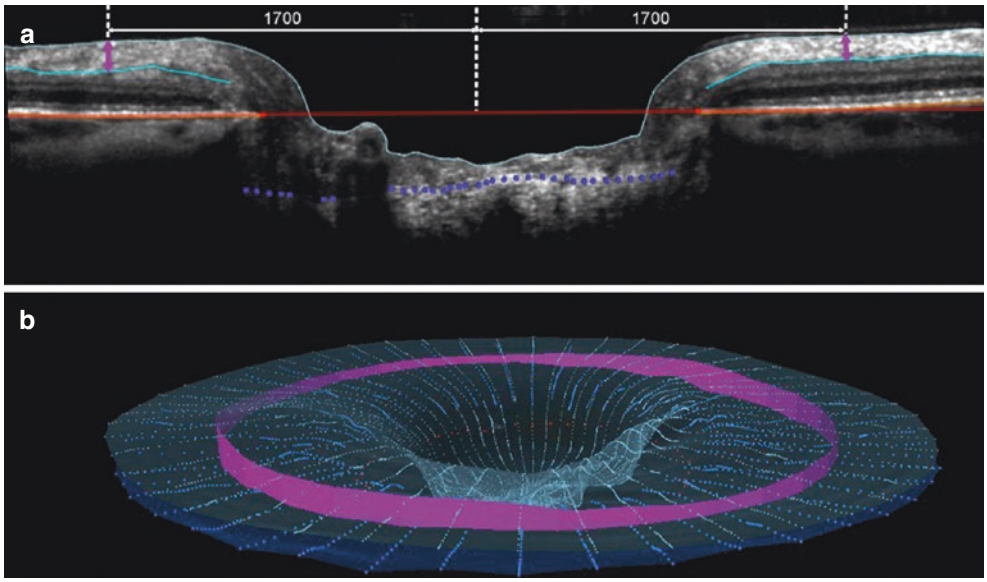

Fig. 29.3 RNFLT measurement is shown (*pink band*). (**a**) RNFLT was measured on either side of the canal at ILM points that are 1700 μm (3.4-mm diameter) from the centroid of the 48 delineated BMO points (the BMO centroid). The perpendicular projection of the BMO centroid is shown as the central *white vertical dotted line*. RNFLT at each ILM point is the minimum distance (*pink arrow*) between the ILM and the posterior RNFL boundary (*turquoise* B-spline *line*). (**b**) 3D representation of interpolated RNFLT (*pink band*) is based on the 24 delineated B-scans (Reproduced with permission from [1])

Table 29.1 Characteristics of the 211 participants and the 211 eyes in the study (Reproduced with permission from [1])

	Mean ± standard deviation	Range
Age (years)	64.3 ± 11.0	33.0–90.0
Central corneal thickness (μm)	556.0 ± 39.2	466.0–735.0
Intraocular Pressure (mmHg)	17.4 ± 3.5	5.0–29.0
Mean deviation (dB)	−0.69 ± 2.94	−16.53 to 3.29
ALCSD (μm)	405 ± 119	178–835
SDOCT RNFLT 1700 (μm)	89 ± 16	36–122
BMO area (mm^2)	1.85 ± 0.43	1.03–3.20
BMO major (μm)	1619 ± 186	1173–2169
BMO minor (μm)	1442 ± 173	1083–1929

ALCSD anterior lamina cribrosa surface depth, *RNFLT* retinal nerve fiber layer thickness; *BMO* Bruch's membrane opening

Two regression lines are shown, based on the equation given above: the solid gray line represents the relationship between ALCSD and age when MD = 0 dB; the dashed gray line represents the same relationship when the MD = −10 dB. Among eyes with no detectable VF loss, there are no significant differences between the ALCSD of young and those of old eyes. However, among eyes with a given amount of VF loss (in this case −10 dB), the anterior lamina surface is deeper in younger eyes than in older eyes. Note that most cases with worse VF status (darker-shaded symbols) are located to the right (older eyes) and toward the top (eyes with relatively shallow lamina cribrosa) of the scatterplot.

Figure 29.5 plots ALCSD against VF MD, with points shaded according to the different ages (darker plots indicate older age). There are also two regression lines shown, based on the same equation as given in Fig. 29.4: solid gray line and dashed gray line represent the situation of different ages. In senior eyes at the age of 75, ALCSD was unrelated to MD. However, in the younger eyes at the age of 55, the deeper ALCSD was, the worse MD was.

Also we found that univariate correlations among the three additional ALCSD parameters ($ALCSD_{max1}$, $ALCSD_{max2}$, and $ALCSD_{central}$) and three outcome parameters (age, IOP, and MD) were similar to those reported for ALCSD (Table 29.2).

Multivariate relationships between the three additional ALCSD parameters and MD were also age-dependent and similar to those reported for ALCSD. The interaction term (MD × Age) was consistently significant, with $P = 0.007$, $P = 0.007$, and $P = 0.004$, respectively.

$ALCSD_{max1} = 472.13–65.87 \times MD - 0.07 \times Age + 0.84 \times MD \times Age$ (MD $P = 0.002$); (Age $P = 0.926$); (MD × Age $P = 0.007$).

$ALCSD_{max2} = 457.40–65.26 \times MD - 0.03 \times Age + 0.83 \times MD \times Age$ (MD $P = 0.002$); (Age $P = 0.972$); (MD × Age $P = 0.007$).

$ALCSD_{central} = 420.28–66.53 \times MD - 0.05 \times Age + 0.86 \times MD \times Age$ (MD $P = 0.001$); (Age $P = 0.947$); (MD × Age $P = 0.004$).

There was no significant univariate relationship between RNFLT and ALCSD ($P = 0.225$, linear regression model) or IOP ($P = 0.226$, linear regression model). However, there was a significant negative relationship between RNFLT and age such that RNFLT = 112.26–0.37 × Age ($P < 0.001$, ordinary least squares regression) (Fig. 29.6).

Table 29.2 Correlations between the four measures of ALCSD and three outcome parameters (age, IOP, MD)

	ALCSD		$ALCSD_{max1}$		$ALCSD_{max2}$		$ALCSD_{central}$	
	R	*P* value	*R*	*P* value	*R*	*P* value	*R*	*P* value
Age	−0.045	0.504	−0.035	0.603	−0.030	0.658	−0.030	0.664
IOP	−0.083	0.222	−0.093	0.170	−0.099	0.143	−0.082	0.226
MD	−0.159	0.019	−0.196	0.004	−0.204	0.002	−0.190	0.005

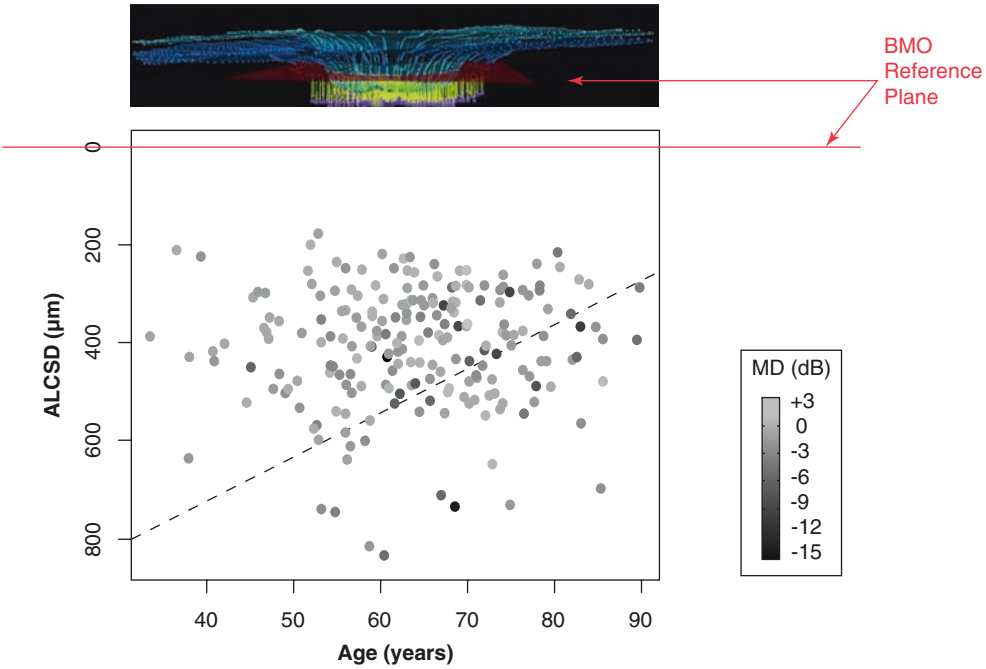

Fig. 29.4 The relationship between ALCSD and age (Reproduced with permission from [1])

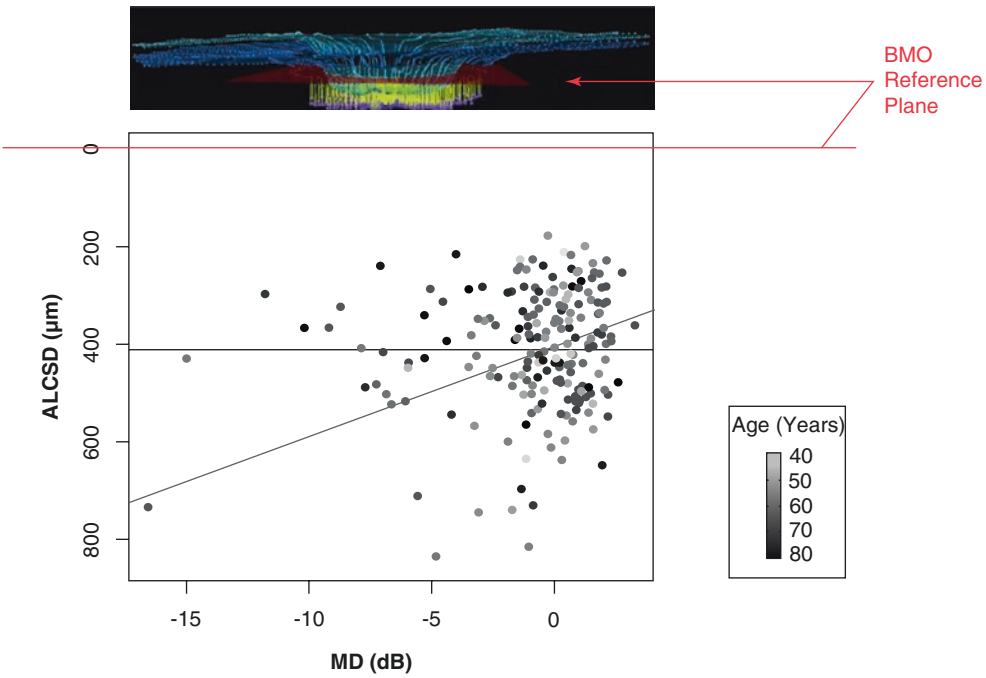

Fig. 29.5 The relationship between ALCSD and VF MD (Reproduced with permission from [1])

Fig. 29.6 The relation between RNFLT and age

Characteristic	Mean ± Standard Deviation	Range
Age, y	64.3 ± 11.0	33.0 – 90.0
Intraocular pressure, mm Hg	17.4 ± 3.5	5.0 – 29.0
Mean deviation, dB	–0.69 ± 2.94	– 16.53 – 3.29
ALCSD, μm	405 ± 119	178 – 835
SDOCT RNFLT, μm	89 ± 16	36 – 122
BMO area, mm^2	1.85 ± 0.43	1.03 – 3.20
BMO major, μm	1619 ± 186	1173 – 2169
BMO minor, μm	1442 ± 173	1083 – 1929

Using RNFLT as a surrogate for the "disease stage" instead of MD, and even though the *P* value of interaction term was not quite significant [(ALCSD = 1021.51−6.22 × RNFLT−8.38 × Age + 0.08 × RNFLT × Age) (RNFLT $P = 0.040$), (Age $P = 0.047$), (RNFLT × Age $P = 0.067$)], the same trend was observed as for MD: the anterior lamina surface was deeper in the eyes with thinner retinal nerve fiber layers; and this effect was greater in the younger eyes, as it was for MD. Moreover, the relationships using each of the three alternative definitions of ALCSD relative to RNFLT appeared to be similar, and the interaction term (RNFLT × Age) for each definition achieved a similar level of significance ($ALCSD_{max1}$, $P = 0.081$; $ALCSD_{max2}$, $P = 0.074$; $ALCSD_{central}$, $P = 0.085$).

In conclusion, the lamina appeared to be deeper in the eyes with greater visual field loss and thinner retinal nerve fiber layer in high-risk ocular hypertension and primary open-angle glaucoma patients. However, in older patients, the lamina is shallower than in younger patients with the same level of function loss and RNFLT.

Our data are consistent with the concept that old eyes are structurally stiffer than young eyes. Structural change in old compared to young eyes includes more neural tissues (thinner retinal nerve fiber layer) and more visual field loss for a given amount of lamina cribrosa deformation.

In the future, a longitudinal study of these same eyes is under way to test our hypothesis regarding age-related differences in structural versus functional progression.

Acknowledgments The authors thank Juan Reynaud, Cindy Blachly, and Michael Whitworth for their SDOCT technical support (JR) and clinical imaging of the P3 participants (CB and MW).

Supported by National Institutes of Health (NIH)/National Eye Institute (NEI) Grant R01-EY-019674 (SD); Legacy Good Samaritan Foundation; Carl Zeiss Meditec; NIH/NEI Grant R01-EY021281 (CFB); and Heidelberg Engineering, GmbH, Heidelberg, Germany.

Claude F. Burgoyne is a consultant to Heidelberg Engineering.

The above listed sponsors/funding organizations had no role in the design or conduct of this research.

The authors alone are responsible for the content and writing of the paper.

The text and figures of this manuscript have appeared previously in our own work: *Ren R, Yang H, Gardiner SK, Fortune B, Hardin C, Demirel S, Burgoyne CF. Anterior lamina cribrosa surface depth, age, and visual field sensitivity in the Portland Progression Project. Invest Ophthalmol Vis Sci. 2014;55(3):1531–9* [1]. They have been partly used with permission and edited for this chapter.

Reference

1. Ren R, Yang H, Gardiner SK, Fortune B, Hardin C, Demirel S, Burgoyne CF. Anterior Lamina Cribrosa surface depth, age and visual field sensitivity in the Portland progression project. Invest Ophthalmol Vis Sci. 2014;55(3):1531–9.

The Importance of Habitual 24-Hour IOP Measurement

30

John H. K. Liu

For this presentation, the habitual intraocular pressure (IOP) is defined as sitting IOP during the day and supine IOP during the night. We will discuss IOP with a period not shorter or longer than 24 h. Since most of our IOP data are obtained using a pneumatonometer that is not considered clinical gold standard, the emphasis will be on the IOP pattern along the day and night instead of the absolute IOP levels.

Several important lessons have been learned after having spent the past 18 years doing related studies in our sleep laboratory. The first lesson: the average IOP is higher at night than during the day. Today we are familiar with the habitual 24-h IOP pattern in glaucoma patients; approximately two thirds of IOP peaks appear at night. If one measures the office IOP only, IOP peaks would be missed two thirds of time. The second lesson: the 24-h IOP fluctuation in glaucoma patients is probably not larger than the IOP fluctuation in normal individuals. While a larger diurnal (daytime) IOP fluctuation is well known in glaucoma patients, data indicate that the 24-h IOP fluctuation may be different. The third lesson: various glaucoma medications may affect 24-h IOP pattern in different ways. Certain glaucoma medications may not work at all during the sleep period and other medications work but not well at night. A better medication is needed for consistent 24-h IOP control. Lastly, are our nighttime data valid when the patients have to open their eyes for the IOP measurements? Our lesson allows us to conclude that these data are not artifacts.

Figure 30.1 shows typical 24-h IOP patterns for healthy individuals and untreated glaucoma patients: the left panel for healthy individuals and the right panel for glaucoma patients. Both healthy eyes and glaucomatous eyes have higher nocturnal supine IOP than diurnal sitting IOP [1]. In addition, the IOP in glaucoma patients is always higher than healthy individuals. Before our studies in the sleep laboratory, most people thought that IOP would go down at night, rather than going up. For the 24-h IOP peaks in habitual body positions [2], 95% of healthy younger individuals have IOP peaks during the nocturnal period. In healthy older individuals (40 and above), nocturnal IOP would peak similarly. Due to a larger IOP fluctuation during the day in glaucoma patients, only two thirds of them have IOP peaks at night. While IOP fluctuation is larger in glaucoma patients than normal during the diurnal period, IOP fluctuation is approximately the same if you look over the 24 h.

Regarding glaucoma medications [3], we first made a comparison of timolol, a beta-blocker, versus latanoprost. Timolol gel form was given once a day in the morning for 4 weeks. Compared with the 24-h baseline, IOP was reduced during the day but not at night. Treatment of latanoprost once in the evening showed effects both during the day and at night, although the nighttime effect was less. Since latanoprost was given prior to sleep, its bioavailability was higher before the patient woke up. However, IOP effect was larger in the morning than at night during the sleep period. We repeated the study of timolol gel form once a day in the morning as the adjunctive therapy. IOP decreased for diurnal sitting and diurnal supine measurements but not for the nocturnal supine measurements. Recently we had another test of timolol's IOP-lowering efficacy using timolol solution twice a day for 4 weeks [4]. Diurnal sitting and diurnal supine IOP decreased under treatment but no effect upon the nocturnal supine IOP. These results affirm the absence of timolol's IOP effect at night. For our sleep laboratory record of testing prostaglandin analogs including 54 patients, approximately 4 mmHg IOP reduction was found for the diurnal sitting and supine IOP but only 2 mmHg for the nocturnal supine IOP. It seems that mechanisms of IOP regulation are different for the day and at night. A study [5] on the habitual 24-h IOP

J. H. K. Liu
Department of Ophthalmology, Shiley Eye Institute,
University of California, San Diego, CA, USA
e-mail: joliu@ucsd.edu

N. Wang (ed.), *Intraocular and Intracranial Pressure Gradient in Glaucoma*,
Advances in Visual Science and Eye Diseases 1, https://doi.org/10.1007/978-981-13-2137-5_30

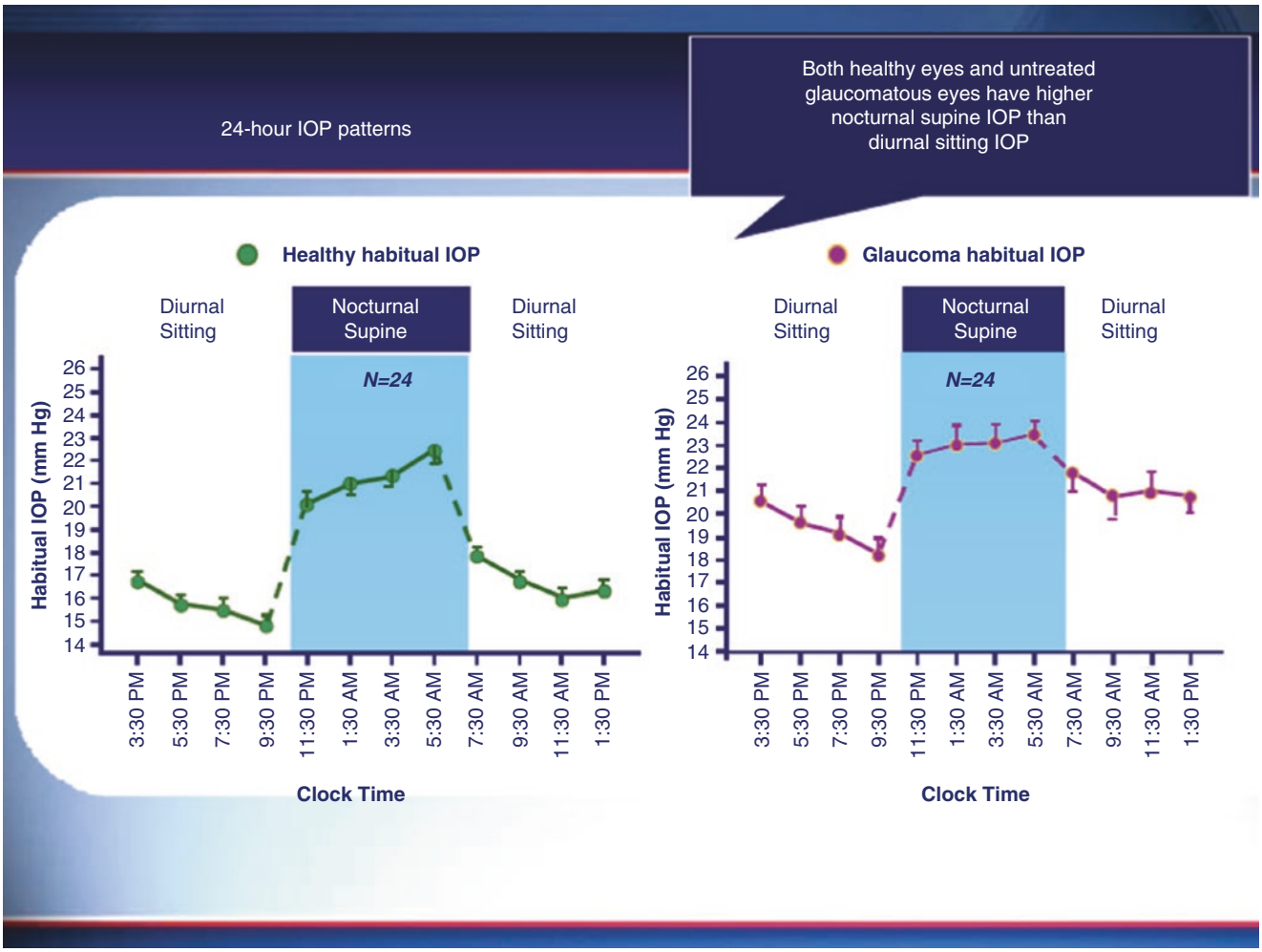

Fig. 30.1 Comparison of 24-hour IOP patterns in healthy and untreated glaucomatous eyes. Error bars represent SEM

pattern with laser trabeculoplasty as the secondary therapy showed that IOP can decrease more during the nocturnal period, indicating the potential of a medication that can act on trabecular meshwork to improve the overall 24-h IOP-lowering efficacy.

Recent development of contact lens-based IOP sensors (CLS) is a new tool to study the 24-h habitual IOP pattern. Figures 30.2 and 30.3 show 24-h data collected by this CLS and pneumatonometer in 30 healthy and contralateral eyes, respectively. There are 288 readings using the CLS and 12 IOP readings using the pneumatonometer. Change patterns using the CLS and pneumatonometer are similar. Considering the fact that there is no definite evidence to link higher IOP at night and glaucoma progression, a power calculation suggests that thousands of patients need to be enrolled for a clinical trial. We are looking forward to the use of CLS home recordings to effectively study the link of nocturnal IOP and glaucoma progression.

We have shown that habitual 24-h IOP at the front of optic nerve head is dynamic. It can be changed by posture, circadian time, and glaucoma medications. A critical question remains: how does intracranial pressure change behind the optic nerve head? Reports in the literature only indicate that the opening cerebrospinal fluid pressure by lumbar puncture is lower in glaucoma patients. We should seek more data of intracranial pressure with different postures, times of the day, and glaucoma medications as well as the role of intracranial pressure in glaucoma pathogenesis.

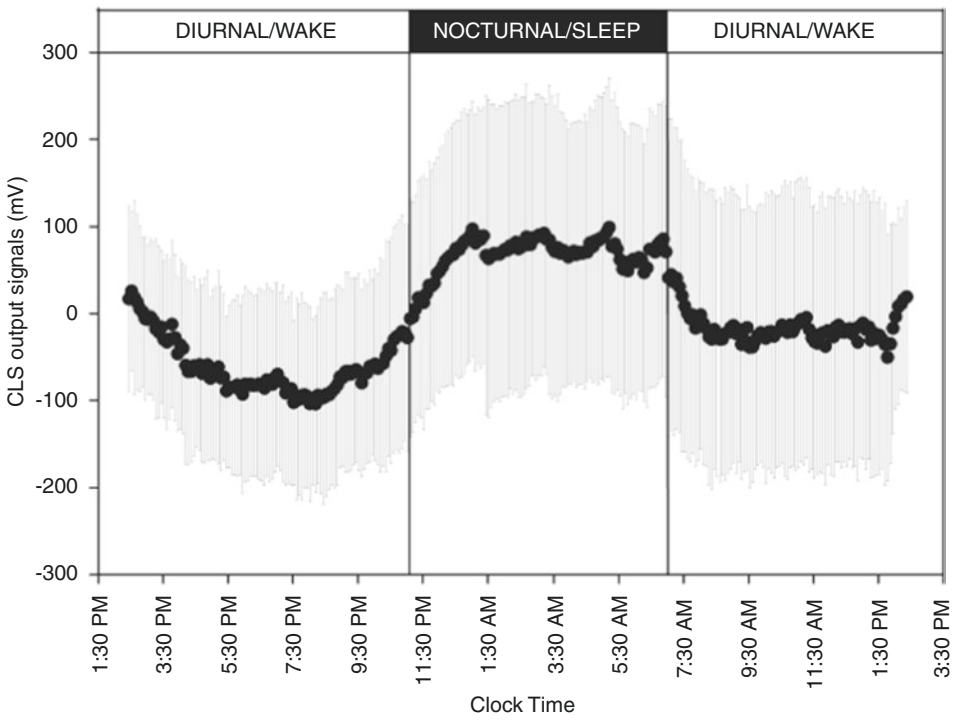

Fig. 30.2 24-hour pattern of output signal from the contact lens sensor in 30 healthy eyes. Error bars represent SD. (Reprinted with permission from Liu J H, Mansouri K, Weinreb R N. Estimation of 24-Hour Intraocular Pressure Peak Timing and Variation Using a Contact Lens Sensor[J]. PLos One, 2015, 10(6):e0129529 [6])

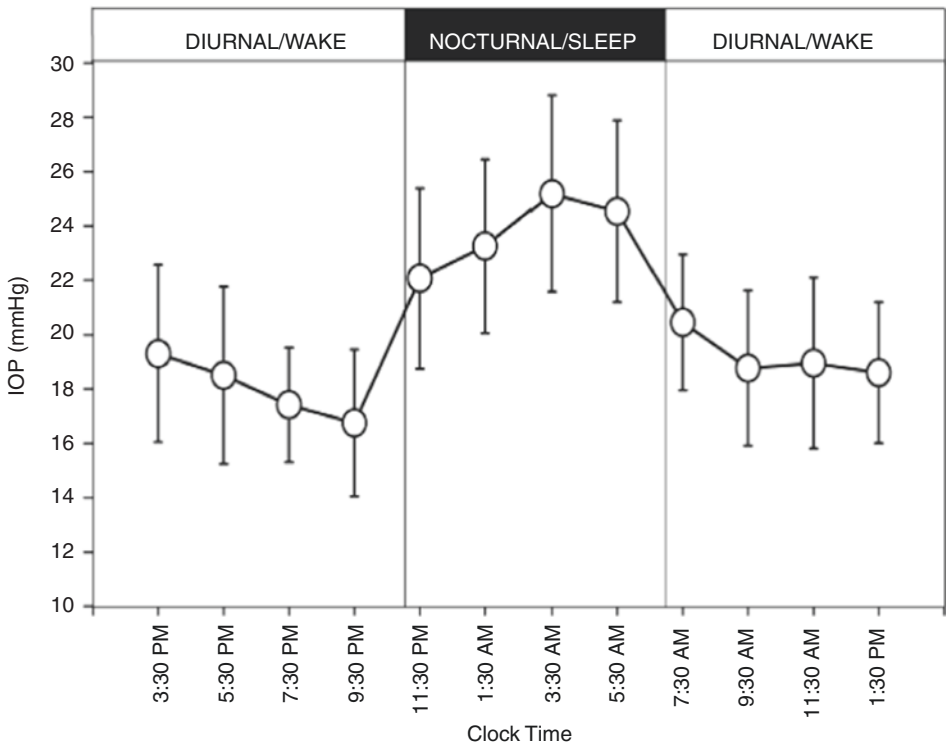

Fig. 30.3 24-hour IOP pattern in 30 contralateral eyes using the pneumatonometer. Error bars represent SD. (Reprinted with permission from Liu J H, Mansouri K, Weinreb R N. Estimation of 24-Hour Intraocular Pressure Peak Timing and Variation Using a Contact Lens Sensor[J]. PLos One, 2015, 10(6):e0129529 [6])

References

1. Liu JH, et al. Twenty-four-hour intraocular pressure pattern associated with early glaucomatous changes. Invest Ophthalmol Vis Sci. 2003;44(4):1586–90.
2. Mosaed S, Liu JH, Weinreb RN. Correlation between office and peak nocturnal intraocular pressures in healthy subjects and glaucoma patients. Am J Ophthalmol. 2005;139(2):320–4.
3. Liu JH, Kripke DF, Weinreb RN. Comparison of the nocturnal effects of once-daily timolol and latanoprost on intraocular pressure. Am J Ophthalmol. 2004;138(3):389–95.
4. Liu JH, et al. Efficacy of latanoprostene bunod 0.024% compared with timolol 0.5% in lowering intraocular pressure over 24 hours. Am J Ophthalmol. 2016;169:249–57.
5. Lee AC, et al. Effect of laser trabeculoplasty on nocturnal intraocular pressure in medically treated glaucoma patients. Ophthalmology. 2007;114(4):666–70.
6. Liu JH, Mansouri K, Weinreb RN. Estimation of 24-hour intraocular pressure peak timing and variation using a contact lens sensor. PLoS One. 2015;10(6):e0129529.

Intracranial Hypotension and Coexistent Normal-Pressure Glaucoma: 5-Year Follow-Up

31

Zhen Li and Ningli Wang

Trans-lamina pressure difference theory is a new theory on pathogenesis of glaucoma. The core of this theory is that it is the trans-lamina pressure difference that causes the change of lamina cribrosa, and the latter leads to the onset of glaucoma.

Lamina cribrosa is the primary site of glaucomatous neuropathy [1] and separates two pressurized circulating fluid compartments: anterior intraocular pressure compartment and posterior intracranial pressure compartment. The trans-lamina pressure difference (TLPD) equals to intraocular pressure minus intracranial pressure. In theory, both increased intraocular pressure and decreased intracranial pressure could cause increased TLPD. High TLPD pushes the lamina cribrosa backward, which initiates the glaucomatous optic neuropathy. On the other side, decreased intraocular pressure, same as increased intracranial pressure, would lead to decreased TLPD, which contributes to the occurrence of papilledema. There are plenty of evidences proving that high intraocular pressure causes high TLPD and then glaucomatous neuropathy in human. Optic disc edema (papilledema) can be observed in the eyes with high intracranial pressure or with low intraocular pressure. At present, solid evidence demonstrating that low intracranial pressure could cause glaucoma in human is lacking.

The major milestone events in the development of this theory are as follows. Trans-lamina pressure difference was first put forward by Volkov in 1976 [2]. He suggested that a low cerebrospinal pressure (CSFP) could be pathogenetically associated with glaucomatous optic neuropathy. Three years later, an animal test in cats conducted by Yablonski and his colleagues [3] confirmed this hypothesis. In 2008, Berdahl [4] reported in their retrospective study that the mean CSFP was significantly higher in the non-glaucomatous patients than in open-angle glaucoma patients. In 2010, Ren and her coworkers [5] carried out a prospective study and found that POAG (include NTG) patients had lower CSFP than non-glaucoma controls. In 2014, Dr. Yang [6] reported the results of animal experiments conducted in the rhesus monkey. They found that experimental and chronic reduction in CSF pressure in monkeys was associated with the development of optic neuropathy.

Existing clinical evidences showed that intracranial pressure (ICP) in NTG patients was lower than control subjects. Animal experiments have confirmed that reduced ICP would have the same effect as increased IOP for the development of glaucoma. Nevertheless, clinical evidence proving that low ICP can lead to NTG is still needed to close the evidence chain (Fig. 31.1).

Fig. 31.1 The evidence chain for low intracranial pressure being one of the etiological factors of glaucomatous neuropathy

Z. Li
Department of Ophthalmology, Xuanwu Hospital, Capital Medical University, Beijing, China

N. Wang (✉)
Beijing Institute of Ophthalmology, Beijing Tongren Eye Center, Beijing Tongren Hospital, Capital Medical University, Beijing, China

Beijing Ophthalmology & Visual Sciences Key Laboratory, Beijing, China
e-mail: wningli@vip.163.com

N. Wang (ed.), *Intraocular and Intracranial Pressure Gradient in Glaucoma*,
Advances in Visual Science and Eye Diseases 1, https://doi.org/10.1007/978-981-13-2137-5_31

31.1 A Clinical Case Report

We once reported a patient with intracranial hypotension and coexistent normal-tension glaucoma [7]. In 2010, a 53-year-old man complained of increasingly painful headache lasting for 1 month. The characteristic of the headaches is orthostatic headache, which eases in supine position and deteriorates in an upright or sitting position.

The man had a head trauma and some clear fluid ran out from his ears 2 years ago. Due to the lack of the examination results of that injury, it cannot be confirmed whether the clear liquid is cerebrospinal otorrhea. Furthermore, the patient also suffered from hypertension and diabetic mellitus.

Neurological examination revealed an increased muscle tone in his left lower limb. Rossolimo's sign and Hoffman's sign were positive on the left side of the body. CSF pressure measured by lumbar puncture was 20 mmH_2O (1.5 mmHg). The neuroimaging findings were consistent with intracranial hypotension syndrome. Therefore, neurologists diagnosed the patient as intracranial hypotension syndrome (Fig. 31.2).

The ophthalmological examination revealed a best corrected visual acuity of 0.80 in both eyes and a normal anterior ocular segment. IOP was 14 mmHg in the right eye and 15 mmHg in the left eye. Central corneal thickness was 494 μm for the right eye and 504 μm for the left eye. In a 24-h intraocular pressure examination, intraocular pressure ranged between 11 and 15 mmHg in both eyes. The glaucomatous changes were observed in both optic nerve heads in this patient's fundus photography. Optical coherence tomography correspondingly showed a thinning of the retinal nerve fiber layer profile, and perimetry showed corresponding defects. Hence, the ophthalmologist diagnosed him as normal-tension glaucoma (Figs. 31.3, 31.4, and 31.5).

We present a patient with both intracranial hypotension and NTG. At the same time, without ophthalmological examination results before the onset of intracranial hypotension, it cannot be affirmed whether the patient's NTG was caused by his low intracranial pressure.

Therefore, two hypotheses were proposed:

1. If TLPD is higher than normal range, the patient's glaucoma would progress.
2. If the TLPD returns to normal range, the patient's glaucoma progression would slow down or come to a stop.

Follow-up observations were continued, and two reviews were conducted in May 2011 and February 2012, respectively. No abnormality was detected in neurological examination and neuroimaging examination. CSF pressure measured by lumber puncture was 50 mmH_2O (3.7 mmHg) in 2011 and 110 mmH_2O (8.2 mmHg) in 2012.

Ophthalmological examinations showed the optic disc was free of hemorrhages during the first review but revealed a new optic disc hemorrhage in the left eye during the second review. While visual field had no significant change, OCT showed a progressive thinning of the retinal nerve fiber layer. Progression of the patient's glaucoma was observed.

The same ophthalmological examinations were performed again in 2015, still without any abnormality detected in the neurological examination and neuroimaging examination. CSF pressure was measured by MRI and calculated CSF pressure was about 12 mmHg. The calculated TLPD returned to normal range, and the progression of the patient's glaucoma obviously slowed down. (This part will be published in another article.)

When the patient first came to hospital, specialists gave him the diagnosis of intracranial hypotension with coexistent normal-tension glaucoma. At that time, the patient's translaminar pressure difference was 12.5 mmHg in the right eye and 13.5 mmHg in the left eye, much higher than normal range (about 4 mmHg). Although his ICP was elevated to 8.2 mmHg 17 months later, which is the normal level of CSF pressure, the trans-lamina pressure differences were 5.8 and 6.8 mmHg in the right eye and left eye, still higher than normal level. In this period, with TLPD higher than normal range, patient's glaucoma progressed. This condition is similar to previous clinical studies [4, 5]. The first hypothesis was confirmed.

In the last examination, with the rise of intracranial pressure, the patient's TLPD gradually resumed to normal, and the progression of his glaucoma markedly slowed down, which was consistent with the second hypothesis.

It is worth noting that because the decreased range of intracranial pressure is significantly smaller than increased range of intraocular pressure, the normal-tension glaucoma caused by low intracranial pressure is similar to high-tension glaucoma caused by mildly increased intraocular pressure. The glaucomatous optic nerve damage could be detected only when the low intracranial pressure sustained for a relatively long time.

The patient's condition was in consistence with all of the above descriptions. We believe that the TLPD must play an important role in the patient's normal-tension glaucoma with intracranial hypotension as one of pathogenic factors that lead to the occurrence and development of normal-tension glaucoma.

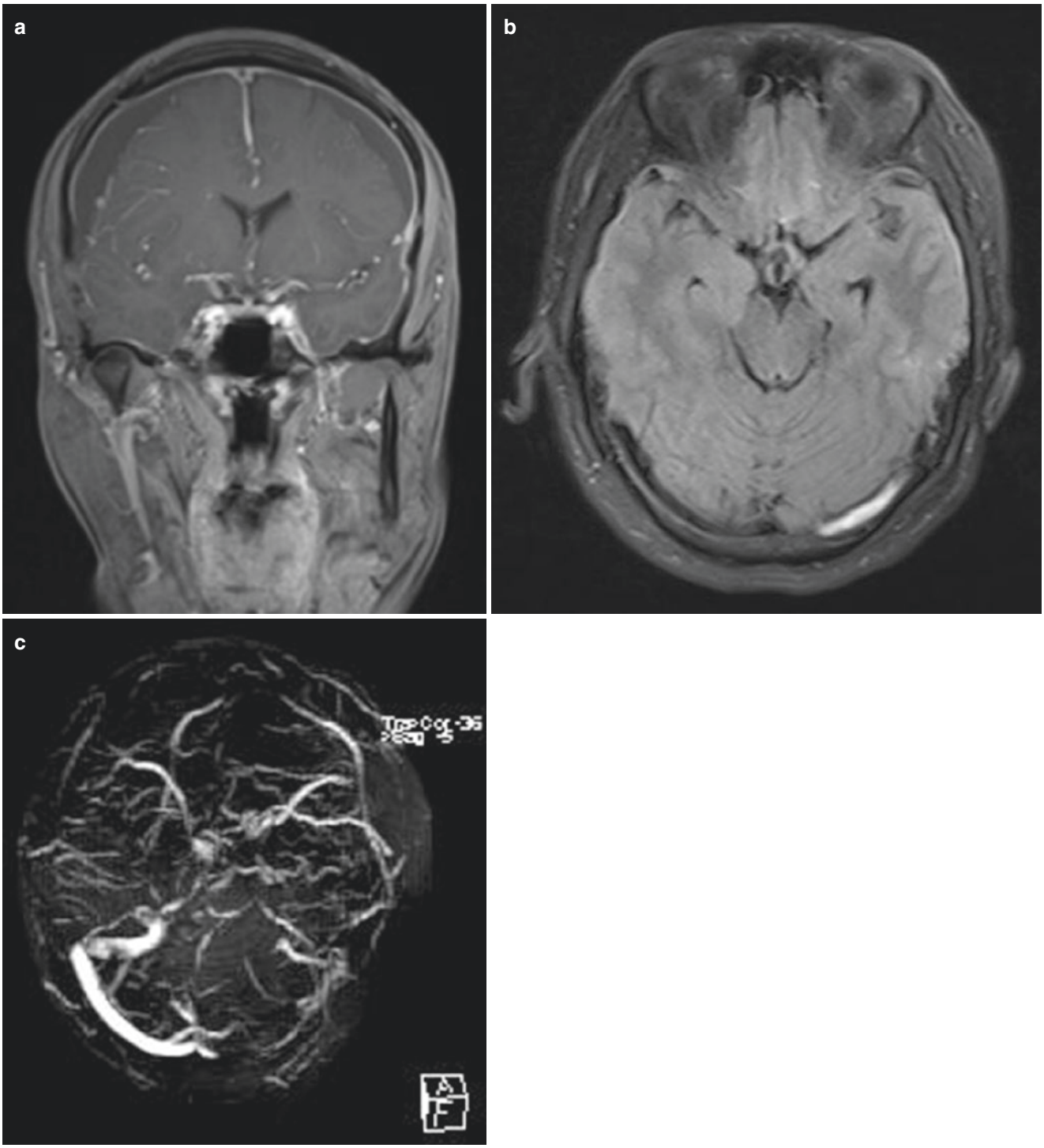

Fig. 31.2 Neuroimaging examination results. (**a**): a coronal MRI head scan photography revealed meningeal thickening and enhancement, subdural effusion, and smaller supratentorial ventricles; (**b**): a flair image showed a venous sinus thrombosis on the left side; (**c**): a MRV figure showed sigmoid sinus being not developed, which indicated the left transverse sinus

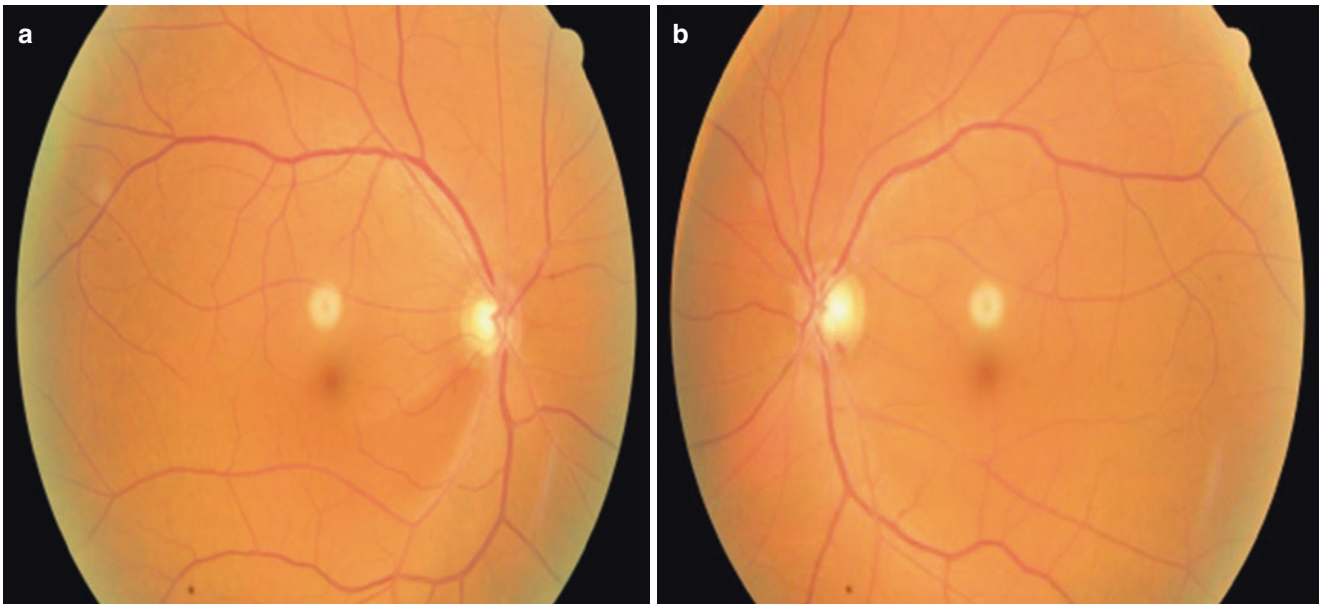

Fig. 31.3 Fundus photographs of the right eye (**a**) and left eye (**b**) of the patient with normal intraocular pressure glaucoma and low CSF pressure. The glaucomatous notch in the temporal inferior neuroretinal rim with corresponding localized retinal nerve fiber defect in the right eye and more diffused neuroretinal rim decrease and splinter-shaped disc hemorrhage in the left eye (Reproduced with permission from [7])

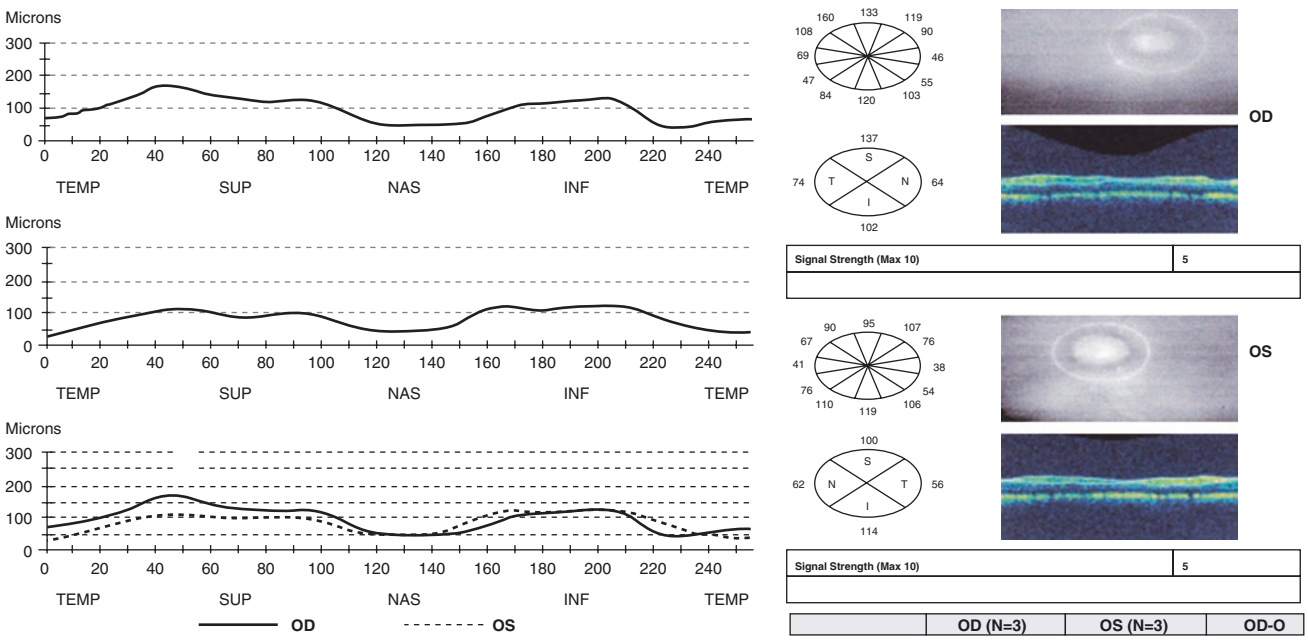

Fig. 31.4 RNFL thickness scanned with OCT nerve fiber layer thinning in the inferior-temporal area in the right eye and more diffused nerve fiber layer thinning in the left eye, especially in superior area

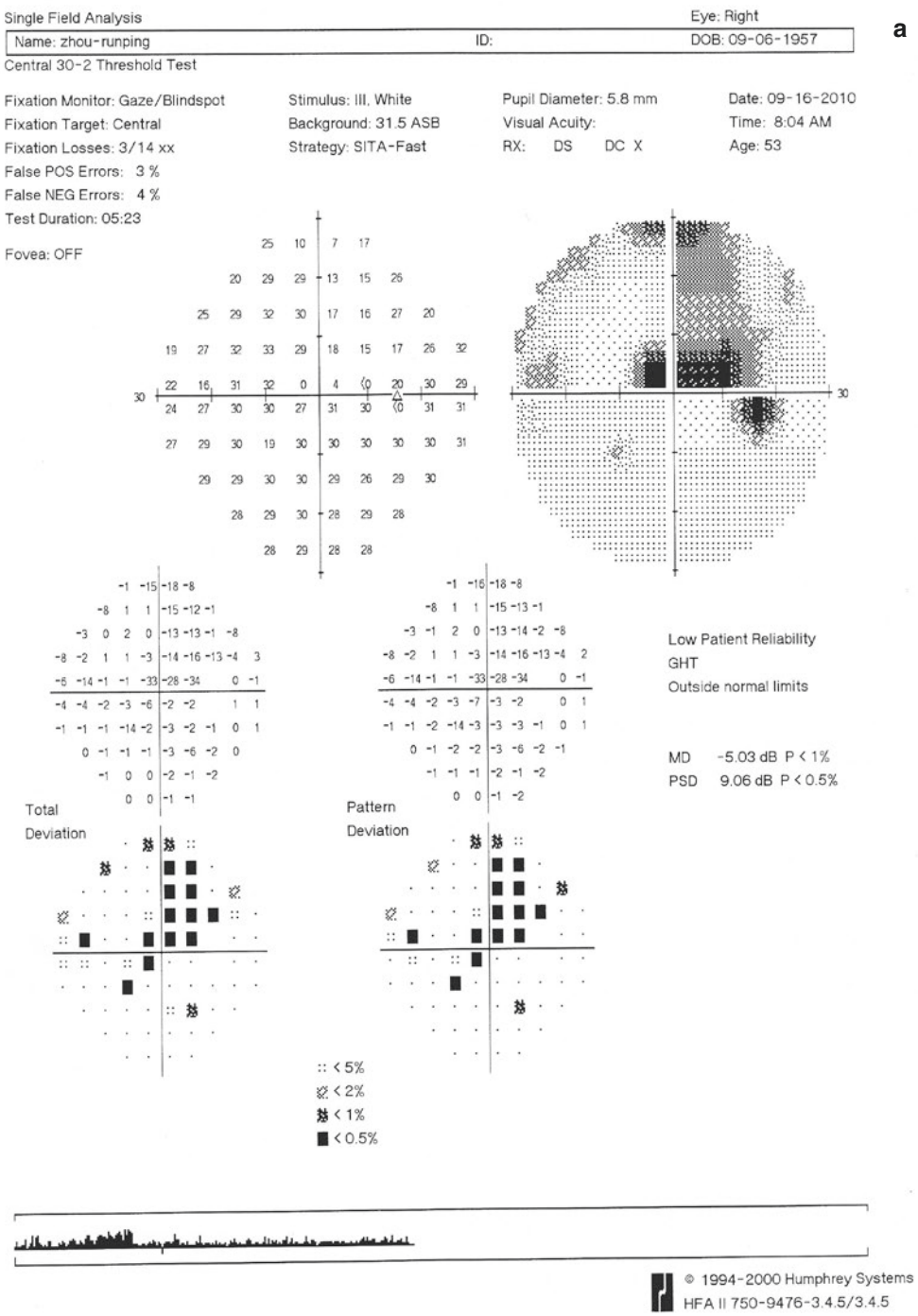

Fig. 31.5 Visual field of the right eye (**a**) and left eye (**b**). Visual field defects in the superior field quadrants of the right eye and inferior field quadrants of the right eye

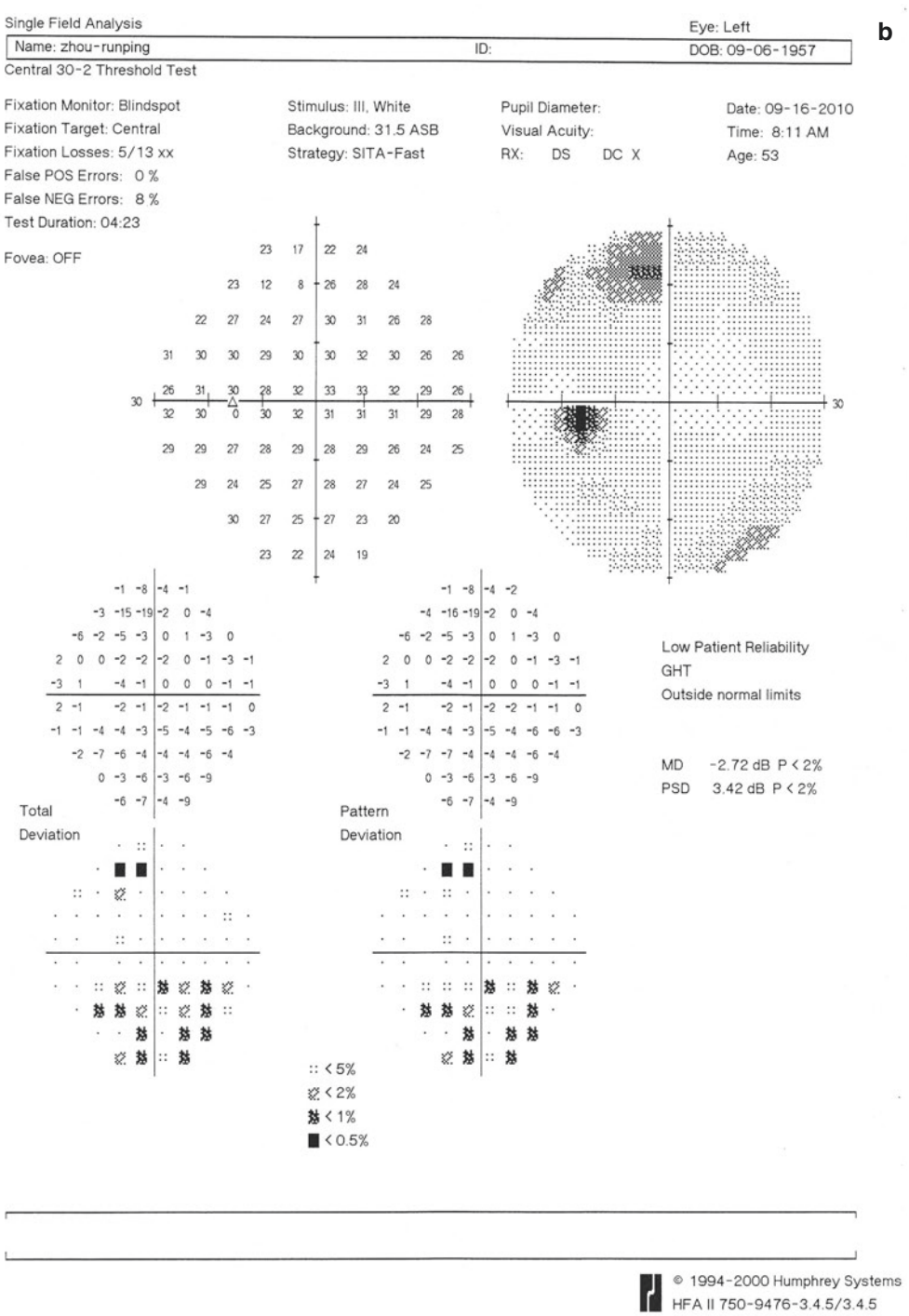

Fig. 31.5 (continued)

References

1. Quigley HA, Addicks EM, Green WR, et al. Optic nerve damage in human glaucoma. II. The site of injury and susceptibility to damage[J]. Arch Ophthalmol. 1981;99(4):635–49.
2. Volkov VV. [Essential element of the glaucomatous process neglected in clinical practice][J]. Oftalmol Zh. 1976;31(7):500–4.
3. Yablonski M, Ritch R, Pokorny KS. Effect of decreased intracranial pressure on optic disc. Invest Ophthalmol Vis Sci. 1979;18((Suppl)):165.
4. Berdahl JP, Allingham RR, Johnson DH. Cerebrospinal fluid pressure is decreased in primary open-angle Glaucoma[J]. Ophthalmology. 2008;115(5):763–8.
5. Ren R, Jonas JB, Tian G, et al. Cerebrospinal Fluid Pressure in Glaucoma[J]. Ophthalmology. 2010;117(2):259–66.
6. Yang D, Fu J, Hou R, et al. Optic neuropathy induced by experimentally reduced cerebrospinal fluid pressure in monkeys[J]. Invest Ophthalmol Vis Sci. 2014;55(5):3067–73.
7. Li Z, Yang DY, Lu Y, et al. Intracranial hypotension and co-existent normal-pressure glaucoma: the Beijing intracranial and intraocular pressure study[J]. Chin Med J (Engl). 2013;126(8):1588–9.

32 Peripapillary Retinal Pigment Epithelium Movement Associated with Acute IOP Elevation

Yaxing Wang and Ningli Wang

Peripapillary atrophy (PPA) is a normal feature in the optic disc region, which might be associated with diseases like glaucoma and myopia. On fundus photography, the PPA is classified into the alpha zone and the beta zone, which is defined as the outer region with irregular hyperpigmentation and hypopigmentation, and the inner region with visible sclera and visible large choroidal vessels [1]. With the help of the optical coherent tomography, the microstructure base of PPA is defined. The traditional beta zone PPA is divided into beta zone with overlying Bruch's membrane and newly gamma zone without overlying Bruch's membrane [2]. The beta zone PPA was widely investigated to be associated with the presence and progression of glaucoma [3, 4]. However, its etiology and the potential interactions with glaucoma development and with the intraocular pressure (IOP) are unknown.

We have conducted a series of studies to investigate the morphological changes based on the IOP rise induced by the dark room prone provocative test (DRPPT), which might be of importance to the understanding of the mechanism of the development of PPA. The DRPPT is a routine clinical diagnostic test for identifying patients with acute angle closure when suspected, which is a combination of the dark room test with the prone test [5]. Eyes with IOP elevation more than 5 or 8 mmHg were deemed as positive clinically.

The prospective comparative study enrolled primary angle closure suspects whom had IOP elevation more than 2 mmHg after a 2 h DRPPT, in a consecutive manner from February 2013 to September 2013. The optic nerve head (ONH) was scanned by spectral domain OCT before the DRPPT and within 5 min after the DRPPT, with both the matrix scanning mode and the star scan mode. A total of 114 eyes from 65 patients (57 women) were enrolled with mean age of 58.6 years. The IOP was 16.0 ± 3.9 mmHg at baseline and 26.1 ± 11.7 mmHg after the DRPPT, with a mean elevation of 10.1 ± 10.9 mmHg (2–47 mmHg).

In the first step, we measured the ONH parameters including Bruch's membrane opening (BMO) diameter, the minimum rim width, the lamina depth, the lamina thickness, the cup width, and the cup depth. When the 114 eyes were all included, most of the above parameters did not change statistically ($P > 0.05$), except for a decrease of the temporal minimal rim width. If we only chose those with markedly IOP rise (>15 mmHg), there was significant change, including an increase in the cup width and cup depth and a decrease in the temporal/nasal minimal rim width and the lamina cribrosa thickness. The lamina cribrosa depth and BMO diameter kept constant from baseline to the end of the DRPPT. These morphological changes of the ONH were found to be IOP elevation dependent ($P < 0.01$). It suggested that a 2-h IOP rise in non-glaucomatous eyes leads to a compression of neuroretinal rim, prelaminar tissue, and lamina cribrosa; however no major changes were present in optic disc size and relative position of the lamina cribrosa surface [6].

Furtherly, we closely observed the detailed changes of the ONH region in eyes with IOP rising more than 15 mmHg. Nineteen eyes from 14 participants were enrolled, with the IOP rise of 32.1 ± 9.5 mmHg (range, 17–47 mmHg), changing from 15.5 ± 2.9 mmHg at baseline to 47.6 ± 10.5 mmHg at the end of the DRPPT. Morphological alterations on the RPE edge close to the peripapillary border of Bruch's membrane were observed in 94.7% of the eyes. Some presented a folding of the RPE end, and some presented a RPE sliding on Bruch's membrane directing away from the optic disc (Fig. 32.1). The same RPE changes were found both in the line-scan mode and the subsequent scans of the radial-scan mode. The RPE changes were found to be located in the

Y. Wang · N. Wang (✉)
Beijing Institute of Ophthalmology, Beijing Tongren Eye Center, Beijing Tongren Hospital, Capital Medical University, Beijing, China

Beijing Ophthalmology & Visual Sciences Key Laboratory, Beijing, China
e-mail: wningli@vip.163.com

N. Wang (ed.), *Intraocular and Intracranial Pressure Gradient in Glaucoma*,
Advances in Visual Science and Eye Diseases 1, https://doi.org/10.1007/978-981-13-2137-5_32

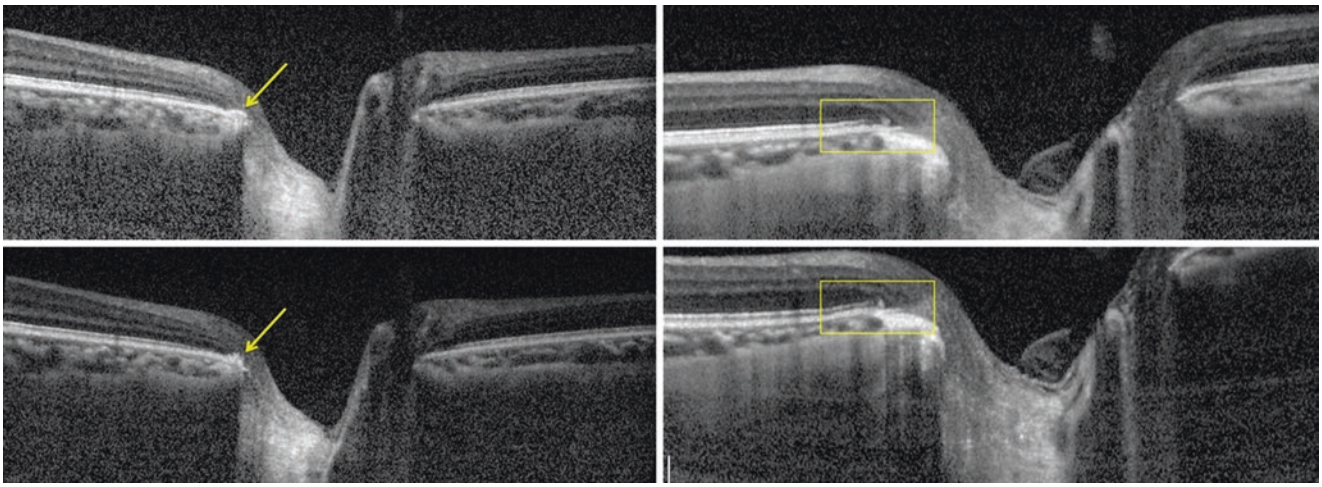

Fig. 32.1 Change in the peripapillary retinal pigment epithelium (RPE) detected before (top) and after rise in IOP (bottom) in two eyes. The left eye showed a RPE folding, and the right eye showed a centrifugal sliding of the RPE end on Bruch's membrane away from the optic disc (Reprinted with permission from [7])

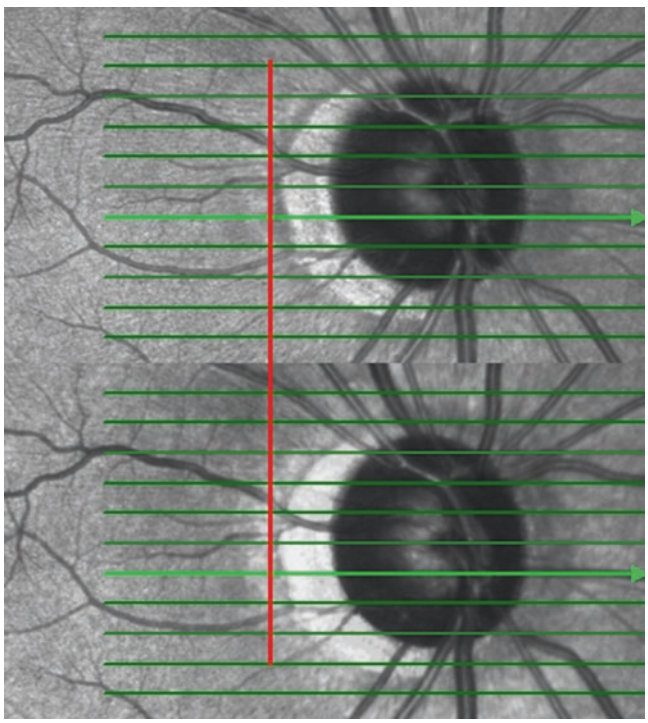

Fig. 32.2 Slight enlargement of peripapillary beta zone (bright peripapillary region) after an acute increase in IOP from 13 mmHg (*above*) to 47 mmHg (*below*) at the end of a 2-h dark room prone provocative test (Reprinted with permission from [7])

temporal region of the ONH, which accounted for 84%. Seven eyes were refollowed on the day after the DRPPT when the IOP returned to normal. The parapapillary end of RPE was found to move back toward the peripapillary Bruch's membrane border [7].

In some eyes with a marked change in the RPE end on the peripapillary Bruch's membrane, an enlarged beta zone at the corresponding location was detected in the scanning laser ophthalmoscopy (SLO) images (Fig. 32.2).

Our study showed the morphological changes of the ONH upon acute IOP rise, especially the dynamic changes of the RPE border on the peripapillary Bruch's membrane, containing a folding and a centrifugal sliding of the end of the RPE away from the ONH center. In some eyes with substantial changes in the RPE observed on the OCT scan, an enlargement of the peripapillary beta zone was also recognized on the SLO images of the optic disc. Such changes were proved to be reversible by observations on the following day after the DRPPT when the IOP returned to normal. In the control group that eyes with minor rise of IOP during the DRPPT were selected, none of the eyes showed comparable alterations.

The short-term IOP rise-associated changes of the peripapillary RPE were found most often at the temporal disc margin. It agrees with the location of peripapillary beta zone which is located most often and which is largest in the temporal peripapillary sector as compared to any other peripapillary sector [1].

These findings suggested that the occurrence of beta zone PPA may be secondary to IOP increase, at least in some occasions. The consistent enlargement of beta zone with the cupping of the ONH responding to acute IOP increase also suggested that PPA and glaucomatous changes may share the same mechanism. These observations may be of interest to elucidate the pathogenesis of PPA in glaucoma.

References

1. Jonas JB, Nguyen XN, Gusek GC, Naumann GO. Parapapillary chorioretinal atrophy in normal and glaucoma eyes. II correlations. Invest Ophthalmol Vis Sci. 1989;30:919–26.
2. Lee EJ, Kim TW, Weinreb RN, Park KH, Kim SH, Kim DM. β-Zone parapapillary atrophy and the rate of retinal nerve fiber layer thinning in glaucoma. Invest Ophthalmol Vis Sci. 2011;52:4422–7.
3. Teng CC, De Moraes CG, Prata TS, Liebmann CA, Tello C, Ritch R, Liebmann JM. The region of largest β-zone parapapillary atrophy area predicts the location of most rapid visual field progression. Ophthalmology. 2011;118:2409–13.
4. Teng CC, De Moraes CG, Prata TS, Tello C, Ritch R, Liebmann JM. Beta-zone parapapillary atrophy and the velocity of glaucoma progression. Ophthalmology. 2010;117:909–15.
5. Hyams SW, Friedman Z, Neumann E. Elevated intraocular pressure in the prone position: a new provocative test for angle-closure glaucoma. Am J Ophthalmol. 1968;66(4):661–72.
6. Jiang R, Xu L, Liu X, et al. Optic nerve head changes after short-term intraocular pressure elevation in acute primary angle-closure suspects. Ophthalmology. 2015;122(4):730–7.
7. Wang YX, Jiang R, Wang NL, Xu L, Jonas JB. Acute peripapillary retinal pigment epithelium changes associated with acute intraocular pressure elevation. Ophthalmology. 2015;122(10):2022–8.

The Relationship Between Cerebrospinal Fluid Pressure and Blood Flow in the Retina and Optic Nerve

33

Alon Harris, Josh Gross, Daniele Prada, Brent Siesky, Alice C. Verticchio Vercellin, Lauren Saint, and Giovanna Guidoboni

33.1 Introduction

Advancements in imaging technologies over the past several decades have allowed for the identification of non-intraocular pressure (IOP) processes involved in glaucomatous optic neuropathy. Perhaps the most commonly cited non-IOP risk factors are impaired ocular circulation and/or faulty vascular regulation and vasospasm [1, 2]. Other important considerations include the possible synergistic interaction between IOP and intracranial pressure (ICP) and their effects on ocular structure and circulation [3]. The ability to assess ICP in glaucoma has been significantly limited by the highly invasive nature of ICP measurements. Recently, the ability to quantify ICP noninvasively has significantly improved, with pilot data suggesting a link between low ICP and glaucoma [4]. Even though the limited data on the topic prevents us from drawing definitive conclusions, the emergence of noninvasive assessment protocols holds great promise to define the pathway of ICP's involvement in glaucoma. In this article, new data and analysis on cerebrospinal fluid pressure (CSFp) and its impact on optic nerve and retinal microcirculation will be explored alongside the broader implications of ICP in glaucoma. One difficulty in interpreting ICP as a risk factor for the onset and progression of glaucoma is the interplay and possible synergies among IOP, ICP, and the ocular circulation. Advances in physically based mathematical modeling have recently allowed for the exploration of glaucoma risk factor interconnectivity [5–9], providing further insight into glaucoma pathophysiology, and eventually may allow for individualized screening and improved patient-specific treatment options [10]. The concepts of ICP, pilot data, and future paradigms in glaucoma management are presented herein, with a focus on comprehensively understanding the role and impact that ICP may have on glaucomatous optic neuropathy.

A. Harris (✉) · J. Gross · B. Siesky · L. Saint
Department of Ophthalmology, Indiana University School of Medicine, Indianapolis, IN, USA
e-mail: alharris@indiana.edu

A. C. Verticchio Vercellin
Department of Ophthalmology, Indiana University School of Medicine, Indianapolis, IN, USA

Glaucoma Unit, Istituto di Ricovero e Cura a Carattere Scientifico, Fondazione G.B. Bietti, Indianapolis, Rome, Italy

University Eye Clinic, Istituto di Ricovero e Cura a Carattere Scientifico (IRCCS), Policlinico San Matteo, Pavia, Italy

D. Prada · G. Guidoboni
Department of Mathematical Sciences, Indiana University Purdue University Indianapolis, Indianapolis, IN, USA

33.2 Eye and Brain

33.2.1 Ocular and Cerebral Embryology

The eye develops its neural and neurovascular tissue, including central retinal artery and vein (CRA and CRV, respectively) and the retinal vessels, from the forebrain [11]. At 22 days of development, the eyes appear as shallow grooves on the sides of the forebrain. In the coming weeks of development, these grooves continue to mature into the optic nerve and retina, which eventually connect to the brain and form the visual pathways. Figures 33.1 and 33.2 represent embryonic development of the eye at 6 and 7 weeks of gestation, respectively [11].

33.2.2 Cerebral and Ocular Hemodynamics and Circulation

According to physiology, many similarities are shared by cerebral and ocular circulations. For example, both circulation systems exhibit pressure autoregulation, ensuring a relatively constant blood flow within the tissues despite changes in arterial pressure, and metabolic autoregulation, ensuring a relatively constant oxygen (O_2) delivery to the tis-

N. Wang (ed.), *Intraocular and Intracranial Pressure Gradient in Glaucoma*,
Advances in Visual Science and Eye Diseases 1, https://doi.org/10.1007/978-981-13-2137-5_33

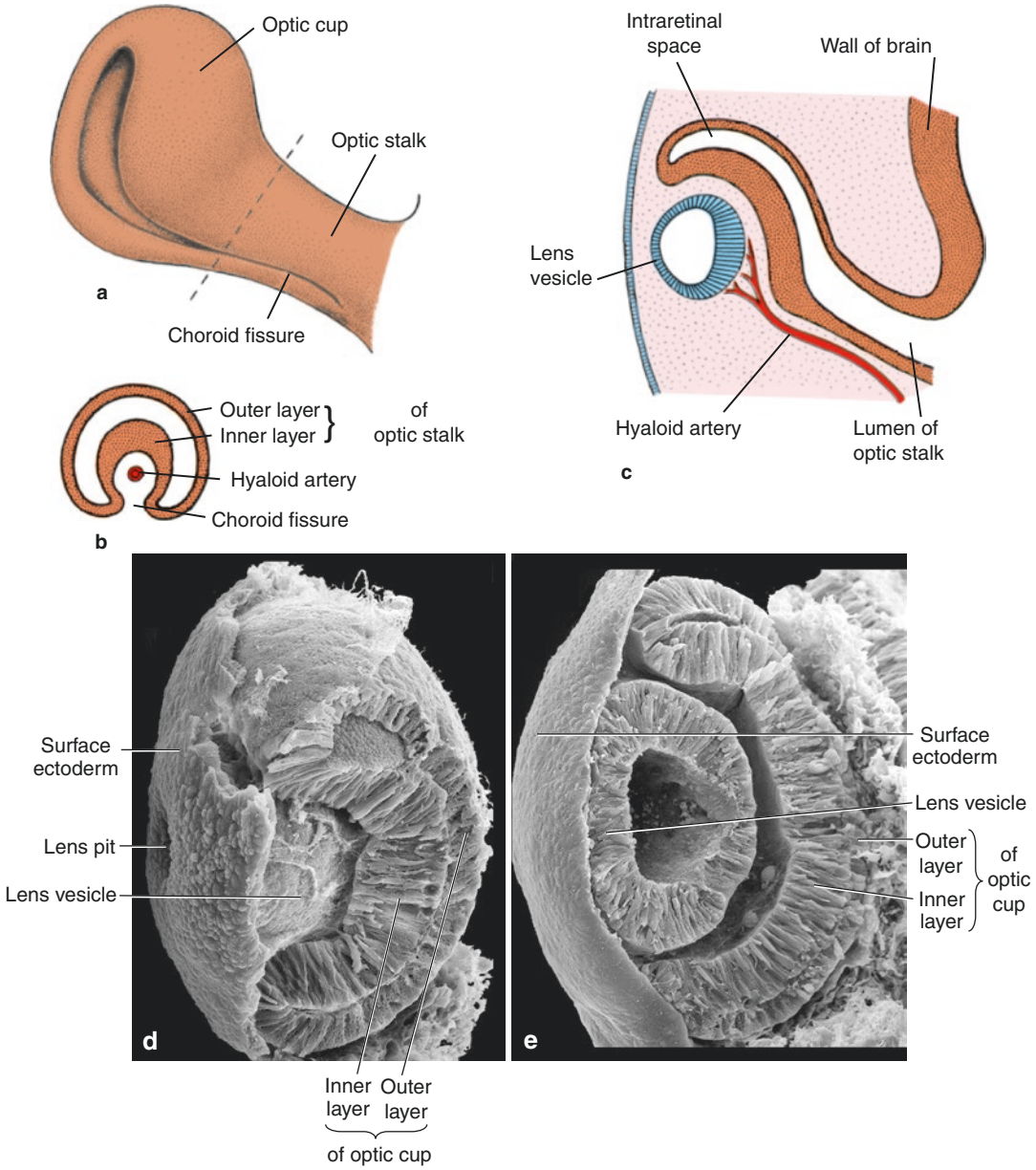

Fig. 33.1 Embryonic development of the human eye at 6 weeks of gestation [11]. (**a**) Ventrolateral view of the optic cup and optic stalk. (**b**) Transverse sections through the optic stalk as indicated by the dashed line in A, showing the hyaloid artery in the choroid fissure. (**c**) A section through the lens vesicle, the optic cup, and the optic stalk at the plane of the choroid fissure. (**d**) Scanning electron microscope (SEM) through the eye showing the lens vesicle and the formation of the two layers of the optic cup. (**e**) SEM of the eye at 6.5 weeks, showing that the lens has completely detached from the surface of the optic cup (Reproduced with permission from [11])

sue despite changes in arterial O_2 content [12, 13]. Furthermore, both systems show minimal sympathetic control and a linear response to the partial pressure of carbonic dioxide (CO_2) [12, 13]. In [14, 15], we found that when CO_2 increased in both retinal and cerebral circulation, the middle cerebral artery and retinal vessels dilated and showed similar responses to this change. Vessels' dilation responding to increasing CO_2 mainly resides in the mechanism that hypercapnia leads to a lower pH, which may cause the higher activity of prostanoid and glibenclamidesensitive K^+ channels, resulting in high concentration of cAMP, cGMP, and nitric oxide [1].

A decrease in available bicarbonate and increase in CO_2 also present a strong rationale for the occurrence of vasodilation. Acetazolamide, a systemic carbonic anhydrase inhibitor (CAI), is known to vasodilate retinal and cerebral tissues [16]. Topical CAIs, like dorzolamide, were

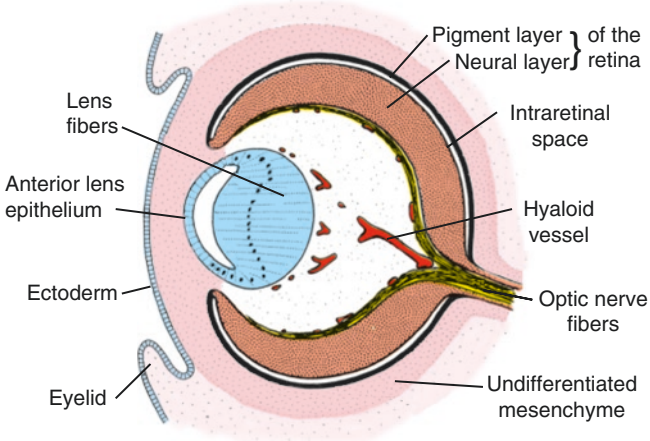

Fig. 33.2 Section through the eye of a 7-week embryo [11]. The eye primordium is completely embedded in mesenchyme. Fibers of the neural retina converge toward the choroid fissure to form the optic nerve (Reproduced with permission from [11])

found to improve retrobulbar velocity in both normal and glaucomatous eyes [17] and continue to show promise of local ocular vasodilation [18]. In low-cerebral blood flow regions, acetazolamide can induce an increased cerebral blood flow and O_2 extraction fraction compared to normal areas, thereby motivating the use of CAIs to investigate and treat cerebral hypoperfusion. In [15], we compared middle cerebral artery (MCA) blood flow velocity between glaucoma patients and the control group at room air and under hyperoxic conditions. We found that the controls had a higher MCA velocity than glaucoma patients at room air (controls, 65.3 ± 23.2 cm/s; glaucoma, 50.2 ± 12.8 cm/s) as well as in conditions with 100% O_2 (controls, 57.7 ± 19.5 cm/s; glaucoma, 49.6 ± 11.8 cm/s), and reduction in MCA velocity with hyperoxia was observed in controls only. These reductions in cerebral blood flow velocity found in both high-tension and normal-tension glaucoma patients suggest that cerebrovascular insufficiency may be associated with glaucoma independently of IOP. The failure of glaucoma patients to reduce MCA flow velocities in hyperoxia implies that O_2 delivery to the brain is not well regulated in these individuals and, instead, rises with arterial O_2 content. Similar trends were also observed in the ocular hemodynamics responses to induced hypercapnia and hyperoxia [19].

These findings suggest that global cerebral vascular insufficiency may play a substantial role in the etiology of glaucomatous optic neuropathy. For this reason, a 5-year population-based follow-up study investigating the association between glaucoma and the risk of stroke development was conducted [20]. After adjusting for age, demographic characteristics, and selected comorbidities, glaucoma patients were found to have a 1.52-fold (95% CI, 1.40–1.72) higher risk of stroke development than the matched comparison cohort.

33.2.3 Age and Circulation

Age is an independent risk factor for glaucoma [21], and increasing age is also associated with vascular changes, particularly in cerebral blood flow [22]. Krejza et al. [23] examined 182 healthy volunteers in a study where the subjects were divided into three age groups: 20–40 years old, 41–60 years old, and over 60 years old. They used color-coded Doppler sonography to measure the blood flow in anterior, middle, and posterior cerebral arteries, with a result of statistically significant differences in the resistive index between age groups 20–40 years old and over 60 years and groups 41–60 years and over 60 years. Harris et al. [24] showed a decrease in the end-diastolic velocity and an increase in the resistivity index of the ophthalmic artery with age in healthy women and men ($p < 0.001$). These results suggest that in healthy subjects of both sexes, changes induced by aging in the retrobulbar hemodynamics are similar to those seen in glaucoma or age-related macular degeneration patients. Hemodynamics changes that occur with age can therefore contribute in increasing the risk for progression in these diseases.

Figure 33.3 [25] shows one paradigm for the influence of age-related mechanisms on hemodynamics alterations and their contribution to age-related disease onset. Aging promotes oxidative stress, endothelial dysfunction, and structural modifications such as thickening of basement membrane in blood vessels and impaired autoregulation, which leads to ischemia. Age-related systemic pathologies, environmental factors, or genetic predisposition represent stressors that may additionally impair ocular blood flow and make the optic nerve susceptible to further damage and disease onset.

Another important consideration about age and glaucoma pathogenesis is related to the effects of aging on CSFp. A significant decrease in the CSFp with age starting in the sixth decade has been shown in clinical studies by Fleischman et al. [26]. Interestingly, the age at which CSFp starts to decrease corresponds with the age when an increase in the prevalence of the glaucomatous optic neuropathy can be observed. These findings suggest that decreased CSFp might represent a risk factor for glaucoma and can explain the underlying mechanisms of the increased prevalence of primary open-angle glaucoma (POAG) with age.

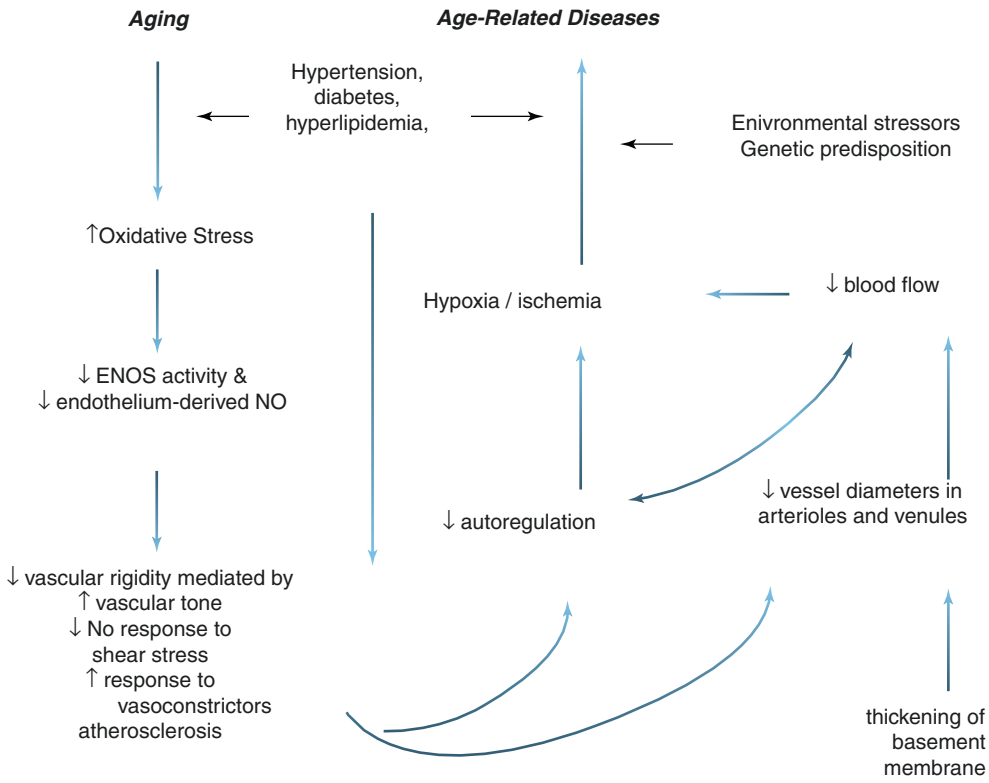

Fig. 33.3 A proposed paradigm for the role of aging in age-related diseases (Reprinted with permission from [24]).

33.3 Blood Flow Detection

With the development of technology, more equipment is available to measure and evaluate ocular blood flow. In various studies, we employed color Doppler, spectral-domain optical coherence tomography (SD-OCT), and Fourier domain OCT to show that total retinal blood flow was lower in POAG compared to the healthy controls. For example, in Harris [27], we found a significant difference in retinal blood flow as measured by Doppler OCT between POAG patients and healthy controls. More precisely, patients with POAG had 23.9% lower total retinal blood flow compared to healthy controls (p = 0.001). Recently, the development of angio-OCT has allowed for the visualization of the blood flow in the deeper regions of the optic nerve head, even at the level of the lamina cribrosa. However, further improvements are needed to better distinguish between blood flow signals coming from different tissue layers [29].

33.3.1 Ocular Perfusion Pressure and Glaucoma

Many population-based studies have been conducted to better understand the role of blood pressure and ocular perfusion pressure (OPP) in the development of glaucoma, with many studies showing how low OPP has consistently been identified as a risk factor for glaucoma [28–37]. The Barbados Eye Study (9-year follow-up) and the Rotterdam Study (9.8-year follow-up) showed that OPP was a risk factor for glaucoma incidence, and the Early Manifest Glaucoma Trial (8-year follow-up) and Low-Pressure Glaucoma Treatment Study Group (40.6-month follow-up) indicated that OPP was a risk factor for glaucoma progression [38–41]. In 2006, the interpretation of initial data from the Thessaloniki Eye Study suggested that both antihypertensive treatment and low diastolic blood pressure (DBP) were independently associated with optic disc structural changes [42]. However, the subgroup analyses led to more accurate findings, namely, that only patients on antihypertensive medications with a low DBP (<90 mmHg) had a significantly associated change in optic disc structure [43]. We hypothesized that OPP status (meaning OPP with or without antihypertensive treatment) may be more relevant to glaucoma pathogenesis than OPP alone. Further subgroup analyses [43] on OPP status confirmed that diastolic OPP (DOPP) was significantly associated with POAG in subjects using antihypertensive treatment in contrast to a negative association between DOPP and POAG in subjects not on antihypertensive treatment, as reported in Fig. 33.4. These data show the importance of determining patients' hemodynamic status along with absolute values of mean arterial blood pressure and IOP.

Effect	In Subjects without Anthypertensive Treatment				In Subjects with Anthypertensive Treatment			
	N	OR	95% CI	*P* Value[j]	N	OR	95% CI	*P* Value[j]
Association with OAG								
DPP (per 10 mm Hg) (unadjusted)	1039[a]	0.72	0.57-0.92	**.008**	1212[c]	0.78	0.66-0.93	**.006**
DPP (per 10 mm Hg) (adjusted)[f]		1.05	0.81-1.35	.731		0.83	0.68-1.01	.062
Association with POAG[i]								
DPP (per 10 mm Hg) (unadjusted)	922[b]	0.80	0.59.1.07	.13	1060[d]	0.69	0.56-0.85	**<.001**
DPP (per 10 mm Hg) (adjusted)[f]		0.98	0.72.1.33	.891		0.78	0.62-0.97	**.028**
Association with PEXG[i]								
DPP (per 10 mm Hg) (unadjusted)	117	0.76	0.51-1.13	.18	152[e]	1.10	0.79-1.52	.58
DPP (per 10 mm Hg) (adjusted)[f]		1.39[g]	0.81-2.37	.235		0.90[h]	0.58-1.41	.653

CI = confidence interval; DPP = diastolic perfusion pressure; OAG = open-angle glaucoma; OR = odds ration; PEXG = pseudoexfoliative glaucoma; POAG = primary open-angle glaucoma.

Excluded from the analyses due to missing values: [a]8 subjects, [b]subjects, [c]2 subjects, [d]1 subjects, [e]1 subjects.

[f]Adjusted results were obtained from logistic regression models adjusting for age, sex, coronary artery bypass or vascular surgery, diabetes treated with insulin, IOP, and IOP-lowering treatment; in OAG, pseudoexfoliation was also included in the adjustments.

[g]Coronary artery bypass or vascular surgery and diabetes treated with insulin were not included in the model, because none of these subjectshad such history.

[h]Diabetes treated with insulin was not included in the model because none of these subjects had such history.

[i]In regression models for POAG, only subjects who did not have pseudoexfoliation were included in the analyses; in regression models for PEXG, only subjects who had pseudoexfoliation were included in the analyses.

[j]Bold characters indicate statistical significance.

Fig. 33.4 Association of diastolic perfusion pressure status with open-angle glaucoma, primary open-angle glaucoma, and pseudoexfoliative glaucoma in the Thessaloniki Eye Study [43] (Reprinted with permission from Topouzis F, Wilson M R, Harris A, et al. Association of Open-angle Glaucoma With Perfusion Pressure Status in the Thessaloniki Eye Study - American Journal of Ophthalmology[J]. American Journal of Ophthalmology, 2013, 155(5):843-851.)

To date, the two most prominent hypotheses for antihypertensive treatment's role in the relationship between DOPP and POAG are:

1. Subjects treated for systemic hypertension experience larger reductions of nocturnal blood pressure (BP), leading to very low OPP values compared to subjects not on antihypertensives.
2. Antihypertensive treatment disrupts the vessel's natural ability to autoregulate at certain OPPs where autoregulation is effective at the same or similar levels of OPP in patients not on antihypertensives.

These hypotheses propose that either low OPP or inadequate or dysfunctional autoregulation at certain OPP levels is associated with aberrant blood flow and glaucomatous structural change. However, a combination of both hypotheses might also underlie the influence of antihypertensives on glaucoma.

The relationship between OPP, IOP, BP, and optic disc structure is indeed very complex and, to date, poorly understood. The translamina cribrosa pressure difference (TLpD), defined as the difference between IOP and CSFp, may affect this relationship as well. Since CSFp and BP are correlated, lower BP leads to lower CSFp to allow cerebral perfusion, and higher BP indicts higher CSFp to prevent cerebral hemorrhage. If BP is medically reduced, then CSFp is also reduced. However, if IOP is relatively constant, this leads to an elevated TLpD that may cause optic disc damage [4, 44]. Ren et al. [44] found that abnormally low CSFp is associated with low arterial BP in many NTG patients, which raised concerns that nocturnal BP dips may be exacerbated with BP lowering treatment, thereby resulting in optic disc damage. When investigating nocturnal BP in glaucoma patients and healthy subjects, we found significant arterial BP reductions during the night in both glaucoma patients and controls [45]. However, our study did not show the same trend of BP reduction in glaucoma patients at night compared with Ren et al., and glaucoma patients showed reduced blood flow regulation compared with agerelated controls. These findings lead to hypothesize that the lack of autoregulation, rather than nocturnal BP per se, may play a crucial role in glaucomatous damage.

33.4 Noninvasive ICP Measurement Technology

ICP monitoring has been used for decades in the fields of neurosurgery and neurology. Multiple invasive and noninvasive techniques are available. Raboel et al. [46] provided an overview of the advantages and disadvantages of the most common and well-known methods, as reported in Fig. 33.5.

In our group, a noninvasive ICP measurement method was utilized that is based on simultaneous and insonation angle-independent blood flow pulsation monitoring in intracranial and extracranial segments of the ophthalmic artery (OA). The intracranial OA segment is compressed by ICP,

Technology	Accuracy	Rate of infection	Rate of hemorrhaging	Cost per patient	Miscellaneous
External ventricular drainage	High	Low to moderate	Low	Relatively low	Can be used for drainage of CSF and infusion of antibiotics
Microtransducer ICP monitoring devices	High	Low	Low	High	Some transducers have problems with high zero drift
Transcranial Doppler ultrasonography	Low	None	None	Low	High percentage of unsuccessful measurements
Tympanic membrane displacement	Low	None	None	Low	High percentage of unsuccessful measurements
Optic nerve Sheath diameter	Low	None	None	Low	Can potentially be used as a screening method of detecting rasied ICP
MRI/CT	Low	None	None	Low	MRI has potential for being used for noninvasive estimation of ICP
Fundoscopy (papilledema)	Low	None	None	Low	Can be used as a screening method of detecting raised ICP, but not in cases of sudden raise in ICP, that is, trauma

Fig. 33.5 Comparisons between different technologies used to measure intracranial pressure (ICP) [46] (Reprinted with permission from Raboel P H, Jr B J, Andresen M, et al. Intracranial Pressure Monitoring: Invasive versus Non-Invasive Methods-A Review[J]. Crit Care Res Pract, 2012, 2012(12):950393.)

whereas the extracranial OA segment is compressed by the controlled external pressure P_e produced by a small inflatable ring cuff placed over the tissues surrounding the eyeball. Transorbital Doppler ultrasonic technology is used for indication of the pressure balance P_e = ICP, which is reached when measured blood flow velocity pulsations in both OA segments are approximately equal. Siaudvytyte et al. [4] used the two-depth orbital Doppler device to measure CSFp in 18 glaucoma patients (9 NTG and 9 high-tension glaucoma (HTG)) and 9 control subjects. The measured CSFp values were 7.4 ± 2.7 mmHg (NTG group), 8.9 ± 1.9 mmHg (HTG group), and 10.5 ± 3.0 mmHg (control group) ($p > 0.05$), and the TLpD was 6.3 ± 3.1 mmHg (NTG group), 15.7 ± 7.7 mmHg (HTG group), and 5.4 ± 3.3 mmHg (control group) ($p < 0.001$). NTG patients showed a lower CSFp and a higher TLpD, leading to decreased neuroretinal rim area (NRA), whereas POAG patients had lower ocular hemodynamic parameters and lower OPP leading to decreased NRA, suggesting that higher TLpD leads to decreased NRA.

The same team has conducted another study to assess the differences in NRA and ocular hemodynamic parameters (IOP, noninvasive ICP, retrobulbar blood flow, and optic nerve disc structural parameters) among NTG patients with differing ICP values [47]. A total of 40 NTG patients (11 males) with a mean age of 61.1 (±11.5) years were included in this prospective clinical study. The study showed that lower ICP was correlated with decreased NRA ($R = 0.51$, $P = 0.001$) ($r = 0.51$, $p = 0.001$). In conclusion, NTG patients having lower ICP have decreased NRA and OA blood flow parameters compared with NTG patients with higher ICP. Siaudvytvte et al. published in 2015 a literature review of five studies (396 patients) on TLpD in glaucoma, finding an association between higher TLpD and lower NRA in NTG patients. No association was observed in healthy subjects and OHT patients. A higher TLpD was found in patients with NTG and HTG, compared with healthy controls. As it has been shown in a recent review [48], the current literature is limited in scope and execution and has significant differences and weaknesses in methodologies utilized. With acknowledgment of these weaknesses, the available data suggests that there is a need for further longitudinal prospective clinical and experimental studies investigating the influence of TLpD on glaucoma occurrence and progression.

33.5 Mathematical Modeling of Ocular Blood Flow

The findings presented by both the Early Manifest Glaucoma Trial ([39, 49] pose interesting thoughts as to whether OPP is more influenced by BP or IOP. Even though IOP appears to be a dominant factor, to date the findings are not conclusive. It must be mentioned that there are limitations to population-based, clinical, and animal studies that make isolating all factors and singling out their influence on ocular physiology in health and disease extremely challenging. To overcome these limitations, alternative options based on interdisciplinary approaches have been explored in recent years, including, for example, physically based mathematical modeling.

Physically based mathematical modeling can be thought of as a "virtual lab" that provides a virtual system designed to replicate physiology, where we may manipulate variables and isolate factors that cannot be easily separated in clinical studies and identify the contribution of each factor on the

system response to particular challenges [10, 50]. The synergy between clinical studies and mathematical modeling holds the potential to advance our understanding of intertwined factors involved in ocular diseases and demystify the role of OPP, BP, and IOP in glaucoma.

33.5.1 Modeling the Influence of BP, IOP, and CSFp on the Hemodynamics in the Central Retinal Vessels and the Retinal Vasculature

In recent years, our team has strived to investigate theoretically the influence of BP, IOP, and CSFp on the hemodynamics in the central retinal vessels and the retinal vasculature. For example, the model proposed in Guidoboni et al. [51] and Carichino et al. [52] calculates stresses and strains in the lamina cribrosa deforming under the action of IOP and CSFp. The model describes the relationship between stresses and strains in the lamina (structure) induced by IOP and CSFp and the blood flow (fluid) in CRA, CRV, and the retinal vasculature driven by the mean arterial pressure (MAP), as depicted in Fig. 33.6.

Another example is the model in [9], where the combination of biomechanics and hemodynamics is used to calculate the blood flow in retinal arterioles, capillaries, venules, CRA, and CRV, leveraging the analogy between blood flowing in a network of vessels and electric current flowing in a circuit, as

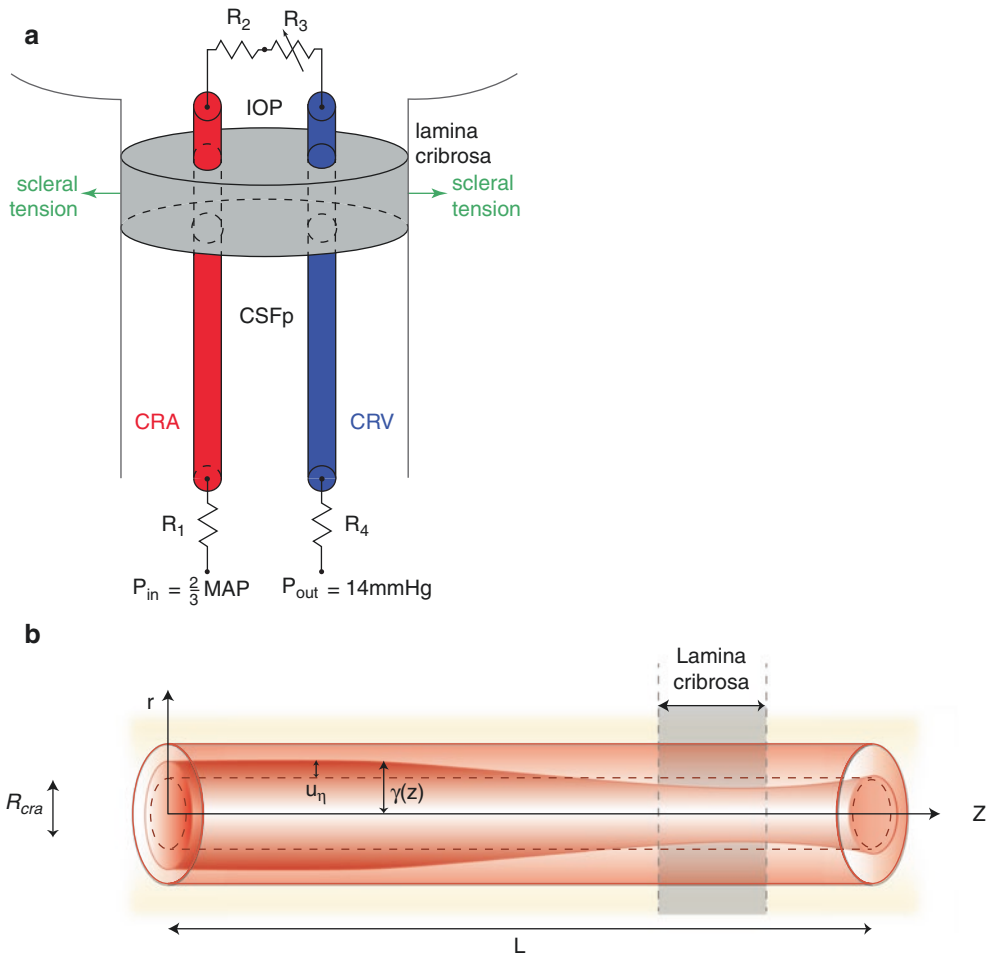

Fig. 33.6 (**a**) Schematic representation of the mathematical model coupling IOP, CSFp, and lamina cribrosa deformations with the blood flow in the central retinal vessels and the retinal vasculature. Based on the analogy between hydraulic and electrical circuits, resistors are used to represent the resistance to flow offered by blood vessels. R_1 and R_4: constant vascular resistances upstream of the CRA and downstream of the CRV. R_2: constant vascular resistance of retinal arterioles and capillaries. R_3: variable vascular resistance of venules describing active and passive diameter changes due to blood flow autoregulation and IOP. The blood flow through the retinal vasculature is driven by P_{in} (equal to 2/3 of the mean arterial pressure MAP) and P_{out}, which represent the blood pressure upstream of the CRA and downstream of the CRV [52] (Reprinted with permission from Guidoboni G, Harris A, Cassani S, et al. Intraocular pressure, blood pressure, and retinal blood flow autoregulation: a mathematical model to clarify their relationship and clinical relevance[J]. Invest Ophthalmol Vis Sci, 2014, 55(7):4105-4118.) (**b**): Domain occupied by the blood flowing inside the CRA. The function $\gamma(z)$ describes the wall/blood interface, R_{cra} is the reference radius of the CRA, and u_η is the radial displacement of the arterial wall. The vertical dashed lines indicate the location of the lamina cribrosa [51]

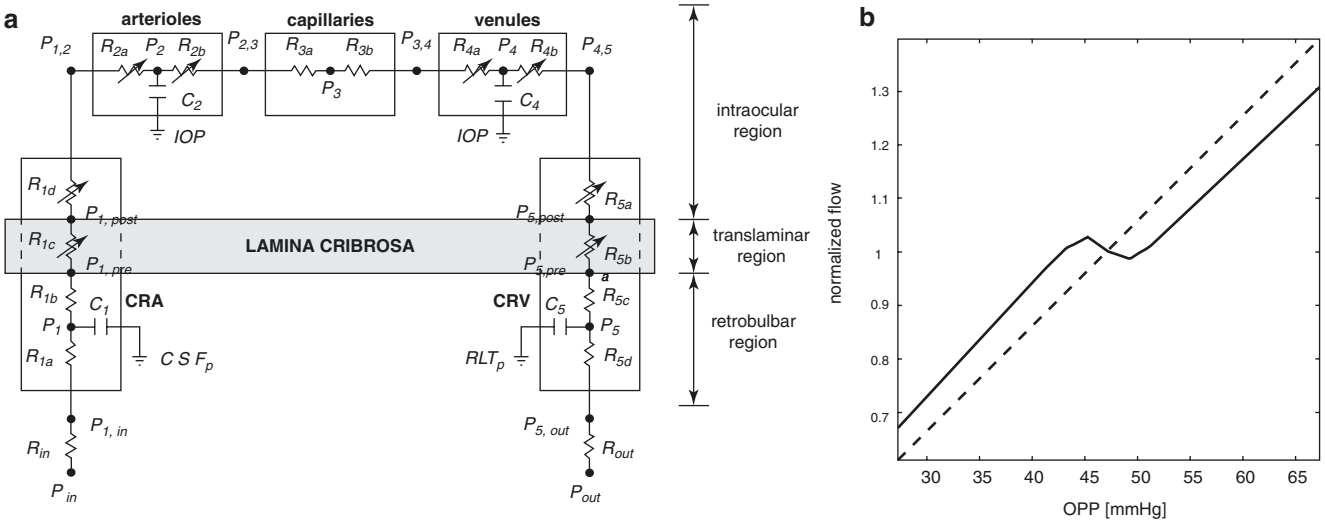

Fig. 33.7 (**a**): Network model for the retinal vasculature. The vasculature is divided into five main compartments: the CRA, arterioles, capillaries, venules, and the CRV. Each compartment includes resistances (R) and capacitances (C). The intraocular segments are exposed to the IOP, the retrobulbar segments are exposed to the CSFp, and the translaminar segments are exposed to an external pressure that depends on the internal state of stress within the lamina cribrosa (gray-shaded area). Diameters of venules and intraocular and translaminar segments of the CRA and CRV are assumed to vary passively with IOP, whereas arterioles are assumed to be vasoactive [51]. (**b**): Normalized blood flow in the retinal vasculature for model simulation with functional (*solid line*) or absent (*dashed line*) autoregulation for various OPPs attained by setting IOP = 15 mmHg and varying MAP [9] (Reprinted with permission from Guidoboni G, Harris A, Cassani S, et al. Intraocular pressure, blood pressure, and retinal blood flow autoregulation: a mathematical model to clarify their relationship and clinical relevance[J]. Invest Ophthalmol Vis Sci, 2014, 55(7):4105-4118.).

depicted in Fig. 33.7. The model simulates the relationship between increase in IOP and collapse of the veins, a phenomenon known as a Starling resistor. In addition, the variable resistance in arterioles can be switched on or off in order to simulate conditions of functional or impaired autoregulation. MAP is the driving force of blood flow inside the vascular circuit and pressurizes the interior of the vessels. IOP enters the system in many ways: (1) it acts as an external pressure compressing the vessels inside the eye globe; (2) it pushes on the lamina whose IOP-induced deformation, in turn, alters the blood flow in the central retinal vessels. The veins are more sensitive to the external pressure since they can collapse and act as Starling resistors (passive variable resistances indicated with arrows). Retinal arterioles, on the other hand, can actively change their diameter to compensate for changes in pressure, thereby masking actual changes in the measurements.

33.5.2 Synergy Between Clinical Studies and Mathematical Modeling

Despite the appeal of these mathematical models, the question still remains as to how they can aid in interpreting clinical data. The Egna-Neumarkt [30] and Rotterdam Studies [31, 41] first proposed the question as to whether IOP or BP is more important in determining OPP. If one is more important than the other, to which degree does this hold? How does OPP's reliance on either variable change with the IOP spectrum? How does IOP elevation influence total retinal blood flow in individuals with different MAP?

To aid in answering these questions, the model in Guidoboni et al. [9] was utilized to run simulations where IOP is artificially increased from 15 to 45 mmHg for three different theoretical patients with different MAP values, and the corresponding retinal blood flow is calculated, as reported in Fig. 33.8. The green line, black line, and blue line represent conditions of low blood pressure (LBP), normal blood pressure (NBP), and high blood pressure (HBP), respectively, with a MAP of 80 mmHg, 93.3 mmHg, and 106.7 mmHg, respectively. In regard to the predicted curve of retinal blood flow versus IOP, the model predicts that (1) if IOP < 26 mmHg, there is blood flow plateau for HBP and NBP, but no plateau for LBP; (2) when 26 < IOP < 36 mmHg, there is the same decreasing slope for HBP, NBP, and LBP; and (3) if IOP > 36 mmHg, steeper slope due to partial venous collapse (Starling resistor effect), with venous collapse starting earlier for LBP. The model predicts that the autoregulation plateau would shift toward higher IOP values as MAP increases. In particular, three areas in the graph can be identified (see dashed red lines on the graph of Fig. 33.8): (1) a plateau for low IOP, indicating the ability of the vascular system to autoregulate and compensate for IOP elevation, (2) an area

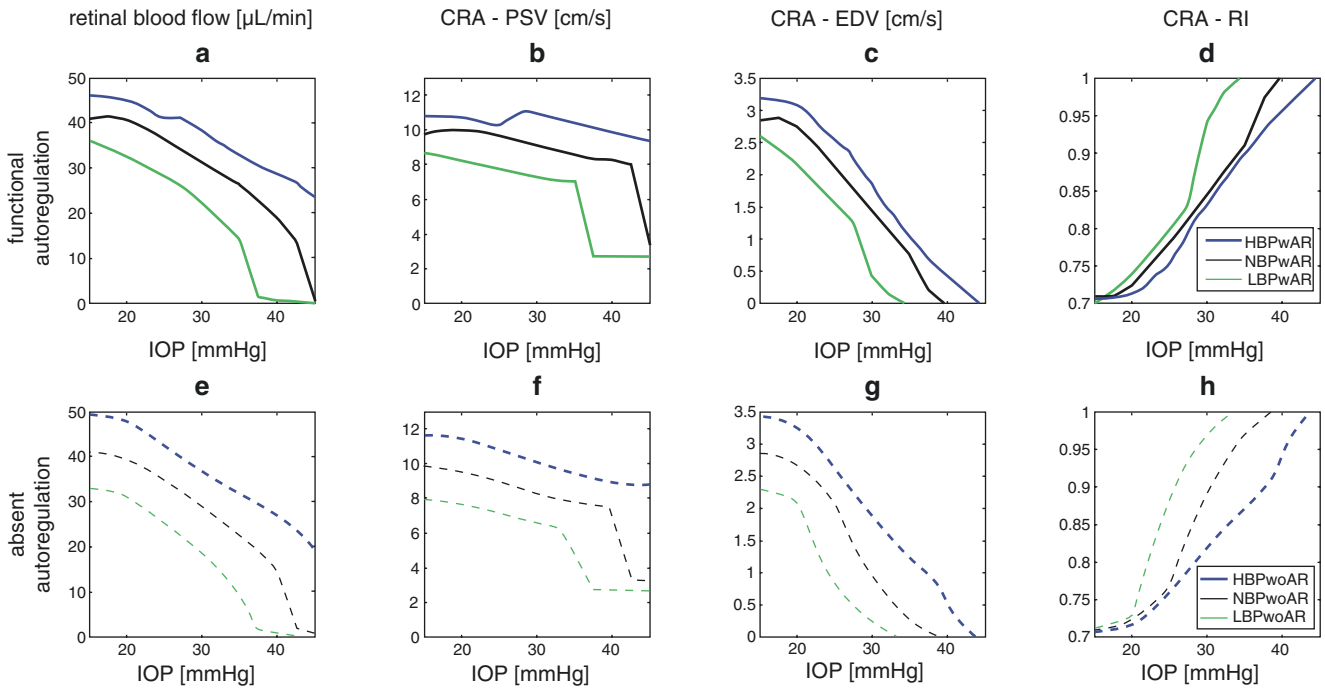

Fig. 33.8 Model predicted values of total retinal blood flow as IOP varies between 15 and 40 mmHg in conditions of low blood pressure (green line), normal blood pressure (black line), and high blood pressure (blue line) [9] (Reprinted with permission from Guidoboni G, Harris A, Cassani S, et al. Intraocular pressure, blood pressure, and retinal blood flow autoregulation: a mathematical model to clarify their relationship and clinical relevance[J]. Invest Ophthalmol Vis Sci, 2014, 55(7):4105-4118.)

in the middle range reflecting a loss of autoregulation capacity by all the three patients, and (3) a third area demonstrating the start of venous collapse. These results are in agreement with the clinical findings reported by Boltz et al. [49].

In the study conducted by Boltz et al. [49] on the relationship between OPP, MAP, IOP, and blood flow, 40 subjects between ages 18 and 29 were instructed to go through a procedure including performing isometric exercise to increase MAP, suction cupping to increase IOP, and then a simultaneous combination of isometric exercise with suction cupping. Measured data showed that optic nerve head blood flow (ONHBF) was autoregulated during both an increase and a decrease in OPP. However, more interestingly, during activity of both combined (increase in both MAP and IOP), inadequate autoregulation of ONHBF occurred at IOP values at 26 mmHg or greater, where blood flow became independent of MAP. Contrastingly, blood flow was always dependent on IOP throughout all data values for MAP. This indicates that IOP is likely the dominant factor in OPP to cause inadequate or dysfunctional autoregulation. The predictions of the mathematical model presented above are in agreement with these clinical findings and, thanks to the single variable manipulation in the "virtual lab", clarify the mechanisms that give rise to these clinical observations.

In the previous study, we focused on how changes in IOP affected retinal blood flow and the hemodynamics in the central retinal vessels. However, the model depicted in Fig. 33.6 was also used to explore conditions at the back of the lamina by investigating how changes in CSFp affected hemodynamics in the same vascular beds (retinal blood flow and central retinal vessels) in comparison to changes in IOP. We remark that, in our theoretical studies, we have assumed that the retrolaminar tissue pressure is equal to CSFp as suggested by Morgan et al. [53]. The model is utilized to simulate how retinal blood flow rate (Q) changes with TLpD, as reported in Fig. 33.9. The black horizontal line represents low CSFp conditions, where changes in TLpD are attained by varying CSFp from 1 to 15 mmHg and holding IOP constant at 15 mmHg. The model predicts that, in this case, Q remains relatively constant. The red line represents high IOP conditions, where changes in TLpD are attained by varying IOP from 15 to 50 mmHg and holding CSFp constant at 7 mmHg. The model predicts that, in this case, Q drastically decreases as TLpD increases. Overall, these theoretical findings suggest that IOP has more effect on retinal blood flow rate than CSFp, especially when CSFp is low and IOP is high.

Figure 33.10 reports the model predicted changes in CRA and CRV blood velocity as TLpD changes due to CSFp and IOP. In each graph, the black horizontal line rep-

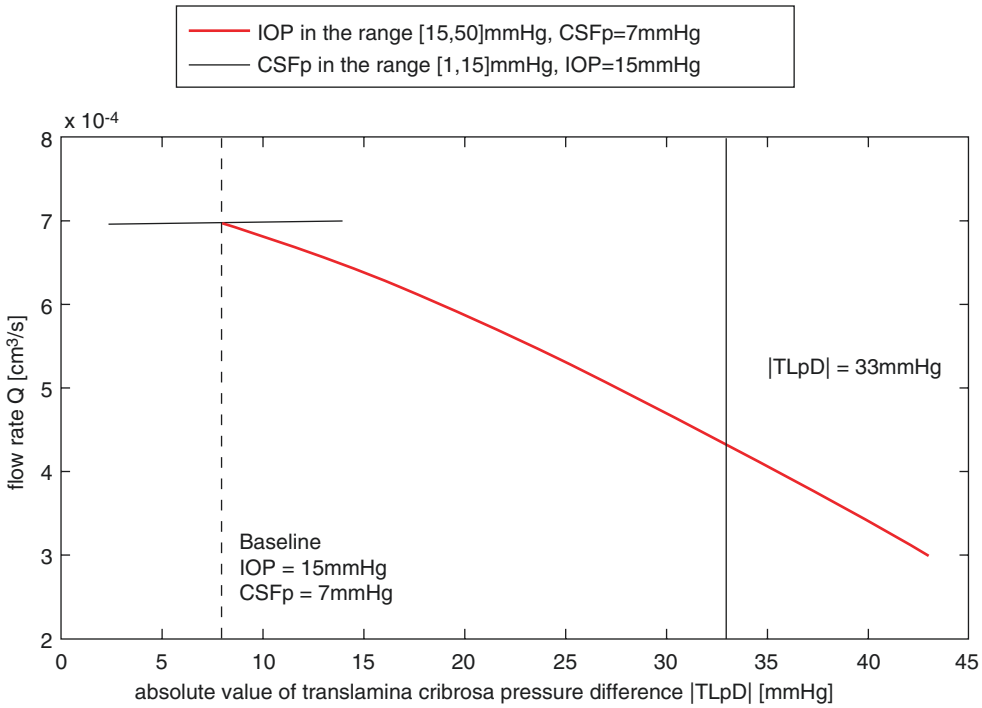

Fig. 33.9 Variations of retinal blood flow Q as function of the absolute value of the translamina cribrosa pressure difference |TLpD|. The black vertical dashed line corresponds to the baseline case IOP = 15 mmHg and CSFp = 7 mmHg, and the black vertical solid line corresponds to an absolute value of TLpD equal to 33 mmHg. This figure has been adapted from Fig. 33.2c in [52]) (Reproduced with permission [52]) (We thank Kugler Publications giving the permission to publish this figure)

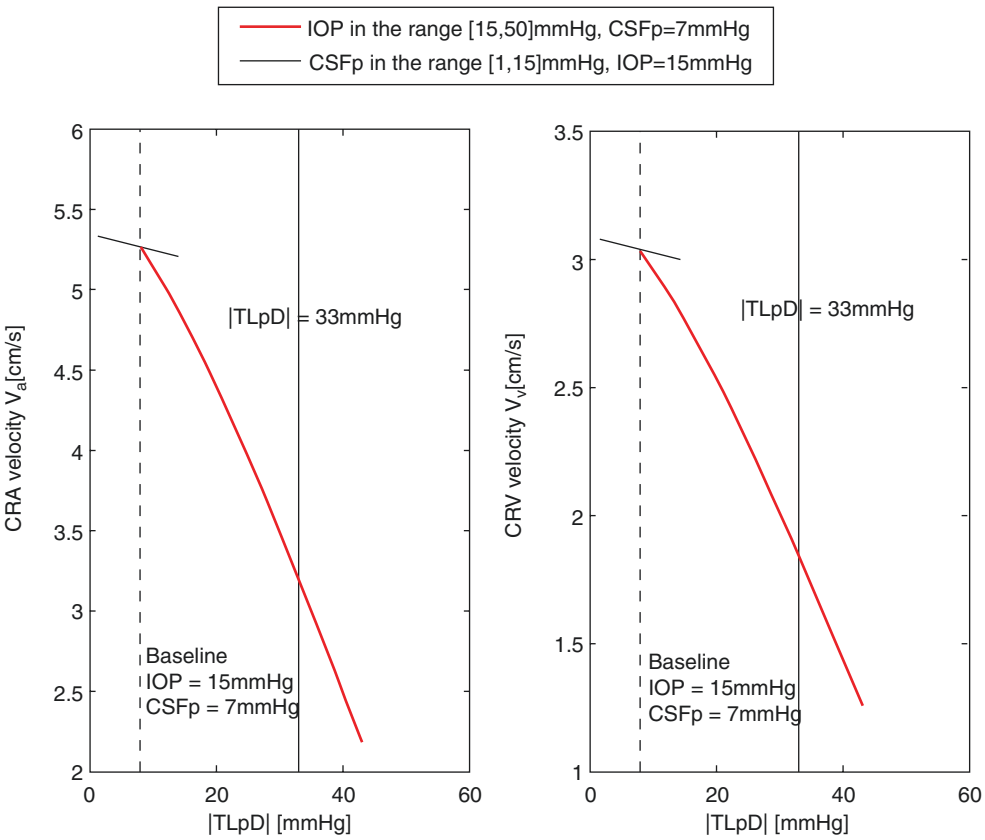

Fig. 33.10 Variations of CRA and CRV mean velocities V_a and V_v in the pre-laminar segment as function of the absolute value of the translamina cribrosa pressure difference |TLpD|. The black vertical dashed line corresponds to the baseline case IOP = 15 mmHg and CSFp = 7 mmHg, and the black vertical solid line corresponds to an absolute value of TLpD equal to 33 mmHg. This figure has been adapted from Fig. 33.2a, b in (Carichino et al. [52]) (Reproduced with permission from) (We thank Kugler Publications giving the permission to publish this figure [52])

resents low CSFp conditions, with CSFp varying from 1 to 15 mmHg and IOP constant at 15 mmHg. As TLpD is increased due to decreasing CSFp, CRA and CRV blood velocity experiences a minimal decrease. On the other hand, the red line in represents high IOP conditions, with IOP varying from 15 to 50 mmHg and CSFp constant at 7 mmHg. As TLpD is increased due to increasing IOP, CRA, and CRV blood velocities experience a drastic decrease. These results indicate that although IOP and CSFp changes might lead to comparable changes in TLpD values, they do not correspond to similar hemodynamic alterations in retinal blood flow and CRA and CRV blood velocities.

33.5.3 Modeling Hemodynamics in the Optic Nerve Head

Recently, we extended our modeling efforts to describe the perfusion of the lamina cribrosa, whose complex structure, depicted in Fig. 33.11a–c, has been analyzed in various studies, including [56], Jonas et al. [57], Burgoyne [54], Downs et al. [58], Kim [59], and Girard et al. [60]). The perfusion of the lamina cribrosa is described by a poro-viscoelastic model [61, 62], where blood vessels are viewed as pores in a viscoelastic solid matrix comprising collagen, extracellular matrix, and neural tissue (see Fig. 33.11d). This model provides a theoretical description of the coupling between lamina biomechanics and hemodynamics. Model simulations show that as external forces (IOP, CSFp) lead to microscopic deformation of the laminar tissues, the pores and the blood vessels inside the lamina would also deform, and this deformation would subsequently influence the perfusion of the lamina. As a consequence, alterations in the lamina biomechanics would have consequences on the hemodynamics within the lamina itself.

Utilizing our mathematical models, we investigated the integrated rate of change of blood kinetic energy treating the lamina as an elastic (Fig. 33.12a) or a viscoelastic (Fig. 33.12b) medium when sudden external forces are applied. By comparing the elastic conditions on the left with the viscoelastic conditions on the right, we see that a sudden force, for example, an increase in IOP due to rubbing of the eye, will correspond to a sudden deformation of the tissue in the elastic model. However, in the viscoelastic model, the deformation will develop more slowly in the tissue, thereby reducing susceptibility to damage. In other words, the viscoelastic biomechanical properties of an intact and healthy lamina cribrosa enable it to absorb sudden changes in force and transfer it slowly to the surrounding structures, including blood vessels and capillaries, thereby lowering the susceptibility to vessel hemorrhage and rupture.

Figure 33.13 shows that the absence or presence of structural viscoelasticity influence noticeably the integrated rate of change of blood kinetic energy (W) as the lamina experiences sudden changes in IOP (Fig. 33.13a). More precisely, without viscoelasticity (Fig. 33.13b, black curve), W exhibits sharp peaks at the IOP switch-on and switch-off times, suggesting perfusion instability. Conversely, in the presence of viscoelasticity (Fig. 33.13b, blue curve), W remains bounded at lower levels. In summary, this theoretical work suggests that (1) if the lamina viscoelasticity is not intact, sudden IOP changes will be translated to lamina hemodynamics, possibly leading to disc hemorrhages, and (2) if the lamina viscoelasticity is intact, sudden changes will be absorbed by the tissue and we will not see perfusion instabilities in the lamina. The importance of viscoelasticity in the tissue has been evidenced in other works as well [63, 64].

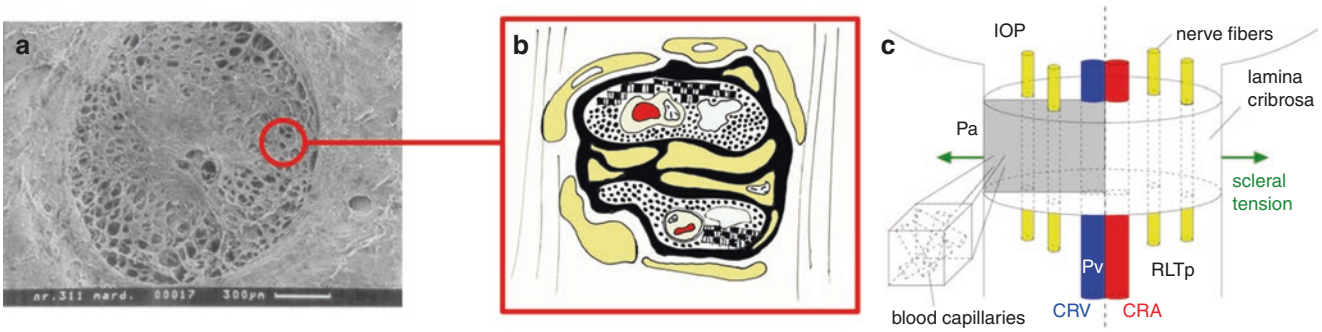

Fig. 33.11 (**a**) Scanning electron micrograph of the lamina cribrosa of a right eye (Jonas 1991). (Reprinted with permission from Jonas J B, Mardin C Y, Shlötzer-Schrehardt U, et al. Morphometry of the human lamina cribrosa surface. Investigative Ophthalmology & Visual Science, 1991, 32(2):401). (**b**) Zoom of the lamina with stippled extracellular matrix, central capillary (red) and surrounding astrocytes (yellow with basement membranes in black). (**c**) Schematic representation of the mathematical model [54]

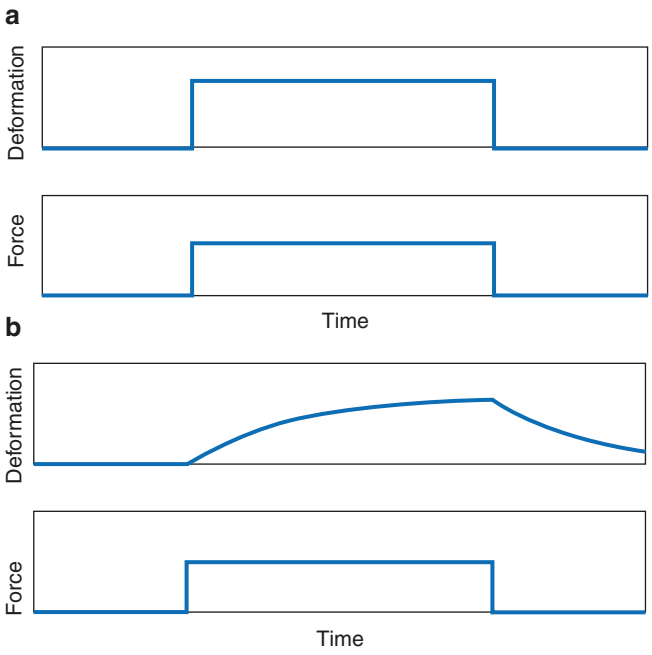

Fig. 33.12 Force-deformation response of elastic (**a**) and viscoelastic (**b**) materials (We thank Dr. Lorenzo Sala giving the permission to publish this figure)

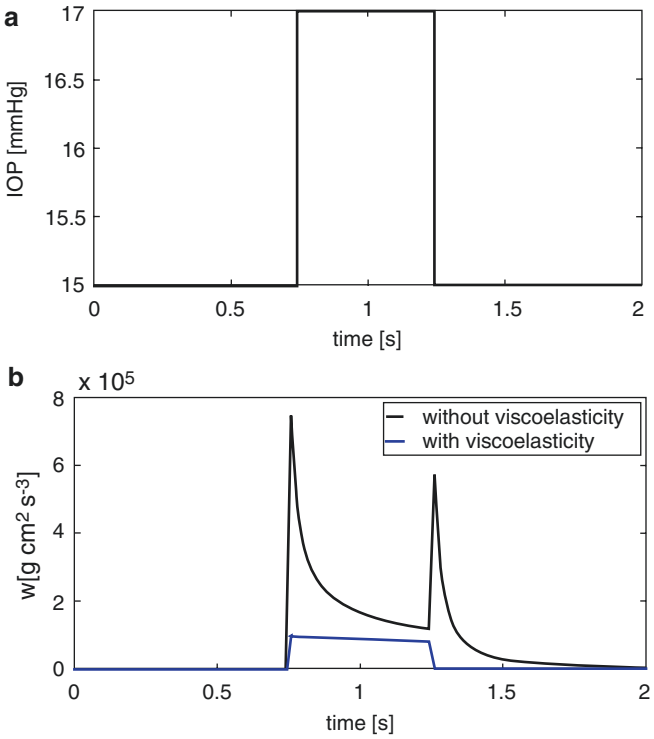

Fig. 33.13 (**a**) IOP fluctuation pattern tested in the model; (**b**) integrated time rate of change of the blood kinetic energy (W) in response to IOP variations without (black curve) and with (blue curve) LC viscoelasticity (Reproduced with permission from [55])

33.6 Conclusions

Recent advances in retinal and optic nerve blood flow detection, noninvasive ICP measurement devices, and mathematical modeling have extended our knowledge of the role of CSFp in glaucoma pathophysiology. With further comprehension, CSFp may be incorporated in future glaucoma management as a risk factor. However, to date the understanding of CSFp in itself and of its interactions with potential risk factors for glaucoma remains complex. Therefore, further investigations are needed to better understand the relationships between IOP, BP, and CSFp and consequent glaucomatous damage, and a synergistic alliance across disciplines will play a crucial role in this direction. In particular, mathematical modeling can serve as an overarching framework to guide and further analyze the invaluable information that is coming from experimental and clinical studies. It is important to recognize that all studies—animal, experimental, clinical, and mathematical modeling—are strongest when considered together.

Disclosures Dr. Alon Harris would like to disclose that he receives remuneration from CIPLA, AdOM and Shire for serving as a consultant. Dr. Harris also holds an ownership interest in AdOM and Oxymap. All relationships listed above are pursuant to Indiana University's policy on outside activities. None of the other authors listed have any financial disclosures.

Funding This work has been partially supported by the NSF DMS-1224195, NIH 1R21EY022101-01A1, a grant from Research to Prevent Blindness (RPB, New York, NY, USA), an Indiana University Collaborative Research Grant of the Office of the Vice President for Research, the Chair Gutenberg funds of the Cercle Gutenberg (France), and the Labex IRMIA (University of Strasbourg, France). The funding parties did not have any role in the study design, collection of data, analysis of data, writing of the manuscript, or decision to submit the manuscript.

References

1. Moore D, Harris A, WuDunn D, Kheradiya N, Siesky B. Dysfunctional regulation of ocular blood flow: a risk factor for glaucoma? Clin Ophthalmol. 2008;2(4):849–61.
2. Moore NA, Harris A, Wentz S, Verticchio Vercellin AC, Parekh P, Gross J, Hussain RM, Thieme C, Siesky B. Baseline retrobulbar blood flow is associated with both functional and structural glaucomatous progression after 4 years. Br J Ophthalmology. 2016; https://doi.org/10.1136/bjophthalmol-2016-308460.
3. Siaudvytvte L, Janulevicience I, Daveckaite A, Ragauskas A, Bartusis L, Kucinoviene J, Siesky B, Harris A. Literateure review and meta-analysis of translaminar pressure difference in open-angle glaucoma. Eye (Lond). 2015a;29(10):1242–50.
4. Siaudvytyte L, Januleviciene I, Ragauskas A, Bartusis L, Meiliuniene I, Siesky B, Harris A. The difference in translaminar pressure gradient and neuroretinal rim area in glaucoma and healthy subjects. J Ophthalmol. 2014;2014:937360.

5. Arciero J, Harris A, Siesky B, Amireskandari A, Gershuny V, Pickrell A, Guidoboni G. Theoretical analysis of vascular regulatory mechanisms contributing to retinal blood flow autoregulation. Invest Ophthalmol Vis Sci. 2013;54(8):5584–93.
6. Carichino L, Harris A, Guidoboni G, Siesky BA, Abegão Pinto L, Vandewalle E, Olafsdottir OB, Hardarson SH, van Keer K, Stalmans I, Stefánsson E, Arciero JC. A theoretical investigation of the increase in venous oxygen saturation levels in advanced glaucoma patients. J Model Ophthalmol. 2016;1(1):64–87.
7. Cassani S, Guidoboni G, Janulviciene I, Carichino L, Siesky BA, Tobe LA, Amireskandari A, Baikstiene DP, Harris A. Effect of trabeculectomy on retinal hemodynamics: mathematical modeling of clinical data. In: Causin P, Guidoboni G, Sacco R, Harris A, editors. Integrated Multidisciplinary Approaches in the Study and Care of the Human Eye. Amsterdam: Kugler Publications; 2014. p. 29–36.
8. Dziubek A, Guidoboni G, Harris A, Hirani AH, Rusjan E, Thistleton W. Effect of ocular shape and vascular geometry on retinal hemodynamics: a computational model. Biomech Model Mechanobiol. 2016;15(4):893–907. [Epub 2015 Oct 7]
9. Guidoboni G, Harris A, Cassani S, Arciero J, Siesky B, Amireskandari A, Tobe L, Egan P, Januleviciene I, Park J. Intraocular pressure, blood pressure and retinal blood flow autoregulation: a mathematical model to clarify their relationship and clinical relevance. Invest Ophthalmol Vis Sci. 2014a;55(7):4105–18.
10. Gross JC, Harris A, Siesky BA, Sacco R, Shah A, Guidoboni G. Mathematical modeling for novel treatment approaches to open-angle glaucoma. Expert Rev Ophthalmol. 2017;12:443–55.
11. Sadler TW. Langman's medical embryology. 12th ed: Lipincott Williams & Wilkins; 2012. p. 330–1.
12. Donnelly J, Budohoski KP, Smielewski P, Czosnyka M. Regulation of cerebral circulation: bedside assessment and clinical implications. Crit Care. 2016;20(1):129.
13. Prada D, Harris A, Guidoboni G, Siesky B, Huang AM, Arciero JC. Autoregulation and neurovascular coupling in the optic nerve head. Surv Ophthalmol. 2016a;61(2):164–86.
14. Harris A, Arend O, Wolf S, Cantor LB, Martin BJ. CO_2 dependence of retinal arterial and capillary blood velocity. Acta Ophthalmol Scand. 1995;73(5):421–4.
15. Harris A, Zarfati D, Zalish M, Biller J, Sheets CW, Rechtman E, Migliardi R, Garzoli HT. Reduced cerebrovascular blood flow velocities and vasoreactivity in open angle glaucoma. Am J Ophthalmol. 2003;135(2):144–7.
16. Siesky B, Harris A, Brizendine E, Marques C, Loh J, Mackey J, Overton J, Netland P. Literature review and meta-analysis of topical carbonic anhydrase inhibitors and ocular blood flow. Surv Ophthalmol. 2009;54(1):33–46.
17. Martinez A, Gonzalez F, Capeans C, Perez R, Sanchez-Salorio M. Dorzolamide effect on ocular blood flow. Invest Ophthalmol Vis Sci. 1999;40(6):1270–5.
18. Siesky B, Harris A, Kagemann L, Stefansson E, McCranon L, Miller B, Bwatwa J, Regen G, Ehrlich R. Ocular blood flow and oxygen delivery to the retina in primary open-angle glaucoma patients: the addition of dorzolamide to timolol monotherapy. Acta Ophthalmol. 2010;88(1):142–9.
19. Hosking SL, Harris A, Chung HS, Jonescu-Cuypers CD, Kagemann L, Roff Hilton EJ, Garzozi H. Ocular haemodynamic responses to induced hypercapnia and hyperoxia in glaucoma. Br J Ophthalmol. 2004;88(3):406–11.
20. Ho JD, Hu CC, Lin CC. Open angle glaucoma and the risk of stroke development: a 5-yr populaiton-based follow up study. Stroke. 2009;40(8):2685–90.
21. Doucette LP, Rasnitsyn A, Seifi M, Walter MA. The interactions of genes, age, and environment in glaucoma pathogenesis. Surv Ophthalmol. 2015;60(4):310–26.
22. Yang D, Cabral D, Gaspard EN, Lipton RB, Rundek T, Derby CA. Cerebral hemodynamics in the elderly: a transcranial doppler study in the Einstein aging study cohort. J Ultrasound Med. 2016;35(9):1907–14.
23. Krejza J, Mariak Z, Walecki J, Szydlik P, Lewko J, Ustymowicz A. Transcranial color Doppler sonography of basal cerebral arteries in 182 healthy subjects: age and sex variability and normal reference values for blood flow parameters. Am J Roetgenol. 1999;172(1):213–8.
24. Harris A, Harris M, Biller J, Garzozi H, Zarfty D, Ciulla TA, Martin B. Aging affects the retrobulbar circulation differently in women and men. Arch Ophthalmol. 2000;118(8):1076–80.
25. Ehrlich R, Kheradiya NS, Winston DM, Moore DB, Wirostko B, Harris A. Age-related ocular vascular changes. Graefes Arch Clin Exp Ophthalmol. 2009;247(5):583–91.
26. Fleischman D, Berdahl P, Zaydlarova J, Stinnett S, Fautsch MP, Allingham RR. Cerebrospinal fluid pressure decreases with older age. PLoS One. 2012;7(12):e52664. Epub 2012 Dec 26
27. Harris et al. Association for Research in Vision and Ophthalmology (ARVO). Presentation entitled, 'Fourier domain optical coherence tomography blood flow assessment in patients with glaucoma: A new blood flow method'. Fort Lauderdale, FL. May 2–6, 2010.
28. Tielsch JM, Katz J, Sommer A, Quigley HA, Javitt JC. Hypertension, perfusion pressure, and primary open-angle glaucoma. A population-based assessment. Arch Ophthalmol. 1995 Feb;113(2):216–21.
29. Koustenis A, Harris A, Gross J, Januleviciene I, Shah A, Siesky B. Optical coherence tomography angiography: an overview of the technology and an assessment of applications for clinical research. Br J Ophthalmol. 2017;101(1):16–20. Epub ahead of print
30. Bonomi L, Marchini G, Marraffa M, Morbio R. The relationship between intraocular pressure and glaucoma in a defined population. Data from the Egna-Neumarkt Glaucoma study. Ophthalmology. 2000;107(7):1287–93.
31. Hulsman CA, Vingerling JR, Hofman A, Witteman JC, de Jong PT. Blood pressure, arterial stiffness, and open-angle glaucoma: the Rotterdam study. Arch Ophthalmol. 2007;125(6):805–12.
32. Leske MC, Connell AM, Wu SY, Hyman LG, Schachat AP. Risk factors for open-angle glaucoma The Barbados Eye Study. Arch Ophthalmol. 1995;113(7):918–24.
33. Quigley HA, West SK, Rodriquez J, Munoz B, Klein R, Snyder R. The prevalence of glaucoma in a population-based study of Hispanic subject: Proyecto VER. Arch Ophthalmol. 2001;119(12):1819–26.
34. Memarzadeh F, Ying-Lai M, Chung J, Azen SP, Varma R, Los Angeles Latino Eye Study Group. Blood pressure, perfusion pressure, and open-angle glaucoma: the Los Angeles Latino Eye Study. Invest Ophthalmol Vis Sci. 2010;51(6):2872–7.
35. Zheng Y, Wong TY, Mitchell P, Friedman DS, He M, Aung T. Distribution of ocular perfusion pressure and its relationships with open-angle glaucoma: the Singapore Malay Eye Study. Invest Ophthalmol Vis Sci. 2010;51(7):3399–404.
36. Deb AK, Kaliaperumal S, Rao VA, Sengupta S. Relationship between systemic hypertension, perfusion pressure, and glaucoma: a comparative study in an adult Indian population. Indian J Ophthalmol. 2014;62(9):917–22.
37. Tieisch JM, Katz J, Sommer A, Quigley HA, Javitt JC. Hypertension, perfusion pressure, and primary open-angle glaucoma. A population-based assessment. Arch Ophthalmol. 1995;113(2):216–21.
38. De Moraes CG, Liebman JM, Greenfield DS, Gardiner SK, Ritch R, Krupin J, Low-pressure Glaucoma Treatment Study Group. Risk factors for visual field progression in the low-pressure glaucoma treatment study. Am J Ophthalmol. 2012;154(4):702–11.
39. Leske MC, Heijl A, Hyman L, Bengtsson B, Dong L, Yang Z, EMGT Group. Predictors of long-term progression in the early manifest glaucoma trial. Ophthalmology. 2007;114(11):1965–72.

40. Leske MC, Wu SY, Hennis A, Honkanen R, Nemesure B, BEBs Study Group. Risk factors for incident open-angle glaucoma: the Barbados eye studies. Ophthalmology. 2008;115(1):85–93.
41. Ramdas WD, Wolfs RC, Hofman A, de Jong PT, Vingerling JR, Jansonius NM. Ocular perfusion pressure and the incidence of glaucoma: real effect or artifact? The Rotterdam study. Invest Ophthalmol Vis Sci. 2011;52(9):6875–81.
42. Topouzis F, Coleman AL, Harris A, Jonescu-Cuypers C, Yu F, Marvoudis L, Anastasopoulos E, Pappas T, Koskosas A, Wilson MR. Association of blood pressure status with the optic disk structure in non-glaucoma subjects: the Thessaloniki Eye Study. Am J Ophthalmol. 2006;142(11):60–7.
43. Topouzis F, Wilson MR, Harris A, Founti P, Yu F, Anastasopoulos E, Pappas T, Koskosas A, Salonikiou A, Coleman AL. Association of open-angle glaucoma with perfusion pressure status in the Thessaloniki Eye Study. Am J Ophthalmol. 2013;155(5):843–51.
44. Ren R, Jonas JB, Tian G, Zhen Y, Ma K, Li S, Wang H, Li B, Zhang X, Wang N. Cerebrospinal fluid pressure in glaucoma: a prospective study. Ophthalmology. 2010;117(2):259–66.
45. Harris A, Evans D, Martin B, Zalish M, Kagemann L, McCranor L, Garzozi H. Nocturnal blood pressure reduction: effect on retrobulbar hemodynamics in glaucoma. Graefes Arch Clin Exp Ophthalmol. 2002;240(5):372–8. Epub 2002 Apr 16
46. Raboel PH, Bartek J, Andresen M, Bellander BM, Romner B. Intracranial pressure monitoring: invasive versus non-invasive methods—a review. Crit Care Res Pract. 2012;2012:950393.
47. Siaudvytvte L, Janulevicience I, Daveckaite A, Ragauskas A, Siesky B, Harris A. Neuroretinal rim area and ocular haemodynamic parameters in patients with normal-tension glaucoma with differing intracranial pressures. Br J Ophthalmol. 2015b;100(8):1134–8.
48. Jóhannesson G, Eklund A, Lindén C. Intracranial and Intraocular Pressure at the Lamina Cribrosa: Gradient Effects Curr Neurol Neurosci Rep. 2018;18(5):25.
49. Boltz A, Schmidl D, Werkmeister RM, Lasta M, Kaya S, Palkovits S, Told R, Napora KJ, Popa-Cherecheanu A, Garhöfer G, Schmetterer L. Regulation of optic nerve head blood flow during combined changes in intraocular pressure and arterial blood pressure. J Cereb Blood Flow Metab. 2013;33(12):1850–6. https://doi.org/10.1038/jcbfm.2013.137. Epub 2013 Aug 7
50. Harris A, Guidoboni G, Arciero JC, Ameriskandari A, Tobe LA, Siesky BA. Ocular hemodynamics and glaucoma: the role of mathematical modeling. Eur J Ophthalmol. 2013;23(2):139–46.
51. Guidoboni G, Harris A, Carichino L, Arieli Y, Siesky BA. Effect of intraocular pressure on the hemodynamics of the central retinal artery: a mathematical model. Math Biosci Eng. 2014b;11(3):523–46.
52. Carichino L, Guidoboni G, Siesky BA, Amireskandari A, Januleviciene I, Harris A. Effect of intraocular pressure and cerebrospinal fluid pressure on the blood flow in the central retinal vessels. In: Causin P, Guidoboni G, Sacco R, Harris A, editors. Integrated multidisciplinary approaches in the study and care of the human eye. Amsterdam: Kugler Publications; 2014. p. 59–66.
53. Morgan WH, Yu DY, Alder VA, Cringle SJ, Cooper RL, House PH, Constable IJ. The correlation between cerebrospinal fluid pressure and retrolaminar tissue pressure. Invest Ophthalmol Vis Sci. 1998;39(8):1419–28.
54. Burgoyne CF. A biomechanical paradigm for axonal insult within the optic nerve head in aging and glaucoma. Exp Eye Res. 2011;93(2):120–32.
55. D. Prada, R. Sacco, B. Cockburn, L. Bociu, J. Webster, B. A. Siesky, A. Harris. Influence of tissue viscoelasticity on the optic nerve head perfusion: a mathematical model. In: ARVO 2016 Annual Meeting, Program Number 3558, Poster Board Number A0256, 2016b.
56. Quigley HA, Hohman RM, Addicks EM, Massof RW, Green WR. Morphologic changes in the lamina cribrosa correlated with neural loss in open-angle glaucoma. Am J Ophthalmol. 1983;95(5):673–91.
57. Jonas JJ, Mardin CY, Schrehardt US, Naumann GOH. Morphometry of the human lamina cribrosa surface. Invest Ophthalmol Vis Sci. 1991;32(2):401–5.
58. Crawford Downs J, Roberts MD, Sigal IA. Glaucomatous cupping of the lamina cribrosa: a review of the evidence for active progressive remodeling as a mechanism. Exp Eye Res. 2011;93(2):133–40.
59. Yong Woo Kim, Byeong Wook Yoo, Jin Wook Jeoung, Hee Chan Kim, Ki Ho Park. Lamina cribrosa pore characteristics in eyes with primary open-angle glaucoma: A swept-source optical coherence tomography study. In ARVO Annual Meeting Abstract, June 2015.
60. M. J. Girard, E. Birgersson, H. L. Leo, A. Thiery, T. Chuangsuwanich. Factors Influencing Lamina Cribrosa Microcapillary Hemodynamics and Oxygen Concentrations. ARVO 2016 Annual Meeting, Program Number: 4711.
61. Bociu L, Guidoboni G, Sacco R, Webster JT. Analysis of nonlinear poro-elastic and poro-visco-elastic models. Arch Ration Mech Anal. 2016;222(3):1445–519. [Epub 2016 Jul 14]
62. Causin P, Guidoboni G, Harris A, Prada D, Sacco R, Terragni S. A poroelastic model for the perfusion of the lamina cribrosa in the optic nerve head. Math Biosci. 2014;257:33–41.
63. Downs JC, Suh JK, Thomas KA, Bellezza AJ, Hart RT, Burgoyne CF. Viscoelastic material properties of the peripapillary sclera in normal and early-glaucoma monkey eyes. Invest Ophthalmol Vis Sci. 2005;46(2):540–6.
64. Palko JR, Iwabe S, Pan X, Agarwal G, Komáromy AM, Liu J. Biomechanical properties and correlation with collagen solubility profile in the posterior sclera of canine eyes with an ADAMTS10 mutation. Invest Ophthalmol Vis Sci. 2013;54(4):2685–95.

34 Intraocular Pressure-Related Factors, Retinal Vessel Diameter, and Optic Disc Rim Area

Qing Zhang, Chen Xin, Chunyu Guo, Ye Zhang, and Ningli Wang

Although elevated intraocular pressure (IOP) is a main risk factor, more and more attention has been paid to other factors contributing to the development and progression of primary open-angle glaucoma (POAG) [1–16]. Among those factors, narrow retinal vessels and IOP-related stress have been found associated with glaucomatous optic neuropathy in many clinical trials and population-based study, which furnishes the basis for the vascular mechanism of POAG [1–7]. Lower lumbar cerebrospinal fluid pressure (CSFP) and narrower orbital cerebrospinal fluid space are found in some normal-tension glaucoma patients, compared with normal subjects and POAG with high IOP [13]. Higher CSFP was found relevant to higher body mass index (BMI), and BMI has been reported to be positively correlated with neuroretinal rim area and retinal nerve fiber layer thickness [10–13, 17]. A proven formula was employed to estimate the CSFP in the Central India Eye and Medical Study, instead of the direct measurement which lacks feasibility in such a population-based study. The same formula was also used in the Beijing Eye Study [8, 9, 18]. Along with the CSFP, the trans-lamina cribrosa pressure difference (TLCPD: IOP minus estimated CSFP) was also estimated. A lower estimated CSFP and a higher TLCPD were found associated with the presence of POAG and the severity of optic nerve damage [8, 9, 18].

Central retinal artery, accompanying with central retinal vein and optic nerve, passes through the optic canal and crosses the lamina cribrosa. Therefore, these three structures subject to the same biomechanical forces. So we presume they correlate with each other and IOP-related pressure (IOP, estimated CSFP, and TLCPD). Although glaucomatous optic nerve damage, IOP-related stress, and the status of retinal vessels have been studied respectively in previous population-based studies, the analysis of the interactions between the three factors is still absent, which was then realized in the Handan Eye Study (HES).

As a rural population-based, longitudinal study, HES employed a stratified, multistaged cluster sampling method, included 6830 participants, and was initiated since October 2006. The methods and other details have been described previously [19–21]. All subjects presented a detailed family and medical history and underwent a comprehensive ocular examination [19, 22–25]. POAG was diagnosed by two definitions: expert consensus and International Society of Geographical and Epidemiological Ophthalmology (ISGEO) classification [26, 27]. In the recruited population, 67 POAG (1.0%) were diagnosed based on expert consensus, while 125 POAG (1.9%) were determined by ISGEO classification [26]. The CSFP was calculated by the formula: CSFP [mmHg] = 0.44 × body mass index [kg/m^2] + 0.16 × diastolic blood pressure [mmHg] − 0.18 × age (years) − 1.91. TLCPD was set as IOP minus CSFP calculated [9, 18, 28–30]. Based on the fundus photographs, arteriolar and venular diameters were measured by a computer-assisted program (IVAN; University of Wisconsin, Madison, WI, USA as a standardized protocol [31]). Only participants with good qualities of HRTII images, gradable retinal photographs, refractive errors not larger than −8 diopters, axial lengths not longer than 26.5 mm, age, diastolic blood pressure (BP), IOP, and BMI were included in the final analysis [24, 32].

Only the data of the right eye was used for analysis. Both univariable and multivariable linear regressions were used to analyze the factors related to the neuroretinal rim area. Finally, 67 POAG patients were identified or diagnosed through expert consensus via propensity score matching, who were then compared with 67 normal controls (age and

Q. Zhang · C. Xin · Y. Zhang · N. Wang (✉)
Beijing Institute of Ophthalmology, Beijing Tongren Eye Center, Beijing Tongren Hospital, Capital Medical University, Beijing, China

Beijing Ophthalmology & Visual Sciences Key Laboratory, Beijing, China
e-mail: wningli@vip.163.com

C. Guo
Department of Epidemiology, School of Public Health, University of Michigan, Ann Arbor, MI, USA

N. Wang (ed.), *Intraocular and Intracranial Pressure Gradient in Glaucoma*,
Advances in Visual Science and Eye Diseases 1, https://doi.org/10.1007/978-981-13-2137-5_34

gender matched). The 125 POAG patients diagnosed with the ISGEO classification system were also compared with normal controls, selected by propensity score matching [33].

Of all the participants, gradable fundus images were absent in 182 subjects; 99 were diagnosed with primary angle-closure glaucoma or other types of glaucoma. Among the left 6549 participants, 67 were POAG patients, and 22 of them had no acceptable HRTII images and five had high myopia. Thus 40 POAG patients and 4194 non-glaucoma subjects were eligible for further analysis. The demographical data of those subjects included and excluded in the final analysis are shown in Table 34.1.

Compared with those excluded, the included participants were younger, possessed lower refractive errors, and higher female-to-male ratio. The univariable analysis spotted several systemic and ocular features which show significant association with narrow neuroretinal rim area (RA). Those parameters include female gender, older age, larger waist/hip ratio (W/H ratio), lower BMI, hypertension, longer axial length (AL), higher refractive error (RE), higher estimated TLCPD, smaller disc area (DA), lower estimated CSFP, and smaller central retinal vessel parameters (Table 34.2).

Table 34.1 Characteristics of included and excluded participants

Parameter	Included	Excluded	*P-value*
Number	4234	2596	
Age (years)	51.1 ± 10.8	54.3 ± 13.80	<0.001
Gender(male%)	1882(44.4%)	1281(49.3%)	<0.001
Refractive error, diopters	0.003 ± 1.1	−0.37 ± 2.7	<0.001
Axial length (mm)	22.80 ± 0.85	22.82 ± 1.28	0.06

Data are shown as "mean ± standard deviation"
$p < 0.05$

However, the association between narrow RA and diabetes or IOP was not significant.

In the multivariable analysis, all the parameters demonstrating significant association with RA in the univariable analysis and IOP were included. The features shown significantly association with reduced RA included smaller disc area, higher IOP, older age, presence of POAG, narrower CRVE, longer axial length, higher refractive error, and lower BMI. The standard deviation (SD) decrease of CRVE and BMI was correlated to the decrease of neuroretinal RA at the ratio of 1:0.08 and 1:0.029. Model 2 included the estimated CSFP and TLCPD as independent variables, and a higher TLCPD was found significantly associated with a smaller RA, while IOP was not significantly relevant. A decrease of 0.028mm^2 in neuroretinal RA was induced by an increase of 1 mmHg in TLCPD. Model 3 omitted age with or without BMI, and the association between reduced RA and narrower disc area was still significant, as well as between reduced RA and presence of POAG, higher IOP, lower CSFP, hypertension, narrower CRVE, longer axial length, higher refractive error, and higher W/H ratio. Each unit of decrease in CSFP induced a decrease of 0.074mm^2 in neuroretinal RA and each unit of decrease in W/H ratio, 0.024mm^2. The Durbin-Watson value in these models ranged from 1.94 to 1.97 (Table 34.3).

Similar results were demonstrated in population without POAG (Table 34.4). In POAG patients, significant associations were observed between narrow neuroretinal RA and other features, including smaller disc area, lower diastolic BP, and higher TLCPD. Multivariable analysis demonstrated a significant association between RA and disc area.

Table 34.2 Univariable analysis: associations of the neuroretinal rim area in all subjects (40 POAG and 4194 non-glaucoma)

Parameters	*P*-value	Regression coefficient B	Standardized coefficient beta	95% confidence interval of B
Age	<0.001	−0.007	−0.237	−0.008, −0.006
BMI, kg/mm^2	0.024	0.003	0.035	0.000, 0.006
W/H ratio	<0.001	−0.338	−0.062	−0.502, −0.173
RE, diopter	<0.001	−0.037	−0.129	−0.046, −0.029
AL, mm	<0.001	−0.035	−0.087	−0.023, −0.047
TLCPD, mmHg	<0.001	−0.012	−0.144	−0.015, −0.010
CSFP, mmHg	<0.001	0.013	0.143	0.010, 0.016
IOP, mmHg	0.167	−0.002	−0.021	−0.006, 0.001
DA, mm^2	<0.001	0.473	0.681	0.458, 0.488
CRAE, μm	<0.001	0.001	0.071	0.001, 0.001
CRVE, μm	<0.001	0.001	0.081	0.000, 0.001
A/V ratio	0.409			
Gender	0.003			
Presence of hypertension	<0.001			
Presence of diabetes	0.386			

BMI body mass index, *W/H* ratio waist/hip ratio, *RE* refractive error, *AL* axial length, *LT* lens thickness, *TLCPD* trans-lamina cribrosa pressure difference, *CSFP* cerebrospinal fluid pressure, *IOP* intraocular pressure, *DA* disc area, *CRAE* central retinal arteriolar equivalent, *CRVE* central retinal venular equivalent, *A/V* ratio retinal vein-to-artery diameter ratio

Table 34.3 Multivariable analysis: associations of the neuroretinal rim area in all subjects (40 POAG and 4194 non-glaucoma)

Parameter	*P*-value	Regression coefficient B	Standardized coefficient B	95% confidence interval for B	Variance inflation factor
Model 1					
Disc area, mm^2	<0.001	0.467	0.667	0.450, 0.483	1.068
Presence of POAG	<0.001	−0.135	−0.119	−0.161, −0.0109	1.021
Age, y	<0.001	−0.003	−0.099	−0.004, −0.002	1.179
CRVE, μm	<0.001	0.001	0.080	0.001, 0.001	1.053
Refractive error, diopters	0.002	−0.012	−0.041	−0.020, −0.004	1.308
Axial length, mm	0.006	−0.014	−0.035	−0.025, −0.004	1.238
BMI, kg/mm^2	0.015	0.002	0.029	0.000, 0.004	1.056
IOP, mmHg	0.016	−0.003	−0.029	−0.006, −0.001	1.077
Model 2					
Disc area, mm^2	<0.001	0.467	0.667	0.450, 0.483	1.068
Presence of POAG	<0.001	−0.135	−0.120	−0.161, −0.109	1.020
Age, years	<0.001	−0.002	−0.084	−0.003, −0.002	1.395
CRVE μm	<0.001	0.001	0.082	0.001, 0.001	1.045
Refractive error, diopters	0.002	−0.012	−0.040	−0.020, −0.004	1.308
Axial length, mm	0.007	−0.014	−0.035	−0.024, −0.004	1.244
TLCPD, mmHg	0.028	−0.002	−0.028	−0.004, 0.000	1.236
Model 3					
Disc area, mm^2	<0.001	0.470	0.672	0.454, 0.487	1.060
Presence of POAG	<0.001	−0.139	−0.124	−0.165, −0.113	1.016
CRVE, μm	<0.001	0.001	0.076	0.000, 0.001	1.060
CSFP, mmHg,	<0.001	0.007	0.074	0.005, 0.009	1.192
Presence of hypertension	0.002	−0.023	−0.038	−0.038, −0.009	1.101
Refractive error, diopters	<0.001	−0.016	−0.055	−0.024, −0.009	1.237
Axial length, mm	0.003	−0.016	−0.039	−0.026, 0.005	1.252
IOP, mmHg	0.025	−0.003	−0.028	−0.006, 0.000	1.124
Waist-to-hip ratio	0.047	−0.130	−0.024	−0.258, −0.002	1.044

Model 1: adjusted stepwise for independent parameters significantly associated with rim area in the univariable analyses plus IOP (estimated CSFP and estimated TLCPD not included). Durbin-Watson value: 1.97.
Model 2: adjusted for the same variables in Model 1 plus estimated CSFP and TLCPD. Durbin-Watson value: 1.94.
Model 3: adjusted for the same variables in Model 2 (age or age and BMI excluded). Durbin-Watson value: 1.95.

When compared with non-glaucomatous controls, the 67 POAG patients were found with smaller mean RA, deeper mean maximum cup, higher mean IOP, and higher mean TLCPD (Table 34.5). The 125 patients identified by ISGEO were found with significantly smaller mean RA, lower mean CRAE and CRVE, deeper mean maximum cup, higher mean IOP, and higher mean TLCPD (Table 34.6).

Our analysis showed several features were associated with the narrow neuroretinal RA, including narrower CRVE, IOP-related pressure factors such as higher estimated TLCPD and lower CSFP, higher IOP, myopia, longer axial length, and lower BMI. Significant association presented in both populations with and without POAG.

There is not yet unified opinion with regard to the relation between the caliber of glaucomatous optic neuropathy and retinal vessels [1, 4, 34, 35]. The association between retinal arteriolar caliber and glaucoma was reported to be stronger than it was between venular caliber and POAG in several hospital- or population-based studies [4, 34, 35]. The association between glaucomatous optic neuropathy and both the calibers of arteries and venules was observed in our study, much closer to the findings in the Singapore Malay Eye Study, and the associations were independent of IOP, which applied to those without POAG [1, 3]. A significant relation between the venular calibers and rim area was also observed.

Our study is consistent with previous results that lower BMIs are related to the higher prevalence and incidence of glaucoma, as well as the worse optic neuropathy [36, 37]. As the BMI is relevant to the CSFP, a significant association between lower BMIs and narrower RA indicated that the low CSFP may play a role in the development and progression of POAG [11, 13, 37–40]. Moreover, our results agreed with some findings of previous studies [8, 9, 18]. Both Beijing

Table 34.4 Multivariable analysis: associations of neuroretinal rim area and ocular and systemic parameters in the population without glaucoma ($n = 4194$)

Parameters	*P*-value	Regression coefficient B	Standardized coefficient B	95% confidence interval for B	Variance inflation factor
Model 1					
Disc area, mm^2	<0.001	0.468	0.678	0.453, 0.483	1.165
Age, y	<0.001	−0.003	−0.099	−0.004, −0.002	1.165
CRVE, μm	<0.001	0.001	0.080	0.001, 0.001	1.055
Refractive error, diopters	0.002	−0.011	−0.039	−0.019, −0.004	1.296
Axial length, mm	0.005	−0.014	−0.035	−0.023, −0.004	1.226
IOP, mmHg	0.010	−0.003	−0.029	−0.006, −0.001	1.069
BMI, kg/mm^2	0.020	0.002	0.026	0.000, 0.004	1.053
Model 2					
Disc area, mm^2	<0.001	0.468	0.678	0.453, 0.484	1.065
Age, years	<0.001	−0.002	−0.083	−0.003, −0.002	1.386
CRVE μm	<0.001	0.001	0.082	0.001, 0.001	1.047
Refractive error, diopters	0.002	−0.011	−0.039	−0.019, −0.004	1.296
Axial length, mm	0.005	−0.014	−0.034	−0.023, −0.004	1.230
TLCPD, mmHg	0.012	−0.003	−0.031	−0.005, 0.000	1.231
Model 3					
Disc area, mm^2	<0.001	0.475	0.688	0. 460, 0.491	1.050
CRVE, μm	<0.001	0.001	0.076	0.000, 0.001	1.065
Refractive error, diopters	<0.001	−0.018	−0.061	−0.025, −0.011	1.186
Axial length, mm	0.004	−0.014	−0.035	−0.024, 0.005	1.223
Waist-to-hip ratio	0.015	−0.150	−0.028	−0.270, −0.029	1.051
CSFP, mmHg	0.001	0.003	0.042	0.001, 0.004	1.238
Presence of hypertension	0.006	−0.021	−0.034	−0.035, −0.006	1.244

Model 1: adjusted stepwise for independent parameters all of those that were significantly associated with rim area in the univariable analyses plus IOP (estimated CSFP and estimated TLCPD not included). Durbin-Watson value: 1.94.
Model 2: adjusted for the same variables in Model 1 plus estimated CSFP and TLCPD. Durbin-Watson value: 1.94.
Model 3: adjusted for the same variables in Model 2 (age or age and BMI excluded). Durbin-Watson value: 1.93.

Table 34.5 Comparison of POAG diagnosed by expert consensus with propensity score matched controls ($N = 67$)

	Non-glaucomatous group ($n = 67$)		POAG group ($n = 67$)		
Parameters[a]		Missing data, n		Missing data, n	*P-value*
Age (year)	61.63 ± 10.43	0	61.64 ± 10.46	0	0.99
Gender (female %)	61.2	0	61.2	0	1
Rim area (mm^2)	1.73 ± 0.25	20	1.43 ± 0.38	13	<0.001[b]
Maximum cup depth (mm)	0.54 ± 0.24	20	0.73 ± 0.18	13	<0.001[b]
SBP (mmHg)	151.39 ± 24.47	3	151.08 ± 24.96	0	0.94
DBP (mmHg)	80.00 ± 13.33	3	78.55 ± 13.86	0	0.54
BMI (kg/m^2)	24.05 ± 3.71	9	24.07 ± 3.27	4	0.97
Axial length (mm)	22.95 (22.33 ~ 23.61)[b]	0	23.33 (22.47 ~ 24.23)[b]	0	0.376[d]
Refractive error (diopter)	0.38 (0.00 ~ 1.25)[b]	6	0.00(−1.16 ~ 0.75)[b]	1	0.002[cd]
Waist-to-hip ratio	0.90 ± 0.04	5	0.91 ± 0.05	0	0.36
IOP (mmHg)	14.44 ± 3.01	9	16.61 ± 3.07	4	<0.001[b]
CSFP (mmHg)	10.66 ± 3.53	9	10.25 ± 3.67	4	0.532
TLCPD (mmHg)	3.88 ± 3.52	14	6.37 ± 4.22	8	0.001[b]
CRAE, μm	152.33 ± 29.04	4	145.77 ± 20.50	0	0.14
CRVE, μm	233.77 (208.06–255.10)[b]	4	222.4(207.94–242.00)[b]	0	0.29[d]
AVR	0.64 (0.60–0.71)[b]	4	0.64(0.59–0.69)[b]	0	0.51[d]

[a]Continuous data are represented as mean ± SD (standard deviation); and categorical data are represented as *n* (%) for gender or median (percentile 25 ~ percentile 75) when comparisons between groups were performed with Wilcoxon's rank-sum test for continuous data
[b]$p < 0.05$, indicates a significant difference found between the two groups
[c]Median (percentile 25 ~ percentile 75)
[d]Comparisons between groups were performed with Wilcoxon's rank-sum test for continuous data

Table 34.6 Comparison of POAG diagnosed using ISGEO Classification with propensity score matched controls ($N = 125$)

Parameters[a]	Non-glaucomatous Group ($n = 125$)	Missing data, n	POAG Group ($n = 125$)	Missing data, n	P Value
Age (year)	56.44±11.36	0	56.44±11.36	0	1
Gender (female %)	44	0	44	0	1
Rim area (mm^2)	1.74±0.30	21	1.60±0.40	24	0.004[c]
Maximum cup depth (mm)	0.54±0.22	21	0.79±0.18	24	<0.001[c]
SBP (mmHg)	138.5 (126.75 ~ 159.25)[b]	3	144 (125 ~ 160)[b]	0	0.361[d]
DBP (mmHg)	77.14±11.62	3	78.59±12.59	0	0.35
BMI (kg/m^2)	24.34±3.36	7	23.95±3.08	4	0.36
Axial length (mm)	22.90 (22.41 ~ 23.66)[b]	0	23.21 (22.60 ~ 23.94)[b]	0	0.07[d]
Refractive error (diopter)	0.13(-0.25 ~ 0.75)[b]	4	0.00(-0.50 ~ 0.38)[b]	3	0.06[d]
Waist-to-hip ratio	0.90±0.04	4	0.91±0.05	1	0.36
IOP (mmHg)	14.48±2.92	8	15.61±3.12	2	0.004[c]
CSFP (mmHg)	11.03±3.55	7	11.09±3.60	4	0.90
TLCPD (mmHg)	3.35±3.75	10	4.42±4.31	6	0.04[b]
CRAE, μm	151.85 (140.72 ~ 169.25) Ω	3	146.31(135.40 ~ 156.81)[b]	0	0.002[c,d]
CRVE, μm	236.41(214.83 ~ 261.42)[b]	3	221.3(202.67 ~ 240.47[b]	0	<0.001[c,d]
AVR	0.65(0.61 ~ 0.69)[b]	3	0.66(0.61 ~ 0.69)[b]	0	0.575[d]

[a]Continuous data are represented as mean ± SD (standard deviation); and categorical data are represented as n (%) for gender or median (percentile 25 ~ percentile 75) when comparisons between groups were performed with Wilcoxon's rank-sum test for continuous data.
[b]Median (percentile 25 ~ percentile 75).
[c]$p < 0.05$, indicates a significant difference found between the two groups.
[d]Comparisons between groups were performed with Wilcoxon's rank-sum test for continuous data.
ISGEO International Society of Geographical and Epidemiological Ophthalmology

Eye study and Central India Eye and Medical Study have reported that compared with IOP, TLCPD was more strongly associated with the optic neuropathy of POAG, as well as the prevalence, which was not observed in primary angle-closure glaucoma (PACG). If taking both TLCPD and CSFP into consideration, it is yet to be explored whether a high TLCPD, independent of the CSFP-BP and CSFP-BMI relationship, is associated with POAG optic neuropathy [8].

The population-based design, the large sample size of patients without glaucoma, multiple-variable statistical analysis, and the high response rate endow our study with the advantages in better understanding the relationships among glaucomatous optic nerve damage, IOP-related stress, and the status of retinal vessels.

Some limitations do exist in our study. Because of the lack of noninvasive measurement, the formula is the merely practical method for CSFP estimation despite the possible shortage of our results. We also proposed that although a reported linear relationship exists, the CSFP is not the pressure in the optic nerve subarachnoid space. Furthermore, some variables composing the formula for CSFP estimation were relevant to POAG themselves. It was impossible to identify the causal relationship between the CSFP and narrower RA. To conclude, this study showed the significant association between decreased optic disc RA and several features, including narrower CRVEs, lower CSFPs, and higher IOPs. It enriched the current multiple principles for the pathogenic mechanism of POAG, which stresses that besides high IOP, biomechanics and vascular microcirculation of optic nerve contribute to the optic nerve damage in POAG [41].

References

1. Amerasinghe N, Aung T, Cheung N, et al. Evidence of retinal vascular narrowing in glaucomatous eyes in an Asian population. Invest Ophthalmol Vis Sci. 2008;49:5397–402.
2. Kawasaki R, Wang JJ, Rochtchina E, Lee AJ, Wong TY, Mitchell P. Retinal vessel calibre is associated with the 10-year incidence of glaucoma: the Blue Mountains Eye Study. Ophthalmology. 2013;120:84–90.
3. Zheng Y, Cheung N, Aung T, Mitchell P, He M, Wong TY. Relationship of retinal vascular caliber with retinal nerve fiber layer thickness: the Singapore Malay Eye Study. Invest Ophthalmol Vis Sci. 2009;50:4091–6.
4. Wang S, Xu L, Wang Y, Wang Y, Jonas JB. Retinal vessel diameter in normal and glaucomatous eyes: the Beijing eye study. Clin Experiment Ophthalmol. 2007;35:800–7.
5. Mitchell P, Leung H, Wang JJ, et al. Retinal vessel diameter and open-angle glaucoma: the Blue Mountains Eye Study. Ophthalmology. 2005;112:245–50.
6. Flammer J, Orgul S, Costa VP, et al. The impact of ocular blood flow in glaucoma. Prog Retin Eye Res. 2002;21:359–93.
7. Wang JJ, Mitchell P, Smith W. Is there an association between migraine headache and open-angle glaucoma? Findings from the Blue Mountains Eye Study. Ophthalmology. 1997;104:1714–9.
8. Jonas JB, Wang N, Yang D, Ritch R, Panda-Jonas S. Facts and myths of cerebrospinal fluid pressure for the physiology of the eye. Prog Retin Eye Res. 2015;46:67–83.
9. Jonas JB, Wang N, Wang YX, et al. Estimated trans-lamina cribrosa pressure difference versus intraocular pressure as biomarker for open-angle glaucoma: The Beijing Eye Study 2011. Acta Ophthalmol. 2015;93(1):e7–e13.
10. Jonas JB, Nangia V, Gupta R, et al. Retinal nerve fibre layer cross-sectional area, neuroretinal rim area and body mass index. Acta Ophthalmol. 2014;92:e194–9.
11. Ren R, Wang N, Zhang X, Tian G, Jonas JB. Cerebrospinal fluid pressure correlated with body mass index. Graefes Arch Clin Exp Ophthalmol. 2012;250:445–6.

12. Ren R, Wang N, Zhang X, Cui T, Jonas JB. Trans-lamina cribrosa pressure difference correlated with neuroretinal rim area in glaucoma. Graefes Arch Clin Exp Ophthalmol. 2011;249:1057–63.
13. Ren R, Jonas JB, Tian G, et al. Cerebrospinal fluid pressure in glaucoma: a prospective study. Ophthalmology. 2010;117:259–66.
14. Wang N, Xie X, Yang D, et al. Orbital cerebrospinal fluid space in glaucoma: the Beijing intracranial and intraocular pressure (iCOP) study. Ophthalmology. 2012;119:2065–73.. e2061
15. Yang H, Williams G, Downs JC, et al. Posterior (outward) migration of the lamina cribrosa and early cupping in monkey experimental glaucoma. Invest Ophthalmol Vis Sci. 2011;52:7109–21.
16. Yang H, Thompson H, Roberts MD, Sigal IA, Downs JC, Burgoyne CF. Deformation of the early glaucomatous monkey optic nerve head connective tissue after acute IOP elevation in 3-D histomorphometric reconstructions. Invest Ophthalmol Vis Sci. 2011;52:345–63.
17. Jonas JB, Xu L, Xu J, Wei WB, Wang YX. Prevalence of diabetic retinopathy and vision loss in the Beijing Eye Study: the potential role of the cerebrospinal fluid pressure. Curr Diab Rep. 2015;15:71.
18. Jonas JB, Nangia V, Wang N, et al. Trans-lamina cribrosa pressure difference and open-angle glaucoma. The central India eye and medical study. PLoS One. 2013;8:e82284.
19. Liang YB, Friedman DS, Wong TY, et al. Rationale, design, methodology, and baseline data of a population-based study in rural China: the Handan Eye Study. Ophthalmic Epidemiol. 2009;16:115–27.
20. Liang YB, Friedman DS, Wong TY, et al. Prevalence and causes of low vision and blindness in a rural Chinese adult population: the Handan Eye Study. Ophthalmology. 2008;115:1965–72.
21. Wang FH, Liang YB, Zhang F, et al. Prevalence of diabetic retinopathy in rural China: the Handan Eye Study. Ophthalmology. 2009;116:461–7.
22. Peng XY, Wang FH, Liang YB, et al. Retinopathy in persons without diabetes: the Handan Eye Study. Ophthalmology. 2010;117:531–7, 537e531–2.
23. Wang NL, Friedman DS, Zhou Q, et al. A population-based assessment of 24-hour intraocular pressure among subjects with primary open-angle glaucoma: the Handan eye study. Invest Ophthalmol Vis Sci. 2011;52:7817–21.
24. Zhang Q, Li S, Liang Y, Wang F, Chen W, Wang N. Characteristics of optic disc parameters and its association in normal Chinese population: the Handan Eye Study. Chin Med J (Engl). 2014;127:1702–9.
25. Liang Y, Friedman DS, Zhou Q, et al. Prevalence and characteristics of primary angle-closure diseases in a rural adult Chinese population: the Handan Eye Study. Invest Ophthalmol Vis Sci. 2011;52:8672–9.
26. Liang YB, Friedman DS, Zhou Q, et al. Prevalence of primary open angle glaucoma in a rural adult Chinese population: the Handan eye study. Invest Ophthalmol Vis Sci. 2011;52:8250–7.
27. Foster PJ, Buhrmann R, Quigley HA, Johnson GJ. The definition and classification of glaucoma in prevalence surveys. Br J Ophthalmol. 2002;86:238–42.
28. Jonas JB, Wang N, Wang YX, et al. Subfoveal choroidal thickness and cerebrospinal fluid pressure: the Beijing Eye Study 2011. Invest Ophthalmol Vis Sci. 2014;55:1292–8.
29. Jonas JB, Wang N, Wang YX, You QS, Yang D, Xu L. Ocular Hypertension: General characteristics and estimated cerebrospinal fluid pressure. The Beijing Eye Study 2011. PLoS One. 2014;9(7):e100533.
30. Xie X, Zhang X, Fu J, et al. Noninvasive intracranial pressure estimation by orbital subarachnoid space measurement: the Beijing Intracranial and Intraocular Pressure (iCOP) study. Crit Care. 2013;17:R162.
31. Yang K, Zhan SY, Liang YB, et al. Association of dilated retinal arteriolar caliber with early age-related macular degeneration: the Handan Eye Study. Graefes Arch Clin Exp Ophthalmol. 2012;250:741–9.
32. Jonas JB, Xu L, Zhang L, Wang Y, Wang Y. Optic disk size in chronic glaucoma: the Beijing eye study. Am J Ophthalmol. 2006;142:168–70.
33. Pattanayak CW, Rubin DB, Zell ER. Propensity score methods for creating covariate balance in observational studies. Rev Esp Cardiol. 2011;64:897–903.
34. Hall JK, Andrews AP, Walker R, Piltz-Seymour JR. Association of retinal vessel caliber and visual field defects in glaucoma. Am J Ophthalmol. 2001;132:855–9.
35. Rankin SJ, Drance SM. Peripapillary focal retinal arteriolar narrowing in open angle glaucoma. J Glaucoma. 1996;5:22–8.
36. Cheung N, Wong TY. Obesity and eye diseases. Surv Ophthalmol. 2007;52:180–95.
37. Xu L, Wang YX, Wang S, Jonas JB. Neuroretinal rim area and body mass index. PLoS One. 2012;7:e30104.
38. Berdahl JP, Allingham RR, Johnson DH. Cerebrospinal fluid pressure is decreased in primary open-angle glaucoma. Ophthalmology. 2008;115:763–8.
39. Berdahl JP, Fautsch MP, Stinnett SS, Allingham RR. Intracranial pressure in primary open angle glaucoma, normal tension glaucoma, and ocular hypertension: a case-control study. Invest Ophthalmol Vis Sci. 2008;49:5412–8.
40. Berdahl JP, Fleischman D, Zaydlarova J, Stinnett S, Allingham RR, Fautsch MP. Body mass index has a linear relationship with cerebrospinal fluid pressure. Invest Ophthalmol Vis Sci. 2012;53:1422–7.
41. Zhang Q, Jan C, Guo CY, et al. Association of intraocular pressure-related factors and retinal vessel diameter with optic disc rim area in subjects with and without primary open angle glaucoma. Clin Experiment Ophthalmol. 2018;46(4):389–99.

New Insights into Ocular Hypertension

35

Translaminar Pressure Gradient Hypothesis and Pressure-Independent Viewpoint

Xiaobin Xie and Ningli Wang

Ocular hypertension (OHT), the same as "normal-tension glaucoma," is not a clinical entity [1]. This term usually refers to a situation in which intraocular pressure (IOP) is consistently elevated, usually an IOP of 22 mmHg or higher on two or more occasions without glaucomatous discs or visual field abnormality [2]. This would distinguish them from patients with "elevated" pressure and clear evidence of glaucomatous optic nerve damage [1]. OHT is often considered the opposite end of the glaucoma spectrum to normal-tension glaucoma. OHT is a condition requiring closer observation for the potential development of glaucomatous damage. The 5-year cumulative incidence of primary open-angle glaucoma (POAG) was 9.5% in the observational ocular hypertensive group without treatment intervention [3].

Glaucomatous optic neuropathy can be regarded as a multifactorial, complex central nervous system neurodegenerative disease. However, the pathogenesis is still not very clear. Study of OHT's mechanism may provide important clues to factors that may play a protective role in glaucoma and to establish comprehensive therapeutic strategies for this disease. This chapter will present some novel viewpoints on the mechanism of OHT.

X. Xie
Eye Hospital, China Academy of Chinese Medical Sciences, Beijing, China

N. Wang (✉)
Beijing Institute of Ophthalmology, Beijing Tongren Eye Center, Beijing Tongren Hospital, Capital Medical University, Beijing, China

Beijing Ophthalmology & Visual Sciences Key Laboratory, Beijing, China
e-mail: wningli@vip.163.com

35.1 Low Translaminar Pressure Gradient Hypothesis of Ocular Hypertension

Several experimental and clinical investigations suggested that an abnormally low orbital cerebral spinal fluid pressure (CSFP) may result in elevated translaminar pressure gradient which may potentially play a role in the pathogenesis of POAG, especially normal-tension glaucoma [4–11]. OHT is often considered the opposite end of the glaucoma spectrum to normal-tension glaucoma. So here comes the hypothesis that a relatively higher orbital CSFP in OHT would partially counterbalance an increased IOP and maybe play a vital protective role in preventing from or in postponing of OHT developing glaucoma.

Several hospital-based studies provided the clinical evidence that, measured by lumber puncture, the CSFP in OHT (13.2–16.0 mmHg) is higher than the controls (11.5–12.9 mmHg) [7, 9]. At the same time, however, the translaminar cribrosa pressure difference in OHT (6.7–8.4 mmHg) is still higher than the controls (1.4–4.4 mmHg) [7, 9]. A point to note here is that in the previous hospital-based study, the CSFP and the translaminar pressure difference in high IOP glaucoma group were 9.6–11.7 mmHg and 6.1–12.5 mmHg, respectively [7, 8].

Own to our data of a recent study (has been submitted and under reviewing), the estimated CSFP value in the 19 ocular hypertensive subjects (14.9 ± 2.9 mmHg) was significantly higher than that in 21 controls (12.0 ± 2.8 mmHg; $P < 0.01$). The estimated translaminar pressure difference was still significantly higher in the ocular hypertensive subjects than in the controls (9.0 ± 4.2 mmHg vs. 3.6 ± 3.0 mmHg $P < 0.01$). Among the ocular hypertensive subjects, the estimated translaminar pressure difference values in 7 (36.8%) were within the range found in the control group; however, the values in 12 (63.2%) were significantly higher than the control group. From the above data, we can see that OHT and POAG shared a range overlap of translaminar pressure difference which might be contributed to the glaucomatous optic nerve damage

N. Wang (ed.), *Intraocular and Intracranial Pressure Gradient in Glaucoma*,
Advances in Visual Science and Eye Diseases 1, https://doi.org/10.1007/978-981-13-2137-5_35

potentially. We would like to suggest that about 63% among the ocular hypertensive subjects should be closely monitored and need appropriate timely intervention.

The Ocular Hypertension Treatment Study (OHTS) demonstrated that a 20% reduction in IOP reduced the incidence of POAG by more than 50% in ocular hypertensive individuals [12]. If the low translaminar cribrosa pressure gradient hypothesis is verified, reasonably raising the CSFP when it is pathologically low would become the new therapeutic target, in addition to lowering IOP [13].

It is interesting to make special mention here of body mass index (BMI). In fact, BMI is positively and independently associated with CSFP [14]. Measuring BMI can partially contribute to evaluating CSFP [15]. The exact mechanism that high BMI increases CSFP remains unclear. Some studies showed that high BMI might increase in venous pressure by increasing intra-abdominal pressure and then consequently increase CSFP [16].

Studies have showed that higher BMI is associated with a lower risk of POAG [17–19]; meanwhile, lower BMI was associated with increased risk for normal-tension glaucoma [20]. In the study mentioned above (not published and under review), the BMI was significantly higher in OHT group than in control group ($P < 0.05$). It's important to note, however, that whether reasonable high BMI is an independent direct protective factor for ocular hypertension or indirectly protects ocular hypertension from developing glaucoma by means of contribution to a higher CSFP remains speculative.

35.2 Pressure-Independent Viewpoint on Ocular Hypertension

35.2.1 CSF Dynamics and Clearance of Neurotoxins

Apart from CSF pressure, both CSF dynamics and composition surrounding the optic nerve might have fundamental significance in the pathogenesis of glaucoma [21]. Recent research revealed similarities in the process leading to retinal ganglion cell death in glaucoma and neuronal cell death in Alzheimer's disease [22–24]. Exploring this possibility could shed new light on the pathogenesis of optic nerve glaucomatous damage. Wostyn, P et al. described a novel hypothesis for glaucoma, which, just like Alzheimer's disease, might be considered as an imbalance between CSF dynamics and clearance of neurotoxins, including amyloid-β or other toxic molecules [25]. As for OHT, Wostyn, P et al. presented that faster cerebrospinal fluid production leads to increased cerebrospinal fluid turnover with enhanced removal of potentially neurotoxic waste products that accumulate in the optic nerve [26].

35.2.2 Vascular Factors in Ocular Hypertension

Under the physiology condition, ocular perfusion pressure status (ocular perfusion pressure with or without antihypertensive treatment), blood pressure, and IOP keep the stabile dynamic balance. Decreases in ocular perfusion pressure (blood pressure-intraocular pressure) and systemic hypotension (especially low diastolic blood pressure) are associated with increased risk for open-angle glaucoma [27–32].

In Beijing Eye Study, a population-based study, systolic and diastolic blood pressure in ocular hypertensive group ($n = 62$; 140 ± 23 mmHg and 76 ± 12 mmHg, respectively) are significantly higher (both $P < 0.001$) than normotensive group ($n = 2757$; 130 ± 21 mmHg and 70 ± 12 mmHg, respectively). However, the percentage difference of suffering from arterial hypertension between the ocular hypertensive group (76.2 ± 5.7%) and the normotensive group 50.4 ± 1.0% was still statistically significant ($P = 0.002$) [33].

May it be speculated that, conversely, higher blood pressure can improve ocular perfusion pressure and then play a protective role of preventing OHT from development of glaucoma? So far, there is no evidence to support the speculation. Actually, there are also cardiovascular safety concerns associated with treatments designed to increase ocular perfusion pressure by elevating blood pressure, especially in old patients [34]. Arterial hypertension also has an important negative effect on ocular perfusion [35]. Nocturnal arterial hypotension, particularly among arterial hypertensive patients taking oral hypotensive medication, may be an important risk factor. Yet, using systemic BP medicine to minimize nocturnal hypotension and avoiding IOP medicine that lowers systemic BP at night (e.g., beta-blockers, alpha-agonists) need to be considered [32].

In short, these abovementioned new, important viewpoints on the mechanism of OHT would shed light on our understanding of the pathogenesis of glaucomatous optic neuropathy and help us to seek more perfect prevention and control measures for OHT and glaucoma.

References

1. Sommer A. Ocular hypertension and normal-tension glaucoma: time for banishment and burial. Arch Ophthalmol. 2011;129(6):785–7.
2. Perkins ES. The Bedford glaucoma survey. I. Long-term follow-up of borderline cases. Br J Ophthalmol. 1973;57(3):179–85.
3. Kass MA, Heuer DK, Higginbotham EJ, et al. The ocular hypertension treatment study: a randomized trial determines that topical ocular hypotensive medication delays or prevents the onset of primary open-angle glaucoma. Arch Ophthalmol. 2002;120(6):701–13. discussion 829-730
4. Morgan WH, Yu DY, Cooper RL, Alder VA, Cringle SJ, Constable IJ. The influence of cerebrospinal fluid pressure on the lamina cribrosa tissue pressure gradient. Invest Ophthalmol Vis Sci. 1995;36(6):1163–72.

5. Jonas JB, Berenshtein E, Holbach L. Anatomic relationship between lamina cribrosa, intraocular space, and cerebrospinal fluid space. Invest Ophthalmol Vis Sci. 2003;44(12):5189–95.
6. Berdahl JP, Allingham RR, Johnson DH. Cerebrospinal fluid pressure is decreased in primary open-angle glaucoma. Ophthalmology. 2008;115(5):763–8.
7. Berdahl JP, Fautsch MP, Stinnett SS, Allingham RR. Intracranial pressure in primary open angle glaucoma, normal tension glaucoma, and ocular hypertension: a case-control study. Invest Ophthalmol Vis Sci. 2008;49(12):5412–8.
8. Ren R, Jonas JB, Tian G, et al. Cerebrospinal fluid pressure in glaucoma: a prospective study. Ophthalmology. 2010;117(2):259–66.
9. Ren R, Wang N, Zhang X, Cui T, Jonas JB. Trans-lamina cribrosa pressure difference correlated with neuroretinal rim area in glaucoma. Graefes Arch Clin Exp Ophthalmol. 2011;249(7):1057–63.
10. Wang N, Xie X, Yang D, et al. Orbital cerebrospinal fluid space in glaucoma: The Beijing Intracranial and Intraocular Pressure (iCOP) Study. Ophthalmology. 2012;119(10):2065–73. e2061
11. Yang D, Fu J, Hou R, et al. Optic neuropathy induced by experimentally reduced cerebrospinal fluid pressure in monkeys. *Invest Ophthalmol Vis Sci. 2014*;55(5):3067–73.
12. Quigley HA, Enger C, Katz J, Sommer A, Scott R, Gilbert D. Risk factors for the development of glaucomatous visual field loss in ocular hypertension. Arch Ophthalmol. 1994;112(5):644–9.
13. Guy AH, Wiggs JL, Turalba A, Pasquale LR. Translating the low translaminar Cribrosa pressure gradient hypothesis into the clinical Care of Glaucoma. Semin Ophthalmol. 2016;31(1–2):131–9.
14. Fleischman D, Berdahl JP, Zaydlarova J, Stinnett S, Fautsch MP, Allingham RR. Cerebrospinal fluid pressure decreases with older age. PLoS One. 2012;7(12):e52664.
15. Xie X, Zhang X, Fu J, et al. Noninvasive intracranial pressure estimation by orbital subarachnoid space measurement: the Beijing intracranial and intraocular pressure (iCOP) study. Crit Care. 2013;17(4):R162.
16. Smit M, Werner MJ, Lansink-Hartgring AO, Dieperink W, Zijlstra JG, van Meurs M. How central obesity influences intra-abdominal pressure: a prospective, observational study in cardiothoracic surgical patients. Ann Intensive Care. 2016;6(1):99.
17. Pasquale LR, Willett WC, Rosner BA, Kang JH. Anthropometric measures and their relation to incident primary open-angle glaucoma. Ophthalmology. 2010;117(8):1521–9.
18. Ramdas WD, Wolfs RC, Hofman A, de Jong PT, Vingerling JR, Jansonius NM. Lifestyle and risk of developing open-angle glaucoma: the Rotterdam study. Arch Ophthalmol. 2011;129(6):767–72.
19. Berdahl JP, Fleischman D, Zaydlarova J, Stinnett S, Allingham RR, Fautsch MP. Body mass index has a linear relationship with cerebrospinal fluid pressure. Invest Ophthalmol Vis Sci. 2012;53(3):1422–7.
20. Leske MC, Connell AM, Wu SY, Hyman LG, Schachat AP. Risk factors for open-angle glaucoma. The Barbados Eye Study. Arch Ophthalmol. 1995;113(7):918–24.
21. Killer HE, Jaggi GP, Flammer J, Miller NR, Huber AR, Mironov A. Cerebrospinal fluid dynamics between the intracranial and the subarachnoid space of the optic nerve. Is it always bidirectional? Brain. 2007;130(Pt 2):514–20.
22. Wostyn P, Audenaert K, De Deyn PP. More advanced Alzheimer's disease may be associated with a decrease in cerebrospinal fluid pressure. Cerebrospinal Fluid Res. 2009;6:14.
23. Guo L, Salt TE, Luong V, et al. Targeting amyloid-beta in glaucoma treatment. Proc Natl Acad Sci U S A. 2007;104(33):13444–9.
24. Nucci C, Martucci A, Martorana A, Sancesario GM, Cerulli L. Glaucoma progression associated with altered cerebral spinal fluid levels of amyloid beta and tau proteins. Clin Exp Ophthalmol. 2011;39(3):279–81.
25. Wostyn P, De Groot V, Van Dam D, Audenaert K, De Deyn PP. Senescent changes in cerebrospinal fluid circulatory physiology and their role in the pathogenesis of normal-tension glaucoma. Am J Ophthalmol. 2013;156(1):5–14. e12
26. Wostyn P, De Groot V, Van Dam D, Audenaert K, Killer HE, De Deyn PP. Fast circulation of cerebrospinal fluid: an alternative perspective on the protective role of high intracranial pressure in ocular hypertension. Clin Exp Optom. 2016;99(3):213–8.
27. Furlanetto RL, De Moraes CG, Teng CC, et al. Risk factors for optic disc hemorrhage in the low-pressure glaucoma treatment study. Am J Ophthalmol. 2014;157(5):945–52.
28. Charlson ME, de Moraes CG, Link A, et al. Nocturnal systemic hypotension increases the risk of glaucoma progression. Ophthalmology. 2014;121(10):2004–12.
29. Leske MC, Wu SY, Hennis A, Honkanen R, Nemesure B, Group BES. Risk factors for incident open-angle glaucoma: the Barbados eye studies. Ophthalmology. 2008;115(1):85–93.
30. Leske MC, Heijl A, Hyman L, et al. Predictors of long-term progression in the early manifest glaucoma trial. Ophthalmology. 2007;114(11):1965–72.
31. Tielsch JM, Katz J, Sommer A, Quigley HA, Javitt JC. Hypertension, perfusion pressure, and primary open-angle glaucoma. A population-based assessment. Arch Ophthalmol. 1995;113(2):216–21.
32. Topouzis F, Wilson MR, Harris A, et al. Association of open-angle glaucoma with perfusion pressure status in the Thessaloniki eye study. Am J Ophthalmol. 2013;155(5):843–51.
33. Jonas JB, Wang N, Wang YX, You QS, Yang D, Xu L. Ocular hypertension: general characteristics and estimated cerebrospinal fluid pressure. The Beijing Eye Study 2011. *PLoS One*. 2014;9(7):e100533.
34. Caprioli J, Coleman AL. Blood pressure, perfusion pressure, and glaucoma. Am J Ophthalmol. 2010;149(5):704–12.
35. Bonomi L, Marchini G, Marraffa M, Bernardi P, Morbio R, Varotto A. Vascular risk factors for primary open angle glaucoma: the Egna-Neumarkt study. Ophthalmology. 2000;107(7):1287–93.

36

Correlation Among Intraocular Pressure, Intracranial Pressure, and Blood Pressure

Zhen Li, Dachuan Liu, and Ningli Wang

Glaucoma is the second leading cause of blindness in the world and the main cause of irreversible blindness [1]. The incidence of glaucoma in general population is about 0.21–1.64%. It is estimated that there were about 60.5 million people with glaucoma in 2010 and will increase to 79.6 million by 2020, with primary open-angle glaucoma (POAG) being the main type [2]. Glaucoma signifies a worldwide public health issue rather than just a disease.

Over the past years, many clinical and experimental researches have been conducted to explore the pathogenesis of POAG. Unfortunately, so far we have not gained a comprehensive understanding of the exact pathogenesis of POAG. Mechanical theory that high intraocular pressure (IOP) is the most important risk factor for the occurrence of optic neuropathy in glaucoma is widely accepted [3]. However, intraocular hypertension cannot explain why the normal-tension glaucoma (NTG) patients develop glaucomatous optic neuropathy with normal IOP and why the ocular hypertension patients with chronically elevated IOP do not develop glaucoma optic nerve injury. People recognized that high IOP is not the only risk factor of glaucoma. At the same time, recent studies have begun to focus on the nature of intraocular pressure, that is, the pressure on the wall of the eyeball. What we call "intraocular pressure" is just the trans-corneal pressure difference, the difference between intraocular pressure and atmospheric pressure around the eyeball. For the optic nerve, however, it is not the trans-corneal pressure difference which counts but the trans-lamina cribrosa pressure difference (which is intraocular pressure minus orbital cerebrospinal fluid pressure) [4]. The change in the concept of "intraocular pressure" also requires us to have a new understanding of the traditional mechanical theory of glaucoma.

Because there were certain limitations in the theory of mechanical pressure of glaucoma, especially it cannot explain the pathogenesis of NTG, people began to look for the role of vascular factors in the pathogenesis of glaucoma. Blood pressure (BP) is considered to be an important factor affecting the incidence of glaucoma. Some of clinical studies showed that NTG patients had lower blood pressure, especially nocturnal hypotension.

Researchers considered that it was the decreased ocular perfusion pressure (OPP) that caused the optic nerve ischemia hypoxia changes and then triggering the oxidative stress reaction and further aggravating the injury of optic nerve. NTG patients are more prone to some vasospastic symptoms when compared with the people without glaucoma [5]. In addition, the decrease of local vascular number and vessel diameter in the optic disc was also considered closely related with ischemia and hypoxia injury in glaucomatous optic nerve. These results of clinical researches suggest that vascular factors play an important role in the pathogenesis of NTG, and some scholars even think that vascular factors are the main causes of NTG.

However, the view that the vascular factor is the most important factor in the pathogenesis of glaucoma optic neuropathy has also been challenged by some evidence. First, some epidemiological studies have found that the prevalence of glaucoma in patients with hypertension is higher than that in the general population. Hypertension is considered to be a risk factor for glaucoma. However, high blood pressure brings high perfusion pressure. There is a contradiction between such phenomenon and the vascular theory of glaucoma, which emphasizes the optic nerve ischemia hypoxia injury induced by low perfusion. Second, it was observed in the clinical studies that decreasing intraocular pressure can also stop or slow down the optic nerve damage in patients

Z. Li · D. Liu
Department of Ophthalmology, Xuanwu Hospital, Capital Medical University, Beijing, China

N. Wang (✉)
Beijing Institute of Ophthalmology, Beijing Tongren Eye Center, Beijing Tongren Hospital, Capital Medical University, Beijing, China

Beijing Ophthalmology & Visual Sciences Key Laboratory, Beijing, China
e-mail: wningli@vip.163.com

N. Wang (ed.), *Intraocular and Intracranial Pressure Gradient in Glaucoma*,
Advances in Visual Science and Eye Diseases 1, https://doi.org/10.1007/978-981-13-2137-5_36

with NTG. It indicates that intraocular pressure also has an important role in the pathogenesis of NTG. Then, what is the interaction between intraocular pressure and vascular factors in the pathogenesis of POAG? Third, the high-tension glaucoma and normal-tension glaucoma showed very similar optic disc morphology changes, including the characteristic expanding and deepening of the optic cup, the loss of rim area, the expansion of peripapillary atrophy (beta zone), and retinal nerve fiber layer defects. A study compared the optic disc morphology of glaucoma and some vascular optic neuropathies (including central retinal artery occlusion, central retinal vein occlusion, diabetic optic neuropathy, and anterior ischemic optic neuropathy). With the only exception of anterior ischemic optic neuropathy, all these vascular optic neuropathies did not show the constriction of rim, which keeps its physiological shape despite the loss of retinal ganglion cells and axons and the pale of the optic discs. The remaining rim typically is not pale in glaucomatous optic neuropathy, which is another morphological difference between glaucoma and the vascular optic neuropathies. How do the vascular factors act on the optic nerve and lead to the typical glaucomatous optic disc and surrounding scleral morphological change? These questions cannot be answered by the present POAG vascular abnormal theory, and therefore the new theory of the pathogenesis of glaucoma needs to be further improved.

The mechanism of POAG optic neuropathy is still not very clear. The traditional mechanical theory and ischemia theory cannot fully explain the cause of glaucoma optic nerve damage and are also questioned by some clinical evidence. At present, the only effective way to treat glaucoma is to reduce the intraocular pressure. However, some patients still experience damage of optic nerve and loss of visual field even when the intraocular pressure is well controlled. The questions that plagued clinicians also remind us that there must be some other risk factors besides intraocular pressure in the pathogenesis of glaucoma and some new and effective targets for the treatment of glaucoma should be sought out.

Based on the current understanding of glaucoma, glaucoma has been defined as a kind of optic neuropathy involving multiple factors. In addition to the factors that have been widely recognized, such as high IOP, age, positive family history, and race, some new glaucoma risk factors, such as hypotension, high myopia, thinning of central cornea thickness, diabetes, and low intracranial pressure, have also been drawing more and more extensive attention. These risk factors affect the metabolism of retinal ganglion cells in different ways, and trigger the apoptosis process of retinal ganglion cells, and then lead to typical visual field defects of glaucoma. Since the function and specific mechanism of these risk factors in the occurrence and progression of glaucoma remain unknown, and some even are under dispute, further study on these risk factors will facilitate a comprehensive understanding of pathogenesis of glaucoma.

Among the aforementioned risk factors, age, corneal thickness, myopia status, diabetes, race, and family history are hard to intervene in the current condition, while intraocular pressure, blood pressure, and intracranial pressure are physiological indicators that can be regulated with physical methods, drug intervention or surgery, and other clinical methods.

The lamina cribrosa always bears the brunt of optic nerve damage in glaucoma. Identification of the risk factors of glaucoma optic neuropathy, such as intraocular pressure, intracranial pressure, and blood pressure, is important in the analysis of the anatomical and biomechanical environment around the lamina cribrosa. Three pressures around the lamina cribrosa form a biomechanical system that maintains a balanced dynamic state through autonomic regulation and mutual adjustment between the pressures. When one or several pressure(s) is (are) out of the normal range that the system can withstand or the mechanism by which the pressure can be regulated is disturbed and cannot function, the original balance of the system is broken, which impacts the morphology of the lamina itself and physiological function of important structures through the lamina cribrosa (optic nerve and central retinal artery and vein), and then leads to the corresponding pathological damage, thereby causing diseases such as glaucoma, papilla edema, and central retinal vein block.

This chapter will focus on and expounds intraocular pressure, intracranial pressure, and blood pressure surrounding the lamina cribrosa and their relationship.

The production and maintenance of intraocular pressure, intracranial pressure, and blood pressure are controlled by three liquid circulation systems, which are the aqueous humor circulation system, the cerebrospinal fluid circulation system, and the blood circulation system**.** These three liquid circulation systems have their respective mechanism of production, circulation, and discharge, but at the same time, they are mutually connected and influence each other on the anatomy and function.

In respect of anatomical structure, these three liquid circulation systems meet at lamina cribrosa. The intraocular space is in front of the lamina cribrosa, and the intraocular pressure acts from anterior to posterior on the lamina cribrosa. The optic nerve tissue pressure and cerebrospinal fluid pressure in subarachnoid around optic nerve are behind the lamina cribrosa. Among the two, the optic nerve tissue pressure is relatively constant. The lamina cribrosa is mainly affected by the cerebral spinal fluid pressure from posterior to anterior. Central retinal artery and central retinal vein travel in the center of the optic nerve and into the inner eye space through the lamina cribrosa and supply the inner layers of the retina.

The blood circulation system is the base of all life activities. The continuous blood circulation is driven by the heart and has many important functions, such as transport, buffer, and immune function.

Most liquid in the cerebrospinal fluid circulation and aqueous circulation comes from the blood circulation and goes back to the blood circulation after playing their respective roles. When the blood pressure changes, the blood flow in the ciliary body choroid plexus and the choroid plexus will change, which, consequently, changes the production of aqueous humor and cerebrospinal fluid and then affects IOP and ICP. When intracranial pressure and intraocular pressure change, the body starts its self-adjustment mechanism in order to protect the metabolism and physiological functions of important organs. The function of this mechanism is to maintain the stability of the original pressure environment by changing the blood pressure and the organ blood flow.

It is known that blood circulation is the base of all the liquid circulation in the body. The blood accounts for about 7–8% of the body weight in normal adult or equivalent to 70–80 mL/kg of body weight. The body moisture content is more in children, with the total amount of blood accounting for 9% of the body weight. The formation of arterial blood pressure is dependent on the presence of sufficient blood filling, cardiac ejection, and peripheral resistance in the circulatory system. In the premise of adequate blood volume, in every cardiac cycle, ventricular contraction causes aortic pressure to increase dramatically and reach the highest value in the middle of the contraction. This highest arterial blood pressure is called the systolic blood pressure (SBP). During diastole, aortic pressure decreases and reaches the lowest value at the end of diastolic phase. This lowest arterial blood pressure is called diastolic blood pressure (DBP). In one cardiac cycle, the mean value of arterial blood pressure at each moment, called mean arterial pressure, is approximately equal to DBP + 1/3 (SBP-DBP).

Cerebrospinal fluid is present in the ventricular system of brain and pools around the brain and the subarachnoid space. The total amount of cerebrospinal fluid in adults is about 150 mL. The production of cerebrospinal fluid is about 800 mL every day, five to six times of total cerebrospinal fluid in the body. Nonetheless, at the same time, the same amount of cerebrospinal fluid is absorbed into the blood. It can be seen that the renewal rate of CSF is high. Cerebrospinal fluid is mainly secreted by the choroid plexus in the lateral ventricle, the third and fourth ventricle. Besides that, ependymocytes can also secrete cerebrospinal fluid. A part of liquid filtrated by pial vessels and brain capillary is reabsorbed; the rest flows into the subarachnoid along the perivascular space and becomes cerebrospinal fluid (CSF). The cerebrospinal fluid in the lateral cerebral chamber flows into the third ventricle and then through the aqueduct into the fourth ventricle and at last into the subarachnoid space.

Cerebrospinal fluid is mainly absorbed by arachnoid villi and goes into the blood in the venous sinus. Arachnoid villi have some valve-like microtubules with diameter of 4–12 μm. When the pressure in subarachnoid is higher than in venous sinus, the pipeline opens, and cerebrospinal fluid flows into blood in the venous sinus. When the subarachnoid space pressure is lower than venous sinus pressure, the pipeline closes, and the liquid cannot flow back from the venous sinus to the subarachnoid space. The cerebrospinal fluid pressure depends on the balance between the formation and absorption.

The CSFP is about 1.3 kPa (10 mmHg) in normal adults in decubitus position, and normal range is 0.67–2 kPa (5–15 mmHg). The main function of cerebrospinal fluid is to serve as a buffer and exert protective effect between the brain and the spinal cord, the cranial cavity, and spinal canal. Brain bathes in cerebrospinal fluid, which can reduce the weight of brain to about 50 g owing to the buoyancy effect. In addition, the cerebrospinal fluid also acts as a mediator between the brain and the blood. There is no lymphatic vessel in the brain, and the cerebrospinal fluid partly plays a role of lymphatic drainage.

The stability of intraocular pressure relies on the balance of aqueous formation and elimination. Aqueous humor is produced by the nonpigmented epithelial cells in the ciliary processes, and its formation mainly contains three physiological processes: water and nonelectrolyte in aqueous diffuse from the capillaries from ciliary processes; aqueous salts are formed through ultrafiltration; higher levels of vitamin C, lactic acid, and some amino acids in aqueous than in plasma are generated through the secretion of the ciliary processes. The aqueous humor enters the posterior chamber after production, flows into anterior chamber through the pupil, and then goes into the Schlemm's canal by trabecular meshwork at the anterior chamber angle. Passage of aqueous humor into the Schlemm's canal depends upon cyclic formation of transcellular channels in the endothelial lining. Efferent channels from the Schlemm's canal (about 30 collector channels and 12 aqueous veins) convey the fluid into the venous system. In addition, there is also a small amount of the aqueous drainage through the uveoscleral pathway (10–20%), and about 5% aqueous is absorbed at the surface of crypts of iris. Aqueous humor uveoscleral flow pathway refers to the route that the aqueous passes between the bundles of the ciliary muscle, enters the superciliary cavity and epichoroidal space, and is discharged through the sclera and scleral periscleral vascular nerve gap.

There is about 0.15–0.3 mL aqueous in normal adult; the formation rate of aqueous humor is about 1.5–3μL/min per minute. Aqueous humor can maintain the metabolism of the intraocular tissue, provide the necessary nutrients to maintain

its normal operation, take away the metabolic waste from these tissues, and keep the integrity of the eye structure. Aqueous humor is also an important component of refractive media. The intraocular pressure is mainly determined by three factors: the formation rate of aqueous humor produced by ciliary processes, the resistance of the aqueous outflow at trabecular meshwork, and the pressure in the episcleral venous network. Understanding of blood circulation, cerebrospinal fluid circulation, and aqueous circulation can help us to better understand the formation and influencing factors of blood pressure, intracranial pressure, and intraocular pressure and to facilitate a better understanding of the interaction between these three pressures.

References

1. Resnikoff S, Pascolini D, Etya D, et al. Global data on visual impairment in the year 2002. Bull World Health Organ. 2004;11(82):844–51.
2. Quigley HA. The number of people with glaucoma worldwide in 2010 and 2020. Br J Ophthalmol. 2006;90(3):262–7.
3. Sommer A, Tielsch JM, Katz J, et al. Relationship between intraocular pressure and primary open angle glaucoma among white and black Americans. The baltimore eye survey. Arch Ophthalmol. 1991;109(8):1090–5.
4. Jonas JB. Role of cerebrospinal fluid pressure in the pathogenesis of glaucoma. Acta Ophthalmol. 2011;89(6):505–14.
5. Hulsman CA, Vingerling JR, Hofman A, et al. Blood pressure, arterial stiffness, and open-angle glaucoma: the Rotterdam study. Arch Ophthalmol. 2007;125(6):805–12.

Part VI

Biomechanics of Trans-laminar Cribrosa Pressure Difference

How to Define a Glaucomatous Optic Neuropathy

37

Claude F. Burgoyne

37.1 Introduction

While RGC axonal insult within the ONH is central to glaucomatous vision loss and its manifestations are the source of all current forms of clinical staging (visual field, retinal nerve fiber layer (RNFL) thickness, etc.), we propose that RGC axonal insult is not the pathophysiology that defines the optic neuropathy of glaucoma. In making this statement, we acknowledge the essential need to preserve RGC axons, soma, and their peripheral connections in all glaucoma patients, because preservation of vision is the goal of all glaucoma therapy. However, we also emphasize that, to date, selectively killing RGC soma or axons alone, by whatever mechanism, has not been shown to create a glaucomatous optic neuropathy (i.e., glaucomatous ONH cupping) [1–6]. We propose that the defining pathophysiology of a glaucomatous optic neuropathy is the deformation, remodeling, and mechanical failure of the ONH connective tissues [7]. The primary goal of this report is to explain the importance of including ONH connective tissue processes in characterizing the phenotype of a glaucomatous optic neuropathy in all species.

37.2 ONH Anatomy and Biomechanics (Figs. 37.1, 37.2, and 37.3)

In a series of previous publications [8, 12–16], we have proposed a framework for conceptualizing the optic nerve head (ONH) as a biomechanical structure (Figs. 37.1, 37.2, and 37.3). Figure 37.2a provides a cut-away diagram of IOP-induced mechanical stress in an idealized spherical scleral shell with a circular scleral canal spanned by a more compliant lamina cribrosa. In this case, the majority of the stress generated by IOP/orbital pressure difference is transferred into a hoop stress borne within the thickness of the sclera and lamina and is concentrated circumferentially around the scleral canal. Note in Fig. 37.2b that the pressure behind the lamina is not simply cerebrospinal fluid pressure (CSFp) but is retrolaminar tissue pressure which has been demonstrated to be approximately $0.82 \times CSF + 2.9$ mmHg by Morgan et al. in dogs [17]. The difference between IOP and the retrolaminar tissue pressure is the translaminar pressure difference (Fig. 37.2c), which generates both a net posterior (outward) force on the surface of the lamina and a hydrostatic pressure gradient (the translaminar pressure gradient) within the neural and connective tissues of the prelaminar and laminar regions. Note that the in-plane hoop stress transferred to the lamina from the sclera is much larger than the stresses induced by the translaminar pressure difference.

CSFp directly influences laminar position through its effect on the translaminar pressure difference. CSFp may also effect scleral flange position within the region; it projects onto the sclera, but in most eyes, because the projection of the cerebrospinal fluid (CSF) space is minimal, this is not likely important (the CSF space within Fig. 37.2b, c is greatly expanded due to perfusion fixation). IOP has a similar direct effect on laminar position but has an additional (and potentially more important) effect on laminar position through the pp-sclera. However, while the magnitude of the translaminar pressure difference may be small relative to the stresses within the sclera and lamina, the axons experience it as the translaminar pressure gradient, the steepness of which is influenced by the thickness of the tissues over which it is experienced. The translaminar pressure gradient, as such, may serve as a primary barrier to axon transport and flow within this region and likely is an important physiologic determinant for the ONH axons and cells.

C. F. Burgoyne (✉)
Devers Eye Institute, Optic Nerve Head Research Laboratory, Legacy Research Institute, Portland, OR, USA
e-mail: cfburgoyne@deverseye.org

N. Wang (ed.), *Intraocular and Intracranial Pressure Gradient in Glaucoma*,
Advances in Visual Science and Eye Diseases 1, https://doi.org/10.1007/978-981-13-2137-5_37

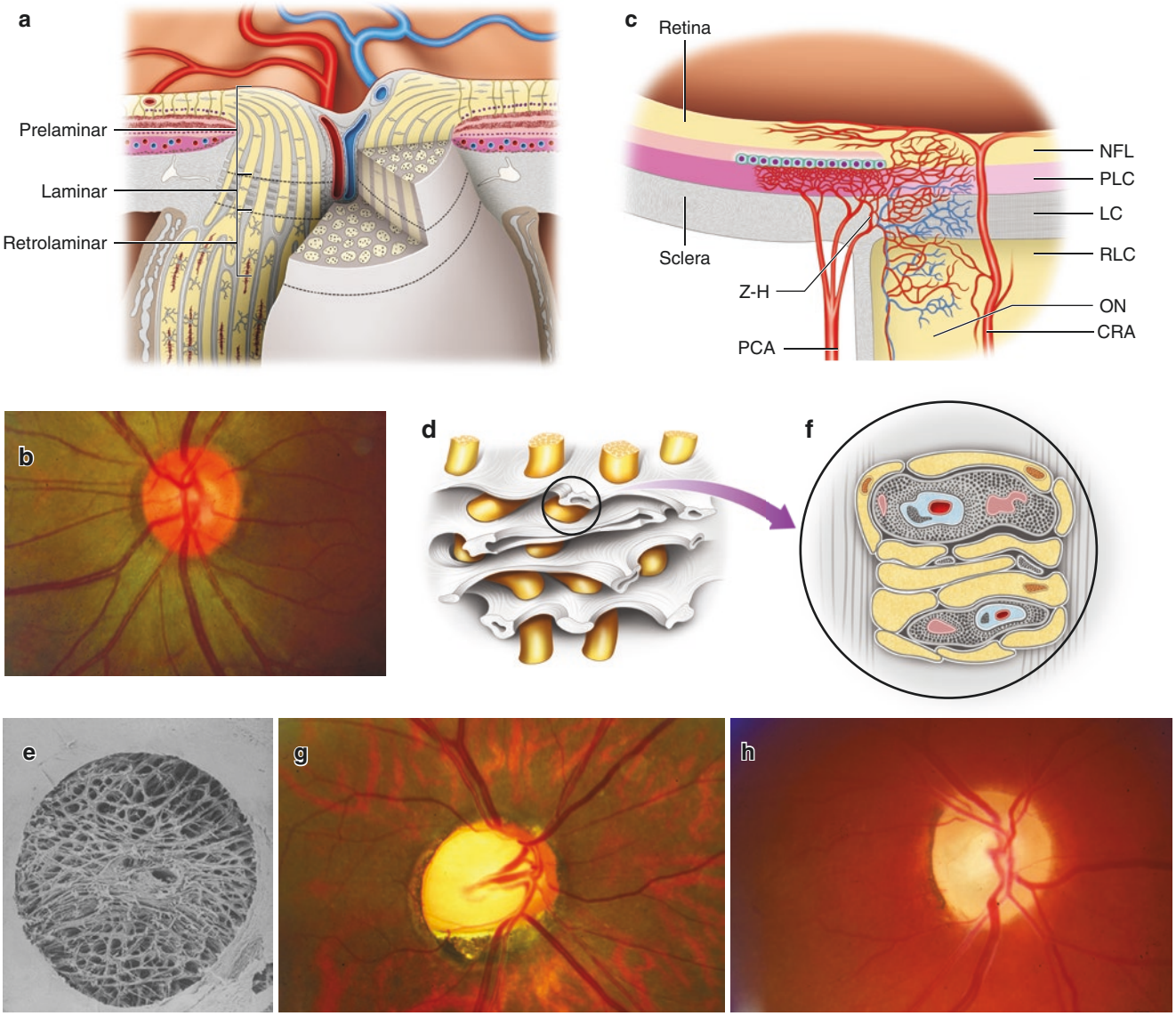

Fig. 37.1 Optic nerve head (ONH) homeostasis is influenced by intraocular pressure (IOP)-related stress and strain at all levels of IOP. (**a**) Prelaminar, laminar, and retrolaminar ONH regions. (**b**) The clinically visible surface of the normal ONH (referred to as the optic disc). Central retinal vessels enter the eye and RGC axons appear pink due to their capillaries. (**c**) The posterior ciliary arteries (PCA) are the principal blood supply to the ONH. (**d**) The lamina cribrosa (LC) is schematically depicted with axon bundles in (**d**), isolated by trypsin digest in a scanning electron micrograph in (**e**) and drawn with stippled extracellular matrix (ECM), central capillary (red), and surrounding astrocytes (yellow with basement membranes in black) (**f**). The clinical manifestation of IOP-induced damage to the ONH is most commonly "deep cupping" (**g**), but in some eyes cupping can be shallower accompanied by pallor (**h**). *Z–H* circle of Zinn–Haller, *PCA* posterior ciliary arteries, *NFL* nerve fiber layer, *PLC* prelaminar region, *LC* lamina cribrosa, *RLC* retrolaminar region, *ON* optic nerve, *CRA* central retinal artery. A - Adapted or reproduced with permission from Arch Ophthalmol.1969;82:800–814. Copyright © (1969) American Medical Association. All rights reserved (Anderson and Hoyt, 1969). B, G, H – Reprinted from J Glaucoma. 2008;17(4):318–28, with permission from Wolters Kluwer Health, Inc. (Burgoyne and Downs, 2008). C - Reprinted courtesy of J. Cioffi and M. Van Buskirk, from The Glaucomas. St. Louis, Mosby: Basic Sciences; 1996:177–197 (Cioffi and Van Buskirk, 1996). D –Reprinted courtesy of Harry Quigley, from Optic Nerve in Glaucoma. Amsterdam: Kugler Publications; 1995:15–36 (Quigley, 1995). E - Adapted or reproduced with permission from Arch Ophthalmol. 1990;108:51–57. Copyright © (1990) American Medical Association. All rights reserved (Morrison et al., 1989). F - Adapted or reproduced with permission from Arch Ophthalmol. 1989;107:123–129. Copyright © (1989) American Medical Association. All rights reserved (Quigley et al., 1990).

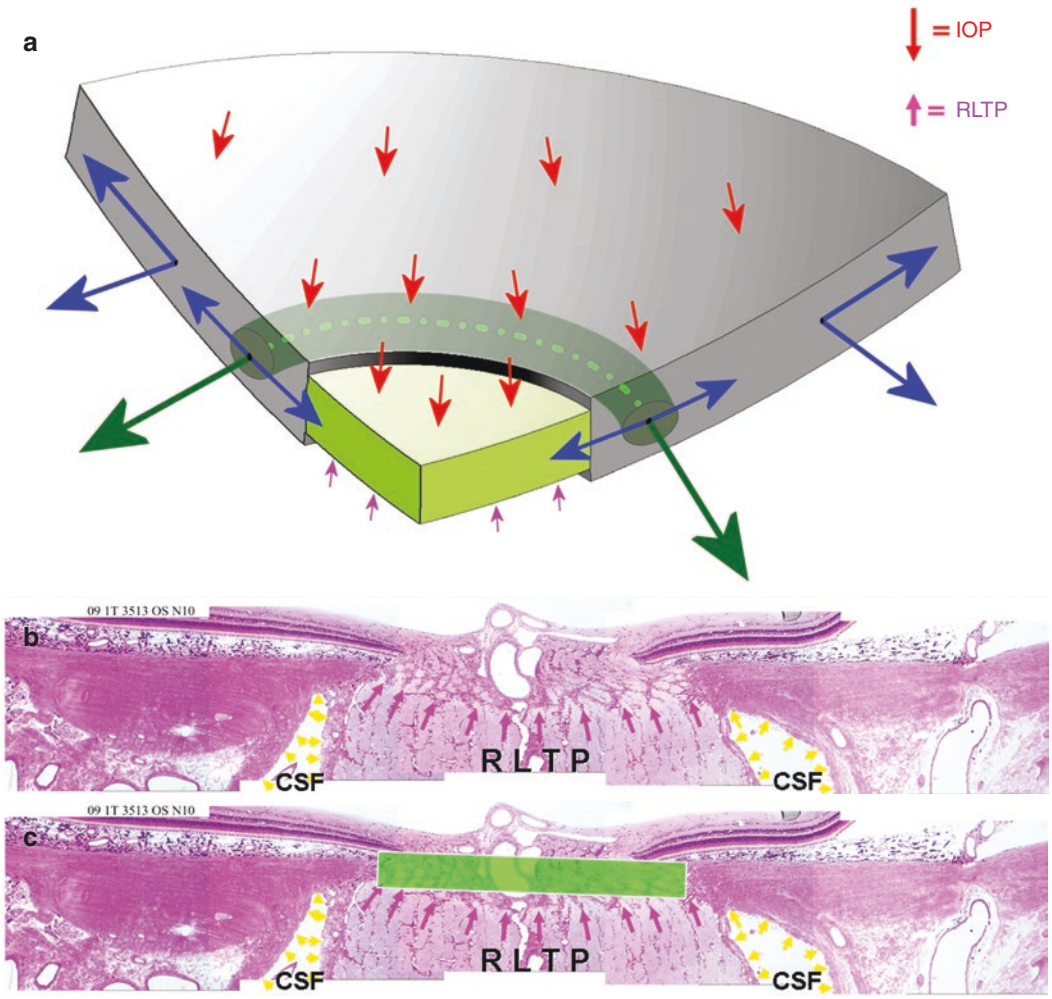

Fig. 37.2 Principal distribution of forces, pressures, and the translaminar pressure gradient within the optic nerve head (ONH). (**a**) Cut-away diagram of intraocular pressure (IOP)-induced mechanical stress in an idealized spherical scleral shell. **Red arrows**, IOP/orbital pressure difference; **green arrows,** peripapillary scleral hoop stress generated by IOP; **blue arrows,** peripapillary tensile stress that is generated by the lamina and delivered to the laminar beams. (**b**) **Pink arrows,** retrolaminar tissue pressure (**RLTP**) which is higher than cerebrospinal fluid pressure (**yellow arrows**). (**c**) The difference between IOP and the retrolaminar tissue pressure is the translaminar pressure difference which generates both a net posterior (outward) force on the surface of the lamina (the red arrows over the lamina) and a hydrostatic pressure gradient (the translaminar pressure gradient—schematically shown in green) within the neural and connective tissues of the prelaminar and laminar regions. Panel **a** (Adapted with permission from Elsevier [11]). Panels **b** and **c** (Reprinted with permission from Elsevier [12])

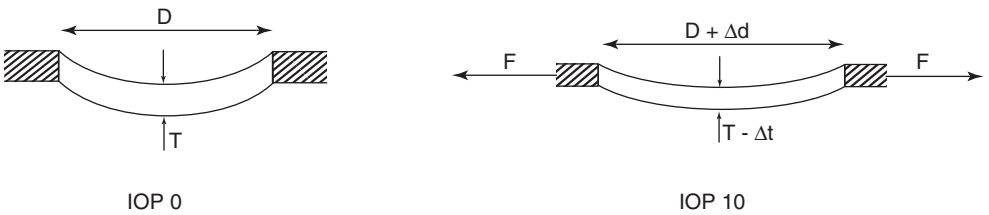

Fig. 37.3 Schematic representation of the laminar/scleral dynamic as experimentally observed in non-pressurized (intraocular pressure (IOP) 0, left) and pressurized (IOP 10, right) monkey control eyes [13]. (**Left**) Thickness (T) of the lamina cribrosa and diameter (D) of the scleral canal opening in an unpressurized (IOP 0) eye. (**Right**) Pressure within the globe generates an expansion of the scleral shell which, in turn, generates (and is resisted by) tensile forces within the sclera. These forces (F) act on the scleral canal wall, causing the scleral canal opening to expand (Ad), which in turn stretches the lamina within the canal. Thus, the lamina is taut (more anteriorly positioned) and thinned (At) in the IOP 10 eye, compared with the IOP 0 eye. Adapted or reproduced with permission from BMJ Publishing Group Ltd. [13]

37.3 The Sclera and Lamina Biomechanically Interact at All Levels of IOP and CSFp (Fig. 37.3)

IOP generates an expansion of the scleral shell, at all levels of IOP, which generates (and is resisted by) tensile forces within the sclera. These forces act on the scleral canal wall, causing the scleral canal opening to expand, which in turn stretches the lamina within the canal. The magnitude of these effects depends upon the level of IOP and the relative structural stiffness of the pp-sclera and lamina, respectively. If the structural stiffness of the sclera is more compliant than the lamina, the lamina will be pulled taut (more anteriorly positioned) and thinned in an eye at IOP 10 compared to the same eye at IOP 0 mmHg. The effects of IOP within the sclera, and the scleral effects on the lamina, are in most models, greater than the direct effects of IOP on the lamina, alone [14, 18–35]. It is important to recognize that CSFp and IOP have fundamentally different effects on the tissues of the ONH because IOP generates profound scleral tensile effects that are delivered to the lamina. CSFp, in most eyes, is not likely to generate similar scleral tensile forces even when it is elevated but particularly when it is low.

37.4 ONH Connective Tissue Deformation, Remodeling, Failed Remodeling, and Mechanical Failure Underlie "Laminar" Cupping (Figs. 37.4 and 37.5)

Early IOP-related damage in the monkey eye (Fig. 37.4) [36–41] includes posterior bowing of the lamina and pp-sclera accompanied by scleral canal expansion, thickening

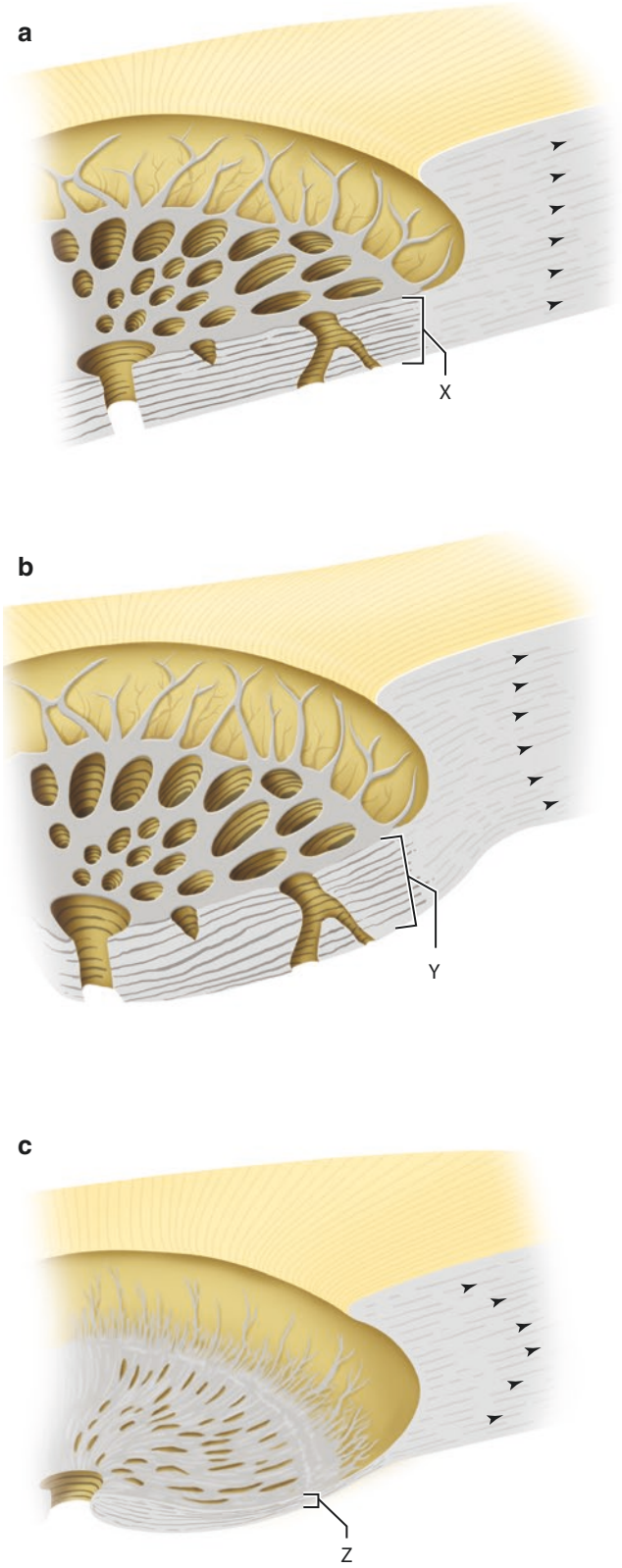

Fig. 37.4 Connective tissue deformation, remodeling, and mechanical failure underlie the "laminar" component of glaucomatous cupping. (**a**) Schematic of normal laminar thickness (*x*) within the scleral canal with scleral tensile forces acting on the scleral canal wall (arrows). (**b**) Early lOP-related damage in the monkey eye includes posterior bowing of the lamina and pp-sclera accompanied by scleral canal expansion (mostly within the posterior (outer) scleral portion), thickening (not thinning) of the lamina (*y*), and outward migration of the laminar insertion from the sclera into the pia mater (not depicted here but seen in Fig. 37.8) (**c**) Progression to end-stage damage is thus along and within the canal wall and includes profound scleral canal wall expansion (clinical excavation) and posterior deformation and thinning of the lamina (*z*)

Reproduced from Yang, H., et al. (2015). "The Connective Tissue Components of Optic Nerve Head Cupping in Monkey Experimental Glaucoma Part 1: Global Change." Invest Ophthalmol Vis Sci 56(13): 7661–7678, with permission from Association for Research in Vision and Ophthalmology (Yang et al., 2015)

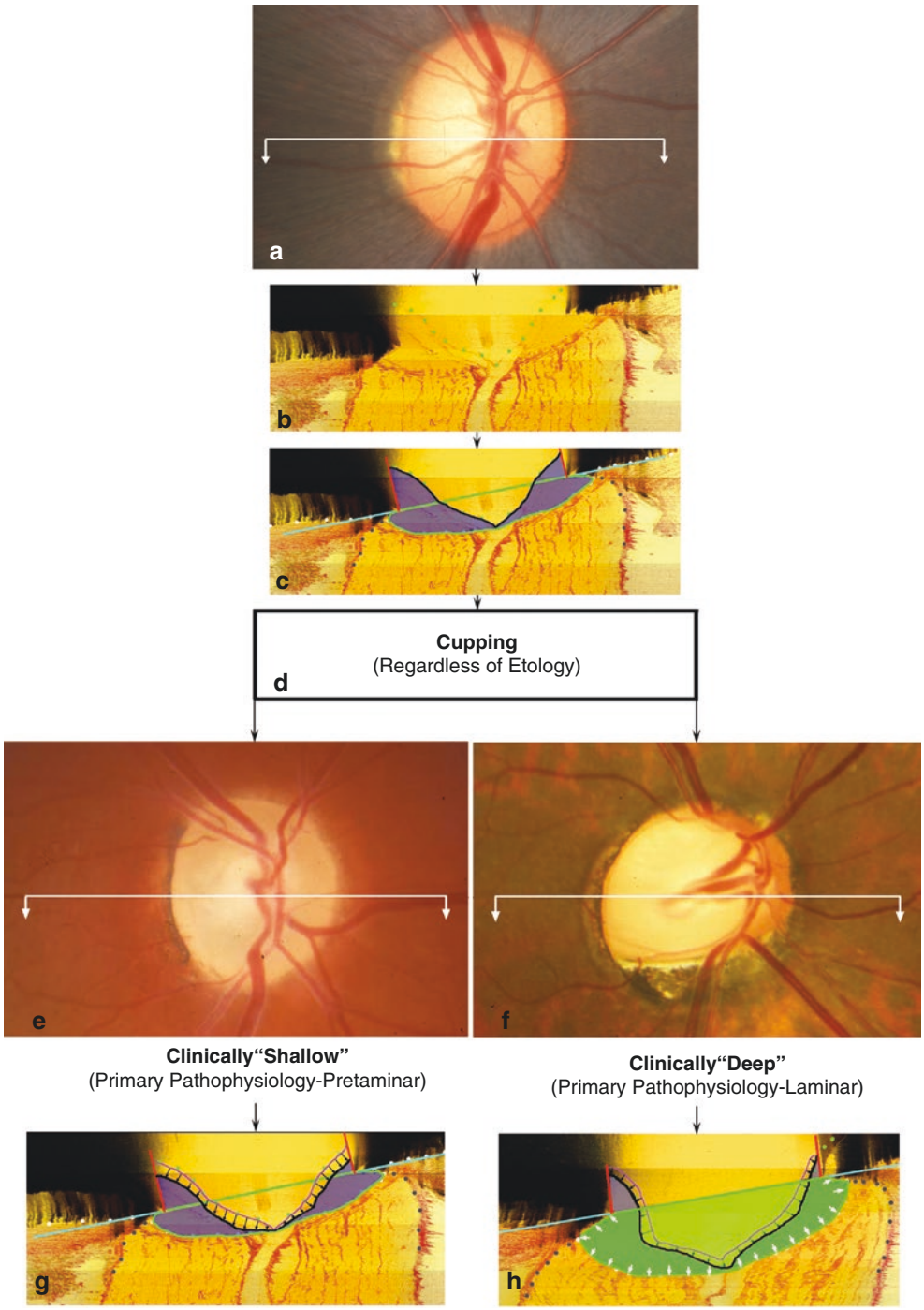

Fig. 37.5 All clinical optic nerve head (ONH) cupping, regardless of etiology, manifests "prelaminar" and "laminar" components. (**a**) Normal ONH. To understand the two pathophysiologic components of clinical cupping, start with (**b**) a representative digital central horizontal section image from a postmortem 3D reconstruction of this same eye (white section line in (**a**))—vitreous top, orbital optic nerve bottom, and lamina cribrosa between the sclera and internal limiting membrane (ILM) delineated with green dots. (**c**) The same section is delineated into principal surfaces and volumes (Black, ILM; purple, prelaminar neural and vascular tissue; cyan blue line, Bruch's membrane opening (BMO) zero reference plane cut in section; green outline, post-BMO total prelaminar area or a measure of the space below BMO and the anterior laminar surface). (**d**) Regardless of the etiology, clinical cupping can be "shallow" (**e**) or "deep" (**f**) (these clinical photos are representative and are not of the eye in (**a**)). A prelaminar, or shallow, form of cupping (**g**, *arrows*) is primarily due to loss of prelaminar neural tissues without important laminar or ONH connective tissue involvement. Laminar or deep cupping (H, small white arrows) follows ONH connective tissue damage and deformation that manifests as expansion of the total area beneath BMO, but above the lamina. Notice in (**h**) that whereas a laminar component of cupping predominates (*white arrows*), there is a prelaminar component as well (*black arrows*). Although prelaminar thinning is a manifestation of neural tissue damage alone, we propose that laminar deformation can occur only in the setting of ONH connective tissue damage followed by permanent (fixed) IOP-induced deformation. Reprinted with permission from the Association for Research in Vision and Ophthalmology [36]

(not thinning) of the lamina, and outward migration of the laminar insertion from the sclera into the pia mater. In our studies to date, this appears to represent mechanical yield (permanent stretching) combined with mechanical failure (physical disruption) of the laminar beams. We propose that while its onset may be diffuse, failure occurs focally within the anterior most laminar beam insertions (into the scleral canal wall and border tissues of Elschnig) and spreads to adjacent beams (both circumferentially and by depth within the canal wall), as the load from failed or disrupted beams is shifted to neighboring beams making them more susceptible to failure. Progression to end-stage damage is likely along and within the canal wall and eventually includes profound scleral canal wall expansion (which underlies the clinical phenomenon of "excavation"), progressive posterior deformation, and eventual thinning of the lamina.

37.5 All Clinical Cupping, Regardless of Etiology, Manifests "Prelaminar" and "Laminar" Components (Fig. 37.5)

Regardless of the etiology, clinical cupping can be "shallow" or "deep" (Fig. 37.5). A prelaminar or "shallow" form of cupping is primarily due to loss (thinning) of prelaminar neural tissues without important laminar or ONH connective tissue involvement. Laminar or "deep" cupping follows ONH connective tissue damage, deformation, and remodeling as schematically depicted in Fig. 37.4. While a laminar component of cupping predominates in a glaucomatous optic neuropathy, it is the prelaminar component that underlies clinical rim thinning. While prelaminar (rim) thinning is a manifestation of neural tissue damage and or "stretching" [42] alone, we propose that "laminar" or "deep" cupping can only occur in the setting of ONH connective tissue deformation and remodeling, regardless of the IOP at which these phenomena occur.

37.6 Connective Tissue Deformation and Remodeling are Unique to the Optic Neuropathy of Glaucoma (Fig. 37.6) and Should be Part of Its Staging (Fig. 37.7)

ONH connective tissue deformation underlies the clinical phenomenon of glaucomatous cupping in the monkey eye (Fig. 37.6). We have identified five morphologically recognizable components of ONH connective tissue alteration in the monkey EG model (Fig. 37.7) [43]: (1) posterior (outward) laminar deformation, (2) scleral canal expansion, (3) posterior (outward) migration of the anterior laminar insertion (ALI) and posterior laminar insertion (PLI) (from the sclera into the pial sheath), (4) laminar thickness change, and (5) posterior (outward) bowing of the pp-sclera. We propose that these five components provide a strategy for morphometrically staging ONH connective tissue change in monkey EG that is independent from the state of RGC axon health. While such a strategy will require careful clinical study, it will lay the scientific foundation for treating certain forms of ONH connective tissue structural abnormality or change as early "structural glaucoma" having determined their power to predict subsequent progression to detectable visual field loss.

37.7 Longitudinal Detection of Laminar Deformation by OCT Precedes Retinal Nerve Fiber Alteration in Monkey Early EG [44]

We previously reported the presence of OCT-detected deep ONH change at the time of confocal scanning laser tomography (CSLT) ONH surface change within the pre-sacrifice OCT data sets of nine rhesus macaque monkeys with chronic, laser-induced, and unilateral IOP elevations [45]. In a follow-up study, both eyes from four young and four old monkeys were tested three times at baseline and then every 2 weeks following laser-induced, chronic unilateral IOP elevation until CSLT-detected ONH surface change was detected and confirmed on two subsequent occasions, at which point each animal was sacrificed. Event- and trend-based definitions of onset in both the control and EG eyes for 11 OCT, CSLT, SLP, and mfERG parameters were explored [44].

For both event- and trend-based analyses, onsets were achieved earliest and most frequently within the ONH neural and connective tissues using OCT. Using event-based analysis, only OCT anterior laminar surface depth relative to BMO reference plane and *rim volume (RimV)* detected change onset in all eight EG eyes. These data demonstrate that detectable deep ONH change precedes detectable RNFL and retinal functional change in the monkey EG model.

37.8 Phenotyping the Optic Neuropathy of Glaucoma in the Monkey and Human Eye Should Include the ONH Connective Tissues (Figs. 37.6, 37.7, and 37.8)

Monkey models for unilateral AION [46, 47], optic nerve transection [3, 48–50] and chronic, optic nerve endothelin exposure [1, 51–53], as well as bilateral optic neuropathy following primary CSFp lowering [6], have been described. Of these, the neuropathies in the AION and optic nerve transection models both demonstrate mild (transection) to profound (AION) disc swelling followed by diffuse pallor without evident "cupping." In a longitudinal OCT study in five unilaterally transected monkeys, we report anterior rather than posterior laminar deformation within weekly post-transec-

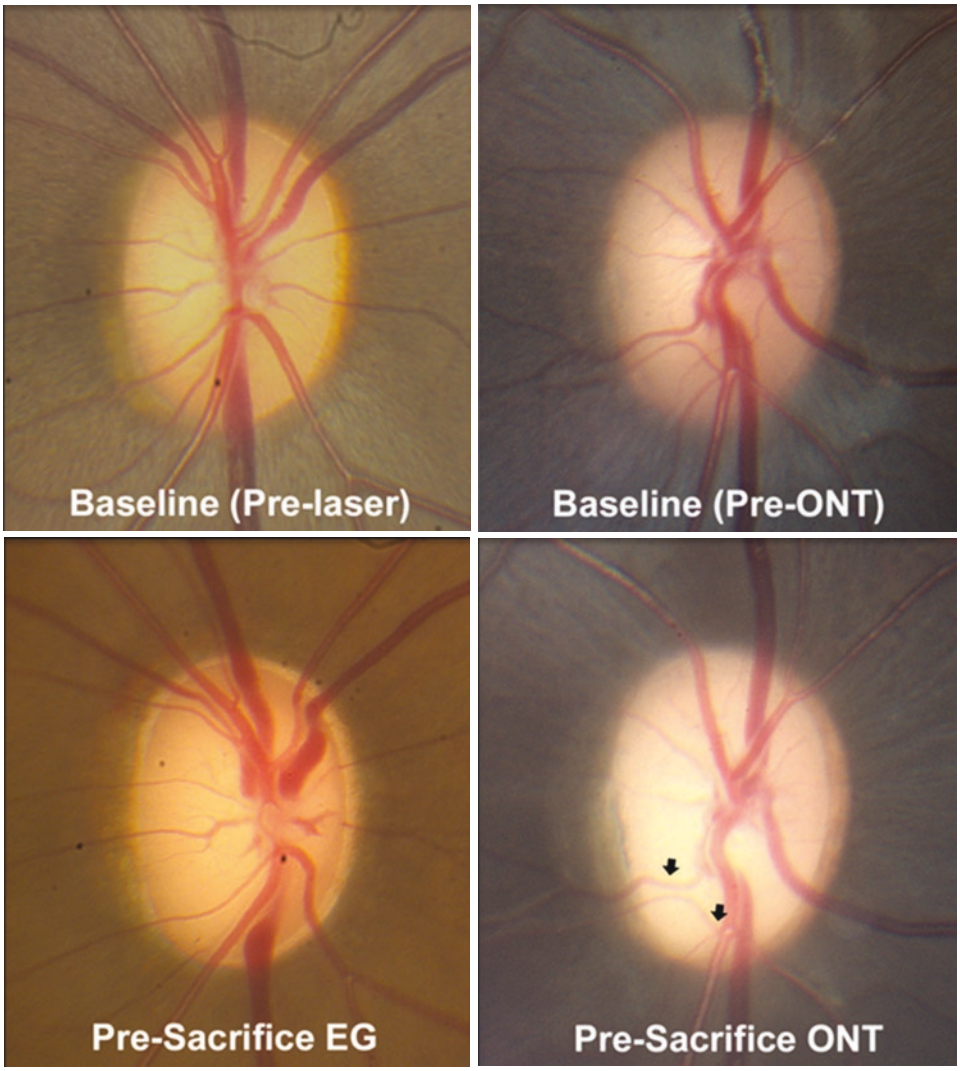

Fig. 37.6 The clinical appearance of cupping in a representative monkey experimental glaucoma (EG, left) and optic nerve transection (ONT) eye [3]. (**Left**) Representative EG eye at baseline prior to laser (above) and near the time of euthanasia (below) from an old (16.1 years of age) animal with 58% axon loss at the time of death. (**Right**) Representative young adult ONT eye (7.8 years old) with 51% axon loss. Both eyes are shown in right eye orientation. In the EG eye (left panels), note the posterior deformation and early excavation of the central retinal artery and veins as they leave the lamina and cross the clinical disc margin. Early "nasalization" of the vessels and "bayoneting" of the inferior vein as well as diffuse loss of the retinal nerve fiber layer (RNFL) striations are also apparent. In the ONT eye (right panels), diffuse pallor and RNFL loss (−41% by OCT) are apparent, as is OCT-detected prelaminar and rim tissue thinning. While the presence of clinical cupping is not obvious, it is suggested by a slight change in the trajectory of the inferior temporal vessels (black arrows). No eye-specific change in anterior lamina cribrosa surface depth was detected by OCT in this eye (see Fig. 37.8). Reprinted with permission from [3], under the CC BY-NC-ND 4.0 license

tion, OCT data sets acquired through the first 60 days post-transection (Fig. 37.8) [3]. However, thinning of the RNFL and prelaminar rim tissue was profound, strongly supporting the concept that "prelaminar" or "shallow" forms of "cupping" can be present in "non-glaucomatous" optic neuropathies, due to prelaminar and rim tissue thinning that is not accompanied by laminar deformation and remodeling.

In the implanted endothelin pump model of unilateral optic nerve vasoconstriction, after preliminary studies in rabbits [54, 55], optic nerve blood flow reduction in monkeys was characterized [51], and localized optic nerve axon loss in the setting of diffuse RNFL loss with shallow cupping was reported in a subset of 12 monkeys [52]. However a follow-up study failed to achieve detectable optic nerve axon loss in the endothelin eyes, and its results were therefore uninterpretable (personal communication from the coprincipal investigators, Jack Cioffi and Claude Burgoyne). In a later study in five rhesus macaques unilaterally implanted with endothelin

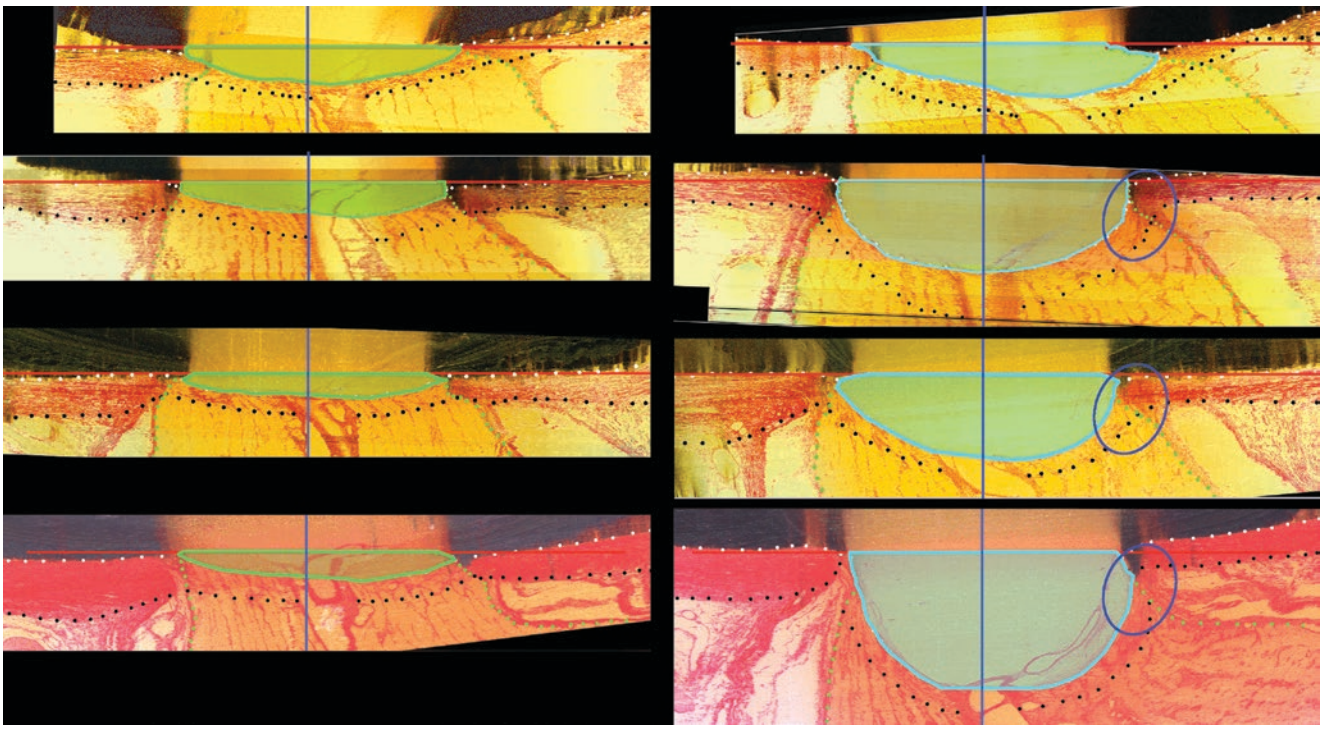

Fig. 37.7 Connective tissue deformation, remodeling, and mechanical failure in the monkey experimental glaucoma (EG) model [15, 43]. Five morphologic phenomena underlie ONH cupping in monkey experimental glaucoma (EG): (1) laminar deformation, (2) scleral canal expansion, (3) laminar insertion migration, (4) laminar thickness change, and (5) posterior bowing of the pp-sclera. The following landmarks are delineated within representative superior temporal (ST) to inferior nasal (IN) digital sections from the control (left) and EG (right) eye of four representative unilateral EG animals (Monkeys 1, 12, 18, and 21, respectively, from the above study): anterior scleral/laminar surface (white dots), posterior scleral/laminar surface (black dots), neural boundary (green dots), BMO reference plane (red line), and BMO centroid (vertical blue line). For each animal, our parameter Post-BMO total prelaminar volume is outlined in both the control (light green, left) and EG (light blue) eyes for qualitative comparison. EG eye *post-BMO total prelaminar volume* expansion is due to the combination of posterior laminar deformation, scleral canal expansion, and outward migration of the anterior laminar insertion. Because it captures three of the five deformation/remodeling phenomena, we use it as a surrogate measure of overall ONH laminar/scleral canal deformation within a given EG eye. *Post-BMO total prelaminar volume* expansion is present within Monkey 1 and progresses through more advanced stages of connective tissue deformation and remodeling (Monkeys 12, 18, and 21). The phenomena that underlie *post-BMO total prelaminar volume* expansion are accompanied by laminar thickening in the EG eyes with the least *post-BMO total prelaminar volume* change (Monkeys 1 and 12), thickening that is progressively diminished in magnitude in eyes with moderate *post-BMO total prelaminar volume* change (Monkey 18), and laminar thinning in the eyes with the largest *post-BMO total prelaminar volume* change (Monkey 21). Outward migration of the laminar insertions from the sclera into the pia is apparent in Monkeys 12, 18, and 21 (blue ovals). Reprinted with permission from Wolters Kluwer Health, Inc. [15]

Fig. 37.8 Representative baseline (left) and pre-euthanasia (right) radial B-scans from the optic nerve transection (ONT) (upper) and control eyes (lower) of five unilateral ONT monkeys [3]**.** Scanning laser ophthalmoscopy image (left) showing radial B-scan location in each eye (green line). Within each baseline and pre-euthanasia radial B-scan, the following landmarks are delineated: internal limiting membrane (ILM, green line); Bruch's membrane opening (BMO) reference plane (red line); and the anterior lamina cribrosa surface (ALCS, yellow dots). ONT eye retinal nerve fiber layer thickness (RNFLT, white arrows) is markedly thinned within the pre-euthanasia compared to the baseline B-scans, while control eye RNFLT remains unchanged in all animals. ONT eye ALCS position relative to the BMO reference plane remains unchanged in M1 and M2 (and moves anteriorly in M3, M4, and M5), while laminar position remains unchanged in all control eyes. Reprinted with permission from [3], under the CC BY-NC-ND 4.0 license

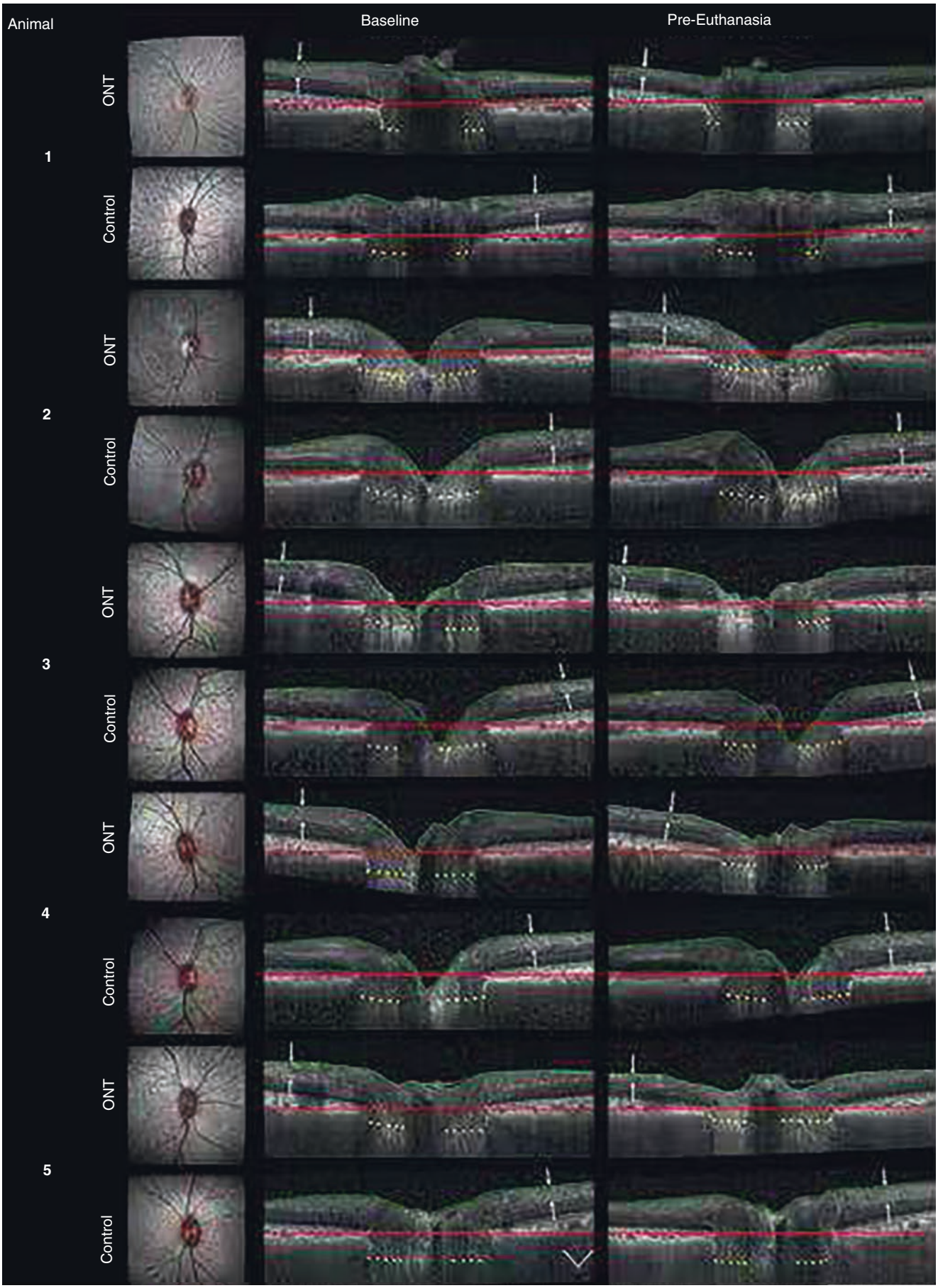
Animal
Baseline
Pre-Euthanasia
1
ONT
Control
2
ONT
Control
3
ONT
Control
4
ONT
Control
5
ONT
Control

pumps and followed for 1.5 years [1], no significant changes in ONH morphology, ONH blood flow velocity, or optic nerve axon counts were detected in the implanted eyes.

Yang and coauthors recently reported diffuse RNFL and optic nerve rim thinning in two of four monkeys following primary surgical CSFp lowering [6]. A third monkey demonstrated a single nerve fiber hemorrhage but no other change. While quantitative assessment was not reported, no qualitative evidence of laminar deformation was present within the published OCT images. Subsequent unpublished quantification has confirmed that there was no OCT-detected laminar deformation within the four studied animals (Personal communication, Ningli Wang). While the appearance of this neuropathy is not glaucomatous by the criteria suggested above, the model is important because it demonstrates that primary CSFp lowering at "normal" levels of IOP is a risk factor for RGC axon loss in a subset of monkey eyes. It therefore also suggests that in a given eye, a relative increase in the translaminar pressure gradient (by whatever cause) may be a risk factor for RGC axon loss at all levels of IOP. However, the fact that primary CSFp lowering in these eyes did not result in laminar deformation and remodeling is also important. It supports the notion that scleral tensile effects on the lamina (Fig. 37.3), even at normal levels of IOP, likely exceed the direct effects of the increased translaminar pressure difference on the lamina that results from CSFp lowering.

37.9 Implications for Phenotyping All Experimental Glaucoma Models

As noted above, there are no experimental models of a glaucomatous optic neuropathy that do not require IOP elevation (i.e., "normal tension glaucoma" models) in the monkey or any other species. Those that have so far been suggested have either presented no characterization of the ONH phenotype [4, 5] or have been shown to possess an ONH phenotype that is non-glaucomatous [1, 6]. Creating a "normal tension glaucoma model" remains an important research target for our field because it will provide insight into how a primary, non-IOP-related insult, such as inflammation [56, 57] or autoimmunity [58], can influence the physiology of the ONH tissues in such a way that the connective tissues become susceptible to deformation and remodeling at "normal levels" of IOP-related stress and strain. The data summarized in this report emphasize the importance of ONH connective tissue deformation and remodeling to the phenotype of glaucoma in the monkey eye. The models of primary CSFp lowering and optic nerve transection, as well as clinical experience with peripheral retinal photocoagulation in humans, tell us that primary insult to the RGC soma and axons outside of the ONH (pan-retinal photocoagulation and optic nerve transection) or within it (CSFp) leads to a pale optic nerve that is non-glaucomatous in appearance and behavior.

37.10 Summary of Core Findings, Concepts, and Predictions

- RGC axonal insult is central to vision loss in glaucoma, but it is not the organizing pathophysiology of ONH aging or the optic neuropathy of glaucoma.
- Optic nerve head connective tissue deformation and remodeling underlie the pathophysiology of a glaucomatous optic neuropathy and should be incorporated into both its staging and phenotyping.
- Primary CSF lowering in the monkey eye kills RGC axons but does not create a glaucomatous form of cupping.

Acknowledgments The text and figures of this manuscript have appeared previously in a Progress in Retinal and Eye Research review of our work: *Yang, H., Reynaud, J., Lockwood, H., Williams, G., Hardin, C., Reyes, L., Stowell, C., Gardiner, S.K., Burgoyne, C.F., 2017. The Connective Tissue Phenotype of Glaucomatous Cupping in the Monkey Eye—Clinical and Research Implications. Prog Retin Eye Re.s Accepted for Publication March, 2017* [7]. They have been used with permission and edited for this chapter. The work reported herein has been supported in part by USPHS grants R01EY011610 (CFB) and R01EY021281 (CFB) from the National Eye Institute, National Institutes of Health, Bethesda, Maryland; a grant from the American Health Assistance Foundation, Rockville, Maryland (CFB); a grant from The Whitaker Foundation, Arlington, Virginia (CFB); a Career Development Award (CFB); The Legacy Good Samaritan Foundation, Portland, Oregon; and the Sears Trust for Biomedical Research, Mexico, Missouri.

References

1. Brooks DE, Kallberg ME, Cannon RL, Komaromy AM, Ollivier FJ, Malakhova OE, Dawson WW, Sherwood MB, Kuekuerichkina EE, Lambrou GN. Functional and structural analysis of the visual system in the rhesus monkey model of optic nerve head ischemia. Invest Ophthalmol Vis Sci. 2004;45:1830–40.
2. Chauhan BC, LeVatte TL, Jollimore CA, Yu PK, Reitsamer HA, Kelly ME, Yu DY, Tremblay F, Archibald ML. Model of endothelin-1-induced chronic optic neuropathy in rat. Invest Ophthalmol Vis Sci. 2004;45:144–52.
3. Ing E, Ivers KM, Yang H, Gardiner SK, Reynaud J, Cull G, Wang L, Burgoyne CF. Cupping in the monkey optic nerve transection model consists of prelaminar tissue thinning in the absence of posterior laminar deformation. Invest Ophthalmol Vis Sci. 2016;57:2598–611.
4. Joachim SC, Reinehr S, Kuehn S, Laspas P, Gramlich OW, Kuehn M, Tischoff I, von Pein HD, Dick HB, Grus FH. Immune response against ocular tissues after immunization with optic nerve antigens in a model of autoimmune glaucoma. Mol Vis. 2013;19:1804–14.
5. Wax MB, Tezel G, Yang J, Peng G, Patil RV, Agarwal N, Sappington RM, Calkins DJ. Induced autoimmunity to heat shock proteins elicits glaucomatous loss of retinal ganglion cell neurons via activated T-cell-derived fas-ligand. J Neurosci. 2008;28:12085–96.

6. Yang D, Fu J, Hou R, Liu K, Jonas JB, Wang H, Chen W, Li Z, Sang J, Zhang Z, Liu S, Cao Y, Xie X, Ren R, Lu Q, Weinreb RN, Wang N. Optic neuropathy induced by experimentally reduced cerebrospinal fluid pressure in monkeys. Invest Ophthalmol Vis Sci. 2014;55:3067–73.
7. Yang H, Reynaud J, Lockwood H, Williams G, Hardin C, Reyes L, Stowell C, Gardiner SK, Burgoyne CF. The connective tissue phenotype of glaucomatous cupping in the monkey eye -clinical and research implications. Prog Retin Eye Res. 2017;59:1–52.
8. Burgoyne CF, Downs JC. Premise and prediction-how optic nerve head biomechanics underlies the susceptibility and clinical behavior of the aged optic nerve head. J Glaucoma. 2008;17:318–28.
9. Jonas JB, Mardin CY, Schlötzer-Schrehardt U, Naumann GO. Morphometry of the human lamina cribrosa surface. Invest Ophthalmol Vis Sci. 1991;32(2):401–5.
10. Shaarawy T, Sherwood MB, Hitchings RA, Crowston JG, editors. Glaucoma. 1st ed. London: W.B. Saunders; 2009.
11. Downs JC, Roberts MD, Burgoyne CF. Mechanical strain and restructuring of the optic nerve head. In: Shaarawy T, Sherwood MB, Hitchings RA, Crowston JG, editors. Glaucoma. 1st ed. London: Saunders; 2009.
12. Burgoyne CF. A biomechanical paradigm for axonal insult within the optic nerve head in aging and glaucoma. Exp Eye Res. 2011;93:120–32.
13. Bellezza AJ, Rintalan CJ, Thompson HW, Downs JC, Hart RT, Burgoyne CF. Anterior scleral canal geometry in pressurised (IOP 10) and non-pressurised (IOP 0) normal monkey eyes. Br J Ophthalmol. 2003a;87:1284–90.
14. Bellezza AJ, Hart RT, Burgoyne CF. The optic nerve head as a biomechanical structure: initial finite element modeling. Invest Ophthalmol Vis Sci. 2000;41:2991–3000.
15. Burgoyne C. The morphological difference between glaucoma and other optic neuropathies. J Neuroophthalmol. 2015;35(Suppl 1):S8–S21.
16. Burgoyne CF, Downs JC, Bellezza AJ, Suh JK, Hart RT. The optic nerve head as a biomechanical structure: a new paradigm for understanding the role of IOP-related stress and strain in the pathophysiology of glaucomatous optic nerve head damage. Prog Retin Eye Res. 2005;24:39–73.
17. Morgan WH, Yu DY, Alder VA, Cringle SJ, Cooper RL, House PH, Constable IJ. The correlation between cerebrospinal fluid pressure and retrolaminar tissue pressure. Invest Ophthalmol Vis Sci. 1998;39:1419–28.
18. Clark AF. The cell and molecular biology of glaucoma: biomechanical factors in glaucoma. Invest Ophthalmol Vis Sci. 2012;53:2473–5.
19. Downs JC. Optic nerve head biomechanics in aging and disease. Exp Eye Res. 2015;133:19–29.
20. Eilaghi A, Flanagan JG, Simmons CA, Ethier CR. Effects of scleral stiffness properties on optic nerve head biomechanics. Ann Biomed Eng. 2010;38:1586–92.
21. Girard MJ, Beotra MR, Chin KS, Sandhu A, Clemo M, Nikita E, Kamal DS, Papadopoulos M, Mari JM, Aung T, Strouthidis NG. In vivo 3-dimensional strain mapping of the optic nerve head following intraocular pressure lowering by trabeculectomy. Ophthalmology. 2016;123(6):1190–200.
22. Girard MJ, Dahlmann-Noor A, Rayapureddi S, Bechara JA, Bertin BM, Jones H, Albon J, Khaw PT, Ethier CR. Quantitative mapping of scleral fiber orientation in normal rat eyes. Invest Ophthalmol Vis Sci. 2011;52:9684–93.
23. Girard MJ, Strouthidis NG, Desjardins A, Mari JM, Ethier CR. In vivo optic nerve head biomechanics: performance testing of a three-dimensional tracking algorithm. J R Soc Interface. 2013;10:20130459.
24. Grytz R, Girkin CA, Libertiaux V, Downs JC. Perspectives on biomechanical growth and remodeling mechanisms in glaucoma. Mech Res Commun. 2012;42:92–106.
25. Lei Y, Rajabi S, Pedrigi RM, Overby DR, Read AT, Ethier CR. In vitro models for glaucoma research: effects of hydrostatic pressure. Invest Ophthalmol Vis Sci. 2011;52:6329–39.
26. Sigal IA, Bilonick RA, Kagemann L, Wollstein G, Ishikawa H, Schuman JS, Grimm JL. The optic nerve head as a robust biomechanical system. Invest Ophthalmol Vis Sci. 2012;53:2658–67.
27. Sigal IA, Ethier CR. Biomechanics of the optic nerve head. Exp Eye Res. 2009;88:799–807.
28. Sigal IA, Flanagan JG, Tertinegg I, Ethier CR. Reconstruction of human optic nerve heads for finite element modeling. Technol Health Care. 2005;13:313–29.
29. Sigal IA, Flanagan JG, Tertinegg I, Ethier CR. Modeling individual-specific human optic nerve head biomechanics. Part I: lOP-induced deformations and influence of geometry. Biomech Model Mechanobiol. 2009a;8:85–98.
30. Sigal IA, Flanagan JG, Tertinegg I, Ethier CR. Modeling individual-specific human optic nerve head biomechanics. Part II: influence of material properties. Biomech Model Mechanobiol. 2009b;8:99–109.
31. Sigal IA, Grimm JL. A few good responses: which mechanical effects of IOP on the ONH to study? Invest Ophthalmol Vis Sci. 2012;53:4270–8.
32. Sigal IA, Grimm JL, Schuman JS, Kagemann L, Ishikawa H, Wollstein G. A method to estimate biomechanics and mechanical properties of optic nerve head tissues from parameters measurable using optical coherence tomography. IEEE Trans Med Imaging. 2014;33:1381–9.
33. Stewart PS, Jensen OE, Foss AJ. A theoretical model to allow prediction of the CSF pressure from observations of the retinal venous pulse. Invest Ophthalmol Vis Sci. 2014;55:6319–23.
34. Wang X, Rumpel H, Lim WE, Baskaran M, Perera SA, Nongpiur ME, Aung T, Milea D, Girard MJ. Finite element analysis predicts large optic nerve head strains during horizontal eye movements. Invest Ophthalmol Vis Sci. 2016;57:2452–62.
35. Zhang L, Albon J, Jones H, Gouget CL, Ethier CR, Goh JC, Girard MJ. Collagen microstructural factors influencing optic nerve head biomechanics. Invest Ophthalmol Vis Sci. 2015;56:2031–42.
36. Yang H, Downs JC, Bellezza A, Thompson H, Burgoyne CF. 3-D histomorphometry of the normal and early glaucomatous monkey optic nerve head: prelaminar neural tissues and cupping. Invest Ophthalmol Vis Sci. 2007a;48:5068–84.
37. Bellezza AJ, Rintalan CJ, Thompson HW, Downs JC, Hart RT, Burgoyne CF. Deformation of the lamina cribrosa and anterior scleral canal wall in early experimental glaucoma. Invest Ophthalmol Vis Sci. 2003b;44:623–37.
38. Burgoyne CF, Downs JC, Bellezza AJ, Hart RT. Three-dimensional reconstruction of normal and early glaucoma monkey optic nerve head connective tissues. Invest Ophthalmol Vis Sci. 2004;45:4388–99.
39. Downs JC, Suh JK, Thomas KA, Bellezza AJ, Hart RT, Burgoyne CF. Viscoelastic material properties of the peripapillary sclera in normal and early-glaucoma monkey eyes. Invest Ophthalmol Vis Sci. 2005;46:540–6.
40. Downs JC, Yang H, Girkin C, Sakata L, Bellezza A, Thompson H, Burgoyne CF. Three-dimensional histomorphometry of the normal and early glaucomatous monkey optic nerve head: neural canal and subarachnoid space architecture. Invest Ophthalmol Vis Sci. 2007;48:3195–208.
41. Yang H, Downs JC, Girkin C, Sakata L, Bellezza A, Thompson H, Burgoyne CF. 3-D histomorphometry of the normal and early glaucomatous monkey optic nerve head: lamina cribrosa and peripapillary scleral position and thickness. Invest Ophthalmol Vis Sci. 2007b;48:4597–607.
42. Fortune B, Reynaud J, Hardin C, Wang L, Sigal IA, Burgoyne CF. Experimental glaucoma causes optic nerve head neural rim tissue compression: a potentially important mechanism of axon injury. Invest Ophthalmol Vis Sci. 2016;57:4403–11.

43. Yang H, Ren R, Lockwood H, Williams G, Libertiaux V, Downs C, Gardiner SK, Burgoyne CF. The connective tissue components of optic nerve head cupping in monkey experimental glaucoma part 1: global change. Invest Ophthalmol Vis Sci. 2015;56:7661–78.
44. He L, Yang H, Gardiner SK, Williams G, Hardin C, Strouthidis NG, Fortune B, Burgoyne CF. Longitudinal detection of optic nerve head changes by spectral domain optical coherence tomography in early experimental glaucoma. Invest Ophthalmol Vis Sci. 2014;55:574–86.
45. Strouthidis NG, Fortune B, Yang H, Sigal IA, Burgoyne CF. Longitudinal change detected by spectral domain optical coherence tomography in the optic nerve head and peripapillary retina in experimental glaucoma. Invest Ophthalmol Vis Sci. 2011;52:1206–19.
46. Chen CS, Johnson MA, Flower RA, Slater BJ, Miller NR, Bernstein SL. A primate model of nonarteritic anterior ischemic optic neuropathy. Invest Ophthalmol Vis Sci. 2008;49:2985–92.
47. Miller NR, Johnson MA, Nolan T, Guo Y, Bernstein AM, Bernstein SL. Sustained neuroprotection from a single intravitreal injection of PGJ(2) in a nonhuman primate model of nonarteritic anterior ischemic optic neuropathy. Invest Ophthalmol Vis Sci. 2014;55:7047–56.
48. Burgoyne CF, Quigley HA, Thompson HW, Vitale S, Varma R. Early changes in optic disc compliance and surface position in experimental glaucoma. Ophthalmology. 1995;102:1800–9.
49. Morrison JC, Dorman-Pease ME, Dunkelberger GR, Quigley HA. Optic nerve head extracellular matrix in primary optic atrophy and experimental glaucoma. Arch Ophthalmol. 1990;108:1020–4.
50. Quigley HA, Anderson DR. The histologic basis of optic disk pallor in experimental optic atrophy. Am J Ophthalmol. 1977;83:709–17.
51. Cioffi GA, Sullivan P. The effect of chronic ischemia on the primate optic nerve. Eur J Ophthalmol. 1999;9(Suppl 1):S34–6.
52. Cioffi GA, Wang L, Fortune B, Cull G, Dong J, Bui B, Van Buskirk EM. Chronic ischemia induces regional axonal damage in experimental primate optic neuropathy. Arch Ophthalmol. 2004;122:1517–25.
53. Orgul S, Cioffi GA, Bacon DR, Van Buskirk EM. An endothelin-1-induced model of chronic optic nerve ischemia in rhesus monkeys. J Glaucoma. 1996a;5:135–8.
54. Cioffi GA, Orgul S, Onda E, Bacon DR, Van Buskirk EM. An in vivo model of chronic optic nerve ischemia: the dose-dependent effects of endothelin-1 on the optic nerve microvasculature. Curr Eye Res. 1995;14:1147–53.
55. Orgul S, Cioffi GA, Wilson DJ, Bacon DR, Van Buskirk EM. An endothelin-1 induced model of optic nerve ischemia in the rabbit. Invest Ophthalmol Vis Sci. 1996b;37:1860–9.
56. Tezel G, Wax MB. The immune system and glaucoma. Curr Opin Ophthalmol. 2004;15:80–4.
57. Tezel G, Yang X, Luo C, Cai J, Powell DW. An astrocyte-specific proteomic approach to inflammatory responses in experimental rat glaucoma. Invest Ophthalmol Vis Sci. 2012;53:4220–33.
58. Grus FH, Joachim SC, Wuenschig D, Rieck J, Pfeiffer N. Autoimmunity and glaucoma. J Glaucoma. 2008;17:79–84.

Pressure Difference and Ocular Morphology Change, From Biomechanical Analysis

38

Xiaoyu Liu and Yubo Fan

The most important structure of the cornea is stroma, which has layer tissue and consists of 200 stromal lamella constructed by parallel collagen fibrils (Fig. 38.1).

Collagen fibrils in the stroma are typically in an ordered arrangement to keep the cornea transparent. However, when the cornea suffers from disease or injury, the layers will show a disordered arrangement, leading to opacity in the cornea (Fig. 38.2).

Figure 38.3 demonstrates the mechanical model of the cornea under IOPs. Using the mathematical formula, we can build the relation between IOP and stress on the cornea.

The collagen fibril morphology revealed that the fibrils in the load-free state present a wave shape, which becomes smaller and straighter with the increase of the stress and finally turns into a disorderly arrangement when the cornea is under high stress.

As demonstrated above, the structure of the cornea varies under different stress states. When the cornea suffers disease or injury, the stress distribution will become complex and difficult to describe. Digital image correlation (DIC) technology was then used to obtain full-field corneal strain. Firstly, ran-

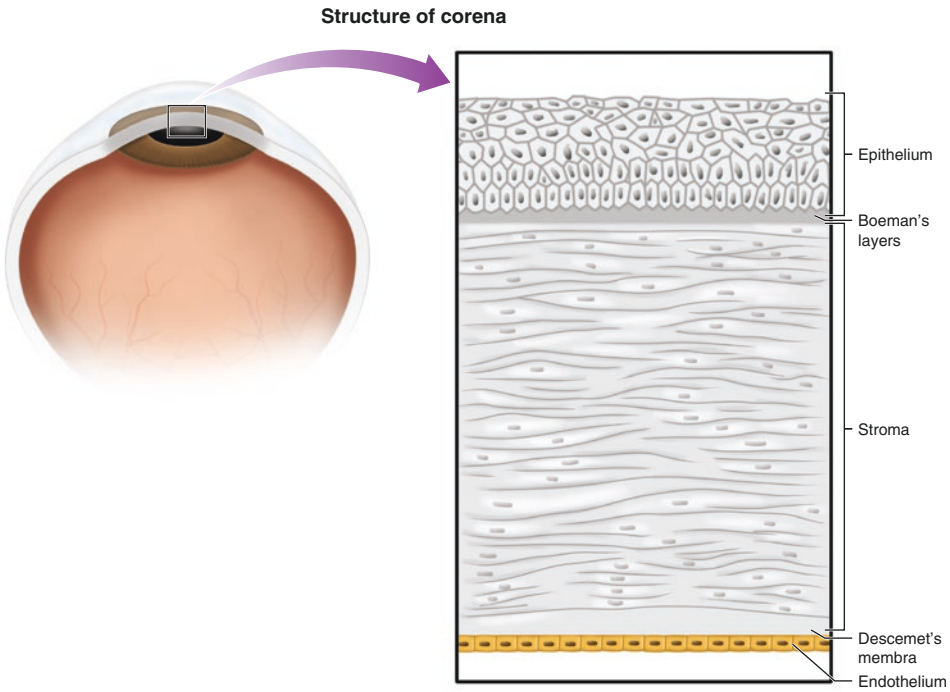

Fig. 38.1 The structure of the cornea

X. Liu · Y. Fan (✉)
Key Laboratory for Biomechanics and Mechanobiology of Ministry of Education, School of Biological Science, and Medical Engineering, Beijing Advanced Innovation Centre for Biomedical Engineering, Beihang University, Beijing, China
e-mail: yubofan@buaa.edu.cn

N. Wang (ed.), *Intraocular and Intracranial Pressure Gradient in Glaucoma*,
Advances in Visual Science and Eye Diseases 1, https://doi.org/10.1007/978-981-13-2137-5_38

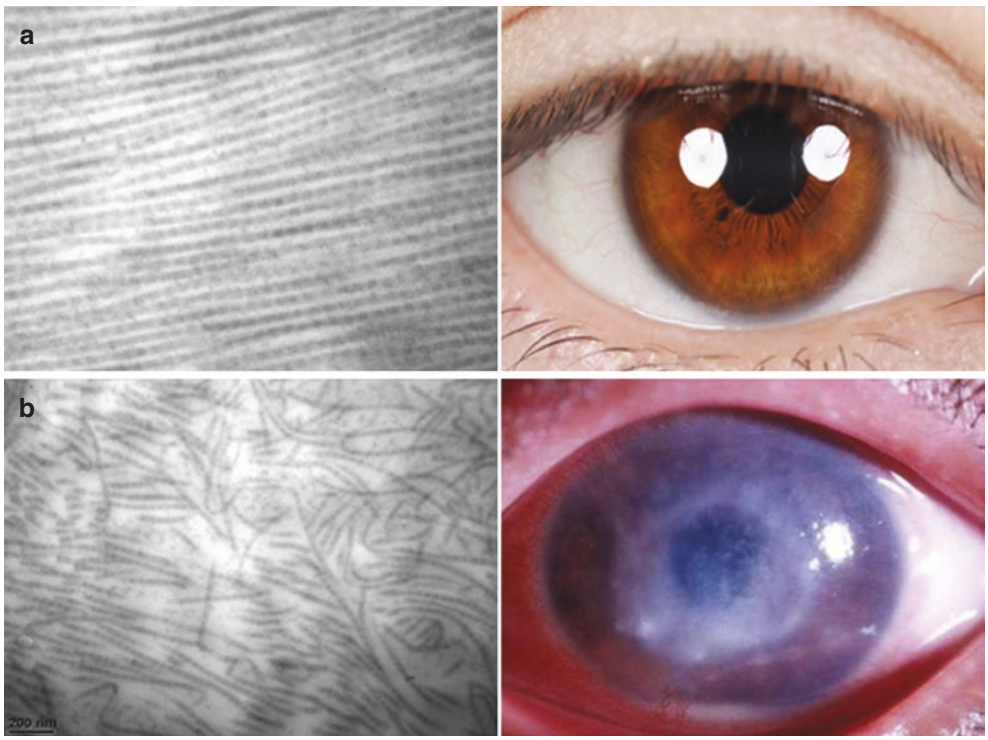

Fig. 38.2 The disordered arrangement of collagen fibrils leads to corneal opacity. (**a**) The organized arrangement of collagen fibrils in the stroma, contributing to transparency of the cornea. (**b**) The disordered arrangement of collagen fibrils in the stroma, leading to the optical opacity

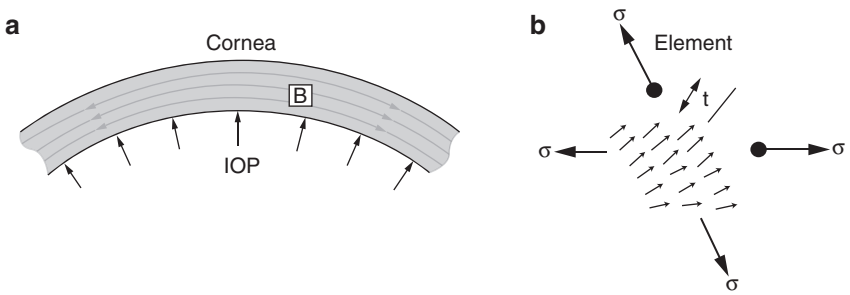

Fig. 38.3 The state of force balance on the cornea. (**a**) The extension state of the cornea under a normal IOP. (**b**) The stress state of the corneal element

dom speckles of cornea were made to produce the image, which was then used to track the points to obtain the points and zone track of cornea under different IOPs (Fig. 38.4).

In this experiment, the injection pump and transducer were employed to control the IOP, and DIC was used to obtain the full-field strain measurement. And the picture shows our instrument working under different pressure patterns including volume loading, volume cycling, pressure loading, and pressure cycling.

Figure 38.5 demonstrates the variation of full-field corneal strain under different IOPs. We found that in abnormal cornea, the distribution of the stress varied obvious in the local area with abnormalities, which can be used to predict the morphological changes of collagen fiber under various mechanical states.

The second work is associated with IOP and retinal detachment.

Retinal detachment caused by trauma accounts for 10% of total cases with retinal detachment. The onset of retinal detachment needs two conditions: (1) retinal break and (2) liquid vitreous passing through the break into the subretinal space (Fig. 38.6). The aim of our work was to investigate how the force caused retinal detachment.

The experiment was designed as the following procedures: In the first step, a dynamic pressure transducer was inserted into a porcine eye which was then put into the 3D printing orbit; gel was used simulating the fat to fill the middle yellow space; and then a computer was used to record the dynamic IOP changes and a pump injection to accurately produce the desired IOP (Fig. 38.7). The eyeball sample was placed into a 3D-printed orbit model. The space between the eyeball and the orbit model was filled with gel (Fig. 38.8).

A negative pressure was measured under the normal IOP and the standard atmosphere. The transient pressure under blunt impact was found to be highly correlated to the IOP, which means the IOP is increased with the force of impact.

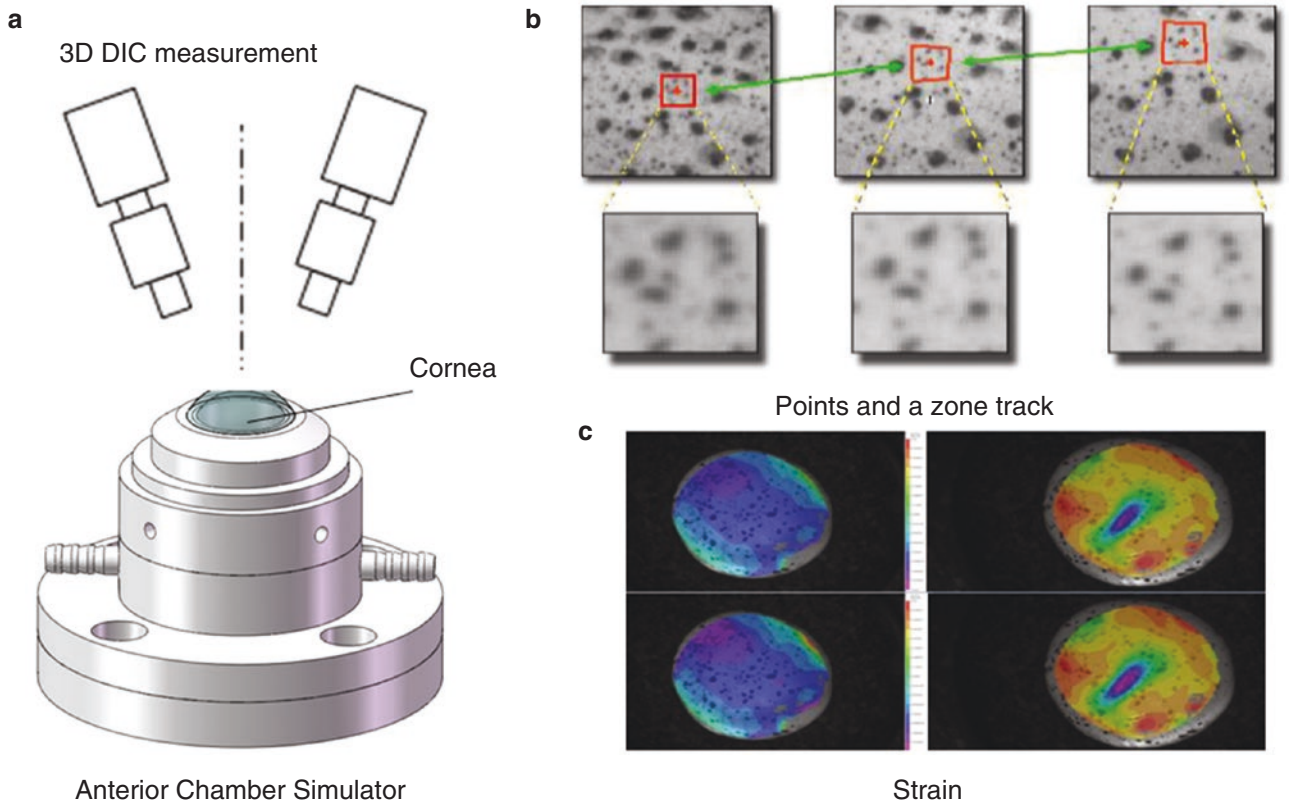

Fig. 38.4 Digital image correlation (DIC) technology for corneal stress distribution. (**a**) A measuring system for assessing the corneal strain in the inflation test. (**b**) The track of points in a zone for the calculation of the strain. (**c**) The measured strains in different corneal samples

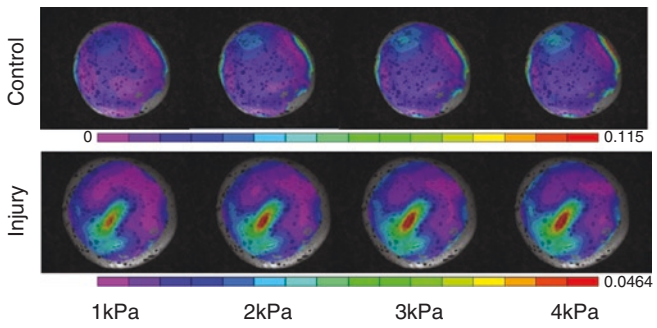

Fig. 38.5 The variation of full-field corneal strain under different IOPs

As has been known that transient positive pressure can cause the damage, so what about the negative pressures? It was believed to be associated with the peel of the retina.

Measurement of the transient pressure under blunt impact revealed its great variation (Figs. 38.8 and 38.9). The negative pressure would peel the retina away from the normal position. We conduct an experiment to study the correlation between retinal detachment and pressure difference (Fig. 38.10).

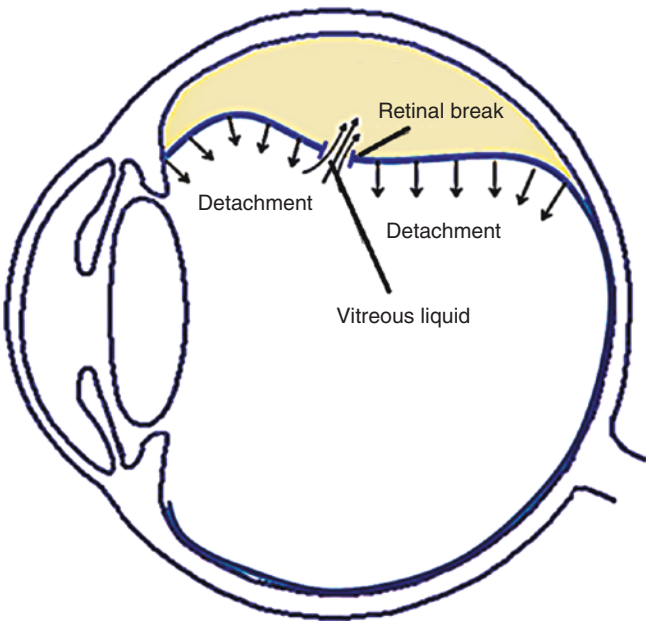

Fig. 38.6 The conditions for retinal detachment

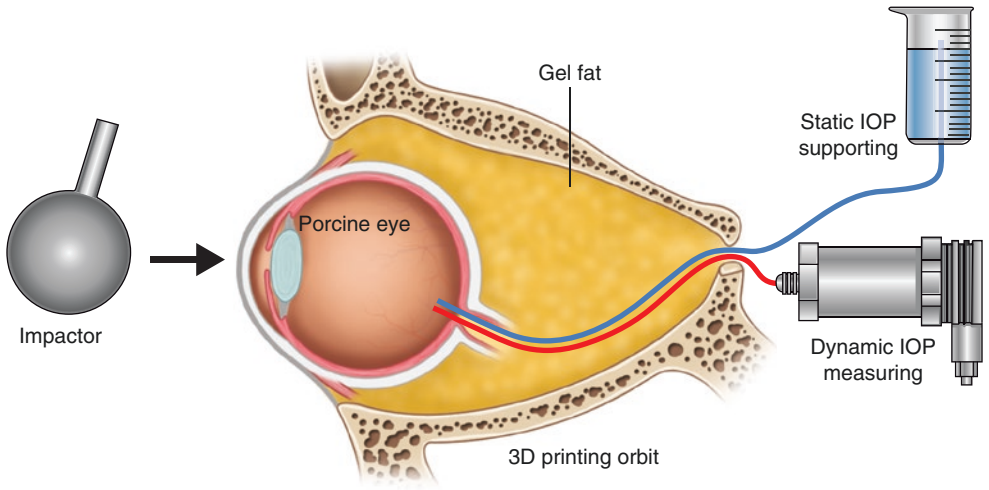

Fig. 38.7 Experimental test for dynamic IOP under blunt impact

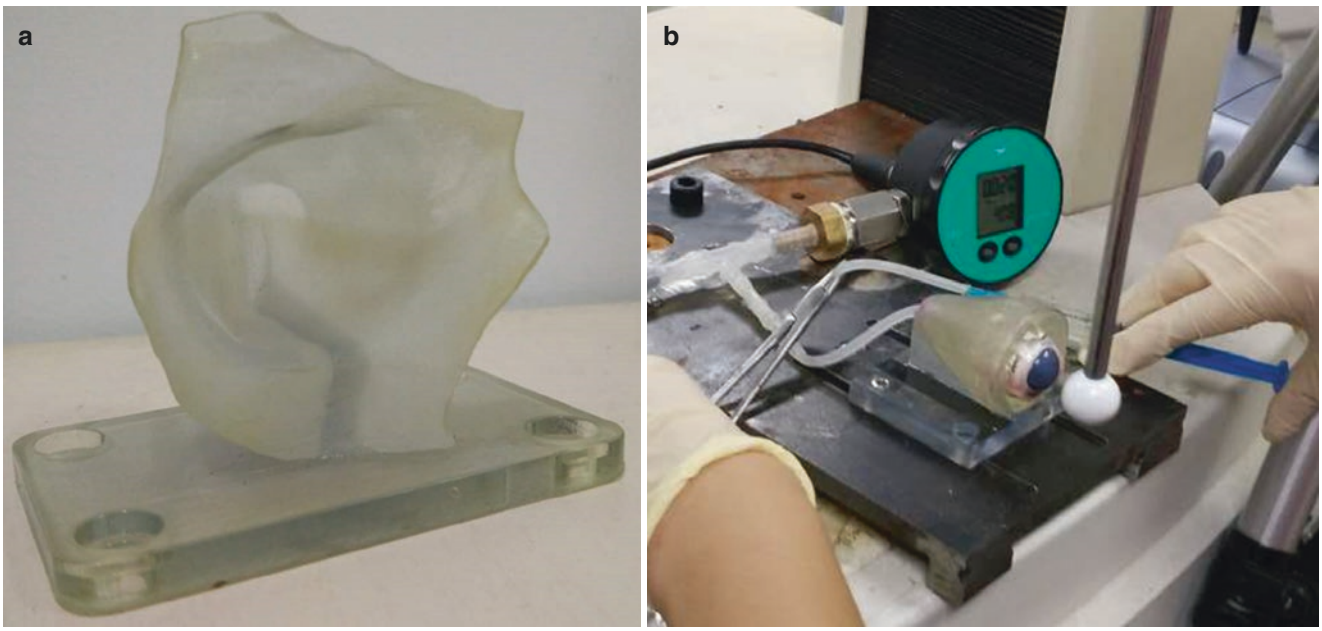

Fig. 38.8 (**a**) a 3D-printed orbit model. (**b**) a setup of the impact test for retinal detachment

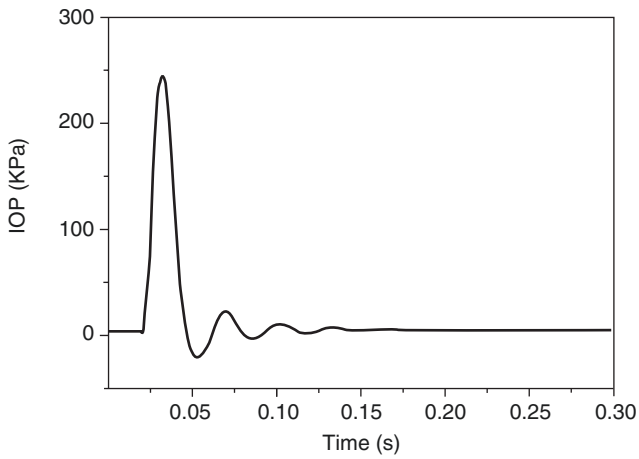

Fig. 38.9 The dynamic pressure during blunt impact

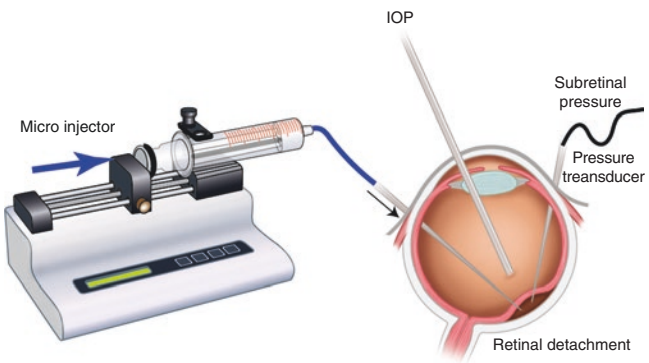

Fig. 38.10 Experimental test for pressure peeling the retina from supporting tissue

The pressure measured at the moment when the bulb suddenly exploded was defined as the pressure causing detachment of the retina (Figs. 38.11 and 38.12).

1. When the pressure increases to a level to damage the retinal adhesion, the retina will be peeled away from the supporting tissues.
2. The average pressure for retina separation is 860 ± 78 Pa.

In order to obtain an accurate measurement of the pressure, we built a finite element model of human eye (Fig. 38.13).

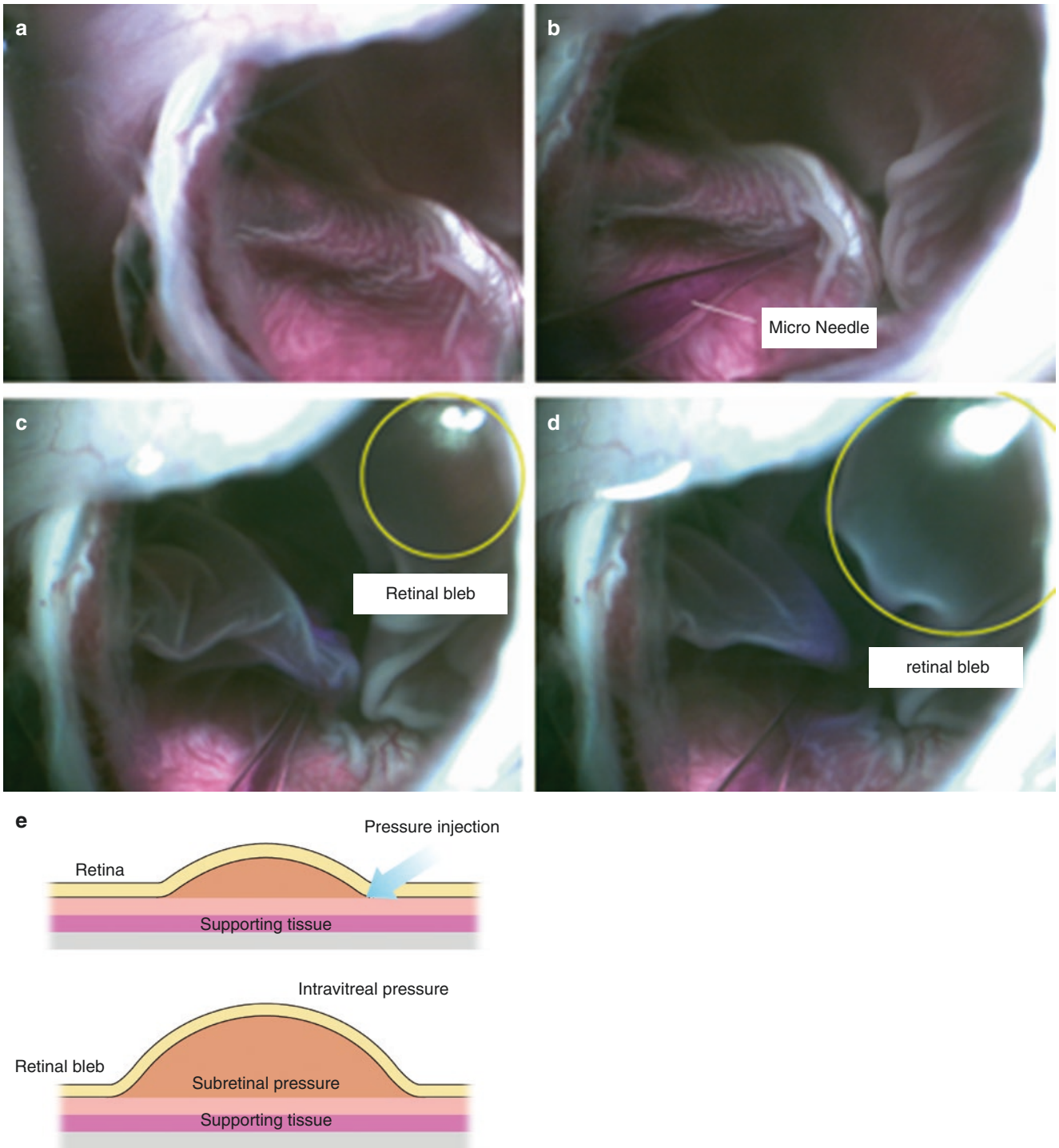

Fig. 38.11 Model and measurement: pressure for retinal detachment. (**a**) The retina tissue under microscope. (**b**) A micro needle was used to insert into the subretinal space. (**c**) A retinal bubble was made by the injection. (**d**) The diameter of the retinal bubble reach a maximum. (**e**) Schematic description of the bubble-make experiment

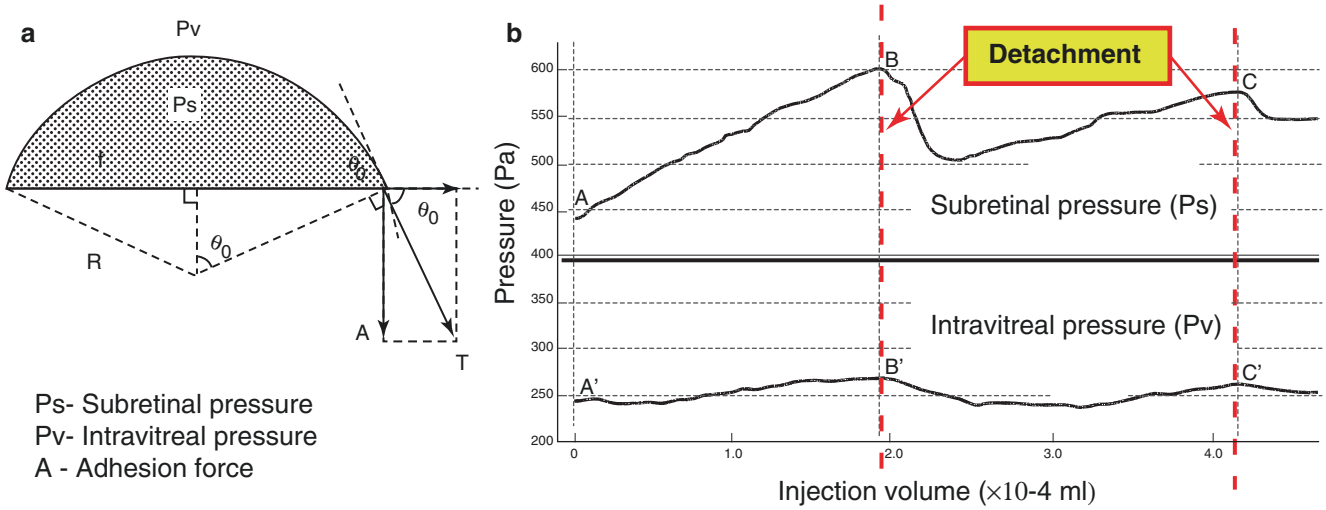

Fig. 38.12 Pressure for retina separating from the supporting tissue. (**a**) Diagram showing the calculation of the retinal adhesive force. (**b**) The pressure variation with the injection volume

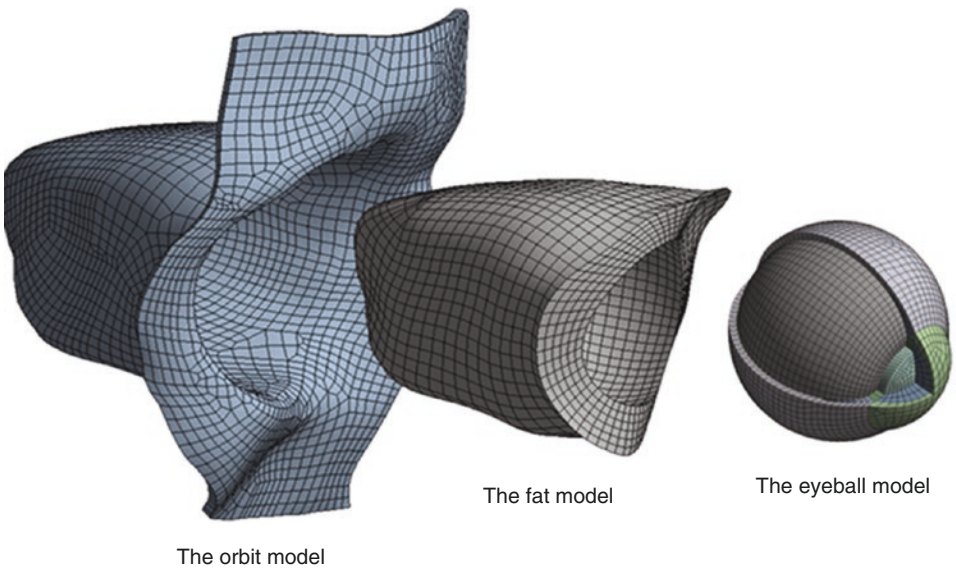

Fig. 38.13 A finite element model of a human eye

We conducted a finite element simulation to investigate the pressure variation in retinal detachment under blunt impact (Fig. 38.14).

A negative pressure was measured at the area of retinal detachment, which was believed to be an important factor for retinal detachment caused by blunt impact.

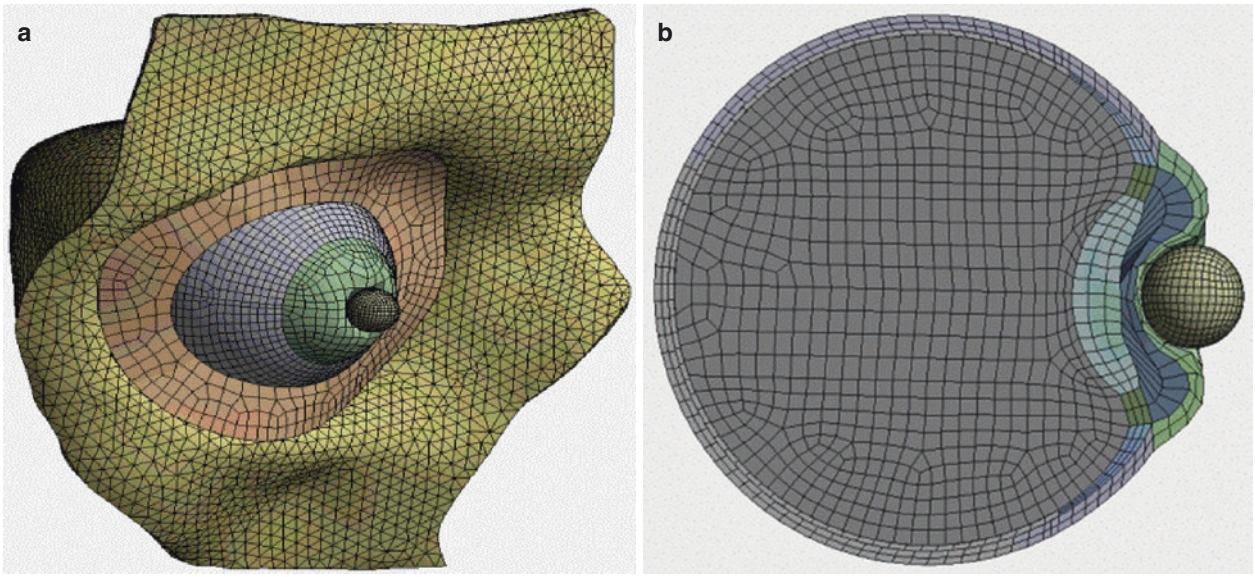

Fig. 38.14 The dynamic responses under blunt eye trauma. (**a**) A full finite element eye model. (**b**) A ball is impacting the eye model

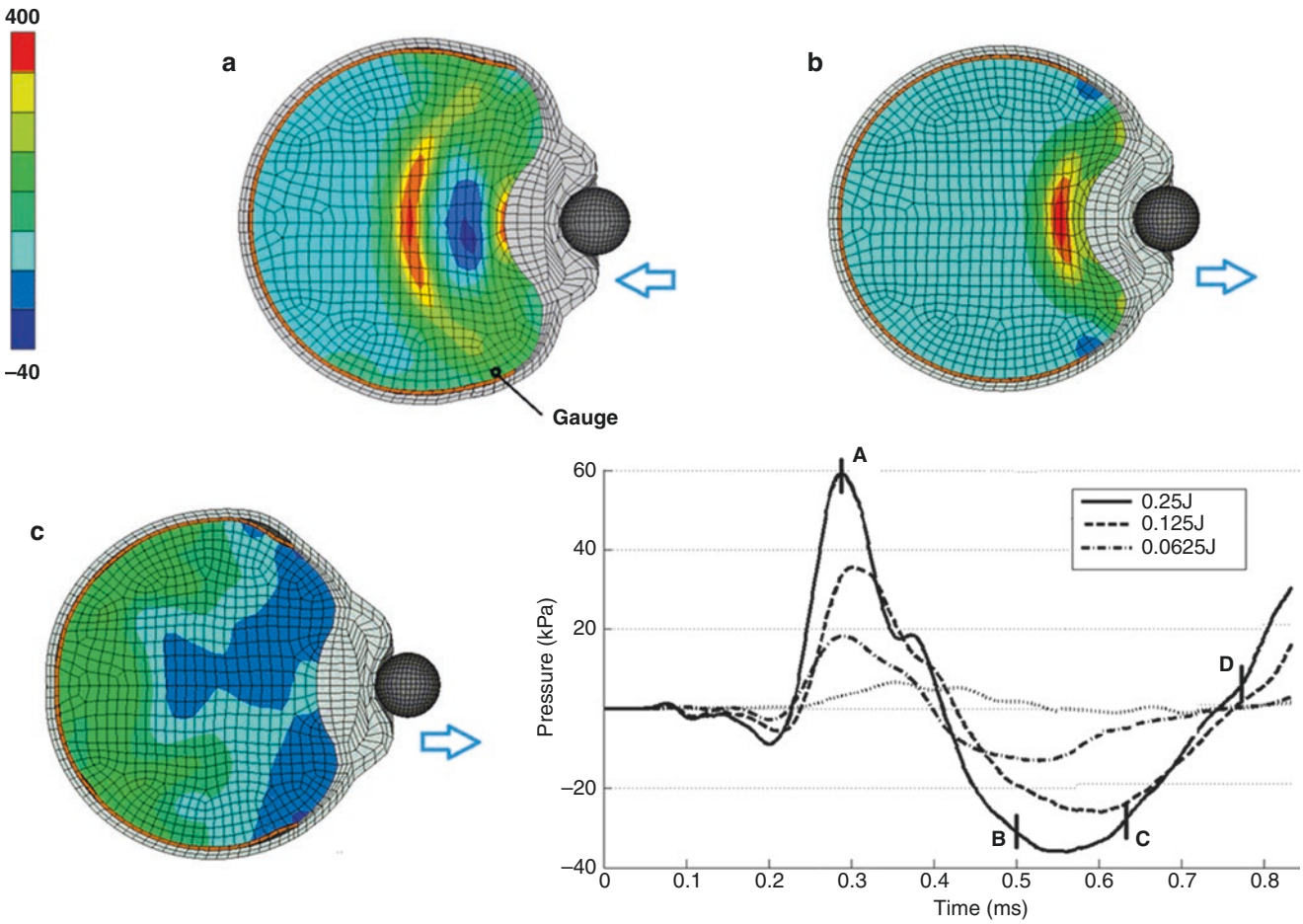

Biomechanical Mechanisms of IOP-/CSFP-Induced Optic Nerve Damage

39

Yingyan Mao and Ningli Wang

39.1 Introduction

Glaucoma, which is characterized by loss of retinal ganglion cell death, is a leading cause of irreversible world vision loss. Traditionally, intraocular pressure (IOP) is considered as the main reason that glaucomatous optic neuropathy develops [1]. However, as well as an elevated IOP, a low cerebrospinal fluid pressure (CSFP) has been proved to be another factor that related to the pathogenesis of glaucomatous optic neuropathy, especially in normal-IOP glaucoma patients [2–10]. The trans-lamina cribrosa pressure difference (TLCPD), which is defined as IOP minus CSFP, may be more important for the development of glaucomatous optic neuropathy [3, 5–8, 11–14]. Study on the damage of optic nerve in reduced CSFP animal models has further supported the hypothesis [15, 16]. However, mechanism of reduced CSFP on the optic nerve damage has not been elucidated yet.

Biomechanically, CSFP- and IOP-induced mechanical strain on optic nerve head is the weak point of the eyeball. With reduced CSFP or elevated IOP, the change of the pressure environment will result in the apoptosis of ganglion cells and the loss of vision [17]. It's worth noting that the threshold of TLCPD is individual difference because it depends on the biomechanical properties and geometry of ONH. Here we will give an improved understanding of biomechanical mechanisms of IOP-/CSFP-induced optic nerve damage in glaucomatous optic neuropathy.

39.2 Pressure Environment of Optic Nerve Head

Anatomically, ONH contains connective tissues, i.e., lamina cribrosa (LC), through which axons of the retinal ganglion cells, central retinal artery, and central retinal vein pass through [18]. ONH is the principal site of insult in glaucoma because it is the weak spot of the whole corneoscleral shell. Therefore, the biomechanical environment of the ONH has attracted much interest in academic circle.

As seen in Fig. 39.1, when considering LC biomechanics, IOP acts directly on the ONH and generates an inside-out force. There are two force vectors generated by IOP on the ONH. Firstly, IOP generates an inside-out force on the ONH because IOP is higher than ONH tissue pressure. Secondly, IOP generates a wall tension which pulls on the perimeter of ONH. It is the tissues around the complex opening in the eyewall that account for both forces, which allows the nerve fiber and the blood vessel pass out of the eye safely under normal pressure conditions [19].

In optic nerve chamber, optic nerve is surrounded by optic nerve sheath which is formed by loosely packed layers of connective tissue. The optic nerve bears subarachnoid space pressure (ONSP) due to the CSFP in the subarachnoid. Therefore, there exists force to ONH transmits by post-laminar tissue from CSFP.

In conclusion, there are IOP from the eye side and CSFP from the brain side across the LC in ONH. Either elevated IOP or reduced CSFP will result to elevated TLCPD, leading to pathological pressure environment around ONH. Such pathological pressure on ONH will cause more stress, strain, and deformations of the tissues, eventually resulting in pressure-related damage to the optic nerve. And, more remarkable, the individual susceptibility to IOP and CSFP of different people is determinated by their anatomy and mechanical properties of the individual eyes.

Y. Mao · N. Wang (✉)
Beijing Institute of Ophthalmology, Beijing Tongren Eye Center, Beijing Tongren Hospital, Capital Medical University, Beijing, China

Beijing Ophthalmology & Visual Sciences Key Laboratory, Beijing, China
e-mail: wningli@vip.163.com

N. Wang (ed.), *Intraocular and Intracranial Pressure Gradient in Glaucoma*,
Advances in Visual Science and Eye Diseases 1, https://doi.org/10.1007/978-981-13-2137-5_39

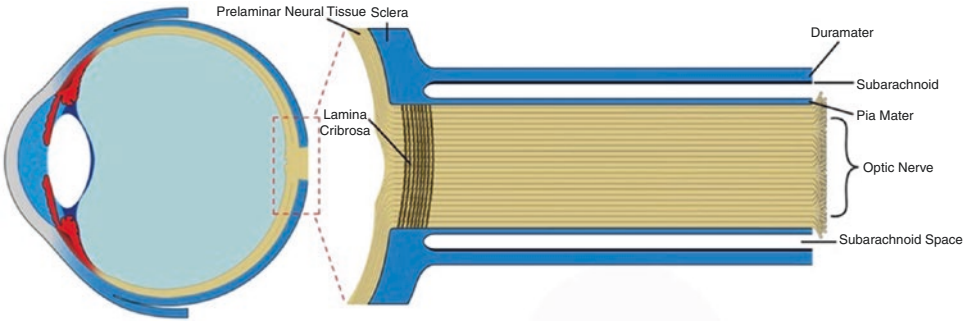

Fig. 39.1 Nonmyelinated intraocular optic fibers traverse the outer layers of the retina, and then the choroid and finally the sclera pass through the lamina cribrosa and become the intraorbital part of the optic nerve

39.3 Stress–Strain Relationship on Mechanical Behavior

Uniaxial stress is defined to be the ratio of the force to the cross-sectional area of the object:

$$\sigma = F / A$$

where F is the applied load [N] and A is the cross-sectional area [m^2].

Stress is a physical quantity that expresses the internal forces that the neighboring particles of a continuous material exert on each other, while strain is the measure of the deformation of the material. The relationship between stress and strain is known as stress-strain curve, which is unique for the difference of the properties of a material.

Under the pressure generated by IOP and CSFP, the ONH tissue resists compressive, tensile, and shear stresses. When ONH is subjected to tension or compression, the elastin fibers of the laminar beams will tend to be longitudinally oriented or compressed. And cross-sectional area changes of ONH are dependent on Poisson's ratio of the ONH tissue material.

39.4 The Biomechanical Effects of IOP–and CSFP–Related Biomechanics on the Connective Tissues

Figure 39.2 shows the undeformed shape of model (only edge) at an IOP and CSFP of 0 mmHg and deformed shape of model at normal TLCPD of 10 mmHg and elevated TLCPD of 18 mmHg resulting from reduced CSFP or elevated IOP, at true scale (left) and with the deformation exaggerated six times (right). When TLCPD increases from 10 mmHg to 18 mmHg, prelaminar neural tissue displaced laterally and posteriorly, and LC had appreciable stretching, and as a result, the prelaminar neural tissue and LC displaced backward and thinned. Comparatively, we observed higher deformations occurring at elevated TLCPD of 18 mmHg resulting from elevated IOP than resulting from reduced CSFP.

The deformation patterns of LC can be further understood by the LC edge deformation versus distance from the center of ONH curves (Fig. 39.3). The curves provide information on how the lamina cribrosa deformed. As shown in Fig. 39.3, the maximum LC deformation occurred at the center of the cup, which is consistent with the results reported. Also, the anterior surface of LC deformation is higher than that of posterior surface of LC deformation; another evidence of the thickness of LC decreased. Moreover, LC displaced more thinned at elevated TLCPD of 18 mmHg resulting from elevated IOP than resulting from reduced CSFP. For example, the laminar cribrosa thickness in the middle decreased by 6.2% at elevated TLCPD of 18 mmHg resulting from elevated IOP and 4.8% at elevated TLCPD of 18 mmHg resulting from reduced CSFP, respectively.

To get a general understanding of how biomechanical response of the optic nerve head is affected by IOP, we set CSFP to 10 mmHg and allowed IOP to vary from 20 mmHg to 50 mmHg. Figure 39.4 shows computed distributions of the first principal strain (left column) and von Mises equivalent stress (right column), under an IOP varying from 20 mmHg to 50 mmHg. As IOP increased, we observed higher stresses and strains. The largest stresses were observed in the relatively stiff sclera and pia mater, compared with the relatively soft neural and laminar tissue. The largest strains were observed in the neural tissue around the sclera ring, because the surrounding fibers are in direct contact with the sclera.

As the nonmyelinated intraocular optic fibers traverse the outer layers of the retina, then the choroid and finally the sclera pass through the lamina cribrosa and become the intraorbital part of the optic nerve. When these fibers traverse the sclera, the surrounding fibers are in direct contact with sclera. Under the action of mechanical force, the optic nerve surrounding the sclera ring bears the maximum strain. With IOP

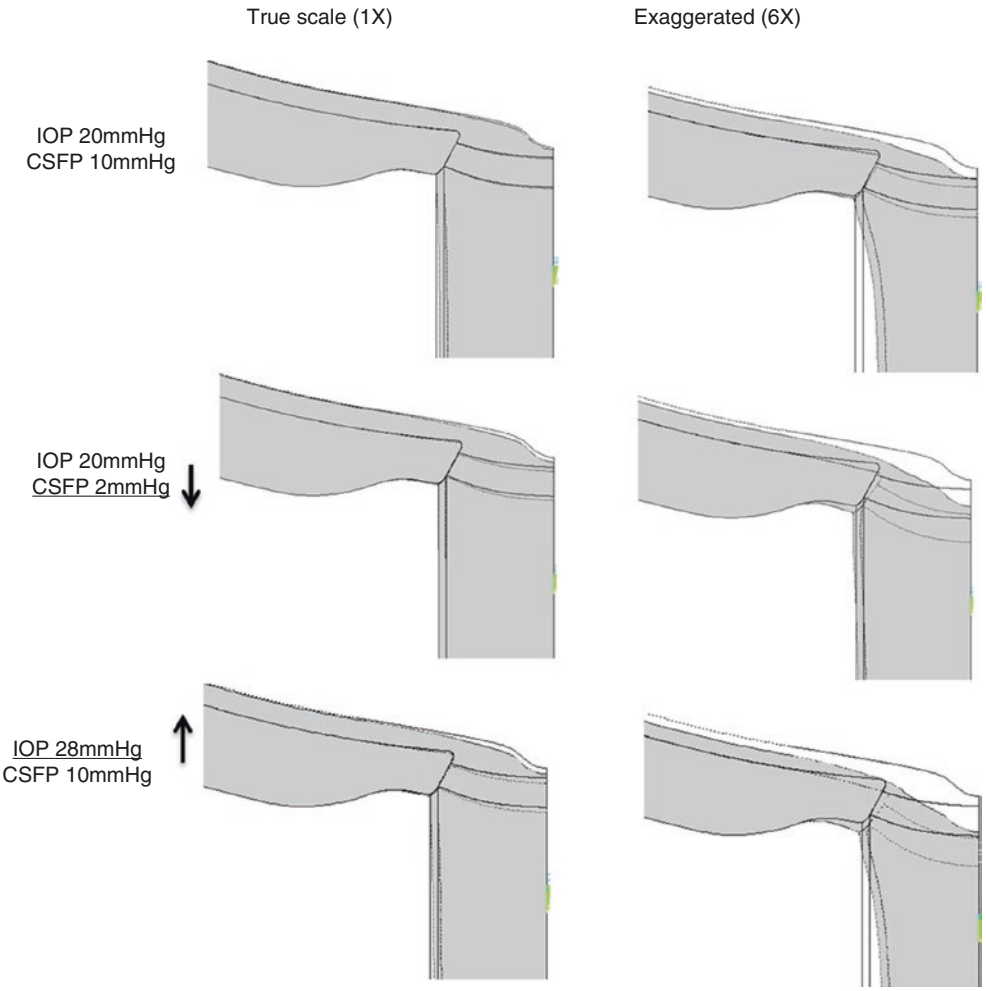

Fig. 39.2 Deformations, true and exaggerated. Left, true scale of the deformations; right, deformations exaggerated six times

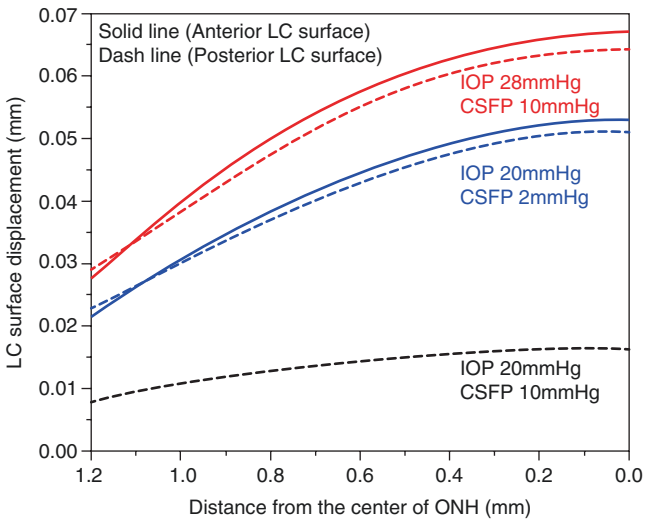

Fig. 39.3 LC edge deformation profiles. Curves of LC displacement versus distance from the center of ONH as TLCPD increased from 10 to 18 mmHg which resulted from elevated IOP or reduced CSFP. (Solid line) LC anterior surface; (dash line) LC posterior surface

evaluated from 20 mmHg to 50 mmHg, both direct mechanic injury and complex pathophysiological mechanism can induce the pathological changes of axon and neuronal soma of the surrounding fibers. Finally, the surrounding fibers are most likely to be first injured. The results are consistent with glaucomatous optic neuropathy model and glaucomatous visual field defect.

As the reduction of CSFP has a limited range, the reduction of CSFP can not have the increase in TLCPD as huge as the elevation of IOP. To further assess how strains in the ONH are affected by mild increase of TLCPD resulting from reduced CSFP or mild elevated IOP, we first set CSFP to 10 mmHg and allowed IOP to vary from 22 mmHg to 28 mmHg. Then we set IOP to 20 mmHg and allowed CSFP to vary from 8 mmHg to 2 mmHg. We compared the different strains of ONH affected by a reduction in CSFP and a mild evaluation of IOP resulting in same TLCPD. It can be seen that mild evaluation of IOP had an appreciable effect on strains within the LC. The effects of CSFP also

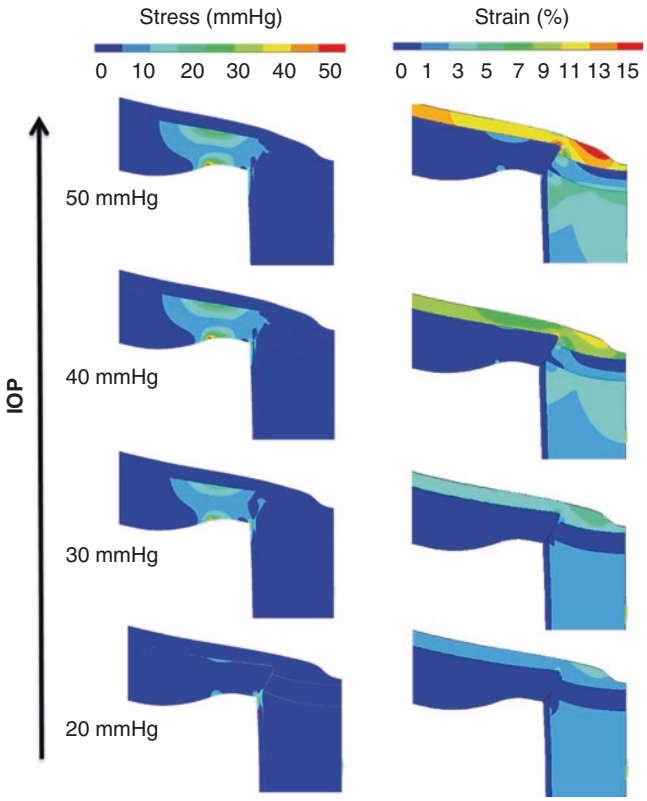

Fig. 39.4 Stress and strain distributions of ONH region. Computed distributions of the first principal strain (left) and von Mises equivalent stress (right) at a CSFP of 10 mmHg and an IOP evaluated from 20 mmHg to 50 mmHg

have some effect on the strains of the ONH tissue. However, the average peak strain within the lamina is relatively more defective with reduced CSFP than with mild elevated IOP, even though at the same TLCPD (Fig. 39.5).

The results showed that reduced CSFP and elevated IOP leading to increased TLCPD were particularly influential. As TLCPD increased from 12 to 18 mmHg by reducing CSFP or elevating IOP, there was a clear effect of increased TLCPD leading to larger peak tensile and compressive strains in the different regions of ONH tissue. Also, we observed higher strains occurring at the prelaminar neural tissue anterior to the LC, compared with the post-laminar neural tissue. From our sensitivity analysis, we found that sclera, annular ring, optic nerve, and LC stiffness had a large effect on ONH strains.

More intuitive understanding of the difference between IOP and CSFP in the deformed shape of optic nerve head can be manifested by C/D ratio. Figure 39.6 shows C/D ratio at different TLCPD. The red line is low CSFP with IOP at 20 mmHg, while the black line is mild high IOP with CSFP at 10 mmHg. The result shows that, at the same TLCPD, low CSFP group exhibits less deformation than those of the mild high IOP group. For example, at an IOP of 20 mmHg, C/D averaged from 0.38 to 0.48 with reduced CSFP from 10 mmHg to 2 mmHg. At a CSFP of 10 mmHg, C/D averaged from 0.38 to 0.43 with elevated IOP from 20 mmHg to 28 mmHg. In comparison, when the TLCPD is up to 16 mmHg, C/D is 0.45 with elevated IOP, while C/D is 0.42 with reduced CSFP.

39.5 Biomechanical Effects in Optic Nerve Head due to IOP/CSFP Changes

As the pressure environment changed, there were biomechanical effects within the ONH, especially within the lamina cribrosa. Specifically speaking, the maximum principle strains resulted from elevated IOP were highest within the neural and laminar regions, especially around the sclera ring, reaching potentially biologically significant levels. Therefore, with acutely elevated IOP, it is plausible that direct mechanical injury could contribute to glaucomatous optic neuropathy. Comparatively, the reduction in CSFP may lead to less strain increase in ONH, as compared to elevated IOP at the same level of TLCPD. It will cause less direct mechanical injury and may cause glaucomatous optic neuropathy by some other pathways. In conclusion, we think that biomechanics will not only determine the mechanic environment within the ONH but also mediate pressure-related cellular responses by various ways.

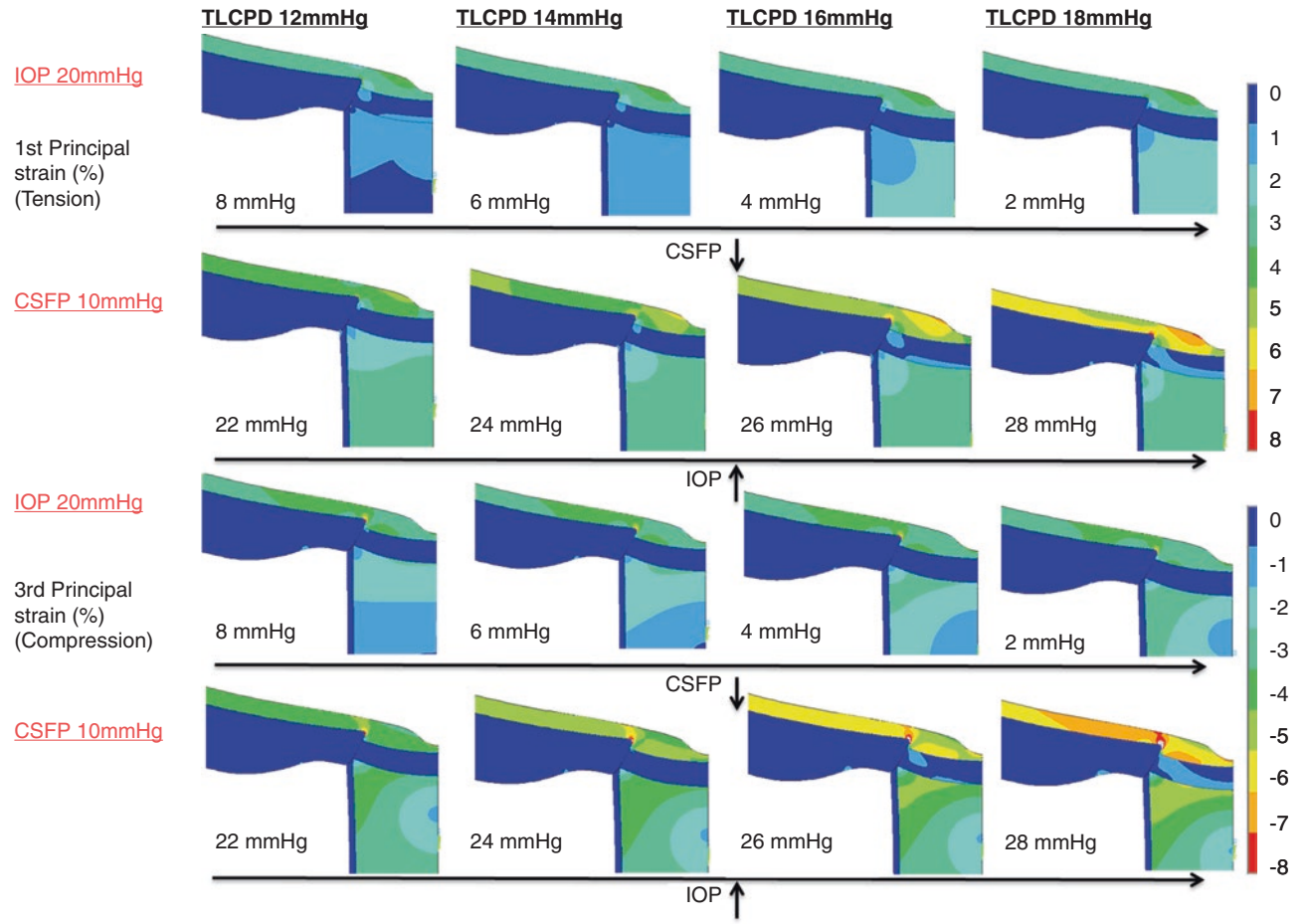

Fig. 39.5 Computed first principal strain and third principal strain in ONH tissues as TLCPD varies from 12 to 18 mmHg resulting from reduced CSFP or elevated IOP. All other parameter values are assigned to the baseline values except IOP or CSFP. Specifically, when increase of TLCPD is resulted from reduced CSFP, IOP is set to 20 mmHg; when increase of TLCPD is resulted from elevated IOP, CSFP is set to 10 mmHg

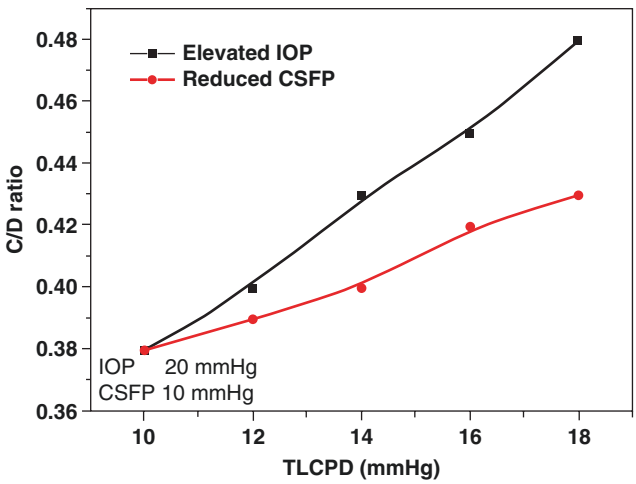

Fig. 39.6 C/D ratio at different TLCPD. The red line is reduced CSFP with IOP at 20 mmHg, while the black line is mild elevated IOP with CSFP at 10 mmHg

References

1. Geijssen HC. Studies on normal pressure glaucoma. Amsterdam: Kugler Publications; 1991.
2. Jonas JB, Berenshtein E, Holbach L. Anatomic relationship between lamina cribrosa, intraocular space, and cerebrospinal fluid space. Invest Ophthalmol Vis Sci. 2003;44:5189–95.
3. Ren R, Jonas JB, Tian G, et al. Cerebrospinal fluid pressure in glaucoma: a prospective study. Ophthalmology. 2010;117:259–66.
4. Morgan WH, Chauhan BC, Yu DY, Cringle SJ, Alder VA, House PH. Optic disc movement with variations in intraocular and cerebrospinal fluid pressure. Invest Ophthalmol Vis Sci. 2002;43:3236–42.
5. Morgan WH, Yu DY, Balaratnasingam C. The role of cerebrospinal fluid pressure in glaucoma pathophysiology: the dark side of the optic disc. J Glaucoma. 2008;17:408–13.
6. Berdahl JP, Allingham RR, Johnson DH. Cerebrospinal fluid pressure is decreased in primary open-angle glaucoma. Ophthalmology. 2008;115:763–8.
7. Berdahl JP, Fautsch MP, Stinnett SS, Allingham RR. Intracranial pressure in primary open angle glaucoma, normal tension glaucoma, and ocular hypertension: a case-control study. Invest Ophthalmol Vis Sci. 2008;49:5412–8.

8. Ren R, Wang N, Zhang X, Cui T, Jonas JB. Trans-lamina cribrosa pressure difference correlated with neuroretinal rim area in glaucoma. Graefes Arch Clin Exp Ophthalmol. 2011;249:1057–63.
9. Wang N, Xie X, Yang D, et al. Orbital cerebrospinal fluid space in glaucoma: the Beijing intracranial and intraocular pressure (iCOP) study. Ophthalmology. 2012;119:2065–2073.e2061.
10. Morgan WH, Yu DY, Cooper RL, Alder VA, Cringle SJ, Constable IJ. The influence of cerebrospinal fluid pressure on the lamina cribrosa tissue pressure gradient. Invest Ophthalmol Vis Sci. 1995;36:1163–72.
11. Yablonski M, Ritch R, Pokorny KS. Effect of decreased intracranial pressure on optic disc. Invest Ophthalmol Vis Sci. 1979;18(Suppl):165.
12. Jonas JB, Budde WM. Optic cup deepening spatially correlated with optic nerve damage in focal normal-pressure glaucoma. J Glaucoma. 1999;8:227–31.
13. Morgan WH, Cringle SJ, Balaratnasingam C, Yu DY. Impaired cerebrospinal fluid circulation and its relationship to glaucoma. Clin Exp Ophthalmol. 2008;36:802–3.
14. Wang N, Xie X, Yang D, Xian J, Li Y, et al. Orbital cerebrospinal fluid space in glaucoma. Ophthalmology. 2012;119:2065–2073.e1.
15. Yang D, Fu J, Hou R, et al. Optic neuropathy induced by experimentally reduced cerebrospinal fluid pressure in monkeys. Invest Ophthalmol Vis Sci. 2014;55:3067–73.
16. Zheng Z, Liu D, Jonas JB, Wu S, Kwong JM, Zhang J, Liu Q, Li L, Lu Q, Yang D, Wang J, Wang N. Axonal transport in the rat optic nerve following short-term reduction in cerebrospinal fluid pressure or elevation in intraocular pressure. Invest Ophthalmol Vis Sci. 2015;56:4257–66.
17. Osborne NN, del Olowns JC, Bellezza A, et al. 3-D histomorphometry of the normal and early glaucomatous monkey optic nerve head: prelaminar neural tissues and cupping. Invest Ophthalmol Vis Sci. 2007;48:5068–84.
18. Hattar S, Liao H-W, Takao M, Berson DM, Yau K-W. Melanopsin-containing retinal ganglion cells: architecture, projections, and intrinsic photosensitivity. Science. 2002;295(5557):1065–70.
19. Quigley HA, Brown A, Dorman-Pease ME. Alterations in elastin of the optic nerve head in human and experimental glaucoma. Br J Ophthalmol. 1991;75:552–7.

Part VII

Nutrition and POAG

Dietary Nitrate Intake and Primary Open-Angle Glaucoma

40

Jae Hee Kang

40.1 Introduction

It has been reported that low BMI is associated with lower CSF pressure, which then translates into higher translaminar cribrosa pressure gradient, a risk factor for glaucoma [1]. Previously, in our epidemiologic studies, we have reported that low BMI was a possible risk factor for POAG. To better understand this association and because POAG is a heterogeneous condition, we previously evaluated the relation between BMI and POAG subtypes based on pattern of visual field loss. We observed that low BMI is more strongly associated with primary open-angle glaucoma where the loss of vision tends to focus on the paracentral region rather than the peripheral vision. Every 10-unit increase in BMI was associated with a 33% lower risk of primary open-angle glaucoma with early paracentral loss, whereas it was not associated with peripheral loss [2, 3]. So we have hypothesized that the paracentral fibers, particularly the inferior, are in the "macular vulnerability zone," as the fovea lies below the disc, and accompanying blood vessels make more acute arcuate turns, creating shear forces that could compromise local blood flow [4, 5].

NO signaling may be important in POAG. Changes in blood flow to the eye differ by POAG case and control status after a NO synthase inhibitor is administered [6]. Also, polymorphisms in *NOS3* (OMIM 163729) were related to POAG [7] as well as lower NO production [8]. Recently, new glaucoma drugs that have nitric oxide as a component have been introduced; however, nitrates from the diet can also increase nitric oxide. Nitrate from diet can be reduced to nitrite by oral/gut bacteria [9] and converted to NO (Fig. 40.1). A few servings of green leafy vegetables yield more nitrate than from the L-arginine NO pathway [10]. A list of vegetables by nitrate content [11] is shown in (Fig. 40.2).

J. H. Kang (✉)
Brigham and Women's Hospital/Harvard Medical School, Boston, MA, USA
e-mail: nhjhk@channing.harvard.edu

Thus, we evaluated dietary nitrate and POAG risk in a large long-term longitudinal study of female nurses and male health professionals.

40.2 Objective

We investigated the relation between intake of nitrates from diet and risk of POAG [12].

40.3 Study Population and Design

Design: Prospective cohort study from the Nurses' Health Study (NHS; 1984–2012) and Health Professionals Follow-up Study (HPFS; 1986–2012).

Participants: 63,893 women in NHS and 41,094 men in HPFS (1) who were at least 40 years of age, (2) without prevalent glaucoma, (3) had eye exams, and (4) had complete dietary nitrate data (from 1984 in NHS and from 1986 in HPFS).

Outcome: Confirmed incident POAG (n = 1483) and POAG subtypes classified by the predominant visual field loss pattern and intraocular pressure (IOP) at diagnosis.

Exposure: Dietary nitrate intake updated every 2–4 years.

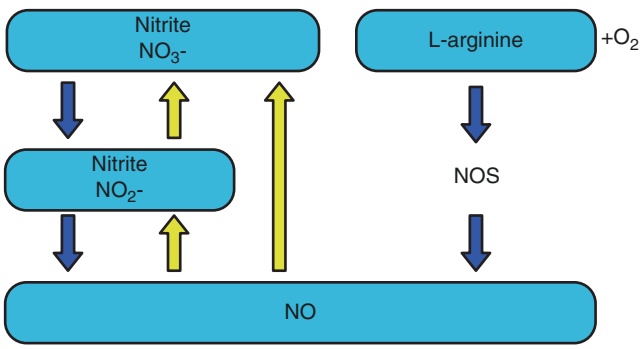

Fig. 40.1 The nitrate-nitrite-NO pathway

N. Wang (ed.), *Intraocular and Intracranial Pressure Gradient in Glaucoma*,
Advances in Visual Science and Eye Diseases 1, https://doi.org/10.1007/978-981-13-2137-5_40

Fig. 40.2 The classification of vegetables according to nitrate content [11]

Nitrate content(mg /100g fresh weight)	Vegetable varieties
Very low, <20	Artichoke, asparagus, broad bean, eggplant, garlic, onion, green Bean, mushroom, pea, pepper, potato, summer squash, sweet potato, tomato, watermelon
Low, 20 to <50	Broccoli, carrot, cauliflower, cucumber, pumpkin, chicory
Middle, 50 to <100	Cabbage, dill, turnip, savoy cabbage
High, 100 to <250	Celeriac, Chinese cabbage, endive, fennel, kohlrabi, leek, parsley
Very high, >250	Celery, cress, chervil, lettuce, red beetroot, spinach, rocket (rucola)

Fig. 40.3 Results—main findings

		Q1	Q2	Q3	Q4	Q5	
Women	Median (mg/day) Cases Person-time	80 210 227,054	114 173 227,827	142 207 226,545	175 199 227,053	238 211 226,982	
Men	Median (mg/day) Cases Person-time	81 98 108,530	117 89 109,243	148 101 108,596	185 111 108,704	254 84 108,180	
Pooled	MV RR (95% CI)	1.00 (ref)	0.78 (0.65, 0.94)	0.82 (0.67, 0.99)	0.81 (0.53, 1.24)	0.67 (0.52, 0.85)	0.01

40.4 Statistical Analysis

The relation between dietary nitrate intake and incident POAG was evaluated with Cox proportional hazard models with time-varying covariates. Analyses were stratified by age in months and period at risk and adjusted for the following variables, ancestry; family history of glaucoma; self-reported history of hypertension; diabetes; body mass index; cumulatively averaged intakes of total energy, alcohol, and caffeine; pack-years of smoking; physical activity; number of eye exams reported during follow-up; and multivitamin use, and in NHS only additionally adjusted for age at menopause and postmenopausal hormone status. We calculated pooled multivariable relative risks (RRs) and their 95% confidence intervals (CIs).

40.5 Results

Main findings (RR in women and men and pooled) are shown in (Fig. 40.3). Compared with those consuming 80 mg/day of dietary nitrate intake (lowest 20%, Q1), the RR for consuming 240 mg/day (highest 20%, Q5) was 0.79 (95%CI: 0.66–0.93). There was a linear dose-response (linear $p = 0.02$).

Figure 40.4 shows the results about the POAG subtype analyses (Fig. 40.4): paracentral (Pc) versus peripheral (Pr) and IOP ≥ 22 mmHg (HTG) versus IOP < 22 mmHg (NTG). The association was more evident ($p = 0.01$) for Pc loss (Q5 RR = 0.56; 95%CI: 0.40–0.79; linear $p = 0.0003$) than for Pr loss only (Q5 RR = 0.85; 95%CI: 0.68–1.06; linear $p = 0.50$). The association did not differ ($p = 0.75$) by IOP (HTG: Q5 RR = 0.82; 95%CI: 0.67–1.01; linear p = 0.11; NTG: Q5 RR = 0.71; 95%CI: 0.53–0.96; linear $p = 0.12$).

Other results are as follows. Green leafy vegetables were the largest contributor of nitrate intake (statistically accounted for 56.7% of nitrate intake differences). Compared to the reference group of 0.31 servings/day, the RR for the group with 1.45+ servings/day was 0.82 (95%CI: 0.69–0.97; linear $p = 0.02$) and RR = 0.52 for paracentral loss (RR = 0.52; 95%CI: 0.29–0.96; linear $p = 0.0002$). Compared to the reference group of 0.11 servings/day of iceberg lettuce, the RR for 0.86 servings/day was 0.89 (95%CI: 0.75–1.06; linear $p = 0.06$) and RR = 0.69 for paracentral loss (95%CI: 0.49–0.97; linear $p = 0.001$).

40.6 Discussions

40.6.1 Consistency of Findings with Prior Literature

Our results are similar to those found by Coleman et al. [13] and Giaconi et al. [14]. In both studies, kale/collard greens were associated with 55–70% lower POAG relative risk.

40.6.2 Biological Mechanism

Alterations of the nitric oxide system may lead to dysregulation of ocular blood flow and elevated IOP, which may be etiologic factors for POAG. Although nitric oxide is mainly generated endogenously via the L-arginine/nitric oxide pathway, when there is hypoxia [15] or when this pathway is compromised as in POAG, the nitrate-nitrite-nitric oxide pathway can be an alternate source of nitric

		Q1	Q2	Q3	Q4	Q5	P-trend	P-het
Pooled§ - POAG with IOP ≥22 mm Hg (n=998 cases)	MV RR (95% CI)	1.00 (ref)	0.85 (0.69, 1.04)	0.93 (0.76, 1.13)	0.90 (0.61, 1.32)	0.82 (0.67, 1.01)	0.11	0.75
Pooled§ - POAG with IOP <22 mm Hg (n=487 cases)	MV RR (95% CI)	1.00 (ref)	0.73 (0.55, 0.98)	0.79 (0.59, 1.05)	0.86 (0.65, 1.13)	0.71 (0.53, 0.96)	0.12	
Pooled§ - POAG with peripheral VF loss only (n=836 cases)	MV RR (95% CI)	1.00 (ref)	0.82 (0.58, 1.15)	0.98 (0.72, 1.34)	1.00 (0.65, 1.54)	0.85 (0.68, 1.06)	.50	0.01
Pooled§ - POAG with early paracentral VF loss (n=433 cases)	MV RR (95% CI)	1.00 (ref)	0.89 (0.67, 1.20)	0.77 (0.57, 1.04)	0.77 (0.57, 1.04)	0.56 (0.40, 0.79)	<.001	

Fig. 40.4 Results—POAG subtype analyses

oxide. The role of nitric oxide in alterations in regulating vascular function was supported by the association with early paracentral loss.

40.7 Limitations

1. Underascertainment of cases due to lack of standardized eye exams for all participants.
2. Misclassification of dietary nitrate intake due to lack of detailed info on soil conditions, storage, etc.
3. Confounding by other dietary factors.
4. Lack of generalizability as most participants were Caucasian.
5. This is the first study to evaluate dietary nitrates and glaucoma, indicating that more confirmation is needed in other studies.

40.8 Summary

Higher intake of nitrate and green leafy vegetables was associated with modestly lower risk of primary open-angle glaucoma; this further supports the role of nitric oxide in glaucoma pathogenesis.

References

1. Marek B, Harris A, Kanakamedala P, Lee E, Amireskandari A, Carichino L, Guidoboni G, Tobe LA, Siesky B. Cerebrospinal fluid pressure and glaucoma: regulation of trans-lamina cribrosa pressure. Br J Ophthalmol. 2014;98(6):721–5. https://doi.org/10.1136/bjophthalmol-2013-303884.. Epub 2013 Dec 4
2. Kang JH, Loomis SJ, Rosner BA, Wiggs JL, Pasquale LR. Comparison of risk factor profiles for primary open angle glaucoma subtypes defined by pattern of visual field loss: a prospective study. Invest Ophthalmol Vis Sci. 2015a;56(4):2439–48.
3. Kang JW, Park B, Cho BJ. Comparison of risk factors for initial central scotoma versus initial peripheral scotoma in normal-tension glaucoma. Korean J Ophthalmol. 2015b;29(2):102–8.
4. Park SC, De Moraes CG, Teng CC, Tello C, Liebmann JM, Ritch R. Initial parafoveal versus peripheral scotomas in glaucoma: risk factors and visual field characteristics. Ophthalmology. 2011;118(9):1782–9.
5. Hood DC, Raza AS, de Moraes CG, Liebmann JM, Ritch R. Glaucomatous damage of the macula. Prog Retin Eye Res. 2013;32:1–21.
6. Polak K, Luksch A, Berisha F, Fuchsjaeger-Mayrl G, Dallinger S, Schmetterer L. Altered nitric oxide system in patients with open-angle glaucoma. Arch Ophthalmol. 2007;125(4):494–8.
7. Dengel DR, Brown MD, Ferrell RE, Reynolds TH, Supiano MA. A preliminary study on T-786C endothelial nitric oxide synthase gene and renal hemodynamic and blood pressure responses to dietary sodium. Physiol Res. 2007;56(4):393–401.
8. Emam WA, Zidan HE, Abdulhalim BE, Dabour SA, Ghali MA, Kamal AT. Endothelial nitric oxide synthase polymorphisms and susceptibility to high-tension primary open-angle glaucoma in an Egyptian cohort. Mol Vis. 2014;20:804–11.
9. Cosby K, Partovi KS, Crawford JH, et al. Nitrite reduction to nitric oxide by deoxyhemoglobin vasodilates the human circulation. Nat Med. 2003;9(12):1498–505.
10. Lundberg JO, Gladwin MT, Ahluwalia A, et al. Nitrate and nitrite in biology, nutrition and therapeutics. Nat Chem Biol. 2009;5(12):865–9.
11. Santamaria P. Nitrate in vegetables: toxicity, content, intake and EC regulation. J Sci Food Agric. 2006;86:10–7.
12. Kang JH, Willett WC, Rosner BA, Buys E, Wiggs JL, Pasquale LR. Association of dietary nitrate intake with primary open-angle glaucoma: a prospective analysis from the nurses' health study and health professionals follow-up study. JAMA Ophthalmol. 2016;134(3):294–303.
13. Coleman AL, Stone KL, Kodjebacheva G, Study of Osteoporotic Fractures Research Group, et al. Glaucoma risk and the consumption of fruits and vegetables among older women in the study of osteoporotic fractures. Am J Ophthalmol. 2008;145(6):1081–9.
14. Giaconi JA, Yu F, Stone KL, Study of Osteoporotic Fractures Research Group, et al. The association of consumption of fruits/vegetables with decreased risk of glaucoma among older African-American women in the study of osteoporotic fractures. Am J Ophthalmol. 2012;154(4):635–44.
15. Kaur C, Foulds WS, Ling EA. Hypoxia-ischemia and retinal ganglion cell damage. Clin Ophthalmol. 2008;2(4):879–89.

Body Mass Index and Primary Open-Angle Glaucoma

41

Jinghong Sang, Qian Zhang, Huaizhou Wang, Diya Yang, and Ningli Wang

Glaucomatous optic neuropathy is the most common cause of irreversible blindness worldwide [1]. Primary open-angle glaucoma (POAG) is characterized by typical glaucomatous optic nerve damage and visual field defects. The elevation of IOP has long been considered as the major risk factor for glaucoma. However, the intraocular pressure of patients within normal range could also be affected with glaucoma, known as normal-tension glaucoma (NTG) [2]. High-tension glaucoma (HTG) and normal-tension glaucoma are the two subtypes of POAG.

In our previous perspective studies, we have investigated that cerebrospinal fluid pressure was abnormally low in normal-tension glaucoma, which may lead a high translamina pressure difference (TLPD) [3, 4]. So, it was thought that TLPD may be the cause of glaucomatous optic neuropathy. TLPD is determined by IOP and CSF pressure. The regulation of cerebrospinal fluid pressure is mainly related with venous pressure and other several systemic factors. The amounts of neurological studies have well established that cerebrospinal fluid pressure was positively correlated with body mass index, which was known as one of cardinal factors of evaluation of adiposity [5, 6]. The body mass index (BMI) is a measure for human body shape based on an individual's mass and height. One possible mechanism for this positive correlation is that subjects with high BMI may have higher CSF pressure due to increased abdomen pressure and high central venous pressure. Therefore, the objective of this study is to investigate whether BMI and other anthropometric measurement factors were associated with POAG.

J. Sang · H. Wang · D. Yang · N. Wang (✉)
Beijing Institute of Ophthalmology, Beijing Tongren Eye Center, Beijing Tongren Hospital, Capital Medical University, Beijing, China

Beijing Ophthalmology & Visual Sciences Key Laboratory, Beijing, China
e-mail: wningli@vip.163.com

Q. Zhang
Department of Nutrition, Beijing Tongren Hospital, Capital Medical University, Beijing, China

All participants recruited in this study underwent a thoroughly ophthalmological examination including visual acuity, intraocular pressure measurement, slit-lamp examination, gonioscopy, measurement of central corneal thickness, stereophotography of the optic nerve head (Nidek 3-Dx simultaneous stereo retinal camera, Nidek Co. Ltd., Gamagori, Japan), and computerized perimetry (central 30-2 full threshold program; Humphrey Field Analyzer; Zeiss Meditec AG, Jena, Germany). The diagnosis of primary open-angle glaucoma included that the recorded IOP measurement is higher than 21 mmHg along with characteristic glaucomatous neuropathy and visual field defect. All patients with normal-tension glaucoma were needed to undertake 24-h IOP measurement without any anti-glaucomatous medications or ceasing to these at least 4 weeks before the IOP measurements. All patients included in this study had underwent anthropometric measurements which included height in meter, weight in kilogram, waist circumference in meter, hip circumference in meter, and blood pressure. Body mass index (BMI) is calculated as weight in kilograms divided by height in meters squared. Waist-to-hip ratio is calculated as waist circumference divided by hip circumference. Moreover, we stratified the NTG group into two subgroups according to patients' maximum IOP. NTG patients whose maximum IOP was less than 18 mmHg during 24-h measurements were defined as low-tension NTG group, and those whose maximum IOP was higher than 18 mmHg during 24-h measurements were defined as high-tension NTG group.

In addition, the participants also had fasting blood biochemistry test mainly including total cholesterol, low-density lipoprotein (LDL) cholesterol, high-density lipoprotein (HDL) cholesterol, and triglycerides.

Exclusion criteria for this study included patients with severe systemic diseases such as liver and renal failure and malignant tumor. Patients with any optic nerve disease other than glaucoma, pregnant women, and patients undergone weight loss should also be excluded in this study.

In this study, we collected 278 patients with primary open-angle glaucoma, including 165 high-tension glaucoma (HTG) and 113 NTG patients from Beijing Tongren

N. Wang (ed.), *Intraocular and Intracranial Pressure Gradient in Glaucoma*,
Advances in Visual Science and Eye Diseases 1, https://doi.org/10.1007/978-981-13-2137-5_41

Table 41.1 Demographic features of the study population

	High-tension glaucoma	Normal-tension glaucoma	*P* value
Number of subjects	165	113	
Age (years)	50.3 ± 15.9	51.1 ± 14.7	0.642
Gender (M/F)	115/50	68/45	0.10
Mean IOP (mmHg)			
OD	16.7 ± 6.5	14.5 ± 2.9	0.001
OS	16.5 ± 6.7	14.5 ± 2.7	0.002

Table 41.2 Anthropometric measurements of the study population

	High-tension glaucoma	Normal-tension glaucoma	*P* value
Height (m)	1.67 ± 0.08	1.68 ± 0.08	0.719
Weight (kg)	68.7 ± 11.9	64.0 ± 10.7	0.001
WC (cm)	86.0 ± 9.8	83.0 ± 9.3	0.043
HC (cm)	97.1 ± 6.4	94.4 ± 5.4	0.003
BMI (kg/m^2)	24.49 ± 3.44	22.70 ± 2.91	<0.01
W/H ratio	0.88 ± 0.07	0.88 ± 0.07	0.48
BP (mmHg)			
Systolic	121 ± 15	117 ± 14	0.019
Diastolic	79 ± 9	78 ± 10	0.499

WC waist circumference, *HC* hip circumference, *BMI* body mass index, *W/H ratio* waist-to-hip ratio, *BP* blood pressure

Hospital. Table 41.1 presents demographic statistics for all participants. It was not statistically significant in age and gender between these two groups (P = 0.642, P = 0.10, respectively). The mean IOP of NTG patients was lower than HTG patients in both the left and right eyes (P = 0.001 for OD; P = 0.002 for OS).

The weight, waist circumference, and hip circumference in the NTG group were lower than the HTG group (P = 0.001, P = 0.043, and P = 0.003, respectively). The BMI in NTG group was 22.70 ± 2.91 kg/m^2 compared to 24.49 ± 3.44 kg/m^2 in HTG group (P < 0.01). The systolic blood pressure was also lower in NTG group than in HTG group (P = 0.019). The height and waist-to-hip ratio did not vary significantly between two groups (Table 41.2).

According to the WHO BMI classification for Asians, there are four levels [7]. The proportion of all the patients' classification of underweight, normal, overweight, and obese based on BMI has been presented in Table 41.3. According to the WHO BMI classification for Asian population, the normal range of BMI is 18.5–22.9 kg/m^2. The adults with BMI less than 18.5 are underweight, and the cutoff points of overweight and obese are 23 and 30, respectively. In our study, 6.2% NTG patients were underweight compared to 1.8% patients in HTG group (P = 0.06). The patients with BMI in normal range differed statistically significant between these two groups. 35.2% vs. 49.6% of patients were overweight in HTG and NTG group (P = 0.016). In particular, only one patient with normal-tension glaucoma was obese whose body mass index was higher than 30 kg/m^2. However, 6.7% patients in HTG group were obese (P = 0.02). In the 1990s, the cooperative meta-analysis group of China Obesity Task Force revised BMI classification adapted for Chinese adult population. According to this revised classification, the differences between two groups were statistically significant in each category (Table 41.4).

Table 41.3 Comparison between patients' BMI in both two study groups based on WHO BMI classification for Asian population

	High-tension glaucoma	Normal-tension glaucoma	*P* value
BMI (kg/m^2)			
<18.5	3 (1.8)	7 (6.2)	0.06
18.5–22.9	58 (35.2)	56 (49.6)	0.016
23–29.9	93 (56.3)	49 (43.4)	0.033
23–24.9	34 (20.6)	28 (24.8)	0.412
25.0–29.9	59 (35.7)	21 (18.6)	0.002
≥30	11 (6.7)	1 (0.9)	0.02

BMI body mass index, percentage of cases in each BMI classification showed in parentheses

Table 41.4 Comparison between patients' BMI in both two study groups based on cooperative meta-analysis group of China Obesity Task Force revised BMI classification for Chinese adult population

	High-tension glaucoma	Normal-tension glaucoma	*P* value
BMI (kg/m^2)			
<18.5	3 (1.8)	7 (6.2)	0.06
18.5–23.9	69 (41.8)	71 (62.8)	0.001
24–27.9	71 (43.1)	32 (28.3)	0.013
≥28	22 (13.3)	3 (2.7)	0.002

Percentage of cases in each BMI classification showed in parentheses

We stratified patients with NTG into two subgroups depending on the cut-off IOP of 18 mmHg during 24-h measurements (Table 41.5). In comparison between these two subgroups, the low-tension NTG group had lower weight (P = 0.007), shorter waist circumference (P = 0.01), less body mass index (P = 0.02), and waist-to-hip ratio (P = 0.02).

In another part of our study, we had totally 143 POAG patients with fast biochemical blood test (Table 41.6). Only the difference of triglycerides was statistically significant between the NTG and HTG group (P = 0.003).

In this study, we found that compared to HTG patients, NTG patients had lower body weight, lower BMI, lower waist and hip circumference, lower systolic blood pressure, and lower level of triglycerides. The subgroup of NTG patients, in which the maximum IOP was less than 18 mmHg, had distinct lean body shape with low BMI, waist circumference, and waist-to-hip ratio.

From our study, it showed that NTG patients had related with lean body shape and more distinguished among those

Table 41.5 Comparison of anthropometric measurements between two normal-tension glaucoma subgroups

	Normal-tension glaucoma		
	Maximum IOP ≤ 18 mmHg	Maximum IOP > 18 mmHg	*P* value
Number of subjects	56	57	
Age (years)	50.9 ± 14.0	51.5 ± 15.4	0.835
Height (m)	1.67 ± 0.08	1.68 ± 0.08	0.481
Weight (kg)	61.3 ± 10.7	66.6 ± 10.1	0.007
WC (cm)	79.7 ± 9.9	85.8 ± 7.9	0.01
HC (cm)	93.1 ± 6.0	95.6 ± 4.6	0.07
BMI (kg/m^2)	21.8 ± 2.9	23.5 ± 2.7	0.002
W/H ratio	0.86 ± 0.07	0.90 ± 0.06	0.02
BP (mmHg)			
Systolic	115 ± 14	119 ± 15	0.131
Diastolic	78 ± 11	78 ± 10	0.694

Table 41.6 Biochemical blood test in two study groups

	High-tension glaucoma	Normal-tension glaucoma	*P* value
Number of patients	110	33	
FBG (mmol/L)	5.28 ± 0.58	5.19 ± 0.62	0.44
Triglycerides (mmol/L)	1.72 ± 1.23	1.24 ± 0.58	0.003
Total cholesterol (mmol/L)	4.71 ± 0.96	4.74 ± 1.10	0.87
LDL (mmol/L)	2.97 ± 0.82	3.0 ± 1.04	0.91
HDL (mmol/L)	1.32 ± 0.37	1.41 ± 0.36	0.24

FBG fast blood glucose

maximum IOP was even lower than 18 mmHg. On the contrary, HTG patients were predisposed to be overweight or have central obesity. One previous study from Asrani et al. presented similar results that NTG patients had less BMI with smaller sample size of patients [8]. Many studies from different ethnics documented a positive association between BMI and IOP [9–13]. In contrast, few studies have directly studied the relation between BMI and POAG, and these studies suggest there may be an inverse association between BMI and POAG [13, 14]. One cohort study had presented that higher BMI was associated with a lower risk of POAG with normal IOP only among women. From our results, we confirmed that the mean BMI of NTG patients was lower than patients with HTG, and the percentage of underweight was higher. Recently, a new term Flammer syndrome described a series of systemic and ocular phenotypes characterized by the main presence of vascular dysregulation, low blood pressure, low body mass index, and other symptoms affected with autonomic nervous system and gene expression. Flammer syndrome also contributed to certain diseases, such as normal-tension glaucoma. The clinical characteristic of our NTG patients also had some signs same as Flammer syndrome [15].

The mechanisms of association of BMI and POAG have not been well understood. Recent clinical and animal model studies have shown that low cerebrospinal fluid pressure and increased trans-lamina pressure difference might be involved the pathogenesis of NTG [3, 4, 16–22]. The correlation between BMI and cerebrospinal fluid pressure has been widely proved [5, 6, 23]. These findings provide supporting evidence that the NTG patients with lean body mass may be predisposed to have lower CSF pressure. Therefore, low body mass index might influence the blood pressure, intraocular pressure, and intracranial pressure, and the abnormally increased trans-lamina pressure might lead to glaucomatous optic neuropathy. However, in our study, the results showed that 16.4% NTG patients had higher BMI above 25 kg/m^2, and, on the other hand, 1.8% HTG patients had BMI less than 18.5 kg/m^2. The pathogenesis of these patients may not be explained by the mechanism of trans-lamina pressure difference increased. Therefore, other factors and mechanisms may also involve the pathogenesis of POAG together. The biochemical results showed that NTG patients had lower triglycerides. There was one report in the literature based on Korean POAG patients that presented no significant differences in hs-CRP and lipid profiles either between NTG patients and healthy controls or between the subgroups of NTG and controls [24]. Other studies in large sample size are needed to investigate the association of lipids level and POAG.

There are some potential limitations of our study. First, it was a hospital-based observational study with the possibility of a bias by the selection of the patients. The recruitment of all patients was from a tertiary referral center. Therefore, it might also have the referral bias. Second, the number of patients included in the study was relatively low, especially after we stratified the NTG into two subgroups.

In conclusion, NTG patients were predisposed to have lean body mass such as lower body weight and lower body mass index. For HTG patients, the proportion of overweight and obese was higher. Further study should be investigated on the mechanism of how the body mass factors involved the risk and pathogenesis of POAG.

References

1. Quigley HA, Broman AT. The number of people with glaucoma worldwide in 2010 and 2020. Br J Ophthalmol. 2006;90:262–7.
2. Kwon YH, Fingert JH, Kuehn MH, Alward WL. Primary open-angle glaucoma. N Engl J Med. 2009;360:1113–24.
3. Ren R, Jonas JB, Tian G, Zhen Y, Ma K, Li S, et al. Cerebrospinal fluid pressure in glaucoma: a prospective study. Ophthalmology. 2010;117:259–66.
4. Wang N, Xie X, Yang D, Xian J, Li Y, Ren R, et al. Orbital cerebrospinal fluid space in glaucoma: the Beijing intracranial and intraocular pressure (iCOP) study. Ophthalmology. 2012;119:2065–73.
5. Berdahl JP, Fleischman D, Zaydlarova J, Stinnett S, Allingham RR, Fautsch MP. Body mass index has a linear relationship with cerebrospinal fluid pressure. Invest Ophthalmol Vis Sci. 2012;53:1422–7.

6. Ren R, Wang N, Zhang X, Tian G, Jonas JB. Cerebrospinal fluid pressure correlated with body mass index. Graefes Arch Clin Exp Ophthalmol. 2012;250:445–6.
7. World Health Organization. Global database on body mass index. http://apps.who.int/bmi/.Accessed 7 June 2011.
8. Asrani S, Samuels B, Thakur M, Santiago C, Kuchibhatla M. Clinical profiles of primary open angle glaucoma versus normal tension glaucoma patients: a pilot study. Curr Eye Res. 2011;36:429–35.
9. Cohen E, Kramer M, Shochat T, Goldberg E, Garty M, Krause I. Relationship between body mass index and intraocular pressure in men and women: a population-based study. J Glaucoma. 2016;25(5):e509–13.
10. Zhao D, Kim MH, Pastor-Barriuso R, Chang Y, Ryu S, Zhang Y, et al. A longitudinal study of association between adiposity markers and intraocular pressure: the Kangbuk Samsung health study. PLoS One. 2016;11:e146057.
11. Pasquale LR, Kang JH. Lifestyle, nutrition, and glaucoma. J Glaucoma. 2009;18:423–8.
12. Lee JS, Lee SH, Oum BS, Chung JS, Cho BM, Hong JW. Relationship between intraocular pressure and systemic health parameters in a Korean population. Clin Exp Ophthalmol. 2002;30:237–41.
13. Pasquale LR, Willett WC, Rosner BA, Kang JH. Anthropometric measures and their relation to incident primary open-angle glaucoma. Ophthalmology. 2010;117:1521–9.
14. Ramdas WD, Wolfs RC, Hofman A, de Jong PT, Vingerling JR, Jansonius NM. Lifestyle and risk of developing open-angle glaucoma: the Rotterdam study. Arch Ophthalmol. 2011;129:767–72.
15. Konieczka K, Ritch R, Traverso CE, Kim DM, Kook MS, Gallino A, et al. Flammer syndrome. EPMA J. 2014;5:11.
16. Killer HE, Flammer J, Miller NR. Glaucoma and cerebrospinal fluid pressure. Ophthalmology. 2008;115:2316–2317, 2317.
17. Berdahl JP, Allingham RR, Johnson DH. Cerebrospinal fluid pressure is decreased in primary open-angle glaucoma. Ophthalmology. 2008;115:763–8.
18. Yang D, Fu J, Hou R, Liu K, Jonas JB, Wang H, et al. Optic neuropathy induced by experimentally reduced cerebrospinal fluid pressure in monkeys. Invest Ophthalmol Vis Sci. 2014;55:3067–73.
19. Killer HE, Miller NR, Flammer J, Meyer P, Weinreb RN, Remonda L, et al. Cerebrospinal fluid exchange in the optic nerve in normal-tension glaucoma. Br J Ophthalmol. 2012;96:544–8.
20. Hou R, Zhang Z, Yang D, Wang H, Chen W, Li Z, et al. Pressure balance and imbalance in the optic nerve chamber: the Beijing intracranial and intraocular pressure (iCOP) study. Sci China Life Sci. 2016;59(5):495–503.
21. Chen BH, Drucker MD, Louis KM, Richards DW. Progression of normal-tension Glaucoma after Ventriculoperitoneal shunt to decrease cerebrospinal fluid pressure. J Glaucoma. 2016;25:e50–2.
22. Li Z, Yang DY, Lu Y, Liu DC, Jia JP, Jonas JB, et al. Intracranial hypotension and co-existent normal-pressure glaucoma: the Beijing intracranial and intraocular pressure study. Chin Med J (Engl). 2013;126:1588–9.
23. Davson H, Segal MB. The intracranial or CSF-pressure. Physiology of the CSF and blood-brain barriers: Boca Raton, FL, CRC Press; 1996. p. 699–705.
24. Choi J, Joe SG, Seong M, Choi JY, Sung KR, Kook MS. C-reactive protein and lipid profiles in Korean patients with normal tension glaucoma. Korean J Ophthalmol. 2009;23:193–7.

Normal-Tension Glaucoma: A "Qi Deficiency" Disease

42

Jing Yu, Jinghong Sang, and Ningli Wang

The unique basic theory of Traditional Chinese Medicine (TCM), an important integral part of the 5000 years of Chinese traditional culture, has been formed over 2000 years ago. Over such a long term of clinical practice, TCM doctors have accumulated valuable experience in the diagnosis and treatment of diseases and developed unique treatment methods. Until now, nearly 10,000 medical books on TCM have been found, and a series of medical management and medical education system have been established.

In western medicine, the doctors make diagnoses relying on lab tests, imaging, etc., and there are lots of available technologies to isolate the smallest possible particle that may be disease-related all the way down to the electrical charge of a molecule. TCM focuses on the larger perceptions unique to our human senses rather than these small units. To put this in another way, TCM doctors observe the whole person with their eyes rather than study the electrical charge of a particular molecule or a cell with a leaky wall; they evaluate the health status of patients by palpating the pulse at the wrist; they can assess the internal condition of the body through the appearance of the tongue; they detect the pathological changes by listening to the breath rhythm of patients.

Traditional Chinese Medicine (TCM) constitution can be classified in different ways. Professor Wang Qi's method of categorizing it into nine types is the most influential and widely used one. And this method has given detailed description on the diagnosis basis and features of the nine types of constitution, namely, normal constitution, Qi deficiency, Yang deficiency, Yin deficiency, Phlegm-dampness, Damp-heat, blood stasis, Qi stagnation, and special constitution. Now it is accepted as a reasonable method of constitution classification. Reaction of the body in the physiological state when exposed to external stimuli is determined by the patients' constitution. The constitution largely determines the susceptibility to some pathogenic factors, the tendency of disease development, and the types of symptoms in the course of disease. The constitution is adjustable that has both relatively stability and dynamic variability. Attachment of more importance to TCM constitution is not only conducive to gaining a good understanding of the occurrence, development, and prognosis of diseases but also an important guidance for the diagnosis, treatment, prevention, and rehabilitation of diseases.

Current research has confirmed that normal-tension glaucoma (NTG) patients have lower intracranial pressure. The lower ICP will lead to a raised translaminar cribrosa gradient when ICP falls below a critical breakpoint, while the intraocular pressure is stable. This may play a role in the development and progression of glaucomatous neuropathy. Evidence indicates the uncoupled relationship between blood pressure, IOP, and ICP is the cause of occurrence and development of glaucoma [1–4]. Clinical study found that NTG patients were mostly in "low functional status" with lower BMI, BP, and weight [5, 6]. They usually experience fatigue and other symptoms of deficiency. These manifestations of NTG patients were consistent with the "Qi deficiency" state of TCM. "Qi deficiency" may cause Yang Qi failing to rise, viscera nutrient deficiency, habitual abortion, organizational slack, organ prolapse, etc. People are prone to fatigue, cold, and other wasting diseases when they have such constitution. The NTG patients have normal IOP, but they still undergo persistent injury of optic nerve and lamina cribrosa collapse finally. These were highly consistent with the "Qi deficiency" theory of TCM. The etiology and pathogenesis of NTG in TCM is that deficiency of vital energy causes failure of Qi activity and nutrition shortage, so the essence and blood fail to nourish the eyes, which eventually develops into the eye disease of NTG.

The Beijing Intracranial and Intraocular Pressure (iCOP) study has confirmed that [7, 8] (1) if primary open-angle glaucoma (POAG) patients do some moderate aerobic exer-

J. Yu · J. Sang · N. Wang (✉)
Beijing Institute of Ophthalmology, Beijing Tongren Eye Center, Beijing Tongren Hospital, Capital Medical University, Beijing, China

Beijing Ophthalmology & Visual Sciences Key Laboratory, Beijing, China
e-mail: wningli@vip.163.com

N. Wang (ed.), *Intraocular and Intracranial Pressure Gradient in Glaucoma*,
Advances in Visual Science and Eye Diseases 1, https://doi.org/10.1007/978-981-13-2137-5_42

cise, IOP will be reduced within a certain range, but excessive exercise will lead to fluctuations in IOP so as to increase the risk of optic nerve injury possibly. This finding is highly compatible with the basic theory of TCM: "the spleen controls the four limbs and muscle." The "spleen-qi deficiency" patients can activate the "spleen-qi" with proper moderate aerobic exercise so that the liquid metabolism is promoted. But excessive exercise will harm the spleen, and then make the condition of "spleen-qi deficiency" worse. This can lead to fluid metabolism disorders, which leads to IOP fluctuation. (2) After 5 min of strenuous exercise, the IOP fluctuation of POAG patients with high myopia was more significant than the POAG patients without high myopia; when both groups were using IOP control eye drops, the IOP of POAG patients with high myopia was much higher than the POAG patients without high myopia, but the 24-h IOP fluctuation was stable in both groups. Its pathogenesis in the theory of TCM mainly includes insufficiency of natural endowment, acquired dystrophy, and excessive use of the eyes, and these developed to deficiency of both Qi and blood. Yi deficiency would contribute to Yang deficiency in the long term, and at last, the Yang would fail to nourish the eyes. Meanwhile, "spleen-Qi deficiency" caused by excessive exercise leads to fluid metabolism disorders and then abnormal fluctuation of the IOP. The conclusion of this study is consistent with the constitution theory of TCM.

Based on the above findings, we hope to find the correlation between the incidence of POAG and TCM constitution by studying the TCM constitution and POAG, so as to define the relationship among the clinical characteristics of different types of POAG patients and different TCM constitutions and to establish the diagnosis, prevention, and treatment system of POAG in TCM.

In our clinic, we found that NTG patients were always thin and weak. With the question "why do NTG patients generally have that appearance?," we began our study, a prospective observational study including 113 NTG and 165HTG patients, without significant differences in age, gender, systolic, and mean arterial blood pressure between two groups (the article has not been published, so the data will not be listed here). And finally, we found that the NTG patients were predisposed to have lean body mass.

Then, what is Qi deficiency disease? In general, Qi can be thought of as "function." There are pathways in the human body wherein Qi flows. What is Qi deficiency state, and is there any relationship between Qi deficiency and NTG? "Qi deficiency" may cause Yang Qi failing to rise, viscera nutrient deficiency, habitual abortion, organizational slack, organ prolapse, etc. The characteristics of Qi deficiency patients are thin, weak, and pale; shortness of breath and unwillingness to speak; spontaneous perspiration; poor appetite; susceptible to cold; fatigue and lassitude; red tongue with tooth marks; and feeble and weak pulse. So with this hypothesis, we continued our study: 116 POAG patients, including 62 HTG and 54 NTG patients, were classified depending on their TCM constitution. Among NTG patients, Qi deficiency constitution accounted for the largest proportion with a ratio of about 34%, while among HTG patients, blood stasis constitution constituted the largest proportion with a ratio of 26%. Therefore, we believe NTG is a kind of Qi deficiency disease. Qi deficiency NTG should be treated with "Bu Zhong Yi Qi" decoction, which can help repair the function of viscera.

Now we draw a conclusion on the relationship between NTG and Qi deficiency. If gene = constitution, while low BMI ICP and BP = Qi deficiency, and the goal for treatment of NTG is to decrease translamina cribrosa gradient, we use "Bu Zhong Yi Qi" decoction. Hence, it is safe to say that the treatment of NTG with TCM and western medicine reaches the same goal by different means.

During the Olympic Games, we saw the dark red circles covering Michael Phelps' body. That is called cupping, an ancient Chinese therapy that uses suction to help circulate blood and relieve muscle tension. Cupping therapy is an alternative Chinese medicinal practice used for healing muscles. Several high-profile Olympic athletes are using it.

Holistic concept as well as syndrome differentiation and treatment is the soul of the basic theory of TCM, and this principle has been well practiced in TCM constitution theory. Those POAG results by iCOP and other researchers were highly consistent with the etiology and pathogenesis of TCM constitution theory. The clinical features coincide with the theory on constitution of TCM. The constitution theory of TCM is a point of penetration to integrate the TCM and western medicine. The guidance of "constitution is adjustable" theory may bring the dawn to the treatment of POAG, especially NTG.

TCM represents a method of diagnosis and treatment that is completely different from western medicine. But they play the same role in different ways.

References

1. Berdahl JP, Allingham RR, Johnson DH. Cerebrospinal fluid pressure is decreased in primary open-angle glaucoma. Ophthalmology. 2008;115:763–8.
2. Ren R, Jonas JB, Tian G, et al. Cerebrospinal fluid pressure in glaucoma. A prospective study. Ophthalmology. 2010;117:259–66.
3. Ren R, Wang N, Zhang X, Cui T, Jonas JB. Trans-lamina cribrosa pressure difference correlated with neuroretinal rim area in glaucoma. Graefes Arch Clin Exp Ophthalmol. 2011;249(7):1057–63.
4. Jonas JB, Wang N. Association between arterial blood pressure, cerebrospinal fluid pressure and intraocular pressure in the pathophysiology of optic nerve head diseases. Clin Exp Ophthalmol. 2011;40(4):e233–4.
5. Pasquale LR, et al. Anthropometric measures and their relation to incident primary open-angle glaucoma. Ophthalmology. 2011;117(8):1521–9.

6. Asrani S, et al. Clinical profiles of primary open angle glaucoma versus normal tension glaucoma patients: a pilot study. Curr Eye Res. 2011;36(5):429–35.
7. Yang Y, Li Z, Wang N, et al. Intraocular pressure fluctuation in patients with primary open-angle glaucoma combined with high myopia. J Glaucoma. 2014;23(1):19–22.
8. Yang YX, Wang NL, Wu L, et al. Effect of high myopia on 24-hour intraocular pressure in patients with primary open-angle glaucoma. Chin Med J (Engl). 2012;125(7):1282–6.

Part VIII

System Disease and POAG

43 Visual Impairment in Astronauts After Long-Duration Space Flight: A Backward of Glaucomatous Optic Neuropathy? Beijing Intracranial and Intraocular Pressure (iCOP) Study

Diya Yang and Ningli Wang

There have been extensive studies on physiologic changes of the astronauts in microgravity environment. However, the effect of this environment on eye remained greatly unknown until recently a report from the National Aeronautics and Space Administration (NASA) documented astronauts presenting visual impairment, anatomical changes in the eye, and elevated cerebrospinal fluid pressure (CSFP) during long-duration space flight [1]. Loss of visual acuity is a significant threat to astronauts' performance, safety, and health. It is therefore important to understand the pathogenesis of this condition.

Beijing iCOP (intracranial and intraocular pressure) study is focused on the anatomical and pathophysiological changes of the eye upon the dynamics of intracranial pressure (ICP or cerebrospinal fluid pressure, CSFP) and intraocular pressure (IOP). Disease conditions like glaucoma, which was largely associated with CSFP and IOP, have been extensively studied by this group. As the current evidences about the visual impairment in long-duration microgravity environment have shown its association with elevated CSFP, a similar paradigm might be found between glaucoma and visual impairment in microgravity environment, and new thoughts might be provoked by reviewing the literatures of iCOP and others.

43.1 Glaucoma: An Optic Neuropathy Correlated with CSFP?

Glaucoma is the primary cause of irreversible blindness worldwide. It affects more than 70 million people in the world [2]. It is characterized by progressive optic nerve degeneration with appearance of optic disk cupping and visual field loss [2, 3]. Elevated IOP is the major risk factor for glaucoma [4]. However, numerous studies have shown that there is a relatively large number of glaucoma patients whose IOP are in the normal range (<21 mmHg) [5]. These patients are then called normal-tension glaucoma (NTG). In population-based Handan Eye Study, it was found that about 80% of Chinese primary open-angle glaucoma (POAG) patients had maximum IOPs less than 21 mmHg over a 24-h period [6]. More interestingly, it was found by The Ocular Hypertension Treatment Study Group (OHTS) that only 9.5% of ocular hypertension patients would develop into glaucomatous optic neuropathy during 5-year follow-up [7]. Why do NTG patients still develop into glaucoma without high IOP? Why do not ocular hypertension (OHT) patients develop into glaucoma with an abnormally high IOP?

Volkov hypothesized that low CSF pressure could be pathogenically associated with glaucomatous optic neuropathy [8]. It was until recently a retrospective chart review study found that CSFP was higher in non-glaucomatous patients than those with open-angle glaucoma and that ocular hypertensive subjects had higher CSFP [9, 10]. In a prospective observational study from iCOP, it was also found that lumbar CSFP was ($P < 0.001$) lower in the normal IOP glaucoma group (9.5 ± 2.2 mmHg) than in the high IOP glaucoma group (11.7 ± 2.7 mmHg) or the control group (12.9 ± 1.9 mmHg) [11]. In a parallel study from iCOP, CSFP was ($P < 0.001$) higher in an ocular hypertensive group (16.0 ± 2.5 mmHg) than in the control group (12.9 ± 1.9 mmHg) [12]. However, whether there is causal relationship between low CSFP and glaucoma remains to be determined.

D. Yang · N. Wang (✉)
Beijing Institute of Ophthalmology, Beijing Tongren Eye Center, Beijing Tongren Hospital, Capital Medical University, Beijing, China

Beijing Ophthalmology & Visual Sciences Key Laboratory, Beijing, China
e-mail: wningli@vip.163.com

N. Wang (ed.), *Intraocular and Intracranial Pressure Gradient in Glaucoma*,
Advances in Visual Science and Eye Diseases 1, https://doi.org/10.1007/978-981-13-2137-5_43

To further understand the role of CSFP in glaucoma, the iCOP group conducted an experimental study on monkeys. Briefly, a continuous low CSFP was resulted by lumbar-peritoneal shunting of the CSF in those monkeys. A bilaterally progressive reduction in RNFL thickness between 12% and 30% and reduction in neuroretinal rim area and volume and increase in cup-to-disk area ratios were shown in two out of four monkeys in the study group. Although no RNFL and cup changes, the third monkey developed a splinter-like disk hemorrhage in one eye. Non-morphologic changes were detected in the fourth monkey, nor did any monkey in the control group [13]. This study first demonstrates that primary CSFP lowering in the nonhuman primate produces an optic neuropathy that is similar to glaucoma in a subset of eyes.

43.2 Trans-laminar Cribrosa Pressure Difference (TLPD) and Its Relation with Glaucomatous Optic Neuropathy

Anatomically, the intraocular space and subarachnoid space of the optic nerve were separated naturally by laminar cribrosa of the eye. From the mechanical point of view, CSFP can act as a counter pressure of IOP; the morphology of the laminar cribrosa and optic disk would be affected by the balancing of the two pressures. Therefore, the difference between IOP and CSFP (trans-lamina cribrosa pressure difference, TLPD) can be important in glaucoma. The iCOP study group found that the TLPD was correlated significantly with neuroretinal rim area and mean visual field defect ($P = 0.008$; $r = 0.38$) in glaucoma patients; moreover, the correlation coefficients of rim area/visual field defect and TLPD were higher than for the associations between rim area/visual field defect and IOP or lumbar CSFP alone [14]. Berdahl et al. also described that TLPD was significantly correlated with cup-to-disk (C/D) ratio ($P < 0.0001$; $r = 0.34$) [15]. These evidences may suggest that TLPD may play a stronger role than IOP or CSFP alone in glaucoma.

However, the assessment of TLPD in the previous mentioned studies was based on lumbar puncture and calculation with IOP but not on a direct measuring of CSFP in the optic nerve subarachnoid space. Whether lumbar CSFP can represent subarachnoid space, CSFP in the optic nerve remains unknown. Due to its invasive and non-practical nature of subarachnoid space CSFP measuring, a noninvasive method is needed. Thus, a 3T-MRI-based imaging technology was developed by iCOP group to measure the subarachnoid space width of the optic nerve as a surrogate for CSFP in site. It was found that NTG group has significantly narrower subarachnoid space width of the optic nerve than the high-pressure group or the control group [16]. This result demonstrated that NTG patients had an abnormally narrow subarachnoid CSF space around the post-laminar optic nerve, suggesting a low CSFP or, as a corollary, a high TLPD.

Based on this technology, the iCOP group developed an algorithm for noninvasive measurement of the intracranial CSFP with MRI-assisted optic nerve subarachnoid space measuring and with intraclass correlation coefficients (ICCs) of 0.87 [17]. Then, an easier formula to estimate the CSFP without measuring of optic nerve subarachnoid space was formed with multivariate analysis (CSFP [mmHg] = 0.44*BMI [kg/m^2] + 0.16*Diastolic Blood Pressure [mmHg] − 0.18*Age [Years] − 1.91). It confirmed previous reports on associations between higher CSFP and younger age, higher BMI, and higher blood pressure [18, 19]. This formula was applied to population-based Beijing Eye Study and Central India Eye and Medical Study. It was found in these population-based studies that calculated TLPD versus IOP showed a better association with glaucoma presence and amount of glaucomatous optic neuropathy [20, 21]. It supports the role of CSFP in NTG.

43.3 Visual Impairment in Long-Duration Space Flight: Another Form of Optic Neuropathy Associated with TLPD?

NASA reported ophthalmic findings of seven astronauts in long-term space flight mission of 6 months. These astronauts present with five disk edema, five globe flattening, five choroidal folds, three cotton wool spots, six retinal nerve fiber layer thickening, and six decreased near vision. Five of seven astronauts with previous near vision complaint a hyperopic shift after back. These five astronauts also showed globe flattening on MRI. For the four astronauts with disk edema, lumbar punctures were performed with opening pressures of 22, 21, 28, and 28.5 cmH_2O on the 60th, 19th, 12th, and 57th day after the mission, respectively. There is also a post-flight questionnaire for 300 astronauts which revealed that approximately 29% and 60% of astronauts on short- and long-duration missions, respectively, experienced a degradation in distant and near visual acuity. Some of these vision changes remain unresolved years after flight [1].

The cause of the above visual impairments and symptoms of the astronauts and the mechanisms behind them are largely unknown. In another study from NASA, 27 astronauts underwent 3T-MRI of the eyeball and optic nerve, which revealed that 96% of the astronauts (26) presented increased diameter of optic nerve sheath. Moreover, in 7 of the 27 astronauts (26%), posterior globe flattening was seen. Other major changes include optic nerve protrusion in 4 (15%) and moderate concavity of the pituitary dome with posterior stalk deviation in 3 (11%) without additional intracranial abnormalities [22]. It was concluded that exposure to microgravity

can result in a spectrum of intraocular and intracranial findings similar to those in idiopathic intracranial hypertension.

Based on the ophthalmic findings and the MRI findings, we proposed that a reverse elevation of TLPD (CSFP > IOP) might be the reason for the visual impairment in long-duration microgravity environment. In the microgravity environment, as the body fluid lost 1-G hydrostatic pressure gradient, there will be a redistribution of the body fluid from lower limbs to the head, causing an elevation of ICP and venous pressure of the precava [23]. Moreover, the elevated venous pressure may also induce cranial venous congestion and an increase in ICP. An elevated ICP may directly transmit elevated subarachnoid CSFP to the perioptic subarachnoid space, which may lead to optic nerve sheath distension and disk edema.

If an elevation of optic nerve subarachnoid space CSFP is not enough to reversely enlarge TLPD, a decreased IOP (hypotony) may also be involved in long-duration space flight. It is recorded that there is an initial spike IOP when exposed to microgravity, and then the IOP would decrease over a period of days. Except for the in-flight studies, post-flight and head-down studies also suggest lowering of IOP possibly occurs during long-term microgravity exposure [1, 24–29].

43.4 TLPD: A Monism for the Causing of Glaucoma or Visual Impairment in Long-Duration Space Flight?

Reversely enlarged TLPD (decrease of pre-laminar IOP and increase of post-laminar CSFP) associated with many symptoms of the long-duration space flight astronauts. Even in 1-G environment (on earth), hypotony of the eye (IOP < 6.5 mmHg) can induce disk edema, posterior globe flattening, choroidal folds, and a hyperopic shift that are similar to the symptoms of astronauts [30]. For idiopathic intracranial hypertension patients, the manifests are also very similar to abovementioned anatomical and pathophysiological changes of the astronauts [31].

More interestingly, all the ocular changes in astronauts during the long-duration space flight, like the distension of optic nerve sheath, disk edema, thickening of retinal nerve fiber layer (RNFL), and flattening of posterior globe, are just as the opposite manner of the changes of glaucoma, in which narrowing of optic nerve subarachnoid space, disk cupping, thinning of RNFL, and posterior bowing of laminar cribrosa are common characteristics [2].

Actually, the pressure gradient (TLPD) between the pre-laminar IOP and post-laminar CSFP across the laminar cribrosa not only has a mechanical effect on the structure of the optic disk, it may also affect the axonal transportation of the optic nerve axons [32] and the ocular blood flow [33]. Hence, when CSFP elevates, ocular vein congestion and blockage of the transportation of anterograde axonal transportation may occur and thereby lead to choroid folds and cotton wool spots in astronauts.

Subsequently, here we might find a clue that a forward elevation of TLPD (IOP > CSFP) may cause optic neuropathy that was similar to glaucomatous changes and a backward elevation of TLPD (CSFP > IOP) may cause optic neuropathy that was similar to idiopathic intracranial hypertension or visual impairment associated with long-duration space flight.

43.5 Conclusion

In summary, microgravity-induced loss of hydrostatic pressure gradients initiates a shift of CSF and vein blood distribution, which may result in the elevation of ICP and CSFP of the optic nerve subarachnoid space. Thus, a reversely enlarged TLPD presents a series of clinical features that are opposite to glaucomatous optic neuropathy. We hypothesized that the dynamic and imbalance of the TLPD play an important role in optic neuropathy like glaucoma and visual impairment of astronauts. Animal model researches are of importance and yet to be continued to elucidate the downstream mechanisms of increased trans-laminar cribrosa pressure difference in this optic neuropathy. Rational and precise procedure of noninvasive measuring of TLPD should be developed in the future. The diagnosis and management of this optic neuropathy based on TLPD are of importance in the following studies.

References

1. Mader TH, Gibson CR, et al. Optic disc edema, globe flattening, choroidal folds, and hyperopic shifts observed in astronauts after long-duration space flight. Ophthalmology. 2011;118(10):2058–69.
2. Weinreb RN, Aung T, Medeiros FA. The pathophysiology and treatment of glaucoma: a review. JAMA. 2014;311(18):1901–11.
3. Hitchings RA, Spaeth GL. The optic disc in glaucoma I: classification. Br J Ophthalmol. 1976;60:778–85.
4. Leske MC, Heijl A, Hussein M, et al. Factors for glaucoma progression and the effect of treatment: the early manifest glaucoma trial. Arch Ophthalmol. 2003;121:48–56.
5. Drance SM. Some factors in the production of low tension glaucoma. Br J Ophthalmol. 1972;56:229–42.
6. Wang NL, Friedman DS, et al. A population-based assessment of 24-hour intraocular pressure among subjects with primary open-angle glaucoma: the Handan eye study. Invest Ophthalmol Vis Sci. 2011;52(11):7817–21.
7. Kass MA, Heuer DK, Higginbotham EJ, Johnson CA, Keltner JL, Miller JP, Parrish RK 2nd, Wilson MR, Gordon MO. The Ocular Hypertension Treatment Study: a randomized trial determines that topical ocular hypotensive medication delays or prevents the onset of primary open-angle glaucoma. Arch Ophthalmol. 2002;120(6):701–13. discussion 829-730

8. Volkov VV. Essential element of the glaucomatous process neglected in clinical practice. Oftalmol Zh. 1976;31:500–4.
9. Berdahl JP, Allingham RR, Johnson DH. Cerebrospinal fluid pressure is decreased in primary open-angle glaucoma. Ophthalmology. 2008;115:763–8.
10. Berdahl JP, Fautsch MP, Stinnett SS, Allingham RR. Intracranial pressure in primary open angle glaucoma, normal tension glaucoma, and ocular hypertension: a case-control study. Invest Ophthalmol Vis Sci. 2008;49:5412–8.
11. Ren R, Jonas JB, Tian G, et al. Cerebrospinal fluid pressure in glaucoma. A prospective study. Ophthalmology. 2010;117:259–66.
12. Ren R, Zhang X, Wang N, Li B, Tian G, Jonas JB. Cerebrospinal fluid pressure in ocular hypertension. Acta Ophthalmol. 2011;89:E142–8.
13. Yang D, Fu J, Hou R, Liu K, Jonas JB, Wang H, Chen W, Li Z, Sang J, Zhang Z, Liu S, Cao Y, Xie X, Ren R, Lu Q, Weinreb RN, Wang N. Optic neuropathy induced by experimentally reduced cerebrospinal fluid pressure in monkeys. Invest Ophthalmol Vis Sci. 2014;55(5):3067–73.
14. Ren R, Wang N, et al. Trans-lamina cribrosa pressure difference correlated with neuroretinal rim area in glaucoma. Graefes Arch Clin Exp Ophthalmol. 2011;249(7):1057–63.
15. Berdahl JP, Allingham RR. Intracranial pressure and glaucoma. Curr Opin Ophthalmol. 2010;21(2):106–11.
16. Wang NL, Xie XB, Yang DY, et al. Orbital cerebrospinal fluid space in glaucoma: the Beijing iCOP Study. Ophthalmology. 2012;119(10):2065–73.
17. Xie X, Zhang X, Fu J, et al. Noninvasive intracranial pressure estimation by orbital subarachnoid space measurement: the Beijing Intracranial and Intraocular Pressure (iCOP) study[J]. Crit Care. 2013;17(4):R162.
18. Berdahl JP, Fleischman D, Zaydlarova J, Stinnett S, Allingham RR, et al. Body mass index has a linear relationship with cerebrospinal fluid pressure. Invest Ophthalmol Vis Sci. 2012;53:1422–7.
19. Ren R, Wang N, Zhang X, Tian G, Jonas JB. Cerebrospinal fluid pressure correlated with body mass index. Graefes Arch Clin Exp Ophthalmol. 2012;250:445–6.
20. Jonas JB, Wang N, Wang YX, You QS, Xie X, Yang D, Xu L. Body height, estimated cerebrospinal fluid pressure and open-angle glaucoma. The Beijing eye study 2011. PLoS One. 2014;9(1):e86678.
21. Jonas JB, Nangia V, Wang N, Bhate K, Nangia P, Nangia P, Yang D, Xie X, Panda-Jonas S. Trans-lamina cribrosa pressure difference and open-angle glaucoma. The central India eye and medical study. PLoS One. 2013;8(12):e82284.
22. Kramer LA, Sargsyan AE, et al. Orbital and intracranial effects of microgravity: findings at 3-T MR imaging. Radiology. 2012;263(3):819–27.
23. Zhang LF, Hargens AR. Intraocular/intracranial pressure mismatch hypothesis for visual impairment syndrome in space. Aviat Space Environ Med. 2014;85(1):78–80.
24. Draeger J, Wirt H, Schwartz R. Tonometry under microgravity conditions. In: Sahm PR, Jansen R, Keller MH, eds. Proceedings of the Norderney Symposium on Scientific Results of the German Spacelab Mission: D1, Nordenerney, Germany, August 27–29, 1986. Koln, Germany: Wissenschaftliche Projektfu¨hrung DI c/o DFVLR; 1987;503–9.
25. Mader TH, Taylor GR, Hunter N, et al. Intraocular pressure, retinal vascular, and visual acuity changes during 48 hours of 10 degrees head-down tilt. Aviat Space Environ Med. 1990;61:810–3.
26. Chiquet C, Custaud MA, Le Traon AP, et al. Changes in intraocular pressure during prolonged (7-day) head-down tilt bedrest. J Glaucoma. 2003;12:204–8.
27. Drozdova NT, Grishin EP. State of the visual analyzer during hypokinesia [in Russian]. Kosm Biol Med. 1972;6:46–9.
28. Mader TH, Gibson CR, Caputo M, et al. Intraocular pressure and retinal vascular changes during transient exposure to microgravity. Am J Ophthalmol. 1993;115:347–50.
29. Nicogossian AE, Parker JF Jr. Space physiology and medicine. Washington, DC: NASA, Technical Information Branch; 1982;158. NASA SP-447.
30. Costa VP, Arcieri ES. Hypotony maculopathy. Acta Ophthalmol Scand. 2007;85:586–97.
31. Jacobson DM. Intracranial hypertension and the syndrome of acquired hyperopia with choroidal folds. J Neuroophthalmol. 1995;15(3):178–85.
32. Almasieh M, Wilson AM, Morquette B, Cueva Vargas JL, Di Polo A. The molecular basis of retinal ganglion cell death in glaucoma. Prog Retin Eye Res. 2012;31(2):152–81.
33. Costa VP, Harris A, Anderson D, Stodtmeister R, Cremasco F, Kergoat H, Lovasik J, Stalmans I, Zeitz O, Lanzl I, Gugleta K, Schmetterer L. Ocular perfusion pressure in glaucoma. Acta Ophthalmol. 2014;92(4):e252–66.

Genetic Insights into Primary Open-Angle Glaucoma

44

Louis R. Pasquale

Primary open-angle glaucoma (POAG) is a public health problem with a projected prevalence of 110 million patients overall by 2040; 40 million of these cases will come from Asia [1]. Therefore a deeper understanding of this disease is an urgent challenge as treatments that address the root cause of POAG are needed. POAG is a seemingly enigmatic disease. The intraocular pressure (IOP) may or may not be elevated. If IOP is elevated, anterior segment examination does not reveal clues as to why this is the case. The optic nerve is excavated and pale, and there is attendant VF loss (Fig. 44.1). Genomics offers an incredible opportunity to gain insights into this IOP-related otherwise idiopathic optic neuropathy.

It's worth reviewing the POAG genetics timeline. As early as 1842, a time that predates Mendel and his pea, Benedict suggested that glaucoma was hereditary. In 1987, Teikara performed classic twin studies that suggested the heritability for POAG was only 13% [2] In 2000, the first draft of the human genome was announced providing a blueprint to understand POAG and other common complex diseases. Fast-forward to 2016, where the International Glaucoma Genetics Consortium and other investigators have discovered over 20 genes for POAG, some of which are depicted in the Manhattan plot shown in Fig. 44.2 [3] The strategy that was used to discover these genes was to form large case-control groups in clinics and populations around the world. These efforts were supplemented with genetic searches for disc area [4], cup area [4], vertical cup-disc ratio (Fig. 44.3) [5], IOP (Fig. 44.4) [5, 6], and central corneal thickness (CCT) [7], as genes for the latter glaucoma-related traits could be excellent candidate genes for POAG.

Associations with vertical CDR (n = 27,878)—multiethnic results.

GWAS for IOP: results from 18 multiethnic cohorts (n = 35,296).

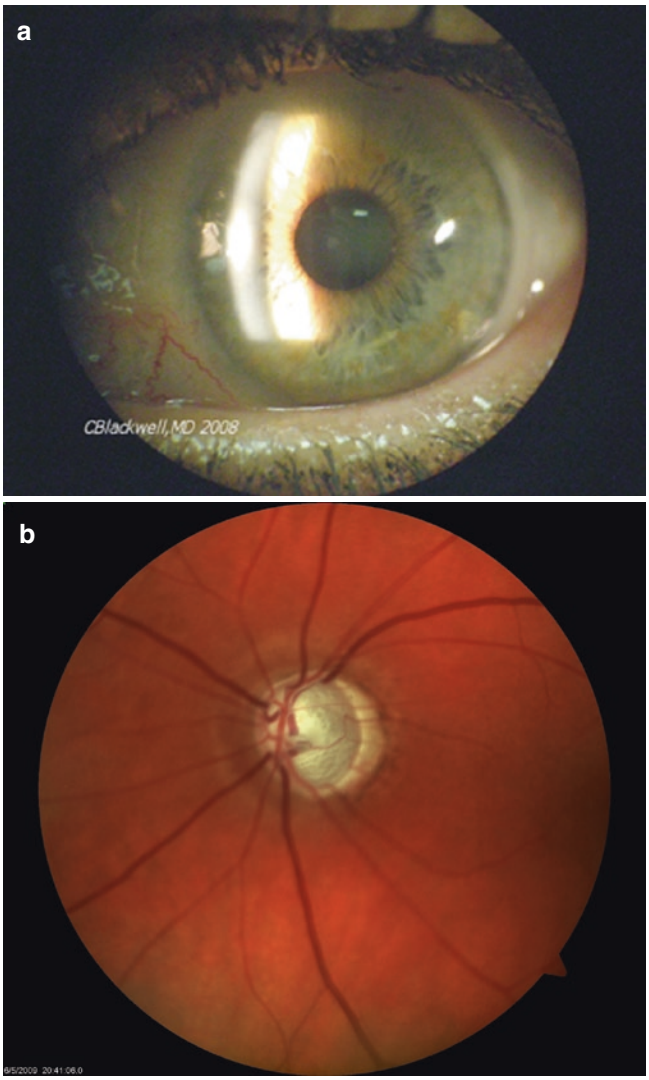

Fig. 44.1 (**a**) A typical patient with advanced primary open-angle glaucoma The anterior segment exam is unremarkable, and the highest known intraocular pressure is only slightly elevated (22 mmHg); (**b**) yet the disc shows advanced cupping

L. R. Pasquale (✉)
Department of Ophthalmology, Icahn School of Medicine at Mount Sinai, New York, NY, USA
e-mail: Louis.Pasquale@mssm.edu

N. Wang (ed.), *Intraocular and Intracranial Pressure Gradient in Glaucoma*,
Advances in Visual Science and Eye Diseases 1, https://doi.org/10.1007/978-981-13-2137-5_44

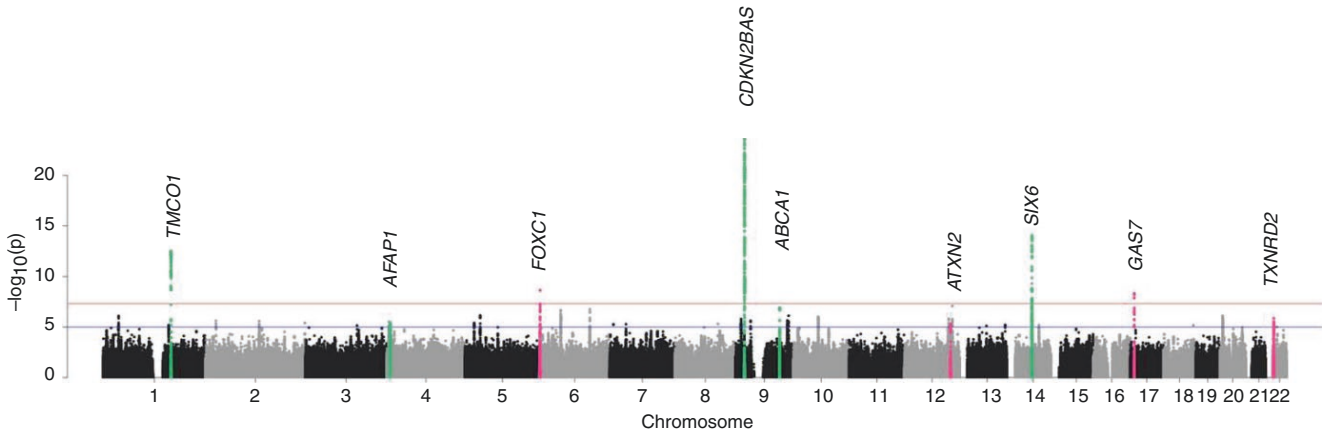

Fig. 44.2 Manhattan plot from a genome-wide association study illustrating several genes associated with primary open-angle glaucoma (Reprinted with permission from Bailey et al. [3])

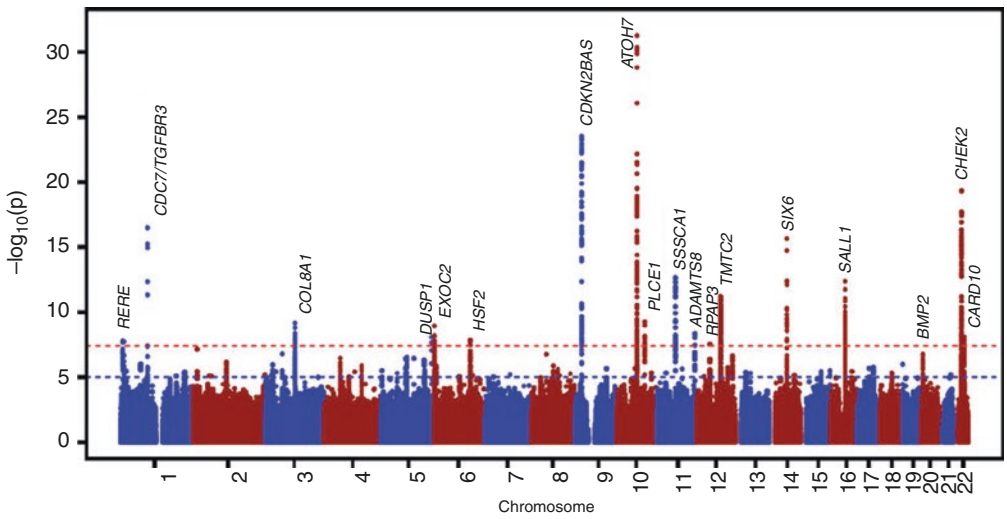

Fig. 44.3 Manhattan plot from a genome-wide association study performed by the International Glaucoma Genetics Consortium investigators illustrating several genes associated with vertical cup-disc ratio (Reprinted with permission from Springelkamp et al. [5])

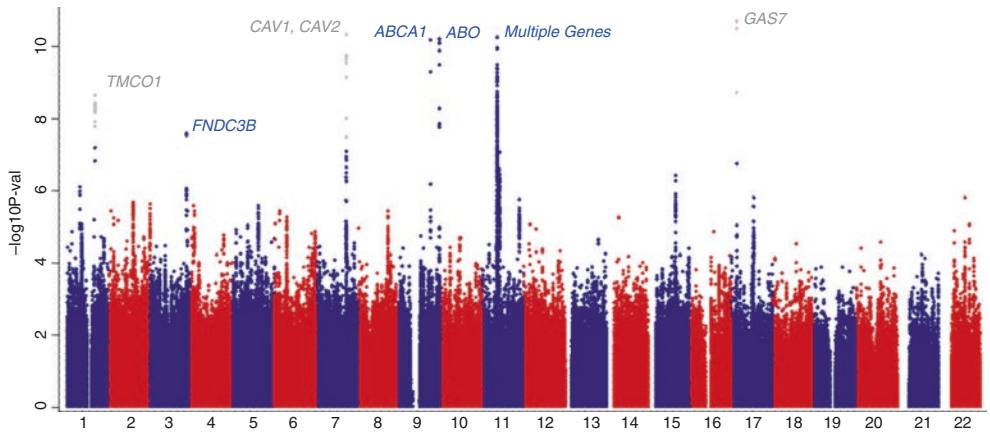

Fig. 44.4 Manhattan plot from a genome-wide association study performed by the International Glaucoma Genetics Consortium investigators illustrating several genes associated with intraocular pressure (Reprinted with permission from Hysi et al. [6])

While these Manhattan plots summarize tremendous achievements in POAG gene discovery, I will summarize five insights that have been revealed from this work.

44.1 First Insight

The first insight relates to the chromosome 9 region containing *CDKN2B-AS*, which contain loci that affect vulnerability to POAG across the IOP spectrum (Fig. 44.5). As we know from the previous studies, some genes are associated with normal-tension glaucoma, and the others seem to be more related with high-tension glaucoma. The *CDKN2B-AS* region has both relationships with HTG and NTG. This *CDKN2B-AS* region plays a role in cell cycling, which may affect the glial support cells that support the retinal ganglion cells (RGCs) which do not turn over. POAG patients with high at-risk *CDKN2B-AS* loci have lower IOP, higher CDR, and more advanced disease than comparable POAG patients without these at-risk loci [8, 9] Furthermore, transgenic mice with a 70 kB deletion syntenic to the human chromosome 9p21 containing *CDKN2B-AS* were observed to be more vulnerable to RGC dropout than wild-type and heterozygous animals [10] In addition, several protective *CDKN2-AS* alleles are conspicuously absent in African-derived populations [11].

CDKN2B-AS is an unexpected major hotspot in the genome, and several diseases such as melanoma, glioma, POAG, coronary artery disease, and diabetes discretely localize there [12]. Perhaps variants related to enhanced cell turnover (leading to glioma) or cellular senescence (leading to glaucoma) are encoded in different aspects of this genomic region.

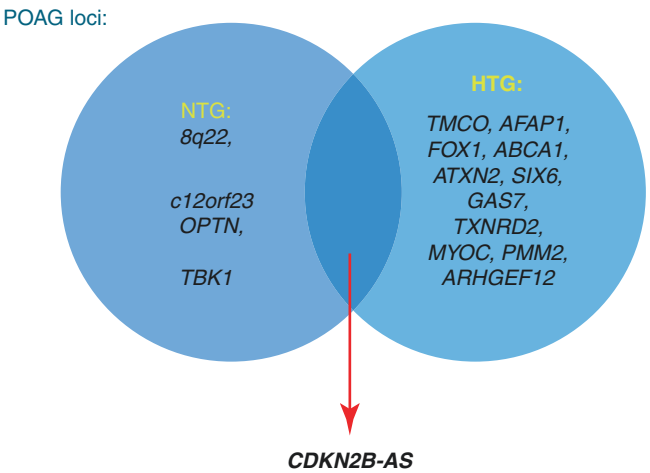

Fig. 44.5 *CDKN2B-AS* represents a gene region that affects vulnerability to POAG across the IOP spectrum. Other genes listed seem more strongly associated with normal-tension glaucoma (NTG) or high-tension glaucoma (HTG)

44.2 Bottom Line

More work is needed to understand how *CDKN2B-AS* loci contribute to RGC biology in general and glaucoma in particular.

44.3 Second Insight

There is a strong overlap between genes associated with variation in disc morphology and POAG [13]. This underscores the fact that disc structure, especially the cup-disc ratio, is central to the glaucomatous process and may explain why normal-tension glaucoma is so prevalent in populations around the world (Fig. 44.6).

44.4 Third Insight

Several genes for IOP are also genes for POAG (*TMCO1*, *CAV1/CAV2*, and *GAS7*), underscoring the importance of IOP in POAG pathogenesis.

44.5 Fourth Insight

A thin central cornea is risk factor for POAG. CCT is one of the most highly heritable traits in medicine (95%). There are 27 known genome-wide common loci for CCT, including one (*ZNF469*), where rare variants produce a Mendelian form of extreme corneal thinning called Brittle cornea syndrome [7]. Yet neither ZNF469 nor most of the other CCT loci were associated with POAG. One CCT gene (*FNDC3B*) was associated with POAG, but the allele associated with a thicker CCT was the at-risk locus for POAG, suggesting this result could be a false-positive finding. These data suggest that, to date, the gene variants associated with CCT are not directly associated with POAG.

44.6 Fifth Insight

Genetic pathway analysis indicates that vascular tone is important in POAG [14] and suggests nitric oxide (NO) signaling is a therapeutic target in this disease. These data are supported by evidence that IOP increases modestly and the optic nerve degenerates in mice with defective NO signaling

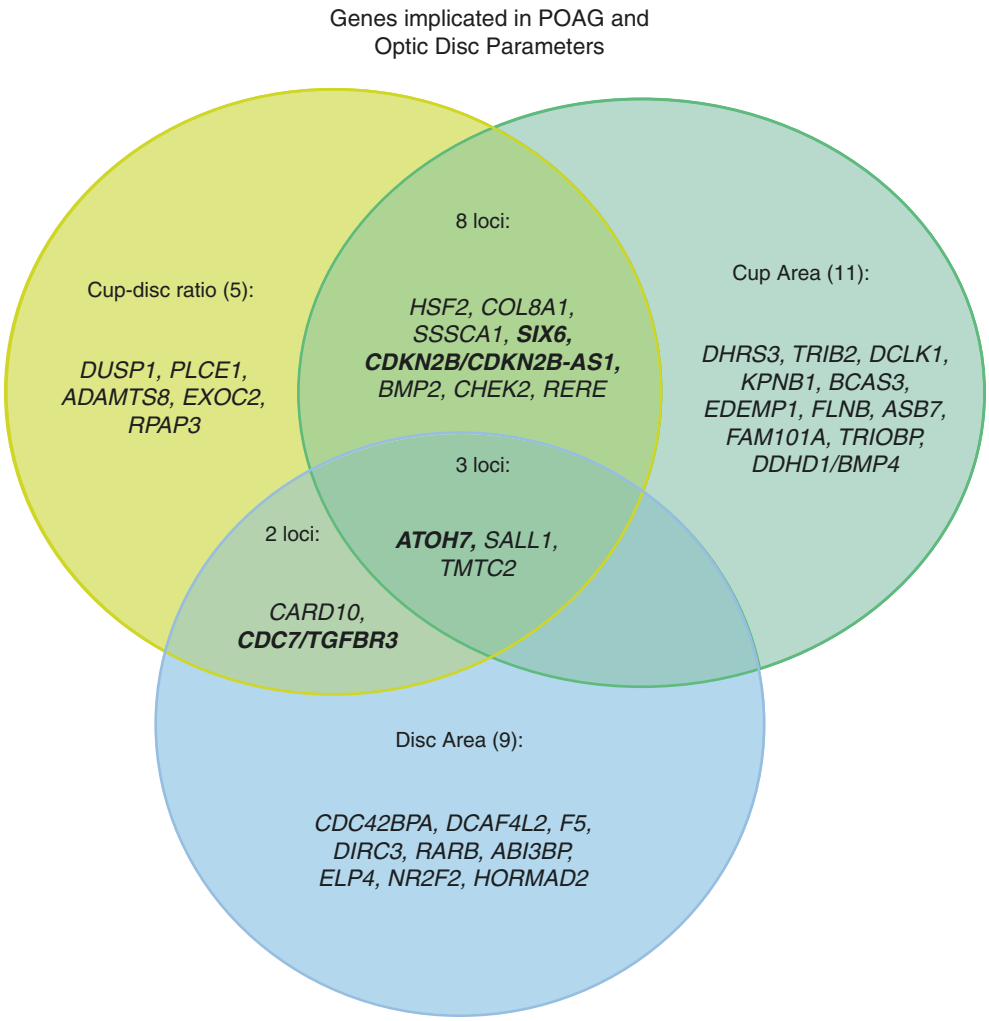

Fig. 44.6 Genetic loci for cup-disc ratio, cup area, and disc area are illustrated. Loci also associated with primary open-angle glaucoma are highlighted in bold font (Reprinted with permission from Iglesias et al. [13])

[15]. NOS3, the enzyme responsible for generating NO, sits adjacent to CAV1 on biological membranes. *CAV1* was the first genome-wide variant for POAG [16] that was independently confirmed [17]. *CAV1* reciprocally works with *NOS3* to regulate NO production. Interestingly, with the emergence of rho kinase inhibitors and NO donators as possible new therapeutic entities for glaucoma, the endothelial cell relaxation pathway is an attractive new target for glaucoma intervention [18, 19].

44.7 Future Directions

An international mega-analysis should be conducted to find more genes for POAG. Existing datasets should undergo HRC (Haplotype Reference Consortium) imputation so to generate genotype calls for alleles with low frequency. Some of these alleles may emerge as new genes for POAG and glaucoma-related traits. Efforts should be made to predict glaucoma features such as age of onset, rate of progression, and response to treatment as well as to identify novel drug targets for POAG.

References

1. Tham YC, Li X, Wong TY, Quigley HA, Aung T, Cheng CY. Global prevalence of glaucoma and projections of glaucoma burden through 2040: a systematic review and meta-analysis. Ophthalmology. 2014;121(11):2081–90.
2. Teikari JM. Genetic factors in open-angle (simple and capsular) glaucoma. A population-based twin study. Acta Ophthalmol (Copenh). 1987;65(6):715–20.
3. Bailey JN, Loomis SJ, Kang JH, et al. Genome-wide association analysis identifies TXNRD2, ATXN2 and FOXC1 as susceptibility loci for primary open-angle glaucoma. Nat Genet. 2016;48(2):189–94.
4. Springelkamp H, Mishra A, Hysi PG, et al. Meta-analysis of genome-wide association studies identifies novel loci associated with optic disc morphology. Genet Epidemiol. 2015;39(3):207–16.
5. Springelkamp H, Hohn R, Mishra A, et al. Meta-analysis of genome-wide association studies identifies novel loci that influence cupping and the glaucomatous process. Nat Commun. 2014;5:4883.

6. Hysi PG, Cheng CY, Springelkamp H, et al. Genome-wide analysis of multi-ancestry cohorts identifies new loci influencing intraocular pressure and susceptibility to glaucoma. Nat Genet. 2014;46(10):1126–30.
7. Lu Y, Vitart V, Burdon KP, NEIGHBOR consortium. GWAS on central corneal thickness identifies a total of 27 associated loci, including six risk loci for keratoconus. Nat Genet. 2012;45(2):155–63.
8. Pasquale LR, Loomis SJ, Kang JH, et al. CDKN2B-AS1 genotype-glaucoma feature correlations in primary open-angle glaucoma patients from the United States. Am J Ophthalmol. 2013;155(2):342–53. e345
9. Burdon KP, Crawford A, Casson RJ, et al. Glaucoma risk alleles at CDKN2B-AS1 are associated with lower intraocular pressure, normal-tension glaucoma, and advanced glaucoma. Ophthalmology. 2012;119(8):1539–45.
10. Gao S, Jakobs TC. Mice homozygous for a deletion in the glaucoma susceptibility locus INK4 show increased vulnerability of retinal ganglion cells to elevated intraocular pressure. Am J Pathol. 2016;186(4):985–1005.
11. Altshuler DM, Gibbs RA, Peltonen L, et al. Integrating common and rare genetic variation in diverse human populations. Nature. 2010;467(7311):52–8.
12. Pasmant E, Sabbagh A, Vidaud M, Bieche I. ANRIL, a long, noncoding RNA, is an unexpected major hotspot in GWAS. FASEB J. 2011;25(2):444–8.
13. Iglesias AI, Springelkamp H, Ramdas WD, Klaver CC, Willemsen R, van Duijn CM. Genes, pathways, and animal models in primary open-angle glaucoma. Eye (Lond). 2015;29(10):1285–98.
14. Kang JH, Loomis SJ, Yaspan BL, et al. Vascular tone pathway polymorphisms in relation to primary open-angle glaucoma. Eye (Lond). 2014;28(6):662–71.
15. Buys ES, Ko YC, Alt C, et al. Soluble guanylate cyclase alpha1-deficient mice: a novel murine model for primary open angle glaucoma. PLoS One. 2013;8(3):e60156.
16. Thorleifsson G, Walters GB, Hewitt AW, et al. Common variants near CAV1 and CAV2 are associated with primary open-angle glaucoma. Nat Genet. 2010;42(10):906–9.
17. Wiggs JL, Hee Kang J, Yaspan BL, et al. Common variants near CAV1 and CAV2 are associated with primary open-angle glaucoma in Caucasians from the USA. Hum Mol Genet. 2011;20(23):4707–13.
18. Ren R, Li G, Le TD, Kopczynski C, Stamer WD, Gong H. Netarsudil increases outflow facility in human eyes through multiple mechanisms. Invest Ophthalmol Vis Sci. 2016;57(14):6197–209.
19. Kaufman PL. Latanoprostene bunod ophthalmic solution 0.024% for IOP lowering in glaucoma and ocular hypertension. Expert Opin Pharmacother. 2017;18(4):433–44.

Alzheimer Disease: Intracranial Pressure and Glaucoma

45

Yan Lu and Ningli Wang

Alzheimer's disease (AD) is a regular, age-related dementia and is also the most common type of senile dementia. Its pathological features include (1) Aβ plaques, (2) neurofibrillary tangles, (3) hyperphosphorylated tau, (4) neuronal degeneration, and (5) amyloid angiopathy. Retina is the extension of central nervous system (CNS), which makes it as the similar source of tissue and anatomical characteristics with CNS; hence, retina can be an indicator of CNS diseases at various circumstances. Several researches testified that the incidence of glaucoma in Alzheimer patients is higher than normal people, the mechanism of which remains unclear.

Clinical research found that the incidence of glaucoma in Alzheimer patients is higher than that of normal people. German study reported that incidence of glaucoma in Alzheimer patients is 25.9% and 5.2% in normal people, whereas Japanese research showed 23.8% in AD patients and 9.9% in normal people [1, 2]. Our study also found a higher incidence of 43.2% in AD patients, versus 12.5% in normal people (Fig. 45.1). Figure 45.2 demonstrates the big optic cup of AD patients.

Both clinical trials and animal experiments discovered that the pathological changes of AD patients in retina correspond to that of optic neuropathy in glaucoma. For example, the number of retinal ganglion cells reduced in both AD mouse and AD patients. Enlargement of C/D and attenuation of retinal nerve fiber were found in AD patients. In our research, it is noted that retinal nerve fiber layer becomes thinner with an obvious attenuation in superior and inferior parts (Fig. 45.3) [3].

Further, we divided patients into four groups according to different stages including mild cognitive impairment (MCI), moderate AD, medium AD, and severe AD. Changes of optic nerve fiber were studied, respectively. We discovered that there is no significant difference in intraocular pressure between every stage of AD and control group. However, attenuation of superior optic nerve fiber layer was detected in every stage of AD, and the apparent thinning of inferior optic nerve fiber layer was noted in severe AD patients. These evidence reveal that damage appears first in superior optic nerve fiber layer in early AD, and then the inferior part got involved with the aggravation of AD, which corresponds to the feature of optic neuropathy in glaucoma (Tables 45.1 and 45.2).

Imageological examination of AD shows atrophy of hippocampus and cerebrum, which leads to decrease of ICP according to the theory of brain reduction. Both the elevation of IOP and decrease of ICP can cause glaucomatous optic neuropathy. Meanwhile, a clinical trial [4] found ICP of AD is lower than normal, with 96.1% (174 out of 181) having a ICP of 103 ± 47 mmH_2O compared to that of normal range of 70–200 mmH_2O (Fig. 45.4). Therefore, we speculate that an increase of trans-lamina cribrosa pressure induced by reduction of ICP might be one of the mechanisms of glaucoma in AD patients.

Our recent research collected amnestic mild cognitive impairment (aMCI) and AD patients, with different exclusion criteria, adding the following protocols: C/D greater than or equal to 0.6 and difference of C/D in binoculus greater than or equal to 0.2. We found that IOP of aMCI and AD patients is lower than that of control groups ($p < 0.05$); see Table 45.3.

Analyze the reason why IOP of aMCI and AD reduces: (1) Blood flow volume of brain in AD and aMCI might cause decrease of aqueous humor secretion; thus a reduction of IOP forms. (2) Reduction of IOP in aMCI and AD patients may be a meaning of self-protection when enduring increase of trans-lamina cribrosa pressure induced by low ICP.

Y. Lu
Department of Ophthalmology, Beijing Shijitan Hospital, Capital Medical University, Beijing, China

N. Wang (✉)
Beijing Institute of Ophthalmology, Beijing Tongren Eye Center, Beijing Tongren Hospital, Capital Medical University, Beijing, China

Beijing Ophthalmology & Visual Sciences Key Laboratory, Beijing, China
e-mail: wningli@vip.163.com

N. Wang (ed.), *Intraocular and Intracranial Pressure Gradient in Glaucoma*,
Advances in Visual Science and Eye Diseases 1, https://doi.org/10.1007/978-981-13-2137-5_45

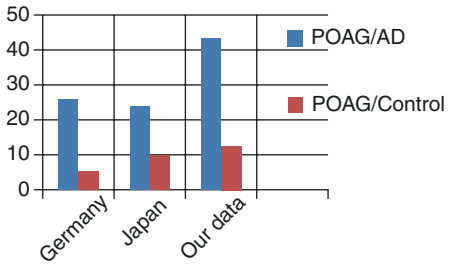

Fig. 45.1 The incidence of glaucoma in Alzheimer patients is higher than that of normal people

Gemany

Glaucoma were found in 29 out of 112 patients with AD (**25.9%**)

When compared to a control group (**5.2%**)

Japan

OAG was found in 41 of the AD patients (**23.8%**)

which was a higher prevalence than that in the control(**9.9%**).

Our data

Glaucoma were found in 32 out of 74 patients with AD (**43.2%**).

When compared to a control group(9/72) (**12.5%**)

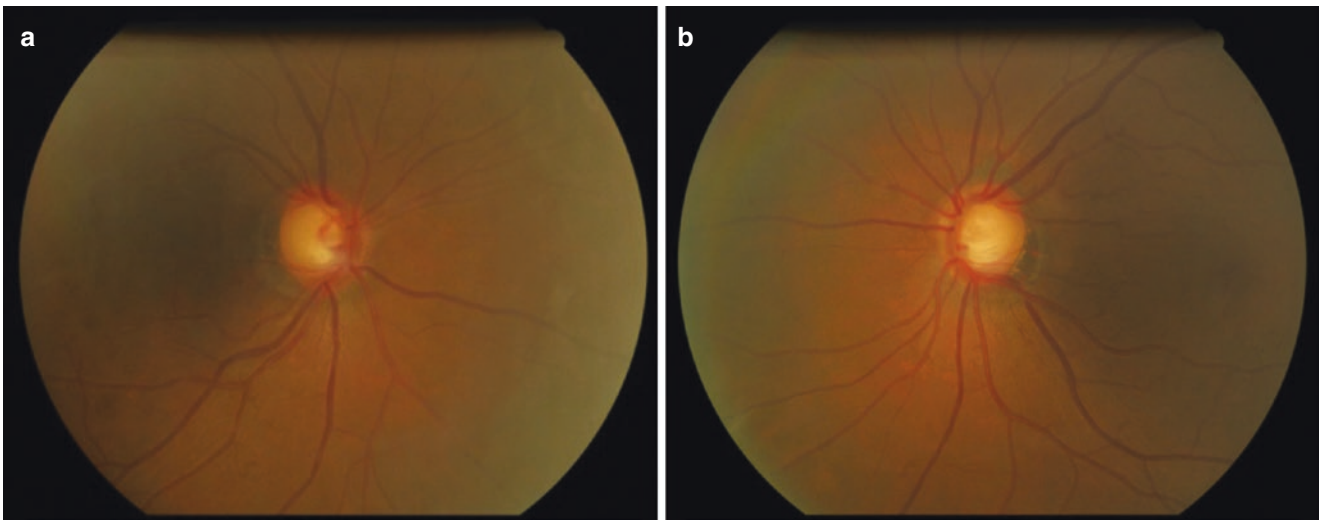

Fig. 45.2 Photograph of fundus in AD patients shows big optic cup

Fig. 45.3 Obvious attenuation of retinal nerve fiber layer especially in superior and inferior parts compares to control group (Reprinted with permission from Lu Y, Li Z, Zhang X, et al. Retinal nerve fiber layer structure abnormalities in early Alzheimer's disease: evidence in optical coherence tomography [J]. Neurosci Lett. 2010, 480(1):69–72)

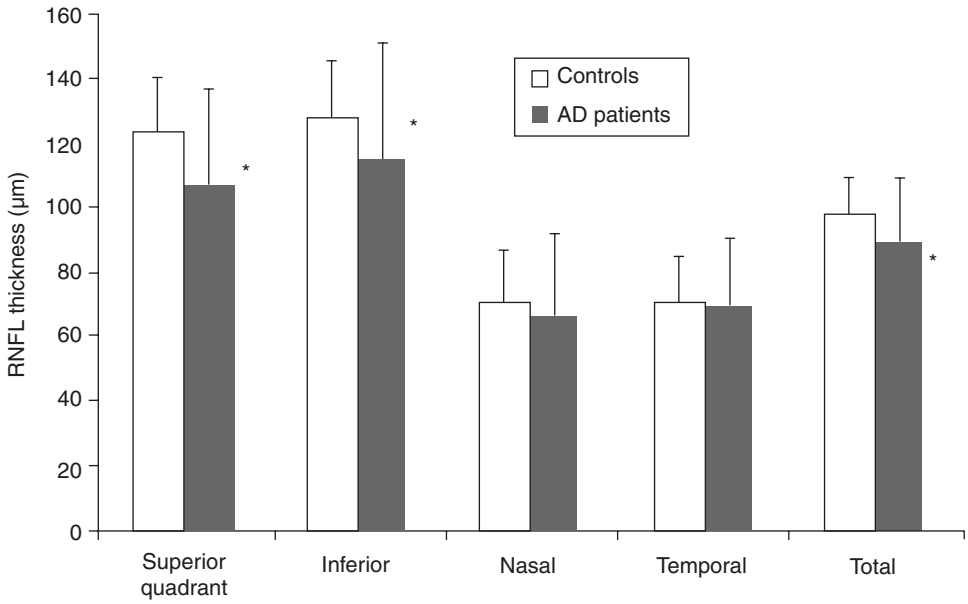

The RNFL thickness is thinner at superior, inferior postion than those in control subjects ($p<0.05$). The value at nasal and temporal position is lower than those in controls, but not reach to a statistical significance. The total average thichness is much lower in the AD patients than those in controls ($p<0.05$).

Table 45.1 Regular characteristics of control group, MCI, and different stages of AD patients

	Control	MCI	Mild AD	Moderate AD	Severe AD	*P*
Number	72	31	27	28	21	–
Sex (F/M)	38/34	18/13	15/12	16/12	11/10	>0.05
Age	70.78 ± 6.48	70.58 ± 7.03	72.74 ± 6.67	72.07 ± 5.06	71.57 ± 7.87	>0.05
IOP	15.6 ± 1.5	15.2 ± 1.9	14.9 ± 1.2	16.1 ± 1.0	15.9 ± 0.9	>0.05

There is no significant difference in intraocular pressure between MCI, every stage of AD, and control group

Table 45.2 Comparison of superior, inferior, nasal, temporal, and total optic nerve fiber layer thickness in control group, MCI, and different stages of AD

	Superior	Inferior	Nasal	Temporal	Total
Control	127.40 ± 16.94	135.75 ± 14.93	80.78 ± 23.90	71.65 ± 15.27	104.53 ± 11.30
MCI	124.19 ± 15.33▲	131.45 ± 14.93	76.80 ± 22.92	71.48 ± 13.66	100.09 ± 12.13▲
Mild	120.00 ± 16.19▲	125.11 ± 11.99	76.93 ± 19.49	63.37 ± 16.05	94.77 ± 8.19▲▲
Moderate	119.71 ± 21.28▲▲■	123.57 ± 14.24	72.71 ± 26.92	71.43 ± 16.36	94.33 ± 10.62▲▲■
Severe	113.80 ± 24.65▲▲■	121.90 ± 14.80▲▲■	65.95 ± 20.32	70.48 ± 16.33	92.16 ± 6.37▲▲▲■
F	2.788*	6.667***	1.880	1.582	9.810***

Attenuation of superior optic nerve fiber layer was detected in every stage of AD compared to control group, and the apparent thinning of inferior optic nerve fiber layer was noted in severe AD patients
Comparison to the control group: ▲$p < 0.05$, ▲▲$p < 0.01$, comparison to MCI: ■$p < 0.05$, F test: $^{*}p < 0.05$, $^{**}p < 0.001$

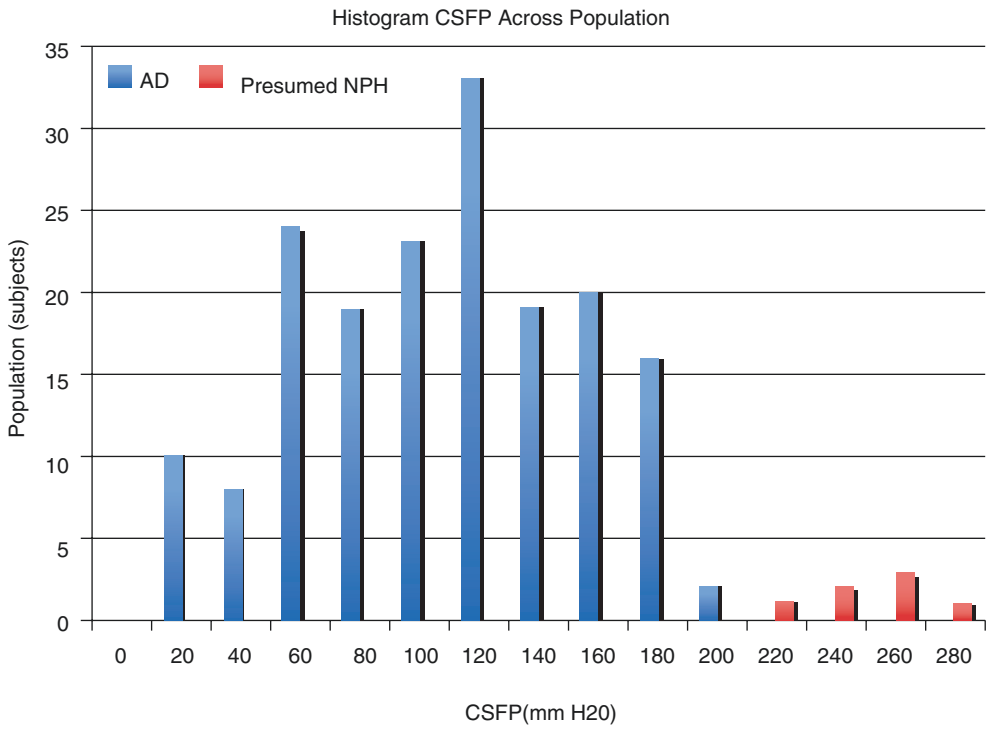

Fig. 45.4 AD patients have lower ICP compared to that of control (Reprinted with permission from Silverberg G, Mayo M, Saul T, et al. Elevated cerebrospinal fluid pressure in patients with Alzheimer's disease [J]. Cerebrospinal Fluid Res. 2006, 3:7)

Table 45.3 IOP comparison of control, AD, and aMCI

	AD ($n = 24$)	aMCI ($n = 22$)	Control ($n = 30$)
IOP Mean ± SE (mmHg)	12.7 ± 2.8*	12.6 ± 3.0**	14.4 ± 3.3

*$P < 0.05$, AD vs. control
**$P < 0.05$, aMCI vs. control

References

1. Tamura H, Kawakami H, Kanamoto T, et al. High frequency of open-angle glaucoma in Japanese patients with Alzheimer's disease[J]. J Neurol Sci. 2006;246(1–2):79–83.
2. Wostyn P, Audenaert K, De Deyn PP. Alzheimer's disease: cerebral glaucoma?[J]. Med Hypotheses. 2010;74(6):973–7.
3. Lu Y, Li Z, Zhang X, et al. Retinal nerve fiber layer structure abnormalities in early Alzheimer's disease: evidence in optical coherence tomography[J]. Neurosci Lett. 2010;480(1):69–72.
4. Silverberg G, Mayo M, Saul T, et al. Elevated cerebrospinal fluid pressure in patients with Alzheimer's disease[J]. Cerebrospinal Fluid Res. 2006;3:7.

46 Surgical Management Strategies for Pseudotumor Cerebri/Idiopathic Intracranial Hypertension

John M. McGregor

Although a rare condition generally, we have seen a growing population of idiopathic intracranial hypertension (IIH) patients over the years. We have evolved better management strategies and improved on our options for diagnosis and treatment. These patients all have elevated intracranial pressures (ICP). Symptomatic presentation varies. The possibilities of visual deterioration and blindness drive our therapeutic interventions. When patients have reached the point where their condition is no longer effectively managed by medical means and lifestyle adjustments, we have developed procedural strategies and surgical interventions to assist in the management. We hope to share these in this presentation.

The pathophysiology of IIH remains unclear. There are several possible explanations with lines of evidence to support them. It is possible that ICP is elevated secondary to decreased absorption or, less likely, increased production of cerebrospinal fluid (CSF) [1]. Some authors have suggested that cerebral blood volume fluctuations may be responsible for the increased pressure, the so-called hyperemic hydrocephalus [2, 3]. There is some evidence that the brain extracellular space has increased fluid within it. A common set of anatomic findings in IIH are that these patients tend to have small cerebral ventricles and small intracranial subarachnoid spaces, and with decompression, either with shunting of CSF in the lateral ventricles or by bone removal of the squamous temporal bone, the brain expands into those spaces [4]. More recent analysis of magnetic resonance imaging (MRI) of the brain in IIH patients, however, does not support these findings [5]. There is also evidence that elevated pressure differentials between CSF and central venous blood pressures are a mechanism for IIH. These may be a consequence of venous hypertension or venous outflow obstruction as in cases of venous sinus stenosis. Therefore, while there are many known causes of intracranial hypertension, so-called secondary IH, there remain many patients whose pathophysiology is truly idiopathic.

We use the modified Dandy criteria to make the diagnosis [6]. First, there need to be signs and symptoms of elevated ICP, including headache, transient visual obscurations, tinnitus, papilledema, or possibly double vision secondary to a cranial nerve palsy. Second, there should be no localizing findings on neurologic exam. Third, all neurodiagnostic studies should be normal with the exception that the ICP should be elevated >25 cmH_2O. MRI findings of elevated ICP are allowed such as an empty sella turcica, a type I Chiari malformation, flattening of the globe, expansion of the optic nerve sheaths in the orbit, thinning or defects of the bone overlying the skull base, and smooth narrowing of the venous sinuses. Fourth, the patient should be awake and alert. Fifth, there are no other causes of the elevated intracranial pressure. These various anatomic findings may in fact point to the likelihood that the underlying causes of the elevated intracranial pressures in IIH condition may in fact be multifactorial.

The IIH condition is noted primarily in obese women of childbearing ages; the mean age is 30 years. Overall the incidence is 0.9 per 100,000 persons, 3.0/100,000 in women, and 19/100,000 in women who are >20% above their ideal body weight. Of the primary IIH patients, 90% are women, and 90% are obese [7]. The World Health Organization (WHO) body mass index (BMI) comparisons have documented that the world population is growing heavier. We are seeing increased weight worldwide, particularly in the USA. The obesity prevalence has gone from 11.5% in 1990 to 33.8% in 2008 in the USA alone [8].

We are seeing an increase in the diagnosis of the condition that may be related to these factors. We have attempted to document the increasing frequency of emergency room (ER) visits due to the IIH condition. We analyzed our ER admissions included only those whose primary diagnosis was IIH. We reviewed the numbers over a 2-year span, 2013 and 2014. Nearly 70 patients annually were seen in our

J. M. McGregor (✉)
Department of Neurological Surgery, The Ohio State University, Columbus, OH, USA
e-mail: John.McGregor@osumc.edu

N. Wang (ed.), *Intraocular and Intracranial Pressure Gradient in Glaucoma*,
Advances in Visual Science and Eye Diseases 1, https://doi.org/10.1007/978-981-13-2137-5_46

emergency room with IIH as their primary diagnosis. As expected, 90% were female patients. These patients required significant resources and time to conclude their ER visits. They spent an average of 9.7 h from arrival to release, undergoing such evaluations as routine blood work; head CT scans; MRI scans; X-rays of shunt implants; consultations with neurologists, ophthalmologists, and neurosurgeons; shunt adjustments; and lumbar punctures, many under fluoroscopy. This incidence analysis underestimates the frequency of the condition because it did not capture patients who may have other primary complaints in association with IIH, such as visual changes or headaches. As you can see, this is a resource intensive condition that is increasing in its incidence worldwide.

The more invasive treatments for IIH patients, such as surgery, are directed toward patients who have failed medical management. After the initial diagnosis, patients undergo lumbar puncture, both for diagnostic and therapeutic purposes, trials of medications, lifestyle changes, and close follow-up for examinations of vision. If the threat of visual loss remains high, or visual deterioration occurs despite medical management, or patients continue to suffer from intractable headaches that are modulated by lumbar puncture, then considerations for interventions with procedures or surgery would be considered. CSF decompression and diversion strategies include serial lumbar punctures, a lumbar drain trial, subtemporal bony decompressions, optic nerve sheath fenestrations/decompressions (OSNF), and shunting.

The OSNF has been shown to stabilize or improve vision in 89% of patients at 2 years [9]. Shunts have been shown to help preserve vision as well, with 95% of patients noting visual stability or improvement at 4 years[9]. Still, visual deterioration can occur, and these patients will continue to need frequent evaluations. Shunts are more frequently recommended in patients with a substantial complaint of intractable headache along with their visual threats. They are not as effective of a headache management tool, however. Ninety-five percent will note headache relief at 1 month, but only 52% continue to note headache relief at 2 years [10].

A relatively recent trend is the identification of venous hypertension due to sinus stenosis leading to the elevated ICP of IIH. There are several studies that have indicated relief from IIH symptoms, both visual and headache improvement, with endovascular venous sinus stenting. Identifying these patients has been somewhat controversial. There is a known narrowing of the sinuses that can occur as a consequence of elevated ICP, and identifying which patients would be amenable to stent placement has been a challenge. Patients with suggestive stenosis on CT angiography or MR angiography must then undergo a formal cerebral angiogram with venous pressure gradient measurements. Any sagittal sinus or bilateral transverse or sigmoid sinus narrowing associated with a 10 mmHg difference across would be amenable to placement of a stent. Patients then will need to be on platelet inhibitors for several months. Still the initial results are compelling with reduction of ICP elevations down to the normal ranges, 80–90% papilledema resolution and 80–100% headache improvement noted at 1.5 years [11, 12].

The indications for the placement of CSF diverting shunts include intractable visual abnormalities despite nonoperative management, rapid visual deterioration in the midst of beginning of medical management, significant ICP elevation with papilledema and vision deficit, and intractable headaches. The decision on type of shunt and its locations can depend on several anatomic factors including ventricular size, abdominal size, previous surgeries, and the presence or absence of a Chiari malformation. Ventricles that are too small may obstruct too soon to make a ventricular shunt successful, and a lumbar shunt may be preferred. The ventricular catheter placement for IIH patients really only became useful with the advent of widely available stereotactic intraoperative image guidance catheter placements because of the small ventricular size that is typical in IIH patients. Lumbar shunts may be more difficult to place in the patient with the larger abdominal girth. They may also be problematic in the patients with a known Chiari I malformation as they may exacerbate this condition making the patients symptomatic secondary to their lumbar CSF diversion. Previous abdominal surgeries or intraperitoneal infections may preclude peritoneal placement and indicate that placement of the distal catheter into either the internal jugular vein or the pleural cavity should be considered.

There are several choices for catheters and valves, but no evidence that any are particularly superior in this patient population. There are catheters of various diameters, and some impregnated with antibiotics. There are valve systems that are fixed pressures, have gravity compensations, have adjustable pressures, and have adjustable pressures that remain locked during MRI scans and systems that are with and without anti-siphon devices. There are surgical adjuncts to the placement of shunts that are useful, including stereotactic image guidance and endoscopic assists for ventricular placement, laparoscopic techniques for peritoneal placements, and ultrasound for percutaneous venous access for jugular vein placements.

As stated above, shunts are an effective treatment tool to assist with visual stabilization and improvement in patients with intractable IIH. They are less effective as a

headache management tool. They do require frequent neurosurgical outpatient visits to assist with shunt pressure adjustments, and they are associated with high revision rates. We reviewed our series of 61 first-time shunt placements from 2003 to 2008 and identified a 51% revision rate irrespective of LP or VP configuration, on average at 4 months post-op, for such things as distal or proximal failure, persistent ICP elevation, intractable low-pressure symptoms, and infections. Additionally we noted an acquired Chiari malformation rate in the lumboperitoneal shunt placements of 29%, occurring between 3 months and 6.5 years post-op, and a need for suboccipital decompression in 14% of the patients.

In summary, those patients with idiopathic intracranial hypertension who have significant visual threat or visual deterioration despite best medical management or whose visual deterioration is rapid enough to warrant urgent intervention should be considered for operative management. CSF diversion with these variously described forms of shunt placements is a useful adjunct in the management of this condition. They are associated with successful visual preservation, moderately successful in headache amelioration, and require frequent monitoring because of a frequent need for additional surgeries. Further understanding of the pathophysiology is needed to help direct more targeted therapeutics including surgery for IIH in the future. Thank you.

References

1. Boulton M, et al. Raised intracranial pressure increases CSF drainage through arachnoid villi and extracranial lymphatics. Am J Physiol. 1998;275:889–96.
2. Dandy WE, et al. Intracranial pressure without brain tumor diagnosis and treatment. Ann Surg. 1937;106:492–513.
3. Bateman GA, et al. Association between arterial inflow and venous outflow in idiopathic and secondary intracranial hypertension. J Clin Neurosci. 2006;13:550–7.
4. Sahs AL, Hyndman OR, et al. Intracranial hypertension of unknown cause: cerebral edema. Arch Surg. 1939;38:428–42.
5. Bastin ME, et al. Diffuse brain oedema in idiopathic intracranial hypertension: a quantitative magnetic resonance imaging study. J Neurol Neurosurg Psychiatry. 2003;74(12):1693–6.
6. Wall M. Idiopathic intracranial hypertension. Neurol Clin. 2010;28(3):593–617.
7. Durcan FJ, et al. The incidence of pseudotumor cerebri. Population studies in Iowa and Louisiana. Arch Neurol. 1988;45:875–7.
8. http://apps.who.int/bmi/index.jsp accessed 11/05/2016.
9. Feldon SE. Visual outcomes comparing surgical techniques for management of severe idiopathic intracranial hypertension. Neurosurg Focus. 2007;23(5):E6.
10. MJ MG, et al. Cerebrospinal fluid shunt placement for pseudotumor cerebri—associated intractable headache: predictors of treatment response and an analysis of long-term outcomes. J Neurosurg. 2004;101:627–32.
11. Donnet A, et al. Endovascular treatment of idiopathic intracranial hypertension: clinical and radiologic outcome of 10 consecutive patients. Neurology. 2008;70(8):641–7.
12. Bussière M, et al. Unilateral transverse sinus stenting of patients with idiopathic intracranial hypertension. AJNR Am J Neuroradiol. 2010;31(4):645–50.

Idiopathic Intracranial Hypertension

47

Ruowu Hou and Ningli Wang

47.1 Introduction

Idiopathic intracranial hypertension (IIH) is the disease with characteristics of higher intracranial pressure (ICP), but the pathogenic mechanism is still not clear. In general population the incidence is about 0.5–2 per 100,000 people per year [1–4]; however, in the obese women, it is around 12–20 per 100,000 people per year [1, 2, 5]. Its typical symptoms include headache, visual dysfunction, pulsatile tinnitus, and neck pain, and the vital one is the visual loss. As the visual acuity loss is highly variable, from mild to severity, and in general the process takes some time, which can cause delays in diagnosis and treatment, it could lead to considerable visual morbidity. The emblematic sign is the papilloedema, but this is not the only sign of IIH, and making diagnosis should exclude the other identifiable secondary causes such as intracranial tumor and hemorrhage. At present, the modified Dandy criteria [6] are usually considered the optimal diagnosis criteria. There are numerous therapeutic methods to treat IIH, but there is no consensus on the best method which is accepted by doctors who come from different departments involving ophthalmology, neurology, and neurosurgery.

In this chapter, we will introduce some progress in the pathogenesis, diagnosis, and treatment, from different viewpoints of ophthalmologist, neurologist, and neurosurgeon. We do not judge who is right or what is the best. We just highlight these latest findings and briefly discuss what we could learn from them and what factors we should consider when we make diagnosis, treatment, and future researches.

47.2 Possible Mechanism

It is not clear about the pathogenesis of idiopathic intracranial hypertension and there is no a universal theory that is accepted by all researchers. However, there are three mechanisms that could not be neglected: CSF hypersecretion, CSF malabsorption, and CSF outflow obstruction. On the other hand, obesity, hormonal and other metabolic causes, etc. are also important factors in the pathogenic mechanisms of IIH [7, 8].

47.2.1 CSF Hypersecretion

In traditional theory, the CSF is mainly produced by choroid plexuses in the lateral and third ventricles, and the rate of CSF formation is about 0.35 to 0.40 mL/min or 500 to 600 mL/day in adults. As the whole nervous system normally contains approximately 140 mL of CSF, the volume of CSF is replaced 3–4 times per day. If the producing rate of CSF increases and the absorbing rate does not rise up accordingly, there are more CSF in the nervous system; that is to say, more than 140 mL of CSF exists in the intracranial cavity. Because of the limitation of the skull, the intracranial pressure (ICP) rises and results in a series of symptoms and signs of intracranial hypertension. However, there are no direct evidences to prove this and some studies do not support this theory [9, 10]. Moreover, in patients of IIH, ventricular enlargement or hydrocephalus does not occur, and on the contrary, the lateral ventricles remain normal size or a little bit smaller like slit, which cannot be explained by secretory increase of CSF.

R. Hou
Department of Neurosurgery, Beijing Tongren Hospital, Capital Medical University, Beijing, China

N. Wang (✉)
Beijing Institute of Ophthalmology, Beijing Tongren Eye Center, Beijing Tongren Hospital, Capital Medical University, Beijing, China

Beijing Ophthalmology & Visual Sciences Key Laboratory, Beijing, China
e-mail: wningli@vip.163.com

N. Wang (ed.), *Intraocular and Intracranial Pressure Gradient in Glaucoma*,
Advances in Visual Science and Eye Diseases 1, https://doi.org/10.1007/978-981-13-2137-5_47

47.2.2 CSF Malabsorption

Classically, the arachnoid granulations are regarded the main absorbing places of CSF. Thus, if there is something wrong with the arachnoid granulations, reduced absorption of CSF would happen and lead to fluid retention in intracranial cavity, resulting in intracranial hypertension. This has been identified by some researches [9, 11] which show that a delay of CSF clearance could be observed by the method of isotope infusion, compared with normal subjects.

Recently, with the development of technology, findings from some research show that in the central nervous system, CSF is not only absorbed by arachnoid granulations but also by lymphatic system which has been identified existing in the brain and perivascular space. Especially, more and more research [12–15] focus on the lymphatic system which may play an important role in the pathophysiology of CSF circulation in the central nervous system and, much more than this, the optic nerve. In spite of this, it brings new light on the mechanism of IIH.

47.2.3 CSF Outflow Obstruction

When discussing CSF outflow pathway, it is necessary to consider venous sinuses because CSF finally is drained into them. The driving force of CSF absorption is the pressure gradient between ICP and venous sinus pressure, which push CSF flow out from the intracranial cavity to the venous system. The rise of venous sinus pressure results in increased CSF outflow resistance and intracranial hypertension. Venous sinus stenosis is a common finding in IIH, which often occurs in the transverse sinus [16–20]. However, it is not clear which one is the initial reason—venous sinus stenosis or intracranial hypertension—because some studies find that after lumboperitoneal shunt, venous sinus stenosis could resolute; that is to say, in idiopathic intracranial hypertension, higher ICP may be caused by the collapse of transverse sinus, while it is also possible that a stenosed sinus may be one of the phenomenon of higher ICP [21, 22]. It is just like to answer the question "which came first, the chicken or the egg?"

47.2.4 Obesity

In most cases of IIH, it is noted that obesity is popular and has strong correlation with intracranial hypertension. Some studies [23–27] suggest that weight loss could be a remedy for IIH. By contrast, weight gain is highly correlated to development and recurrence of IIH [28, 29]. However, the mechanism why weight loss could lower ICP and treat IIH is not clear. The possible theory is focusing on the mechanical changes of pressures because of abdominal fat accumulation. The hypothesis [30] is obesity could raise the abdominal and intrathoracic pressures which increase the venous pressure, and so accordingly the venous sinus pressure rise can prevent CSF drainage into venous system, resulting in intracranial hypertension. Nevertheless, for one thing, the incidence of IIH is just higher in obese women but not in obese men, with a reported female-to-male ratio of 8:1 [26, 27, 31]. For the other thing, some people who is overweight do not suffer IIH and the mass alone of weight is not a convincing illustration for clinical observation because BMI is not strongly related to CSF opening pressure measured by lumbar puncture [32, 33].

Notwithstanding, it cannot be denied that the patients of IIH could benefit from weight loss. The improvement in symptoms and signs such as headache and papilloedema is noticeable after weight reduction not only in obese patients but also in nonobese cases [28, 29]. Therefore, obesity cannot never be overlooked when we research on the mechanism of IIH.

47.2.5 Others

There are some other hypotheses to explain the mechanism of IIH including hormones, vitamin A, and iron deficiency anemia, but no one could be a perfect explanation for IIH. Obviously, it is a long way to identify the real mechanism of IIH.

47.3 Diagnosis

In 1937, Dandy—one of the most famous neurosurgeons—proposed the diagnostic criteria for IIH. However, the Dandy criterion was only focused on the symptoms and signs without efficient radiographic evidence because of restrictions of the time. After that, with the development of imaging technology, especially high-quality CT and MRI scans available, some studies proposed the modified Dandy criteria [34, 35]. Accordingly, the diagnosis of IIH is not only based on the clinical expression but on the positive findings by CT and MRI which reflect raised ICP, and at the same time, the secondary causes such as tumors or hemorrhage resulting in intracranial hypertension should be excluded. On the other hand, through CTV or MRV, it is possible to get more details about venous sinuses, specifically, venous sinus thrombosis or stenosis. For the former, it may be the cause of acute intracranial hypertension and sometimes it needs endovascular treatments like thrombolysis or stents. For the later, it gives us a look-in to understand the mechanism of IIH [19, 36–40].

Regarding the diagnosis of IIH, ICP is the vital factor that cannot be denied. Because it is impossible to measure ICP

directly, in general, the lumbar puncture is done to identify the level of ICP, in which patients should be in lateral decubitus, bending knees, and coxa. But after success of punctuation, patients, on the contrary, should relax and breathe smoothly. So, when interpreting results of measured pressures by lumbar puncture, it should be a caution whether CSF opening pressures is the real one because there are just too many factors that could influence the results of measurement, not to mention one snapshot. Nevertheless, more than 250 mmH_2O in lumbar puncture are still deemed as the necessary diagnostic criteria of IIH, and components such as protein should be normal.

The newest revised diagnostic criteria of IIH were proposed by Friedman et al. [6] in which papilloedema and the sixth cranial nerve—abducens nerve—were specified. Moreover, the correlation between the optic nerve and higher ICP was of importance in the diagnosis of IIH, including flattening of the posterior eyeball, widening of the subarachnoid space of the optic nerve, projecting of the optic papilla, and distorting of the optic nerve [41–45].

47.4 Treatment

Because the mechanism of IIH is still not clear and no consensus among all of researchers on one therapy is better than the others, there are several management strategies—weight loss, acetazolamide, optic nerve sheath fenestration, CSF diversion like L-P shunt, and dural venous sinus stenting—accepted, respectively, by clinical doctors coming from different departments including neurologists, neurosurgeons, ophthalmologists, and neuroradiation-interventional physicians. Some clinical trials or reviews have been done, but good-quality randomized controlled ones are still absent [46–52].

47.4.1 Weight Loss

Although the link between weight loss and IIH is not confirmed, it could not be denied that patients of IIH, either obese or not, could benefit from weight reduction only or when combined with other treatments. [53–57]. Recently, some reviews further highlight the effectiveness of weight reduction in treating IIH not only relieving headaches but also improving visual acuity and papilloedema [7, 23, 58]. In another study, patients reducing weight less than 3.5% of BMI though could influence the ICP insignificantly ($p = 0.6$). Furthermore, weight loss is not only a remedy for IIH but a main predictor of a favorable outcome in terms of CSF opening pressure of lumbar puncture [59].

In order to prevent or cure IIH, generally weight loss is firstly recommended by physicians. However, in the process of treatment, the most challenging thing is to maintain the effectiveness of weight loss not just for a short while but rather over a long time. To achieve this goal, bariatric surgery is just the beginning, and the lifestyle modification is indeed the endpoint. Typically, the specialists would give the patients some advice including diet control, physical activity, and behavioral therapy. Clinicians also could rely on some programs like Weight Watchers or Nutrisystem, showing promising efficiency [60].

Furthermore, bariatric surgery is also used in weight loss, and it is an effective and quick weight reduction method for IIH [61, 62]. Finding from some reviews and meta-analysis [58, 63–65], after bariatric surgery, not only papilloedema could be alleviated but ICP be reduced. Therefore, bariatric surgery is quite prospecting in the treatment of IIH. Notwithstanding, as a surgical procedure, surgical complications like small bowel obstruction and anastomosis leak are not avoided [62]. Moreover, the correlation between weight loss and ICP is not explicit, and the long-term effectiveness of bariatric surgery for IIH is still not established. It should be cautious to apply this surgical method to treat IIH.

47.4.2 Acetazolamide

Acetazolamide now is popularly used to control intraocular pressure (ICP) in glaucoma and ICP in idiopathic intracranial hypertension because it inhibits the enzyme carbonic anhydrase located in the choroid plexus and ciliary epithelial cells to reduce secretion of CSF and aqueous fluid [66–69]. However, originally, the first studies [52] could not provide confirmed evidence for the efficacy of acetazolamide even though they are open-label randomized pilot study, but it did not recruit enough patients in the treatment group and placebo group. Until 2014, the idiopathic intracranial hypertension treatment trail (IIHTT) [70], a multicenter, randomized, double-blind placebo-controlled trial, has established firm evidences for the efficacy of acetazolamide. In this trail, both test group and placebo group are not treated only by acetazolamide but combined with low-salt weight-reduction diet; that is, the strategy of diet control plus acetazolamide is better than just diet alone. Compared with improvement in visual field, the scores of headache and visual acuity in both groups are not different significantly, which still need more research.

47.4.3 Optic Nerve Sheath Fenestration

As the impaired vision is the main complaint of IIH, they most often firstly see ophthalmologists. From the findings of MRI, subarachnoid space around optic nerve expands in patients, and it is reasonable that the CSF pressure in optic nerve subarachnoid space (ONSP) is the main cause of optic nerve damage. Thus, fenestrating the optic nerve sheath to

release ONSP is a rational remedy. Some researches [71–75] also prove this hypothesis in clinic. They reported that papilloedema, visual field, and visual acuity can be improved after fenestration; even more, undergoing optic nerve sheath fenestration in unilateral side provided clinical relief in both sides. The mechanism is not clear why unilateral optic nerve sheath fenestration can reduce papilloedema in the contralateral side, improving visual function in both optic nerves; moreover, there is no need to do operations on both optic nerves. However, other studies [76, 77] showed that visual function may deteriorate after operation. On the other hand, there are a number of complications such as transient or permanent visual loss, diplopia, retrobulbar hemorrhage, and ischemic optic neuropathy, even though in terms of blindness, based on a series of studies [78–81], it is not too high and under acceptable area.

However, for example, regardless of the complications, optic nerve sheath fenestration cannot solve headache, a main complain of IIH, which is sometimes serious and patients of IIH could not bear. Thus, it could be seen that there are two major weakness of optic nerve sheath fenestration. The first one is although fenestration could release CSF pressure around the optic nerve, it cannot decrease ICP which is the main cause of a series of symptoms and signs of IIH such as headache,abducens nerve paralysis, and tinnitus. The other is regarding the visual loss, in general, patients of IIH complain on both eyes, and operating on one side could solve both sides is still suspicious, though some research [71, 72] report that it could happen in some patients.

47.4.4 CSF Diversion

Although the pathophysiology of IIH is not very clear, all researchers admit that high ICP is the first and foremost factor which causes papilloedema, headache, and so on. Therefore, lowering ICP is a reasonable remedy of IIH. How can we lower ICP and maintain ICP in a lower level? The CSF diversion is used by neurosurgeons to treat IIH, which include lumboperitoneal shunt, ventriculoperitoneal shunt, ventriculojugular shunt, and ventriculoatrial shunt. Because of considering the safety and efficacy, the lumboperitoneal and ventriculoperitoneal shunts are the most popular ones. Comparing the two methods, because ICP is higher in IIH, the ventricles are in general smaller than the normal ones or sometimes lateral ventricles are slit, and so it is difficult to punctuate the lateral ventricle and insert the catheter, and the lumboperitoneal shunt is more often applied in CSF division for patients of IIH.

There are some complications of lumboperitoneal shunt such as obstruction of catheter, infection, intracranial hypotension, and even tonsillar herniation. However, all these complications happen because of technological limitations. With the development of technology, especially the programmable valve used in the CSF diversion, if the setup pressure before operation is not suitable for the patient after CSF diversion, it is possible to change the setting pressure gradually to fit the patient and to reduce the incidence of complications such as intracranial hypotension and tonsillar herniation [82–85].

47.4.5 Dural Venous Sinus Stenting

From MRV or CTV scans, venous stenosis is a typical finding in IIH, and some researchers hypothesized that it is the reason of higher ICP because when venous sinus pressure is higher, CSF cannot flow into venous system normally and that would cause CSF malabsorption. From this hypothesis, it is reasonable that dural venous sinus stenting which is able to solve venous stenosis is an established treatment for IIH. Higgins et al. found that in 12 patients of IIH, venous pressure gradients were decreased after interventional therapy [86, 87]. However, there have been no prospective, randomized controlled trials until present, and long-term effectiveness is not clear in spite of complications like stent thrombosis, stent migration, and restenosis which are sometimes more dangerous than IIH [88–90].

From another point of view, it is unclear about the causality between venous stenosis and higher ICP. More research should be done in the future.

47.5 Conclusion

The mechanism of IIH is unclear, and with gradual understanding, people get more information about its pathophysiology to guide management and achieve much better therapeutic efficacy in advance. Moreover, accompanying with improvements in medical imaging such as CT and MRI, it is possible to provide more evidence on diagnosis and treatment of IIH.

It is interesting that with the development of modern society, obesity is popular in the world, and there is tendency that the incidence of IIH increases gradually, together with more people that need to be treated in clinics. Weight loss seems to be not only a promising treatment for the patient of IIH but also an effective method for preclinical people to prevent IIH. In addition to weight loss, acetazolamide, optic nerve sheath fenestration, CSF division, and dural venous sinus stenting have their own advantages and disadvantages. Based on the present comprehension, it is unable to judge which one is better than the other one, and further research is needed to assess the short-term and long-term efficacy on these therapeutic methods.

References

1. Raoof N, et al. The incidence and prevalence of idiopathic intracranial hypertension in Sheffield. UK Eur J Neurol. 2011;18(10):1266–8.
2. Durcan FJ, Corbett JJ, Wall M. The incidence of pseudotumor cerebri. Population studies in Iowa and Louisiana. Arch Neurol. 1988;45(8):875–7.
3. Idiculla T, et al. The incidence and prevalence of idiopathic intracranial hypertension in south Sharaqiah region, Oman. Oman J Ophthalmol. 2013;6(3):189–92.
4. Kesler A, et al. The incidence of idiopathic intracranial hypertension in Israel from 2005 to 2007: results of a nationwide survey. Eur J Neurol. 2014;21(8):1055–9.
5. Radhakrishnan K, et al. Idiopathic intracranial hypertension (pseudotumor cerebri). Descriptive epidemiology in Rochester, Minn, 1976 to 1990. Arch Neurol. 1993;50(1):78–80.
6. Friedman DI, Liu GT, Digre KB. Revised diagnostic criteria for the pseudotumor cerebri syndrome in adults and children. Neurology. 2013;81(13):1159–65.
7. Sinclair AJ, et al. Low energy diet and intracranial pressure in women with idiopathic intracranial hypertension: prospective cohort study. BMJ. 2010;341:c2701.
8. Newborg B. Pseudotumor cerebri treated by rice reduction diet. Arch Intern Med. 1974;133(5):802–7.
9. Malm J, et al. CSF hydrodynamics in idiopathic intracranial hypertension: a long-term study. Neurology. 1992;42(4):851–8.
10. Eisenberg HM, McComb JG, Lorenzo AV. Cerebrospinal fluid overproduction and hydrocephalus associated with choroid plexus papilloma. J Neurosurg. 1974;40(3):381–5.
11. Johnston I. The definition of reduced CSF absorption syndrome: a reappraisal of benign intracranial hypertension and related conditions. Med Hypotheses. 1975;1(1):10–4.
12. Ludemann W, et al. Ultrastructure of the cerebrospinal fluid outflow along the optic nerve into the lymphatic system. Childs Nerv Syst. 2005;21(2):96–103.
13. Zakharov A, Papaiconomou C, Johnston M. Lymphatic vessels gain access to cerebrospinal fluid through unique association with olfactory nerves. Lymphat Res Biol. 2004;2(3):139–46.
14. Johnston M, et al. Evidence of connections between cerebrospinal fluid and nasal lymphatic vessels in humans, non-human primates and other mammalian species. Cerebrospinal Fluid Res. 2004;1(1):2.
15. Johnston M, Papaiconomou C. Cerebrospinal fluid transport: a lymphatic perspective. News Physiol Sci. 2002;17:227–30.
16. Morris PP, et al. Transverse Sinus Stenosis Is the Most Sensitive MR Imaging Correlate of Idiopathic Intracranial Hypertension. AJNR Am J Neuroradiol. 2017;38(3):471–7.
17. Carvalho GB, et al. A new index for the assessment of transverse sinus stenosis for diagnosing idiopathic intracranial hypertension. J Neurointerv Surg. 2017;9(2):173–7.
18. Riggeal BD, et al. Clinical course of idiopathic intracranial hypertension with transverse sinus stenosis. Neurology. 2013;80(3):289–95.
19. Ridha MA, et al. MRI findings of elevated intracranial pressure in cerebral venous thrombosis versus idiopathic intracranial hypertension with transverse sinus stenosis. Neuroophthalmology. 2013;37(1):1–6.
20. Connor SE, et al. The relationship of transverse sinus stenosis to bony groove dimensions provides an insight into the aetiology of idiopathic intracranial hypertension. Neuroradiology. 2008;50(12):999–1004.
21. Stevens SA, et al. Idiopathic intracranial hypertension and transverse sinus stenosis: a modelling study. Math Med Biol. 2007;24(1):85–109.
22. McGonigal A, Bone I, Teasdale E. Resolution of transverse sinus stenosis in idiopathic intracranial hypertension after L-P shunt. Neurology. 2004;62(3):514–5.
23. Subramaniam S, Fletcher WA. Obesity and weight loss in idiopathic intracranial hypertension: a narrative review. J Neuroophthalmol. 2017;37(2):197–205.
24. Naarden MT, et al. Idiopathic intracranial hypertension and obesity. Ned Tijdschr Geneeskd. 2015;159:A7980.
25. Banik R. Obesity and the role of nonsurgical and surgical weight reduction in idiopathic intracranial hypertension. Int Ophthalmol Clin. 2014;54(1):27–41.
26. Andrews LE, Liu GT, Ko MW. Idiopathic intracranial hypertension and obesity. Horm Res Paediatr. 2014;81(4):217–25.
27. Schwartz R, et al. The obesity pattern of idiopathic intracranial hypertension in men. Graefes Arch Clin Exp Ophthalmol. 2013;251(11):2643–6.
28. Daniels AB, et al. Profiles of obesity, weight gain, and quality of life in idiopathic intracranial hypertension (pseudotumor cerebri). Am J Ophthalmol. 2007;143(4):635–41.
29. Ko MW, et al. Weight gain and recurrence in idiopathic intracranial hypertension: a case-control study. Neurology. 2011;76(18):1564–7.
30. Sugerman HJ, et al. Increased intra-abdominal pressure and cardiac filling pressures in obesity-associated pseudotumor cerebri. Neurology. 1997;49(2):507–11.
31. Hannerz J, Ericson K. The relationship between idiopathic intracranial hypertension and obesity. Headache. 2009;49(2):178–84.
32. Whiteley W, et al. CSF opening pressure: reference interval and the effect of body mass index. Neurology. 2006;67(9):1690–1.
33. Bono F, et al. Obesity does not induce abnormal CSF pressure in subjects with normal cerebral MR venography. Neurology. 2002;59(10):1641–3.
34. Friedman DI, Jacobson DM. Diagnostic criteria for idiopathic intracranial hypertension. Neurology. 2002;59(10):1492–5.
35. Smith JL. Whence pseudotumor cerebri? J Clin Neuroophthalmol. 1985;5(1):55–6.
36. Piette JC, Wechsler B, Vidailhet M. Idiopathic intracranial hypertension: don't forget cerebral venous thrombosis. Am J Med. 1994;97(2):200.
37. Sylaja PN, et al. Differential diagnosis of patients with intracranial sinus venous thrombosis related isolated intracranial hypertension from those with idiopathic intracranial hypertension. J Neurol Sci. 2003;215(1–2):9–12.
38. Lin A, et al. Occurrence of cerebral venous sinus thrombosis in patients with presumed idiopathic intracranial hypertension. Ophthalmology. 2006;113(12):2281–4.
39. Nithyanandam S, Joseph M, Mathew T. Clinical profile of cerebral venous thrombosis and the role of imaging in its diagnosis in patients with presumed idiopathic intracranial hypertension. Indian J Ophthalmol. 2011;59(2):169. author reply 169-70
40. Hardin JS, et al. Idiopathic intracranial hypertension progressing to venous sinus thrombosis, subarachnoid hemorrhage, and stroke. J Neuroophthalmol. 2017;38(1):60–4.
41. Saindane AM, et al. Association of MRI findings and visual outcome in idiopathic intracranial hypertension. AJR Am J Roentgenol. 2013;201(2):412–8.
42. Lee SH, et al. MRI and ultrasonographic findings in idiopathic intracranial hypertension. Cephalalgia. 2013;33(2):139–40.
43. Alperin N, et al. MRI evidence of impaired CSF homeostasis in obesity-associated idiopathic intracranial hypertension. AJNR Am J Neuroradiol. 2013;34(1):29–34.
44. Mandelstam S, Moon A. MRI of optic disc edema in childhood idiopathic intracranial hypertension. Pediatr Radiol. 2004;34(4):362.
45. Manfre L, et al. Idiopathic intracranial hypertension: orbital MRI. Neuroradiology. 1995;37(6):459–61.

46. Kalyvas AV, et al. Efficacy, complications and cost of surgical interventions for idiopathic intracranial hypertension: a systematic review of the literature. Acta Neurochir. 2017;159(1):33–49.
47. Hui FK, Abruzzo T, Ansari SA. Endovascular Interventions for Idiopathic Intracranial Hypertension and Venous Tinnitus: New Horizons. Neuroimaging Clin N Am. 2016;26(2):289–99.
48. Sivasankar R, et al. Imaging and interventions in idiopathic intracranial hypertension: a pictorial essay. Indian J Radiol Imaging. 2015;25(4):439–44.
49. Piper RJ, et al. Interventions for idiopathic intracranial hypertension. Cochrane Database Syst Rev. 2015;8:CD003434.
50. Spitze A, Malik A, Lee AG. Surgical and endovascular interventions in idiopathic intracranial hypertension. Curr Opin Neurol. 2014;27(1):69–74.
51. Uretsky S. Surgical interventions for idiopathic intracranial hypertension. Curr Opin Ophthalmol. 2009;20(6):451–5.
52. Lueck C, McIlwaine G. Interventions for idiopathic intracranial hypertension. Cochrane Database Syst Rev. 2005;3:CD003434.
53. Wong R, et al. Idiopathic intracranial hypertension: the association between weight loss and the requirement for systemic treatment. BMC Ophthalmol. 2007;7:15.
54. McIlwaine G, Lueck C. Weight loss in idiopathic intracranial hypertension. Ophthalmology. 1999;106(12):2232–3.
55. Kupersmith MJ, et al. Effects of weight loss on the course of idiopathic intracranial hypertension in women. Neurology. 1998;50(4):1094–8.
56. Johnson LN, et al. The role of weight loss and acetazolamide in the treatment of idiopathic intracranial hypertension (pseudotumor cerebri). Ophthalmology. 1998;105(12):2313–7.
57. Sugerman HJ, et al. Effects of surgically induced weight loss on idiopathic intracranial hypertension in morbid obesity. Neurology. 1995;45(9):1655–9.
58. Manfield JH, et al. Bariatric surgery or non-surgical weight loss for idiopathic intracranial hypertension? A systematic review and comparison of meta-analyses. Obes Surg. 2017;27(2):513–21.
59. Skau M, et al. Disease activity in idiopathic intracranial hypertension: a 3-month follow-up study. J Neurol. 2011;258(2):277–83.
60. Gudzune KA, et al. Efficacy of commercial weight-loss programs: an updated systematic review. Ann Intern Med. 2015;162(7):501–12.
61. Perez-Sanchez JR, et al. Treatment of idiopathic intracranial hypertension with bariatric surgery. Neurologia. 2016;114(1):34–9.
62. Garb J, et al. Bariatric surgery for the treatment of morbid obesity: a meta-analysis of weight loss outcomes for laparoscopic adjustable gastric banding and laparoscopic gastric bypass. Obes Surg. 2009;19(10):1447–55.
63. Cazzo E, et al. Bariatric surgery as a treatment for pseudotumor cerebri: case study and narrative review of the literature. Sao Paulo Med J. 2017;136(2):182–7.
64. Fridley J, et al. Bariatric surgery for the treatment of idiopathic intracranial hypertension. J Neurosurg. 2011;114(1):34–9.
65. Handley JD, et al. Bariatric surgery as a treatment for idiopathic intracranial hypertension: a systematic review. Surg Obes Relat Dis. 2015;11(6):1396–403.
66. Masuzawa T, Saito T, Sato F. Cytochemical study on enzyme activity associated with cerebrospinal fluid secretion in the choroid plexus and ventricular ependyma. Brain Res. 1981;222(2):309–22.
67. Buxton N, Punt J. Choroid plexus papilloma producing symptoms by secretion of cerebrospinal fluid. Pediatr Neurosurg. 1997;27(2):108–11.
68. Keep RF, et al. Choroid plexus ion transporter expression and cerebrospinal fluid secretion. Acta Neurochir Suppl. 1997;70:279–81.
69. Damkier HH, Brown PD, Praetorius J. Cerebrospinal fluid secretion by the choroid plexus. Physiol Rev. 2013;93(4):1847–92.
70. Committee, N.I.I.H.S.G.W, et al. Effect of acetazolamide on visual function in patients with idiopathic intracranial hypertension and mild visual loss: the idiopathic intracranial hypertension treatment trial. JAMA. 2014;311(16):1641–51.
71. Agarwal MR, Yoo JH. Optic nerve sheath fenestration for vision preservation in idiopathic intracranial hypertension. Neurosurg Focus. 2007;23(5):E7.
72. Alsuhaibani AH, et al. Effect of optic nerve sheath fenestration on papilledema of the operated and the contralateral nonoperated eyes in idiopathic intracranial hypertension. Ophthalmology. 2011;118(2):412–4.
73. Obi EE, et al. Optic nerve sheath fenestration for idiopathic intracranial hypertension: a seven year review of visual outcomes in a tertiary centre. Clin Neurol Neurosurg. 2015;137:94–101.
74. Pineles SL, Volpe NJ. Long-term results of optic nerve sheath fenestration for idiopathic intracranial hypertension: earlier intervention favours improved outcomes. Neuroophthalmology. 2013;37(1):12–9.
75. Starks V, et al. Effect of optic nerve sheath fenestration for idiopathic intracranial hypertension on retinal nerve fiber layer thickness. Orbit. 2016;35(2):87–90.
76. Fonseca PL, et al. Visual outcomes of surgical intervention for pseudotumour cerebri: optic nerve sheath fenestration versus cerebrospinal fluid diversion. Br J Ophthalmol. 2014;98(10):1360–3.
77. Spoor TC, McHenry JG. Long-term effectiveness of optic nerve sheath decompression for pseudotumor cerebri. Arch Ophthalmol. 1993;111(5):632–5.
78. Brodsky MC, Rettele GA. Protracted postsurgical blindness with visual recovery following optic nerve sheath fenestration. Arch Ophthalmol. 1998;116(1):107–9.
79. Flynn WJ, Westfall CT, Weisman JS. Transient blindness after optic nerve sheath fenestration. Am J Ophthalmol. 1994;117(5):678–9.
80. Mudumbai RC. Optic nerve sheath fenestration: indications, techniques, mechanisms and, results. Int Ophthalmol Clin. 2014;54(1):43–9.
81. Russo RR, et al. Progressive visual loss due to obstruction of an optic nerve sheath fenestration demonstrated on SPECT/CT radionuclide cisternography. Clin Nucl Med. 2010;35(3):208–10.
82. Abubaker K, et al. Idiopathic intracranial hypertension: lumboperitoneal shunts versus ventriculoperitoneal shunts--case series and literature review. Br J Neurosurg. 2011;25(1):94–9.
83. Alkherayf F, Abou Al-Shaar H, Awad M. Management of idiopathic intracranial hypertension with a programmable lumboperitoneal shunt: early experience. Clin Neurol Neurosurg. 2015;136:5–9.
84. El-Saadany WF, Farhoud A, Zidan I. Lumboperitoneal shunt for idiopathic intracranial hypertension: patients' selection and outcome. Neurosurg Rev. 2012;35(2):239–43. discussion 243-4
85. Hammers R, et al. Laparoscopic-assisted lumboperitoneal shunt placement for idiopathic intracranial hypertension. Semin Ophthalmol. 2008;23(3):151–5.
86. Higgins JN, et al. Venous sinus stenting for refractory benign intracranial hypertension. Lancet. 2002;359(9302):228–30.
87. Higgins JN, et al. Idiopathic intracranial hypertension: 12 cases treated by venous sinus stenting. J Neurol Neurosurg Psychiatry. 2003;74(12):1662–6.
88. Radvany MG, et al. Visual and neurological outcomes following endovascular stenting for pseudotumor cerebri associated with transverse sinus stenosis. J Neuroophthalmol. 2013;33(2):117–22.
89. Fields JD, et al. Dural venous sinus angioplasty and stenting for the treatment of idiopathic intracranial hypertension. J Neurointerv Surg. 2013;5(1):62–8.
90. Qiu MJ, et al. Dural venous sinus angioplasty and stenting for treatment of Idiopathic intracranial hypertension. Chin Med J. 2017;130(7):879–80.

Acknowledgement

This book was supported by National Natural Science Foundation of China (81730027, 81271005, 81300767), Beijing Municipal Administration of Hospitals' Youth Program (QML20180208), Beijing Natural Science Foundation (7122038) and the Capital Health Research and Development of Special Foundation, "Yangfan Plan" (ZYLX201501).

N. Wang (ed.), *Intraocular and Intracranial Pressure Gradient in Glaucoma*,
Advances in Visual Science and Eye Diseases 1, https://doi.org/10.1007/978-981-13-2137-5